Vertebrate Paleobiology and Paleoanthropology Series

Lawrence J. Flynn
Wen-Yu Wu
Editors

Late Cenozoic Yushe Basin, Shanxi Province, China: Geology and Fossil Mammals

Volume II: Small Mammal Fossils of Yushe Basin

Springer

Late Cenozoic Yushe Basin, Shanxi Province, China: Geology and Fossil Mammals

Vertebrate Paleobiology and Paleoanthropology Series

Edited by

Eric Delson
Vertebrate Paleontology, American Museum of Natural History
New York, NY 10024, USA
delson@amnh.org

Eric J. Sargis
Anthropology, Yale University
New Haven, CT 06520, USA
eric.sargis@yale.edu

Focal topics for volumes in the series will include systematic paleontology of all vertebrates (from agnathans to humans), phylogeny reconstruction, functional morphology, Paleolithic archaeology, taphonomy, geochronology, historical biogeography, and biostratigraphy. Other fields (e.g., paleoclimatology, paleoecology, ancient DNA, total organismal community structure) may be considered if the volume theme emphasizes paleobiology (or archaeology). Fields such as modeling of physical processes, genetic methodology, nonvertebrates or neontology are out of our scope.

Volumes in the series may either be monographic treatments (including unpublished but fully revised dissertations) or edited collections, especially those focusing on problem-oriented issues, with multidisciplinary coverage where possible.

More information about this series at http://www.springer.com/series/6978

Late Cenozoic Yushe Basin, Shanxi Province, China: Geology and Fossil Mammals

Volume II: Small Mammal Fossils of Yushe Basin

Edited by

Lawrence J. Flynn

Department of Human Evolutionary Biology, Harvard University, Cambridge, MA, USA

Wen-Yu Wu

Laboratory of Paleomammalogy, Institute of Vertebrate Paleontology and Paleoanthropology, Chinese Academy of Sciences, Beijing, China

Springer

Editors
Lawrence J. Flynn
Department of Human Evolutionary Biology
Harvard University
Cambridge, MA
USA

Wen-Yu Wu
Laboratory of Paleomammalogy
Institute of Vertebrate Paleontology
and Paleoanthropology
Chinese Academy of Sciences
Beijing
China

ISSN 1877-9077 ISSN 1877-9085 (electronic)
Vertebrate Paleobiology and Paleoanthropology Series
ISBN 978-94-024-1049-5 ISBN 978-94-024-1050-1 (eBook)
DOI 10.1007/978-94-024-1050-1

Library of Congress Control Number: 2016963174

Cover Illustration: View of Nan Zhuang Gou area in Yushe Basin with the early Pliocene upper Gaozhuang Formation in the middle ground. The yellow band in the middle ground is a marl marker bed. Younger Red Loess drapes over the outcrops on the upper right. The inset is a skull of the rabbit *Alilepus*, about 5 cm long (see Chapter 4). Background photo, 1988, by L. Flynn.

Printed on acid-free paper

This Springer imprint is published by Springer Nature
The registered company is Springer Science+Business Media B.V.
The registered company address is: Van Godewijckstraat 30, 3311 GX Dordrecht, The Netherlands

Preface

This second volume of the Springer series *Late Cenozoic Yushe Basin, Shanxi Province, China: Geology and Fossil Mammals* focuses on small mammal fossils about 6.5 to 1 million years old from an area of North China that played a role in the emergence of vertebrate paleontology as a modern science. Yushe Basin fossils present a view of changes in Northeast Asian terrestrial faunas during the Late Neogene, and therefore are a key to developing the biochronology for a vast part of the continent. Yushe strata record in one area a succession of faunas that has figured prominently in the definition of land mammal ages in the North Asian biogeographic province. Much of the basis for this system of ages has been the large mammal fauna, and now we can add the small mammals. Field and laboratory work of the last quarter century has added a rich small mammal component to the paleontology of Yushe, which greatly increases the understanding of evolution of its faunas as paleobiological communities. This volume presents the small mammal fossil record of Yushe Basin in the biostratigraphic framework dated by magnetostratigraphy, as developed by Neil Opdyke (University of Florida) and colleagues in Volume I of the Late Cenozoic of Yushe Basin.

The advances in micromammal paleontology presented in Volume II, "Small Mammal Fossils of Yushe Basin" were made possible by a team approach organized around the principle of attention to biostratigraphic detail. A large number of individuals carefully built and dated a stratigraphic framework in which fossil localities were placed relative to their horizons of occurrence. This approach yielded vastly better resolved provenance data for individual finds than were recorded in early historical collections. Secondly, we applied modern wet-screen techniques to process large volumes of sediment from fossiliferous concentrations. This provided improved representation of the micromammal assemblages preserved at individual localities and reduced bias toward representation of "large" small mammals at the expense of species characterized by small body size.

The Yushe teams were inspired by co-leaders Zhan-Xiang Qiu (Institute of Vertebrate Paleontology and Paleoanthropology, IVPP) and Richard H. Tedford (American Museum of Natural History, AMNH), who designed the project to maximize the biostratigraphic potential of Yushe Basin. They established a collegial atmosphere for collaboration by individuals from many institutions of China, the United States, and other countries. Figure 1 shows many of our group from 1987, the first full field season, including visitors S. Mahmood Raza and I.U. Cheema from Pakistan, and an army of paleontologists who made numerous surface finds of small mammal fossils.

Fig. 1 The Yushe Basin Team at the outset of field work, in front of the Yushe County Guest House. Left to right, front row, second from left, De-Fa Yan, fourth to seventh are Wen-Yu Wu, Zhan-Xiang Qiu, Richard Tedford, Will Downs, and at far right, Yi-Zheng Li; back row, left, is Tai-Ming Wang of the Yushe County Museum, fourth from left, Neil Opdyke, S. Mahmood Raza, I.U. Cheema, Xiao-Feng Chen, Jie Ye, and Gen-Zhu Zhu. Photo: September, 1987, by L.J. Flynn

The principal small mammal researchers for the Yushe project were Wen-Yu Wu, Zhu-Ding Qiu, and Lawrence J. Flynn, all of whom would admit that the great success of our work was due to the creativity, drive, and imagination of our colleague William R. Downs. Will, now deceased, prepared numerous fossil finds. Our team developed the succession of small mammal assemblages of Yushe to accompany the large mammal record in a comprehensive biostratigraphy by screening many new fossil localities throughout the succession of strata. The assemblages we developed represent changes in the small mammal community of the Yushe Basin, revealed on a fine scale not previously achieved. Detailed systematic studies on small mammal groups proceeded under the care of specialists, as presented in the chapters of this volume.

Acknowledgments

We express our deep gratitude to all the institutions and individuals, local and more broadly, who warmly supported the Yushe Project in various ways. We thank the people of the town of Yushe for their help and hospitality, and particularly the staff of the Yushe Hotel, who tolerated our screening program in their parking lot. For financial support we thank the National Natural Science Foundation (NSFC, China), the National Science Foundation (NSF, USA), and the Chinese Academy of Sciences. The two NSF grants EAR 8709221 and BSR 9020065 enabled our field work; later synthesis was supported under EAR grants 0716186 and 0958178. We acknowledge the authorities and our colleagues of the Institute of Vertebrate Paleontology and Paleoanthropology, the Tianjin Natural History Museum, and the American Museum of Natural History.

We thank especially our mentors, Zhan-Xiang Qiu and Dick Tedford, who created the atmosphere of scientific inquiry in which our project flourished. Their encouragement and support made our work possible. Sadly, Dick Tedford's health declined in recent years, and he

passed away in 2011, but the inspiration behind the project remained. We also think of Will Downs. Will died prematurely before he could see this volume published, but he steadfastly supported our work. Will found many of the fossils we present and processed most of them from the concentrate produced by screening. His spirit of scientific inquiry and enthusiasm carried us all forward as we developed a series of superposed small mammal horizons that span the entire Late Neogene sequence of Yushe Basin. He is sorely missed. Volume II benefitted from the contributions of many colleagues and associates of IVPP in Beijing and staff members of AMNH in New York, especially Frank Ippolito, Judy Galkin, Susan Bell, Ruth O'Leary, Alejandra Lora, Chester Tarka, and Loraine Meeker. Some of Frank's artwork developed with Dick Tedford for Volume I was adapted for Volume II.

Comparative collections are crucial to realize success in systematic work. For the small mammal fossils studied here, we relied heavily on the comparative collections of IVPP and the Paleontology Division at AMNH, but also on the mammal collections of various institutions. We thank their curators and collection managers. The Department of Mammalogy (currently under the day to day care of Eileen Westwig) at AMNH holds important reference collections, as do the Museum of Comparative Zoology, Harvard University (Judith Chupasko and Mark Omura), and Kunming Institute of Zoology (Song Li). We thank all for opening their collections to us.

We thank the entire Springer staff, particularly Sudeshna Das, for their help in realizing the Yushe Basin volumes. The meticulous efforts of series editors Eric Sargis and Eric Delson are deeply appreciated. They encouraged the maturation of the final product and its artwork. Finally, we acknowledge the constructive help of external manuscript reviewers. They devoted considerable time to help us to improve and update the following systematic accounts. Their careful reading led to increased clarity throughout the volume.

Lawrence J. Flynn
Wen-Yu Wu

Contents

Contributors

Lawrence J. Flynn
Department of Human Evolutionary Biology, and the Peabody Museum of Archaeology and Ethnology, Harvard University, Cambridge, MA, USA

Qiang Li
Key Laboratory of Vertebrate Evolution and Human Origins of Chinese Academy of Sciences, Institute of Vertebrate Paleontology and Paleoanthropology, Chinese Academy of Sciences, Beijing, People's Republic of China

Zhu-Ding Qiu
Laboratory of Paleomammalogy, Institute of Vertebrate Paleontology and Paleoanthropology, Chinese Academy of Sciences, Beijing, People's Republic of China

Wen-Yu Wu
Laboratory of Paleomammalogy, Institute of Vertebrate Paleontology and Paleoanthropology Chinese Academy of Sciences, Beijing, People's Republic of China

Xiaofeng Xu
Shuler Museum, Southern Methodist University, Dallas, TX, USA

Ying-Qi Zhang
Key Laboratory of Vertebrate Evolution and Human Origins of Chinese Academy of Sciences, Institute of Vertebrate Paleontology and Paleoanthropology, Chinese Academy of Sciences, Beijing, People's Republic of China

Shao-Hua Zheng
Laboratory of Paleomammalogy, Institute of Vertebrate Paleontology and Paleoanthropology, Chinese Academy of Sciences, Beijing, People's Republic of China

Chapter 1
Small Mammal Exploration in Yushe Basin, Shanxi Province

Lawrence J. Flynn and Wen-Yu Wu

Abstract Yushe Basin is an intermontane basin at the eastern edge of the Loess Plateau in northern China. Its fluvial, lake and superposed loess deposits accumulated during the last 7 myr and contain many fossiliferous horizons. Small mammal fossils occur throughout, and some fossil horizons produce diverse assemblages that appear to faithfully represent the micromammal component of Yushe paleocommunities. Yushe Basin includes assemblages that represent the late Baodean age (latest Miocene) microfaunas of North China, and document contrasting younger assemblages that characterize a distinct Pliocene Yushe chronofauna. Pliocene fossils represent two successive microfaunas that distinguish the Gaozhuangian and Mazegouan land mammal stage/ages. These are in turn distinct from the Pleistocene assemblages of Yushe that correlate with Nihewan and later faunas. The Sino-American project, especially in the interval of 1987–1991, developed the small mammal biostratigraphy of the Yuncu subbasin of Yushe Basin. Small mammal fossils occur in every Yuncu formation, from the Baodean age Mahui Formation, through the Pliocene Gaozhuang and Mazegou formations, to the early Pleistocene Haiyan Formation. Important elements of later Pleistocene faunas occur in overlying loess. Field teams collected specimens exposed on eroded surfaces and followed indications of small mammal concentrations to excavate bulk samples and process them for fossils by wet screening. Wet screening revealed a rich component of micromammal diversity to complement the wealth of larger species that previously had been known as surface finds.

Keywords Yushe Basin • Late Neogene • Biochronology • Small Mammals • North China • Screen Wash

L.J. Flynn (✉)
Department of Human Evolutionary Biology, and the Peabody Museum of Archaeology and Ethnology, Harvard University, Cambridge, MA 02138, USA
e-mail: ljflynn@fas.harvard.edu

W.-Y. Wu
Laboratory of Paleomammalogy, Institute of Vertebrate Paleontology and Paleoanthropology, Chinese Academy of Sciences, 142 Xizhimenwai Ave., Beijing 100044, People's Republic of China
e-mail: wuwenyu@ivpp.ac.cn

1.1 Introduction

The history of scientific exploration of Yushe Basin over the last century was chronicled in Chap. 2, Volume I, of the Springer series Late Cenozoic Yushe Basin, Shanxi Province, China: Geology and Fossil Mammals. Fossils from Yushe Basin have been known for nearly 100 years, and exploration culminated in the late 20th century in a joint Sino-American expedition led by members of the Institute of Vertebrate Paleontology and Paleoanthropology, Academia Sinica, (IVPP) and the American Museum of Natural History (AMNH). Important fossil sites had been found in the first half of the 20th century throughout Shanxi Province in North China (Fig. 1.1), including the classical Baode faunas (Kurtén 1952), localities in the Wuxiang area, lesser known finds from Shouyang, and the pivotal Yushe Basin. Yushe Basin was key because in one area "*Hipparion*" faunas of "Pontian" and younger age were overlain by Pleistocene faunas bearing the modern horse *Equus* (Licent and Trassaert 1935). The physical setting for fluvial and lacustrine deposition of the Late Neogene formations of Yushe in basins underlain by Triassic age bedrock was described in Volume I, Chapter 3.

Since the 1930s, special attention was given to the small mammal fossils preserved in the formations of Yushe Basin. Paleontologists Pierre Teilhard de Chardin and C.C. Young (1933) surveyed the Yushe area in 1932 and recognized the importance of Yushe Basin for its small mammal record. Teilhard de Chardin (1942) completed a monographic treatment of larger body size rodents that were well represented as fossils. Young embarked on a long career of study

Lawrence J. Flynn and Wen-Yu Wu (eds.), *Late Cenozoic Yushe Basin, Shanxi Province, China: Geology and Fossil Mammals, Volume II: Small Mammal Fossils of Yushe Basin*, Vertebrate Paleobiology and Paleoanthropology,
DOI 10.1007/978-94-024-1050-1_1

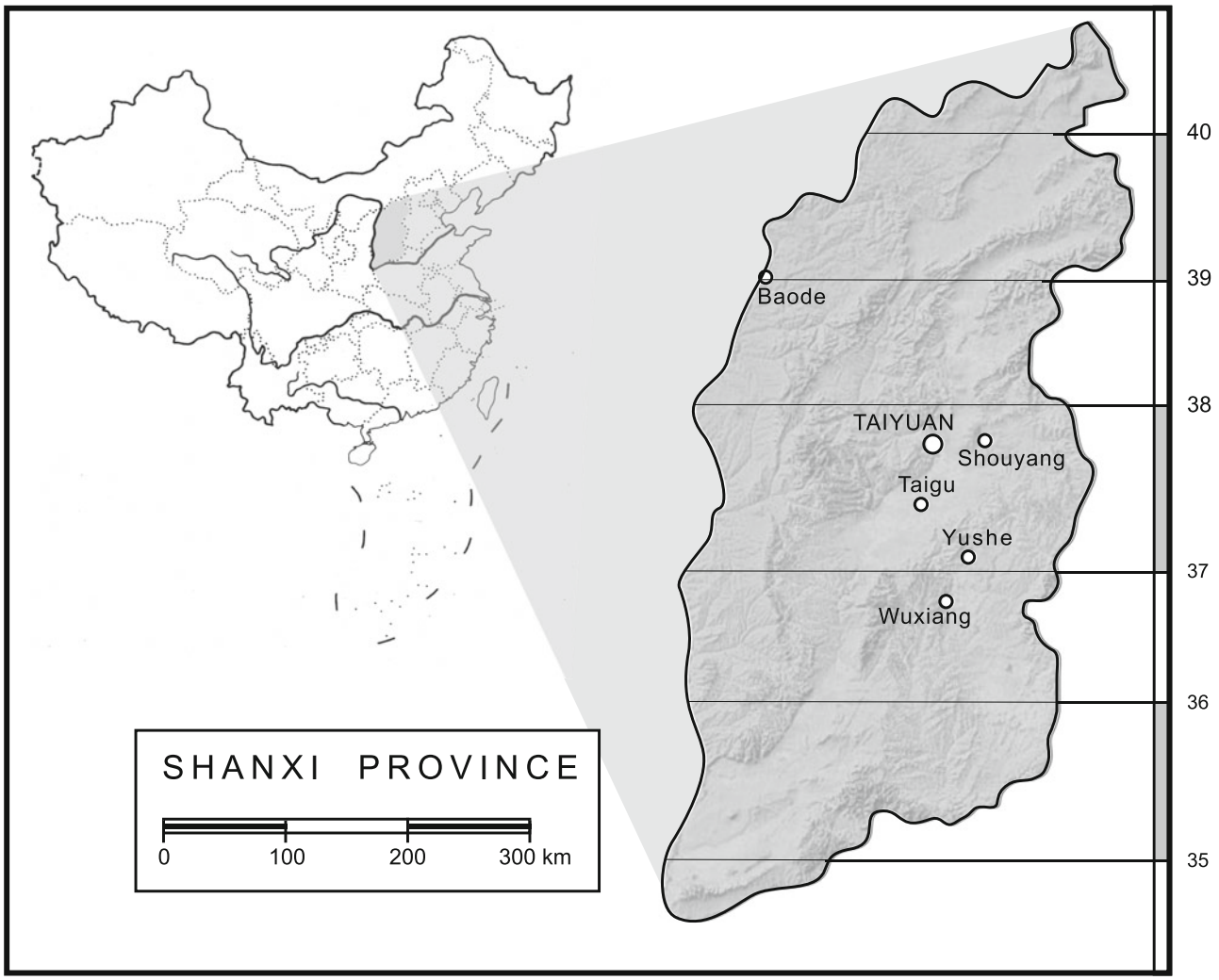

Fig. 1.1 Location of Shanxi Province within North China, indicating important fossil-producing regions: Baode, Shouyang, Yushe, and Wuxiang. Artwork by Frank Ippolito (AMNH) adapted from Fig. 1.1 of Volume I of this series

of small mammal fossils that in repeated instances influences the modern interpretation of Yushe microfaunas, as will be seen in the following chapters. Young (Chungchien Young, Zhong-Jian Yang) may be seen as the father of modern vertebrate paleontology in China.

Fossils were entombed throughout the deposits of Yushe Basin, so that superposed assemblages today represent successive samples of past biotas. The sediments were mainly gravels, sands and silts that accumulated to an aggregate thickness of about 800 m, and the entire series was blanketed by loess. Given generally limited cementation, fossils that accumulate on modern surface exposures due to erosion can be extracted easily from adhering matrix. The dating of Yushe sediments was presented in Chap. 4 of Volume I (Opdyke et al. 2013) in a tandem analysis of fossils and paleomagnetism: given an understanding of approximate age from fossils, characteristic magnetozones were correlated with the known magnetic time scale. In the case of Yushe, Late Neogene in age and known to contain early Pleistocene fossils at the top, the magnetochrons could be identified with characteristic chrons C1r to C3An, including the classical Matuyama, Gauss, and Gilbert chrons. In millions of years (Ma, megaannum) these date to about 2 to 6–7 Ma, with younger fossils from the loess. As noted in Volume I we use the prevailing concept of the Pleistocene beginning at about 2.6 Ma (Mascarelli 2011).

The modern epoch of research on Yushe Basin faunas began in 1978 when Zhan-Xiang Qiu and IVPP began stratigraphically controlled reconnaissance. It was clear (Qiu 1987) that the subbasins of Yushe (the Yuncu, Nihe, Ouniwa, Tancun, and Zhangcun subbasins) offered a laboratory in which to study on a fine scale mammalian biostratigraphy for North China. The Yuncu subbasin in particular presented a series of formations that spanned late

Miocene to early Pleistocene time. By 1987, Zhan-Xiang Qiu and Richard H. Tedford (AMNH) had mounted a collaborative Sino-American investigation of the geology and fossil mammals of Yushe Basin. Their teams concentrated on the Yuncu and Tancun subbasins of Yushe, collecting fossils throughout, and documenting nearly 200 fossil sites (Fig. 1.2a–c). Stratigraphic provenance was carefully controlled for each locality, which was numbered in sequence of study and given a prefix YS for "Yushe site". The present volume focuses on the micromammal component of the fossils produced from Yushe.

1.2 Small Mammal Recovery

Through most of the 20th century, Yushe small mammals appeared in field collections that had been retrieved as surface finds (Teilhard de Chardin 1942). These fossils represented mainly large body-size species of rabbits, beavers, bamboo rats, and zokors (the latter, an evolutionary radiation of subterranean muroids endemic to northeastern Asia). Such surface finds were comparable to those of large mammals found while prospecting: opportunistic finds, usually of single individuals. However, there was a strong bias against representation among fossils of small-body size. Today, important specimens are still found by prospecting, as by current field teams supported by the Yushe County Museum.

A fundamentally different approach for collecting small mammals was introduced to Yushe Basin in 1987 when the Sino-American group began a campaign of wet-screening productive sites. Figure 1.2a–c highlight many of the most important localities that were screened in Yuncu subbasin in 1987 and 1988, and in Tancun subbasin in 1991. Localities were found by prospecting, surface finds indicating concentrations of remains. Where the fossils indicated preservation of small mammals, the team quarried bulk samples of sediment (Fig. 1.3).

Of the eighty localities producing small mammals, the Sino-American team selected two dozen that appeared to be particularly productive. The Sino-American field team sacked bulk samples of loosely consolidated matrix for processing. The Town of Yushe Hotel allowed us to process these samples on the premises; this involved drying (samples spread out on tarps), soaking in buckets, and screening the wet sediment (Fig. 1.4). We used tandem screen boxes made of wood, a coarse mesh in the bottom of a small inner box, which fitted neatly into a larger fine-mesh box. The fine screen had a mesh size of 0.5 mm on a side. The screening took place by agitating boxes in large tubs to wash water over the sediment. This removed clays, and the water could be reused. Most lithologies were amenable to soaking and screening, but some clayey materials were broken down by flocculation induced by kerosene pre-treatment. The many pairs of screen boxes allowed processing samples from multiple localities at the same time. Our Appendix lists fossils retrieved by both surface collection and initial sorting of bulk test samples from all YS localities that yielded small mammals. The appendix includes invertebrates and non-mammal vertebrates and lists small mammals prior to the systematic study of the following chapters.

In 1991, Zhu-Ding Qiu added a complement to this procedure. He brought a large pair of aluminum boxes modeled after a design used by Volker Fahlbusch. Mesh sizes differed slightly: 2 mm coarse screen and 0.5 mm fine screen. This was particularly useful for processing large volumes of sediment from single localities. A further advantage was that the boxes could be set up for washing in the field. A hose carrying water from a pond or stream and powered by a pump supplied a continuous spray washing over the fossiliferous sediment (Fig. 1.5).

A key to screening by either technique was assuring that the matrix was thoroughly dry. After drying fresh samples completely, we screened matrix, dried again, and screened at least one more time. The second or third wash removed most of the remaining clays – if the sediment was dry (Fig. 1.6). The resulting concentrate of sand grains and bone was then processed for fossils. The large fraction (smaller volume) could be sorted by hand, but the fraction remaining in the fine screen, a large volume, was too fine to sort reliably, even with magnification. Will Downs took charge of this concentrate and sorted out the fossils by means of heavy liquids. He used a settling tube of sodium polytungstate to float off the sediment from the higher density bones and teeth. Will processed many kilograms of concentrate in his laboratory in Flagstaff, Arizona, carefully retrieved small teeth and bones by microscope, and then prepared these for study.

1.3 Small Mammal Study

Microfossils collected during the joint Sino-American campaigns are in the permanent collections of IVPP in Beijing. They have been assigned V numbers. Some old specimens have revised RV numbers – see explanation by Qiu and Tedford (2013). Older collections bear various numbering schemes, including collections of the Tianjin Natural History Museum (TNHM) which have THP or TNP prefixes, and materials of the Frick Collection (AMNH) with the F:AM prefix. The Tianjin Natural History Museum was known, years ago, under the French name *Musée Hoang-ho Pai-ho de Tientsin*, with acronym HHPHM. Some fossils, including

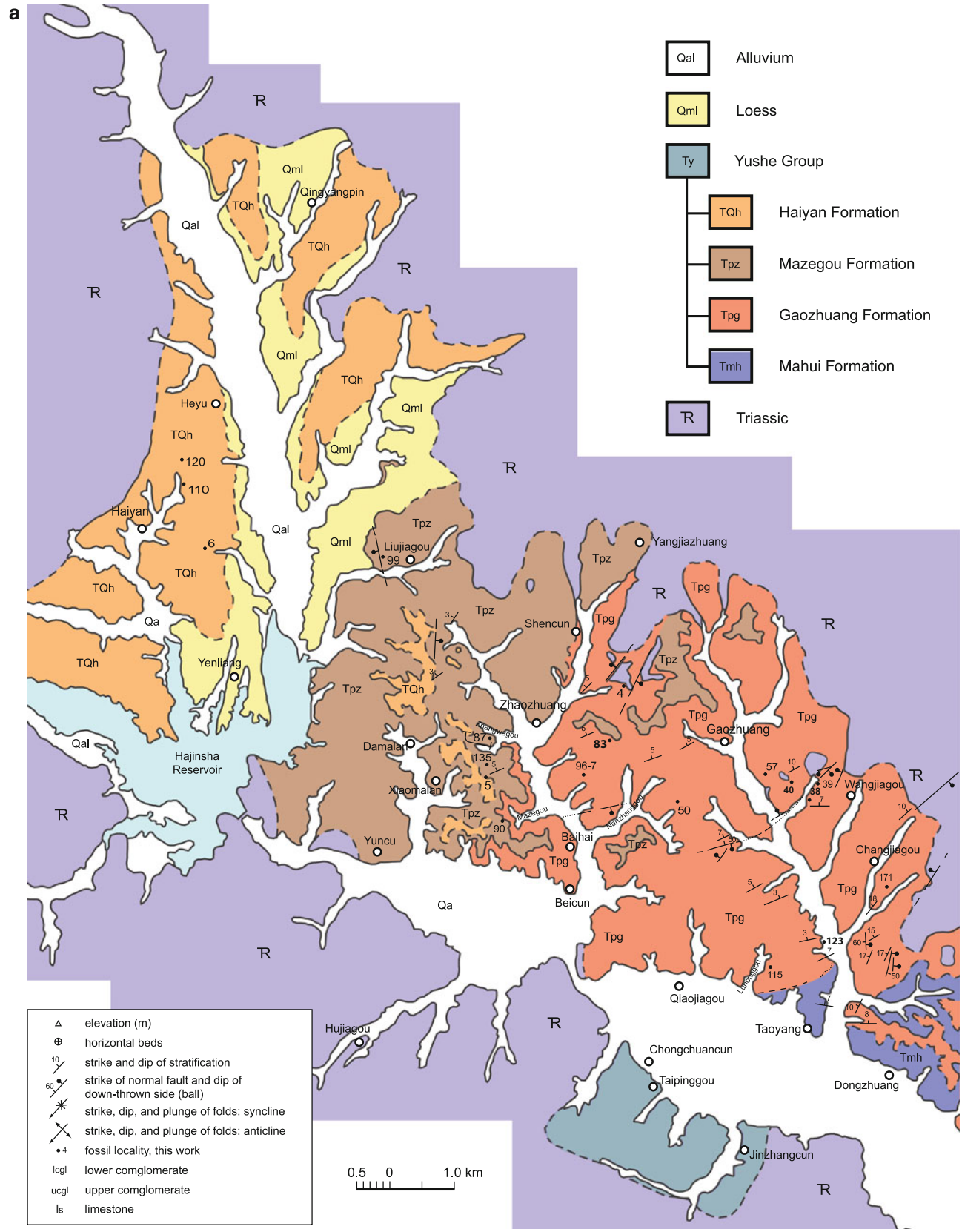

Fig. 1.2 **a**–**c**. Geological maps of Yushe subbasins prepared by the Sino-American mapping teams (1987–1998), showing lithostratigraphy, structure, and fossil localities. Figure 1.2a, formations exposed in Yuncu subbasin. Figure 1.2b, the northern Yushe subbasins (Nihe-Ouniwa area) and northern part of the Tancun subbasin. Figure 1.2c, most of the Tancun subbasin and lower Yuncu subbasin deposits on opposite sides of the Zhuozhang River. Maps by Frank Ippolito (AMNH) adapted to illustrate the distribution of small mammal localities

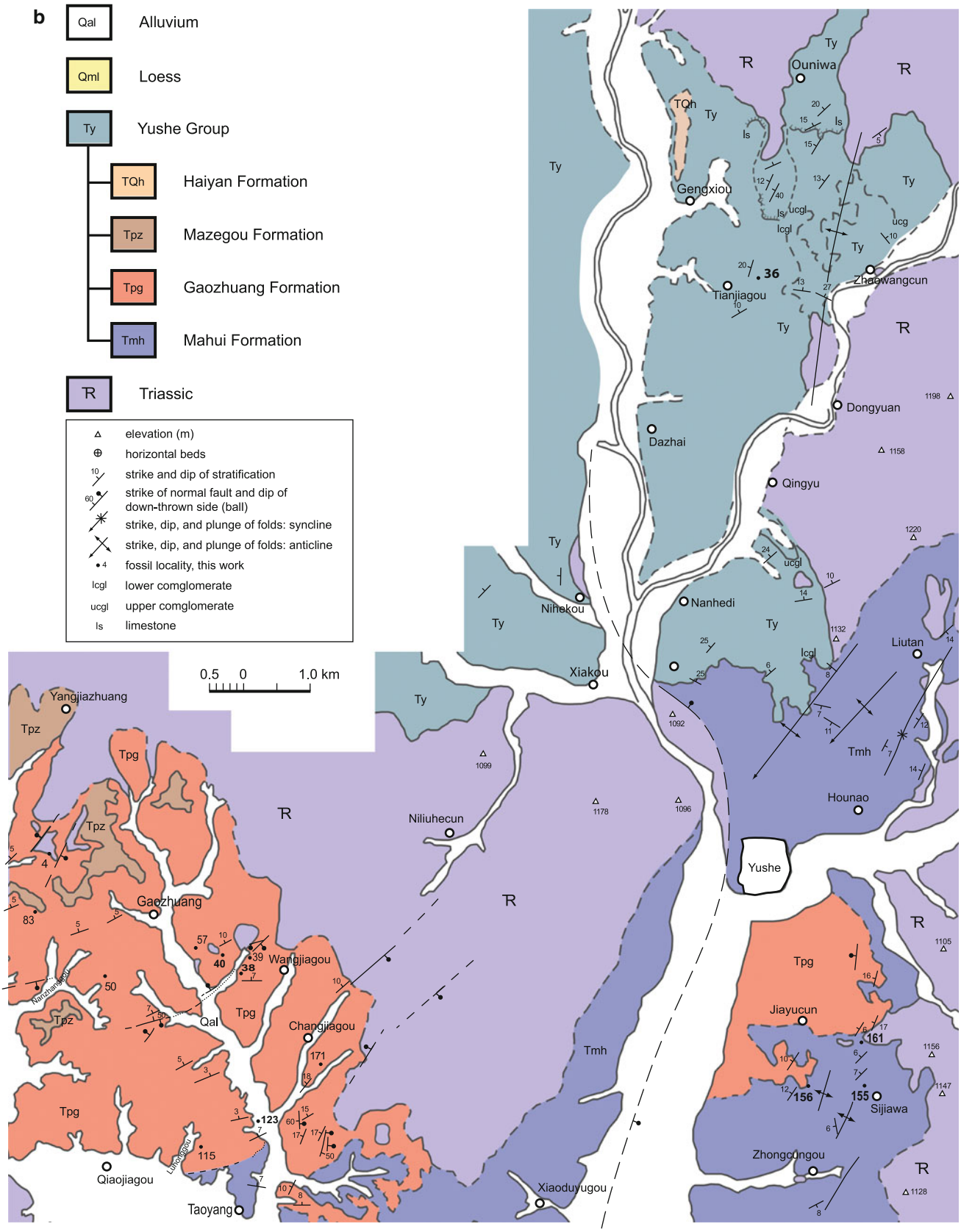

Fig. 1.2 (continued)

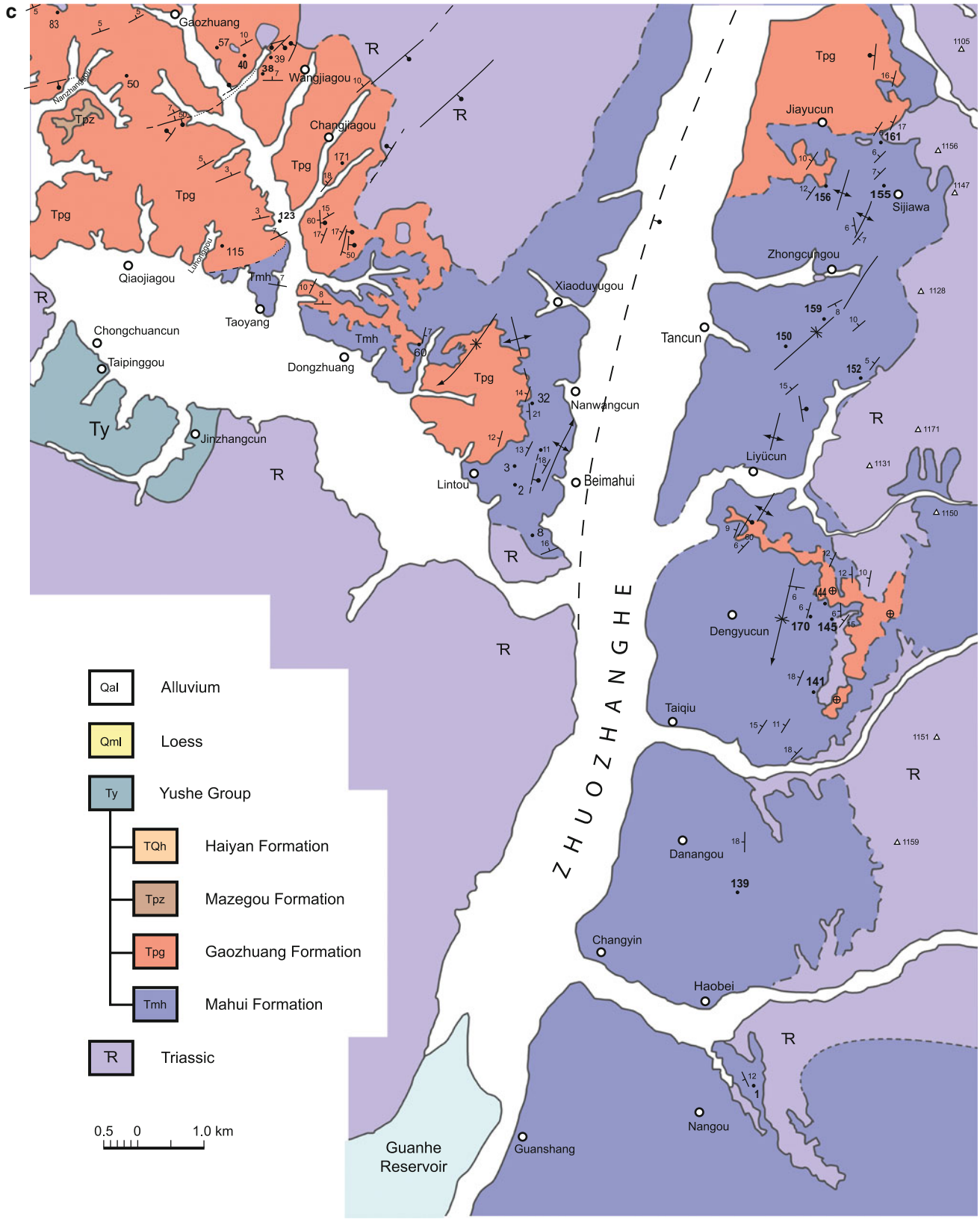

Fig. 1.2 (continued)

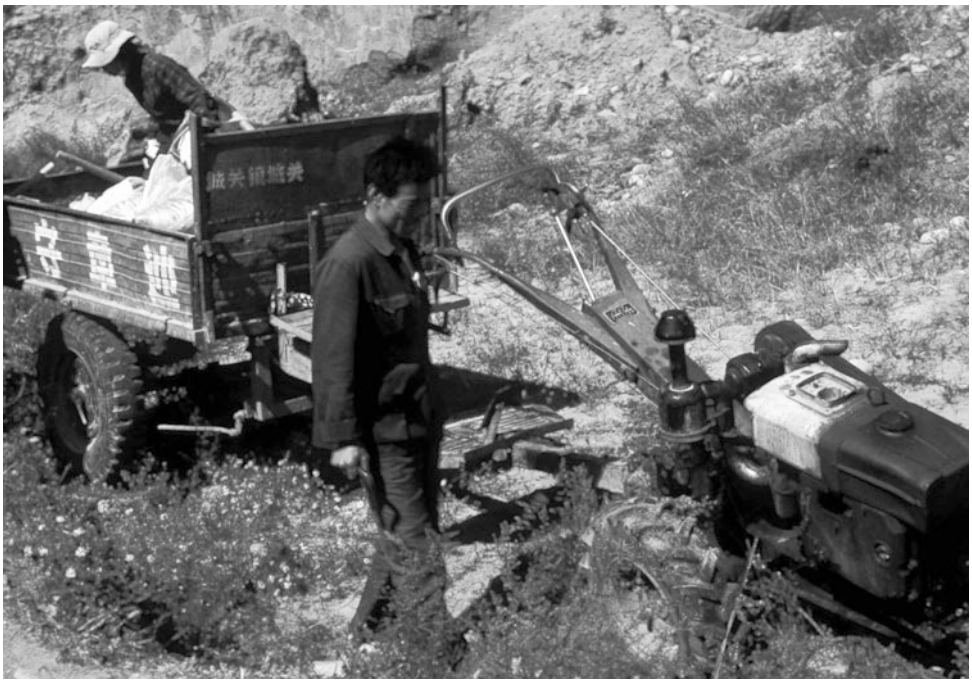

Fig. 1.3 Wen-Yu Wu collecting bulk samples of sediment for screening near Beimahui, utilizing one of the methods of hauling tons of material (Photo by L. Flynn, Sept. 1987)

Fig. 1.4 Screening operation at the Yushe Hotel, showing tandem screen boxes, drying tarps for discrete samples, buckets to soak the dried sediment in water, and wash tubs in which the boxes are agitated (Photo by L. Flynn, Sept. 1987)

Fig. 1.5 Zhu-Ding Qiu in Taiqiu area, Tancun subbasin, with tandem aluminum screens (coarse fraction visible, hose from pond supplying water), and curious admirers. L. Flynn, Sept. 1991

Fig. 1.6 Will Downs carefully drying washed sediment prior to rewashing, while keeping locality matrix separated. Downs then processed concentrated matrix by heavy liquids and retrieved microfauna by microscope examination (Photo by L. Flynn, Sept. 1991)

rodents studied by Teilhard de Chardin (1942), were published with the HHPHM acronym.

The Sino-American team was fortunate in greatly expanding the small mammal representation of the communities that evolved in Yushe Basin. Diverse shrews and moles, squirrels and dormice, dipodids, hamsters, and mice were faunal elements that had been poorly represented or completely absent from older collections. The studies of the material presented here are collaborative, and due to richness of the fossils, the editors engaged specialists to study some groups. To facilitate current and future comparative work, we have made molds and casts of much of the material.

Editors Flynn and Wu most depended on the experience and advice of Zhu-Ding Qiu. Qiu specifically undertook description of dipodids and squirrels, but encouraged us in many ways. In the course of his dissertation undertaken at Southern Methodist University, Dallas, Texas, under Professor Louis L. Jacobs, Xiaofeng Xu studied the beavers; this effort was later advanced by Qiang Li. Shao-Hua Zheng, authority on zokor evolution, undertook the analysis of Myospalacinae. Recently Ying-Qi Zhang kindly took on study of the Yushe voles. Remaining groups were the responsibility of the editors, but in all tasks we depended on the help of the staff of IVPP who care for the collections, and the curators who freely share information.

Our Yushe project localities were plotted on the composite biostratigraphy developed in Volume I (Fig. 1.7). We modified the biostratigraphy of Fig. 4.8 of Volume I, original artwork by Frank Ippolito, to combine both parts and present localities in a single figure. While the entire membership of our field teams participated in this, it was the guidance of R.H. Tedford and Z.-X. Qiu that inspired the fine scale biostratigraphic control that we use. This framework was developed by careful attention in the field and by the insistence, particularly by Dick Tedford, of tying physical localities to master sections. The age relationships of individual sites are well resolved. Localities of historic importance for fossil occurrences developed by Licent, Frick collectors, and later by IVPP were also placed in the sequence.

Small mammals occur in all stratigraphic units of Yuncu subbasin. The oldest small mammals are from middle to upper parts of the Mahui Formation, about 6.5 Ma. The youngest sites, other than those in the red and yellow loess, are from high in the Haiyan Formation, about 2.2 Ma. This biostratigraphic and dating framework for the Yuncu subbasin (Fig. 1.7) is used throughout this volume. The composite biostratigraphy unifies the separate but complementary studies by different authors on the various groups of small mammals. For some groups significant fossil material came from localities from Tancun subbasin. These fossils can be projected into the Yuncu master chronology by means of stratigraphic distance from the chron 3An-chron 3r reversal recognized in both subbasins in Chap. 4 of Volume I (Opdyke et al. 2013, p. 75).

While Yushe Basin played an important role in the history of paleontology of China, the small mammal component to Yushe faunas was heretofore poorly known. Our studies since 1990 have led to the description of 18 new species of small mammals. We are now able to characterize the diverse small body-size organisms of the Late Neogene communities of this region. They document changes in the Pliocene mammalian faunas of northeastern Asia, and play a role in understanding development of modern Asian communities. They constitute an important element in definition of

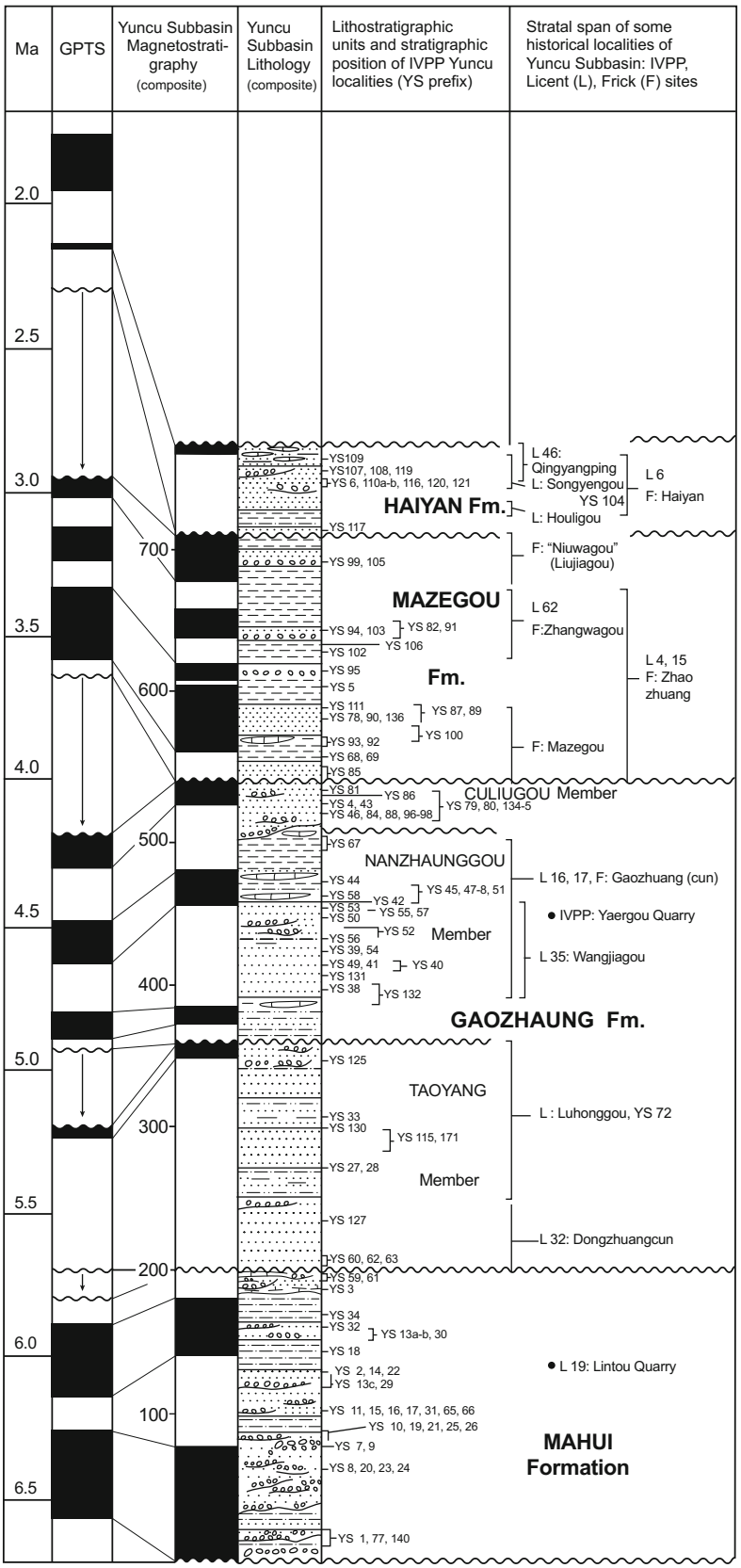

Fig. 1.7 Composite Yuncu subbasin lithology with observed magnetostratigraphy and correlation to the GPTS of Cande and Kent (1995). Adapted from Volume I to show relative positions of fossil localities mentioned in the text

Pliocene biochrons, the Gaozhuangian and Mazegouan Land Mammal Stage/Ages (Qiu et al. 2013). The Yushe small mammals complement the faunal history of the region in a continuous record from approximately 6.5 to 2 Ma.

Acknowledgements First, we acknowledge again our friend and micromammal colleague, the late Will Downs. His energy, tenacity, and sharp wit lie at the foundation of the success of our small mammal collecting. He is part of every chapter in this volume, and a part of every volume of the Yushe series. In addition, he embodied the good will and productivity of the Sino-American team, which co-leaders Zhan-Xiang Qiu and Dick Tedford nurtured. We thank reviewers Louis Jacobs, Jon Baskin, and Lou Taylor for their constructive reviews of this chapter. We appreciate their efforts and those of all reviewers who consistently supported our efforts in producing this volume.

References

Flynn, L. J., Tedford, R. H., & Qiu, Z.-X. (1991). Enrichment and stability in the Pliocene mammalian fauna of North China. *Paleobiology, 17,* 246–265.

Kurtén, B. (1952). The Chinese Hipparion fauna. *Societas Scientiarium Fennica. Commentationes Biologicae, 13*(4), 1–82.

Licent, E., & Trassaert, M. (1935). The Pliocene lacustrine series in central Shansi. *Bulletin of the Geological Society of China, 14,* 211–219.

Mascarelli, A. L. (2011). Quaternary geologists win timescale vote. *Nature, 459,* 624.

Opdyke, N. D., Huang, K., & Tedford, R. H. (2013). The paleomagnetism and magnetic stratigraphy of the Late Cenozoic sediments of the Yushe Basin, Shanxi Province, China. In R. H. Tedford, Z.-X. Qiu, & L. J. Flynn (Eds.), *Late Cenozoic Yushe Basin, Shanxi Province, China: Geology and fossil mammals Volume I: History, geology, and magnetostratigraphy* (pp. 69–78). Dordrecht: Springer.

Qiu, Z.-X. (1987). Die Hyaeniden aus dem Ruscinium und Villafranchium Chinas. *Münchener Geowissenschaftliche Abhandlungen, A9,* 1–110.

Qiu, Z.-X., Deng, T., Qiu, Z.-D., Li, C.-K., Zhang, Z.-Q., Wang, B.-Y., et al. (2013). Neogene land mammal ages of China. In X. Wang, L. J. Flynn, & M. Fortelius (Eds.), *Fossil mammals of Asia: Neogene biostratigraphy and chronology* (pp. 29–90). New York: Columbia University Press.

Qiu, Z.-X., & Tedford, R. H. (2013). History of scientific exploration of Yushe Basin. In R. H. Tedford, Z.-X. Qiu, & L. J. Flynn (Eds.), *Late Cenozoic Yushe Basin, Shanxi Province, China: Geology and fossil mammals Volume I: History, geology, and magnetostratigraphy* (pp. 7–34). Dordrecht: Springer.

Teilhard de Chardin, P. (1942). New rodents of the Pliocene and lower Pleistocene of North China. *Publications de l'Institut de Géobiologie, Pékin, 9,* 1–101.

Teilhard de Chardin, P., & Young, C. C. (1933). The late Cenozoic formations of S. E. Shansi. *Bulletin of Geological Society of China, 12,* 207–248.

Chapter 2
The Lipotyphla of Yushe Basin

Lawrence J. Flynn and Wen-Yu Wu

Abstract Insectivoran mammals have been recovered by Sino-American field teams from various localities in each formation of the Yuncu and Tancun subbasins. They were an important component of late Miocene through Pliocene faunas of North China. One hedgehog has been found in late Pliocene and Pleistocene localities. Moles, however, are diverse and occur throughout the Miocene and Pliocene section, with one early Pliocene record of the water mole *Desmana*. The Yushe collection includes the Pliocene talpine *Scaptochirus*, which is at present the oldest fossil of this genus. Shrews are also diverse, including multiple representatives of the tribes Soricini, Nectogalini, and Beremendiini. Presence of a blarinine suggests immigration of this element from North America by 6 Ma, and morphological similarity with beremendiines suggests that recognition of these groups should be reviewed. The early Pleistocene Haiyan Formation has yielded only *Sorex*, and to date only *Crocidura* has emerged from the Pleistocene loess. Declining insectivoran diversity corresponds with a hypothetical decline in mean annual temperature. The insectivoran component of Yushe shows affinity with fossil and living faunas of North China, and a majority of elements are shared broadly across Eurasia. Two taxa at least (*Yunoscaptor* and *Soriculus*) also occur in South China, indicating former wide distribution of these genera, and suggesting southward retraction of their preferred paleohabitat from Shanxi Province since the Pliocene.

Keywords Yushe Basin • North China • Late Neogene • Lipotyphla • Insectivores • Shrews • Moles

2.1 Introduction

Across North China, Late Cenozoic deposits reveal high species richness among micromammals of late Miocene and Pliocene age. Certain productive localities, such as Ertemte and Bilike, both Inner Mongolia (Fahlbusch et al. 1983; Qiu and Storch 2000), attest to this diversity within the insectivoran component of small mammal communities. Yushe Basin demonstrates this richness for Shanxi Province as well. One aspect of the importance of Yushe is in its aggregate of successive localities. While no single Yushe sample is as large as that of Ertemte or Bilike, in aggregate, the Yushe localities show great insectivoran richness. Of the many insectivoran specimens described in this chapter, nearly all were recovered by our field parties. An exception is the excellent (large) specimen of *Erinaceus* found in 1935 for Childs Frick and the American Museum of Natural History (AMNH) by Quan-Bao Gan.

The diversity of insectivorans as preserved in the Late Cenozoic deposits of Yushe Basin matches that seen today in North China, although some taxa imply changes in distribution. The composition of the fauna also suggests that the Yushe region insectivoran fauna showed significant differences from both South China and northern Asia (Inner Mongolia northwards).

Our progress in this study depended not only on the fine fossil collections of the Institute of Vertebrate Paleontology

Note: This chapter includes one or more new nomenclatural-taxonomic actions, registered in Zoobank, and for such purposes the official publication date is 2017.

L.J. Flynn (✉)
Department of Human Evolutionary Biology, and the Peabody Museum of Archaeology and Ethnology, Harvard University, Cambridge, MA 02138, USA
e-mail: ljflynn@fas.harvard.edu

W.-Y. Wu
Laboratory of Paleomammalogy, Institute of Vertebrate Paleontology and Paleoanthropology Chinese Academy of Sciences, 142 Xizhimenwai Ave., Beijing 100044, People's Republic of China
e-mail: wuwenyu@ivpp.ac.cn

Lawrence J. Flynn and Wen-Yu Wu (eds.), *Late Cenozoic Yushe Basin, Shanxi Province, China: Geology and Fossil Mammals, Volume II: Small Mammal Fossils of Yushe Basin*, Vertebrate Paleobiology and Paleoanthropology,
DOI 10.1007/978-94-024-1050-1_2

and Paleoanthropology (IVPP) in Beijing, but also on the recent mammal collections of the AMNH and of the Museum of Comparative Zoology (MCZ) at Harvard University, and of the Kunming Institute of Zoology (KIZ). Measurements are in millimeters unless otherwise noted.

2.2 Systematics

The relationships of the higher categories of small mammals loosely called "insectivores" remain controversial. Insectivorans, as traditionally conceived, are not monophyletic, but the core group of hedgehogs, moles and shrews is a natural group and most workers (e.g., McKenna and Bell 1997) utilize the higher taxon Lipotyphla Haeckel, 1866 for them. Currently, it appears that Solenodontidae is sister taxon to Lipotyphla (Douady and Douzery 2009) and the more inclusive group is modified as Eulipotyphla. Because the possible relationships of Erinaceidae, Talpidae, and Soricidae have varying support, we list them in that order without subordinal grouping.

2.2.1 Family Erinaceidae Fischer, 1814

Erinaceus Linnaeus, 1758
Erinaceus olgae Young, 1934

Referred material: V8893, complete left m1 from late Pliocene locality YS5. F:AM 76707, right mandible bearing complete dentition, including enlarged lower incisor (damaged tip) and three antemolars between it and p4, plus three molars; minor breakage anteriorly and at the condyle, the angle, and the coronoid process. Specimen collected in 1935 from the Nan Zhuang Gou area by Q.-B. Gan ("Buckshot"), who was employed by Childs Frick.

Distribution: Hypodigm material from Zhoukoudian (Localities 1, 2). Additional material from Yushe Basin: V8893 collected in 1987 from locality YS5, Mazegou Formation, 3.3 Ma; Nan Zhuang Gou specimen from a unit, probably loess, overlying the mid-Pliocene sediment.

Revised diagnosis: Large species of *Erinaceus* characterized by reduced paraconid on p4: paraconid is low and the paralophid is directed anterolingually; cingulum is absent on p4 and weak on lower molars.

Remark on nomenclature: Young (1934) named this species to honor Mrs. Olga Hempel-Gowen, "indefatigable secretary of the Cenozoic Laboratory". The published spelling of the species was "olgai", which is corrected here as *Erinaceus olgae*.

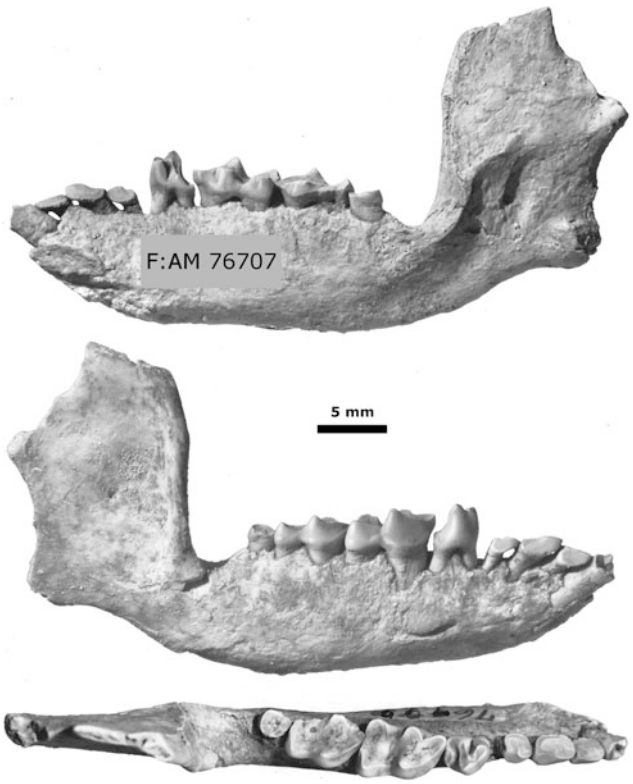

Fig. 2.1 *Erinaceus olgae*, right dentary with dentition, F:AM 76707, in medial (above), lateral, and dorsal (below) views (photography by Chester Tarka, AMNH)

Description: F:AM 76707 is a well-preserved dentary with moderately worn dentition (Fig. 2.1). The dentary bone is comparable in living *Erinaceus amurensis*, whose present range includes the Yushe area (Corbet 1988). The ventral border of the dentary is straight, depth uniform at about 8 mm from p4 to m3. Anterior from p4, the dentary bears a laterally thickened and strong symphysis that accommodates the long root of the enlarged incisor. Posteriorly the ramus narrows, with rising angle. The ascending ramus is vertical and coronoid is high. The condyle is positioned 5 mm above the tooth row. The mental foramen is low on the dentary, below the posterior part of p4, and the mandibular foramen is in the ascending ramus behind m3.

The dentition includes the procumbent incisor, generally considered the homologue of i2. It is followed by three simple antemolars, the middle one largest, and usually considered the canine. These teeth are worn, with a longitudinal crest located buccal to their midline. Each has a single root that projects posteriorly. The three are crowded together, combined length of 7.6 mm, and are followed by a small diastema. The second and third antemolars have low

posterior heels, suggesting structures comparable to the p4 talonid. Of the three antemolars, only the second suggests a hint of a buccal cingulum. The two-rooted p4 has a high trigonid and low talonid shelf below the level of the occlusal surface of m1. The trigonid is shortened longitudinally. Its paralophid projects anterolingually, but does not reach as far lingually as the metalophid, and bears a paraconid smaller and lower than the protoconid. The nearly transverse metalophid plunges steeply lingually, has a sloping wear facet, and bears a very low metaconid at the lingual border of the tooth. The talonid is hardly more than a posterior cingulum with enamel slightly raised posterolabially.

Molars decrease in size posteriorly. The first two are elongated, with large trigonids. Metalophids are transverse, and paralophids project anterolingually, reaching nearly as far lingually as metalophids, their smooth external walls gently curved. The protoconid is the highest cusp. The hypoconid and entoconid dominate the talonid basin. The cristid obliqua joins the base of the protoconid. At this state of wear, a small entocristid anterior to the entoconid is evident, and is apparently larger on m2. The reduced m3 is a worn, rounded basin. If its developmental homologue is a trigonid, it appears to have a strong metaconid. A weak cingulum is present on m1-2, strongest anterobuccally and between protoconid-hypoconid, faint at the protoconid. The first molar is wider posteriorly than anteriorly; m2 is wider anteriorly.

The fresh m1, V8893, is beautifully preserved, with two large roots, and is smaller than m1 of F:AM 76707 (Table 2.1). It shows a small entocristid, not yet worn and in the form of a small cusp. A low marginal crest extends anteriorly from the entocristid, but the entocristid is isolated from the large entoconid immediately posterior to it. A weak, intermittent cingulum occurs anterobuccally, between hypoconid-protoconid, and posteriorly. The posterior cingulum continues buccally from an entoconid shelf. The shelf is evident but nearly hidden in F:AM 76707, and neither m2 nor m3 show a posterior cingulum on that specimen.

Discussion: Both Yushe specimens represent a large *Erinaceus*. They conform to the descriptions of *Erinaceus olgae* from Zhoukoudian 1 and 2 (=*Erinaceus olgai* Young, 1934), sites assigned an age close to the Brunhes/Matuyama boundary, ca. 0.7 Ma. The provenance of V8893 is clear, given the local setting (YS5 is the top of a small hill), and is dated paleomagnetically to 3.3 Ma. Given the preservation and circumstance of collection in 1935, F:AM 76707 probably did not come from the early Pliocene deposits of Nan Zhuang Gou, but from overlying Pleistocene deposits, likely ~1 Ma in age. In addition to size appropriate for *E. olgae*, this specimen displays a reduced p4 with shelflike talonid and compressed trigonid with low paraconid and metaconid. The diagnostic value of this premolar morphology is largely untested, but the fossil specimens assigned to this species appear to be distinct from *Erinaceus* presently living in China. Specimen V8893 of significantly greater age is appreciably smaller (see Table 2.1), but matches size of some specimens from Zhoukoudian (Young 1934). Both Yushe specimens have only a vestigial cingulum on the molars. V8893 would represent the oldest known specimen of *E. olgae*, and therefore a taxon that ranged through the Plio/Pleistocene faunal turnover of Yushe Basin (Flynn et al. 1991).

Other late Cenozoic records of *Erinaceus* in China include "*E. mongolicus*" Schlosser (1924) from Ertemte. Contrary to original indications, Fahlbusch et al. (1983) pointed out that this is a small hedgehog; it may represent the genus *Hemiechinus*. *E. koloshanensis* Young and Liu, 1950, was named for material from the early Pleistocene of Sichuan. Also assigned to this smaller *Erinaceus* is material from the Nihewan area described by Teilhard and Piveteau (1930). Corbet (1988) notes that careful comparisons with *Hemiechinus* are lacking. As concerns the lower dentition, it

Table 2.1 Dimensions (length, width) for teeth and total p4 − m3 length in described insectivoran mandibular specimens (mm)

	p4	m1	m2	m3	p4 − m3
Erinaceus olgae					
V8893		5.2, 3.3			
F:AM 76707	3.4, 2.8	6.2, 4.4	5.7, 4.0	2.7, 2.0	16.9
Yanshuella yushensis					
V8915	1.45, 1.00	2.53, 1.80	2.75, 2.30	2.38, 1.63	8.73
V8916	1.53, 1.03	2.33, 2.03	*	2.35, 1.60	8.05
V8917 (worn)		2.20, 1.93	2.45, 2.05		
Soriculus praecursus					
V8898.1	1.48, 0.95	1.71, 1.09	1.62, 0.95	1.48, 0.76	5.07
V8898.2			1.52, 0.95	1.14, 0.58	
Beremendia pohaiensis					
V2671		2.90, 1.86	2.33, 1.48	1.48, 0.86	
V8900		3.00, 1.86	2.43, 1.67	1.71, 1.05	

* p4 − m3 length may be underestimated due to absence of m2

appears that *Hemiechinus* more typically has a highly reduced metalophid/metaconid, lacks a cingulum, and has m3 relatively more reduced than does *Erinaceus*. If these features are valid at the generic level, then *E. koloshanensis* and *E. olgae* appear to be correctly assigned to genus. However, *E. olgae* would be unusual for *Erinaceus* in its reduced molar cingulum.

2.2.2 Family Talpidae Fischer, 1814

Subfamily Talpinae Fischer, 1814
Tribe Talpini Fischer, 1814
Scaptochirus A. Milne-Edwards, 1867
Scaptochirus sp.

1991 *Scaptochirus* Tedford et al., in part
1994 *Scaptochirus* sp. Flynn and Wu

Referred material: V8913, right humerus from YS93 in the Mazegou Formation, about 3.5 Ma; V8910, broken left lower molar from YS4 (talonid width, 1.5 mm), Gaozhuang Formation, 4.3 Ma, both of Yuncu subbasin (Figs. 2.2a, and 2.3a).

Description: The well-preserved humerus shows damage of only the spike-like tip of the deltoid process and the ectepicondylar process (terminology of Hutchison 1968). The specimen is much like that of extant *S. moschatus* in being relatively broad, indicating strong fossorial adaptation. Humerus measurement (Table 2.2) follows Storch and Qiu (1990), who modified somewhat the measurement categories of Storch and Qiu (1983). The proximal breadth approaches total length. The greater tuberosity and teres tubercle are flared out with associated crests to dominate the humerus.

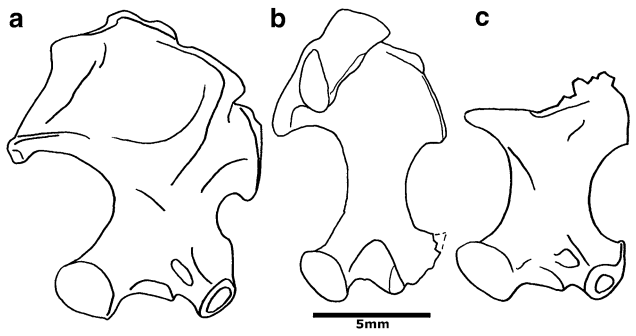

Fig. 2.2 Comparisons of talpid humeri: **a** *Scaptochirus* sp., right humerus V8913; **b** *Yunoscaptor* sp., left humerus V8840; **c** *Yanshuella yushensis*, right humerus V8914. *Yunoscaptor* V8840 shown in posterior view for comparison with the others in anterior view; its small deltoid spike is reconstructed from V8921, in which the spike is preserved. Scale bar = 5 mm for all

Distally, the condyles are widely separated with the capitulum and fossa for the M. flexor digitorum ligament marginal in position; this yields a broad measurement 6, well over half the length of the humerus. The shaft is stout, its breadth nearly half the length (Table 2.2). The long axis of the head is angled medially with respect to the long axis of the humerus as in talpines and scalopines. The pectoral prominent ridge is relatively distal, due to the greatly expanded proximal end of the humerus and distal extension of the teres tubercle. It borders a triangular proximal depression on the anterior side of the bone, extends distally nearly two thirds the humerus length, and ends in a low pectoral tubercle. In keeping with other Talpini, the scalopine ridge is an undeveloped faint line and the notch between head and lesser tuberosity is shallow (see Hutchison, 1968). The teres tubercle and the entepicondylar process are so expanded that the medial reentrant between them is only a small, circular hole, as in living *Scaptochirus*.

The broken molar (Fig. 2.3a) preserves a slightly worn talonid, but the trigonid is broken off at the base of the metalophid. The tooth is consistent with m2 of *Scaptochirus* in size (width, 1.5 mm) the presence of a strong entostylid (terminology of Engesser, 1980) low and posterior to the entoconid, and in that the talonid is as wide as the metalophid. The hypoconid (height, 2 mm) arches upward and lingually. The cristid obliqua reaches the middle of the metalophid. The V-shaped talonid basin is open lingually.

Discussion: This record is a welcome surprise for the Yushe fauna. The humerus is fully modern and of appropriate size for *Scaptochirus moschatus*, which lives today in northeastern China. It is also highly comparable with material from Zhoukoudian that has been given the name *Scaptochirus primitivus* Zdansky, 1928. Although subsequent workers have disputed the distinctness of these two species, the presence of *Scaptochirus* in the Zhoukoudian fossil record is well supported there by dentitions. Zhoukoudian material is plentiful and includes the distinctive hypertrophied p2 of the genus.

The Yushe molar resembles both living and fossil specimens. Furthermore, unpublished Frick collection material from Shouyang supports presence of the same taxon elsewhere in the late Neogene of Shanxi Province. The Yuncu specimens represent the oldest (Pliocene) records of *Scaptochirus* pending evaluation of the Shouyang fossil occurrence. Yushe material is close to *S. moschatus* in size, but differs from the smaller species *S. jiangnanensis* from the early Pleistocene of Anhui Province (Jin and Liu 2008).

Table 2.2 Dimensions of talpid humeri (following Storch and Qiu 1990)

Measurement	1	2	3	4	5	6
Specimen						
Scaptochirus sp.						
V8913	14.10	10.08	4.61	5.29	8.48	11.52
Yanshuella yushensis						
V8914		10.43	6.38	3.90	7.64	
Yunoscaptor sp.						
V8894	12.13	9.62	6.96	2.76	5.66	7.73
V8895	12.86	9.16	6.15	2.70	6.53	6.8+
V8919	12.04	9.37	6.43	2.76	5.69	7.64
V8920			6.92	2.99	6.21	
V8921		8.30	5.59	2.64	5.57	

Measurements (1) length, (2) length from distal end of teres tubercle to condyles, (3) length from proximal end of teres tubercle to condyles, (4) shaft breadth (parallel to condyles), (5) condyle breadth, (6) proximal breadth

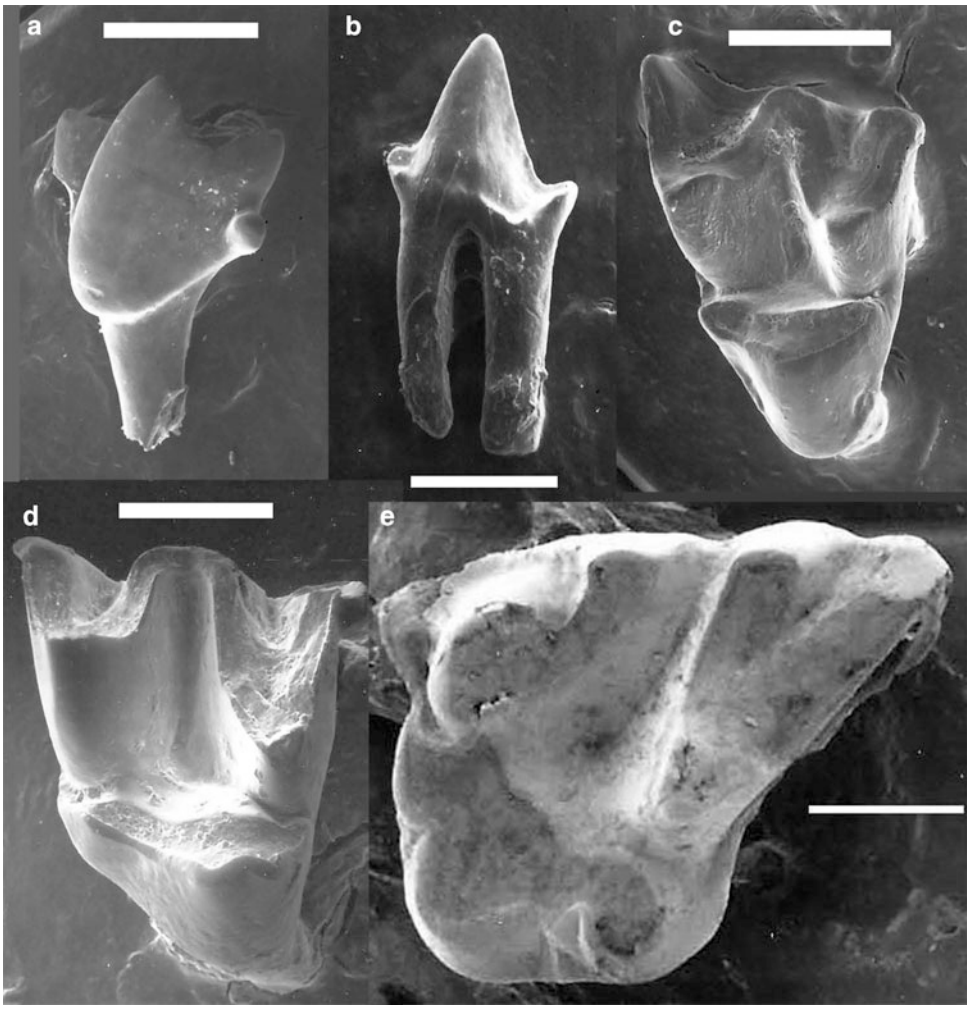

Fig. 2.3 Scanning Electron Microscope (SEM) views of talpid teeth. **a** *Scaptochirus* sp. talonid V8910 in posterobuccal view; **b** and **c** *Yunnoscaptor* sp., p4 V8908.3 in buccal view and M2 V8906 in occlusal view, respectively; **d** *Yanshuella yushensis* sp. nov., M2 V8912 in occlusal view; **e** *Desmana* sp., M2 V8905 in occlusal view. Scale bars are 1 mm

Tribe Scalopini Fischer, 1814
Yanshuella Storch and Qiu, 1983
Yanshuella yushensis sp. nov.

1991 *Yanshuella primaeva* Tedford et al.
1991 *Yanshuella primaeva* Flynn et al.
1994 *Yanshuella primaeva* Flynn and Wu.
1997 *Yanshuella primaeva* Flynn et al.

Holotype: V8915, right dentary broken anteriorly and at superior and posterior parts of the ascending ramus, with enlarged alveolus for i3, single alveolus for c1, and preserved p2–4, m1–3 (Fig. 2.4).

Type locality: YS161, Jiayucun, Tancun subbasin of Yushe Basin, uppermost part of Mahui Formation, about 5.8 Ma.

Hypodigm: V8915; V8916, left dentary with i3 alveolus, canine stub, p2–4, m1, and m3 from YS159; V8917, right dentary fragment with m1–2 from YS143; both Mahui Formation of Tancun subbasin; V8911, broken left M2 from YS8, and V8912, right M2 in maxilla fragment from YS9 (Fig. 2.3d), both Mahui Formation of the Yuncu subbasin. All sites 6.3–5.8 Ma. Referred right humerus fragment V8914 from YS99, Mazegou Formation of Yuncu subbasin, about 3 Ma.

Etymology: Species name in reference to the geographic setting.

Distribution: Presently known only from the Yushe Basin.

Diagnosis: Largest species of *Yanshuella*; p2 and p3 two-rooted; p4 robust, but lacking strong anterior cusp; cristid obliqua of m2–3 joins the metalophid lingual to the midline; weak buccal cingula on lower dentition; M2 with symmetrical W-shaped ectoloph, curled parastyle and metastyle, moderately cleft mesostyle, strong metaconule and smaller paraconule, weak and broken ectocingulum, short metacingulum and abbreviated paracingulum.

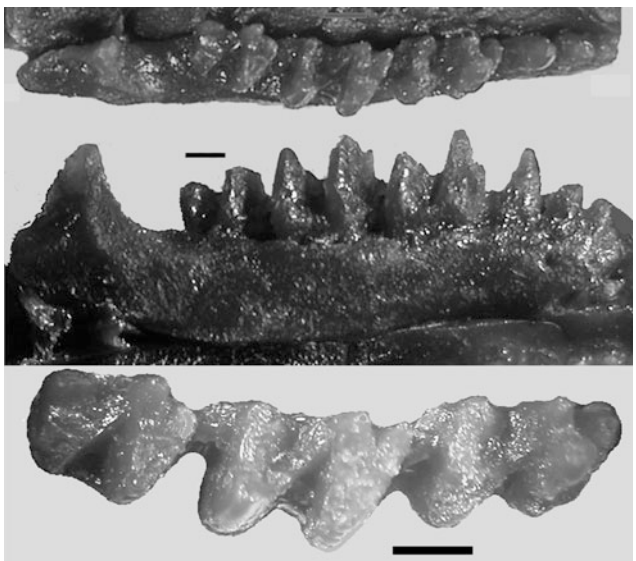

Fig. 2.4 Photograph of holotype V8915, right dentary with dentition of *Yanshuella yushensis*, in dorsal (above) and lateral (middle) views; molar dentition expanded below. Scale bars = 1 mm

Description: This large mole is represented by mandibles and a few isolated elements. The holotype dentary preserves enough of the ascending ramus to indicate that it arose perpendicularly from the horizontal axis. The ventral border of the mandible undulates slightly, rising to its highest point above the anterior portion of m1. Depth is 2.7 mm below m2. The one prominent mental foramen lies below the anterior portion of p4; a second one occurs behind p4 in V8917. The symphysis ends below p2–p3 boundary. A retromolar gap of 1.5 mm lies between m3 and the ascending ramus.

Tooth formula of the dentary includes a large i3 rooted below p3, canine, p2–4, m1–3. The anterior dentition is crowded, the canine small, the premolars two-rooted. The crowded condition is suggested by the *en echelon* nature of p2–3, whose long axes are oblique to the tooth row. Canine and incisors procumbent, but premolars less so. From anterior tip of inclined p2 through vertical p4, the premolar row is 3.4 mm in V8915; it is 3.6 mm in V8916. Anterior border of canine alveolus to posterior wall of p4 is 3.9 and 3.8 mm, respectively. Anterior border of canine alveolus to posterior wall of m3 is 10.7 and 10.3 mm, respectively. The molar row is longer in the holotype, but p4 is larger in V8916. The base of the small canine preserved in V8916 is anteroposteriorly compressed, slightly oblique and oriented posterolingually. Its orientation anticipates the oblique aspect of p2–3, whose roots are obliquely placed, one anterolabial and one posterolingual, and whose crowns are correspondingly oblique. There is one principal cusp on these teeth, with a weak posterolingual ridge plunging to a small basal shelf or cingulum at that corner of the tooth. The canine appears to be smallest, followed by p2 in size; p3 is larger, and its cingulum, though faint, appears to encircle the tooth and supports a small basal posterolingual cusp.

Table 2.1 records measurements of p4 and molars. The former is markedly larger than anterior teeth, wide relative to some moles, and is dominated by a high cusp. The cusp is central medio-laterally, but anterior in position and with a posterolingual ridge that plunges to a shelflike posterior cingulum. The cingulum squares the back of the tooth and bears a distinct posterolingual cusp. Though faint labially, the cingulum is prominent along the lingual side of the tooth and bears a small anterolingual tubercle in V8916 (V8915 is damaged). The more worn V8916 bears a distinct posterolingual wear facet.

Molars are high-cusped, especially buccally, with trigonids higher than talonids, and with m2 largest, m1 wider posteriorly, m3 wider anteriorly. Trigonids and talonids are open lingually, except for m3, in which the talonid is blocked by an entocristid running anteriorly from the entoconid. The trigonid of m1 is less acute than that of the other molars. Its paraconid is lower and smaller than in the other molars. Anterior walls of trigonids are slightly convex and bear a weak cingulum; posterior walls of trigonids and of

talonids are parallel, straight, vertical walls. The anterior cingulum terminates lingually in a low cusp, the parastylid. The parastylid of each molar abuts the talonid cusp of p4 or the entostylid of m1 and m2. The parastylid increases in prominence posteriorly. Entostylid is lacking in m3. The labial cingulum is undeveloped except between protoconid and hypoconid. The cristid obliqua intersects the trigonid lingual to the midline in m1, more lingually in m2–3. In the latter teeth, it approaches the metaconid, which bears a posterior fold, reminiscent of an undifferentiated metastylid.

The paracone and metacone of M2 (Fig. 2.3d) are nearly symmetrical, except that the paracone extends somewhat more lingually. Parastyle and metastyle are curled and add to the symmetry, as does the divided mesostyle, which in occlusal view is a smooth inverted U-shape. The tooth is wider than long (length, width = 2.38, 2.73). The protocone has a broadly open V-shape. The metaconule is prominent, but the paraconule is smaller. Cusp walls are rather tall; metacingulum and paracingulum descend steeply from metaconule and protocone, respectively. Short metacingulum ends below metacone base; paracingulum ends lingual to paracone. The ectocingulum is undeveloped, except in valleys buccal to paracone and metacone. Three roots including a large lingual root are present, plus a small rootlet below the paracone.

The broken humerus (Fig. 2.2c) is associated here based on size (larger than those attributed to *Yunoscaptor*; see below) and similarity to that of *Yanshuella primaeva*. It is more heavily built, with thicker shaft and more distal teres tubercle (apparently more adapted toward fossorial behavior), than is that of *Yunoscaptor*. Broken proximally, measurements 1 and 6 cannot be made. One additional feature consistent with assignment as *Yanshuella* is the slight development of the pectoral ridge and absence of a pectoral tubercle at its distal terminus.

Discussion: Storch and Qiu (1983) described abundant and complete mole material from Ertemte, Inner Mongolia, recognizing two forms. The more common and larger mole was present in original collections described by Schlosser (1924) under the name of *Scaptochirus primaevus*. Storch and Qiu (1983) were able to describe this taxon definitively, and gave it the new generic name *Yanshuella*. As isolated teeth were discovered in Yushe Basin, it was believed that the same species was present there (Flynn et al. 1991, 1997). More material, including mandibles and a humerus, show that the Yushe species differs from *Yanshuella primaeva*. In addition to larger size, the Yushe taxon shows two roots on anterior premolars, more lingual intersection of the cristid obliqua with the trigonid, and weaker cingula on both upper and lower teeth. These features show that while the common large mole of Yushe is similar to that of Mongolia, it is not the same, although its long chronologic span at Yushe likely encompasses the age of Ertemte and Harr Obo. *Y. yushensis* is also larger than *Y. columbianus* (Hutchison, 1968) of Oregon.

Most of the specimens referred to *Yanshuella primaeva* occur in the Mahui Formation of Tancun and Yuncu subbasins of Yushe Basin from localities clustering about 6.3 to 5.8 Ma. The referred humerus occurs in much younger deposits, the upper part of the Mazegou Formation (Yuncu subbasin) at 3 Ma. The humerus, also large for *Y. primaeva*, implies an independent lineage for this mole in Yushe Basin.

Yunoscaptor Storch and Qiu, 1990
Yunoscaptor sp.

Referred material: V8906 right M2 from YS97, (length, width = 2.02, 2.46); V8907.1, left m2 fragment, and V8907.2, right m2 or m3 trigonid from YS4; V8908.1, left M2 (worn, 2.25, 2.70), V8908.2, right p3, V8908.3, left p4, and V9808.4, right m2 or m3 trigonid, from YS 50; all Gaozhuang Formation localities, about 4.3 to 4.7 Ma. V8918, right m2 from YS143, and five humeri V8909, 8840, 8919, 8839, 8921 from YS1, YS151, YS152, YS154, YS157, respectively, all Mahui Formation of the Tancun subbasin, about 6 Ma (Fig. 2.3b, c).

Distribution: *Yunoscaptor scalprum* Storch and Qiu, 1990 was named for material from the late Miocene Shihuiba Formation, Lufeng County, Yunnan. In the Yushe Basin the related mole occurs in Mahui and Gaozhuang formations of Yuncu subbasin (YS 50 near Nanzhuanggou, YS4 between Gaozhuang and Zhaozhuang, and YS97, Chuan Ze Gou, 0.8 km northwest of Nan Zhuang Gou). YS143 and all humeri are from the Mahui Formation of the Tancun subbasin. Temporal range is >6.0 to 4.3 Ma.

Description: This mole is smaller and lower crowned than the other common mole of Yushe, *Yanshuella yushensis*. Its molars are more gracile and its smaller humerus is less heavily built. M2 is asymmetrical externally in that the metacone wing of the ectoloph extends straight posterolabially much farther than does the paracone wing. The parastyle is curled in V8908.1, not in V8906. The mesostyle is undivided. There is no noticeable metastyle. The metaconule is prominent and the paraconule is a faint bulge on the preprotocrista. The ectocingulum is present in the paracone and metacone valleys only. There is a weak cingulum around the protocone, and the metacingulum and paracingulum are short. There are three major roots and a small, central rootlet.

Both specimens attributed to this taxon as premolars are two-rooted. V8908.2 is a blunt and low crowned p3 with larger anterior root. Its main cusp is anterior in position, lateral to the midline of the tooth. Dominating the cingulum is a posterior heel with a small cusp. V8908.3 is a sharp-cusped p4 (length, width = 1.4, 0.8). Its trenchant main cusp is compressed mediolaterally, nearly vertical lingually and curving inward buccally. A cingulum encircles

the tooth, bears a small anterior cusp, and a posterior raised heel capped by a transverse talonid cusp. Of the two long roots, the posterior is heavier.

Lower molars are represented by a corroded tooth and fragments. V8918 is missing enamel labially. Its length, 2.05 mm, may be somewhat reduced by corrosion. This tooth is considered to represent m2 because trigonid and talonid are subequal in size, the cristid obliqua intersects the trigonid near the lingual side of the tooth at a metastylid, the talonid is closed by an entocristid, there is a prominent cusp (parastylid) anterolingually, and there is a small entostylid (possibly abbreviated by enamel loss). V8907.2 is a trigonid of similar size and dimensions, but its parastylid is much smaller. V8908.4 also has a small parastylid, but is larger, with more widely open trigonid (relatively longer) and appears to have a more labial cristid obliqua. Despite its larger size it may represent m1 (possibly another taxon).

The humerus (Fig. 2.2b) is represented by four left specimens, three nearly complete, and one right fragment. These are scalopine in structure, as evidenced by the mediodistally-directed head and the prominent, raised scalopine ridge. The shaft is relatively slender. The teres tubercle does not extend as far distally as in other moles (hence measurement 3 is relatively large). The pectoral ridge terminates lateral to the midline of the humerus in a small, raised pectoral tubercle. Other features correspond to those of *Y. scalprum*.

Discussion: In all features, the Yushe sample of *Yunoscaptor* matches the type species of the genus *Y. scalprum* from Lufeng, Yunnan, although that locality is older, perhaps near 7 Ma. Discrepancies are minor and, at present, can be attributed to individual variation. A few humeri seem relatively large, but m2 (V8918) is a bit small. M2 is consistent in ectoloph shape, mesostyle simplicity, and length-width ratio. Lower p4 is consistent in cusp disposition, including the anterior cingulum cusp. Lower molars show the metatstylid. The scalopine humerus shows a medial pectoral tubercle. Still, the material is insufficient to demonstrate occurrence of the same species in Yushe Basin, and we cite it as indeterminate at the species level.

Subfamily Desmaninae Mivart, 1871
Desmana Güldenstaedt, 1777
Desmana sp.

1991 *Desmana kowalskae* Flynn et al.
1994 *Desmana kowalskae* Flynn and Wu
1997 *Desmana kowalskae* Flynn et al.

Referred material: V8905, left M1 (3.72, 2.89 mm); Fig. 2.3e.

Locality and age: YS50, early Pliocene Gaozhuang Formation, Yuncu subbasin, 4.7 Ma.

Distribution: *Desmana* is widespread, if uncommon, throughout Eurasia. A similar form, probably identical, is known from the Bilike fauna of Inner Mongolia, also early Pliocene in age (Qiu and Storch 2000).

Description: The molar is trapezoidal in outline with nearly parallel short lingual and long buccal walls. The anterior wall is transverse, but the distal wall is oblique due to the posteriorly-jutting metacone-metacrista, which makes a large, oblique shearing crest. The protocone is large, but worn low, the paracone is small, and the metacone is a high cusp. The protocone is anterior in position, more anterior than the paracone. Posterior to the protocone is a smaller metaconule, inflated as an independent cusp. The metaconule joins the protocone via a small accessory cusp between them, but is isolated from the metacone. A short lingual cingulum spans the gap between protocone and metaconule. The paraconule is a swelling of the thick protoloph. Its posterior arm joins the paracone, and its anterior arm is confluent with the thin anterolabial cingulum. The external border of V8905 is slightly convex, consisting of an isolated parastyle, a postparacrista, and a pre- and postmetacrista. The postparacrista and premetacrista lead to a double mesostyle that is broadly divided. The deep trigon basin drains lingually between the two mesostyles. The pre- and postmetacrista make a narrow V-shape, terminating posterolabially in a metastyle. The metastyle lies at the end of the posterior cingulum; the parastyle is bordered by a cingulum at the anterobuccal corner of the tooth. There are three roots plus a small, central rootlet.

Discussion: The low crown height, construction of the metacone and paracone, and strength of the metaconule are all consistent with reference to *Desmana*. Among known *Desmana*, V8905 represents a large species, but it is smaller than living *D. moschata* or Pliocene *D. thermalis*. Its size and width/length ratio (0.78) are consistent with *D. kowalskae*. Flynn et al. (1991) used this identification, but Rzebik-Kowalska (1994) considered the species indistinguishable from *D. nehringi*. In addition, Qiu and Storch (2000) noted differences from *D. kowalskae* in their larger desman sample from Bilike, Inner Mongolia. Therefore, we now consider the Yushe desman as indeterminate to species.

This large talpid indicates aquatic habitat, for example streams or ponds. It is therefore a strong indicator of moist conditions with permanent water. No desmans occur in eastern Asia today. Their presence in both Bilike and Yushe Basin speak to widespread mesic conditions throughout much of Asia during early Pliocene time.

2.2.3 Family Soricidae Fischer, 1814

Subfamily Soricinae Fischer, 1814
Tribe uncertain
Paenelimnoecus Baudelot, 1972
cf. *Paenelimnoecus* sp.

Referred material: V8841.1, left lower incisor; V8841.2-3, right upper incisors.

Locality and age: YS145, upper Mahui Formation of Tancun subbasin, about 5.8 Ma.

Description: This small shrew is represented by three specimens of anterior dentition from one locality. While lacking red pigmentation, the generally off-white teeth show faint yellow tinges that may indicate leached pigment. This is most convincingly demonstrated by the yellow cusp tips of V8841.2, in contrast to the rest of the tooth, which is white. V8441.1, lower incisor broken at the base (2.1 mm length preserved), is simple and bicuspulate, posterior to the tip. Upper incisors show a posterior cusp that in lateral view is short relative to the principle cusp. The principle cusp is simple, and the talon supporting the posterior cusp is relatively long in labial view. The better preserved V8441.2 (1.43 mm long) shows a strong labial cingulum.

Discussion: *Paenelimnoecus*, a small shrew known across Eurasia, has been considered an allosoricine, but is here unaffiliated with a tribe. *P. obtusus* Storch (1995) was named for the late Miocene Ertemte fauna of Inner Mongolia, and this species or a related form occurs in the early Pliocene Bilike fauna of Inner Mongolia (Qiu and Storch 2000). Presence of a similar shrew in the late Miocene of Tancun subbasin, Yushe Basin, would not be surprising. The Yushe specimens are close in size to those of Bilike, but a bit smaller than typical for the type material of *P. obtusus* from Ertemte. The specimens from locality YS145 attest, in any case, to presence of a small shrew in the late Miocene of Yushe Basin.

Tribe Soricini Fischer, 1814
Sorex Linnaeus, 1758
Sorex sp.

1991 *Sorex* sp. Flynn et al.
1994 *Sorex* sp. Flynn and Wu
1997 *Sorex* sp. Flynn et al.

Referred material: V8894.1, left M1; 8894.2, right dentary fragment with worn m1; 8894.2, right upper incisor, and 8894.3, left upper incisor.

Locality and age: YS120, Haiyan Formation, Yuncu subbasin, ~2.2 Ma, reversed lower part of the Matuyama chron.

Description: Specimens are heavily pigmented red, the pigment generally well preserved. M1 is nearly as long as it is wide (1.15, 1.30; Fig. 2.5a). The posterior wing of the ectoloph is longer than the anterior end due to an elongate postmetacrista. The ectoloph is W-shaped, with the mesostyle lingual to the line joining the parastyle and metastyle. Conules are not developed. The metaloph is a weak ridge intersecting the posterior arm of the protocone. No protoloph is evident. Other than the strong anterior arm of the protocone, which intersects the paracone low on its anterior face, there is no anterior cingulum. Lingual and posterior to the protocone is a short cingulum that is confluent with the posterior cingulum. The hypocone, weakly connected to the protocone, shows a posterior spur. Posterior emargination of the hypocone flange is moderate.

The upper incisor (lengths, 1.25, 1.35 mm; Fig. 2.5b) is strongly arcuate in profile. Its posterior cusp is prominent. The major cusp is weakly fissident (possessing a slight bifurcation near the apex). Its labial cingulum is weak.

V8894.2 is a dentary fragment lacking the posterior end and broken in front of m1. It contains a worn m1 and the roots of m2–3. Alveolus length of m1–3 is 3.64 mm. The mental foramen is below the anterior root of m1. The worn first molar (length, width relative to the long axis of the tooth row = 1.60, 0.85) overhangs the dentary on its lateral side. The paraconid and metaconid are widely spaced, the trigonid draining lingually. The cristid obliqua intersects the posterobuccal corner of the protoconid. The entoconid-entocristid closes the talonid basin.

Discussion: The material of this mid-to-large-size shrew is insufficient to establish identity with similar known species. It is consistent with *Sorex* in pigmentation, the fissident incisor, and in morphology of the molars. It is about the size of living *S. excelsus* from Yunnan, but perhaps more similar morphologically to the smaller northern *S. cinereus*. The material presents enough information to rule out identification with *Sorex* species previously described from the late Miocene Ertemte (Storch 1995). It is approximately the same size as *S. pseudoalpinus* identified at Ertemte, but has a less fissident incisor, and smaller hypocone with weak metaloph present. The Yushe material resembles "*Sorex* sp." from Zhoukoudian Locality 3 described by Pei (1936).

Tribe Nectogalini Anderson, 1879
Subtribe Neomyini Repenning, 1967
Soriculus Blyth, 1854
Soriculus praecursus Flynn and Wu, 1994

1991 *Episoriculus* n.sp. Flynn et al.
1994 *Soriculus praecursus* Flynn and Wu
1997 *Soriculus praecursus* Flynn et al.

Holotype: V8898.1, complete left dentary with all teeth.

Hypodigm: V8898.1; 8898.2, left dentary fragments with m2–m3; 8898.3–0.4, two isolated right M2 (Fig. 2.5c–f).

Type Locality and age: YS50, early Pliocene Gaozhuang Formation, Yuncu subbasin, 4.7 Ma, presently known only from Yushe Basin.

Diagnosis: Smaller than *S. nigrescens* (Gray, 1842), about the size of *S.* (*Chodsigoa*) *lamula*, Thomas, 1912 with

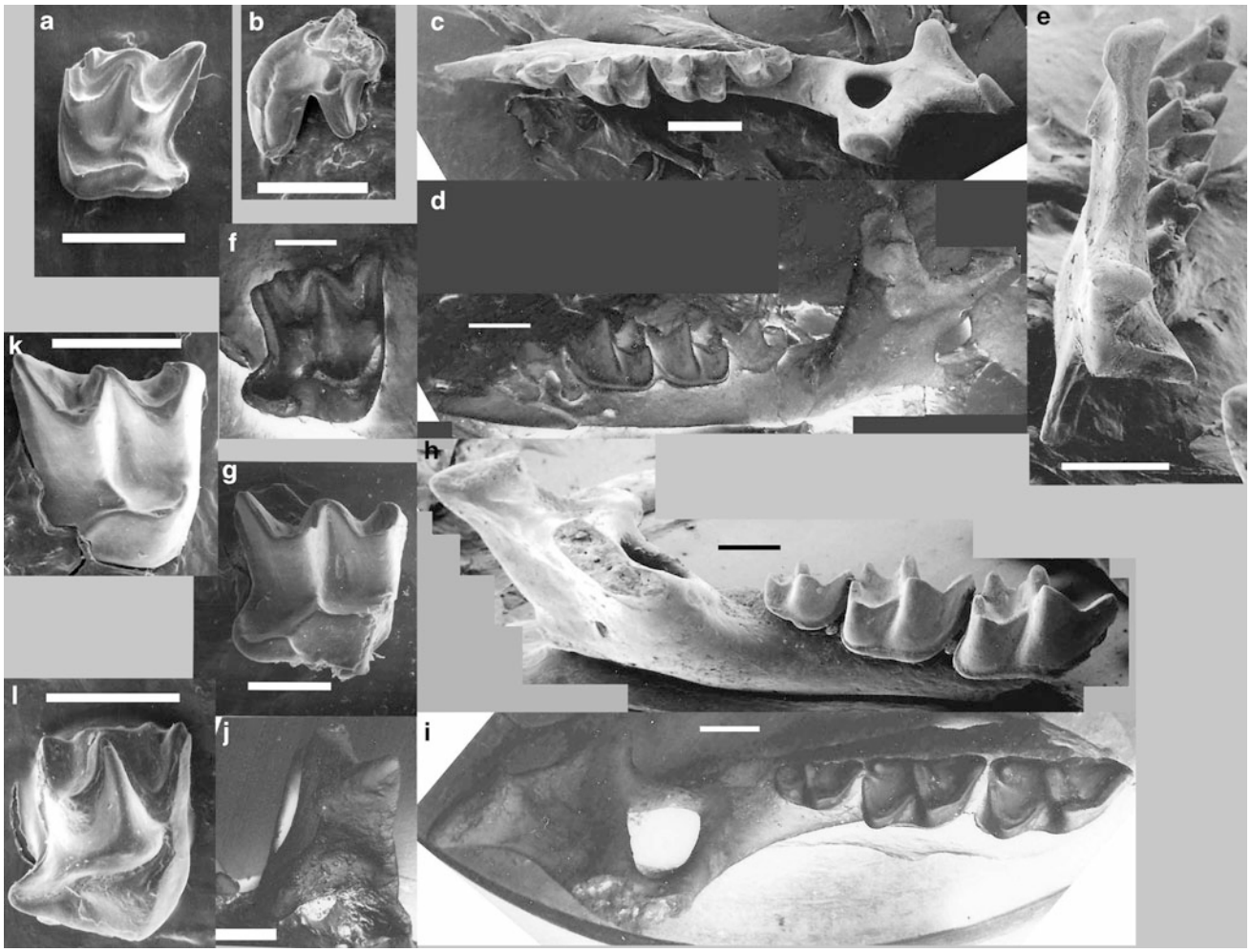

Fig. 2.5 SEM views of shrew mandibles and molars. **a**, **b** Sorex sp., left M1 V8894.1 and V8894.2, right upper incisor; **c**–**e** V8898.1 *Soriculus praecursus* left mandible, in **c** dorsal view, **d** lateral view, **e** posterior view of articulation, and **f** V8898.3 *Soriculus praecursus* right M2; **g** V 8895.1 *Lunanosorex lii* right M1; **h**–**j** V8900 *Beremendia pohaiensis* right mandible, in **h** dorsolateral view, **i** dorsal view, **j** posterior view of articulation; **k** V8897 cf. *Sulimskia* sp. right M1; V8899 *Crocidura* sp. right M2. Scale bars: 1 mm

crowded anterior dentition, labial incisor flange ending below back of p4; lower condyle not transversely elongated and not anterior in position; coronoid process strong and high, inclined slightly, with short spicule midway to upper sigmoid notch; lower cheek teeth uncompressed laterally, differing from the smaller *S.* (*Episoriculus*) *caudatus* (Horsfield, 1851); m3 not greatly reduced; M2 with weak hypocone and not deeply emarginated.

Description: No new material has been assigned to this taxon since its description (Flynn and Wu 1994), but new measurements are presented in Table 2.1. The structure of the mandible is much like closely related living forms that cluster as Subtribe Neomyini. The double articulation is L-shaped, the interarticular area being a slender, sculpted ridge (Fig. 2.6). The upper arm of the articulation and the coronoid process tilt laterally from the ramus in posterior view. The lower articulation is separated from the lower sigmoid notch by a reentrant. These features are similar to the condition in the larger *Soriculus nigrescens* and *Neomys fodiens* (Pennant, 1771), and to *S.* (*E.*) *caudatus,* although the coronoid of the former two has a distinct anterior inclination of its tip. *S.* (*Chodsigoa*), although similar in size to *S. praecursus* differs also in its heavier condyle, anteriorly displaced lower articulation, and more tilted coronoid process. The small coronoid spicule extends half way down the sigmoid notch. Position and relatively large size of the internal temporal fossa and mandibular foramen resemble *S.* (*E.*) *caudatus*. Mental foramen lies below the middle of m1.

The lower incisor shows both wear and damage, but appears relatively short and suggests that accessory cusps were minor. A low posterior cusp is suggested by a widening of the wear surface, dorsally on the enamel; any more anterior cusps are not in evidence. Incisors of some living soriculines (e.g., *Chodsigoa*) are also weakly cuspulate. *Episoriculus* tends to have two cuspules. The incisor has

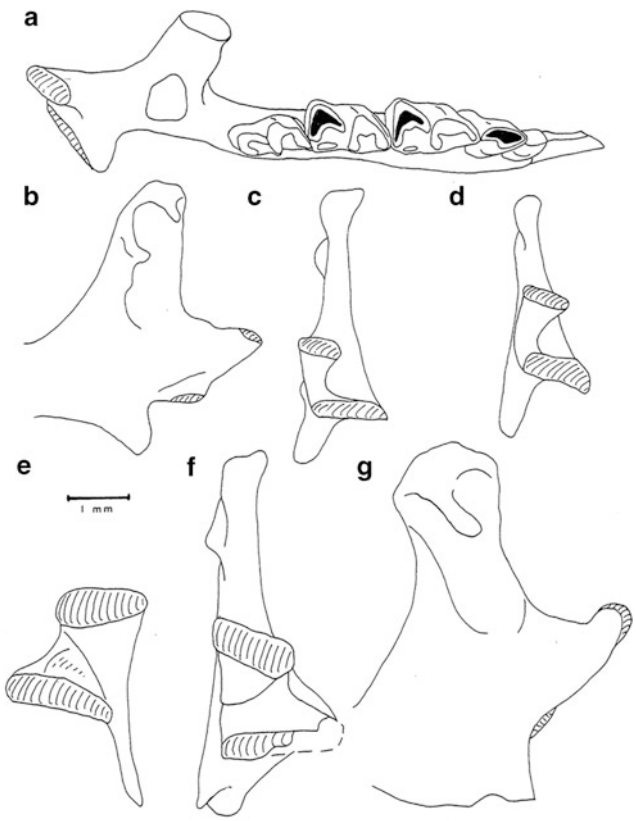

Fig. 2.6 Drawings of shrew mandibles featuring articulation morphology. **a–c** *Soriculus praecursus* holotype V8898.1 in dorsal, lateral and posterior view; **d** posterior view of modern *Episoriculus caudatus* (MCZ 20726); **e** posterior view of articulation of *Beremendia pohaiensis* (V8900); **f**, **g** *Lunanosorex lii* (V8895.4) in posterior and lateral views

strong lingual and buccal cingula, and its exposure extends rather far posteriorly on the buccal side to below p4 and the trigonid of m1. Posterodorsal to this is the mental foramen, below the front of the talonid of m1. Premolars are damaged buccally, but show a cingulum on both sides. The first antemolar, known as a1, shows one elongate wear facet, is crowded between the incisor and the following premolar (p4), and extends on the lateral side under half of p4. The buccal flange of p4 sweeps posteriorly much farther than does the lingual part of the tooth, to a point below the middle of the trigonid of m1, and well below the level of the base of the molar row. The tooth is elongate, highest crowned along its median axis. Its apex is a relatively small trigonid, which wears as a lingually sloping triangular surface. There is an abbreviated talonid, with high buccal wall that continues the trigonid wear facet. The talonid is open and drains lingually.

The molar row is 4.33 mm long. The first molar is largest and overhangs the talonid of p4. The trigonid V shape is broadly open lingually due to the anteriorly projecting paraconid. The paraconid is the lowest cusp of the trigonid; the protoconid is highest, its apex at the midline of the tooth. The molar is widest posteriorly at the acute-angle hypoconid. The cristid obliqua intersects the protoconid. The entoconid is high and slopes anteriorly to close the talonid basin, but lacks an entoconid crest. There is a narrow trough posterior to the entoconid. A cingulum encircles the tooth. The second molar is similar, but the trigonid makes a more acute angle, the paraconid being less anteriorly directed, and the anterior and posterior widths are equal. The last molar is smallest, its talonid reduced as is typical for m3. Its cingulum is fainter than in m1–2. The talonid is a double-cusped, small and enclosed basin. The cristid obliqua is directed toward the metaconid. The two specimens show variation in size, the m3 being relatively smaller in V8898.2.

The fossil upper molars are identified as M2 due to their proportions (width slightly greater than length) and the nearly symmetrical ectoloph. The ectocingulum is limited to the external paracone and metacone valleys. The crescentic hypocone is joined to the protocone by a low ridge. The hypocone flange, sculpted posteriorly, is continuous with the posterior cingulum. The pre- and postprotocristas make a symmetrical V-shape. The preprotocrista intersects the base of the paracone, but other than locally at the intersection, there is no precingulum. The postprotocrista terminates as a wear feature short of the metacone, but is continued by a weak and low metaloph.

Two upper incisors from YS50 were briefly mentioned by Flynn and Wu (1994). These large specimens are assigned to *Lunanosorex* (below).

Discussion: Hoffman (1986) and McKenna and Bell (1997) consider *Soriculus* as a genus containing a number of species previously assigned to distinct genera *Chodsigoa* and *Episoriculus*. The differences between living species are minor and their polarities are undemonstrated, so the latter taxa are retained as subgenera. Affinity of Pliocene fossils to a living subgenus would be difficult to defend. The Yushe shrew, while unlike living species, is therefore assigned to *Soriculus*, *sensu lato*, without implying subgeneric relationship.

Taxa related to *Soriculus* (*Soriculus*) other than *Neomys* show little pigment, and pigment is at best doubtfully preserved in the fossils. Living *Chodsigoa* and *Chimarogale*, for example, show almost none. *Soriculus* has a bit more pigment, *Episoriculus* more. Concerning mandibular morphology, there are resemblances to *Episoriculus*, but also to *Soriculus* and *Neomys*. *Chodsigoa* is distinct in its heavier and more twisted articulation. One distinction of the fossil mandible is that the tip of its coronoid process inclines slightly anteriorly, while that of *Episoriculus* is nearly vertical. Dentally, the Yushe taxon resembles *Episoriculus* in that the anterior dentition is crowded, the external flange of p4 reaches well below the level of the molar row, and the talonid of m3 is basined with two cusps. *Chodsigoa* has a more reduced m3 talonid and lesser p4 flange reaching only somewhat below the level of the molars. *Soriculus*

nigrescens, a more fossorial species, also has a conservative p4, and its molars appear laterally compressed. The Yushe species resembles *Chodsigoa* in incisor morphology, both having weak dorsal cuspules. *Episoriculus* p4 has a more prominent posterior (pigmented) cusp, and tendency to show a second cuspule. Living *Soriculus* species tend to have a more sectorial p4, without a triangular trigonid wear facet. In p4 morphology, then, the Yushe shrew is likely primitive. Since it shows a mosaic of soriculine as well as distinctive features, we assign the new species as *Soriculus praecursus* without attribution to subgenus.

Other fossil soriculines include a Pleistocene species from Zhoukoudian. Originally "*Neomys bohlini*," Repenning (1967) transferred the species to *Chodsigoa*, based partly on jaw morphology. *Soriculus* (*Chodsigoa*) *bohlini* (Young 1934) has a different jaw articulation and is smaller than *Soriculus praecursus*. Kotlia (1991) named an Indian form *Episoriculus repenningi* from 2.4 Ma deposits in Kashmir. This diminutive species occurs near the range of living *Episoriculus*, exhibits two cuspules on the lower incisor, and p4 extending below the molar row, making subgeneric assignment reasonable. Jin and Liu (2008) named *Soriculus fanchangensis,* an early Pleistocene species from Anhui Province, which is much smaller than *S. praecursus*.

Late Pliocene *E. giberodon* from Poland was assigned to *Episoriculus* by Repenning (1967) when he reviewed soriculines, and raised the subgenera to generic rank. De Bruijn et al. (1970) added good material from the Isle of Rhodes, Greece. In distinction from other subgenera, the assignment is defended by a number of features that remain to be evaluated for polarity. Recognition of this material as having affinity to living *Episoriculus caudatus*, if valid, would indicate an extraordinarily wide distribution for this group of shrews.

On balance, *Soriculus praecursus* seems to share most features with *Episoriculus*, but there are differences in p4 morphology, simplicity of the incisor, and apparent lack of pigment. The Yushe species is somewhat larger than *E. caudatus*, slightly smaller than *Chodsigoa hypsibia*, and near the present geographic range of *Chodsigoa*. Because the generic status of the living subgenera and their cohesiveness with fossil species remain untested, we do not attempt formal affiliation with a living subgenus. The Yushe taxon probably points toward the suite of features that were primitive for the last common ancestor of the *Soriculus* group.

Tribe Beremendiini Reumer, 1984

Beremendia Kormos, 1934

Beremendia pohaiensis (Kowalski and Li, 1963)

1991 *Peisorex* n.sp. Flynn et al.

1994 *Peisorex pliocaenicus* Flynn and Wu

1997 *Peisorex pliocaenicus* Flynn et al.

1996a *Beremendia pohaiensis*, in part, Jin and Kawamura.

Referred material: V8900, right dentary with m1–m3 (Fig. 2.5h–j).

Locality and age: YS5, Mazegou Formation, Yuncu subbasin, late Pliocene about 3.3 Ma.

Distribution: In addition to Yushe Basin, the species is known from Plio-Pleistocene deposits of Liaoning (Haimao) and Hebei (near Tangshan) Provinces (Jin and Kawamura 1996a).

Description: The single Yushe specimen is a large dentary with molars, broken below m1 through the mental foramen, which is below the front of the talonid of m1. The coronoid process is broken so that anterior inclination cannot be evaluated, but enough is present to show that the process diverges strongly laterally from the horizontal ramus. The condyle is preserved, showing a large, protruding, and ventrally shifted lower articulation, and triangular upper articulation with broad interarticular area. The internal temporal fossa is enormous, but the mandibular foramen is not as large as in other specimens of the species.

Molars decrease markedly in size posteriorly, the first being largest, the third less than half its size. Their lingual walls are arrayed in a straight line, with the small m3, therefore, in a relatively lingual position. Teeth are measured with respect to this major axis. Roughly parallelograms, therefore, length is measured with reference to the posterolabial corner of the tooth and tip of the protolophid (width is the maximum perpendicular to length; see Table 2.1). Tooth color is dark in the fossil, but it is not clear whether this reflects original iron staining. While m1 widens slightly posteriorly, m2 is nearly as wide posteriorly as anteriorly. Trigonids are widely open lingually, having a long, anteriorly directed protolophid. Paraconids are nearly as tall as the metaconids. The cristid obliqua intersects the trigonid wall lingual to the protoconid. The sharp entoconid has an entoconid crest that continues anteriorly to the trigonid, closing off the talonid. However, there is a narrow trough posterior to the entoconid and adjacent to the posterolophid that traverses the back of the talonid from the hypoconid. The trigonid of m3 is a small version of that of m2, but the tooth is markedly smaller, in large part due to the diminutive talonid. The tiny talonid is encircled by a low crest that originates (like the cristid obliqua) at a point lingual to the protoconid, passes the position of the hypoconid and posterolophid, and stops at the position of the entoconid, leaving a gap between it and a lingual crest running from the trigonid. There is a strong buccal cingulum on all of the molars. The lingual cingulum is weak in m1, faint on m2, and is only hinted anteriorly on m3.

Discussion: This large shrew is represented by only one specimen in Yushe Basin. Flynn and Wu (1994) realized its similarity to *Peisorex pohaiensis* Kowalski and Li 1963, but were impressed by difference in size. The type specimen of

Peisorex pohaiensis, V2671, has m1–m3 length of 6.12 mm, while that of V8900 is 6.64 mm (remeasured). This difference of V8900 being 8.5% bigger is less than the 15% reported by Flynn and Wu (1994), but explained by three factors. First, the teeth of V8900 are slightly larger than those of holotype V2671. Second, the dental arcade is curved in V2671, with m2 and m3 successively slightly lingually canted with respect to m1. Third, m3 is relatively smaller in V2671 (see Table 2.1). Although m1 and m2 are not much different in size between the two specimens, the impression from the total molar row is that V8900 is larger.

In their important study of new fossils of large shrews from Haimao, near Dalian, Liaoning Province, Jin and Kawamura (1996a) recognized that a sample including a skull and mandibles represents the genus *Beremendia*, well known from Europe. Their skull material compares quite well to *Beremendia fissidens*. The Haimao material was seen to be conspecific with *Peisorex pohaiensis* and assessed as showing sufficient variation to include V8900. Thus, *Peisorex* is a junior synonym of *Beremendia*, and *P. pliocaenicus* Flynn and Wu 1994, is a junior synonym of *B. pohaiensis*. The differences noted between V8900 and V2671 are minor, and Jin and Kawamura (1996a) quite rightly note that the sizes of m1 and m2 are close. Among known specimens, the largest are the oldest and new fossils possibly will suggest a size decrease in this lineage after 3.3 Ma, the age of the Yushe specimen.

Lunanosorex Jin and Kawamura, 1996b

Lunanosorex lii Jin and Kawamura, 1996b

1991 Blarinini Flynn et al.

1994 cf. *Blarinoides* sp. nov. Flynn and Wu

1997 cf. *Blarinoides* sp. Flynn et al.

Referred material: V8895.1, right M1 (Fig. 2.5g); V 8895.2, left M1; V8895.3, right m1; V8895.4, a posterior portion of a left dentary (Fig. 2.6); all from locality YS87; V8896.1, broken right M2, and V8896.2,–0.3, two upper right incisors, from YS50.

Distribution: Yushe material from YS87, Mazegou Formation, Yuncu subbasin, 3.5 Ma, and from YS50, early Pliocene Gaozhuang Formation, Yuncu subbasin, 4.7 Ma. Type material from Yinan, Shandong Province, and referred material from Bilike, Inner Mongolia.

Description: The dentary fragment preserves the coronoid, slightly damaged condyle, and short angular process. It represents a large shrew (tip of coronoid to inferior border of dentary is 6.5 mm), but is not as big as *Beremendia pohaiensis*. The specimen is figured in Flynn and Wu (1994). The condyle has a broad interarticular area and is not greatly deflected medially. The lower articulation is not shifted anteriorly in position and is slightly visible in labial view. The superior pterygoid fossa is a small, shallow basin with a weak spicule. The shallow external temporal fossa extends down the coronoid to the level of the superior sigmoid notch. The coronoid process is spatulate, with a strong, high coronoid spicule; masseteric fossa small and shallow. Internal temporal fossa uninflated, but with a trough-like depression rising up the coronoid. Below this level is the small mandibular foramen. The coronoid is labially deflected and tilted slightly anteriorly.

Except for the projecting metastylar wing, M1 (Fig. 2.5g) is nearly square in outline (dimensions of V8895.1 = 2.43, 2.38; slightly damaged V8895.2 = 2.29, 2.38). The ectoloph is somewhat asymmetrical, the metacone being larger than the paracone; also there is a strong parastyle, an arcuate mesostyle, and no metastyle. The protocone, opposite the paracone, and the metacone border a deep trigon basin. Preprotocrista approaches the paracone, but ends in a minute paraconule at the base of the paracone. The postprotocrista makes a slightly raised intersection with an oblique ridge running posterolingually to the hypocone. The intersection could be homologous to a metaconule, and from it a transverse ridge extends to the base of the metacone. The expansive hypocone flange is gently emarginated near the midline of the tooth. Lingually, a crest rims the flange and the small hypocone is located on this marginal crest. The crest is continuous with a postcingulum. From the hypocone, a weak lingual cingulum runs to and fades at the protocone. The anterior face of the protocone is furrowed vertically, without precingulum.

The referred M2 from the older locality YS50 is nearly as wide (2.28 mm) as the first molars. Its hypocone flange is broken off, but preserved length is 1.81 mm. The ectoloph is symmetrical. Its parastyle is cusplike, but the mesostyle and metastyle are uninflated. As in M1, there is a small paraconule and a raised area in the position of a metaconule, where a faint ridge leads to the hypocone. There is a weak anterior cingulum. V8895.3 is broken, missing its lingual third and anterior termination of the protolophid. Preserved length is 2.6 mm. It is considered m1 because talonid width (at least 1.7) would be considerably greater than trigonid width. The cristid obliqua intersects the back of the trigonid at the midline of the tooth, relatively more lingually than in *Beremendia*. Although damaged, the entoconid and entoconid crest appear to close the talonid basin. The buccal cingulum is prominent.

Two upper incisors are referred here. One is broken at the base but shows a long, curved, laterally compressed root. The other, 3.09 mm long, has a procumbent and large major cusp. It is not fissident, consistent with observations on this tooth by Qiu and Storch (2000).

Discussion: Previously, Flynn and Wu (1994) compared V8895.4 to *Blarinoides*, a blarinine from the Pliocene of Europe. Jin and Kawamura (1996b) referred it to their new genus *Lunanosorex*, currently considered a member of Tribe Beremendiini. *Lunanosorex* shares with *Bermendia* a

massive jaw articulation with large interarticular area, and *Beremendia* had been grouped among Blarinini, due largely to this feature. However, Reumer (1984) recognized a suite of features to defend tribal attribution to Beremendiini: pigmented teeth, upper incisor fissident, upper antemolars diminish in size posteriorly with A4 hidden, M3 and m3 small, robust ramus with anterolaterad inclination of coronoid process and short, blunt angular process, curved and acuspulate lower incisor. *Bermendia pohaiensis* matches this diagnosis (Jin and Kawamura, 1996a), but the upper incisor of *Lunanosorex* is not fissident and its lower incisor is weakly bicuspulate (Qiu and Storch 2000). As to pigmentation, we suspect that the color is leached from the Yushe specimens. There is some coloration of specimens, but not the obvious pattern of shrew pigmentaion. Interestingly, the coloration of V8895.2 and V8895.3 appears reversed, with areas near cusp tips bleached light and the rest of the crowns darker (reddish to beige in the case of V8895.3). As more specimens become available, it will be appropriate to review the diagnoses of Blarinini and Beremendiini.

The species level identification for the Yushe material could be taken as tentative. Qiu and Storch (2000) decided that the smaller dental sizes in the Bilike sample of *Lunanosorex* prevented secure identification as *L. lii*. The Yushe sample includes somewhat younger material and appears to be of appropriate size for the type specimen of *L. lii*. We see no morphological evidence to contradict that assignment.

Tribe Blarinini Stirton, 1930
Sulimskia Reumer, 1984
cf. *Sulimskia* sp.

1994 cf. Blarinini, Flynn and Wu

Referred specimen and age: V8897 (Fig. 2.5k), right M1 from Yuncu subbasin locality YS32, Mahui Formation, 6.0 Ma.

Description: The M1 (buccal length 1.62, width 1.95 mm) is wider than long, although length could be underestimated due to breakage of the hypocone flange. The paracone and metacone are high-walled with narrow, straight wings that comprise a high ectoloph. The ectoloph does not extend deeply into the tooth, due to presence of a buccal shelf at both the paracone and metacone. The protocone is also relatively high, with steep buccal wall, so that the trigon basin is deep. The parastyle is weakly cuspate. Unlike the more symmetrical ectoloph of M1 in *Lunanosorex*, the ectoloph of V8897 is asymmetrical because the metacone wing is longer than the paracone wing. The preprotocrista ends at a small paraconule, which is located at the base of the paracone. The postprotocrista joins the metacone without distinct metaconule. A ridgelike crest descends posteriorly from the midpoint of this crista to the hypocone. However, the hypocone and its flange are broken away. Apparently the flange extends less than half way across the tooth, again unlike *Lunanosorex*, and continues bucally as a narrow posterior cingulum. There is a faint internal and posterior cingulum, but no apparent buccal cingulum.

Discussion: This specimen is insufficient for species identification. It is of appropriate size for *Sulimskia*, but does not match closely known species. Morphologically, with the deep trigon basin, high paracone and metacone with buccal shelf, hypocone ridge and small hypocone flange, and the weak cingula, it matches the description of *Sulimskia zieglerl* from Bilike, Inner Mongolia. However, based on this material, a small species of *Lunanosorex* could not be ruled out. *Sulimskia* is another genus that calls for review of the content of Blarinini and Beremendiini.

Subfamily Crocidurinae Milne-Edwards, 1868
Crocidura Wagler, 1832
Crocidura sp.

1994 *Crocidura* Flynn and Wu
1997 *Crocidura* Flynn et al.

Referred specimen and age: V8899 (Fig. 2.5l), right M2 from YS83, Red Lishi loess of Yuncu subbasin, Yushe Basin, early Pleistocene.

Description: This white molar is worn and damaged buccally, but shows several important features. It is relatively wide with W-shaped ectoloph, deep transversely, but ectoflexus (buccal border) shallowly sculpted. The metacone is larger than the paracone; conules are absent. The protocone is not pinched, its arms defining an angle >90°. The preprotocrista or protoloph abuts the paracone. There is no metaloph directed toward the metacone. Instead, a postprotocrista is directed posteriorly toward the hypocone, which is low and uninflated. There is a weak lingual cingulum. The small hypocone flange slopes gently labially, is invaginated less than half way across the tooth, and is continued by a cingulum extending to the buccal margin of the tooth. Lingual length: 1.57; width: 1.76 mm.

Discussion: The common living *Crocidura* in Shanxi Province and eastward throughout Hebei and Liaoning is *C. shantungensis* (Jiang and Hoffmann 2001). This small species is considerably smaller than the Yushe specimen, but about the size of *C. wongi* named by Pei (1936) for samples from Zhoukoudian. Pei (1936), however, felt that *C. wongi* was smaller than *C. coreae*, the latter now seen as a synonym of *C. shantungensis* (Jiang and Hoffmann 2001). Whether or not *C. wongi* should be subsumed under *C. shantungensis*, the Yushe white-toothed shrew is quite different.

The Yushe *Crocidura* is clearly smaller than *C. fuliginosa*. Today, *C. attenuata* lives west of the Yellow River (Jiang and Hoffmann 2001), not far from Yushe, and V8899 is of comparable size, but the two differ. Structures of upper molars of *C. attenuata* are compressed anteroposteriorly, such that the ectoloph appears to make a narrower and

deeper W-shape, and the trigon is wider transversely. *C. vorax* of Yunnan is somewhat smaller, but a better structural match. No further conclusion can be supported about V8899, other than that it attests to presence of a large *Crocidura* in the early Pleistocene of Yushe.

2.3 Conclusions

Like other well-represented faunas in China, the Yushe insectivores are diverse. The late Miocene of Yushe records two moles, *Yanshuella* and *Yunoscaptor*, and at least two shrews, a blarinine and a smaller form represented by indeterminate fragments. Pliocene Gaozhuang and Mazegou assemblages retain the Miocene mole genera, and add the derived, extant mole *Scaptochirus* and the water mole *Desmana*. Yushe Pliocene shrews include two large beremendiinines, a soriculine, and the small cf. *Paenelimnoecus*. There appears to be a decline in insectivoran diversity toward the end of Pliocene time, although the large hedgehog, *Erinaceus olgae*, persisted in Yushe Basin. Haiyan Formation localities yield only *Sorex*, and the Pleistocene loess produces *Crocidura*. This decline in diversity, if not a sampling effect, may echo cooling climate; Reumer (1984) hypothesizes that lower mean annual temperature corresponds with lower insectivoran diversity. Jin et al. (1999) saw a similar decline in diversity and modernization among insectivores in the Pliocene of North China.

Of the common moles in the terminal Miocene and Pliocene of Yushe Basin, we have recognized two taxa that otherwise have separate northern and southern distributions. Tedford et al. (1991) noted *Yanshuella* in the Gaozhuang Formation and more recently we found it in the Mahui Formation. The Yushe species *Yanshuella yushensis* has close affinity with northern *Y. primaeva* from Ertemte and Harr Obo, Inner Mongolia, but shows some differences. The Yushe taxon ranges well into the Pliocene, presumably younger than either latest Miocene Ertemte or early Pliocene Harr Obo. The Yushe material demonstrates a size difference and some morphological differences, including two roots on anterior premolars, which distinguish the species from *Y. primaeva*.

The second common Yushe mole was difficult to characterize until the Lufeng material of *Yunoscaptor* was described (Storch and Qiu 1990) and more Yushe material was found. The Yushe specimens are somewhat younger than the Lufeng *Y. scalprum*, but do not demonstrate different species level status. This mole suggests a level of faunal similarity with South China in the late Miocene. A less common mid-Pliocene mole, an early record in China of *Scaptochirus*, is closely related to living northeast China *S. moschatus*.

Shrews include large species assigned to *Beremendia* and *Lunanosorex*. Previously we felt that the latter was a blarinine (Flynn and Wu 1994). Although current workers place it in Beremendiini, we suggest that its tribal affinity may need review. A smaller shrew is a soriculine, but it does not preserve autapomorphies of any living subgenus. For that reason it is classified as *Soriculus* without reference to an extant subgenus. Concerning the younger records of small shrews, neither *Sorex* nor *Crocidura* from Yushe are easily matched with living species. Other regions of China record *Anourosorex* Milne-Edwards, 1872 in the Pleistocene (Zheng 1985), but this southern genus is not in evidence at Yushe.

Our recognition of shrew taxa relies largely on condyle structure of the dentary bone and on molar morphology. Tooth pigmentation has limited usefulness: it appears to be leached diagenetically from some specimens. Interestingly, cusp tips of teeth attributed to *Beremendia* are lighter in color than the main bodies of crowns.

Paleobiogeographically, the Yushe Lipotyphla show considerable affinity with eastern China (region around Hebei and Liaoning) and especially with Zhoukoudian. The hedgehog, *Scaptochirus*, *Lunanosorex*, *Beremendia*, and *Sorex* all compare closely with taxa from sites in eastern China (Cai 1987; Jin and Kawamura 1996a, b). Some genera (*Yanshuella*, the erinaceid) show a degree of faunal similarity with continental interior localities of Inner Mongolia and some lypotyphlans such as *Beremendia, Soriculus* and *Desmana* were widespread across northern Eurasia (Kretzoi 1959). Also, a degree of faunal communication with North America is suggested by presence of a late Miocene blarinine. The taxa shared with southern China, *Yunoscaptor* and *Soriculus*, may indicate mild climate with adequate moisture that allowed northward expansion of taxa having southern ranges. The Yushe Lipotyphla attest to some biogeographic fluidity of its members, but share affinity primarily with nearby localities of eastern China, a coastal subprovince of North China.

Acknowledgements We thank reviewers, especially William Korth and Nick Czaplewski, for their help in improving this chapter. Ruth O'Leary kindly verified the correct number for the F:AM jaw of *Erinaceus olgae.*

References

Cai, B.-Q. (1987). A preliminary report on the late Pliocene micromammalian fauna from Yangyuan and Yuxian, Hebei. *Vertebrata PalAsiatica, 25,* 124–136.

Corbet, G. B. (1988). The family erinaceidae: A synthesis of its taxonomy, phylogeny, ecology and zoogeography. *Mammal Review, 18,* 117–172.

De Bruijn, H., Dawson, M.R., & Mein, P. (1970). Upper Pliocene Rodentia, Lagomorpha and Insectivora (mammalia) from the Isle of

Rhodes (Greece). I, II and III. *Proceedings Koninklijke Nederlandse Akademie van Wetenschappen B73*, 535–584.

Douady, C. J., & Douzery, E. J. P. (2009). Hedgehogs, shrews, moles, and solenodons (Eulipotyphla). In S. B. Hedges & S. Kumar (Eds.), *The timetree of life* (pp. 495–498). Oxford: Oxford University Press.

Engesser, B. (1980). Insectivora und Chiroptera (Mammalia) aus dem Neogen der Turkei. *Schweizerische Paläontologische Abhandlungen, 102,* 47–149.

Fahlbusch, V., Qiu, Z.-D., & Storch, G. (1983). Neogene Mammalian faunas of Ertemte and Harr Obo in Nei Monggol, China. 1. Report on field work in 1980 and preliminary results. *Scientia Sinica, B26,* 205–224.

Flynn, L. J., Tedford, R. H., & Qiu, Z.-X. (1991). Enrichment and stability in the pliocene mammalian fauna of North China. *Paleobiology, 17,* 246–265.

Flynn, L. J., & Wu, W.-Y. (1994). Two new shrews from the Pliocene of Yushe Basin, Shanxi Province, China. *Vertebrata PalAsiatica, 32,* 73–86.

Flynn, L. J., Wu, W.-Y., & Downs, W. R. (1997). Dating vertebrate microfaunas in the late Neogene record of northern China. *Palaeogeography, Palaeoclimatology, Palaeoecology, 133,* 227–242.

Hoffmann, R. S. (1986). A review of genus *Soriculus* (Mammalia: Insectivora). *Journal of the Bombay Natural History Society, 82,* 459–481.

Hutchison, J. H. (1968). Fossil Talpidae (Insectivora, Mammalia) from the later Tertiary of Oregon. *Museum of Natural History Bulletin, University of Oregon, 11,* 1–117.

Jiang, X.-L., & Hoffmann, R. S. (2001). A revision of the white-toothed shrews (*Crocidura*) of southern China. *Journal of Mammalogy, 82,* 1059–1079.

Jin C.-Z., & Kawamura Y. (1996a). The first reliable record of *Beremendia* (Insectivora, Mammalia) in East Asia and a revision of *Peisorex* Kowalski and Li, 1963. *Transactions of the Proceedings of the Palaeontological Society of Japan*, *N.S. 182*, 432–447.

Jin C.-Z., & Kawamura Y. (1996b). A new genus of shrew from the Pliocene of Yinan, Shandong Province, northern China. *Transactions of the Proceedings of the Palaeontological Society of Japan*, *N.S. 182*, 478–483.

Jin, C.-Z., & Liu, J.-Y. (2008). *Paleolithic Site – The Renzidong Cave, Fanchang, Anhui Province*. Beijing: Science Press.

Jin, C.-Z., Kowamura, Y., & Taruno, H. (1999). Pliocene and Early Pleistocene insectivore and rodent faunas from Dajushan, Qipanshan and Haimao in North China and the reconstruction of the faunal succession from the Late Miocene to Middle Pleistocene. *Journal of Geosciences, 42,* 1–19. Osaka City University.

Kormos, T. (1934). Neue Insektenfresser, Fledermäuse und Nager aus dem Oberpliozän der Villanyer Gegend. *Földani közlöny, 64,* 296–321.

Kotlia, B. S. (1991). Pliocene Soricidae (Insectivora, Mammalia) from Kashmir Intermontane Basin, northwestern Himalaya. *Journal of the Geological Society of India, 38,* 253–275.

Kowalski, K., & Li, C.-K. (1963). A new form of the Soricidae (Insectivora) from the Pleistocene of North China. *Vertebrata PalAsiatica, 7,* 138–143.

Kretzoi, M. (1959). Insectivoren, Nagetiere und Lagomorphen der Jüngstpliozänen Fauna von Csarnóta im Villanyer Gebirges (Sündungarn). *Vertebrata Hungarica, 1,* 237–246.

McKenna, M. C., & Bell, S. K. (1997). *Classification of mammals above the species level*. New York: Columbia University Press.

Pei, W. C. (1936). On the Mammalian remains from locality 3 at Choukoutien. *Palaeontologica Sinica, C, 7*(5), 1–107.

Qiu, Z.-D., & Storch, G. (2000). The early Pliocene micromammalian fauna of Bilike, Inner Mongolia, China (Mammalia: Lipotyphla, Chiroptera, Rodentia, Lagomorpha). *Senckenbergiana Lethaea, 80,* 173–229.

Repenning, C. A. (1967). Subfamilies and genera of the Soricidae. *Geological Survey Professional Paper, 565,* 1–74.

Reumer, J. W. F. (1984). Ruscinian and early Pleistocene Soricidae (Insectivora, Mammalia) from Tegelen (The Netherlands) and Hungary. *Scripta Geologica, 73,* 1–173.

Rzebik-Kowalska, B. (1994). Pliocene and Quaternary Insectivora (Mammalia) of Poland. *Acta Zoologica Cracoviensia, 37,* 77–136.

Schlosser, M. (1924). Tertiary vertebrates of Mongolia. *Palaeontologica Sinica C, 1*(1), 1–133.

Storch, G. (1995). The Neogene mammalian faunas of Ertemte and Harr Obo in Inner Mongolia (Nei Mongol), China. 11. Soricidae (Insectivora). *Senckenbergiana Lethaea, 75,* 221–251.

Storch, G., & Qiu, Z.-D. (1983). The Neogene mammalian faunas of Ertemte and Harr Obo in Inner Mongolia (Nei Mongol), China. 2. Moles (Insectivora: Talpidae). *Senckenbergiana Lethaea, 64,* 89–127.

Storch, G., & Qiu, Z.-D. (1990). Insectivores (Mammalia: Erinaceidae, Soricidae, Talpidae) from the Lufeng Hominoid Locality, Late Miocene of China. *Géobios, 24,* 601–6212.

Tedford, R. H., Flynn, L. J., Qiu, Z.-X., Opdyke, N. D., & Downs, W. R. (1991). Yushe Basin, China: Paleomagnetic calibrated mammalian biostratigraphic standard for the late Neogene of eastern Asia. *Journal of Vertebrate Paleontology, 11,* 519–526.

Teilhard de Chardin, P., & Piveteau, J. (1930). Les Mammifères fossiles de Nihowan (Chine). *Annales de Paléontologie, Pékin, 19,* 1–132.

Young, C. C. (1934). On the Insectivora, Chiroptera, Rodentia and Primates other than *Sinanthropus* from Locality 1 at Choukoutien. *Palaeontologica Sinica, C, 8,* 1–160.

Young, C. C., & Liu, P. T. (1950). On the mammalian fauna at Koloshan near Chungking, Szechuan. *Bulletin of the Geological Survey of China, 30,* 43–90.

Zdansky, O. (1928). Die Säugetiere der Quartärfauna von Chou-k'ou-tien. *Palaeontologica Sinica, C, 5,* 1–146.

Zheng, S.-H. (1985). Remains of the genus *Anourosorex* (Insectivora, Mammalia) from Pleistocene of Guizhou District. *Vertebrata PalAsiatica, 23,* 39–51.

Chapter 3
The Bats of Yushe

Lawrence J. Flynn

Abstract The screen-washing activities of three field seasons by the Sino-American Yushe teams processed tons of sediment from two dozen localities. Of the many micromammals recovered from Late Neogene deposits, only five chiropteran (bat) teeth were found. These are from five localities dated between 6 and 3 Ma. The bat fossils are assignable or very close to modern genera. In distribution, three of the genera occur in North China today, while at least one is currently of more southerly distribution, occurring to the southwest in Sichuan Province. Together with Pleistocene records, the Yushe Basin fossils suggest that current bat distributions are reduced with respect to early Pleistocene species ranges.

Keywords Yushe Basin • Late Neogene • Bats • Chiroptera • North China

3.1 Introduction

No fossil Chiroptera had been recovered from Yushe Basin until the joint Sino-American expeditions of the late 1980s. "Chiroptera", Greek for "hand-wing", include some large body size taxa, but the characteristic bats of North China are small, and the dominant Family Vespertilionidae contains some quite small species. The records presented here are based on small teeth. Not surprisingly, Yushe bats have been recovered only with the advent of fossil screening.

Taphonomy also plays a role. Bats roost in rock crevices, tree cavities, or caves, spending most of the time in settings that are not usually preserved in the fossil record. Otherwise they are volant, an activity that usually is not conducive to preservation. Therefore, while bats are quite diverse and locally abundant in natural settings, they are not well-represented in fossil accumulations. The number of recovered fossils does not reflect relative abundance, and the number of taxa greatly under-represents composition of the paleocommunity. As for Yushe, Engesser (1980) found Chiroptera to be poorly represented in the rich material from the many Miocene sites in Turkey that otherwise includes many lipotyphlans. The efforts of the Yushe expeditions have produced five specimens from five localities, representing quite possibly five different taxa (Fig. 3.1). Their descriptions follow.

3.2 Systematics

Order Chiroptera Blumenbach, 1779
Family Rhinolophidae Gray, 1825
Rhinolophus Lacépède, 1799
Rhinolophus sp.

Referred material: V8901, broken left m2 (talonid width = 1.45 mm; Fig. 3.1a).

Locality and age: YS37, early Pliocene, Nihe subbasin (no nearby magnetostratigraphy).

Description: Large lower molar, moderately high crowned unilaterally, lacking the anterior part of the trigonid. The metaconid lies at the end of a straight metalophid. The protoconid is broken but would tower above the height of the metaconid. Weak buccal cingulum, talonid wider than trigonid, cristid obliqua intersects in the middle of the trigonid. Entoconid strong and conical, widely spaced from trigonid and isolated from posterolophid by a trough. Hypoconulid is indistinct and incorporated into the posterolophid terminus.

Discussion: Although fragmentary, V8901 is distinctive in its large talonid and its shape relative to the trigonid (with high protoconid), isolation of the conical entoconid, high position of the weak hypoconulid, and weak labial cingulum.

L.J. Flynn (✉)
Department of Human Evolutionary Biology, and the Peabody Museum of Archaeology and Ethnology, Harvard University, Cambridge, MA 02138, USA
e-mail: ljflynn@fas.harvard.edu

Lawrence J. Flynn and Wen-Yu Wu (eds.), *Late Cenozoic Yushe Basin, Shanxi Province, China: Geology and Fossil Mammals, Volume II: Small Mammal Fossils of Yushe Basin*, Vertebrate Paleobiology and Paleoanthropology,
DOI 10.1007/978-94-024-1050-1_3

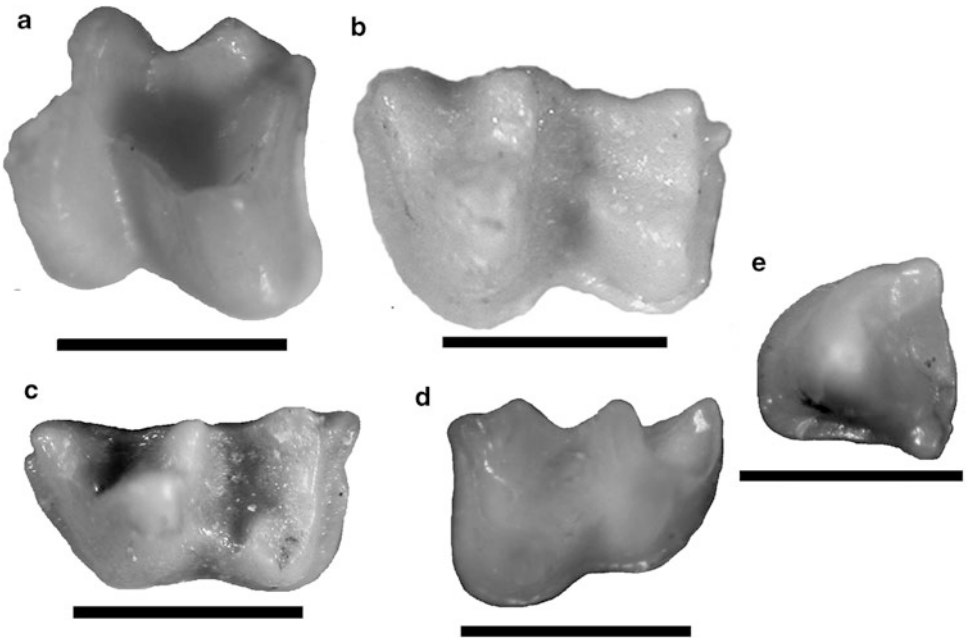

Fig. 3.1 **a**–**e** Isolated chiropteran teeth from Yushe Basin, in occlusal view. **a** *Rhinolophus* sp. V8901, broken left m2; **b** *Myotis* sp. V8902, left m3; **c** cf. *Murina* sp. V8904, left m1; **d** *Kerivoula* sp. V8838, right m1; **e** Vespertilionidae, genus indet. V8903, left lower premolar. Scale bars = 1 mm; **a**–**c** anterior to left; d, anterior to right, e, lingual to right

In addition to diverse living *Rhinolophus*, there are many fossil records in the Neogene of Eurasia. V8901 is about the size of living *R. rouxii* from China, and *R. pleistocaenicus* from Zhoukoudian (Young 1934).

Family Vespertilionidae Gray, 1821
Myotis Kaup, 1829
Myotis sp.

Referred material: V8902, left m3 (1.7 × 1.1, talonid width = 1.0 mm; Fig. 3.1b).

Locality and age: YS4, 4.3 Ma, early Pliocene.

Description: A last lower molar, with talonid narrower than trigonid, somewhat higher crowned buccally than lingually, with strong and continuous anterior-buccal-posterior cingulum. Paraconid and the slightly larger metaconid are somewhat higher than talonid cusps, but the massive protoconid dominates the trigonid. Trigonid is V-shaped with angle of about 45°, metalophid is transverse. Posterior to the trigonid at the middle of m3, the talonid is constricted and its buccal and lingual walls are low; the cristid obliqua intersects the trigonid at a point slightly lingual to the midline of the tooth. A sharp, vertical entoconid is located in the posterolingual corner of the tooth; a ridge slopes anteriorly from it as the lingual margin of the basin. The transverse posterior wall of m3 is straight and parallel to the metalophid. A small hypoconulid lies low on the cingulum, posterior to the entoconid.

Discussion: Several vespertilionids show a strong cingulum, low hypoconulid, and similar dimensions of the trigonid and talonid as in V8902. However, the large molar size and extreme lingual position of the cristid obliqua rule out all genera but *Myotis*. The specimen compares well with living *Myotis chinensis*. *Myotis* is well known from Zhoukoudian (Zdansky 1928; Young 1934; Pei 1936).

Murina Gray, 1842
cf. *Murina* sp.

Referred material: V8904, left m1 (1.55 × 0.9 mm; Fig. 3.1c) in dentary fragment.

Locality and age: YS87, 3.4 Ma, late Pliocene.

Description: Elongate molar in dentary fragment that preserves alveoli for a two-rooted p4. Trigonid is slightly narrower and somewhat higher than the talonid. Uninflated paraconid and metaconid lie on crests of equal height; protolophid and shorter metalophid make a near-right angle; notch separates paraconid and protoconid. Protoconid is large and inflated; hypoconid large, but cusp tip is broken. Talonid is a large basin with the cristid obliqua intersecting buccally, at the middle of the protoconid. There is a small notch in the buccal talonid wall, anterior to the hypoconid. A strong, low hypoconulid posterior to an angular entoconid is developed from but located above the cingulum. The moderately strong cingulum runs from below the paraconid, along the buccal margin (faint at the protoconid), to the posterolingual corner of the tooth. A cingulum also blocks the broad trigonid lingually. Two roots are present, the posterior root oriented transversely.

Discussion: Characteristic features of V8904 include the broad trigonid angle with a notched protolophid and lingual cingulum, buccal position of the cristid obliqua, and lingual

and low position of the hypoconulid posterior to the entoconid. V8904 resembles *Murina*, a genus recognized by Pei (1936) from Zhoukoudian, but the talonid seen in the latter sample is shorter anteroposteriorly. The Yushe fossil represents a species somewhat larger than extant *Murina aurata*. *Kerivoula* has a more acute metalophid-protolophid angle, but is similar in other features to V8904.

Kerivoula Gray, 1842
Kerivoula sp.

Referred material: V8838, isolated right m1 (1.25 × 0.80 mm; Fig. 3.1d).

Locality and age: YS145, Mahui Formation ~6 Ma, late Miocene.

Description: Sharp-cusped V8838 shows little wear. Its maximum talonid width contrasts with the narrow trigonid (0.65 mm wide), and it is identified as m1. It is a small lower molar with high talonid cusps, hypoconid the second largest cusp, and entoconid taller than small metaconid or uninflated paraconid. The straight metalophid and longer, gently curved protolophid give the trigonid an acute angle of about 50°. The entoconid is elongated anteroposteriorly and confluent with entoconid crest on the lingual wall of talonid; the hypoconulid juts from the lingual terminus of the posterolophid, above the cingulum. A strong, continuous cingulum encircles the anterior, buccal and posterior margins of the molar, but is weakest at the protoconid. There are two roots.

Discussion: This very small vespertilionid resembles *Kerivoula* to the exclusion of other genera. It shares the features of a tall hypoconid (rivaling the protoconid) and sharp entoconid, relatively elongated m1, trigonid making an acute angle, and trigonid width on m1 distinctly less than talonid width. There are minor differences from living species. V8838 is larger than m1 of extant *Kerivoula picta* and *K. hardwickei*. Its m1 trigonid in relation to the talonid is narrower than that of living species. *Kerivoula* occurs in the Pliocene of the Czech Republic and possibly older sites in Europe (Horáček 1986).

Vespertilionidae, genus indet.

Referred material: V8903, left lower premolar (length width = 1.0 × 1.05 mm; Fig. 3.1e).

Locality and age: YS134, 4.3 Ma, early Pliocene.

Description: The lower cheek tooth, triangular in outline, is wider than long. It is unicuspid and single-rooted, rounded anterobuccally, straight lingually and posteriorly. The high major cusp has a steep and flattened internal side, with near-vertical anterolingual and posterolingual ridges, the anterior one showing a shear facet on its mesial face. A strong posterior and buccal cingulum diminishes anterolingually and ends at a small, low cusp; linked to it by a weak lingual cingulum is a stronger posterolingual cusp.

Discussion: The size of this specimen is appropriate for p4 of several bats, but a premolar locus of a more anterior position in a large vespertilionid cannot be ruled out. Vespertilionids have one or two cheek teeth anterior to p4. V8903 shows some resemblance to the p4, or possibly the anteromost premolar in species of *Myotis*. The tooth between these is too small. In that the tooth is unicuspid, unlike a trigonid, the main cusp is moderately tall, and there is a straight internal margin but no talonid. However, the p4 of *Myotis chinensis* is more rectangular in occlusal view. There are some similarities to *Nyctalus* and *Eptesicus*, which have only two, crowded premolars, but the p4 of these genera is very sharp-cusped and its base is molded around the neighboring teeth. V8903 is approximately of the appropriate size for the taxon represented by the m3 V8902. V8903 resembles p4 of *Miniopterus*, which is known also from Zhoukoudian (Kowalski and Li 1963), but this is a smaller bat with a relatively taller main cusp.

3.3 Conclusion

The five specimens appear to represent at least four bat species. None are more than about six million years old, and each shows similarity to living species, so they are assigned to extant genera. One specimen represents a rhinolophid bat; the others are vespertilionids. Of the vespertilionids, *Kerivoula* is from the late Miocene Mahui Formation, while the others are Pliocene in age, from both the Gaozhuang and Mazegou formations. The rhinolophid comes from site YS37 in the Nihe subbasin, which otherwise produced very few specimens.

The Yushe fossils demonstrate diversity, but there is no potential in the present collection for recognizing biostratigraphic significance among them. Further sampling would certainly increase apparent diversity. From a biogeographic point of view, the widespread *Rhinolophus* and *Myotis* are not unexpected in the fossil record of Yushe. For example, both genera occur in the early Pleistocene of Dalian (Hu et al. 1992). Known from many Late Neogene age localities, *Myotis* is reported also from the late Miocene of Lufeng, Yunnan (Qiu et al. 1985). *Murina* is widespread in South China, but occurs in Shanxi Province and Inner Mongolia (Wang 2003). The early Pliocene locality, Bilike, Inner Mongolia, records *Murina* and *Myotis* (Qiu and Storch 2000). Jin et al. (1999) and Jin and Liu (2008) record *Rhinolophus*, *Myotis* and *Hipposideros* from the Pliocene and Pleistocene of Anhui and Shandong Provinces. Records of these genera are duplicated in the early Pleistocene of Zhoukoudian in North China (Zdansky 1928; Young 1934; Pei 1936; Kowalski and Li 1963). In South China, Qiu et al. (1984) recovered *Rhinolophus*, *Myotis*, and other genera

from the Pleistocene of Yunnan. However, Shanxi Province is north of the distribution for *Kerivoula* (and *Miniopterus*). *Kerivoula* ranges into Sichuan Province, and *Miniopterus* occurs across South China. Providing that *Kerivoula* is accurately identified in the fossil record of Yushe Basin, the bat species of Yushe Basin on balance would suggest expansion into Shanxi Province of taxa that had a predominantly southerly distribution.

Bats were almost certainly numerous and diverse in the succession of Late Neogene communities of Yushe Basin. The fossils found by the Sino-American Yushe expedition hint at this diversity, but are greatly underrepresented in the recovered assemblages due to their small size and preferred habitat, including sheltered roosts. One or more of the Yushe bats today are restricted to a South China distribution. As late as the early Pleistocene, some southern bats ranged into North China.

Acknowledgements I thank Will Downs and Wen-Yu Wu for their careful labors during the screening, and Tai-Ming Wang for field work in the Nihe subbasin, which produced the Nihe bat tooth. The collections of the Museum of Comparative Zoology at Harvard University under the care of Judith Chupasko and Mark Omura were invaluable for identifications. Reviewers Nick Czaplewski, Bill Korth, Mark Omura, and Wen-Yu Wu offered many improvements.

References

Engesser, B. (1980). Insectivora und Chiroptera (Mammalia) aus dem Neogen der Türkei. *Schweizerische Paläontologische Abhandlungen, 102,* 47–149.

Horáček, I. (1986). *Kerivoula* (Mammalia, Chiroptera), fossil in Europe? *Acta Universitatis Carolinae – Geologica, Špinar 2,* 213–222.

Hu, Q.-Q., Jin, C.-Z., Li, Y., & Hou, L.-H. (1992). *Dalian Haimao Fauna*. Dalian: Scientific and Technological University of Dalian Press.

Jin, C.-Z., Kowamura, Y., & Taruno, H. (1999). Pliocene and Early Pleistocene insectivore and rodent faunas from Dajushan, Qipanshan, and Haimao in North China and the reconstruction of the faunal succession from the Late Miocene to Middle Pleistocene. *Journal of Geosciences, Osaka University, 42,* 1–19.

Jin, C.-Z., & Liu, J.-Y. (2008). *Paleolithic Site – The Renzidong Cave, Fanchang, Anhui Province*. Beijing: Science Press.

Kowalski, K., & Li, C.-K. (1963). Remarks on the fauna of bats (Chiroptera) from Locality 1 at Choukoutien. *Vertebrata PalAsiatica, 7,* 144–150.

Pei, W. C. (1936). On the mammalian remains from Locality 3 at Choukoutien. *Palaeontologica Sinica, C7*(5), 1–107, 6 plates.

Qiu, Z.-D., Han, D.-F., Qi, G.-Q., & Liu, Y.-F. (1985). A preliminary report on a micromammalian assemblage from the hominoid locality of Lufeng, Yunnan. *Acta Anthropologica Sinica, 4,* 13–32.

Qiu, Z.-D., Li, C.-K., & Hu, S.-J. (1984). Late Pleistocene micromammal fauna of Sanjiacun, Kunming. *Vertebrata PalAsiatica, 22,* 281–293.

Qiu, Z.-D., & Storch, G. (2000). The early Pliocene micromammalian fauna of Bilike, Inner Mongolia, China (Mammalia: Lipotyphla, Chiroptera, Rodentia, Lagomorpha). *Senckenbergiana Lethaea, 80,* 173–229.

Schlosser, M. (1924). Tertiary vertebrates of Mongolia. *Palaeontologica Sinica, C*1(1), 1–133.

Wang, Y.-X. (2003). *A complete checklist of mammal species and subspecies in China: A taxonomic and geographic reference*. Beijing: China Forestry Publishing House.

Young, C. C. (1934). On the Insectivora, Chiroptera, Rodentia and Primates other than *Sinanthropus* from Locality 1 at Choukoutien. *Palaeontologica Sinica, C*8(3), 1–160.

Zdansky, O. (1928). Die Säugetiere der Quartärfauna von Chou-k'ou-tien. *Palaeontologica Sinica, C5*(4), 1–146, 16 plates.

Chapter 4
The Lagomorphs (Ochotonidae, Leporidae) of Yushe Basin

Wen-Yu Wu and Lawrence J. Flynn

Abstract Of historical collections of small mammals recovered from the Yushe Basin, fossil lagomorphs comprise a significant proportion because they are relatively large fossils and dentaries with teeth occur on the surfaces of exposures. Key fossils recovered prior to 1940 from various parts of North China, including the Yushe Basin, formed the basis for early systematic studies of both ochotonids and leporids. Several Yushe Basin specimens were important in that early phase of research, and continue to be important in current revisions of Lagomorpha. This systematic treatment of the Yushe Lagomorpha embraces collections made by modern teams and classical collections of the Tianjin Natural History Museum, the American Museum of Natural History, and the Institute of Vertebrate Paleontology and Paleoanthropology. For Yushe our study recognizes an array of *Ochotona* (pikas) and species of the larger genus *Ochotonoides*. Leporids are diverse for the late Neogene deposits of Yushe Basin, and included the genera *Alilepus, Hypolagus, Trischizolagus*, and *Sericolagus*; overlying Pleistocene loess yielded *Lepus* as well. These findings, including four new species, are important for lagomorph systematics, but also for the chronology of lagomorph evolution, because the Yushe sequence improves understanding of the relative ages of isolated Late Neogene deposits in China, and more broadly across Asia.

Keywords Yushe Basin • North China • Late Neogene • Lagomorpha • Leporidae • Ochotonidae

4.1 Introduction

Previously, Lagomorpha from the Yushe Basin included several specimens purchased and later described by Teilhard (1942), but these lacked precise stratigraphic and locality data. There were four genera and five species recognized from Yushe Basin: *Alilepus annectens, Hypolagus* cf. *brachypus, Ochotonoides complicidens, Ochotona (Pika) alpina,* and *Ochotona (Ochotona) daurica.* Today the Late Miocene through Pleistocene Yushe deposits are known to yield at least 17 lagomorphs, both pikas and leporids (hares and rabbits), based on all known specimens, including those collected nearly a century ago and those retrieved during the Sino-American cooperative research expeditions. These are not all contemporaries but occur throughout the late Miocene to early Pleistocene sedimentary record. Pikas include two *Ochotonoides* species, one new, and six or seven species of *Ochotona*. Among leporids are two *Alilepus*, one new, at least two *Hypolagus* (one new), a new species of *Sericolagus*, two *Trischizolagus*, one *Lepus*, and several indeterminate leporids that may indicate further diversity, one recalling the morphology of *Nekrolagus*. New specimens are not numerous but have precise stratigraphic control and, consequently, provide a relatively reliable foundation for the biostratigraphy of this order in the Yushe Basin. The Lagomorpha also serve as a foundation for correlation between this basin and other regions in North China and adjacent territories. In the course of this study, reevaluations of older published data promote reconsideration of the taxonomy and systematics of the group.

Note: This chapter includes one or more new nomenclatural-taxonomic actions, registered in Zoobank, and for such purposes the official publication date is 2017.

W.-Y. Wu (✉)
Laboratory of Paleomammalogy, Institute of Vertebrate Paleontology and Paleoanthropology, Chinese Academy of Sciences, 142 Xizhimenwai Ave., Beijing 100044, People's Republic of China
e-mail: wuwenyu@ivpp.ac.cn

L.J. Flynn
Department of Human Evolutionary Biology, and the Peabody Museum of Archaeology and Ethnology, Harvard University, Cambridge, MA 02138, USA
e-mail: ljflynn@fas.harvard.edu

Lawrence J. Flynn and Wen-Yu Wu (eds.), *Late Cenozoic Yushe Basin, Shanxi Province, China: Geology and Fossil Mammals, Volume II: Small Mammal Fossils of Yushe Basin*, Vertebrate Paleobiology and Paleoanthropology,
DOI 10.1007/978-94-024-1050-1_4

Methods. Our systematic review incorporates information from previous collections, and we studied both published and unpublished fossils at various institutions. We benefitted from material recovered by field parties of the early 20th century, now residing in collections of the Tianjin Natural History Museum (TNHM), and the Frick collection (F:AM) of the American Museum of Natural History, New York. Later IVPP and Sino-American field parties recovered a number of specimens as surface finds, with good provenance data and these are included here. Most of these bear YS field numbers; some sites with prefix "QY" (Qiu, Yushe) were prospected in the late 1970s–early 1980s. In addition, screening produced a number of isolated teeth, which contribute to the following study of Ochotonidae (pikas) and Leporidae (rabbits and hares). Dental measurements are expressed normally as length times width (L × W, with talonid width added for lower molariform teeth) in mm when not specified. Specimen illustrations utilized the Wild M7A binocular stereomicroscope, unless otherwise noted. The nomenclature used in the descriptions follows Boule and Teilhard (1928) and Erbajeva (1988).

4.2 Systematics

4.2.1 *Ochotonidae Thomas, 1897*

Ochotonoides Teilhard and Young, 1931
Ochotonoides teilhardi, sp. nov.

Type: Right mandible with i2, p3-m3 and part of the ascending ramus and angular process (V11200.1, Fig. 4.1a).

Paratype: Right P2 with slightly damaged labial side (V11200.2, Fig. 4.1f).

Type locality: YS5, Late Pliocene, 3.3 Ma, Mazegou Formation, Yushe Basin, Shanxi Province.

Referred material: From YS5, left mandible with i2, m1-3 and part of the ascending ramus and angular process (V11200.3), seven fragmentary mandibles including one with a pair of incisors (V11200.4-10), an anterior maxilla with left and right premaxillae bearing I2 and I3 (V11200.11), three maxillae, two with P3 and the zygomatic arch (V11200.12-13) and one with P4-M2 (V11200.14); two P3 (V11200.15-16), two cheek teeth (V11200.17-18, not differentiable as P4/M1/M2),

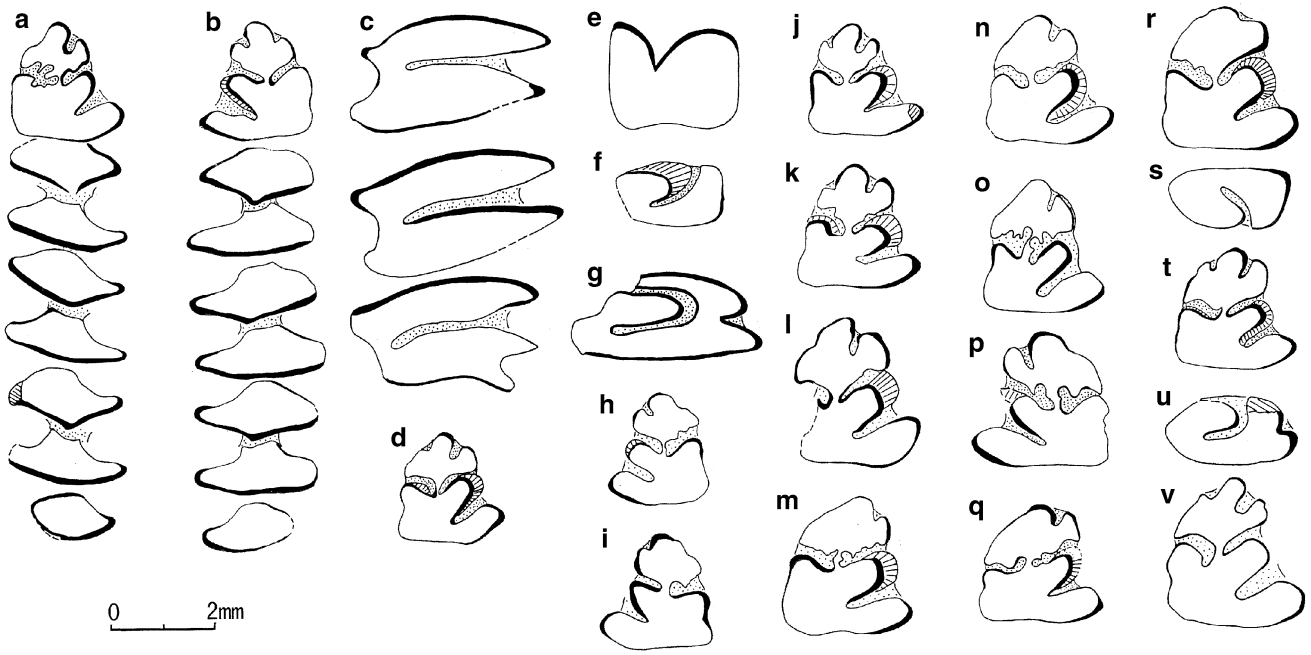

Fig. 4.1 *Ochotonoides teilhardi* sp. nov. from Yushe Basin (**a**–**j**) compared with *Ochotonoides complicidens* from various localities in China (**k**–**v**). *Ochotonoides teilhardi:* **a** Holotype right p3-m3 from YS5 (V11200.1); **b** left p3-m3 from YS99 (V11202.1); **c** right P4-M2 from YS5 (V11200.13); **d** right p3 from YS6 (V11204.1); **e** left I2 from YS6 (V11204.5); **f** paratype, right P2 from YS5 (V11200.2); **g** right P3 from YS5 (V11200.15); **h** left p3 purchased from Baihai (THP14191); **i** left p3 purchased from Malan (THP14212); **j** right p3 purchased from Malan (THP14208). *O. complicidens*: **k** right p3 purchased from Malan (THP14218); **l** right p3 purchased from Gaozhuang (THP14242); **m** right p3 purchased from Baihai (THP14190); **n**–**q** four p3 from Zhoukoudian Loc.18 (CP108); **r** right p3 from Yulin Loc.14 (c/100); **s**–**t** left P2 and right p3 from Gongwangling (V5407); **u**–**v** right P2 and right p3 from Chenjiawo (V3155). Anterior is upward for all but 4.1s

two I2 (V11200.19-20) and one p4/m1/m2 (V11200.21). From Zhaozhuang: field site QY-98, a right mandible with i2, p4-m3 (V11201); and unstudied skull F:AM 116228. YS99, left mandible with i2, p3-m3 and part of ascending ramus (V11202.1), damaged premaxilla with I2 and I3 (V11202.2), pair of I2 (V11202.3) and a P3 (V11202.4). YS118, right mandible with i2 and p4-m3, incomplete ascending ramus and angular process (V11203). YS6, right p3, anterior portion of p3, one P4 or M1, one i2, paired I2, and fragment of premaxilla with left I2 and both I3 (V11204.1-6).

Age of referred material and stratigraphic position: Mazegouan and Nihewanian Age, Late Pliocene-Early Pleistocene, Mazegou and Haiyan Fms., about 3.3 to 2 Ma.

Etymology: Patronym for Teilhard de Chardin, for his previous studies of *Ochotonoides* in the Yushe Basin.

Diagnosis: Small *Ochotonoides*, average p3 size 2.33 × 2.17 mm (n = 5). The mandible of *Ochotonoides teilhardi* has a long diastema. The p3 trigonid is narrow anteriorly with shallow antero-internal reentrant and deep antero-external reentrant, but some specimens retain the trifoliate anterior lobe; the development of plications within the external and internal reentrants is variable among individuals, absent in some. The second external fold (colonette) of p3 exceeds the first and third folds buccally, but is not greatly laterally expanded as it is in *O. complicidens*. The P2 has only a single anterior reentrant. Cementum is moderately developed in reentrants.

Differential diagnosis: Size intermediate between *Ochotona lagreli* and the larger species *Ochotonoides complicidens* (Tables 4.1, 4.2). Like *O. complicidens*, *Ochotonoides bohlini* Erbajeva, 1988 is larger than *Ochotonoides teilhardi*. *Ochotonoides primitivus* Zheng and Li, 1982 is smaller and a synonym of *O. lagreli* (Qiu 1987). The mandible of *Ochotonoides teilhardi* resembles that of *O. complicidens* in general morphology and in having a long diastema and high

Table 4.1 Dental comparison of *Ochotonoides teilhardi* sp. nov. with *Ochotonoides complicidens* and *Ochotona lagreli* (mm)

Species	Locality	P2	p3	p3-m3
Ochotonoides teilhardi sp. nov.	YS5	1.27 × ~ 2.35	2.35 × 2.25	10.35
	YS99		2.35 × 2.27	10.24
	YS6		2.30 × 2.15	
Ochotonoides complicidens	Heshui, Gansu		2.25 × 2.05	
	Nihewan		2.25 × 2.05	
	Loc. 18		2.45–2.74 × 2.25–2.65 (n = 4); $\bar{x}$ 2.60 × 2.39	11.1 (n = 1)
	Gongwangling, Lantian	1.25–1.27 × 2.15–2.54 (n = 2)	2.35–2.74 × 2.05–2.45 (n = 18) $\bar{x}$ 2.48 × 2.30	10.2–10.9 (n = 3) $\bar{x}$ 10.5
	Laochihe		2.60 × 2.40	10.8
	Qingyang, Gansu (type)		2.60 × 2.65	10.9
	Chenjiawo, Lantian	1.60 × 2.70	2.70–3.30 × 2.50–2.90 $\bar{x}$ 2.90 × 2.60 (n = 4)	11.66–12.80 $\bar{x}$ 12.23 (n = 2)
	Yulin, Shaanxi	– × 2.70 (?)	3.00 × 2.70	12.15
	Guide, Qinghai		2.70 × 2.00	11.02
Ochotona lagreli	Ertemte (Qiu 1987)	0.75–1.15 × 1.50–2.45 $\bar{x}$ 0.93 × 1.88 (n = 75)	1.50–2.30 × 1.50–2.40 $\bar{x}$ 1.86 × 1.88 (n = 106)	

Table 4.2 Further comparisons of *Ochtonoides teilhardi* sp. nov. with *O. complicidens* from various localities (mm)

Taxon	Specimen No.	Diastema length	p3-m3 length		Dentary ht. at p4	p3 L × W	Locality
			Crown	Alveoli			
Ochotonoides teilhardi	THP14208	8.0	10.46	10.95	10.30	2.30 × 2.15	Malan
	THP14191	–	–	–	–	2.35 × 2.05	Baihai
Ochotonoides complicidens	THP14190	–	11.5	12.15	12.4	2.74 × 2.40	Baihai
	THP14242	10.5	13.12	13.77	13.2	2.93 × 2.25	Gaozhuang
Ochotonoides teilhardi	V11200.1	9.20	10.40	11.50	9.80	2.35 × 2.25	YS5
	V11202.1	~9.20	10.00	11.80	10.30	2.35 × 2.27	YS99
	V11204.1	–	–	–	–	2.30 × 2.15	YS6
Ochotonoides complicidens	CP 110	~9.00	11.10	11.60	10.80	$\bar{x}$ 2.60 × 2.39	Loc. 18
	V3155	–	$\bar{x}$ 12.23	–	11.80	$\bar{x}$ 2.90 × 2.60	Chenjiawo
	C/100	10.90	12.15	13.45	11.90	3.00 × 2.70	Yulin

ratio of mandible diastema length/p3-m3 alveolar length, features differing from *Ochotonoma*. The p3 is not as derived as that of *O. complicidens*, and the latter species has a deeper anterior reentrant plus a shallow lateral groove on P2.

Description: This description emphasizes the type and paratype from YS5, and p3s from YS99 and YS6. The diastema of the mandible of the type specimen, V11200.1, is 9.2 mm long and the ramus is 9.8 mm high beneath the p4. Incisor terminates beneath the p4 lingually. An anterior mental foramen is situated at the posterior margin of the p3, and a posterior mental foramen lies beneath the posterior margin of the m2, both being 3.3 mm from the ventral margin of the ramus. The p3 (Fig. 4.1a) antero-external reentrant is deep while the antero-internal reentrant is a shallow depression. The fold that lies between the antero-external and the external reentrants (equivalent to "la colonette 2" of Boule and Teilhard 1928) extends externally slightly past the fold that is anterior to it and the fold posterior to it ("colonettes 1 et 3"). This fold clearly does not reach the level of the well-developed postero-external lobe (colonette 4). The anterior lobe extends postero-internally to compose a triangle. Plications within the internal reentrant are intense in V11200.1, while on the external reentrant they are slight on the anterior wall. The internal reentrant is nearly perpendicular to the longitudinal axis of this tooth, while the external reentrant extends postero-internally to intersect with this axis at an angle. Cementum is moderately developed.

The Paratype P2 (V 11200.2, Fig. 4.1f) is ovoid with a principle anterior reentrant that extends anterointernal-posteroexternally and divides the tooth into two nearly equal lingual and labial lobes. A lingual reentrant is absent.

The mandible V11200.3, diastema length of 9.6 mm, is large and robust, but p3 is not preserved. The ramus is 10.6 mm high beneath the p4, has p3-m3 alveolar length of 12.3 mm, and is distinctly inflated at the lingual side of the incisor. An anterior mental foramen is located at the anterior p3, and a posterior foramen is located at the posterior margin of the m2, quite unlike specimen V11200.1, and is provisionally regarded to reflect individual variation.

The p3 from the YS99 mandible (V11202.1, Fig. 4.1b) is narrow anteriorly with distinct antero-external and antero-internal reentrants that make it noticeably trifoliate, although the antero-internal reentrant is slightly shallower than the antero-external reentrant. Colonette 2 extends externally slightly beyond colonettes 1 and 3, but does not exceed colonette 4. The antero-internal fold extends postero-internally. Enamel on the internal and external reentrants is smooth, and lacks plications. The major reentrants isolating the trigonid intersect the longitudinal axis of the tooth at an angle. Cementum filling is moderate.

The anterior lobe of the YS6 p3 (V11204.1, Fig. 4.1d) is relatively broader than the anterior part of the posterior lobe of the tooth. The antero-external reentrant is deep while the antero-internal reentrant is rather shallow. Colonette 2 is distinctly externally extended to surpass colonettes 1 and 3 but not the 4th. The antero-internal fold extends internally and the internal reentrant is nearly perpendicular to the longitudinal axis of the tooth, causing its anterior portion to be triangular. The external reentrant intersects the longitudinal axis at an angle.

Comparison and Discussion: The three p3 of *Ochotonoides teilhardi* vary in anterior breadth, depth of antero-internal reentrants, plications on internal and external reentrants, and orientation of internal reentrant. Nevertheless, the character shared among all is the defining character for the genus *Ochotonoides*: colonette 2 surpasses colonettes 1 and 3. The p3 from YS99 (V11202.1) resembles several specimens of *Ochotona lagreli* in being narrow anteriorly, trifoliate in architecture, with colonette 2 very slightly surpassing colonettes 1 and 3. But compared to the majority of specimens, it is rather complex anteriorly. Measurements (Table 4.1) indicate the P2 and p3 specimens to be larger than those of *O. lagreli* from Ertemte (Qiu 1987), although their breadths match the largest values of the range. Morphology and size place these specimens within *Ochotonoides*, but p3 and P2 are not as derived as those of *O. complicidens.*

Ochotonoides complicidens, derived from basal gravels of the Qingyang loess, was initially assigned to the genus *Ochotona* by Boule and Teilhard (1928: 95–96). Compared to the other species within the genus, it is larger and has a p3 with colonette 2 extending past colonettes 1 and 3 and is nearly equivalent to colonette 4. Teilhard and Young (1931: 30–31), upon studying Cenozoic mammal faunas from the North China regions of western Shaanxi, western Shanxi, and Gansu, erected the genus *Ochotonoides* based upon a well preserved right mandible and its closely associated skull collected from the North China locality of Yulin (Loc. 14), Shaanxi Province. This was intended to represent the type specimen for *Ochotonoides complicidens* by Teilhard and Young (1931). However, Boule and Teilhard (1928) had already assigned the Qingyang specimen as the type specimen for that species. Therefore the "type" designated by Teilhard and Young (1931) is not the species name bearer according to the International Commission on Zoological Nomenclature (1999), and the specimen from Qingyang, Gansu, remains the type of *Ochotonoides complicidens*.

Successive discoveries of this taxon occurred during the following decades in Pleistocene faunas of the North China provinces Shanxi, Shaanxi, Gansu, Hebei, and Qinghai. The majority of specimens were fragmentary jaws and isolated teeth with occasional cranial elements. All of the specimens

were assigned to the species *O. complicidens* until Zheng and Li (1982) erected *O. primitivus* from the late Miocene of Tianzhu, Gansu. The latter specimens were later included in *Ochotona lagreli* by Qiu (1987) in his comparison with large samples from Ertemte, Inner Mongolia. Still later the Tianzhu pika was recognized as *Ochotonoma primitiva* by Qiu and Li (2008). In South China, *O. complicidens* was noted for an edentulous mandible from the early Pleistocene of Yuanmou, Yunnan (Lin et al. 1978).

The genus *Ochotonoma* was created by Sen (1998) for Pliocene (MN15) material from Çalta, Turkey. The type species *O. anatolica* is characterized by the following features: small size; p3 anteroconid is triangular in shape but with one internal or two (internal and external) reentrants filled with cement or unfilled (when the reentrant is shallow), and the posteroconid (talonid) occasionally with a deep or shallow intero-reentrant (the "mesoflexid" of Sen); the mandible has a short diastema and thus a low ratio of diastema length/length of p3-m3 alveoli (0.52, in Sen 1998: 372). As we observed, the p3 of *Ochotonoma anatolica* is similar to that of *Ochotonoides teilhardi* sp. nov. in morphology of p3, but it is much smaller and lacks the plication on the internal and external reentrants. We have measured the diastemas and lengths of p3-m3 alveoli for several mandibles of *Ochotonoides teilhardi* and *Ochotonoides complicidens* from different localities of China (Table 4.3). Both species of *Ochotonoides* have higher ratios (0.73–0.84; our Table 4.3) than *Ochotonoma*; thus *Ochotonoides* had a longer snout than *Ochotonoma,* which should be considered a key criterion to distinguish the genera. Further, the *Ochotonoides* p3 has frequent plications on internal and external reentrants whereas the *Ochotonoma* p3 has no plication on the internal and external reentrants. These features confirm the assignment of Yushe *Ochotonoides teilhardi*. As for the late Miocene *Ochotonoma primitiva* from Shengou, Qinghai, it is dimensionally comparable with *Ochotonoides teilhardi*. We distinguish *Ochotonoma primitiva* p3 specimens mainly by the absence of plications on the external and internal reentrants. Development of the "mesoflexid" is not a definitive criterion for *Ochotonoma* because this structure occurs on *Ochotonoides* specimens as well.

To date, Chinese localities that have produced *Ochotonoides complicidens* include Qingyang in Gansu and Nihewan in Hebei (Boule and Teilhard 1928; Teilhard and Piveteau 1930); Yulin (Shaanxi), Xujiaping, Zhongyang (Shanxi), Xiapodi, Daning (Shanxi), Jingle (Shanxi) (Teilhard and Young 1931); CKT Loc. 18 (Huiyu, west of Beijing; Teilhard 1940); Yushe, Shanxi (Teilhard 1942); Chenjiawo, Shaanxi (Chow and Li 1965); Laochihe (Ji 1976); Gongwangling (Hu and Qi 1978); Heshui, Gansu (Zheng 1976); Luochuan, Shaanxi, (Zheng et al. 1985b, c); and Guide, Qinghai (Zheng et al. 1985a); Dali, Shaanxi (Wang 1988), and more recently from Yunxian, Hubei (Liu et al. 1997), Lingtai, Gansu (Zheng and Zhang 2000, 2001; Erbajeva and Zheng 2005). Detailed study is yet lacking to cover the various stratigraphic levels and geographic regions, particularly description of cranial and postcranial remains. Consequently, phylogenetic relationship is poorly understood.

After studying the new Yushe specimens and comparing described as well as undescribed earlier collections from Yushe and presently known material of *O. complicidens* from elsewhere in China (Table 4.2), we make the following preliminary observations.

1. The type specimen of *O. complicidens* comes from Qingyang, Gansu, considered early Pleistocene in age (Table 4.1).

Table 4.3 Comparison of *Ochotonoides* to *Ochotonoma:* ratio of mandible diastema length to p3-m3 alveolar length

Taxon	Locality	Length of mandible diastema	Length of p3-m3 alveoli	Ratio of mandible diastema/p3-m3 alveoli length
Ochotonoides complicidens	Gongwangling	9.2–9.8 (n = 5)	11.4–12.5 (n = 5)	0.78–0.83
	Laochihe	9.3–10.2 (n = 2)	11.4–12.1 (n = 2)	0.82–0.84
	Yulin (C/100)	10.9	13.45	0.81
	Yulin Loc. 14[a]	9	12.3	0.73
	Loc.18 (CP110)	~9.00	11.60	0.78
	Yushe (THP14242)	10.5	13.77	0.76
Ochotonoides teilhardi	YS99 (V11202.1)	~9.2	11.8	0.78
	YS5 (V11200.1)	9.2	11.5	0.80
	Yushe (THP14208)	8.0	10.95	0.73
Ochotonoma anatolica	Anatolia, Turkey[b]	–	–	0.52

[a]After Teilhard and Young (1931)
[b]After Sen (1998)

More specimens derive from the early Pleistocene sites of Gongwangling and Loc. 18. Two P2 and 18 p3 specimens from Gongwangling (Fig. 4.1s, t), and four p3 specimens from Loc. 18 (Fig. 4.1n–q) were studied. The two P2 specimens from Gongwangling are ovoid, possess a single principle anterior reentrant and lack a lingual reentrant. No P2 from Loc.18 being available, Teilhard's descriptions and figures indicate that they are rectangular in occlusal morphology and lack a lingual reentrant. The p3 has a relatively well-developed antero-external reentrant and an antero-internal reentrant that is shallow or absent, the anterior lobe is broad, the lingual side extends postero-internally, and the terminus of the internal reentrant frequently curves anteriorly. The specimen we illustrate from Loc.18 (Fig. 4.1p) is very similar to the type specimen from Qingyang. The other early Pleistocene specimens are from Laochihe, Nihewan and Heshui. The p3 from Heshui and an undescribed p3 from Nihewan (stored at IVPP) resemble the Gongwangling specimens, but are slightly smaller in size (see Table 4.1).

2. *O. complicidens* from the middle Pleistocene Loc.14 of Yulin, Shaanxi, is large with a P2 that has a lingual reentrant in addition to the main anterior reentrant, and a p3 (Fig. 4.1r) that lacks an antero-internal reentrant, has a shallow antero-external reentrant, and its lingual margin of the anterior lobe extends postero-internally. Middle Pleistocene specimens from Chenjiawo (a single P2 and four p3, Fig. 4.1u, v) resemble the specimens from Yulin in size and morphology, and the teeth from these two localities are larger than those from early Pleistocene sites.

3. *Ochotonoides teilhardi* from Yushe is closer to the Nihewan and Heshui specimens in both size and morphology, but differs from these in the narrower anterior lobe of p3, which is variably trifoliate in shape. (There are only p3 specimens from Nihewan and Heshui). The P2 is similar to those of Gongwangling and Loc.18 sites in the absence of lingual reentrant on P2.

4. The single p3 from Guinan, Qinghai (Zheng et al. 1985b) differs from all of the above in that the length of the lingual side of the posterior section greatly exceeds the labial side, and hence may be reassigned as *O. bohlini*.

Comparatively, P2 and p3 specimens from Yushe sites YS5, YS99, and YS6 are smaller. They are distinctly smaller than specimens from Yulin, Shaanxi, and Chenjiawo but fall within the lower region of size variation for those of Gongwangling. Morphologically, they may be regarded as one taxon regardless of several distinctions in the p3. The YS99 p3 is anteriorly trifoliate which resembles several specimens of *O. lagreli* from Ertemte, but none of the specimens from Gongwangling display trifoliate morphology. Consequently, the extreme disparity of *O. complicidens* from the Type locality (Qingyang, Gansu) and those from Gongwangling, Yulin, and Chenjiawo clearly warrants separate species recognition, for which the new species *Ochotonoides teilhardi* applies. The range in age of *Ochotonoides teilhardi* may be recognized as Mazegouan (late Pliocene) to earliest Nihewanian and is arguably a descendent of *O. lagreli* or its close relatives. This now constitutes the most primitive *Ochotonoides* species in China, and is probably ancestral to *O. complicidens*.

It is interesting that the Early Pleistocene specimens of *O. complicidens* from Qingyang, Heshui, Nihewan, Zhoukoudian Loc.18, Gongwangling and Laochihe are smaller than those from the Middle Pleistocene sites, and in turn the Late Pliocene–earliest Pleistocene *Ochotonoides teilhardi* is smaller than the Early Pleistocene *O. complicidens*. In addition, there exist also morphological differences between these three forms from the three different time periods. Possibly, with increased and more detailed study of more material the Middle Pleistocene *Ochotonoides* may be excluded from *O. complicidens* as a new species of this genus. The three morphotypes demonstrate an evolutionary trend. Because the *Ochotonoides teilhardi* from YS6 is distinctly more primitive in smaller size and its trifoliate lobe of p3 than the *Ochotonoides* from Loc.18, the lower Haiyan Formation is considered to predate Loc.18.

In addition to China, *Ochotonoides* is reported from Mongolia, Kazakstan, Siberia, Hungary and Ukraine (Erbajeva 1988, 1994, 1996; Tjutkova 1992; Tjutkova and Kaipova 1996; Kretzoi 1959a, b; Topachevskij and Skorik 1977). Kretzoi described the early Pliocene species *Ochotonoides csarnotanus* from Hungary and Tjutkova (1992) erected a Late Pliocene species *O. progressivus* from Kazakhstan. These two species are close to *O. teilhardi* in size but differ from the latter in morphology. *O. csarnotanus* has a p3 without cement, and the internal reentrant extends backwards and parallels the longitudinal axis of the tooth. The p3 anterior lobe of *O. progressivus* is small, short rhomboid-shaped with only antero-external reentrant. *O. kujalnikensis* from early Villafranchian of the Odessa Black Sea area is however obviously smaller than *O. teilhardi* and with different p3 pattern. Erbajeva (1988) erected *O. bohlini* based on specimens recovered at Kirghizia in the former USSR and further reassigned two p3 recovered from Olan-Chorea, Inner Mongolia (Bohlin 1942: Fig. 14) to this species. It differs from both *O. complicidens* and *O. teilhardi* in that the p3 postero-internal length (the lingual length of the posterior section of p3) greatly exceeds its labial length.

Ochotonoides complicidens (Boule and Teilhard, 1928)

Holotype: mandible from Qingyang, Gansu Province.

Referred material: unpublished mandibular and cranial fragments in the collections of IVPP, the Tianjin Museum of Natural History (Table 4.2), and from AMNH.

Twelve mandibles, all preserving their p3, are housed at the Tianjin Museum of Natural History, 15 mandibles (five

bearing p3) are housed at IVPP, and a skull with mandibles studied by Teilhard (1942) bearing P2 and p3 derive from different stratigraphic positions. The Frick AMNH collection contains two specimens (F:AM 116224-5), likely from loess overlying the Yushe Group, and a skull and mandible (F:AM 116228) from loess in the "Tsao Chuang" area; all are assignable to *O. complicidens* (Flynn 2011). There is relatively large variation in p3 size and morphology, and among these specimens, some may be assigned to *O. teilhardi* while others can be identified as *O. complicidens.* We have examined most of this material, which generally lacks precise provenance data. *Ochotonoides* specimens that are relatively smaller with anteriorly trifoliate premolars are assigned to *O. teilhardi*; *Ochotonoides* that are relatively large with a broad p3 anterior section and lacking antero-internal reentrants are assigned as *O. complicidens*.

Ochotona Link, 1795

Ochotona lagreli Schlosser, 1924

Material by locality, stratigraphic unit:

YS39c: Anterior half skull with I2-I3, and left and right dentitions (nasals and cranium posterior to the M2 are absent), Nanzhuanggou Member, Gaozhuang Fm. (V11208.1).

YS161: Two posterior right mandibles, one with p4-m3 and one with m2-m3 lacking the ascending rami and angular processes; fragmentary left mandible with the m2 and partial m1; right anterior portion of mandible with p3-p4 alveolae, all Gaozhuang Fm. (V11209.1-4).

YS115: A right posterior mandible with m2-m3 lacking the ascending ramus and with incomplete angular process from the Taoyang Member, Gaozhuang Fm. (V11210).

YS60: A right fragmentary mandible bearing the m1 and a right fragmentary mandible with damaged m1-m3 from the Taoyang Member, Gaozhuang Fm. (V11211.1-2).

YS32: A right P4, Mahui Fm. (V11212).

YS11: A damaged left maxilla with P4-M1, Mahui Fm. (V11213).

YS169: Left jaw fragment with talonids of m1 and m2, and with m3, Mahui Fm. (V11214).

YS156: A right P4/M1, Mahui Fm. (V11215).

YS150: Isolated left P2, isolated right P3, right P4/M1, Mahui Fm. (V11216.1-3).

YS139: Left mandible with p4-m2 and right p4/m1, Mahui Fm. (V11217.1-2).

Stratigraphic Range: Late Miocene Mahui Formation through the early Pliocene Gaozhuang Formation.

Skull Description: The morphology and size of mandibular and dental specimens are consistent with previous descriptions of *Ochotona lagreli*. Most notable is the Yushe Basin specimen V11208.1 from YS39c, the most precisely documented skull of the species (Fig. 4.2; Table 4.4).

V11208.1 preserves the anterior portion of the skull and complete dentition. Nasals and cranium posterior to the M2 are missing while that remaining portion has undergone lateral compression distortion such that the palate overlaps itself. From a dorsal perspective the rostrum is short and broad. It may be determined from the naso-premaxilla suture that the greatest breadth of nasals was approximately 7 mm, while posteriorly they constrict to 5 mm. Distinct parallel supraorbital crests are 1 mm thick. The interorbital region is distinctly concave and is 5.2 mm wide at its narrowest. At the zygomatic arch the skull is approximately 24 mm wide.

From a ventral perspective the diastema is approximately 14 mm long. The premaxilla-maxilla suture is 3.2 mm anterior to P2 where the rostrum is 9.4 mm broad. The incisive and palatal foramina are confluent and pear-shaped (14.6 mm long, at least 6 mm wide posteriorly). Its posterior margin is at the level of the anterior margin of the P4. Anteriorly, at the premaxilla-maxilla suture, this foramen is slightly constricted. The vomer divides the foramen at the middle and extends beyond the premaxilla-maxilla suture, but its terminus is indeterminable. The anterior margin of the choana lies probably between the P4 and M1 with parallel lateral walls posteriorly. A premolar foramen lies opposite the hypostria of P4. The maxillary process is situated at the level between P3 and P4. At the same level is the triangular maxillary-masseteric tubercle with a distinct depression on it. The left and right tubercles differ in size with the left being 3.9 mm long and 2.2 mm wide, while the right one is 6 mm long and 2.7 mm wide.

In lateral view the maxilla possesses a triangular fenestra (infraorbital foramen) bounded dorsally by the nasal process of frontal. The fenestral surface inclines ventrolaterally, and its posterodorsal angle approaches 90°. It seems that another smaller triangular fenestra is located ventral to the infraorbital foramen, dorsal to the P2. The anterior end of the nasal process of the frontal is linked to the dorsal end of the maxilla-premaxilla suture. A masseteric fossa laterally on the zygomatic process of the maxilla is well developed and circular in lateral perspective, 6.5 mm in diameter.

P2-M2 is 9 mm long and alveolar length is 10.4 mm, with dental measurements all falling within the range of variation for *Ochotona lagreli* (Table 4.4). There is slight morphological discrepancy between the left and right P2 as the right displays a single principle anterior reentrant that divides the tooth into a lingual and labial lobe. The left P2, however, possesses a second distinct reentrant (antero-external reentrant) that lies parallel and lateral to it, and is approximately half the length of the principle reentrant.

Locality YS39c is early Pliocene and lies at the base of the Nanzhuanggou Member of the Gaozhuang Formation (see Fig. 1.7). Diverse fossil species of *Ochotona* from North China include Late Miocene to Early Pliocene *O. largreli*

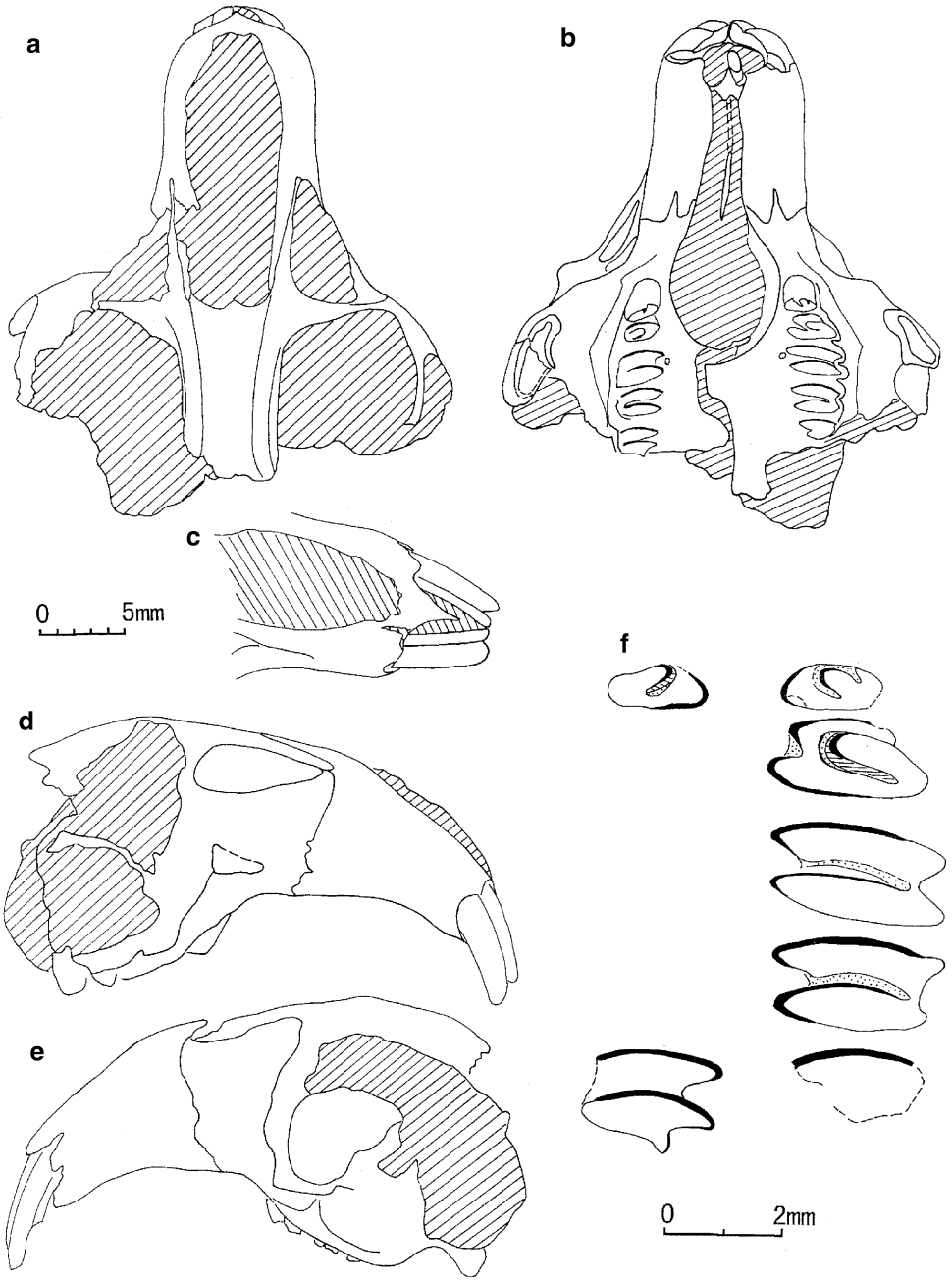

Fig. 4.2 *Ochotona lagreli* from YS39c, Gaozhuang Fm., anterior part of a skull with upper dentition (V11208.1). **a** dorsal aspect, **b** ventral aspect, **c** dorsal aspect of premaxilla with incisors, **d**, **e** Lateral (right and left) aspects of V11208.1; **f** upper dentition showing left P2-M1, partial M2, and right P2 and M2, separate scale

and *O. minor* from many localities, the Late Miocene Tibetan *O. guizhongensis,* and the early Pleistocene *O. nihewanica* Qiu, 1985 from Nihewan. The YS39c specimen is distinctly larger than *O. minor,* and differs from *O. nihewanica* in its larger size, developed supraorbital crests, concave interorbital region, longer rostrum, and larger maxillary-masseteric tubercle. Dentally *O. nihewanica* differs in its rectangular P2 possessing a shallow and broad antero-internal reentrant and its P3 with two lingually reduced lobes. *O. gizhongensis* is a relatively poorly preserved specimen consisting of fragmentary maxillae with cheek tooth row falling completely within the size range of *O. lagreli* (Ji et al. 1980), but obviously larger than V 11208. 1, and the posterior margin of the incisive and palatal foramina is more anteriorly situated than on the YS39c skull. A single maxilla of *O. lagreli* from Ertemte, Inner Mongolia, is consistent with the YS39c specimen in the morphology of the maxillary-masseteric tubercle, with an anteroposterior

Table 4.4 Measurements (mm) for *Ochotona* species from Yushe Basin: lower teeth with length × width of trigonid, width of talonid; upper cheek teeth below (length × width)

Species		p3	p4	m1	m2	m3
Ochotona lagreli	Ertemte (after Qiu 1987)	1.5–2.3 × 1.5–2.4 (n = 106)	1.60–2.25 × 1.60–2.40, 1.50–2.50 (n = 144)*			0.65–0.9 × 1.3–1.7 (n = 15)
	YS39c					
	YS161		1.96 × 1.96, 2.05	1.86 × 2.00, 2.15	1.76–1.95 × 2.05–2.15, 1.96–2.15	0.78 × 1.47–1.57
	YS115				2.05 × 2.05, 1.96	0.88 × 1.96, 1.56
	YS60		2.05 × 1.96, 2.05			
	YS32					
	YS11					
	YS169					0.78 × 1.37
	YS156					
	YS150					
	YS139		1.96 × 2.17, 2.25	1.96 × 2.26		
O. cf. lagreli YS36		1.37 × 1.42	1.47 × 1.76	1.50 × 1.76, ~ 1.66	1.56 × ~ 1.66, 1.65	0.68 × >1.27
O. cf. lagreli YS39				1.50 × 1.56, 1.50	1.42 × 1.50, 1.42	0.60 × 1.22
O. nihewanica? YS110b			1.29 × 1.39, 1.48	1.37 × 1.56, 1.56	1.37 × 1.52, 1.45	0.59 × 1.02
Ochotona sp. 4 YS39b		1.56 × 1.83	1.86 × 1.91, 2.00	1.85 × 2.15, 2.05	1.90 × 2.05, 1.95	0.88 × 1.42

		P2	P3	P4	M1	M2
Ochotona lagreli	Ertemte (Qiu 1987)	0.75–1.15 × 1.5–2.45 (n = 75)	1.2–1.8 × 2.15–3.4 (n = 104)	1.20–2.10 × 2.20–3.72 (n = 196)		1.35–2.30 × 2.2–3.4 (n = 105)
	YS39c	L 0.88 × 1.86 R 0.85 × 1.81	1.37 × 3.02	1.66 × 3.33	1.61 × 3.13	R 1.86 × 2.54
	YS32			1.91 × 3.33		
	YS11			1.96 × ~ 3.13		
	YS156			1.66 × 2.93		
	YS150	0.78 × 1.37	1.18 × 2.15	1.42 × 2.54		

* measurements are observed dimensions for all p4, m1, m2 from Ertemte: lengths × widths of trigonid; widths of talonid

length of 3.8 mm, and as such specimen V11208.1 is assigned to this species. However, on the Ertemte specimen, the premolar foramen lies between the P3 and P4. The presence of an antero-external reentrant on P2 of this specimen may represent individual variation.

Discussion: Teilhard (1942: 88–89, Figs. 55–56) described four skulls from the "red clay" (which differ widely in morphology and lack exact locality information). He distinguished "Type A" (*Ochotona (Pika) alpina*), and "Type B" (*Ochotona (Ochotona) daurica*) on the basis of supraorbital crest development, depression of interorbital region, and constriction of the incisive-palatal foramina at the level of premaxilla-maxilla suture. These specimens require a thorough reassessment. The YS39c specimen is distinct from the aforementioned in its concave interorbital region and development of the supraorbital crests, in the condition of incisive and palatal foramina, and the trace of the premaxilla-maxilla suture.

When Erbajeva and Zheng (2005) reviewed all ochotonids from the late Miocene to Pleistocene of North China, they established six new species of *Ochotona*: *O. plicodenta*, *O. magna*, *O. lingtaica*, *O. gracilis*, *O. youngi* and *O. zhangi*. We can distinguish them from *O. lagreli* simply by p3 morphology: p3s of *O. plicodenta*, *O. magna*, *O. lingtaica* and *O. youngi* have their internal reentrant much deeper than the external reentrant; *O. gracilis* is characterized by the p3 rhomboid anteroconid, the four sides being almost equal; and *O. zhangi* differs from *O. lagreli* in the rectangular anteroconid of p3. Erbajeva et al. (2006) added three new *Ochotona, O. tedfordi, O. chowmincheni,* and *O. gudrunae*, based on old material collected from China in the 1930s and stored in the Frick collection of the American Museum of Natural History. The YS39c skull (V11208.1) is most similar to *Ochotona tedfordi* in upper cheek tooth morphology and size, especially the presence of an anterior-external reentrant on P2. However,

it differs from the latter in having developed supraorbital crests and more concave interorbital region, wider rostrum, larger triangular infraorbital foramen, convexity of the skull at the frontal instead of at the frontal-parietal suture. Whether V11208.1 should be assigned to *O. tedfordi* or *O. tedfordi* is a junior synonym requires further study. The fragmentary Yushe material limits further detailed comparisons.

Ochotona cf. *O. lagreli* Schlosser, 1924

Material by locality, and stratigraphic position: YS36: anterior left mandible with i2, p3, and p4 trigonid (V11218.1; Fig. 4.3b); mid-portion of a left mandible with p4-m3 and a small portion of its ascending ramus (V11218.2) both from the Nanzhuanggou Member of the Gaozhuang Fm. YS159: right posterior mandible with m1-m3 (V11221) from the Mahui Fm.

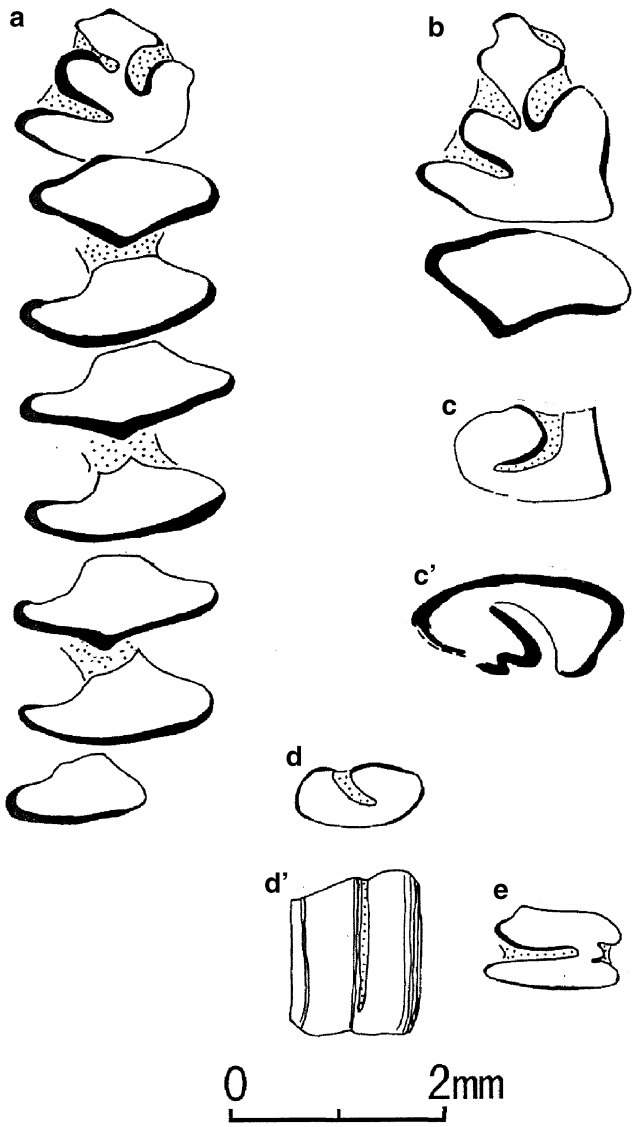

Fig. 4.3 *Ochotona* species from various localities of Yushe Basin. **a** *Ochotona* sp. 4 from YS39b, left p3-m3 (V11242), anterior upward; **b** *Ochotona* cf. *O. lagreli* from YS36, left p3 and partial p4 (V11218.1); **c**, **c′** *Ochotona* sp. 3 from YS99, juvenile right P2, occlusal view and view from root (V11206.1); **d**, **d′** *Ochotona* sp. 1, juvenile left P2 (occlusal and anterior views) (V11220.1) from YS 97; **e** *Ochotona* sp. 1, right M2 (V11220.2) from YS97

Description: These three mandibles are distinct in small size. V11218.1 has a diastema of 4.3 mm; labially the mandible is 4.0 mm deep beneath the p3, and lingually the mandible is 5.3 mm deep beneath the p4. Four nutrient foramina are present labially. V11218.2 and V11221 are slightly smaller than *O. lagreli* but slightly larger than *O. nihewanica* (measurements in Table 4.4). The p3 on V11218.1 resembles the Type for *O. lagreli*, but it is smaller than the lowest values in the range of variation, larger than *O. minor,* and approaching *O. nihewanica* in size. These specimens are provisionally assigned to *O. lagreli*.

Ochotona cf. *O. nihewanica* Qiu, 1985

Material by locality: YS110b: posterior left mandible with p4-m3 (V11219). YS108: right posterior portion of mandible with the alveoli of m1-m3 (V11241). Both lack the ascending ramus and angular process and are from the Haiyan Fm.

Description: Both mandibles are extremely small (Table 4.4), with size between *O. lagreli* and *O. minor.* At present the range of variation for lower teeth of *O. minor* is unknown as the only comparable specimen is the Type. Hence, the two Yushe specimens are assigned provisionally to *O. nihewanica* partly due to their stratigraphic occurrence in the Haiyan Fm.

Other *Ochotona* morphotypes

Ochotona sp. 1 (V11220.1-2) occurs at YS97 from the Culiugou Member, Gaozhuang Fm., and is represented by a juvenile left P2 and right M2 (Fig. 4.3d, e). The two teeth are extremely small, even smaller than *O. minor* (P2: 0.64 × 1.27 mm, 1.71 mm high; M2: 0.88 × 1.37, 1.47 mm, 2.44 mm high, and an embryonic posterior process on its posterior lobe). Identification is difficult due to the early ontogenetic condition.

Ochotona sp. 2 (V11205) from YS116 is represented by an anterior left premaxilla with I2 and I3 from the Haiyan Fm. Measurements are 1.9 (medial-distal length) × 1.2 (anter-posterior diameter) mm and 0.49 × 0.91 mm, respectively. Also YS107, Haiyan Fm. (V11207), damaged right mandible with m1-m3 (m1: 1.96 × 2.22, 2.10 mm; m2: 2.00 × 2.14, 2.01; m3: 0.88 × 1.37; *O. lagreli* size) lacking the ascending ramus and angular process.

Ochotona sp. 3 (V 11206.1-3) from YS99 is represented by a right P2, a left P4/M1 and a fragmentary left M2 from Mazegou Fm. These low-crowned teeth are very small, and belong to a juvenile individual (Fig. 4.3c, c′).

Ochotona sp. 4 (V11242.2) (Fig. 4.3a; Table 4.4) from the base of the Nanzhuanggou Member, Gaozhuang Fm. at YS39b is a mandible with i2 and p3-m3 but lacking ascending ramus and angular process. The specimen is barely fossilized and encased in loose sand, such that there is a possibility that it was derived from the overlying loess. The diastema is 6.5 mm, depth of mandible is 7.8 mm lingually at p4. Small nutrient foramina lie labially ventral to the p3 and a posterior mental foramen is at the midlevel of the mandible beneath the posterior margin of the m3. Incisor terminates approximately at the posterior margin of the p4. The p3-m3 crown length is 8.26 mm. Dental measurements fall within the range of variation for *O. lagreli* from Ertemte, Inner Mongolia, but the anterior lobe of p3 is extremely short and broad, and the internal reentrant extends parallel to the long axis of the tooth and extends posteriorly beyond the posterior end of the external reentrant. This differs greatly from the Ertemte sample but these features occur in the larger extant *O. daurica*, which today occurs in Shanxi Province.

The shape of the p3 resembles that of *Ochotona youngi* Erbajeva and Zheng (2005), especially the anteroconid and its oblique dentine bridge to the posteroconid, but V11242.2 is much larger than *O. youngi*, surpassing the maximum value for p3 of the latter. *O. youngi* is early to middle Pleistocene in age at Danangou, Yuxian County, Hebei Province.

4.2.2 Leporidae Gray, 1821

Alilepus Dice, 1931

Alilepus annectens (Schlosser, 1924)

Referred material by locality, stratigraphic position: Mahui Fm. of the Tancun Subbasin.

YS156 (V11222.1-3), incomplete p3, a right M2, and a fragmentary left maxilla with P3-M2, M3 alveolus, zygomatic masseter tuberosity, and palatal bridge; YS159 (V11223.1-2), right p3 and right P3; YS167 (V11230), pair of mandibles united by the symphysis but lacking incisors, ascending rami, and angular processes; YS139 (V11240), juvenile left P3.

From the Yuncu Subbasin: YS23 (Mahui Fm., V11229), right P4 or M1; YS115 (Taoyang Member, Gaozhuang Fm., V11231), left P3.

Age range: Late Miocene about 6.5 to 5.4 Ma.

Description: The right p3 from YS156 (V11222.1, Fig. 4.4c) is damaged, but displays a broad antero-external reentrant and a postero-external and postero-internal reentrant; the antero-internal reentrant is absent low on the preserved part of the crown. The postero-external reentrant is distinctly deeper than the postero-internal reentrant with a wide dentine bridge separating the two. Its measurements are approximately 2.54 × 2.45 mm. On the right M2 of V11222.2 (Fig. 4.4b) the hypostria is slightly less than two-thirds the breadth of the tooth and lacks enamel plication on the anterior and posterior walls.

The left maxilla (V11222.3, Fig. 4.4a) has a P3 that has been severed halfway up the tooth but its crosssection is distinct. Seven plications lie on the anterior wall of the hypostria but the posterior wall is flat and smooth with the exception of a single labial plication. Plications on the anterior and posterior walls of the P4 hypostria are slightly more intense than on the P3. The hypostria is slightly deeper than one-half the crown breadth. The palatal process of maxilla is distinctly longer than the palatine, distinct posterior palatine foramen lies on the maxillary palatal process-palatine suture. The zygomatic masseter tuberosity is well developed. In ventral view its antero-posterior length is 10 mm and posterior breadth is 3.4 mm. A deep masseteric fossa of the zygomatic arch contains numerous nutrient foramina. The dorsal and ventral crests of this fossa are smooth and rounded. Dental measurements lie within the range of variation for *A. annectens* from Ertemte, Inner Mongolia, with values of P3: 2.25 × 4.3 mm (at cross-section), P4: ~2.25 × 3.91 mm, M1: 2.25 × 3.91 mm, and M2: 2.2 × 3.2 mm. As these three specimens come from the same locality, they are likely conspecific.

Stratigraphically lower than YS156, YS159 (Fig. 4.4d, e) produced a right p3 (V11223.1: 3.13 × 2.66, 3.05 mm) that is typical for *Alilepus* in its postero-external reentrant that is slightly deeper and slightly more posterior than the postero-internal reentrant. This locality also yielded a right P3 (V11223.2: 2.4 × 3.82, 4.70 mm) with a hypostria slightly deeper than one half the tooth breadth, and plications present on both anterior and posterior walls. Their measurements fall within the range of variation for *A. annectens* from Ertemte, Inner Mongolia.

YS167, stratigraphically below YS156, produced a pair of mandibles (V11230) lacking their p3; the remaining dentition is seriously damaged, prohibiting measurements. The diastema length is approximately 16 mm, mandible height on the labial side of p3 is approximately 11 mm, and 12 mm at the p4. The flat symphyseal surface is broad. A mental foramen is located labially slightly beneath the diastema surface and is approximately 4.5 mm anterolabial to the p3. Breadth of the mandibles at the level of mental foramina is 12.8 mm. Labially, there are several small nutrient foramina. Size and morphology are close to "*Lepus annectens*" from Ertemte as described by Schlosser (1924: Pl. III, Fig. 12), but specimen V11230 has lost the posterior part of the ramus and therefore it is impossible to comment on this region. The single *Alilepus* jaw from Ertemte is an anterior fragment (Qiu 1987).

A P3 from YS139 is a juvenile (Fig. 4.4h; V11240, 1.56 × 2.54, 3.23 mm) with a hypostria that is slightly less than one-half the breadth of the tooth, enamel walls are unplicated, and an enamel islet lies opposite the labial side of the hypostria. The P3 from YS115 is large (2.05 × 3.18, 4.68 mm), the length of the hypostria exceeds one-half the

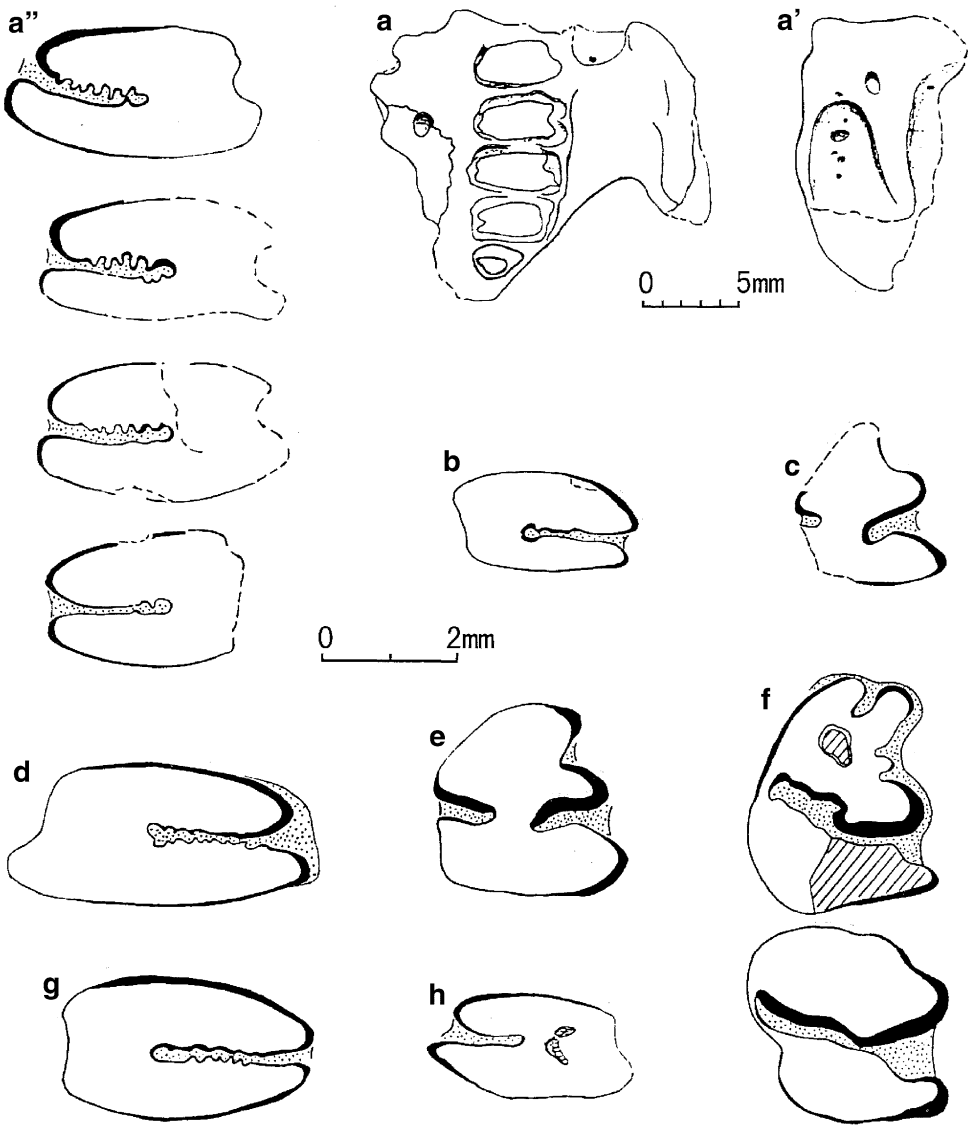

Fig. 4.4 *Alilepus annectens* from Yushe Basin. **a** fragmentary left maxilla from YS156 (V11222.3), showing (**a**) ventral and (**a′**) lateral aspects of the maxilla, and (**a″**) the occlusal view of P3-M2; **b** right M2 from YS156 (V11222.2); **c** fragmentary right p3 from YS156 (V11222.1); **d** right P3 from YS159 (V11223.2); **e** right p3 from YS159 (V11223.1); **f** cf. *Nekrolagus* sp. from QY-87: p3-4 from a right lower jaw (V11238); **g** right P4/M1 from YS23 (V11229); **h** left P3 (juvenile) from YS139 (V11240). Note two scale bars; anterior is upward

width of the tooth but the plications on the anterior and posterior walls are not as complex as seen in *Trischizolagus*. Measurements fall within the range of variation for *Alilepus annectens* from Ertemte.

The anterior and posterior lobes of V11229 (P4 or M1 from YS23), are nearly equivalent in breadth (2.25 × 3.81, 3.86 mm) with a hypostria more than one-half the breadth of the tooth (Fig. 4.4g). Plications occur on the anterior and posterior walls of this reentrant but are not nearly as strong as on *Trischizolagus* from YS50 (discussed below).

Discussion: *Alilepus annectens* was named for a collection from the latest Miocene Ertemte locality, Inner Mongolia. Without doubt the specimens from YS156 and YS159 represent *Alilepus annectens*. At 6.0 Ma, this record may antedate Ertemte. The specimens from the four other localities extend the range of the species in Yushe Basin from about 6.3 to 5.3 Ma. Further documentation (more fossils) will clarify the total residence time in Yushe Basin. The Yushe specimen described by Teilhard (1942, Fig. 52) was not relocated for evaluation. At present, *Alilepus annectens* appears to be a characteristic form of the Mahui Formation and continues into the base of the Gaozhuang Formation.

Alilepus parvus sp. nov.

Type: F:AM 116221 (specimen in the Frick Collection of AMNH). Nodule of hard matrix containing most of the skull

Fig. 4.5 *Alilepus parvus* sp. nov. Skull of type specimen F:AM 116221, from Tancun village of the Tancun Subbasin (Late Miocene, Mahui Fm), left half of mandible removed. Left lateral view above, ventral view below. Scales are 5 mm

(minus occiput and basicranium) and the mandible, only known specimen (Figs. 4.5, 4.6, Table 4.5).

Type locality, stratigraphic position: Tancun village, Late Miocene Mahui Formation of the Tancun Subbasin. There is no paleomagnetic section in the vicinity of the village, but being well below the top of the formation, 6 to 6.5 Ma is the estimated age.

Etymology: *parvus*, from the Latin for little.

Diagnosis: Small size, length of skull from parietals to nasals, 46.4 mm, and the dentition is the smallest of any known species of *Alilepus*. P2 shows a single arcuate, central anterior reentrant. Lower p3 trigonid unelongated, with broad, shallow anteroexternal reentrant, semicircular in crosssection with smooth enamel; central connection between trigonid and talonid is broad, and posterior internal and external reentrants are nearly equally deep. P3-M2 have slightly crenulated enamel in the lingual reentrants (hypostria), p4-m2 without crenulation.

Differential diagnosis: *Alilepus parvus* is smaller than North American *Alilepus*, including the small Pliocene *Alilepus wilsoni* White, 1991, which has p3 average size 2.6 × 2.3 mm, and does not overlap *A. parvus* in size. Single p3 of genotypic species *Alilepus annectens* (Schlosser, 1924) increase in size toward the base (Qiu 1987), meaning that an old individual measured at the occlusal surface appears to be larger in size than a young individual. The smallest teeth of *A. annectens* are larger than F:AM 116221. Like *A. annectens*, *A. parvus* has simple reentrants in p3, the posteroexternal being only somewhat deeper than the posterointernal reentrant, and the trigonid-talonid bridge being strong; *A. longisinuosus* Qiu and Han, 1986 has a weak to absent bridge. *A. laskarewi* Khomenko, 1914 is like *A. parvus* in its relatively large trigonid, but is much bigger in absolute size. *A. elongatus* Winkler et al., 2011, like *A. lii* Jin, 2004, both larger than *A. parvus*, differ also in crenulation of enamel in the main reentrants of lower cheek teeth. *A. meini* Angelone and Rook, 2011 has deep, distally recurved posteroexternal and posterointernal reentrants that yield a relatively short p3 talonid. Other European species of *Alilepus* are all significantly larger than *A. parvus*.

Description: F:AM 116221 (Fig. 4.5) preserves the mandible and most of the skull of a young adult (it has an adult dentition, but the lower incisor increases posteriorly very slightly in width, indicating youth). The posterior part of the skull (interparietal, occipitals to basioccipital, and bullae) is lost. Overall, this skull represents a small leporid, the skull not antero-posteriorly elongated as is *Lepus*, or deepened dorsoventrally. Length from parietals to nasal tips is 46.4 mm (49.3 to face of the procumbent incisor); breadth at zygomatic arches, 32.6 mm; dorsal height from M1 to skull roof, 19.3 mm; upper diastema is 14.8 mm long.

The frontals are gently convex (not flat or concave). The fenestration of maxillae is well developed. Cheek tooth capsules are not as greatly developed, so the maxilla is not as expanded dorsally as in *Lepus*. Zygoma is rooted opposite to P3-P4, not extended posteriorly to M1. The palate reaches posteriorly to the anterior wall of M2.

The upper incisor (breadth × antero-posterior length, 1.95 × 1.30) bears a broad V-shaped longitudinal groove medial to its midline (Fig. 4.5). Enamel is rounded on both sides of the groove, more strongly medially, but wrapping half way around the lateral side. The lower incisor (2.05 × 2.10 mm) is roughly triangular in cross section, with a flat medial side and flattened ventrolateral enamel face; the dorsolateral side is rounded. Enamel barely wraps around lateral and medial corners. The lower incisor is rooted anterior to the p3 root, not extending below the premolars.

The upper cheek tooth row is 8.8 mm long at the occlusal surface; the lower cheek tooth row is 9.0 mm (dental rows flare out toward the roots). P2 has a single arcuate anterior reentrant filled with cementum; it is deep, extending half way into the tooth (Fig. 4.6). P3-4, M1-2 have a generous amount of cementum lingually. Lingual reentrants (hypostriae) cross the tooth half way, and the thin reentrant enamel is only gently wrinkled.

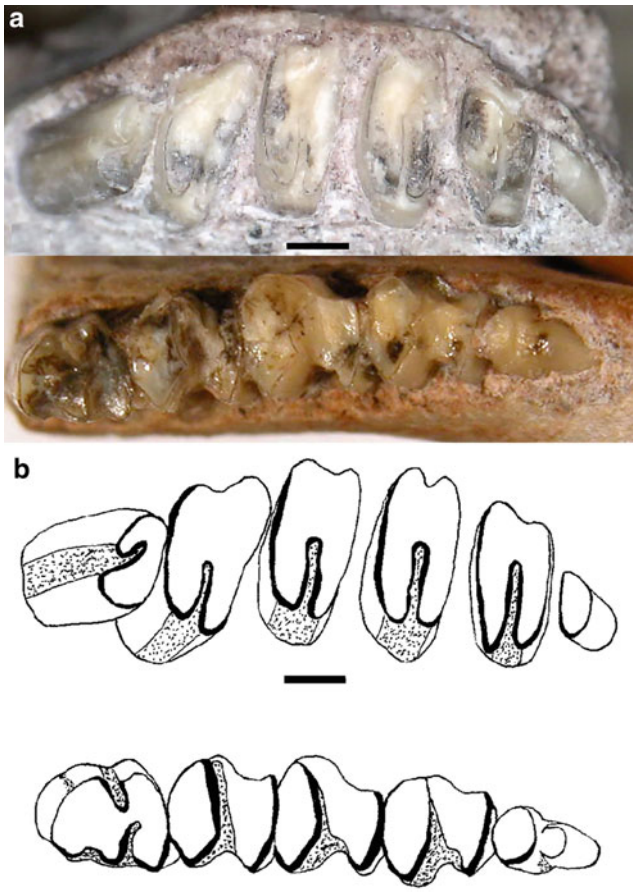

Fig. 4.6 *Alilepus parvus* sp. nov. Dentition of type specimen F:AM 116221, left P2-4 M1-3 and left p3-4 m1-3. a, photograph of specimen, b, interpretive line drawings, anterior to left for both. Upper dentition above, and lower dentition below for both a and b. Scales are 1 mm

Table 4.5 Cheek tooth dimensions (mm) for Yushe Basin *Alilepus parvus* sp. nov. (F:AM 116221)

Left dentition			
P2	1.20 × 1.85		
P3	1.65 × 3.05	p3	2.25 × 1.75, 1.8[a]
P4	1.70 × 2.95	p4	1.80 × 2.0, 2.2
M1	1.65 × 3.05	m1	1.95 × 2.05, 1.6
M2	1.50 × 2.55	m2	1.90 × 1.80, 1.55
M3	0.75 × 1.05	m3	1.40 × 1.20

[a]p3 measured midshaft; third measurement is talonid width

Dentary depth below m1 is 8.4 mm. Its p3 is only slightly longer than wide, with short anteroexternal reentrant, no anterior reentrant, and a gentle anterointernal sulcus. Its dimensions increase slightly toward the base of the tooth, so measurements (Table 4.5) are taken along the shaft, rather than at the crown surface. There is a broad central connection between trigonid and talonid; posterior internal and external reentrants about equal, the posteroexternal reentrant being somewhat deeper and extending slightly more posteriorly. The p3 enamel is not wrinkled. Cementum is developed in the anteroexternal reentrant, heavy in posterior internal and external reentrants. Heavy cementum fills buccal reentrants on molariform teeth (slight on m3). The m1-2 talonids are much narrower than trigonids and pinched buccally; m3 with two collonettes. The trigonids of p4, m1, and m2 are diamond-shaped. Lower molars (Fig. 4.6) are lightly worn and the enamel is not breached on the lingual sides of the trigonids; on m3 it is worn only on the trigonid.

Discussion: This unique skull, part of the Frick Collection in the American Museum of Natural History, was collected in 1935 by Quan-Bao Gan, given a field number (B-674) and recorded as coming from "T'a Tsun". Today we know this as the town Tancun which, located near the local stream (Fig. 1.2c), would have been a general depot for fossils found in the surrounding exposures. Consequently, provenance is not precise but the nearest measured sections indicate that the local rock is equivalent to the Mahui Formation, probably 6–6.5 Ma.

This specimen is distinctive. The structure of the p3 is simple, as in *Alilepus annectens*, and there is very little wrinkling of the enamel. The specimen is small in size, no other Asian *Alilepus* being even close to it. For example, the p3 dimensions of 2.25 × 1.80 mm are well below the smallest of any species tabulated by Angelone and Rook (2011) or Winkler et al. (2011). Skull structure is modern leporine. The age of this small species, is approximately two million years younger than the introduction of *Alilepus*-like leporines into the Old World from North America (Flynn et al. 2014). There is no indication that it represents a separate dispersal from North America, and in the absence of other evidence, we presume that *Alilpus parvus* evolved small size in eastern Asia from immigrant *Alilepus* stock.

Hypolagus Dice, 1917

Two species of *Hypolagus* have been recognized in the Late Neogene of China. Teilhard (1940) based *Hypolagus schreuderi* on fossils from Locality 18, west of Beijing. Earlier C.C. Young (1927) had described *Caprolagus brachypus* from Huiyu, approximately 10 km north of Sanjiadian, near Beijing (noted as Loc. 60, actually the same site as Loc. 18). Schreuder (1937), studied leporids from Shouyang, and declared Young's species as representing *Hypolagus* based upon p3 morphology (Young 1935: Fig. 2). Notably, Bohlin (1942) reevaluated *H. brachypus* specimens from Huiyu, published detailed illustrations of the specimens, and asserted that they were more appropriately assigned to the genus *Alilepus* instead of *Hypolagus*. Some subsequent researchers concurred (Gureev 1964: 124; Qiu

1987: 383). Over the past several decades, a number of specimens from various localities of China have been considered related to *Hypolagus brachypus* including Yushe *H.* cf. *brachypus* (Teilhard 1942), "*C. brachypus*" from Loc. 22, Shouyang (Young 1935) and Loc. 2, Gaojiaya of Jingle (Teilhard and Young 1931), *H. brachypus* from Heshui of Gansu (Zheng 1976), "*Caprolagus* cf. *brachypus*" from Jinniushan of Liaoning (Zhang 1993), *H.* cf. *brachypus* from the East and West Caves of Taipingshan near Zhoukoudian, Beijing (Cheng et al. 1996), and "*Alilepus brachypus*" from Sunjiashan of Zibo, Shandong (Zheng et al. 1997). The Pliocene Yangyuan mandible described by Cai (1989) is not *H. schreuderi* because of its short diastema.

Averianov (1996) restudied the material of *Caprolagus brachypus* described by C.C. Young, recognizing distinctive features, and established new genus *Sericolagus* for this species. In parallel research on fossils from Ningyang, Shandong, and by thorough comparison of available specimens of "*Caprolagus*" *brachypus*, Zhang (2001) systematically excluded the species from *Caprolagus*, *Hypolagus*, *Alilepus* and *Pratilepus*, specifying distinctive features, and creating the new genus name *Brevilagus*. The consensus is that *Brevilagus* Zhang (2001) is a junior synonym of *Sericolagus* Averianov, 1996.

At the turn of the new century for the Late Neogene of China only *Hypolagus schreuderi* was accepted as a member of that genus. Within a few years, however, *Hypolagus fanchangensis* was found in the early Pleistocene of Fanchang, Anhui (Jin and Xu 2009). Here we add a third species for China.

For our study of new material from Yushe, we reviewed the specimens of *H.* cf. *brachypus* described by Teilhard (1942), including 12 mandibles housed at the Tianjin Museum of Natural History, and three mandibles at IVPP illustrated by Teilhard. There was also a skull with mandibles that had suffered compressional distortion and breakage, but the Yushe cranium was not relocated, so the following comparisons are restricted to mandibles. All had been conferred as *Hypolagus* cf. *H. brachypus* due to smaller size than seen in *H. schreuderi* from Loc. 18.

Careful analysis of all mandibles and teeth shows that the Yushe leporids (including new material) encompass four morphotypes that differ distinctly and correspond to a new species of *Hypolagus* described here, the morphologically different *Hypolagus* sp., a third fossil of uncertain generic allocation, and *Sericolagus yushecus,* sp. nov., defined below. Comparisons indicate that all are distinguishable from *Caprolagus brachypus* Young (1927). No *C. brachypus* occurs in Yushe Basin. Furthermore, the Yushe mandibles and teeth display morphological characters and measurements differing from *H. schreuderi* of Loc. 18 (shown in Fig. 4.7).

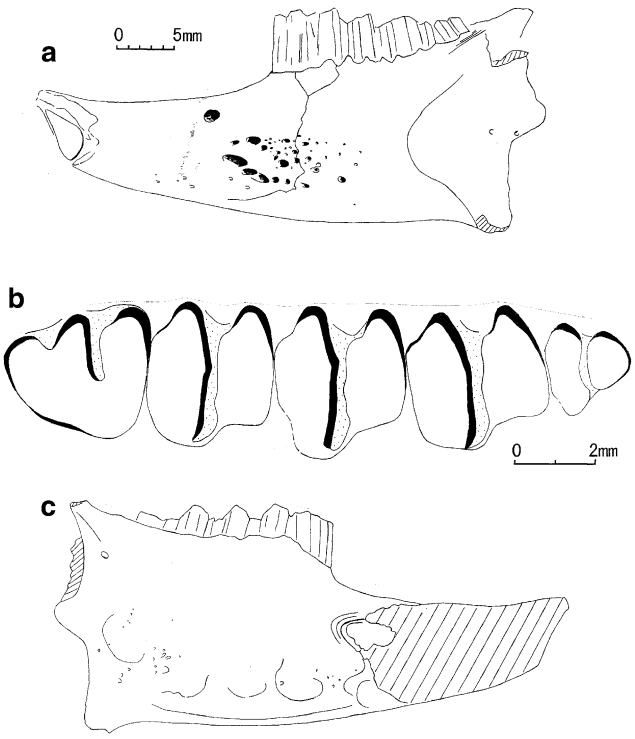

Fig. 4.7 *Hypolagus schreuderi* from Zhoukoudian Loc.18, a left mandible with p3-m3 (29:5:37) showing: **a** lateral aspect, **b** occlusal view of the dentition, anterior to left, **c** lingual aspect

Hypolagus mazegouensis sp. nov.

1942 *Hypolagus* cf. *brachypus*, Teilhard Fig. 53c

1991 *Hypolagus* sp., in part, Tedford et al.

Holotype: A single left p3 (V11224.1)

Type locality, age and stratigraphic position: YS5, 3.3 Ma, Late Pliocene; lower part of Mazegou Formation, Yuncu subbasin.

Referred material by locality, age and stratigraphic position: YS5: damaged right mandible with p4-m3, and a single right P3 (V11224.2-3). Qizigou (field locality QY-74, stratigraphically equivalent to YS5): left mandible with p4-m3 (V11239) lacking the ascending ramus and angular process. Also, left mandible with incisor and p3-m3 housed in IVPP (RV 42019 = 29486) and 7 mandibles housed in TNHM (THP14178, 14184, 14185, 14186, 14188, 14223 and 14245). According to the Tianjin Natural History Museum catalogue these specimens were purchased from Baihai, Haiyan, Gaozhuang and Quanzhitou villages, probably all late Pliocene Mazegou Formation (Figs. 4.8, 4.9a–c; Table 4.6).

Etymology: Indicating the stratigraphic position of the Type of the new taxon.

Diagnosis: A species smaller than *Hypolagus schreuderi* with diastema distinctly longer than the height of the mandible, nearly straight ventral border of the mandible, low

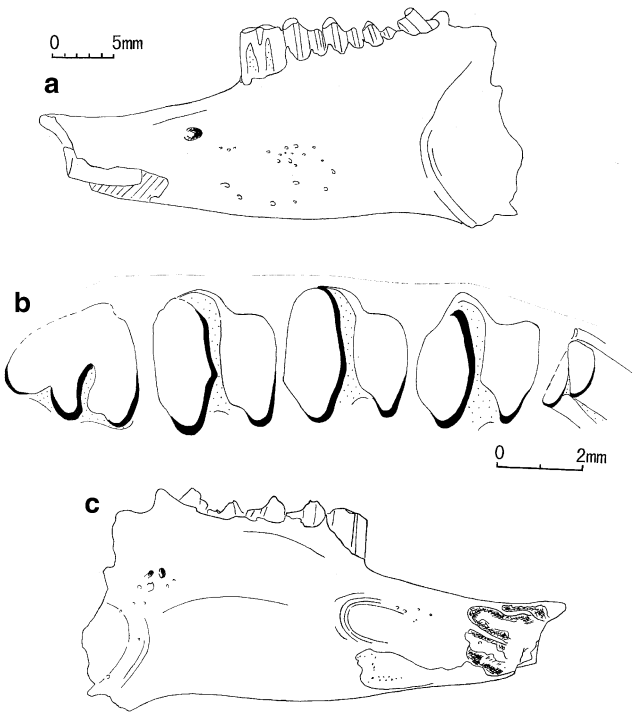

Fig. 4.8 *Hypolagus mazegouensis* sp. nov. from Yushe Basin; a left mandible with p3-m3 (29486 = RV42019): **a** lateral aspect, **b** occlusal view of the dentition, anterior to left, **c** lingual aspect

curvature of lower incisor, which terminates beneath p3, and smooth enamel on the posterior wall of external reentrant of lower cheek teeth (postero-external reentrant for p3).

Differential Diagnosis: *Hypolagus mazegouenesis* differs from *H. schreuderi* in smaller size and less relatively elongate mandibular diastema. *Hypolagus fanchangensis* Jin and Xu, 2009 is small (lower tooth row length = 14.67 mm), comparable to *H. mazegouensis*, but its lower incisor extends farther posteriorly and buccal reentrants of lower cheek teeth have wrinkeled enamel. *Hypolagus igromovi* is generally larger, with a very deep anteroexternal reentrant. *H. brachygnathus* has a short muzzle with reduced diastema and averages larger than *H. mazegouensis* (Fostowicz-Frelik 2003). Erbajeva (1996) described the late Pliocene *Hypolagus multiplicatus* (larger than the Mazegou species) and *H. transbaicalicus. H. transbaicalicus* overlaps *H. mazegouensis* in size, but its anteroconid is reduced (narrow and short) and the anteroexternal reentrant is quite shallow, less deep than in *H. mazegouensis*. *Hypolagus mazegouensis* differs from Late Neogene *H. petenyii* and *H. brachygnathus* in smaller average size of p3, and in its mandibular diastema longer than alveolar length of p3-m3; the lower incisor of *H. brachygnathus* has higher curvature (Cermák and Wagner 2013, Fig. 6).

Compared with various species from North America, *Hypolagus mazegouensis* is distinctly larger than *H. fontinalis*, *H. furlongi*, *H. edensis*, *H. tedfordi* and *H. voorhiesi*. It differs from the type species *H. vetus* in having shallower AER (antero-external reentrant) and the uncrenulated TN (=posterior wall of the p3 posteroexternal reentrant) but it is comparable in size with *H. vetus*. The p3 TN of *H. vetus* is slightly crenulated in 15 of 60 specimens that White (1987) examined. *H. mazegouensis* differs from *H. parviplicatus* in its deeper AER, uncrenulated TN, and slightly larger size, and from *H. edensis* in having shallower and wider AER. *H. furlong* and *H. voorhiesi* have crenulated TN. TN is crenulated in 38% examined specimens of *H. gidleyi*, which also has a deeper AER. *H. regalis* has a crenulated TN of p3, and deeper AER. *H. mazegouensis* differs from *H. apachensis* in the absence of antero- and postero- internal reentrants on p3 and in larger size, differs from *H. arizonensis* in larger size, shallower external reentrants, and uncrenulated TN, and differs from *H. oregonensis* and *H. ringoldensis* in shallower AER, and lack of an anterior reentrant.

Description: The holotype p3 from YS5 (V11224.1, 3.23 × 2.74, 3.13 mm, Fig. 4.9c), slightly damaged postero-internally, is approximately 13 mm tall and has a rather deep antero-external reentrant. Its postero-external reentrant is slightly longer than one-half the breadth of the tooth, is basically parallel to the posterior margin of the tooth and is unplicated. Measurements of the holotype fall low in the range of variation for the specimens of *Hypolagus schreuderi* from Locality 18 (Table 4.6). The isolated P3 (V11224.3, 2.45 × 4.89 mm, 10.3 mm tall) has a hypostria that is two-thirds the breadth of the tooth, with plicated anterior and posterior walls, more complex anteriorly.

Mandible V11224.2 (Fig. 4.9b) is much smaller than that of *H. schreuderi* with measurements of the broken cheek teeth as follows: p4: 2.6 × 2.45, 3.13; m1: 2.74 × 2.25, 2.93; m2: – × 2.54, 2.74 mm. The dentary V11239 from Qizigou may be an aged individual. It is robust, larger than specimens from YS5, has a straight ventral margin, and slight curvature of incisor which terminates beneath p3. The diastema is 16.5 mm long, mandibular height is 14 mm at the lingual side of p4, 14 mm on the lingual side of m1, and 15.4 mm on the lingual side of m3. A mental foramen is located approximately 2.4 mm anterolabial to the p3 on the diastema. Relatively deep nutrient foramina of varying sizes are anteroexternal to the m1. The masseteric fossa is deep and the mandible is lingually slightly inflated where the cheek teeth end. The p4-m2 crown length is 10.21 mm and p3-m3 alveolar length is 15.5 mm. Other measurements are: p4: 2.74 × 2.69, 3.42; m1: 2.74 × 2.62, 3.13; m2: 2.64 × 2.54, 2.64; m3: 1.96 × 1.17, 1.86 mm.

Table 4.6 Measurements of some leporids from Yushe Basin in comparison with *Hypolagus schreuderi* from CKT Loc. 18

Taxon	Specimen	Diastema length	Dentary height on lingual side			Length p3-m3		L × W of p3	Locality of collection or purchase
			at p4	at m1	at m3	Crown	Alveoli		
Sericolagus yushecus sp. nov.	RV 42021	10.53	12.64	12.64	–	–	–	2.89 × 2.45	?
	14201	~13.00	12.96	12.96	13.40	–	15.07	3.03 × 2.64	Malan
	14206	–	12.30	12.00	11.66	–	–	– × –	Malan
	14211	10.53	11.66	12.15	–	–	–	2.93 × 2.64	Malan
Hypolagus mazegouensis sp. nov.	14178	16.85	13.93	13.93	14.10	13.45	14.58	3.03 × 2.74	Baihai
	14184	–	12.31	12.31	–	–	15.50	– × –	Baihai
	14185	–	13.77	–	–	–	–	2.93 × 2.84	Baihai
	14188	16.20	13.77	13.61	–	–	–	3.03 × 2.93	Baihai
	14223	16.70	13.12	13.12	13.77	–	–	3.10 × 3.13	Haiyan
	14245	–	–	–	–	–	–	3.13 × 3.13	Quanzhitou Village
	RV 42019	16.85	14.58	14.58	15.71	14.74	16.36	3.33 × 3.13	Gaozhuang
	14186	–	–	–	–	–	–	3.33 × 3.33	Baiha
Hypolagus schreuderi	1	22.22	15.10	15.20	16.40	15.20		3.42 × 3.18	Zhoukoudian Loc. 18
	2	22.10	15.90	15.60	16.40	16.20		3.50 × –	
	3	~21.20	16.30	16.30	17.00	16.93		3.67 × 3.23	
	4	~21.20	16.20	16.30	17.10	16.30		3.62 × 3.38	(3, 4 same individual)
	5	22.00	16.50	15.40	16.40	14.74		3.33 × 3.18	
	6	21.40	14.80	14.70	15.40	13.77		3.18 × –	
	7	21.20	14.50	14.50	15.40	~14.30		3.23 × ~2.93	
	8	–	16.80	16.50	17.50	16.70		3.72 × 3.33	
	9	–	~15.60	~16.20	–	–		3.72 × 3.23	
Hypolagus mazegouensis sp. nov.	V11224.1	–	–	–	–	–	–	3.23 × 3.13	YS5
	V11224.2 (juvenile)	11.70+	11.80	12.20	12.80	–	–		YS5
	V11239	16.50	14.00	14.00	15.40	–	15.50	–	Qizigou, QY74
Hypolagus sp.	V11225	–	–	–	–	–	–	2.30 × 2.10	YS46
Leporid indet.	RV42020	12.15	11.50	11.50	–	–	–	2.54 × 2.64	Yuncu

RV42019 (THP29486) housed in IVPP(Fig. 4.8, Table 4.6) as well as other jaws residing in TNHM described by Teilhard (1942) match the Type and V11239 in both morphology and size.

Discussion: The newly erected species resembles *Hypolagus schreuderi* in tooth morphology, the nearly straight ventral margin of the mandible, the slight curvature of lower incisor, and diastema longer than mandible height. However, it differs from the latter in smaller size, lower diastema/mandible body height ratio, more posterior incisor termination point (the incisor terminates just anterior to p3 in *H. schreuderi*) and less distinct lingual inflation where the cheek teeth end. Although some specimens of the new species are close to small individuals of *H. schreuderi* in mandible height, size of p3, and length of p3-m3, their diastemas are always shorter than those of *H. schreuderi.* The YS5 jaw (V11224.2) referred to the new species is smaller than other *H. mazegouensis* mandibles; its diastema is close to its mandible height and incisors terminate at the mesial wall of p3; its early stage of ontogeny is a factor in these differences from mature individuals. The comparison of the new species with *H. schreuderi* suggests evolutionary trends from *H. mazegouensis* to *H. schreuderi* in: increased p3 and mandible size, diastema length, hypsodonty (hence the more distinct lingual inflation where the cheek teeth terminate), and anterior retraction of incisor termination.

Hypolagus mazegouensis and *H. schreuderi* represent a lineage of *Hypolagus* in North China that is characterized by a very long diastema. Based on the late Pliocene Mazegou Formation sample, *H. mazegouensis* may be close to the ancestry of *H. schreuderi* as represented at early Pleistocene deposits such as Loc.18. Evolution of this lineage would have involved increasing size and relative length of the diastema. Adhering matrix suggests that some specimens of *H. mazegouensis* may have come from the Haiyan Formation, so the species may have ranged into the earliest Pleistocene. If true, the Haiyan Formation would likely be older than Loc.18.

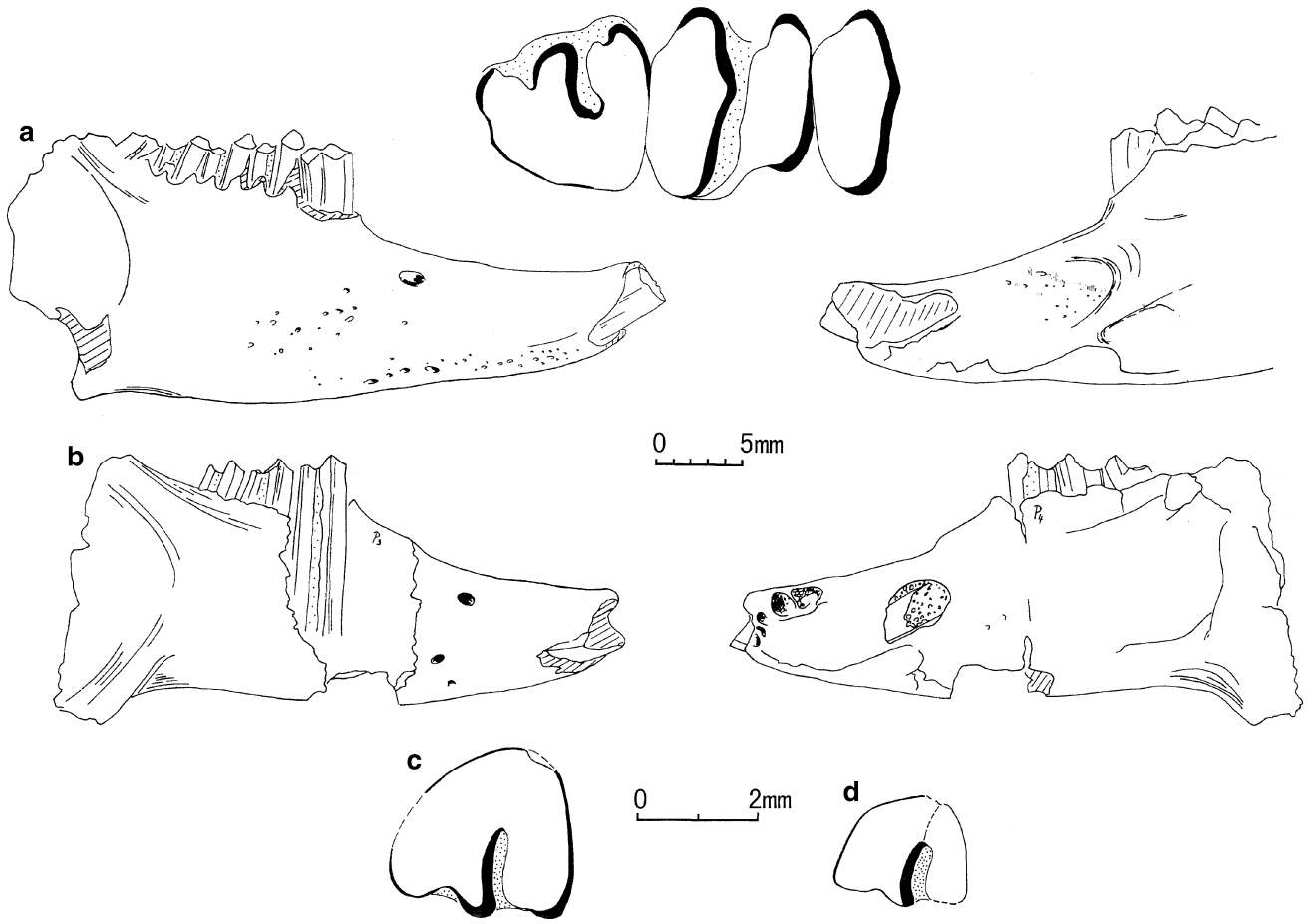

Fig. 4.9 *Hypolagus* from Yushe Basin. **a** *Hypolagus mazegouensis* sp. nov.: right mandible with p3-p4 and the trigonid of m1 (THP14178 purchased from Baihai), showing the lateral aspect (left), lingual aspect (right) and occlusal view of the dentition (above). **b** *Hypolagus mazegouensis* sp. nov.: right fragmentary mandible with p4-m2 from YS5 (V11224.2), showing lateral (left) and lingual aspects of the mandible. **c** *Hypolagus mazegouensis* sp. nov., holotype: left p3 (V11224.1) from YS5, showing occlusal view. **d** *Hypolagus* sp. left p3 (V11225) from YS46 in occlusal view. Note different scale bars for occlusal and mandible views; anterior to left for occlusal views

Hypolagus sp.

Material, locality, stratigraphic position: V11225, a single left p3, slightly damaged posterointernally, from YS46 in the Culiugou Member, Gaozhuang Fm., Yuncu Subbasin (Fig. 4.9d). Measurements are 2.30 × 2.10 mm, preserved height = 9.8 mm.

The p3 crown is slightly posteriorly recurved and barely varies in size along its length. The tooth is narrow anteriorly with a shallow antero-external reentrant. The length of the straight postero-external reentrant is one-half the breadth of the tooth. V11225 differs from YS5 specimens of *H. mazegouensis* in much smaller size (Table 4.6), and the shallower antero-external reentrant. We do not assign this single tooth to species.

Leporidae indet.

The single specimen considered here is a fragmentary right mandible with p3-m1 (RV42020 = 25637; Fig. 4.10b) among the specimens described by Teilhard (1942, Fig. 53A) as *Hypolagus* cf. *brachypus* stands apart from the rest. It is a small form (Table 4.6) with a diastema that is slightly longer than mandible height (longer than typical *Sericolagus*, too short for *Hypolagus mazegouenesis*), a nearly straight ventral mandibular margin, incisors terminating at the anterior part of p3 which has an unplicated postero-external reentrant, but an enclosed postero-internal reentrant or islet. These characters and size isolate it from other Yushe leporids, but the enclosed postero-internal islet occurs in *Sericolagus*. Whether or not the postero-internal enamel islet may occasionally occur in any *Hypolagus* or *Alilepus* is unclear.

Sericolagus Averianov, 1996

Sericolagus yushecus sp. nov.

1942 *Hypolagus* cf. *brachypus*, Teilhard Fig. 53B

Holotype: Fragmentary left mandible with incisor and p3-m3 (RV42021 = 27388), deposited at IVPP (Fig. 4.10a; Table 4.6).

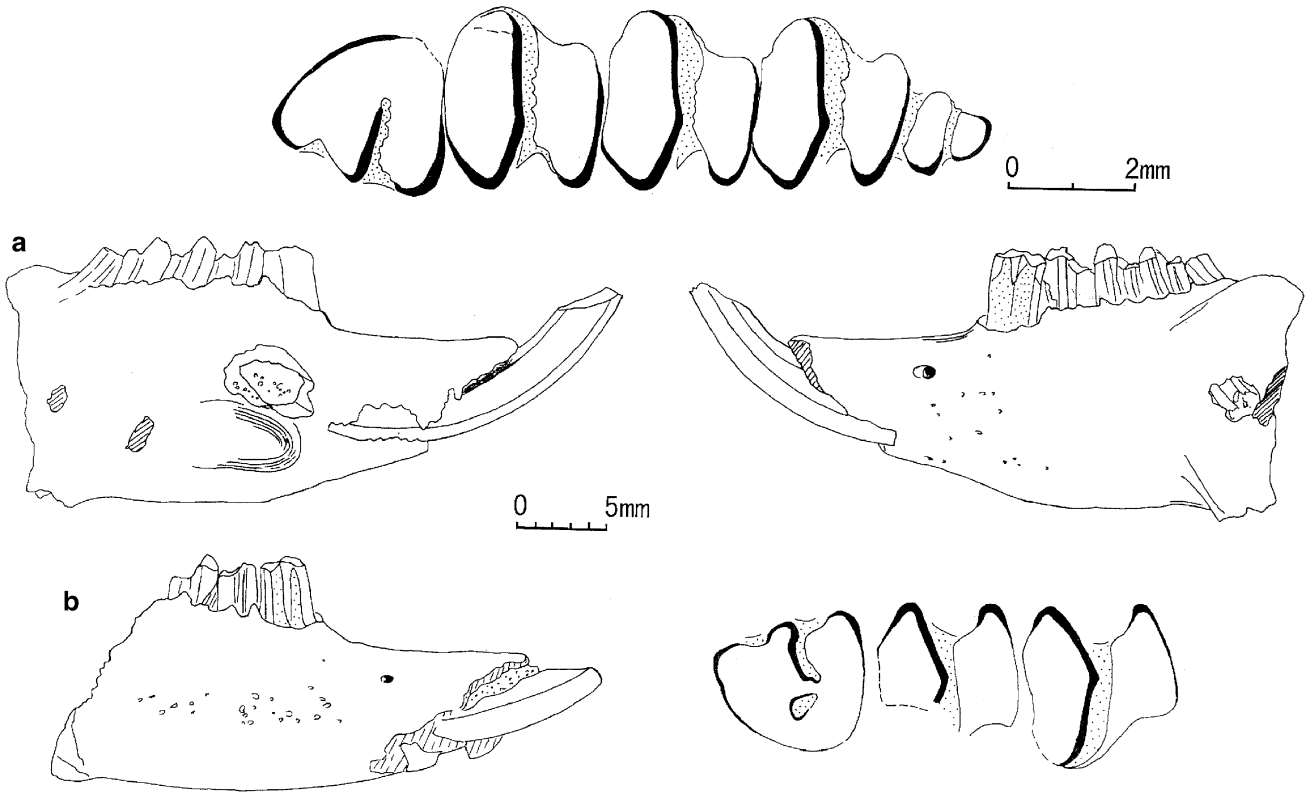

Fig. 4.10 *Sericolagus yushecus* sp. nov. from Yushe Basin: **a** left mandible with p3-m3 (27388 = RV42021): occlusal view of the dentition (above), lingual (left) and lateral (right) aspects of the mandible. Leporidae indet. from Yushe Basin: **b** right mandible with p3-m1 (25637 = RV42020): lateral aspect of the mandible (left) and the occlusal view of the dentition (right). Note different scale bar for occlusal views, for which anterior is to the left

Type locality and age: Unknown

Referred specimens: 3 fragmentary mandibles (THP 14201, 14206, 14211).

Age of referred specimens and stratigraphic position: Purchased from Malancun, Yushe County. No stratigraphic information, but likely Mazegou Formation and/or Haiyan Formation, late Pliocene or early Pleistocene.

Etymology: Yushe, the county of origin of the specimens assigned to this new taxon.

Diagnosis: Diastema shorter than, or equivalent to the height of the mandible, mandible anteroventral margin bends distinctly dorsally, with lower incisor strongly curved and terminating beneath the p4, posterior wall of the p3-m3 postero-external reentrant plicated, posterointernal islet or reentrant usually absent in p3.

Differential Diagnosis: Size similar to *S. brachypus*, but the posterointernal islet or reentrant is absent in known p3. *Hypolagus fanchangensis* Jin and Xu, 2009 (early Pleistocene of Fanchang, Anhui) is similar to *Sericolagus yushecus* in extent of the incisor beneath p4 and crenulation of enamel in lower cheek teeth, but it is smaller (p3: 2.76 × 2.67). Possibly *Hypolagus fanchangensis* should be transferred to genus *Sericolagus.* Other leporids like *Hypolagus parviplicatus* Dawson, 1958 have crenulated reentrants, but that species has a short incisor and very shallow antero-external reentrant on p3.

Description: The Type specimen is small in size. The diastema is 10.5 mm long, shorter than the mandible height 12.64 mm beneath p4 at the lingual side and 12.64 mm beneath m1 at the lingual side. The anteroventral margin of the mandible warps dorsally from p3/p4 forward, and its incisor has high curvature, terminating posteriorly beneath p4, a character of the genus (Zhang 2001). The p3 (2.89 × 2.45 mm) is morphologically similar to *Hypolagus,* but possesses distinct plication on the posterior wall of the postero-external reentrant; similarly the posterior wall of the external reentrants on molariform lower teeth is plicated. The referred specimens show this also. The length of p3 is close to that of *Hypolagus mazegouensis*, but is shorter in *Sericolagus yushecus*. Type specimen RV42021 was described and illustrated by Teilhard (1942, Fig. 53b), but the enamel plication on lower cheek teeth was not noted due to incomplete preparation of the occlusal surface.

Discussion: The features described above differ strongly from those of *Hypolagus mazegouensis*: diastema shorter than or equivalent to the height of the mandible, mandible

anteroventral margin distinctly dorsally warped, lower incisor strongly curved and terminating posteriorly beneath p4, plicated posterior wall of the p3 postero-external and p4-m3 external reentrants.

Having studied original specimens previously called *H. brachypus*, *C. brachypus,* or *H.* cf. *brachypus* and now recognized as *Sericolagus brachypus,* we note that the Yushe species resembles fossils from Loc. 60, Huiyu (Young 1927), Loc. 2 of Gaojiaya, Jingle (Teilhard and Young 1931), Loc. 22 of Shouyang (Young 1935), Heshui, Gansu Province (Zheng 1976), and the East and West Caves near Zhoukoudian (Cheng et al. 1996). Resemblances are morphological as well as size, compelling us to consider the Yushe species to represent *Sericolagus*. However, all Yushe specimens (other than indeterminate RV42020 above) differ in the absence of a postero-internal islet or reentrant on p3. This difference is stable for all four Yushe mandibles and we separate them from *Sericolagus brachypus* as *Sericolagus yushecus*, sp. nov.

Concerning the provenance of the Yushe specimens, we know that they were purchased at Malancun, so they probably derive from the Mazegou Formation (late Pliocene) and/or Haiyan Formation, early Pleistocene. Zhang (2001) indicates a similar range of age estimates for *Sericolagus brachypus*. Provisionally we speculate that Chinese *Sericolagus* could represent an independent immigration of a North America lineage with crenulated lower cheek tooth enamel.

Trischizolagus Radulesco and Samson, 1967

Trischizolagus aff. *T. dumitrescuae* Radulesco and Samson, 1967

Material: isolated teeth, 4 p3, p4/m1/m2, 3 m3, 3 P3, P4/M1, and M2 (V11226.1-13).

Locality and stratigraphic position: YS50, Nanzhuanggou Member, Gaozhuang Fm., Yuncu Subbasin, Yushe, Shanxi Province, 4.7 Ma (Fig. 4.11); right mandible THP14.217 purchased from Malancun (Fig. 4.12c).

See Tables 4.7 and 4.8. Measurements of new material (mm): p3 (V11226.1-4): 3.23 × 2.74, 3.13; 2.84 × 2.15, 2.71; 2.64 × 2.05, 2.35 (Table 4.7); – × 2.35, 2.69.

p4/m1/m2 (V11226.5): 2.05 × 1.86, 2.35.

m3 (V11226.6-8): 1.86 × 1.66, 1.18; 1.27 × 1.27, 0.73; 0.68 × 1.17.

P3 (V11226.9-11): 2.38 × 3.52, 4.3; 2.05 × 3.52, 4.5; 2.35 × 3.72, 4.3.

P4/M1 (V11226.12): 2.06 × 3.15.

M2 (V11226.13): 1.81 × 3.4, 3.6.

Description: The morphologies of the four p3 are similar, being rounded triangles with an anterior lobe and a posterior lobe. The anterior portion is further subdivided into four smaller lobes. The antero-external reentrant is most prominent, stronger than the antero-internal reentrant, which is variable (weak in two teeth), and the anterior reentrant is narrow but clear. The anterior and posterior lobes are separated by postero-external and postero-internal reentrants, with the internal reentrant slightly shorter than the external reentrant, and a relatively wide dentine bridge dividing them. The labial terminus of the postero-internal reentrant is slightly anterior to the lingual terminus of the postero-external reentrant. The reentrants are all infilled with cementum. At the base of one of the specimens the postero-external reentrant composes an elliptical enamel islet that is sealed approximately 1 mm from the base of the colonette. The lingual angle of the posterior lobe is in the shape of a rounded right angle (in three instances) or arc. Enamel thickens at many localities: on the posterior walls of the antero-internal and antero-external reentrants, the anterior walls of the postero-internal and postero-external reentrants, and the labial wall of the posterior lobe. The enamel is predominantly smooth but there are slight plications at the antero-external corner of the postero-internal reentrant, and the antero-internal corner of the postero-external reentrant (one instance). The anterior lobe is twice the length of the posterior lobe.

The posterior lobe of p4, m1, or m2 is distinctly narrower than the anterior lobe, and the enamel on the anterior wall of the posterior lobe is unplicated. The m3 anterior lobe is slightly posteriorly curved and is distinctly broader than the posterior lobe; neither is in contact labially. There is a great size disparity among the three m3 specimens.

The P3 anterior lobe is distinctly narrower than the posterior lobe. The length of the hypostria is slightly more than two-thirds the breadth of the tooth with the enamel of the anterior wall strongly plicated and distinctly thicker than the posterior wall.

The P4 or M1 specimens have anterior and posterior lobes of equivalent breadth and hypostria that are two-thirds the breadth of the tooth. The M2 posterior lobe is narrower than the anterior lobe, and the labial wall is inclined postero-internally. The hypostria is slightly less than two-thirds the breadth of the tooth. For posterior upper cheek teeth (Fig. 4.11o, p), the enamel of anterior walls of the hypostria is thick and plicated. The posterior walls have thin enamel that is either weakly plicated or unplicated.

Discussion and Comparison: *Trischizolagus* contains at least five species occurring in Late Tertiary Eurasian localities. The Type species *T. dumitrescuae* is derived from the Pliocene of Malusteni and Beresti, Romania (MN14b after Fejfar and Heinrich 1987). *T. crusafonti* was named for specimens from the late Miocene (MN13) of La Alberca (Janvier and Montenat 1970). *T. maritsae* is documented from the Pliocene (MN14b) of Maritsa, Greece, and Rousillion, France. Apparently related, *T.* cf. *T. maritsae* is recognized in the late Miocene at La Alberca, Alcoy N, Salobreña and other localities in Spain (López-Martínez 1977). Specimens from the Pliocene (MN14) of Pul-e Charkhi, Kabul Basin, Afghanistan (Sen 1983) are also

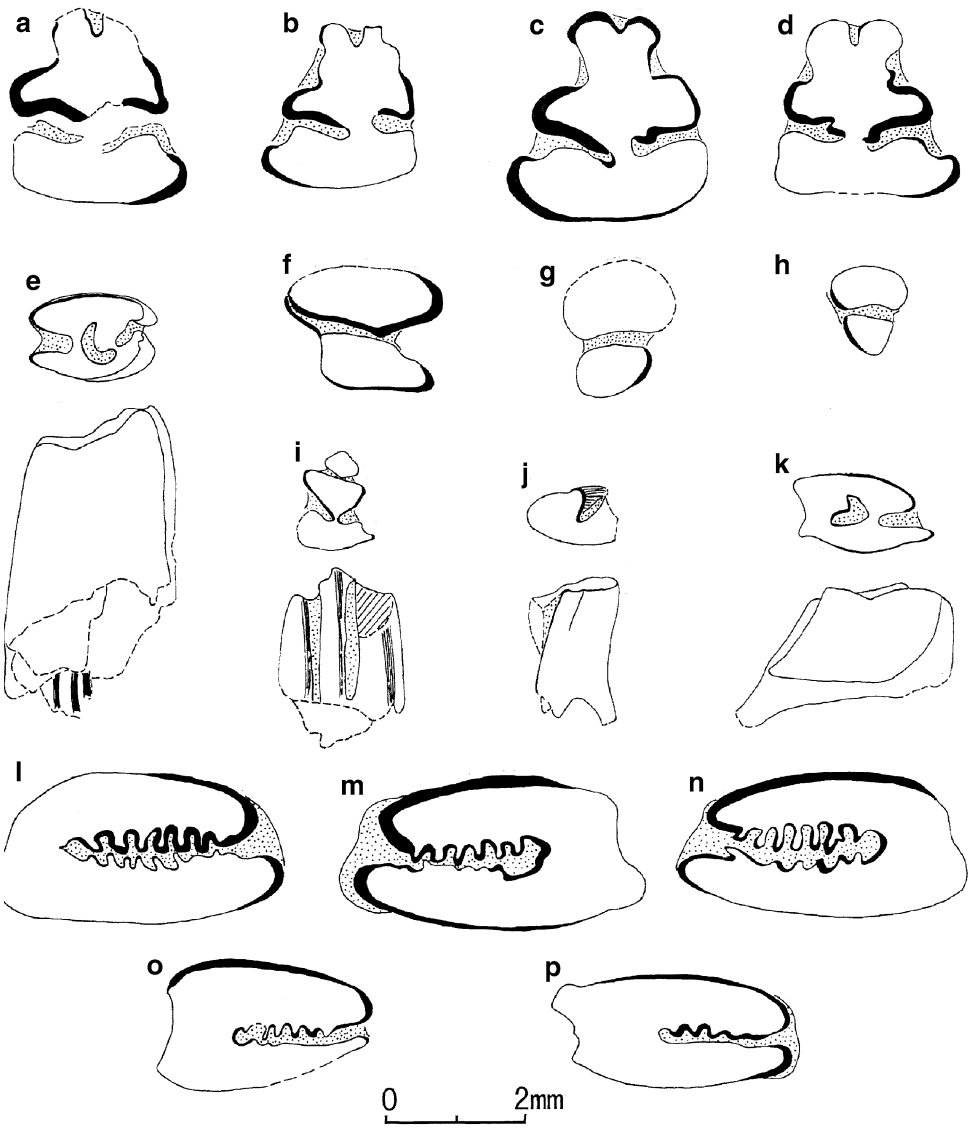

Fig. 4.11 *Trischizolagus* aff. *T. dumitrescuae* from YS50. **a** right p3 (V11226.4); **b** left p3 (V11226.2); **c** left p3 (V11226.1); **d** right p3 (V11226.3); **e** left juvenile P4 or M1 (V11226.16) in occlusal (above) and posterior (below) views; **f** right molariform tooth (p4 or m1 or m2, V11226.5); **g** right m3 (V11226.6); **h** left m3 (V11226.7); **i** left dp3 (V11226.21) in occlusal (above) and buccal (below) views; **j** right DP2 fragment (V11226.14) in occlusal (above) and anterior (below) views; **k** right DP3 (11226.15) in occlusal (above) and anterior (below) views; **l** right P3 (V11226.11); **m** left P3 (V11226.9); **n** left P3 (V11226.10); **o** right P4 or M1 (V11226.12); **p** right M2 (V11226.13). Anterior is upward for occlusal views

listed tentatively as *T.* cf. *maritsae*. *T. mirificus* is named at the early Pliocene of Bilike, Inner Mongolia (MN14 Qiu and Storch 2000) and *T.* sp. is found in the latest Miocene/earliest Pliocene of Kholobolchi Nor, Mongolia (Flynn and Bernor 1987). Tomida and Jin (2005) reassigned *Pliopentalagus nihewanensis* (Cai 1989) from the lower part of Daodi Formation, Hebei (MN 16) to *Trischizolagus*. "*Alilepus*" *gambariani* from early Pliocene of Armenia (MN14, Melik-Adamyan 1986) was reassigned to *T. dumitrescuae* by Averianov and Tesakov (1997), but Cermák and Wagner (2013) held it as a separate species of *Trischizolagus* based on the predominance of the '*Nekrolagus*' morphotype of p3 (see Averianov and Tesakov 1997, Table 2).

The morphology of the Yushe YS50 p3 specimens differs distinctly from *T. maritsae* from Greece, *T.* cf. *maritsae* from Spain and Afghanistan, and *T.* sp. from Mongolia in that the latter forms all have a weak postero-internal reentrant, shallow to absent, or in the form of an enamel islet, while the YS50 specimens have a relatively stable and rather well developed postero-internal reentrant (four specimens). However one Yushe specimen (V11226.2) does have an elliptical enamel islet at the base of the crown. Though similar in size the Yushe material differs from *T. mirificus* in

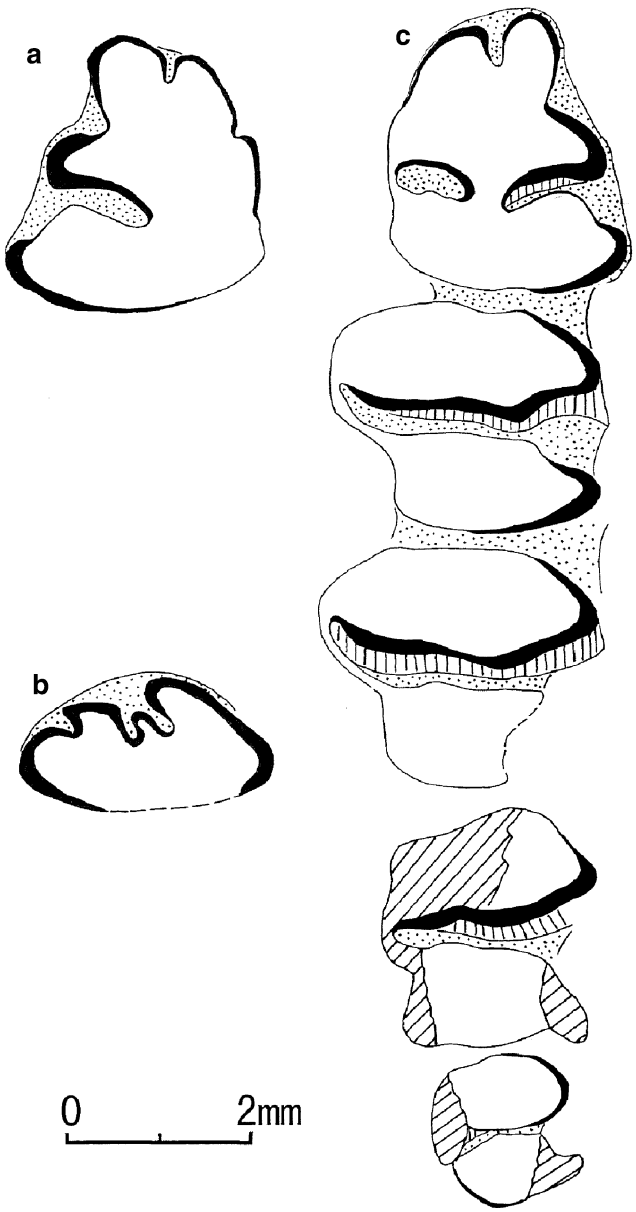

Fig. 4.12 *Trischizolagus* from Yushe Basin. **a** occlusal view of left p3 of *Trischizolagus mirificus* from YS132 (V11227); **b** view from root of right P2 of cf. *Trischizolagus* sp. from YS143 (V11228); **c** occlusal view of right lower dentition of *Trischizolagus* aff. *T. dumitrescuae* (Malancun purchase, THP14.217). Anterior is upward

its strong anterior reentrant and the usually more developed antero-internal reentrant, as well as the ever-present postero-intenal reentrant. The Yushe specimens are very similar to the Type species *T. dumitrescuae* in the anterior lobe being twice the length of the posterior lobe, persistent presence of a postero-internal reentrant that occasionally forms an enamel islet, postero-internal reentrant always shorter than the postero-external reentrant and situated slightly anteriorly with a relatively wide dentine bridge separating the two. Yushe specimen measurements lie between and overlap those of *T. dumitrescuae* and *T. maritsae* (Tables 4.7, 4.8). Further comparison is limited by the small sample for the time being. We prefer now to designate the Yushe form as *Trischizolagus* aff. *T. dumitrescuae*, acknowledging some differences, such as the constant and stronger postero-internal reentrant, but considering plausible a relatively close relationship to *T. dumitrescuae*.

The upper dentition of *T. dumitrescuae* is still unknown from the Type locality, but we refer a number of upper molars from YS50, which yields the *Trischizolagus* p3s. A potentially significant character for the taxon is the P3-M2 hypostria length of generally two-thirds or more the width of the tooth. Additional specimens include a half DP2, 1 DP4, 3 P4 or M1, 2 M2 and 1 dp3 (V11226.14-21), all of which appear to be juveniles and which present difficulties for comparisons. As there are no other lagomorphs from YS50, they are probably referable to the same *Trischizolagus*. Measurements are as follows: DP2: 0.88 × –; DP4: 1.32 × 1.95, 2.05; P4 or M1: 1.37 × 1.95, 2.05; 1.26 × 2.0, 2.15; 1.56 × 2.93; M2: 0.78 × 1.66, 1.37; 1.37 × 2.15, 1.9; dp3: 1.56 × 1.22.

Other material: A pair of mandibles housed at the Tianjin Natural History Museum may be referred here, but the anterior portions of both are broken. The left mandible contains the p3-m2 (THP14.217) and is 7.8 mm deep at the p4, while right mandible THP14.220 contains the p3-m3 with an occlusal length of 8.12 mm and dental alveolus length of 9.29 mm. The state of occlusal wear, mandibular morphology, and condition of preservation suggest that they belong to the same individual. Incisor termini are lingually inflated and are situated beneath the p3. Nutrient foramina

Table 4.7 Comparison of *Trischizolagus* aff. *T. dumitrescue* p3 from Yushe to *T. maritsae* from Greece, *T. dumitrescue* from Romania, and *T. mirificus* from Bilike, Inner Mongolia. Measurements are length × trigonid width; talonid width (mm)

Taxon	N	Range	Mean
T. aff. *T. dumitrescuae*	3	2.64–3.13 × 2.05–2.74; 2.35–3.13	2.90 × 2.31; 2.76
T. maritsae[a]	4	1.50–2.70 × 1.60–2.30; 1.70–2.80	2.20 × 1.93; 2.13
T. dumitrescuae[b]	7	2.85–3.78 × 2.36–2.90; 2.80–3.56	3.41 × 2.77; 3.21
T. mirificus[c]	28	2.25–3.45 × 2.05–3.25	2.98 × 2.79

[a]After De Bruijn et al. (1970)
[b]After Radulesco and Samson (1967)
[c]After Qiu and Storch (2000)

Table 4.8 Dental measurements (mm) of Yushe *Trischizolagus* specimens from the Tianjin Natural History Museum (length × width trigonid; width talonid)

Specimen	p3	p4	m1	m2	m3
THP14.217	3.24 × 2.43, 2.75	2.45 × 2.93, 2.35	2.60 × 2.90, 2.25	2.70 × 2.90, 2.25	
THP14.220	3.03 × 2.45, 2.70	2.60 × 3.00, 2.30	2.80 × 3.03	2.74 × 2.90, 2.00	1.96 × 1.76, 1.27

are present on the ramus dorsolabially and particularly ventral to the p3. The specimens differ from the YS50 specimens in the p3 lacking an antero-internal reentrant, which is replaced merely by an extremely shallow depression, the postero-internal reentrant exists as an enamel loop, the p4, m1 and m2 posterior lobes are relatively narrow with a breadth that is 69–80% of the anterior lobe. However, size and other characters suggest resemblance to the YS50 specimens despite individual variation. Museum records indicate that the specimens were purchased from the village of Malancun. They are well lithified and dark gray with a surrounding matrix of white mudstone, similar to the lithology at YS50.

Trischizolagus mirificus Qiu and Storch, 2000

Material: A single left p3 (V11227, Fig. 4.12a).

Locality and stratigraphic position: YS132, equivalent to YS38 in the lower portion of the Nanzhuanggou Member of the Gaozhuang Fm., 4.8 Ma.

Description and discussion: This p3 has a distinct anterior reentrant that divides the anterior lobe of the tooth into two unequal lobes, with the labial lobe distinctly longer and broader than the lingual one. The antero-external reentrant is broad and deep but the antero-internal reentrant is only a shallow notch. The postero-external reentrant extends slightly more than half the breadth of the tooth but the postero-internal reentrant is only a shallow inflection of the enamel. All reentrants become shallower toward the base. Approximately 10 mm of the tooth is preserved. Crown measurements are 3.22 × 2.54, 3.03 (posterior lobe much wider than anterior).

The YS132 tooth is characterized by the extremely shallow postero-internal reentrant, which contrasts greatly with *Trischizolagus* aff. *T. dumitrescuae* from YS50. In size and morphology the specimen most closely resembles the single specimen of *Trischizolagus* sp. from the Khunuk Fm. of Kholobolchi Nor of Mongolia described by Flynn and Bernor (1987), and *T. mirificus* from Bilike, Inner Mongolia. Chronologically, the specimen is consistent with *Trischizolagus* sp. as YS132 is earliest Pliocene with a paleomagnetic age of 4.8 Ma and the Mongolian Khunuk Fm. is near the Miocene/Pliocene boundary in age. The Bilike fauna is probably somewhat older than the YS50 small mammalian assemblage, possibly near YS132 in age. Two forms of *Trischizolagus* reported from Lingtai, Gansu Province (Zhang and Zheng 2000; Zheng and Zhang 2000, 2001), seem identical with the Yushe species.

cf. *Trischizolagus* sp.

Material: Single right P2 (V11228, Fig. 4.12b) YS143 from the Late Miocene Mahui Fm.; left P4 or M1 (V11232) collected from YS161, Gaozhuang Fm., both Tancun Subbasin.

Description: The P2 specimen, 1.81 × 3.52 mm, has undergone occlusal wear and is heavily waterworn, and as such the discernible morphology lies only at the base of the crown. The central anterior reentrant extends postero-externally into P2 and bifurcates as two parallel reentrants; these are distinct only through the basal half of the crown. The central reentrant divides the P2 into lingual and buccal lobes of roughly equivalent width. An additional shallow reentrant penetrates the lingual lobe. *Trischizolagus* has a complex P2, but coeval *Alilepus* and *Hypolagus* are both simpler in morphology than this specimen. The P2 assigned as *T.* cf. *maritsae* from the Afghanistan locality of Pul-e Charkhi is similar to Yushe specimen, as are the P2s of the Ruscinian (MN14-15) *T. dumitrescuae* from Ukraine and Moldova (Averianov and Tesakov 1997) so V11228 is provisionally referred to the genus *Trischizolagus*.

The left P4/M1 (V11232, 2.45 × 4.52, 4.54 mm) is consistent with YS50 *Trischizolagus,* but is much larger. The hypostria length is two-thirds the width of the tooth, and enamel plication on anterior and posterior walls is extremely complex. Despite large size, it may be a member of this genus.

Discussion: Although the Yushe *Trischizolagus* data are limited, it is an important occurrence of the genus in China. The YS50 sample of *Trischizolagus* aff. *T. dumitrescuae* and YS132 *Trischizolagus mirificus* are derived from two stratigraphic levels, the upper and lower portions respectively, of the Nanzhuanggou Member of the Gaozhuang Fm. Morphologically the p3 specimens are noticeably different and may represent two species. The early Pliocene (MN14) European *T. maritsae* possesses a p3 that has either lost or has reduced its postero-internal reentrant. The Pliocene (MN14b) Type *T. dumitrescuae* displays a postero-internal reentrant that is well developed or formed as an enamel islet and is always present. De Bruijn (1970) considered the undeveloped postero-internal reentrant of *T. maritsae* a primitive character. The Yushe data corroborate this observation as the lower YS132 record has an extremely shallow postero-internal reentrant, while the higher YS50 sample has its postero-internal reentrant well developed. Other localities producing *Trischizolagus* confirm this trend, as evidenced

by the Mongolian locality at Kholoboichi Nor, which is near the Miocene-Pliocene boundary in age, and where *Trischizolagus* sp. has a p3 lacking a postero-internal reentrant. The same phenomenon also occurs on specimens yet to be described from Lingtai, Gansu, which are nearly contemporaneous with the two Yushe species, which may also support this evolutionary trend.

cf. *Nekrolagus* sp.

Material, locality, and stratigraphic position: V11238 is a pair of associated rami that have undergone compressional distortion, the right side preserving p3-m3 and left side preserving p4-m2, but the crowns have all been broken such that there remain only portions in the alveoli. Collected in 1979 by Z.-X. Qiu and others from fine sands, probably the Mahui Formation, of Danangou, Tancun Subbasin (QY-87).

Description and discussion: The right mandible is 14 mm high labially at the p4, and length of p3-m2 is 14.6 mm. The upper portion of the p3 is broken off, with a remnant colonette height of approximately 10 mm. The crosssection is irregular because the fracture surface is uneven, yielding an outline difficult to trace (Fig. 4.4f). The cross section measurements are roughly 3.62 × 2.84, 3.12. Anterior reentrant is deep, trending posterointernally approximately one-sixth the length of the tooth. The antero-external reentrant invades approximately one-third the width of the tooth, and has an associated islet lingual to it. The postero-external reentrant is deep, extending diagonally anteriorly nearly to the lingual side of the tooth, and has thickened, sinuous enamel on its anterior wall. The anterior lobes are distinctly longer (and with thickened enamel) than posterior lobes on p4-m2 (Fig. 4.4f).

The p3 morphology and size indicate possible assignment to *Lepus, Sylvilagus,* or *Nekrolagus*. White (1991, pp. 77–78) stated that the distinctions between *Sylvilagus* and *Lepus* lie in the fusion of the second and third cervical vertebrae in the former and the condition of the interparietal, which in adults of *Lepus* becomes fused with the occiput. The distinction between *Nekrolagus* and *Lepus* is slight since 11% of *Nekrolagus* p3s resemble those of *Lepus* (White, 1991, p. 76). Currently *Sylvilagus* is known only in North America from Pliocene to Recent. *Lepus* originated in North America and dispersed to Eurasia in the Pleistocene, with a first occurrence in China in the late early Pleistocene (Zhang, 2010). *Nekrolagus,* ranging from middle Miocene to Pliocene in North America is not known otherwise in the Old World. A late Miocene record at Danangou is unexpected, but within this range. Because there is only one specimen, we note that it should be compared to the genus.

Other Yushe Group Leporidae

Leporines occur in low abundance as isolated teeth at many localities of the Yushe Basin. Unlike p3 and more complete fossils assigned variously above, these specimens are difficult to diagnose. Noteworthy records with stratigraphic provenance are mentioned here. They may be assigned to *Alilepus*, *Trischizolagus* or *Hypolagus*.

Right I2, left P2 and P4/M1 (V11233.1-3) were collected fromYS49, lower Nanzhuanggou Member of the Gaozhuang Fm. The broken I2 is 2.47 × 1.96 mm. The P2 is 1.17 × 2.59 mm with a distinct anterior reentrant and a single shallow sulcus on the lingual and labial lobes, and is slightly smaller than *Alilepus annectens* from Ertemte and Harr Obo, Inner Mongolia. The P4 or M1 is 2.25 × 3.23 mm, with anterior and posterior lobes being nearly equivalent in breadth, hypostria two-thirds of the tooth breadth. It has a moderately plicated anterior wall, and the posterior wall is nearly unplicated.

Left P2, right P4 or M1, and a p4, m1 or m2 (V11234.1-3) were collected at YS4 from the Culiugou Member of the Gaozhuang Fm. in addition to a fragmentary juvenile right maxilla with loose P3-M1 (V11234.4). The P2 measures 1.17 × 2.36 and displays two anterior reentrants, the antero-external of which is shallower. The P4/M1, 2.54 × 4.69 mm and 11.95 mm high, has a hypostria that is two-thirds the breadth of the tooth, and anterior wall with thicker and more plicated enamel than the posterior wall. The p4/m1/m2 is 3.23 × 3.8, 2.65 mm height = 11.66 mm.

V11234.4 is a juvenile P3, P4, and half M1 measuring 1.56 × 2.48, 2.93; 1.66 × 2.84, 2.93; M1 = 1.78 wide. The P3 hypostria is short and has yet to penetrate the lingual enamel islet. The P4 hypostria is long, approximately one half the breadth of the tooth, and nearly penetrates the enamel islet. The M1 hypostria is longer than that on the P4 and slightly exceeds one-half the breadth of the tooth. In occlusal view, all teeth appear unplicated, but their bases show slight plication.

YS99 from the Mazegou Fm. produced a right P2, left P4/M1, and the posterior lobe of a p4, m1 or m2 (V11236.1-3). The P2, 1.47 × 2.95 mm, possesses a single anterior reentrant. The P4/M1 measures 2.35 × 4.45, 4.62 mm, has a relatively narrow anterior lobe, a hypostria length that is two-thirds the breadth of the tooth, and an anterior wall that has thicker and strongly plicated enamel. The p4, m1 or m2 posterior lobe is 1.47 × 2.93 mm. Stratigraphic position and comparable size suggest assignment to *Hypolagus*.

A single right p4/m1 (V11235) from YS87 of the Mazegou Fm., measures 2.24 × 2.4, 1.86 mm. V11050 from YS6 of the Haiyan Fm. is a left I2, I3, and damaged m3; I2 and I3 cross-sections are 3.13 × 2.2 and 1.64 × 1.02 mm.

Lepus Linnaeus, 1758

Lepus capensis Linnaeus, 1758

Referred material: Palate, F:AM 116223 with right P2-M2 and left P3-M2, and right mandible, F:AM 116222

Table 4.9 Cheek tooth dimensions (mm) for Yushe Basin *Lepus capensis* (F:AM 116223, 116222) of the Frick collection, AMNH

P2	1.55 × 3.05	p3	2.80 × 2.25
P3	2.20 × 4.45	p4	2.30 × 2.45, 2.0[a]
P4	2.50 × 4.90	m1	2.45 × 2.40, 2.05
M1	2.45 × 4.35	m2	2.40 × 2.30, 1.80
M2	2.20 × 4.20	m3	1.35 × 1.30

[a]Third measurement for lower teeth is talonid width

with p3-m3 (no incisor), in the Frick collection of AMNH, from village Nan Zhuang Gou; likely from loess (see Flynn 2011).

Description and discussion: These specimens in matrix suggestive of loess overlying Pliocene Yushe Group deposits of the Nan Zhuang Gou, bear separate numbers, but may represent the same hare individual. They resemble closely *Lepus wongi* named by Young (1927) for fossils from Zhoukoudian Locality 2. Zhang (2010) shows that these hares are indistinguishable from, and a junior synonym of, *Lepus capensis*. The fossils represent a large species (Table 4.9) comparable to modern *L. capensus* MCZ 37230 (Museum of Comparative Zoology, Harvard University). The alveolar length of the maxilla is 15.8 mm, and length of lower tooth row is 11.3 mm (12.6 at the alveoli). Intermolar distance between left and right M1 is 10.6 mm. P2 has two anterior reentrants, the deepest centrally located, and the other shallower reentrant lateral to this (not lingual). The P3-M2 have moderately wrinkled enamel in the hypostria (P4 is largest, 2.5 × 4.9). Lower p3 is typically modern, with a deep posteroexternal reentrant that nearly intersects the lingual wall of the tooth; its path shifts anteriorly half way across the talonid. There is a single anterior reentrant. The largest lower cheek tooth is m1 (2.45 × 2.4 mm; talonid narrower: 2.05).

The Yushe hare is indistinguishable from the population studied by C.C. Young from Zhoukoudian Locality 2. It thus joins *Erinaceus olgae*, *Scaptochirus*, and several shrews and bats as faunal elements in late Pleistocene deposits of eastern North China that were distributed westward from the coast, at least as far as Yushe Basin in Shanxi Province.

4.3 Conclusion

Tertiary lagomorphs from the Yushe Basin are represented by the following pikas *Ochotonoides complicidens, Ochotonoides teilhardi* sp. nov., *Ochotona lagreli, Ochotona* cf. *O. lagreli, Ochotona nihewanica?* and *Ochotona* spp. 1-4 and leporids *Alilepus annectens, Alilepus parvus* sp. nov., *Hypolagus mazegouensis* sp. nov., *Hypolagus* sp., *Sericolagus yushecus* sp. nov., *Trischizolagus* aff. *T. dumitrescuae, Trischizolagus mirificus*, cf. *Nekrolagus* sp., and the modern hare *Lepus capensis*. Additional indeterminate material may hint at higher diversity.

To date, *Ochotonoides teilhardi* constitutes the most primitive and oldest member of the genus with a morphology and size that lie between *Ochotonoides complicidens* and *Ochotona lagreli*. A reevaluation of the original Yushe data indicates the presence of both *O. teilhardi* and *O. complicidens* in the Yushe Basin. The new taxon is produced from the late Pliocene Mazegou Fm. and lower levels of the Haiyan Fm., while the latter taxon comes from younger deposits of loess and possibly the upper part of the Haiyan Fm. The Haiyan *Ochotonoides teilhardi* is distinctly more primitive than the *Ochotonoides* at Locality 18, indicating an age older than Loc. 18 for the Haiyan deposits.

Ochotona lagreli records in Yushe Basin span the Miocene Mahui Fm. to early Pliocene Gaozhuang Fm., preceding *Ochotonoides teilhardi* in the late Pliocene Mazegou Fm. *Ochotonoides teilhardi* appears to replace *Ochotona lagreli*.

Two species of *Alilepus* occur in Yushe Basin: *A. annectens* and *A. parvus* sp. nov. *Alilepus annectens* is recovered from the Mahui Fm. and Taoyang Member, low in the Gaozhuang Fm. The Mahui Formation *Alilepus annectens* fossils appear to represent the oldest documented stratigraphic record for the species. The smaller *Alilepus parvus* occurs low in the Mahui Fm.

The stratigraphic range for genus *Hypolagus* in the Yushe Basin includes the Culiugou Member of the Gaozhuang Fm., the Mazegou Fm. and the Haiyan Fm. *Hypolagus* sp. is stratigraphically lower, and *Hypolagus mazegouensis* comes from the Mazegou Fm. Early finds from Yushe Basin formerly identified as *Hypolagus* cf. *brachypus* Teilhard, 1942 are now recognized as three taxa. Among them, *Hypolagus mazegouensis* sp. nov. forms a clade of long-snouted leporids (long diastema) with *H. schreuderi* from early Pleistocene deposits in North China. We propose an ancestral/descendant relationship between them. Again, we consider the age of the Haiyan sediments to predate Loc. 18. *Sericolagus yushecus* sp. nov. represents a separate lineage; of uncertain provenance, it is late Pliocene or early Pleistocene in age.

The Yushe *Trischizolagus* of the Gaozhuang Formation is early Pliocene in age. The two species of *Trischizolagus*, the older being smaller, probably represent two distinct evolutionary stages. A single, derived leporid specimen may represent *Nekrolagus*; this record in the Gaozhuang Fm. would be the first for the genus in China. It further illustrates the diversity of Lagomorpha in the Pliocene of Yushe Basin. Pleistocene age deposits record the introduction of the modern hare *Lepus* into the area.

Acknowledgements Our reviewers Alisa Winkler, Zhao-Qun Zhang and Yukimitsu Tomida devoted much effort to helping us to improve the manuscript and we thank them for their time. We also thank Miss Si H.-W. for helping us to produce the final illustrations.

References

Angelone, C., & Rook, L. (2011). *Alilepus meini* nov. sp. (Leporidae, Lagomorpha) from the early Messinian of Tuscany (central-western Italy). *Géobios, 44,* 151–156.

Averianov, A. O. (1996). On the systematic position of rabbit "*Caprolagus*" *brachypus* Young, 1927 (Lagomorpha, Leporidae) from the Villafranchian of China. *Russian Academy of Sciences Proceedings of the Zoological Institute St. Petersburg, 270*, 148–156 (in Russian with English summary).

Averianov, A. O., & Tesakov, A. S. (1997). Evolutionary trends in Mio-Pliocene Leporinae, based on *Trischizolagus* (Mammalia, Lagomorpha). *Paläontologische Zeitschrift, 71*(1/2), 145–153.

Bohlin, B. (1942). A review of the fossil Lagomorpha in the Paleontological Museum, Upsala. *Bulletin of the Geological Institution of the University Upsala, 30*(6), 117–154.

Boule, M., & Teilhard de Chardin, P. (1928). Paléontologie. In M. Boule, H. Breuil, E. Licent, & P. Teilhard (Eds.), *Le Paléolithique de la Chine* (pp. 27–102). Paris: Archives de l'Institut de Paléontologie Humaine Mémoire 4.

Cai, B.-Q. (1989). Fossil lagomorphs from the Late Pliocene of Yangyuan and Yuxian, Hebei. *Vertebata PalAsiatica, 27,* 170–181 [in Chinese with English summary].

Čermák, S., & Wagner, J. (2013). The Pliocene record of *Trischizolagus* and *Pliopentalagus* (Leporidae, Lagomorpha, Mammalia) in Central Europe, with comments on taxonomy and evolutionary history of Leporinae. *Neues Jahrbuch für Geologie und Paläontologie, Abhandlungen, 268,* 97–111.

Cheng, J., Tian, M.-Z., Cao, B.-X., & Li, L.-Y. (1996). *The new mammalian fossils from Zhoukoudian (Choukoutien), Beijing, and their environmental explanation*. Beijing: China University of Geosciences Press (in Chinese with English abstract).

Chow, M.-C., & Li, C.-K. (1965). Mammalian fossils in association with the mandible of Lantian Man at Chenchia-ou, in Lantian, Shensi. *Vertebrata PalAsiatica, 9,* 377–394 (in Chinese with English summary).

de Bruijn, H., Dawson, M. R., & Mein, P. (1970). Upper Pliocene Rodentia, Lagomorpha and Insectivora (Mammalia) from the Isle of Rhodes (Greece). *Proceedings Koninklijke Nederlandse Akademie van Wetenschappen, B73*(5), 535–584.

Erbajeva, M. A. (1988). *Cenozoic pikas (taxonomy, systematics, phylogeny)* (pp. 1–224). Moscow: Nauka (in Russian).

Erbajeva, M. A. (1994). Phylogeny and evolution of Ochotonidae with emphasis on Asian ochotonids. In Y. Tomida, C.-K. Li, & T. Setoguchi (Eds.), *Rodent and lagomorph families of Asian origins and diversification* (pp. 1–13). Tokyo: National Science Museum Monographs 8.

Erbajeva, M. A. (1996). Lagomorphs from a Villafranchian sequence in Transbaikalia and their paleoenvironmental implications. *Acta zoologica cracoviensia, 39,* 131–135.

Erbajeva, M. A., Flynn, L. J., Li, C.-K., & Marcus, L. (2006). New Late Cenozoic ochotonids from China. *Beiträge zur Paläontologie, 30,* 133–141.

Erbajeva, M. A., & Zheng, S.-H. (2005). New data on Late Miocene—Pleistocene ochotonids (Ochotonidae, Lagomorpha) from North China. *Acta zoologica cracoviensia, 48A,* 93–117.

Fejfar, O., & Heinrich, W. D. (1987). Zur biostratigraphischen Gliederung des Jüngeren Känozoikums in Europa an Hand von Muriden und Cricetiden (Rodentia, Mammalia). *Časopis pro Mineralogii a Geologii, 32,* 1–15.

Flynn, L. J. (2011). Microtine rodents in the Frick Collection from Yushe Basin, Shanxi Province. *Palaeontologia Electronica, 14.3.33A*, 9 p. http://www.palaeo-electronica.org/toc.htm.

Flynn, L. J., & Bernor, R. L. (1987). Late Tertiary mammals from the Mongolian People's Republic. *American Museum Novitates, 2872,* 1–16.

Flynn, L. J., Winkler, A. J., Erbaeva, M., Alexeeva, N., Anders, U., Angelone, C., et al. (2014). The leporid datum: A late Miocene biotic marker. *Mammal Review, 44,* 164–176.

Fostowicz-Frelik, L. (2003). Species distribution and differentiation of Eurasian *Hypolagus* (Lagomorpha, Leporidae). In J. W. F. Reumer & W. Wessels (Eds.), *Distribution and migration of Tertiary mammals in Europe. A volume in honour of Hans de Bruijn. Deinsea 10*, 197–216.

Gureev, A. A. (1964). *Fauna of USSR: Lagomorpha. 3*(10), 1–276. Moscow-Leningrad: Nauka (in Russian).

Hu, C.-K., & Qi, T. (1978). Gongwangling Pleistocene mammalian fauna of Lantian, Shaanxi. *Palaeontologia Sinica, New Series, C, 21,* 1–64 (in Chinese with English summary).

International Commission on Zoological Nomenclature (1999). *International code of zoological nomenclature*. London: The International Trust for Zoological Nomenclature.

Janvier, P., & Montenat, C. (1970). Le plus ancient Leporidae d'Europe occidentale, *Hispanolagus crusafonti* nov. gen. nov. sp. du Miocène supérieur de Muricia (Espagne). *Bulletin Muséum Nationale d'Histoire Naturelle, Ser. 2, 42*, 780–788.

Ji, H.-X. (1976). The middle Pleistocene mammalian fossils of Laochihe, Lantian District, Shaanxi. *Vertebrata PalAsiatica, 14,* 59–66 (in Chinese with English summary).

Ji, H.-X., Xu, Q.-Q., & Huang, W.-B. (1980). The *Hipparion* fauna from Guizhong basin, Xizang. In Chinese Academy of Sciences (Eds.), *The comprehensive scientific expedition to the Qinghai-Xizang Plateau: Paleontology of Xizang, Book 1* (pp. 18–32). Beijing: Science Press (in Chinese with English abstract).

Jin, C.-Z., & Xu, F. (2009). Lagomorpha. In C.-Z. Jin & J.-Y. Liu (Eds.), *Paleolithic site—The Renzidong Cave, Fanchang, Anhui Province* (pp. 162–166, 400–401). Beijing: Science Press.

Kretzoi, M. (1959a). Insectivoren, Nagetiere und Lagomorphen der Jüngstpliozänen Fauna von Csarnóta im Villányer Gebirge (Südungarn). *Vertebrata Hungarica, 1*(2), 237–246.

Kretzoi, M. (1959b). Fauna und Faunenhorizont von Csarnóta. *A Magyar Állami Földtani Intézet Évi Jelentése az 1959, Budapest, 1962,* 297–395.

Lin, Y.-P., Pan, Y.-R., & Lu, Q.-W. (1978). Early Pleistocene mammal fauna of Yuanmou Basin, Yunnan. In Institute of Vertebrate Paleontology and Paleoanthropology, Chinese Academy of Sciences (Eds.), *Treatise on Paleoanthropology* (pp. 101–125). Beijing: Science Press (in Chinese).

Liu, L.-P., & Zheng, S.-H. (1997). Note on the Late Cenozoic lagomorphs of Danjiang Reservoir Area in Hubei and Henan. *Vertebrata PalAsiatica*, *35*, 130–144 (in Chinese, with English summary).

López-Martínez, N. (1977). *Revision sistematica y biostratigraphica de los Lagomorpha (Mammalia) del Neogeno y Cuaternario de España*. Doctoral thesis, Universidad Madrid.

Melik-Adamyan, G. U. (1986). New data on the Pliocene terrestrial vertebrates of Armenian SSR. *Doklady Akademii Nauk Armyanskoy SSR, 83,* 135–139 (in Russian).

Qiu, Z.-D. (1985). A new ochotonid from Nihewan Bed of Yuxian, Hebei. *Vertebrata PalAsiatica, 23,* 276–286 (in Chinese with English summary).

Qiu, Z.-D. (1987). The Neogene mammalia faunas of Ertemte and Harr-Obo in Inner Mongolia (Nei Mongol), China. 6. Hares and Pikas – Lagomorpha: Leporidae and Ochotonidae. *Senckenbergiana lethaea, 67,* 375–399.

Qiu, Z.-D., & Han, D.-F. (1986). Fossil Lagomorpha from the hominoid locality of Lufeng, Yunnan. *Acta Anthropologica Sinica, 5,* 41–53 (in Chinese with English summary).

Qiu, Z.-D., & Li, Q. (2008). Late Miocene micromammals from the Qaidam Basin in the Qinghai-Xizang Plateau. *Vertebrata PalAsiatica, 46,* 284–306.

Qiu, Z.-D., & Storch, G. (2000). The early Pliocene micromammalian fauna of Bilike, Inner Mongolia, China (Mammalia: Lipotyphla, Chiroptera, Rodentia, Lagomorpha). *Senckenbergiana lethaea, 80,* 173–229.

Qiu, Z.-X., Deng, T., & Wang, B.-Y. (2004). Early Pleistocene mammalian fauna from Longdan, Dongxiang, Gansu, China. *Palaeontologia Sinica, New Series, C, 27,* 1–198 (in Chinese with English summary).

Radulesco, C., & Samson, P. (1967). Contributions à la connaissance du complèxe faunique de Malusteni-Beresti (Pléistocène inférieure), Roumanie. I. Ord. Lagomorpha, Fam. Leporidae. *Neues Jahrbuch für Geologie und Paläontologie, 9,* 544–563.

Schlosser, M. (1924). Tertiary vertebrates from Mongolia. *Palaeontologia Sinica, C, 1,* 1–132.

Schreuder, A. (1937). *Hypolagus* from the Tegelen clay; with a note on recent *Nesolagus*. *Archives Néerlandaises de Zoologie, 2,* 225–239.

Sen, S. (1983). Rongeures et lagomorphes du gisement Pliocène de Pul-e Charkhi, bassin de Kabul, Afganistan. *Bulletin Muséum National d'Histoire Naturelle* (*Paris*), *C*(5), 33–74.

Sen, S. (1998). Pliocene vertebrate locality of Çalta, Ankara, Turkey. 4. Rodentia and Lagomorpha. *Geodiversitas, 20,* 359–378.

Tedford, R. H., Flynn, L. J., Qiu, Z.-X., Opdyke, N. D., & Downs, W. R. (1991). Yushe Basin, China: Paleomagnetically calibrated mammalian biostratigraphic standard for the Late Neogene of eastern Asia. *Journal of Vertebrate Paleontology, 11,* 519–526.

Teilhard de Chardin, P. (1940). The fossils from Locality 18 near Peking. *Palaeontologia Sinica, New Series, C, 9,* 1–100.

Teilhard de Chardin, P. (1942). New rodents of the Pliocene and lower Pleistocene of North China. *Publications de l'Institut de Géobiologie, Pékin, 9,* 1–101.

Teilhard de Chardin, P., & Piveteau, J. (1930). Les Mammifères fossiles de Nihowan (Chine). *Annales de Paléontologie, 19,* 1–134.

Teilhard de Chardin, P., & Young, C. C. (1931). Fossil mammals from the late Cenozoic of Northern China. *Palaeontologia Sinica C, 9,* 1–89.

Tjutkova, L. A. (1992). Rodents and lagomorphs of the late Pliocene Kiikbay fauna (Southeastern Kazakhstan). *Paleontological Journal, 26*(4), 118–124.

Tjutkova, L. A., & Kaipova, G. O. (1996). Late Pliocene and Eopleistocene micromammal faunas of southeastern Kazakhstan. *Acta zoological cracoviensia, 39*(1), 549–557.

Tomida, Y., & Jin, C.-Z. (2005). Reconstruction of the generic assignment of "*Pliopentalagus nihewanensis*" from the Late Pliocene of Hebei, China. *Vertebrata PalAsiatica, 43,* 297–303.

Topachevskij, V. A., & Skorik, A. F. (1977). The first finds of large pikas of the genus *Ochotonoides* (Lagomorpha, Lagomyidae) and a sketch of the history of the Lagomyidae in Eastern Europe. *Vestnik Zoologii, 6,* 45–52 [in Russian with English Summary].

Wang, H. (1988). An early Pleistocene mammalian fauna from Dali, Shaanxi. *Vertebrata PalAsiatica, 26,* 59–72 [in Chinese with English abstract].

White, J. A. (1987). The Archaeolaginae (Mammalia, Lagomorpha) of North America, excluding *Archaeolagus* and *Panolax*. *Journal of Vertebrate Paleontology, 7,* 425–450.

White, J. A. (1991). North American Leporinae (Mammalia, Lagomorpha) from late Miocene (Clarendonian) to latest Miocene (Blancan). *Journal of Vertebrate Paleontology, 11,* 67–89.

Winkler, A. J., Flynn, L. J., & Tomida, Y. (2011). Fossil lagomorphs from the Potwar Plateau, northern Pakistan. *Paleontologia Electronica, 14*(3), 38A, 16 p.

Young, C. C. (1927). Fossile Nagetiere aus Nord-China. *Palaeontologia Sinica, C, 5*(3), 1–82.

Young, C. C. (1935). Miscellaneous mammalian fossils from Shansi and Honan. *Palaeontologia Sinica C, 9*(2), 1–56.

Zhang, S.-S. (1993). Comprehensive study on the Jinniushan Paleolithic site. *Memoirs of Institute of Vertebrate Palaeontology and Palaeoanthropology, Academia Sinica, 19,* 1–153.

Zhang, Z.-Q. (2001). Fossil mammals of early Pleistocene from Ningyang, Shandong Province. *Vertebrata PalAsiatica, 39,* 139–150.

Zhang, Z.-Q. (2010). Revision of Chinese Pleistocene *Lepus* (Leporidae, Lagomorpha). *Vertebrata PalAsiatica, 48,* 262–274.

Zhang, Z.-Q., & Zheng, S.-H. (2000). Late Miocene-early Pliocene biostratigraphy of Loc. 93002 section Lingtai, Gansu. *Vertebrata PalAsiatica, 38,* 274–286.

Zheng, S.-H. (1976). Small mammals of middle Pleistocene in Heshui, Gansu. *Vertebrata PalAsiatica, 14,* 112–119 [in Chinese].

Zheng, S.-H., & Li, Y. (1982). Some Pliocene lagomorphs and rodents from Loc. 1 of Songshan, Tianzu Xian, Gansu Province. *Vertebrata PalAsiatica, 20,* 35–44 [in Chinese with English abstract].

Zheng, S.-H., Wu, W.-Y., Li, Y., & Wang, G.-D. (1985a). Late Cenozoic mammalian faunas of Guide and Gonghe Basins, Qinghai Province. *Vertebrata PalAsiatica, 23,* 89–134 [in Chinese with English summary].

Zheng, S.-H., Yuan, B.-Y., Gao, F.-Q., & Sun, F.-Q. (1985b). Fossil mammals. In T.-S. Liu (Ed.), *Loess and the Environment* (pp. 113–141). Beijing: China Ocean Press [in Chinese].

Zheng, S.-H., Yuan, B.-Y., Gao, F.-Q., & Sun, F.-Q. (1985c). Fossil mammals with special evidence of the evolution of *Myospalax*. In T.-S. Liu (Ed.), *Loess and the environment* (pp. 67–72). Beijing: China Ocean Press [in English].

Zheng, S.-H., & Zhang, Z.-Q. (2000). Late Miocene-Early Pleistocene micromammals from Wenwanggou of Lingtai, Gansu, China. *Vertebrata PalAsiatica, 38,* 58–72 [in Chinese with English summary].

Zheng, S.-H., & Zhang, Z.-Q. (2001). Late Miocene-Early Pleistocene biostratigraphy of the Leijiahe Area, Lingtai, Gansu. *Vertebrata PalAsiatica, 39,* 215–228 [in Chinese with English summary].

Zheng, S.-H., Zhang, Z.-Q., & Liu, L.-P. (1997). Pleistocene mammals from fissure-filling of Sunjiashan hill, Shandong, China. *Vertebrata PalAsiatica, 35,* 215–221 [in Chinese with English summary].

Chapter 5
Yushe Squirrels (Sciuridae, Rodentia)

Zhu-Ding Qiu

Abstract Squirrels (Sciuridae) have been rarely recognized among surface finds of Yushe Basin. The sciurids described here are small samples of mainly isolated teeth recovered from the fossil deposits of Yushe Basin by screening in 1987 and 1988 with additions from 1991, but include six species from two subfamilies. They are *Tamias* cf. *T. ertemtensis* (Qiu 1991), *Sciurus* sp., *Sinotamias* sp., *Marmota* sp. of Sciurinae, and *Pliopetaurista rugosa* Qiu 1991 and *Hylopetes yuncuensis* sp. nov. (Pteromyinae). Among these squirrels, three taxa (*Tamias* cf. *T. ertemtensis, Pliopetaurista rugosa*, and *Hylopetes yuncuensis*) occur in more than one formation, with a temporal interval of 6.3 Ma to 3.4 Ma indicated by paleomagnetic stratigraphy. Morphological comparisons with species related to the chipmunk and the flying squirrel indicate agreement with a geologic span of late Miocene to early Pliocene for the fossil-bearing beds. The Yushe sciurid fauna is most similar in composition to those of Ertemte and Harr Obo of Inner Mongolia, strongly implying chronological similarity and biogeographical affiliation of these assemblages. However, the Yushe fauna contains proportionally more arboreal sciurids than the two Inner Mongolian faunas, and lacks the ground squirrel genus *Prospermophilus*, which is considered indicative of semi-arid grassland and is abundant in the Inner Mongolian faunas. This discrepancy highlights ecological distinctions between the Shanxi fauna and Inner Mongolian faunas, Yushe Basin being moister.

Keywords Yushe Basin • Sciuridae • North China • Late Neogene • Squirrels

5.1 Introduction

The fossil Sciuridae of the Yushe Basin were virtually unknown until the collaborative Sino-American intensive sediment screening campaign of 1987–1991. Brief mention of squirrel remains was made by Teilhard de Chardin (1942), and records in the Yushe County Museum make note of more recent surface finds. Micromammal field teams found squirrels to be a small but usual component of well-sampled microfaunas. Although the collected remains of this family are still few for the basin as a whole, they indicate some diversity (six species in two subfamilies) and are useful paleoecological indicators.

Specimen prefixes used herein: THP (Tianjin Huang Pei), Tianjin Natural History Museum; IVPP V, Institute of Vertebrate Paleontology and Paleoanthropology; Y, Yushe County Museum.

5.2 Systematics

Family Sciuridae Fischer von Waldheim, 1817

5.2.1 *Subfamily Sciurinae Fischer von Waldheim, 1817*

Tamias Illiger, 1811
Tamias cf. *T. ertemtensis* (Qiu, 1991)

Note: This chapter includes one or more new nomenclatural-taxonomic actions, registered in Zoobank and for such purposes the official publication date is 2017.

Z.-D. Qiu (✉)
Laboratory of Paleomammalogy, Institute of Vertebrate Paleontology and Paleoanthropology, Chinese Academy of Sciences, 142 Xizhimenwai Ave., Beijing 100044, People's Republic of China
e-mail: qiuzhuding@ivpp.ac.cn

Lawrence J. Flynn and Wen-Yu Wu (eds.), *Late Cenozoic Yushe Basin, Shanxi Province, China: Geology and Fossil Mammals, Volume II: Small Mammal Fossils of Yushe Basin*, Vertebrate Paleobiology and Paleoanthropology,
DOI 10.1007/978-94-024-1050-1_5

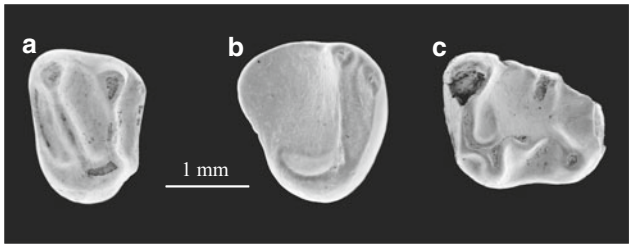

Fig. 5.1 Occlusal view of *Tamias* cf. *T. ertemtensis* from Yushe. **a** M1/2, V 13076.1; **b** M3, V 13076.4; **c** m3, V 13076.2

Material: From locality YS11 (6.2 Ma), one right M1/M2, IVPP V 13076.l and from YS32 (6.0 Ma), left m3, V 13076.2, both late Miocene Mahui Fm. From YS4 (4.7 Ma), one M1/M2 with broken anterior portion, V 13076.3, and from YS50 (4.3 Ma), right M3, V 13076.4, both early Pliocene Gaozhuang Fm. (Fig. 5.1).

Measurements (mm): M1/2: 1.90 × 1.65 (V13076.1), − × 1.70 (V13076.3); M3: 1.80 × 2.00; m3: 1.75 × 1.90.

Description: The M1/2 is subquadrate in occlusal outline. The protocone is the largest cusp and is located mediolingually. The paracone is larger than the metacone. The protoloph and metaloph are continuous, low, and saddle-shaped (lowest in the middle). The protoloph is slightly transverse, and the metaloph is anterolingually-posterolabially inclined to the longitudinal axis of the molar. Both lophs are slightly inflated at their centers, and converge toward the protocone. Protoconule and metaconule are absent. Anteroloph and posteroloph are continuous, and both are lower than the protoloph and metaloph. Parastyle is poorly developed. There is no mesostyle, but a very low connection between the paracone and metacone is present. There is one large lingual root and two labial roots.

The M3 is heavily worn, wider than long, and not very expanded posteriorly. The protoloph is complete, but protoconule, metacone and metaloph are absent. Three roots are present. The m3 is slightly damaged. It is moderately expanded posteriorly and has a well-developed mesoconid, a visible entoconid, a relatively broad and spacious labial valley, and three roots.

Comparison and Discussion: The sizes and morphologies of these specimens correspond to the diagnosis for extant chipmunks from the Palaearctic Region. These characters include small size, upper molar protocone not distinctly antero-posteriorly extended, M1 and M2 subquadrate, protoloph and metaloph tending to converge toward the protocone, absence of protoconule and metaconule, and m3 moderately expanded posteriorly with a small mesoconid and a broad and spacious labial valley.

In size, the Yushe specimens approach *Heterotamias sihongensis* (Qiu and Lin, 1986) from the early Miocene Xiacaowan Fauna of Sihong, Jiangsu Province, but they differ in lacking the distinct protoconule and metaconule on M1 and M2, and an M3 that lacks any vestige of a metaloph or metaconule (see Qiu 2015). Morphologically, the Yushe chipmunk shares many similarities with *Tamias wimani* Young, 1927 from the Quaternary of Choukoutien (=Zhoukoudian), and the extant *T. sibiricus,* but the dimensions of the Yushe specimens are slightly smaller and the protoconule and metaconule are less distinct. The Yushe specimen morphology most closely resembles *T. ertemtensis* Qiu 1991 from Ertemte, and Harr Obo, Inner Mongolia, and the size falls within the range of variation for this species. It also matches the sample of *T. ertemtensis* from the early Pliocene Bilike site, Inner Mongolia (Qiu and Storch 2000).

Tamias orlovi (Sulimski, 1964) from the Pliocene of Poland and *T. urialis* (Munthe, 1980) from the middle Miocene Siwaliks of Pakistan differ from the Yushe chipmunk in that *T. orlovi* has a distinct M1 and M2 mesostyle, and *T. urialis* is slightly smaller with a metaloph that is constricted at the protocone.

The Yushe chipmunk most closely resembles the species from Ertemte in morphology, and as such is probably conspecific with the latter, however, the Yushe sample is small. Moreover, morphology and size of the *Tamias* dentitions recovered from Pliocene sediments of northeast Asia appear very conservative. These isolated teeth from Yushe are assigned to *Tamias* and are considered tentatively to conform to *T. ertemtensis.*

Sciurus Linnaeus, 1758

Sciurus sp.

Material: One left P4 (V 13080), 2.70 × 2.45 mm, from locality YS87 (late Pliocene, Mazegou Fm., 3.4 Ma; Fig. 5.2d).

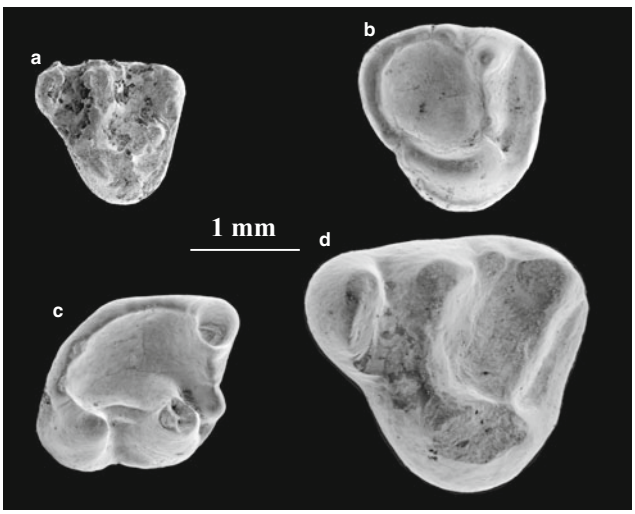

Fig. 5.2 Occlusal view of *Sinotamias* sp. and *Sciurus* sp. from Yushe. *Sinotamias* sp. **a** DP4, V 13079.1; **b** M3, V 13079.2; **c** m1/2, V 13079.3; *Sciurus* sp. **d** P4, V13080

Description: The P4 is subtriangular in shape with low, thick and blunt lophs and cusps. The protocone is robust and slightly elongated anteroposteriorly. The paracone is smaller and lower than the metacone. A well-developed parastyle is anteriorly extended and exceeds one-half the width of the tooth. A small mesostyle is also present. The protoloph and slightly oblique metaloph are complete and lack a protoconule and metaconule, respectively. A posteroloph is continuous but lower than both the protoloph and metaloph.

Discussion: The P4 described above is assigned to the squirrel genus *Sciurus* because its cusps and lophs are low and blunt, the protocone is extended anteroposteriorly, the protoloph and metaloph are continuous and nearly parallel, and a small mesostyle is present. It represents a species of *Sciurus* slightly larger than the living *S. vulgaris*, and differs from it in having a P4 with a more pronounced and anteriorly projected parastyle, and a complete metaloph.

Neogene species of *Sciurus* are poorly recorded in the Holarctic and represented almost exclusively by isolated teeth, frequently considered species indeterminate (see Heller 1930, 1933, 1936; Brunner 1933; Dehm 1962). In Europe, the only named species *S. warthae* is known from the early Pliocene of Węże, Poland. In China, the earliest record of the genus is *S. lii* from the late early Miocene of Shanwang, Shandong. In addition, other indeterminate handfuls of isolated teeth are documented from the Late Miocene of Lantian, Shaanxi, and Ertemte and Harr Obo, Inner Mongolia (Sulimski 1964; Black and Kowalski 1974; Qiu 1991; Qiu and Yan 2005; Qiu et al. 2008). The size of the Yushe P4 is even larger than that of specimens assigned to *S. warthae* from Węże and the indeterminate *Sciurus* sp. from Ertemte and Harr Obo, but the morphology is roughly similar to them, except for displaying a better-developed parastyle that is more anteriorly extended. The Yushe species is easily distinguished from *S. lii* by its stronger parastyle.

Sciurus was also reported from the Pleistocene of Choukoutien (Zhoukoudian) by Pei (1936) and Teilhard de Chardin (1936, 1938), and the late Oligocene of Tabenbuluk by Bohlin (1946), but these citations have been excluded from the genus (see Qiu 1991; Qiu and Yan 2005). "*Sciurus* cf. *davidianus*" and "*?Sciurus* sp." recorded by Pei from Choukoutien Locality 3 and "*Sciurus* sp." recorded by Teilhard de Chardin from Locality 12 (Teilhard de Chardin 1938 synonymized Pei's *S.* cf. *davidianus* with his *Sciurus* sp. from Locality 12) are indeed morphologically similar to the extant *Sciurotamias davidianus* in having nearly elliptical teeth, thick and blunt cusps, protocone well-developed and elongated anteroposteriorly, an indistinct entoconid corner, and a narrow labial valley on lower molars. Systematists currently assign the species *davidianus* to the genus *Sciurotamias* and not *Sciurus*. Consequently, it is believed here that the specimens mentioned above as *Sciurus* cf. *davidianus,* and the other indeterminate species from the Quaternary of Choukoutien, should all be reassigned to *Sciurotamias*. Another adjustment involves "*Sciurus*" sp. from Locality 9 (Teilhard de Chardin 1936) and "?*Sciurus*" sp. from Locality 13 (Pei 1936), which should be transferred to *Tamias* based on having relatively small size, length of lower molar noticeably greater than width, entoconid entirely confluent with posterolophid, and a perfectly rounded entoconid corner.

The Yushe specimen shows some similarities in size and morphology with the P4 from Yuanmou, Yunnan (Qiu and Ni 2006), which is indeterminate at the genus and species level, except for its larger anterostyle, longer anteroloph and slightly curved metaloph.

This late Pliocene YS87 P4 differs from all other Yushe squirrels and any named Chinese taxon. It likely represents a new species of *Sciurus* or a related tree squirrel genus. In view of the single attributed specimen, it is best to assign this Yushe squirrel as an indeterminate species of *Sciurus.*

Sinotamias Qiu, 1991

Sinotamias sp.

Material: Left DP4, right M3, and a right m1/m2 (V 13079.1-3) from locality YS4 (early Pliocene Gaozhuang Fm., 4.3 Ma, Fig. 5.2a–c).

Measurements (mm): DP4: 1.45 × 1.40; M3: 1.70 × 1.65; m1/2: 1.80 × 1.65.

Description: The DP4 is subtriangular with a well-developed parastyle that is distinctly anteriorly projected. The parastyle width is slightly less than half the breadth of the tooth. The protocone is not elongated anteroposteriorly. The paracone is smaller than and located slightly anterior to the protocone. The metacone is nearly equivalent in size and height to the paracone. The continuous protoloph is slightly anteriorly extended, lacks a protoconule, and weakens as it approaches the protocone. The discontinuous metaloph possesses a metaconule, weakens as it approaches the protocone, and does not connect with the metacone. A posteroloph is continuous but extremely low.

The M3 is subrounded and is not very expanded posteriorly. The protocone is anteroposteriorly extended somewhat. The paracone is conical. A metacone is absent. A small mesostyle connects with the paracone. The protoloph is low and nearly complete, maintains an indistinct protoconule, but becomes constricted as it approaches the protocone. A metaloph is absent. The anteroloph is complete and weakly connects with the protocone and anterior margin of the paracone. A posteroloph arises from the posterior margin of the protocone, thickens and curves as a semicircle to connect weakly with the mesostyle. The talon basin is wide, spacious, smooth, and enclosed.

The m1/2 is sub-rhomboidal with robust cusps. The protoconid is the most robust and the metaconid is the highest cusp. The indistinct entoconid is completely

incorporated into the well-developed, curved posterolophid and the entoconid corner is rounded. The lingual wall descends and abuts the metaconid at its base. Absent are a mesoconid and mesostylid. The anterolophid touches the protoconid at a low point, and bears a small anteroconid. The low ectolophid is continuous, directed slightly posterolingually from the protoconid, and turns posterolabially to join the hypoconid. The posterolophid is high and thick, arising from the posterolingual side of the hypoconid and extending continuously but lowering upon reaching the metaconid. The short metalophid is directed lingually from the protoconid to descend and terminate in the talonid basin. The labial valley is short and narrow.

Comparison and discussion: The size of these teeth is comparable to *Tamias* cf. *T. ertemtensis* described above, but the posterior portion of the M3 has a prominent rounded loph that lacks a metacone, the m1/2 has neither an entoconid nor a mesoconid, and the ectolophid is short and firmly joins the hypoconid. These features contrast with the characters of *Tamias,* but are consistent with those of *Sinotamias.*

To date, three species of *Sinotamias* have been named: *S. minutus* Zheng and Li, 1982, from Songshan, Gansu Province, *S. primitivus* Qiu, 1996, from Tunggur, Inner Mongolia, and *S. gravis* Qiu, 1991, from Harr Obo and Ertemte, Inner Mongolia. Both *S. minutus* and *S. gravis* are late Miocene or early Pliocene in age, while *S. primitivus* is middle Miocene. The Yushe specimens are relatively similar to *S. minutus* in their well-developed cusps and lophs, but differ in having slightly lower crowned teeth with relative weakness of the metalophid, the slight height difference between the talonid and trigonid basins, and the anterolabial side of the trigonid basin that tends to be open. Noticeable characters of *Sinotamias gravis* that differ from the Yushe specimens include the larger size, relatively robust cusps and lophs, long metalophid, and a labial valley that extends more distinctly posterolingually. *Sinotamias primitivus* can be distinguished from the Yushe squirrel by its smaller size and more developed metalophid. An indeterminate species of *Sinotamias* was recorded by Zheng and Zhang (2000) from the Pliocene of Lingtai, Gansu, but material from this locality is too scarce to confirm *Sinotamias*. Teilhard de Chardin (1942: 94) noted a squirrel from Yushe that may represent the same species. The few specimens from Yushe do not allow definitive determination at the species level.

Marmota Blumenbach, 1779
Marmota sp.

Marmot remains have been noted as surface finds in Yushe Basin (see Teilhard de Chardin 1942). Marmots are notable as latest Pliocene or younger immigrants from North America (Erbajeva and Alexeeva 2009). Provenance for early finds from Yushe is not clear, and we suspect that some remains are from the early Pleistocene loess. For example, *Marmota* specimen THP 12036 in the Tianjin Museum lists Wangjiagou as its locality, which could indicate derivation from loess or the underlying Gaozhuang Formation. Given that the middle part of the Gaozhuang Formation in this area would be early Pliocene in age, preservation in Pleistocene loess is more likely. THP 12036 is a left dentary fragment with all three molars positioned somewhat *en echelon*, and giving a length of 16 mm for m1-3 (m1 = 4.6 × 5.0, m2 = 5.0 × 5.7, m3 = 6.5 × 6.4 mm).

Modern fossil collections of Yushe Basin appear to demonstrate that *Marmota* was an element of the early Pleistocene Haiyan Formation. A partial skull in the collection of the Yushe County Museum from Xia Chi Yu (Y0131) has dentition on both sides, including large erupting P3 but lacking M3; length of P3-M2 = 18.2 mm. This locality in the Haiyan Formation is an early record for the genus in Yushe Basin, probably greater than 2 Ma.

Marmots from the Yushe Basin are generally called *Marmota robusta*, which is currently considered a synonym of *M. himalayana* (Hodgson, 1841). Some Yushe fossils have been attributed to extant *Marmota bobak,* but identification as *M. himalayana* seems more likely based on modern distributions. The size of Y0131 is at the large end of the range observed for either living species.

5.2.2 Subfamily Pteromyinae Brandt, 1855

Pliopetaurista Kretzoi, 1962
Pliopetaurista rugosa Qiu, 1991

Emended diagnosis: Relatively large with relatively well-developed accessory crests. P4 with a distinct protoconule, and parastyle that is not extremely extended. P4-M2 with a well-developed protocone and hypocone, protocone positioned anteriorly, continuous protoloph and metaloph, extremely strong metaconule that connects to the posteroloph, and well-developed mesostyle crest. Lower molars maintain a conspicuous hypoconulid.

Material: YS8: one broken left maxilla with P3-M3, V 13081.l; YS 2: one left P4, V 13081.2; YS50: one left m1/2 and a posterolateral section of an m1/2, V 13081.3,4; YS90: one right p4 with damaged posterior section, V 13081.5; Shencun village: one damaged right mandible with broken p4, m1-3 (Y0124, kept in the Yushe County Museum); YSl: one left m1, V 13081.6; YS139: one right P4, one right m2, V 13081.7,8; YS170: one damaged m1/2, V 13081.9; YS150: one left M3, V 13081.10; the Yushe County Museum also conserves an unnumbered left jaw fragment with p4, m1-2 from Gaozhuang, a major early Pliocene collecting area. See Fig. 5.3.

Stratigraphic occurrence and age: YSl, YS2, YS8, YS139, YS150, YS170, late Miocene Mahui Fm. (6.3–5.9

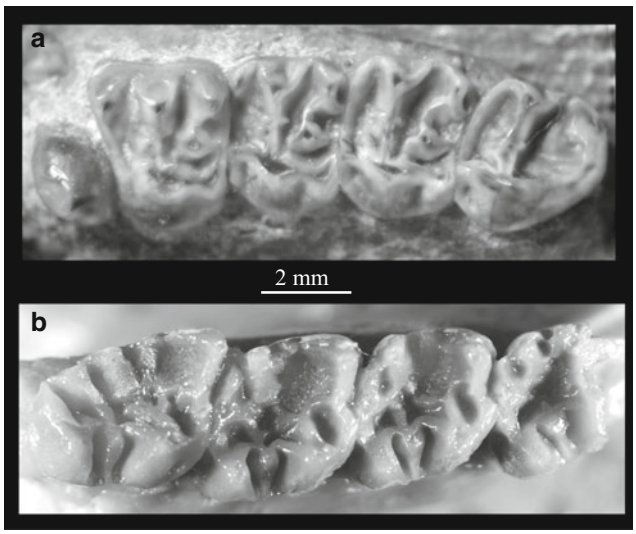

Fig. 5.3 Occlusal view of *Pliopetaurista rugosa* from Yushe. **a** Broken left maxilla with P3-M3, V 13081.l. **b** Damaged right mandible with p4-m3 (Y0124)

Ma); YS50, early Pliocene Gaozhuang Fm., 4.7 Ma; YS90 and the Shencun locality, late Pliocene Mazegou Fm., 3.5 to 3.4 Ma.

Measurements (mm): P3: 1.60 × 2.20; P4: 3.00 × 3.85, 2.80 × 3.45; M1: 2.40 × 3.40; M2: 2.55 × 3.50; M3: 2.80 × 3.15, 2.60 × 2.70; p4: − × 3.00; m1: 2.95 × 3.10; m2: 3.00 × 3.25; m1/2: 2.95 × 3.10, 2.55 × 3.00, 2.75 × 2.95, 2.75 × −; m3: 4.15 × 3.40.

Description: Maxilla and mandible are damaged. The posterior part of P4 lies beneath the posterior margin of the anterior branch of the zygomatic arch. Length of mandibular row of alveolae is approximately 12.4 mm. The masseteric fossa is deep, and the crest, not entirely distinguishable, ends below the posterior root of p4. The deep diastema is about 6 mm long, and a mental foramen is located at its deepest part, anterior to p4.

The P3 is oval with a single cusp that lies in the center of the tooth. A divided crest extends both lingually and labially. Lingually this crest is robust, gradually it descends labially, stretches to the posterior margin, and then recurves to the anterolingual side of the tooth. Labially the crest is extremely weak but is inflated at its terminus.

The P4 is quadrate with its lingual side narrower than the labial side. The cusps and lophs are distinct, with the protocone being the most robust cusp on the tooth, situated anteriorly, and extending slightly anterolabially-posterolingually. The hypocone is the lowest of the major cusps. The paracone and metacone are equivalent in size. At the posterolingual side of the metacone there is a short crest that connects with the posteroloph. The parastyle is prominent, separate from and slightly smaller than the paracone, and not expanded anteriorly. A metastyle is absent but on one P4 there is an extremely small mesostyle. The protoloph and metaloph are weak, the former straight and the latter oblique. The lophs form a V-shape converging at the protocone. A protoconule is small and a metaconule is large with a short posterior crest directed toward the posteroloph. The anteroloph and posteroloph are continuous but lower than the protoloph and metaloph. Short accessory lophs extend anteriorly and posteriorly from the protoloph between the paracone and protoconule. The lingual wall of the tooth is irregular, reflecting terminated wings of the paracone and metacone. There is a shallow anterolingual valley, and a small posterolabial embayment. Three roots are present.

The M1 is rectangular. Similar to the P4, it has distinct cusps and lophs and relatively narrow valleys. The principle cusps are also similar in morphology and arrangement to those of the P4, but the hypocone is relatively more developed. The paracone and metacone are relatively smaller. The parastyle is much less developed than on the P4 and the protoconule is also smaller. The protoloph and metaloph converge at the protocone with the former displaying distinct accessory crests. The anteroloph and posteroloph are less robust than on the P4 but are still continuous. The anteroloph extends nearly to the lingual margin of the tooth and makes a distinct anterior lingual valley with the anterior arm of the protocone. The posteroloph extends to the labial margin of the tooth and with the posterolingual arm of the metacone forms a narrow, open posterolabial valley. A posterolabial wing of the paracone descends labially to a marginal mesostyle, and forms the anterior wall of a deep, open transverse valley that extends to the base of the protocone; this deep transverse valley of the P4, M1-2 is a distinctive feature of the taxon. The mesostyle lies at the mouth of the transverse valley. The M2 is slightly larger than the M1 but displays the same outline, cusp and loph morphology, and arrangement. The hypocone is smaller on M2, absent or indistinct on M3.

The large M3 is expanded posteriorly, with inflation of the metacone. The shape and structure of the trigon is similar to that of the M2, but the protoconule and metaconule are small or indistinct. Both hypocone and metaloph are absent. The metacone is fused with the posteroloph, which sweeps posterolabially from the protocone as a semicircle around the posterior portion of the tooth. A sulcus on the posterior arm of the protocone indicates the position of the undeveloped hypocone and the anterior end of the posteroloph. The enamel in the talon basin is very irregular.

The p4 is triangular with the protoconid and metaconid located closely together but separated by a narrow shallow valley. A distinct anteroconid is absent but a strong crest extends anteriorly from the protoconid to the anterior margin of the tooth. The distinct hypoconid and entoconid are small and lower than the two main anterior cusps. A small mesoconid and short mesolophid are present. A short loph joins the mesoconid to the hypoconid. The mesoconid

possesses two accessory crests, one of which descends to the exterior through the labial valley, the other reaching into the talonid basin. The mesostylid is situated close to the metaconid, with a weak crest between them. A hypoconulid is nearly as well developed as the entoconid, to which it is joined by a crest. The posterolophid is continuous, arising from the hypoconid, passing the hypoconulid and reaching the entoconid. The talonid basin enamel is thick and coarse and the labial valley is wide and deep.

The m1 is subquadrate with the metaconid as the highest cusp; the protoconid is smaller and lower than the metaconid, and the hypoconid and entoconid are subequal but smaller than the protoconid. The metaconid is equidistant from the protoconid and entoconid. The mesoconid and mesostylid are prominent but slightly weaker, compared to those on the p4. The mesoconid possesses an accessory cusp that extends through the talonid basin to connect with the hypoconulid-entoconid crest. The mesostylid also possesses a thick and free labial accessory crest. The degree of development of the hypoconulid and its relationship to the neighboring cusps and crests do not differ from the p4. The protoconid anterior arm joins the metalophid; the protoconid posterior arm abuts the posterolabial extremity of the metaconid. The anterolophid is complete and lacks an anteroconid, although the central part of the anterolophid is swollen, sealing the trigonid basin. A posterolophid is relatively large, comparable to size of the hypoconid and entoconid which join the posterolophid, respectively, labially and lingually. The talonid basin enamel is thick and coarse with well-developed accessory crests.

The m2 is very similar to the m1, such that isolated teeth are difficult to distinguish, but two specimens preserve associated teeth. The m2 is slightly larger, the distance between the protoconid and metaconid is slightly greater, the mesoconid and mesostylid are slightly weaker, and the lingual hypoconulid-entoconid crest is absent.

The m3 is posteriorly lengthened but its hypoconulid is shifted labially and the larger hypoconid, positioned more posteriorly, has a posterolingually-directed posterolophid. The trigonid is similar to that of the m2. The larger entoconid links with the protoconid, and the hypoconulid is elongated anterolabially. The hypoconulid and entoconid are isolated, not joined by the posterolophid. The mesoconid is prominent, and the mesostylid is inflated to cusp size. Accessory crests within the talonid basin are well developed. On the posterior margin of the mesoconid there is an accessory crest that connects to the hypoconulid.

Discussion and comparison: The descriptions above show complete consistency with the dental morphology of *Pliopetaurista* Kretzoi, 1962 (Ref. Mein 1970), a flying squirrel of moderate size with P4 larger than M1, parastyle of P4 separated from paracone, a fundamentally simplified dental structure, dental basins appropriately crenulated, metaloph absent on M3, a V-shaped protoloph and metaloph that meet at the protocone, an extremely large metaconule, upper molars with a mesostyle crest extending from the paracone, lower molars with a mesostylid that is not isolated, and m3 with an accessory cusp resembling a hypolophid.

It is quite evident that this relatively large sciurid cannot be included in the small genera *Hylopetes* Thomas, 1908 or *Blackia* Mein, 1970. It cannot be referred to *Hylopetodon* Qiu, 2002, because of its smaller size, larger P4 relative to M1, better developed hypocone and metaconule of P4-M2, and presence of hypolophid on m3. Its size is consistent with Neogene Old World taxa including *Miopetaurista* Kretzoi, 1962, *Albanensia* Daxner-Hőck and Mein, 1975, *Forsythia* Mein, 1970, *Parapetaurista,* Qiu and Lin, 1986, and *Aliveria* de Bruijn et al., 1980. It also approaches the North American *Petauristodon* Engesser, 1979. Structurally, however, it differs from *Miopetaurista* and *Parapetaurista* by the presence of a robust hypocone, protoloph and metaloph that converge at the protocone, and no anterolabial valley. It differs from *Albanensia* in its relatively smooth enamel and lack of metaloph on the M3. *Forsythia* is distinguished by its P4 being smaller than the M1, a contracted protocone, relatively small hypocone, and M3 possessing posterior crests. *Aliveria* differs greatly from the Yushe flying squirrel in its relatively simple dental structure, resembling the generalized sciurid condition, possessing an isolated mesostyle on upper molars, hypocone being weak or absent, having a metaloph remnant on M3, lacking a hypoconulid on lower molars. *Petauristodon,* the only flying squirrel recognized from the Late Tertiary of North America, was originally referred to as *Sciuropterus* by James (1963) and Lindsay (1972). This genus is easily distinguished from the Yushe material in the relatively weak hypocone and metaconule of P4-M2, its nearly parallel protoloph and metaloph and well developed protolophule, and its lower molars with an isolated mesostylid, but no hypoconulid.

The P4 size and morphology are consistent with the type of *Pliopetaurista rugosa* from Harr Obo, Inner Mongolia. General morphology of the Yushe and Inner Mongolian specimens is basically consistent, with the exception of a slightly smaller M3 in the Yushe sample. Consequently, the Yushe flying squirrel is regarded as conspecific with the Inner Mongolian taxon. *Pliopetaurista rugosa* material from Ertemte, Inner Mongolia, is extremely limited, such that the Yushe specimens greatly increase the knowledge of this species. The Yushe sample not only verifies the generic allocation, but also advances supplementary observations to confirm the diagnostic characters for this species.

Another named species of *Pliopetaurista*, *P. speciosa* and an indeterminate species were recorded from the Late Miocene of Leilao, Yuanmou, Yunnan (Qiu and Ni 2006). The

Yushe flying squirrel differs from them in better developed accessory crests on the basins and larger mesoconid on lower molars. *P. speciosa* is also smaller than *P. rugosa*.

In addition to the Chinese species of *Pliopetaurista* there are several European species including *P. bressana* Mein, 1970; *P. dehneli* Sulimski, 1964; *P. pliocaenica* Deperet, 1893; and *P. meini* Black and Kowalski, 1974. *P. rugosa* differs from *P. bressana* in being relatively larger, P4-M2 with relatively well developed hypocone, a continuous metaloph, lower molars with hypoconulid, and relatively distinct accessory crests within the dental basins. The late Miocene-early Pliocene Chinese form differs from *P. dehneli* (MN14) in its conspicuous protocone and hypocone, and in p4-m3 with strong hypoconulid and relatively well developed accessory crests. *Pliopetaurista rugosa* approaches *P. pliocaenica* in size and shares several morphologic characters such as a pronounced protocone and hypocone on P4-M2, a hypoconulid on lower molars, and other features. The Chinese species differs, however, in possessing a parastyle on P4 that does not extend as far anteriorly, in its protocone on P4-M2 being situated more anteriorly, the metaconule in contact with the posteroloph, and the relatively distinct hypoconulid on lower teeth. *Pliopetaurista rugosa* may be readily distinguished from *P. meini* by its conspicuous accessory crests and the well developed continuous protoloph and metaloph on P4-M2.

Based upon the conclusions of Mein (1970, p. 42) regarding *Pliopetaurista, P. rugosa* is clearly more derived than the European late Miocene *P. bressana* (Turolian, MNl l) because it is larger, the m3 is posteriorly extended, and it possesses distinct hypocones and mesostyles on P4-M2 and hypoconulids on the lower molars. Based on morphology and size *P. rugosa* most closely resembles European Pliocene *P. pliocaenica* (MN15), but its parastyle does not extend as far anteriorly on P4, molars lack a parastyle, and the metaconule is still connected to the posteroloph, all of which indicate that *P. rugosa* retains some primitive characters compared to *P. pliocaenica.* Overall, *P. rugosa* and *P. pliocaenica* display a similar stage of evolution.

Hylopetes Thomas, 1908

Hylopetes yuncuensis sp. nov.

Holotype: Left m1/2 (V 13077), 2.05 mm × 1.80 mm Fig. 5.4f.

Type Locality: YS4, 1.7 km ENE of Zhaozhuang, Yushe, Shanxi Province; early Pliocene Culiugou Member, Gaozhuang Fm., 4.3 Ma.

Etymology: Contemporary Chinese for the region producing the type specimen.

Diagnosis: Small-sized species of *Hylopetes*. M1-2 with protocone not extended greatly anteroposteriorly, and without a mesoloph. Lower m1-2 with entoconid moderately merged with the posterolophid, obtuse entoconid corner, interrupted metalophid, small mesoconid and mesostylid, a deep notch between the entoconid and the mesostylid, and the anterolophid joining the protoconid at a low position; m3 not greatly posteriorly expanded.

Referred specimens: YS8: left DP4 and anterior half of right m2 (V 13078.1, 2); YS50: right P4 and left half of M1/2 (V 13078.3, 4); YS97: right dp4, (V 13078.5); YS4: left M3 with broken protocone, and a left m3 (V 13078.6, 7); YS90: left m1/2, its enamel nearly completely corroded away (V 13078.8); YS87: right M1/2 with broken labial side (V 13078.9). See Fig. 5.4.

Stratigraphic range and age: YS8, late Miocene Mahui Fm., 6.3 Ma; YS50, YS97, YS4, early Pliocene Gaozhuang Fm., 4.7-4.3 Ma; Y S90, YS87, late Pliocene Mazegou Fm., 3.4 Ma.

Measurements (mm): DP4: 1.55 × 1.60; P4: 1.90 × 1.95; M1/2: 1.85 × −, − × 2.25; M3: 2.20 × −; dp4: 1.60 × 1.25; m3: 2.15 × 2.00.

Description: The DP4 parastyle is lophate, and its anterior projection gives the tooth a subtriangular shape. The protocone is robustly conical and situated mediolingually. The paracone and metacone are equivalent in size and much lower and smaller than the protocone. The protoloph and metaloph are continuous, thick, blunt, and nearly parallel. No protoconule or metaconule are visible. As the metaloph approaches the protocone it becomes extremely attenuated. The anteroloph is crescentic in shape, running from the paracone, through the parastyle, to the center of the protoloph. The complete posteroloph extends from the protocone and descends rapidly to the labial margin of the tooth. Both the anteroloph and posteroloph are lower and weaker than the protoloph and metaloph. A mesostyle is indistinct.

The morphology of the P4 is generally similar to that of the DP4 but the anteroloph is relatively long and hence the outline of the tooth is not as conspicuously triangular as DP4. An extremely small mesostyle is present. There are three roots: a robust lingual root and two small labial roots.

The M1 and M2 cusps and lophs are relatively low and blunt. The protocone is slightly extended anteroposteriorly. The protoloph and metaloph are continuous, with the former transverse and the latter slightly anterolingually inclined, thinning and lowering as it approaches the protocone. Both lophs become confluent at the protocone. Protoconule and metaconule are absent.

The M3 is moderately expanded posteriorly with a broad basin circled by a crest from the protocone to the paracone. The protoloph is continuous, but a protoconule, metacone, and metaloph are absent.

The dp4 is trapezoidal. The metaconid is the largest and highest cusp. The protoconid is distinctly separated from the metaconid, and is positioned relatively posteriorly. The hypoconid is slightly higher and more conspicuous than the protoconid. The loph connecting the hypoconid to the

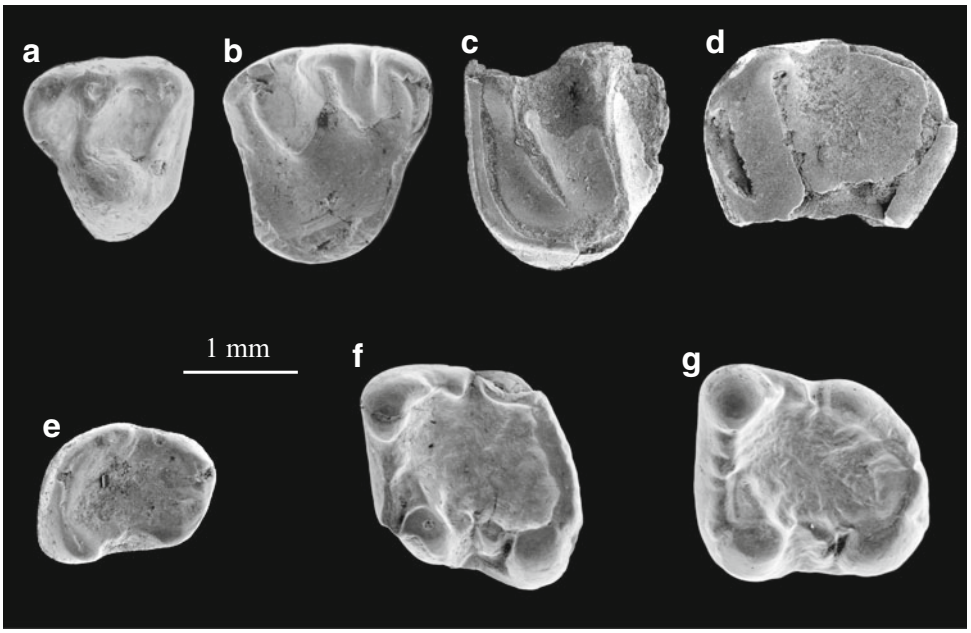

Fig. 5.4 Occlusal view of *Hylopetes yuncuensis* sp. nov. from Yushe. **a** DP4, V 13078.1; **b** P4, V 13078.3; **c** M1/2, V 13078.9; **d** M3, V 13078.6; **e** dp4, V 13078.5; **f** m1/2, holotype, V 13077; **g** m3, V 13078.8

entoconid is rather high and well developed. The ectolophid is low and weak. Neither anteroconid nor distinct mesoconid are present. The labial valley is broad and shallow.

The m1/2 is sub-quadrangular with rather blunt cusps and lophs. The metaconid is highest and sharply pointed. The heights and sizes of the protoconid and hypoconid are nearly equivalent, slightly less than the metaconid. The entoconid is smaller than the other cusps, and the entoconid corner forms an obtuse angle. The anterolophid is low, directed labially from the metaconid to terminate freely anterior to the protoconid and short of the labial tooth margin. The ectolophid is low and narrow, but bears a small mesoconid. The low metalophid is very short, ending at the midpoint of the anterolophid, thus failing to close the high trigonid basin. A small mesostylid is present, which is connected to the metaconid by a short crest but separated from the entoconid by a narrow valley. The talonid basin is broad with finely rugose enamel, and the labial valley is wide and shallow. Four roots are present.

The m3 is larger but not greatly expanded posteriorly, and the posterior half of the tooth is nearly as broad as the anterior half. The protoconid and metaconid are large, the hypoconid is low and gently rounded, the entoconid is smaller than the hypoconid and placed slightly anterior relative to the hypoconid. The morphology and structure of the lophs and cusps in the anterior half are similar to those on anterior molars. The thick, continuous posterolophid unites the entoconid and hypoconid. A mesoconid and small mesostylid are present. There is a small and narrow trigonid basin. The enamel of the talonid basin is rugose. Three roots are present, two anterior and a fused posterior root complex.

Comparison and discussion: The teeth described above resemble those of *Tamias* and *Spermophilinus*, but they display several distinguishing characters. In comparison with the corresponding teeth of *Tamias*, these specimens are larger, cusps and lophs are commonly lower, the upper molar protocone is relatively anteroposteriorly elongated, the protoloph and metaloph are more parallel and completely lack a protoconule and metaconule, and the lower molars have a rather delimited entoconid and well developed mesoconid and mesostylid. They are different from those of *Spermophilinus* in having more parallel arrangement of protoloph and metaloph, and metaloph less contracted at the protocone on M1 and M2, and in having a distinct entoconid and mesostylid with deep notch between them, and higher position of the anterolophid at the protoconid on m1 and m2. The differences from *Tamias* and *Spermophilinus* are similarities with *Hylopetes*, *Sciurus*, and *Palaeosciurus* Pomel, 1853. The Yushe taxon differs from Recent *Sciurus vulgaris*, as well as the indeterminate species of the genus from Lantian, Ertemte and Harr Obo of Late Neogene age, in its smaller size, relatively thinner and blunt cusps and lophs, less anteroposteriorly extended protocone, protoloph and metaloph less parallel, the m1 and m2 less quadrate with more obtuse entoconid corner and less distinct notch between the entoconid and the mesostylid, and the m3 less posteriorly expanded with narrow trigonid basin. These differences from *Sciurus* correspond to characters shared

with *Palaeosciurus* and *Hylopetes* (especially size), the M1/2 with less extended protocone, less blunt protoloph not parallel to metaloph, the absence of protoconule on upper molars, the m1/2 with more obtuse entoconid corner, more conspicuous mesoconid and a deep notch between the entoconid and mesostylid, and the finely rugose enamel of the talonid (Dehm 1950; Vianey-Liaud 1974; Ziegler and Fahlbusch 1986; Bouwens and de Bruijn 1986). However, these specimens cannot be referred to the genus *Palaeosciurus* mainly because of the less expanded protocone, the more parallel arrangement of protoloph and metaloph and absence of a metaconule (or of the metaloph being constricted in the vicinity of a metaconule), and the less pronounced entoconid on m1/2. In addition, the Yushe specimens show some similarities to those of the extant *Tamiasciurus hudsonicus* of North America in morphology, such as the blunt cusps and lophs, the more or less extended protocone, the presence of distinct entoconid, mesoconid and mesostylid, and the moderately expanded M3 and m3. Nevertheless, *T. hudsonicus* is larger in size with prominent mesostyles on the upper cheek teeth, and pronounced mesostylids on the lower ones. Additionally, the protoloph and metaloph of *T. hudsonicus* are more parallel. The small size and the combined characters of these teeth (brachydonty, low and blunt cusps and lophs, nearly quadrilateral outline of M1/2 and m1/2, the constricted protocone and sub-parallel protoloph and metaloph bearing no protoconule and metaconule on M1/2, the delimited entoconid, the pronounced mesoconid and mesostylid, the angular entoconid corner on m1/2, and the finely wrinkled enamel on the basins) tend to ally this squirrel with *Hylopetes* rather than *Palaeosciurus* or *Tamiasciurus*. *Hylopetes* (=*Petinomys*) is an extant pteromyine genus with dental pattern of generalized squirrels. The teeth in the Yushe collection resemble those of *H. phayrei* (=*Petinomys electilis*) from Hainan, China, rather than other extant species of this genus from South Asia, such as *H. genibarbis* and *H. sagitta*, due to size, absence of a short mesoloph on M1/2, and less distinct mesoconid on lower cheek teeth (see Bouwens and de Bruijn 1986). Fossil *Hylopetes* are known as *H. auctor* from Ertemte and Harr Obo and *H. hungaricus* and *H. macedoniensis* from Europe (Black and Kowalski 1974; Daxner-Hőck 1975; Bouwens and de Bruijn 1986; Qiu 1991). In view of the morphological differences of these teeth from those of the known species, the Yushe specimens are treated as a new species of *Hylopetes*.

The Yushe *Hylopetes yuncuensis* sp. nov. is larger than *H. auctor* in size, with stronger cusps and lophs on cheek teeth. It is close to *H. hungaricus* in size, but differs from the European species in the absence of a mesoloph on M1/2 and in having a less developed metalophid on m1/2. The new species is smaller than *H. macedoniensis* and differs from it in having a less labially constricted metaloph on M1/2, the anterolophid less separated buccally from the protoconid on m1/2, a less posteriorly expanded m3, and more sculpted enamel surface in lower molar basins.

In early stages of description, the Yushe material was thought to be assignable to the genus *Tamiasciurus* and the author considered naming it *Tamiasciurus yusheensis*, now nomen nudum. Qiu and Storch (2000) compared specimens from Bilike, Inner Mongolia, with the unpublished Yushe fossils, using the invalid name. That assignment should be corrected and the Bilike squirrel should be reallocated as *Hylopetes yani* Qiu and Li, 2016. It differs from *H. yuncuensis* in its slightly smaller size and in having a complete metalophid enclosing the trigonid on m1 and m2.

5.3 Conclusion

Five species of sciurids described above were retrieved by screening from the Mahui, Gaozhuang, and Mazegou formations. Based on faunal composition, the biochronologic ages of these formations correspond to late Baodean, Gaozhuangian and Mazegouan Chinese Neogene Land Mammal Stage/Age (Qiu et al. 2013). Among these squirrels, three taxa, *Tamias* cf. *T. ertemtensis, Pliopetaurista rugosa,* and *Hylopetes yuncuensis* sp. nov. occurred in more than one formation. Age determinations by magnetostratigraphy indicate that the age range of cf. *Tamias ertemtensis* was 6.2 to 4.7 Ma, and that the latter two taxa span about 3 million years, 6.3 to 3.4 Ma. These are minimum observed ranges. Because the Yushe fossil sample is small, and due to the extremely conservative nature of the sciurid dentition, evolutionary trends cannot be observed *vis a vis* stratigraphic relationship. Evolutionary estimates are thereby influenced by the limitations on collections and past taphonomic conditions. The relative paucity of *Sinotamias* sp. (three teeth) and *Sciurus* sp. (single specimen) fossils from the Gaozhuang and Mazegou formations, respectively, may be in keeping with their limited use in age determination. However, a morphological comparison of *Pliopetaurista rugosa* with known European species of the genus gives a clear evolutionary grade consistent with early Pliocene age for the Chinese taxon. The Yushe chipmunk, close to *Tamias ertemtensis*, otherwise known for the latest Miocene and Early Pliocene of Inner Mongolia, also suggests late Miocene to early Pliocene age.

Squirrels are not common in the Pleistocene deposits of Yushe Basin. This is certainly, in part, a sampling artifact. Teilhard de Chardin (1942) does note a Yushe squirrel of Plio-Pleistocene age that appears to be a ground squirrel. Yushe Basin fossil *Marmota* is discussed briefly here. Generally from old collections, the *Marmota* fossils have poor provenance but a few specimens appear to indicate discovery in the Haiyan Formation, and suggest that by the early Pleistocene, climatic changes were underway in the

Yushe area, which would include loss of extensive tree habitat and the spread of grasslands. Indeed, no tree squirrels are known from the Pleistocene deposits of Yushe.

Among the older Yushe sciurids are two flying squirrel species, one tree squirrel species, one chipmunk species, and one ground squirrel species (resembling extant rock squirrels). These five taxa represent several habitats, with the flying and tree squirrels being arboreal and demanding some extent of tree cover, the chipmunk indicating cover of at least dense thickets, and rock squirrels tolerating partly vegetated rock exposures. The presence of chipmunks, flying squirrels and tree squirrels, indicates that the Yushe Basin was partly forested at that time.

In China, Late Neogene localities producing numerous fossil sciurids include Sihong, Jiangsu (early Miocene); Tunggur, Inner Mongolia (middle Miocene); Lufeng and Yuanmou, Yunnan (late Miocene); and Ertemte (late Miocene), Harr Obo and Bilike (early Pliocene), Inner Mongolia. The Yushe sciurids are more similar to those of Ertemte and Harr Obo, and secondarily to Lufeng. The Lufeng fauna contains numerous arboreal elements (Qiu 2002) including *Callosciurus*, *Tamiops*, and *Dremomys*, which suggest a quite distinct tropical or subtropical environment. Three Yushe genera co-occur at Ertemte and Harr Obo, strongly suggesting chronological similarity as well as biogeographical affiliation. These two Inner Mongolian faunas contain an element that is absent at Yushe, the genus *Prospermophilus* which is representative of semi-arid grassland (Qiu and Storch 2000). Also, ground squirrels and chipmunks predominate in Inner Mongolia, whereas at Yushe the situation differs relatively by the predominance of arboreal sciurids. This discrepancy highlights the ecological distinctions between the two areas: Inner Mongolian Ertemte and Harr Obo faunas indicate open habitat comparable to modern grasslands, while the Yushe faunas indicate a more forested habitat.

Acknowledgements Sincere thanks are due reviewers, especially Everett Lindsay and Yuri Kimura, whose careful efforts led to improving this chapter.

References

Black, C. C., & Kowalski, K. (1974). The Pliocene and Pleistocene Sciuridae (Mammalia, Rodentia) from Poland. *Acta Zoologica Cracoviensia, 30,* 461–486.

Bohlin, B. (1946). The fossil mammals from the Tertiary deposit of Tabenbuluk, western Kansu. Part II: Simplicidentata, Carnivora, Artiodactyla, Perissodactyla, and Primates. *Palaeontologia Sinica, New Series, C5,* 1–259.

Bouwens, P., & de Bruijn, H. (1986). The flying squirrels *Hylopetes* and *Petinomys* and their fossil record. *Koninklijke Nederlandse Akademie van Wetenschappen Proceedings, B89,* 113–123.

Brunner, G. (1933). Eine präglaziale Fauna aus dem Windloch bei Sackdilling (Oberpfalz). *Neues Jahrbuch für Geologie und Paläontologie. Abhandlungen, B71,* 303–328.

de Bruijn, H. (1998). Vertebrates from the Early Miocene lignite deposits of the opencast mine Oberdorf (Western Styrian Basin, Austria): 6. Rodentia 1 (Mammalia). *Annalen des Naturhistorischen Museums in Wien, 99A,* 99–137.

de Bruijn, H. (1999). Superfamily Sciuroidea. In G. Rőssner & K. Heissig (Eds.), *The Miocene land mammals of Europe* (pp. 271–280). München: Verlag Dr. Friedrich Pfeil.

de Bruijn, H., van der Meulen, A. J., & Katsikatsos, G. (1980). The mammals from the Lower Miocene of Aliveri (Island of Evia, Greece). Part 1. The Sciuridae. *Koninklijke Nederlandse Akademie van Wetenschappen Proceedings, B83,* 214–261.

Dehm, R. (1950). Die Nagetiere aus dem Mittel-Miozän (Burdigalium) von Wintershof-West bei Eichstätt in Bayern. *Neues Jahrbuch für Mineralogie, Geologie und Paläontologie, Abhandlungen, B91,* 321–428.

Dehm, R. (1962). Altpleistozäne Säuger von Schernfeld bei Eichstätt in Bayern. *Mitteilungen der Bayerische Staatssammlung für Paläontologie und Historische Geologie, 2,* 17–61.

Engesser, B. (1979). Relationships of some insectivores and rodents from the Miocene of North America and Europe. *Carnegie Museum Bulletin, 14,* 1–64.

Erbajeva, M. A., & Alexeeva, N. V. (2009). Pliocene-Recent Holarctic marmots: Overview. *Ethology, Ecology & Evolution, 21,* 339–348.

Heller, F. (1930). Eine Forest-Bed-Fauna aus der sackdillinger Höhle (Oberfalz). *Neues Jahrbuch für Mineralogie, Geologie und Paläontologie, Abhandlungen, 63,* 247–293.

Heller, F. (1933). Ein Nachtrag zur Forest-Bed-Fauna aus der Sackdillinger Höhle (Oberpfalz). *Centalblatt für Mineralogie, Geologie und Paläontologie, B1,* 60–68.

Heller, F. (1936). Eine oberpliozäne Wirbeltierfauna aus Rheinhessen. *Neues Jahrbuch für Mineralogie, 76,* 99–160.

James, G. T. (1963). *Paleontology and nonmarine stratigraphy of the Cuyama Valley Badlands, California* (Vol. 45, pp. 1–45). University of California Publications in Geological Science.

Lindsay, E. (1972). *Small mammal fossils from the Barstow Formation, California* (Vol. 93, pp. 1–104). University of California Publications in Geological Science.

Mein, P. (1970). Les Sciuroptères (Mammalia, Rodentia) Néogènes d'Europe Occidentale. *Géobios, 3,* 7–77.

Munthe, J. (1980). Rodents of the Miocene Daud Khel Fauna, Mianwali District, Pakistan. Part I. Sciuridae, Gliridae, Ctenodactylidae, and Rhizomyidae. *Milwaukee Public Museum Contributions in Biology and Geology, 34,* 1–36.

Pei, W. C. (1936). On the mammalian remains from Locality 3 at Choukoutien. *Palaeontologia Sinica, C, 7*(5), 1–120.

Qiu, Z.-X., Qiu, Z.-D., Deng, T., Li, C.-K., Zhang, Z.-Q., Wang, B.-Y., et al. (2013). Neogene land mammal stages/ages of China: Toward the goal to establish an Asian land mammal stage/age scheme. In X. Wang, L. J. Flynn, & M. Fortelius (Eds.), *Fossil mammals of Asia – Neogene biostratigraphy and chronology* (pp. 29–90). New York: Columbia University Press.

Qiu, Z.-D. (1991). The Neogene mammalian faunas of Ertemte and Harr Obo in Inner Mongolia (Nei Mongol), China – 8. Sciuridae (Rodentia). *Senckenbergiana lethaea, 71,* 223–255.

Qiu, Z.-D. (2002). Sciurids from the Late Miocene Lufeng hominoid locality, Yunnan. *Vertebrata PalAsiatica, 40,* 177–193 (in Chinese).

Qiu, Z.-D. (2015). Revision and supplementary note on Miocene sciurid fauna of Sihong, China. *Vertebrata PalAsiatica, 53,* 219–237 (in Chinese).

Qiu, Z.-D., & Li, Q. (2016). Neogene rodents from central Nei Mongol, China. *Palaeontologia Sinica 198*, New Series C30, 1–684. Beijing: Science Press.

Qiu Z.-D., & Lin, Y.-P. (1986). The Middle Miocene vertebrate fauna from Xiacaowan, Sihong, Jiangsu Province – 5. Sciuridae. *Vertebrata PalAsiatica*, *24*, 191–205 (in Chinese).

Qiu, Z.-D., & Storch, G. (2000). The early Pliocene micromammalian fauna of Bilike, Inner Mongolia, China (Mammalia: Lipotyphla, Chiroptera, Rodentia, Lagomorpha). *Senckenbergiana lethaea, 80,* 173–229.

Qiu, Z.-D., & Yan, C.-L. (2005). New sciurids from the Miocene Shanwang Formation, Linqu, Shandong. *Vertebrata PalAsiatica, 43,* 194–207.

Qiu, Z.-D., & Ni, X.-J. (2006). Small mammals. In G.-Q. Qi & W. Dong (Eds.), *Origin of early humans and environmental background, Monograph II, Lufengpithecus hudienensis site* (pp. 113–129). Beijing: Science Press.

Qiu, Z.-D., Zheng, S.-H., & Zhang, Z.-Q. (2008). Sciurids and zapodids from the Late Miocene Bahe Formation, Lantian, Shaanxi. *Vertebrata PalAsiatica, 46,* 111–123.

Sulimski, A. (1964). Pliocene Lagomorpha and Rodentia from Węże-l (Poland). *Acta Palaeontologia Polonica, 9,* 149–224.

Tedford, R. H., Flynn, L. J., Qiu, Z.-X., Opdyke, N. D., & Downs, W. R. (1991). Yushe Basin, China: Paleomagnetically calibrated mammalian biostratigraphic standard for the Late Neogene of eastern Asia. *Journal of Vertebrate Paleontology, 11,* 519–526.

Teilhard de Chardin, P. (1936). Fossil mammals from Locality 9 of Choukoutien. *Palaeontologia Sinica, C, 7*(4), 1–63.

Teilhard de Chardin, P. (1938). The fossils from Locality 12 of Choukoutien. *Palaeontologia Sinica New Series, C5,* 1–49.

Teilhard de Chardin, P. (1942). New rodents of the Pliocene and Lower Pleistocene of North China. *Publications de l'Institut Géobiologie, Pékin, 9,* 1–101.

Vianey-Liaud, M. (1974). *Palaeosciurus guti* nov. sp., écureuil terrestre de l'Oligocène moyen du Quercy. Données nouvelles sur l'apparition des Sciuridés en Europe. *Annales de Paléontologie (Vertébrés), 60,* 103–122.

Young, C. C. (1927). *Fossile Nagetiere aus Nord-China. Palaeontologia Sinica, 3*(3), 1–82.

Zheng, S.-H., & Li, Y. (1982). Lagomorpha and Rodentia from Locality 1, Songshan, Tianzhu, Gansu Province. *Vertebrata PalAsiatica, 20,* 35–45 (in Chinese).

Zheng, S.-H., & Zhang, Z.-Q. (2000). Late Miocene-Early Pleistocene micromammals from Wenwanggou of Lingtai, Gansu, China. *Vertebrata PalAsiatica, 38,* 58–71 (in Chinese).

Ziegler, R., & Fahlbusch, V. (1986). Kleinsäuger-Faunen aus der basalen Oberen Süßwasser-Molasse Niederbayerns. *Zitteliana, 14,* 3–80.

Chapter 6
The Beavers (Castoridae) of Yushe Basin

Xiaofeng Xu, Qiang Li, and Lawrence J. Flynn

Abstract We review the systematics and key features of the fossil beavers of Yushe Basin, which encompass much of the taxonomic diversity of Late Neogene Castoridae in China. Larger samples now available reduce some of the diversity that was apparent previously. For example, the North American genus *Eucastor* is no longer recognized in the Yushe Group; specimens previously considered to represent that genus are attributed to *Trogontherium* and *Sinocastor*. Modern fieldwork improves our understanding of provenance and allows discernment of biostratigraphic patterns. The Yushe Basin deposits are characterized by long lineages of the aquatic beavers *Dipoides* and *Sinocastor*, the latter being very close to living beavers and considered a subgenus of *Castor* herein. The older (late Miocene) levels of Yushe Basin contain a species of *Dipoides* that can be distinguished from the form that characterizes Pliocene age deposits. *Castor* (*Sinocastor*) shows a different pattern; there are perhaps two Miocene representatives, with one persisting through the Pliocene as a long lived lineage. The large castoroidine *Trogontherium* appears in the Pleistocene Haiyan Formation, late in the record of Yushe Basin.

Keywords Yushe Basin • Castoridae • North China • Late Neogene • Beavers

6.1 Introduction

Beavers from the Yushe Basin, five species and three genera, comprise a large portion of the known fossil beaver diversity of the late Cenozoic of China (Xu 1994). They include *Trogontherium cuvieri*, *Dipoides anatolicus*, *Dipoides majori*, *Castor* (*Sinocastor*) *zdanskyi*, and *Castor* (*Sinocastor*) *anderssoni*.

The Yuncu subbasin stratigraphic sections, tied by lithological, superpositional, and paleomagnetic evidence, traverse the Mahui Formation, Gaozhuang Formation, Mazegou Formation, and Haiyan Formation, and all yield beavers. The Mahui Formation is late Miocene in age (6.5 to 5.8 Ma), the Gaozhuang and Mazegou formations range from the end of the Miocene through most of the Pliocene Epoch (5.7 to 2.9 Ma), and the Haiyan Formation falls in the early Matuyama magnetic chron, therefore between about 2.6 and 2.2 Ma (Tedford et al. 1991, ages adjusted to time scale of Cande and Kent 1995), and considered early Pleistocene.

The occurrences of the fossil beavers are found to have biostratigraphic importance. *Dipoides anatolicus* occurs in the Mahui Formation, but it is uncertain whether the species survived into Pliocene time. *Dipoides majori* characterizes the Gaozhuang and Mazegou formations. *Sinocastor zdanskyi* is found in the Mahui Formation, and *Sinocastor anderssoni* has a long stratigraphic range, being encountered in the Mahui, Gaozhuang, and Mazegou formations. *Trogontherium cuvieri*, found in the Haiyan Formation, is a Pleistocene age hallmark for North China.

Abbreviations

AMNH The American Museum of Natural History, New York

X. Xu (✉)
Shuler Museum, Southern Methodist University, Dallas, TX 75275, USA
e-mail: xu2005xiaofeng@gmail.com

Q. Li
Key Laboratory of Vertebrate Evolution and Human Origins of Chinese Academy of Sciences, Institute of Vertebrate Paleontology and Paleoanthropology, 142 Xizhimenwai Ave., Beijing 100044, People's Republic of China
e-mail: liqiang@ivpp.ac.cn

L.J. Flynn
Department of Human Evolutionary Biology, and the Peabody Museum of Archaeology and Ethnology, Harvard University, Cambridge, MA 02138, USA
e-mail: ljflynn@fas.harvard.edu

Lawrence J. Flynn and Wen-Yu Wu (eds.), *Late Cenozoic Yushe Basin, Shanxi Province, China: Geology and Fossil Mammals, Volume II: Small Mammal Fossils of Yushe Basin*, Vertebrate Paleobiology and Paleoanthropology,
DOI 10.1007/978-94-024-1050-1_6

F:AM	Specimen number prefix for Frick Collection of the AMNH
IVPP	Institute of Vertebrate Paleontology and Paleoanthropology, Academia Sinica, Beijing, People's Republic of China
IVPP V	IVPP specimen number; other numbers noted in brackets are previously used specimen numbers, sometimes published
IVPP RV	Revised specimen number, replacing numbers formerly used
QY	Field numbers for Yushe Basin collections made by Zhan-Xiang Qiu, 1979−1981
THP	Prefix for specimen numbers of the Tianjin Natural History Museum
YM	Field number prefix, Yushe Mammal
YS	Field locality number, Yushe Site

All specimens recovered by the Sino-American project, and many collected previously are housed in IVPP. Terminology for describing beaver dental morphology follows Stirton (1935), Woodburne (1961), and Xu (1994), and beaver size classes are those of Xu (1994, 1996). Biochronology follows Qiu et al. (2013).

6.2 Systematics

Family Castoridae Hemprich, 1820
Subfamily Castorinae Hemprich, 1820
Castor Linnaeus, 1758
Castor (*Sinocastor*) *anderssoni* (Schlosser, 1924)

1924 *Chalicomys anderssoni*, Schlosser, pp. 22−27, pl. II.
1931 *Chalicomys broilii*, Teilhard & Young, pp. 4−8, Fig. 1, pl. I.
1934 *Sinocastor anderssoni*, Young, pp. 57−58.
1934 *Sinocastor broilii*, Young, pp. 57−58.
1935 *Castor anderssoni*, Stirton, pp. 447.
1942 *Sinocastor anderssoni*, Teilhard de Chardin, pp. 4−8, Figs. 4−10.
1942 *Eucastor youngi,* Teilhard de Chardin, pp. 14−16, Fig. 13.
1994 *Castor anderssoni*, Xu, pp. 87−88.
1994 *Eucastor youngi*, Xu, pp. 83−84.
2010 *Sinocastor anderssoni*, Rybczynski et al., pp. 10−11.

Type Series: A collection of cranial and mandibular material from Ertemte, Inner Mongolia (late Baodean age) was used by Schlosser to characterize the species, and Stirton (1935) designated the right jaw THP 30.723 from Yushe as lectotype.

Lectotype: IVPP V 10474 (THP 30.723), fragmentary right dentary with p4m1-3, Fig. 6.1. Teilhard de Chardin (1942) lists specimens for the Pliocene of Yushe Basin.

Referred material: IVPP V 10475 (19.897), right dentary fragment with p4m1-3; IVPP V 10476, fragmentary skull with all cheek teeth except left P4 from Gaozhuang, Yushe (Fig. 6.1b); IVPP V 10483 (QY116), right M1 or M2 purchased from Haobei, Yushe; IVPP V 2650, left dentary fragment with m1-2 purchased from Yushe in 1955, horizon unknown. Also, Tianjin Museum material under the catalogue numbers THP 12038, 12044, 18915, from Wang Jia Gou, Shen Zhuang Cun, and Gaozhuang, all likely Gaozhuang Formation. IVPP V 10471, incomplete skull with full upper dentition from Gaozhuang, Yushe. IVPP V 10462.1-3, isolated right M1/2, right M3 and right m1/2 attributed to the "White Beds" of Zhangcun, Yushe Basin, likely early Pliocene. We note in addition from Shouyang, Shanxi Province, F:AM 64070, mandible with complete lower dentition, F:AM 64072, partial skull with complete upper dentition, F:AM 64074, nearly complete skull with full upper dentition.

Description of mandible and teeth: Medium size beaver with the shape of the rear margin of the palate similar to that of *Castor fiber*. Cheek tooth enamel is smooth, without complex surface folds in occlusal view. Cheek teeth high crowned and with roots initially open, closed and weak in old individuals. The anterior enamel surface of the incisors is weakly convex; large individuals are grooved faintly, but small (young) incisors are not grooved. Hypoflexus is opposite to paraflexus, and hypoflexid inserts between meso- and metaflexids. Hypostriids (-striae) reach or closely approach the crown base, and para-, meso-, and metastriids (-striae) do not reach the base. The anterior branch of the insertion scar of the masseter medialis on the lateral side of the mandible descends ventrally about 1/2 the depth of the mandible below and between p4 and m2 (Fig. 6.1a). The scar is not as strong as in *Sinocastor zdanskyi*. The mental foramen is anterior to the line connecting the anterior basal edge of p4 and the "chin" process of the symphyseal area on the mandible.

Discussion: Skull morphology is known primarily from Baode and Shouyang specimens. Xu (1994) summarized his methodology and determinations that morphometrically the *Sinocastor* skull clustered between specimens of living *Castor fiber* and *Castor canadensis*. For that reason, he synonymized *Sinocastor* with *Castor*. An alternative view could retain *Sinocastor*, but would require utilization of distinct subgenera or genera for *C. fiber* and *C. canadensis*. Chinese *Sinocastor* has the following characteristics: (1) the suture between jugal and maxilla is more posterior than in

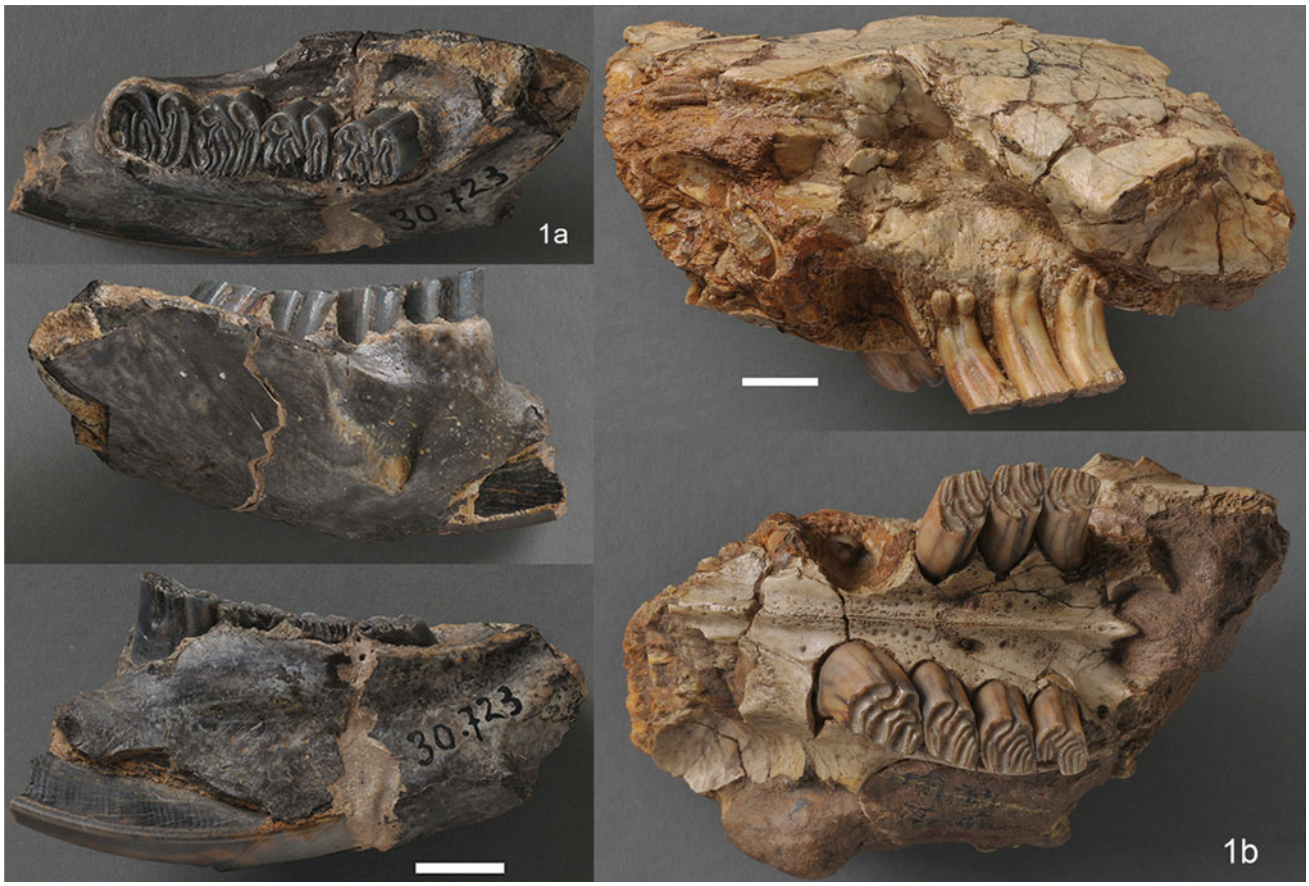

Fig. 6.1 *Sinocastor anderssoni* from Yushe Basin. Figure 6.1a, IVPP V 10474 (30.723), fragmentary right dentary with p4m1-3, exact provenance unrecorded, in occlusal (above), medial (middle), and lateral views; Fig. 6.1b, IVPP V 10476, fragmentary skull with all cheek teeth except left P4 from Gaozhuang, Yushe, in left lateral and occlusal view (Fig. 6.1b). Centimeter scale bars

Castor canadensis, (2) the mental foramen is anterior to the line connecting the anterior base of p4 and the digastric eminence, (3) the shape of the prominent depression in the basioccipital is narrower anteriorly than posteriorly, (4) the posterior margin of the palatine has a short spine rather than the long, thin spine of *C. canadensis* (see Xu 1994).

In these features, *S. anderssoni* more closely resembles European *C. fiber* than American *C. canadensis,* which may reflect relationship (Xu 1994). Troszyñski (1975) considered the shape of nasals, the foramen magnum, the mandible in lateral view, and the interparietal as criteria to distinguish *C. canadensis* from *C. fiber*. Kretzoi (1977) thought that nasal shape was important for distinguishing the two living species. However, all of these characters show individual variations as observed in about ten skulls of *C. canadensis* and five of *C. fiber* (Xu 1994), and they are not stable in either modern species.

Rybczynski et al. (2010) present a new geometric morphometric analysis in which they see the distinction between living beaver species, but *Sinocastor* falls basal to them, not between them. They choose to recognize *Sinocastor* at the generic level, but here we regard *Sinocastor* as a subgeneric lineage of *Castor*, its phylogenetic relationships to other *Castor* species undefined. Under either the (Xu 1994) or the Rybczynski et al. (2010) morphometric analysis, the nomen *Sinocastor* is useful to designate a distinctive Chinese lineage, one that appeared later than the oldest European *Castor* specimens. The scant Miocene material from Europe has not been assessed for morphometric analysis, and whether it is correctly attributed at the genus level remains to be seen. It could represent a taxon basal to other lineages that are lumped currently under the name *Castor*.

The holotype of "*Chalicomys broilii*" from Locality 108 of Baode, V 10472, was synonymized with *S. anderssoni* by Xu (1994). Teilhard de Chardin and Young (1931) also considered the status of the specimen and proposed that it represents the skull of *S. zdanskyi*. The skull is retained under *S. anderssoni* because its smaller size and uncomplicated enamel folds on cheek teeth resemble those features in *S. anderssoni*. We clarify the numbering of this specimen. Originally designated C/9 it is now formally catalogued as V 10472, not V 10471. It is well-illustrated in both Teilhard de

Chardin and Young (1931) and Rybczynski et al. (2010). The number V 10471 applies to a Gaozhuang skull which is included above among Yushe referred material. Correcting Xu (1994), the Gaozhuang specimen should not bear the designation C/9.

Eucastor youngi was based on three isolated teeth that are close in size to *S. anderssoni*, so very large for typical *Eucastor*. With transferal of "*?Eucastor stirtoni*" to *Trogontherium* (Xu 1994), the presence of *Eucastor* in China became arguable. However, Teilhard de Chardin (1942) considered the specimens as similar to geologically older *Eucastor* from North America, and was impressed by the morphology of one tooth in particular (his Fig. 13C). He interpreted this as a lower molar, and therefore considered it derived, but our analysis shows it to be an upper molar consistent with those of *Sinocastor*. The species is therefore a junior synonym, and *Eucastor* is removed from the roster of Yushe beavers.

The first occurrence of *Sinocastor* in China is in the Baode faunas, probably no earlier than 7 Ma (Li et al. 1984; Qiu et al. 2013). Wang (2005) described a much younger lower jaw from Longdan, Gansu, as *Sinocastor anderssoni*. This rich fauna includes many early Pleistocene elements and can be correlated to the earliest Matuyama magnetic chron, approximately the same age as Yushe Haiyan assemblages (which lack *Sinocastor* but contain *Trogontherium*). The Longdan fossil represents a late record of the genus in China, and appears to show a temporal range of over 4 million years for the species.

Castor (*Sinocastor*) *zdanskyi* Young, 1927

1927 *Castor zdanskyi*, Young, pp. 10−11, tafel 1
1934 *Sinocastor zdanskyi*, Young, pp. 57−58
1935 *Castor zdanskyi*, Stirton, pp. 448
1942 *Sinocastor zdanskyi*, Teilhard de Chardin, pp. 8−11, Fig. 11
1994 *Castor zdanskyi*, Xu, pp. 88−90.

Holotype: The type specimen (stored in Paleontology Museum, Uppsala University, Sweden) of this species is from Locality 108 of Baode County, Shanxi.

Referred material: IVPP V 10473 (30.956), right dentary with p4m1-2 from Yinjiaocun, in the Mahui Formation (Fig. 6.2). IVPP RV 42013 (30.721) right dentary with dp4m1-m3 (Teilhard de Chardin 1942, Fig. 18).

Description: Medium size beaver (Xu 1994), skull and upper dentition unknown. Cheek teeth high crowned and weakly rooted, on average somewhat larger than *S. anderssoni* (Table 6.1). Anterior enamel surface of incisors weakly convex and faintly grooved, but angular at lateral edge. Enamel of cheek teeth with complex folds. Hypostriids reach crown base, and para-, meso-, and metastriids nearly reach the base of the crown. Premolar consists of two lobes because mesoflexid and hypoflexid meet in occlusal view. Strong insertion scar on the front branch of the masseter medialis on the lateral side of the mandible below p4-m2, extends ventrally over 3/5 the depth of the dentary, below and between p4 and m1 (Fig. 6.2). Mental foramen anterior to the line connecting the anterior basal edge of p4 and the digastric eminence.

Fig. 6.2 *Sinocastor zdanskyi* from Yushe Basin. IVPP V 10473 (30.956), right dentary with p4m1-2 from Yinjiaocun, in the Mahui Formation; occlusal (above), medial (middle), and lateral views. Scale bar = 1 cm

Discussion: At present, this species is known only by mandibular material. The cheek tooth enamel folds are more complicated, and the muscle insertion scar on the mandible is larger in known specimens of *S. zdanskyi* than in *S. anderssoni*. Specimens of *S. zdanskyi* are marginally larger than those of *S. anderssoni*. These small differences taken together lead some systematists to regard them as two separate species, although they are very close. The morphological features may, however, reflect individual variation or individual age (Xu 1994; our ongoing research). A large

Table 6.1 Measurements (mm) of cheek teeth of *Sinocastor* species in comparison to *Castor fiber* (sample sizes in parentheses)

Measurement	*Castor fiber*	*Sinocastor anderssoni*	*Sinocastor zdanskyi*
Length of p4	8.1–11.2 (12)	9.2–12.3 (9)	12.1
Width of p4	6.5–9.5 (12)	7.3–9.3 (9)	7.5
Length of m1	8.0–9.9 (8)	7.0–8.9 (12)	8.6–9.8 (2)
Width of m1	7.8–9.8 (8)	7.3–9.7 (12)	8.2–10.2 (2)
Length of m2	7.9–9.4 (8)	7.3–8.8 (11)	8.7–9.9 (2)
Width of m2	7.4–8.7 (8)	7.4–10.0 (11)	8.7–10.3 (2)
Length of m3	7.2–8.6 (6)	6.6–8.2 (7)	9.3
Width of m3	6.3–6.4 (6)	6.6–8.3 (7)	7.8

sample of *S. anderssoni* from Siberia (Kowamura and Takai 2009) includes one specimen of *S. zdanskyi* morphotype. Difference in size of cheek teeth between the two species is not significant and the size ranges overlap (Table 6.1). Apparently all records of *S. zdanskyi* are Baodean in age, late Miocene, so there may be temporal significance to the ranges of the species. Although we are inclined to synonymize these species, we treat them as distinct to recognize their places in the history of research of Yushe Basin.

Subfamily Castoroidinae Allen, 1877
Dipoides Schlosser, 1902
Dipoides anatolicus Ozansoy, 1961

1903 *Dipoides majori*, Schlosser, p. 40, plate 2, Fig. 14
1927 *Dipoides majori*, Young, pp. 11–13, plate 1, Fig. 5
1942 *Dipoides majori*, Teilhard de Chardin, in part, pp. 17–20, Fig. 17
1961 *Dipoides anatolicus*, Ozansoy, pp. 89–92, plate II.
1994 *Dipoides anatolicus*, Xu, p. 84.

Referred material from Yushe Basin: IVPP V10468.1-15, isolated upper cheek teeth including 2P4, 12 M1/M2, and 1 M3; IVPP 10469.1-8, isolated lower cheek teeth including a p4 and 7 molars; IVPP V 10470 (QY-85), right dentary with p4m1-3 from Danangou probably Mahui Formation, (Fig. 6.3); three isolated upper cheek teeth figured by Teilhard de Chardin (1942, Fig. 17A–C).

Description: The insertion muscle scar for the masseter medialis (anterior branch) on the lateral side of the mandible, and the temporalis fossa between the ascending ramus and the m3, are relatively less developed than in *Dipoides majori*. The dental pattern is exactly like that of *D. majori*, but the cheek teeth are smaller (Table 6.2). Enamel anterior surface of incisors is convex. Cheek tooth roots open and ever-growing. Cheek teeth, except for p4 and M3, display typical "S" pattern. The mesoflexus of M3 is hook-like, and p4 has a well-developed parastriid. The size of m3 is remarkably small, compared to the other molars.

Discussion: This species is smaller and stratigraphically older than *Dipoides majori*, and is considered assignable to *D. anatolicus* because it has the same dental pattern and size (Xu 1994). It is represented in the Baode area by a fine skull described by Young (1927) and housed at Uppsala University in Sweden (collected from Tai Chia Kou, 30 li = 10 miles, east northeast of Loc. 30). This skull is similar to *Dipoides smithi* described by Wagner (1983) from North

Fig. 6.3 *Dipoides anatolicus* from Yushe Basin. IVPP V 10470 (QY-85), right dentary with p4m1-3 from Danangou, likely Mahui Formation; occlusal (above), medial (middle), and lateral views. Scale bar = 1 cm

Table 6.2. Measurements (mm) of lower cheek teeth of Yushe *Dipoides* in comparison to the genotypic species *Dipoides problematicus* (sample sizes in parentheses)

Measurement	*D. problematicus*	*Dipoides anatolicus*	*Dipoides majori*
Length of p4	5.0−7.3 (5)	5.3−6.5 (16)	6.8−7.9 (13)
Width of p4	4.6−5.2 (5)	4.0−5.1 (16)	5.0−6.5 (13)
Length of m1	4.2−5.8 (9)	4.0−5.1 (13)	5.6−7.2 (10)
Width of m1	4.3−5.3 (9)	3.8−4.7 (13)	5.2−6.2 (10)
Length of m2	4.2−5.7 (8)	3.7−5.3 (9)	5.7−6.8 (9)
Width of m2	4.9−5.8 (8)	3.9−4.7 (9)	5.0−5.9 (9)
Length of m3	3.5−4.5 (6)	3.9−4.4 (4)	5.5−6.1 (6)
Width of m3	3.2−5.0 (6)	3.8−4.0 (4)	4.6−5.5 (6)
Length of P4	4.2−5.7 (10)	4.3−5.2 (8)	6.4−7.5 (5)
Width of P4	4.7−5.9 (10)	3.8−4.8 (8)	4.8−6.3 (5)
Length of M1	3.4−4.8 (7)	3.6−5.4 (12)	5.6−7.4 (14)
Width of M1	3.7−5.5 (7)	3.4−5.0 (12)	5.0−6.7 (14)
Length of M2	3.7−5.6 (7)	3.7−4.9 (11)	5.5−7.4 (12)
Width of M2	3.4−5.2 (7)	4.0−4.2 (11)	4.8−6.5 (12)
Length of M3	4.2−4.7 (4)	4.2−5.0 (6)	5.8−6.4 (5)
Width of M3	3.9−4.7 (4)	3.4−3.9 (6)	4.1−4.6 (5)

America (morphometric comparison of Xu 1994), which may imply close relationship between the two species.

Dipoides majori Schlosser, 1903

1924 *Dipoides* cf. *majori*, Schlosser, pp. 27−30, plate II

1942 *Dipoides majori*, Teilhard de Chardin, pp. 17−20, Figs. 14−16

1994 *Dipoides majori*, Xu, pp. 84−85

Holotype: Unnumbered dentary with full dentition; Tianjin drugstore, poor provenance.

Referred material from Yushe Basin: IVPP V 10480 (YM1), fragmentary right dentary with m1-2, and IVPP V 22701 (YM2), left dentary with p4m1-3 (Fig. 6.4), both from the Gaozhuang Formation. IVPP V 10485.1-4 (YM3), isolated lower incisor and 3 lower cheek teeth purchased from the Gaozhuang area. Isolated teeth from Gaozhuang Formation field sites: V 8835 from YS38, V 8836.1 and 8836.2 from YS40 and YS49, V 8837 from YS132. The following material, perhaps all assignable to the Gaozhuang Formation or equivalent strata: IVPP V 10463.1-34, isolated upper cheek teeth, including a P4, 29 M1 or M2, and 4 M3, from the Pliocene "White Beds"; V 10464.1-28, isolated lower cheek teeth, including 7 p4, and 21 molars, also from the "White Beds"; V 10465 (5VII29 written on specimen; this odd number is in the form of a date), premaxilla with incisors; V 10467 (12.040), left dentary with p4 m1-3, and V 10466 (12.039), left dentary with p4 m1-2 from the "White Beds"; IVPP RV 42022.1-2 (Teilhard de Chardin 1942, Fig. 16A, B), two isolated upper cheek teeth. Additional Tianjin Museum material under the catalogue numbers THP 14224–14229 from near Yang Jia Zhuang and Zhaozhuang, all Mazegou Formation or equivalent.

Fig. 6.4 *Dipoides majori* from Yushe Basin. IVPP V 22701 (YM2), left dentary with p4m1-3 from Gaozhuang; occlusal (above), medial (middle), and lateral views. Scale bar = 1 cm

Description: Cheek teeth of *Dipoides majori* are most similar to *D. anatolicus*. However, several characters distinguish them: *D. majori* has a stronger masseteric scar on the mandible, and cheek teeth of *D. majori* average 20% larger (Table 6.2). The three lophs of each cheek tooth in *D. majori* are almost equal in size, but the anterior loph in *D. anatolicus* is smaller than the two posterior lophs in lower teeth, and the posterior loph is smaller than the two anterior lophs in upper teeth. Upper incisors have strongly convex enamel faces. The lower last molar is not greatly reduced in size.

Trogontherium Fischer, 1809

Trogontherium cuvieri Fischer, 1809

1928 *Trogontherium* cf. *cuvieri*, Zdansky, pp. 52−53, tafel 5, Fig. 3.

1934 *Trogontherium* cf. *cuvieri*, Young, pp. 52−56, plates 4−5.

1942 *Sinocastor anderssoni*, in part, Teilhard de Chardin, p. 5, Fig. 7.

1942 ?*Eucastor stirtoni*, Teilhard de Chardin, pp. 12−14, Fig. 12.

1994 *Trogontherium cuvieri*, Xu, pp. 81−83.

Referred material: From Yushe Basin – IVPP V 10459 (old number 30.726, Fig. 6.5a, b), right dentary fragment with m1-3, probably Haiyan Formation; IVPP V 10481, palate with left and right P4M1-2, purchased from Shanghai drugstore, Yushe "White Beds"; V 10477.1-2 (YM4, left m1-2 and right p4) and V 10478 (YM5, left dentary with p4m1-2 from Heyugou), both from Haiyan Formation, Yushe Basin. Also IVPP V 10460 (C/C 1039), two upper right incisors, and IVPP V 10458 (C/I 240), left dentary with p4m1-3 from the middle Pleistocene of Jiajiashan, Tangshan, Hebei Province (plate 1e in Xu 1994); IVPP V 10461.1 (palate) and V 10461.2 (right dentary) from the late middle Pleistocene of Hexian, Anhui Province (Fig. 6.6).

Description: Due to a lack of skull material from Yushe, most of the following observations are on the dentition and mandible. Mandibles are heavy and swollen, and there is a remarkably large temporalis fossa between m3 and the ascending ramus. Cheek teeth are high crowned, with intermediately long roots, and they lack cementum. The lower premolar has a short metaconid; the m3 is long relative to anterior molars (Fig. 6.5). The hypoflexid inserts between the mesoflexid and metaflexid, and the flexids are relatively straight in occlusal view. Striids extend along half the crown height. Comparison of the Yushe mandible with a larger late middle Pleistocene specimen (Fig. 6.6) suggests that *Trogontherium* body size increased over its temporal range. This was also implied by Teilhard de Chardin (1942) in his comparison of Yushe material with the large Tangshan jaw IVPP V 10541. Lower cheek teeth in lateral view form a flat occlusal surface (concave in *Castor*).

Fig. 6.5 *Trogontherium cuvieri* from Yushe Basin. IVPP V 10459 (30.726), right dentary fragment with m1-3, probably Haiyan Formation; occlusal (above), medial (middle), and lateral views. Scale bar = 1 cm

Preserved upper dentitions are few, but a palate is known from the Hexian Man site of Anhui Province (Fig. 6.6). This specimen shows the characteristic greatly inflated P4, and the elongated M3 (to match m3). P4 and M3 have an additional flexus or fossette posterior to the metaflexus or metafossette (Schreuder 1929; Mayhew 1978). Unlike P4 and M3, other upper and lower cheek teeth have no additional flexus (flexid) or fossette (fossettid). The hypoflexus intersects the paraflexus anteriorly.

The chewing movement between upper and lower cheek teeth yields very smooth enamel areas on the occlusal surfaces of the lower cheek teeth. The polished areas provide information for reconstructing the chewing mechanics of these beavers, as well as for microwear analysis. The

Fig. 6.6 *Trogontherium cuvieri* from Hexian, Anhui. IVPP V 10461.1 (palate, above) and V 10461.2 (right dentary in lateral, occlusal and medial view) from middle Pleistocene of Hexian. Scale bars = 1 cm

chewing surface and the temporalis fossa are associated functionally. According to Butler's (1980) model, the chewing movement in *Trogontherium* is mainly anteroposterior because the flexi and flexids are nearly transverse (derived feature). The occlusal surface should be concave or convex, not flat, if the grinding force is both forward and backward, as in *Castor*. The well-developed temporalis fossa for the muscle insertion indicates that the dominant movement is antero-posterior on the mandible. The temporalis muscle exerts compressive force during the power stroke, and the large fossa implies a strong temporalis muscle.

The large fossa and the smooth occlusal surfaces are two important characters of *Trogontherium cuvieri*. Teilhard de Chardin (1942) misidentified fragmentary mandible IVPP V 10459 (formerly 30.726) as *Sinocastor anderssoni*, but he noticed the anomalous character of "the remarkable width of the fossa extending between m3 and the ascending ramus." In addition, the specimen has the typical *Trogontherium* dental pattern, that is, relatively straight flexids or fossettids, and flat and polished occlusal surfaces. This specimen is illustrated in plate 1 g of Xu (1994). Teilhard de Chardin (1942) had assigned with question a palate acquired at a Shanghai drugstore to *Eucastor*, but noted several similarities with *Trogontherium*, specifically the Tangshan jaw IVPP V 10458. We follow his intuition and include IVPP V 10481 in *T. cuvieri*, together with the Yushe specimens.

6.3 Conclusions

Chinese beavers probably derive from southward invasions of northern Asian Corridor faunas, which are Holarctic in many respects, and therefore have ties to European and North American faunas (Xu 1996). The beavers of Yushe Basin are sensitive to dynamic events resulting in faunal exchange between Eurasia and North America. Three groups of beavers occur in Yushe Basin: *Dipoides*, *Sinocastor* and *Trogontherium*. There is no record of *Eucastor* there. Yushe beavers have biochronological significance because they document dispersal events and represent several first occurrences of beavers in China (Flynn et al. 1991; Xu 1994).

The first occurrence of *Dipoides* in China is represented by *Dipoides anatolicus* from the Mahui Formation, about 6.5 Ma (Flynn 1997). This species is also known from Ertemte, Inner Mongolia, near the Miocene/Pliocene boundary (Fahlbusch et al. 1984). The type material is from the late Miocene of Turkey (Ozansoy 1961), and indicates a broad biogeographic distribution of this beaver at the end of the Miocene. *Dipoides problematicus* of Europe is considerably older (MN 11−13; some possible earlier

records), which may indicate earlier invasion of *Dipoides* from North America, at the beginning of the late Miocene. Hugueney (1999) notes the alternative view that European "*Dipoides*" may have evolved in the Old World from older *Eucastor*-like species. The latter scenario opens as a possibility the immigration of *Dipoides* to China from Europe, not North America.

Dipoides majori appeared near the Miocene-Pliocene boundary after the immigration of *D. anatolicus* into China, possibly evolving within the biogeographic region of northeastern Asia. *D. majori* is similar to *D. anatolicus* except for its larger size and more enhanced masseteric muscle scar. Biostratigraphically, *D. majori* spans the Gaozhuang Formation and most of the Mazegou Formation, about 5.5 to 3 Ma.

Trogontherium cuvieri first appears in China in the early Pleistocene Yushe Basin Haiyan Formation (before 2.2 Ma). Chinese *Trogontherium* was traditionally considered an important index fossil in China for the middle Pleistocene. The record from Yushe Basin demonstrates that *T. cuvieri* arrived in eastern Asia from Europe by early Pleistocene time. The lineage survived into the late Pleistocene (Zhang 1981) and may involve increasing body size during its range.

Previously (Xu 1994, 1996), the *Sinocastor* lineage was considered to be embedded within the genus containing *Castor fiber* and *Castor canadensis*. *Sinocastor* would be a junior synonym of *Castor*, or alternatively under this scenario, taxonomic usage might retain *Sinocastor* as a subgenus parallel to two extant subgenera, one for each living species. Rybczynski et al. (2010) emphasize distinctions of *Sinocastor* from both living *Castor* species, place the taxon basal to the living forms, and resurrect *Sinocastor* as an independent genus. *Castor* (*Sinocastor*) is employed here as a subgenus for the Yushe species, excluding both living lineages from it. This allows, at least temporarily, retaining *Castor* as a larger taxon to accommodate rare early late Miocene *Castor*-like fossils from Europe (Hugueney 1999) and later *Castor* records. Early European *Castor* could represent the origin for *Sinocastor* and both living species. Under this scenario, the direction of dispersal of *Sinocastor* into China would have been west to east.

As mentioned above, *Sinocastor zdanskyi* is questionable as a distinct species, and is possibly a synonym of *S. anderssoni*. In Yushe Basin, specimens assigned to *S. zdanskyi* occur in the upper Mahui Formation, 6.5 to 6 Ma, and *S. anderssoni* ranges through the Gaozhuang and Mazegou formations, without clear Mahui Formation records, so would span roughly 5.5 to 3 Ma in Yushe Basin. The late Miocene Qingyang and other faunas of western North China contain fossils attributed to both *S. anderssoni* and *S. zdanskyi* (Li et al. 1984). Possibly there is only one *Sinocastor* lineage in China from late Miocene through Pliocene. The origin of *Castor* in North America is presumably from the west (Siberia), and the genus has been used as a distinctive immigrant in defining a North American biotic event (Tedford et al. 2004). Now the earliest record of *Castor* in North America, >7 Ma (Samuels and Zancanella 2011), likely about 8 Ma (Carpenter and Smith 2011) is seen to antedate the known record of *Sinocastor* in eastern China. Resolution of the generic or subgeneric relationships of early European *Castor*, late Miocene *Castor* in North America, and *Sinocastor* in China remains elusive and probably requires more complete material of early species than is presently available.

Acknowledgements The authors thank Chuan-Kui Li and Zhan-Xiang Qiu for guidance, advice, and access to unpublished fossils. Louis Jacobs and Dick Tedford supplied information and encouragement at many stages of the research. Dale Winkler kindly provided copies of the tables from the first author's dissertation, and Ms. Jin Chen updated fossil curation with care. Wen-Yu Wu carefully read the manuscript, correcting several details, and reviewers Bill Korth, Louis Jacobs, and Natalia Rybczynski helped immensely to improve the presentation and discussion.

References

Butler, P. M. (1980). Functional aspects of the evolution of rodent molars. *Palaeovertebrata, Mémoire Jubilaire, R. Lavocat,* 249–262.

Cande, S. C., & Kent, D. V. (1995). Revised calibration of the geomagnetic polarity timescale for the late Cretaceous and Cenozoic. *Journal of Geophysical Research, 97B,* 13917–13951.

Carpenter, N. E., & Smith, G. R. (2011). Biostratigraphy of early Hemphillian beavers (Rodentia: Castoridae) from the Pacific northwestern USA. *Society of Vertebrate Paleontology 2011 Program and Abstracts*, 84.

Fahlbusch, V., Qiu, Z.-D., & Storch, G. (1984). Neogene micromammal faunas from Inner Mongolia: Recent investigations on biostratigraphy, ecology and biogeography. In R.O. Whyte (Ed.), *The Evolution of East Asian environment, Volume II, Palaeobotony, palaeozoology, and palaeoanthropology* (pp. 697–707). Hong Kong: The University of Hong Kong.

Flynn, L. J. (1997). Late Neogene mammalian events in North China. *Actes du Congrès BioChrom '97, Mémoire Travaux E.P.H.E., Institut Montpellier, 21,* 1183–192, Montpellier, France.

Flynn, L. J., Tedford, R. H., & Qiu, Z.-X. (1991). Enrichment and stability in the Pliocene mammalian fauna of North China. *Paleobiology, 17,* 246–265.

Hugueney, M. (1999). Family Castoridae. In G. E. Rössner & K. Heissig (Eds.), *The Miocene land mammals of Europe* (pp. 281–300). Munich: Verlag Dr. Friedrich Pfeil.

Kowamura, Y., & Takai, M. (2009). Pliocene lagomorphhs and rodents from Udunga, Transbaikalia, eastern Russia. *Asian Paleoprimatology, 5,* 15–44.

Kretzoi, M. (1977). Die *Castor*-Reste aus den Travertinen von Taubach bei Weimar. *Quartär-paläontologie, 2,* 389–400.

Li, C.-K., Wu, W.-Y., & Qiu, Z.-D. (1984). Chinese Neogene: Subdivision and Correlation. *Vertebrata PalAsiatica, 22,* 163–178 (in Chinese with English summary).

Mayhew, D. F. (1978). Reinterpretation of the extinct beaver *Trogontherium* (Mammalia, Rodentia). *Royal Society of London, Philosophical Transactions, B281,* 407–438.

Ozansoy, F. (1961). Sur quelques mammifères fossiles (*Dinotherium*, *Serridentinus*, *Dipoides*) du Tertiare d'Anatolie Occidentale-Turquie.

Bulletin of Mineral Research and Exploration, Institute of Turkey, 56, 85–93.

Qiu, Z. X., Deng, T., Qiu, Z.-D., Li, C.-K., Zhang, Z.-Q., Wang, B.-Y., et al. (2013). Neogene land mammal stages/ages of China. In X. Wang, L. J. Flynn, & M. Fortelius (Eds.), *Fossil mammals of Asia: Neogene biostratigraphy and chronology* (pp. 29–123). New York: Columbia University Press.

Rybczynski, N., Ross, E. M., Samuels, J. X., & Korth, W. W. (2010). Reevaluation of *Sinocastor* (Rodentia: Castoridae) with implications on the origin of modern beavers. *PLoS ONE, 5,* e13990. doi:10.1371/journal.pone.0013990.

Samuels, J. X., & Zancanella, J. (2011). An early Hemphillian occurrence of *Castor* (Castoridae) from the Rattlesnake Formation of Oregon. *Journal of Paleontology, 85,* 930–935.

Schlosser, M. (1902). Beiträge zur Kenntniss der Säugetierreste aus den Süddeutschen Bohnerzen. *Geologische und Palaeontologische Abhandlungen, 5*(3), 1–144.

Schlosser, M. (1903). Die fossilen Säugetiere Chinas nebst einer Odontographie der recenten Antilopen. *Abhandlungen der Königlich Bayerischen Akademie der Wissenschaften, 22,* 1–221.

Schlosser, M. (1924). Tertiary vertebrates from Mongolia. *Palaeontologia Sinica, C1,* 1–119.

Schreuder, A. (1929). *Conodontes* (*Trogontherium*) and *Castor* from the Teglian Clay compared with the Castoridae from other localities. *Archives du Musée Teyler, III, 6*(3), 99–319.

Stirton, R. A. (1935). *A review of the Tertiary beavers* (Vol. 23, pp. 391–458). University of California Publications, Department of Geological Sciences.

Tedford, R. H., Albright, L. B., III, Barnosky, A. D., Ferrusquia-Villafranca, I., Hunt, R. M., Jr., Storer, J. E., et al. (2004). Mammalian biochronology of the Arikareean through Hemphillian interval (late Oligocene through early Pliocene epochs). In M. O. Woodburne (Ed.), *Late Cretaceous and Cenozoic mammals of North America* (pp. 169–231). New York: Columbia University Press.

Tedford, R. H., Flynn, L. J., Qiu, Z.-X., Opdyke, N. D., & Downs, W. R. (1991). Yushe Basin, China: Paleomagnetically calibrated mammalian biostratigraphic standard from the late Neogene of eastern Asia. *Journal of Vertebrate Paleontology, 11,* 519–526.

Teilhard de Chardin, P. (1942). New rodents of the Pliocene and lower Pleistocene of North China. *Publications de l'Institut Géo-Biologie, Pékin, 9,* 1–101.

Teilhard de Chardin, P., & Young, C. C. (1931). Fossil mammals from the Late Cenozoic of Northern China. *Palaeontologia Sinica, C9,* 1–66.

Troszyñski, W. (1975). The main difference in the structure of the skull of both the Canadian and the European beaver. *Przeglad Zoologiczny, 19,* 481–486.

Wagner, H. M. (1983). The cranial morphology of the fossil beaver *Dipoides smithi* (Rodentia: Mammalia). *Natural History Museum of Los Angeles County, Contributions in Sciences, 346,* 1–6.

Wang B.-Y. (2005). Beaver (Rodentia, Mammalia) fossils from Longdan, Gansu, China – Addition to the early Pleistocene Longdan mammalian fauna (1). *Vertebrata PalAsiatica, 43,* 237–242, in Chinese with English summary.

Woodburne, M. O. (1961). Upper Pliocene geology and vertebrate paleontology of part of the Meade Basin, Kansas. *Papers of the Michigan Academy of Science, Arts, and Letters – Paleontology, 46,* 61–95.

Xu, X.-F. (1994). Evolution of Chinese Castoridae. In Y. Tomida, C. K. Li, & T. Setoguchi (Eds.), *Rodent and lagomorph families of Asian origins and diversification* (pp. 77–98). Tokyo: National Science Museum Monograph 8.

Xu, X.-F. (1996). Castoridae. In D. R. Prothero & R. J. Emry (Eds.), *The terrestrial Eocene-Oligocene transition in North America* (pp. 417–432). New York: Cambridge University Press.

Young, C. C. (1927). Fossile Nagetiere aus Nord-China. *Palaeontologia Sinica, C, 5*(3), 1–82.

Young, C. C. (1934). On the Insectivora, Chiroptera, Rodentia, and Primates other than *Sinanthropus* from Locality 1 in Choukoutien. *Palaeontologia Sinica, C, 8*(3), 1–140.

Zdansky, O. (1928). Die Säugetiere der Quartärfauna von Chou-K'ou-Tien. *Palaeontologia Sinica, C, 5*(4), 3–146.

Zhang, Z.-H. (1981). Humans and the culture of the Paleolithic period from Liaoning District. *Vertebrata PalAsiatica, 19,* 184–192 (in Chinese with English summary).

Chapter 7
Yushe Dipodoidea

Zhu-Ding Qiu

Abstract The few Dipodoidea recorded as fossils in the Late Neogene deposits of Yushe Basin are isolated teeth recovered by screening in 1987 and 1988. They include small zapodids, and remains of a larger dipodid. The fossils recorded at YS8 in the late Miocene Mahui Formation are referable to *Lophocricetus* and to the extant genus *Sicista*. Both also co-occur in late Miocene and early Pliocene localities of central Inner Mongolia, Balunhalagen, Shala, Baogeda Ula, Ertemte, Harr Obo, and Bilike. The Yushe specimens are most comparable to those of Shala and Baogeda Ula, demonstrating somewhat primitive characters for those populations. The dipodid, from younger Yushe formations, is referred to *Dipus* cf. *D. fraudator* and shows a slightly more derived state than the specimens of *D. fraudator* known from Ertemte. The Yushe Pliocene *Dipus* records postdate Ertemte, and an early Pleistocene *Dipus* from the Haiyan Formation is small in size, suggesting phyletic change in the lineage.

Keywords Yushe Basin • Dipodidae • North China • Late Neogene • *Sicista* • *Lophocricetus*

7.1 Introduction

Remains of dipodoids in the Neogene deposits of Yushe Basin were unknown until the sediment screening campaign by the Sino-American team directed by Z.-X. Qiu and R.H. Tedford. This superfamily seems to have been a minor component in the succession of micromammalian faunas of Yushe. Only several isolated teeth have been recovered from the Yushe Basin, but they represent two families and constitute the first discovery of this group in the region. Yushe fossil dipodoids include members of two living genera, the birchmouse *Sicista* and the jerboa *Dipus*, and extinct *Lophocricetus*.

There are differences of opinion in regards to higher-level systematics of jumping mice, birch mice, and jerboas. Before the phylogenetic classification is settled, I follow palaeontologists, such as Simpson (1945) and Daxner-Höck (1999) in grouping these rodents in the superfamily Dipodoidea distributed in two families Zapodidae (for jumping mice and birchmice) and Dipodidae.

7.2 Systematics

Superfamily Dipodoidea Fischer, 1817
Family Zapodidae Coues, 1875
Subfamily Lophocricetinae Savinov, 1970
Lophocricetus Schlosser, 1924
Lophocricetus cf. *L. grabaui* Schlosser, 1924

Locality and Material: YS 8 (late Miocene, Mahui Fm., 6.3 Ma): right M1, right M2, left M3, V 13083.1-3 (Fig. 7. 1).

Measurements (mm): M1: 1.80 × 1.20; M2: 1.35 × 1.15; M3: 0.70 × 0.80.

Description: The M1 is rectangular with slightly posteriorly inclined cusps. A distinct protocone is situated slightly lingual to the longitudinal axis of the tooth. The paracone is located posterior to the protocone and is slightly anteroposteriorly compressed; its anterolingual side is continuous with the protoloph and connects with the protocone. The hypocone is robust and forms the posterolingual corner of the tooth. The metacone is situated slightly more posteriorly than the hypocone, with a morphology and size similar to the paracone, and joins the posterior arm of the hypocone by a long and robust metaloph. The mesocone is an oblique

Z.-D. Qiu (✉)
Laboratory of Paleomammalogy, Institute of Vertebrate Paleontology and Paleoanthropology, Chinese Academy of Sciences, 142 Xizhimenwai Ave., Beijing 100044, People's Republic of China
e-mail: qiuzhuding@ivpp.ac.cn

Lawrence J. Flynn and Wen-Yu Wu (eds.), *Late Cenozoic Yushe Basin, Shanxi Province, China: Geology and Fossil Mammals, Volume II: Small Mammal Fossils of Yushe Basin*, Vertebrate Paleobiology and Paleoanthropology,
DOI 10.1007/978-94-024-1050-1_7

ellipse, smaller than the principal cusps, with major axis in the anterolabial-posteroligual direction and passing through the endoloph to connect with the posterior arm of the paracone and anterior arm of the hypocone. A mesoloph is lacking, but a low "endomesoloph" extends anterolingually from the mesocone and reaches the lingual margin. The protostyle (equals the anterostyle of Qiu 1985) is prominent, columnar, and tightly appressed to the posterolingual side of the protocone. A hypostyle (posterostyle of Qiu 1985) is absent. The anteroloph is extremely low and weak but there is a relatively well developed anterior accessory cusp. The posteroloph is short and high, slightly expanded transversely, and joins the posterior base of the metaloph, near the metacone. Four roots are present.

The M2 is trapezoidal in shape, anteriorly expanded, with the hypocone slightly larger and longer than the protocone. The paracone and metacone are columnar, distinctly smaller but relatively higher than the lingual cusps. The small anterocone, at the anterolabial corner of the tooth, is lophate and connects through the anteroloph with the anterior arm of the protocone. The anterocone continues posterolabially to join the paracone and enclose an anterolabial atoll. The protostyle is fused with the protocone and situated slightly posterior to it. A mesocone is lacking. The protoloph and metaloph are complete, the former being slightly anterolinglual-posterolabially directed, and the latter nearly transverse. An endoloph is oriented oblique to the tooth axis and weakly connected at a low position to both the posterior wall of the protoloph (to the anterior) and the anterior arm of the hypocone (to the posterior). The single anteroloph descends lingually from the protostyle and terminates short of the lingual margin. The high posteroloph firmly joins the hypocone and metacone posteriorly, to enclose the posterior endosinus.

The small M3 is subtriangular and slightly broader than long, with a well-developed protocone that forms the anterolingual corner of the tooth. The lophate anterocone dominates the anterolabial margin of the tooth, and connects the protocone to the paracone while enclosing the anterior ectosinus. The hypocone, metacone, and posteroloph are all fused to compose a strong posterolingual crest (metaloph), which connects with the protocone lingually and the paracone labially to enclose the exterior mesosinus. The protoloph is robust and anterolingual-posterolabially directed. An endoloph is undeveloped.

Comparison and discussion: The structures of the teeth described above are consistent with the genus *Lophocricetus* in the cricetid-like cusp and loph morphology, and the presence of distinct protostyles on M1 and M2. The author follows Zazhigin et al. (2002) in allocation of the species of *Lophocricetus* into two subgenera, *Lophocricetus* (*sensu stricto*) and *Paralophocricetus*. The Yushe specimens are referred to the former genus based on the absence of a hypostyle on M1 and M2.

The range of the genus *Lophocricetus* is restricted to the Upper Miocene and Lower Pliocene of northeast to central Asia. It was possibly derived from the middle Miocene genus *Heterosminthus,* apparently following the evolutionary trends of increasing body size, increasing crown height, strengthening of a protostyle on M1 and M2, weakening of the mesocone and mesoloph, and labial shifting of the endoloph (from the protoloph to paracone) and the posteroloph (from the metaloph to metacone). There are two named species of *Lophocricetus* (*Lophocricetus*) known in China, *L. xianensis* from Lantian, Shaanxi, and Shengou, Qinghai, early late Miocene, and *L. grabaui* from the younger sites Ertemte and Harr Obo, Inner Mongolia (Schlosser 1924; Qiu 1985; Qiu et al. 2008; Qiu and Li 2008). *L. xianensis* Qiu et al., 2008, shows more primitive characters: smaller size, weakly developed protostyles, but distinct mesocone and mesoloph on M1 and M2, and the endoloph connected with the protoloph and the posteroloph with the metaloph in the majority of M1. *L. grabaui* is more derived in being larger, in having distinctly developed protostyles but no mesoloph on M1 and M2, and in connection on M1 of the endoloph to the paracone and the posteroloph to the metacone on M1.

In general morphology, the Yushe lophocricetine shares consistent characters with *Lophocricetus grabaui* from Ertemte and Harr Obo (see Qiu 1985). The minor differences

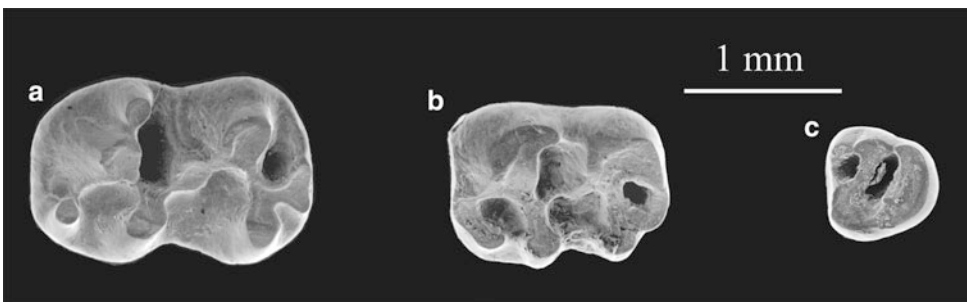

Fig. 7.1 Occlusal views of *Lophocricetus* cf. *L. grabaui* from Yushe Basin, anterior to left **a** M1, V 13083.1; **b** M2, V 13083.2; **c** M3, V 13083.3

from the latter include less height of cusps, the posteroloph connecting with the metaloph rather than metacone, the presence of an endomesoloph on M1, and on M2 the more pronounced anteroloph and posteroloph, and the endoloph connecting with the protoloph. Size of the specimens is within the range of variation for the Inner Mongolian taxon *L. grabaui*, but the Yushe specimens fall toward the small end of the size range. The Yushe M1 is similar to the corresponding tooth of *L. xianensis* from Lantian and Shengou in connecting the posteroloph to the metaloph, but differs in its larger size, lacking a mesoloph, and the endoloph joining the paracone and the protoloph. The Yushe jumping mice appear to indicate a more derived status than *L. xianensis*, but more primitive than *L. grabaui*.

The Yushe lophocricetine resembles *Lophocricetus minisculus* Savinov, 1970 from the late Miocene of Kazakhstan and *L. complicidens,* lower Meotian of Ukraine, in their relative height of crown and comparatively weak cusps. However, the Yushe form is larger and lacks the mesoloph on M1, which is a more derived condition. The Yushe *Lophocricetus* is close to *L. vinogradovi* Savinov, 1970 in size, but differs from the latter in lacking the mesoloph on M1, having a posteroloph-metaloph connection on M1, and its single anteroloph on M2.

The Yushe species most closely resembles *Lophocricetus grabaui*, but shows a slightly more primitive state: the apparently smaller size, the lower crown height, the more lingual position of the posteroloph-metaloph contact on M1, the stronger endoloph connecting to the protoloph on M2. A possibility that these specimens may represent a new species cannot be excluded, for the above characters plus the presence of an endomesoloph on the M1 and the well-developed anteroloph and posteroloph on the M2. Nevertheless, it is considered inadvisable to create a new species based on only three teeth, so they are referred provisionally to *Lophocricetus* cf. *L. grabaui.*

Subfamily Sicistinae Allen, 1901
Sicista Gray, 1827
Sicista sp.

Locality and Material: YS8 (late Miocene Mahui Fm., 6.3 Ma); two left M2 (V 13084.1, 1.00 × 1.00 mm; V 13084.2, 0.95 × 1.00 mm; Fig. 7.2).

Description: Both M2 show a large anterior interdental facet and a short lingual anteroloph, are subquadrate in occlusal outline and wider anteriorly than posteriorly. The greatest tooth length is measured through the paracone and metacone, while the greatest width is measured through the protocone and paracone. The four principle cusps are nearly equivalent in height, but the protocone is largest. Protocone and hypocone morphology are similar and are more or less anterolingual-posterolabially compressed. Paracone and metacone morphology are also similar although the former is

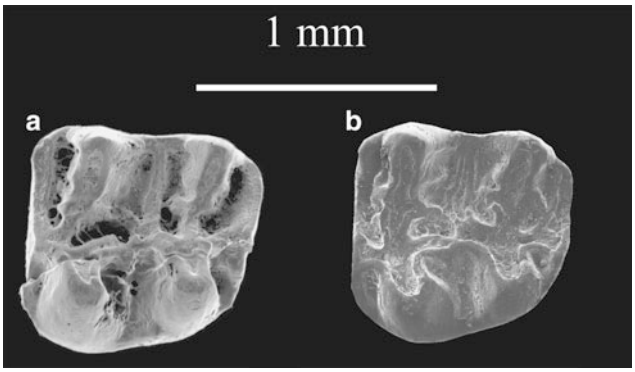

Fig. 7.2 Occlusal views of *Sicista* sp. from Yushe **a** M2, V 13084.1; **b** M2, V 13084.2

larger than the metacone. The anteroloph is low, straight, and extends from the protocone to the labial margin of the tooth. In one tooth the protoloph is located slightly more anteriorly and joined to the anterior arm of the protocone, which in turn joins the anteroloph lingual to the midline of the tooth; in the other tooth the nearly transverse protoloph joins the anterior part of the protocone. In both M2, a mesoloph is rather low and weak but extends to the lateral margin from the endoloph. The posteroloph is continuous, lingually connecting near the center of the tooth to the hypocone by a prominent crest. The moderately developed endoloph is short, slightly curved, and connects the posterior arm of the protocone with the anterior arm of the hypocone. An indistinct mesocone is submerged in this loph. In addition to a transverse mesoloph running from the endoloph, there is an anterolabially-extended accessory loph that connects weakly to the protoloph posterior wall. Another accessory loph extends lingually to reach the posterior base of the protocone. Short accessory lophs are also present on both the anterior and posterior protoloph and metaloph. One root is present lingually and two are present labially.

Sicista ranges broadly throughout the Palaearctic Region with an earliest occurrence in the early Miocene (Kimura 2011), and persists to the present with over ten species. The large size and more complicated occlusal pattern distinguish the Yushe *Sicista* from *S. primus* Kimura, 2011 of Gashunyinadege, Inner Mongolia, but the close size and similar morphology of other named species make it difficult to assess the Yushe birchmouse based on the literature alone and given the small sample sizes. Occlusal morphology roughly differentiates birchmice with relatively simple patterns as in *S. wangi* Qiu and Storch (2000; early Pliocene, Bilike, Inner Mongolia) and *S. pliocaenica* Erbajeva (1976; late Pliocene, Beregovaya, Transbaikalia) from complicated *S. bagajevi* Savinov (1970; late Miocene, Pavlodar, Kazakhstan) and *S. vinogradovi* Topachevsky (1965; early Pliocene, Nogaisk, Ukraine). The Yushe specimens, with rather developed secondary ridges and spurs, can be referred to the

latter pattern. They seem to be smaller than *Sicista vinogradovi*, close to *S. bagajevi* in size, but the secondary ridges are weaker than those of *S. bagajevi*.

Remains of birchmice are commonly encountered in the late Miocene localities of central Inner Mongolia, and rather abundant material is recorded from the latest Miocene and Pliocene localities of Ertemte, Harr Obo, Bilike and Gaotege, mostly reported as indeterminate species (except for *Sicista wangi* from Bilike; see Fahlbusch et al. 1983; Qiu 1988; Qiu and Storch 2000; Qiu et al. 2006). Preliminary observations indicate that the two Yushe teeth fall entirely within the size range for the Shala-Ertemte-Harr Obo samples, but they are smaller than those of Bilike and Gaotege. As for the occlusal pattern, the Yushe teeth are more or less similar to those of Ertemte and Harr Obo, but simpler than those of Shala with poorly developed secondary ridges, and more complicated than those of Bilike and Gaotege with relatively distinct ridges. In addition, cusps of the corresponding teeth from Shala are less anteroposteriorly compressed, cusps and crests in the Bilike and Gaotege samples are relatively striking, and the metaloph is more anteriorly oriented. Erbajeva (1976) described *Sicista pliocaenica* and reviewed Late Neogene *Sicista* in northern Asia. Due to limited material and lack of comparative samples, the Yushe Basin species is considered as indeterminate.

Family Dipodidae Fischer, 1817
Dipodinae Fischer, 1817
Dipus Zimmermann, 1780
Dipus cf. *D. fraudator* (Schlosser, 1924)

Material: YS50 (early Pliocene Gaozhuang Fm., 4.7 Ma), right m1 V 13085.1; YS90 (late Pliocene Mazegou Fm., 3.5 Ma), left M1 lacking its most posterior portion, V 13085.2; YS 120 (early Pleistocene Haiyan Fm., 2.5 to 2.2 Ma), left m1 V 13085.3 (see Fig. 7.3).

Measurements (mm): M1: – × 1.85 (V 13085.2); m1: 2.25 × 1.85 (V 13085.1), 2.20 × 1.55 (V 13085.3).

Description: The M1 protocone is noticeably large, slightly anteroposteriorly compressed with an anterolabial ridge, and located slightly anterior to the paracone. The paracone is anterolingually-posterolabially compressed and smaller than the protocone. The hypocone and metacone are missing, but it may be estimated that their morphologies resemble the anterior cusps, and their sizes are also either nearly equivalent or slightly larger. A mesocone is absent. Protoloph and metaloph are short, posteriorly curved and relatively strongly continuous. A robust endoloph is directed obliquely to link the hypocone and paracone. An extremely weak anterior cingulum lies between the protocone and paracone. The medial sinus is transverse or slightly anteriorly-directed, while laterally it surpasses one-half the breadth of the tooth. The posterolingually extended labial sinus is broad and spacious. An anterolingual sinus is small and narrow.

The m1 principle lingual and labial cusps are in alternate configuration. The metaconid is relatively robust, conical, and situated anterior to the protoconid. The protoconid is smaller than the metaconid and anterolingually-posterolabially compressed. The size and shape of the entoconid are equivalent to the protoconid, which is slightly more transversely directed. The hypoconid is distinctly posteriorly situated, more robust than the entoconid, and anteroposteriorly compressed. The metalophid is short, weak, and extends posterolabially. The hypolophid, which is stronger than the metalophid, is directed anterolingually. The ectolophid is obliquely directed to connect the protoconid to the entoconid. On the smaller specimen (YS120, V 13085.3) there is an extremely weak, cingulum-like anteroconid within the anterolabial sinusid. This specimen also has a reduced posterior cingulum nearly incorporated into the hypoconid, and thus differs from the m1 from YS50 (V 13085.1), which is larger with a cusp-like posterior cingulum attached to the posterolingual side of the hypoconid. The four sinusids are alternate, with the anterolingual and posterolabial sinusids the most spacious. Tooth roots are paired.

Comparison and discussion: Size and morphology of the Yushe specimens are consistent with *Dipus* from central and northern Asia. Fossil species of this genus were formerly assigned to *Sminthoides* or *Scirtodipus* (Schlosser 1924; Savinov 1970; Qiu 2003).

In addition to Yushe, the genus is recovered from several Neogene localities in northern China, including Shala, Ertemte, Harr Obo, and Bilike of Inner Mongolia, Daodi of

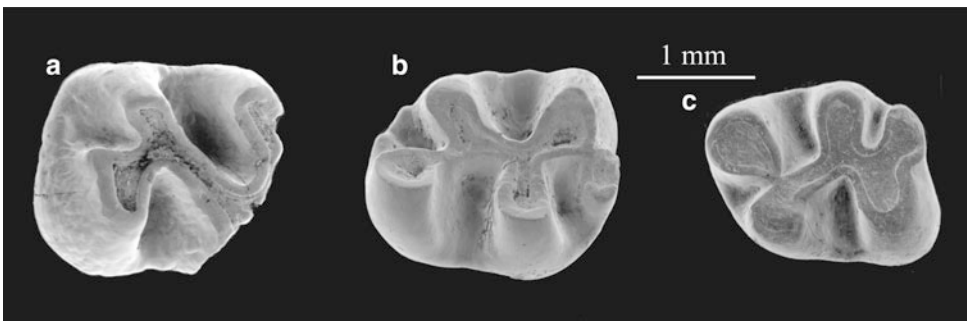

Fig. 7.3 Occlusal views of *Dipus* cf. *D. fraudator* from Yushe Basin, anterior to left **a** M1, V 13085.2; **b** m1, V 13085.1; **c** m1, V 13085.3

Hebei; and the Pleistocene locality of Heshui, Gansu (see Zheng 1976; Fahlbusch et al. 1983; Cai 1987; Qiu and Storch 2000; Qiu et al. 2006). Most of the materials from these localities were referred to the type species *Sminthoides fraudator* or considered indeterminate within the genus. Li and Qiu (2005) made a reallocation of those jerboas to extant *Dipus* and found that the genus underwent little change in dental morphology over the last six million years. Minor changes probably include a tendency toward an increase in crown height with the enlargement of cusps and crests, gradual labial shifting of entoloph on M1 and M2, narrowing of parasinus on M1 and metasinusid on m2, less frequent presence of anteroconid but higher frequency of metalophid on m1. The Pliocene age Yushe jerboa is larger with greater crown height than the early late Miocene *Dipus* sp. from Shala, but falls within the tooth size range for the Ertemte, Harr Obo, Bilike and Gaotege samples. The Yushe M1 seems to be more similar to those of Bilike and Gaotege than to Ertemte and Harr Obo in the endoloph joining the paracone. As the Yushe data are insufficient for precise diagnosis, the three isolated teeth are provisionally referred to *Dipus* cf. *D. fraudator*. However, the few teeth from Yushe span most of the Pliocene Epoch, and the youngest specimen from YS120 in the Haiyan Formation, with small size and strong connection of the posterior cingulum and hypoconid, may represent a second species.

Three species of the genus, *Dipus conditor, D. essedum* and *D. singularis*, of similar size and morphology, were recognized from the late Miocene and early Pliocene of Mongolia by Zazhigin and Lopatin (2000). They may be valid taxa, but the intraspecific variability is difficult to evaluate from the scarce specimens and literature.

A new genus *Scirtodipus* was erected by Savinov (1970) in his description of Neogene dipodids from Kazakhstan. He recognized it as distinct from *Sminthoides* (*Dipus*) in its smaller size, principle cusps lacking spurs, M1 and M2 with relatively well developed cingula, paracone being more posteriorly positioned than protocone, m1 anteroconid small and metaconid relatively narrow, and entoconid relatively lingually inclined. Comparisons with known fossils from North China indicate that the size range for *Scirtodipus* falls completely within the range of variation for *Dipus*. The Chinese specimens also lack spurs on the principle cusps, and distinct variability exists regarding the degree of development of anterior cingula on M1-2, and the anteroconid on the m1. Sometimes these features are present or absent, and sometimes strong or weak. The inclination of the cusps is largely dependent upon the degree of occlusal wear. It is therefore believed here that the Kazakhstan specimens do not display characters that differentiate them from *Dipus*. Interestingly, Zazhigin and Lopatin (2000) synonymized *Sminthoides* with *Dipus*, but retained *Scirtodipus* as distinct. They emphasized the reduction of P4, the development of anteroloph and anterocone on M1, the alternate arrangement of paracone and protocone, the connection of endoloph to paracone on M1 and M2. Separate generic status for some *Dipus*-like species may be warranted (see also Qiu and Storch 2000; Li and Qiu 2005).

7.3 Conclusion

The dipodoid fossils of Yushe Basin are few and very likely underrepresented in the fossil record. We suspect higher diversity in the paleofauna than is indicated by the three recovered taxa. The taxa are endemic to central and northern-eastern Asia. They radiated in drier parts of Asia, and Yushe Basin apparently sampled only the edge of that distribution. By reference to the Miocene and Pliocene deposits of Kazakhstan and the Mongolian plateau, the presence of these taxa in Yushe Basin is to be expected. The lophocricetine *Lophocricetus* and sicistine *Sicista* are comparable to Ertemte elements, and the lophocricetine shows slightly more primitive characters than *L. grabaui* from Ertemte. These occurrences are in the Mahui Formation at locality YS8, estimated at about 6.3 Ma. The only large dipodoid recovered is *Dipus*. The remains, referable to *D.* cf. *D. fraudator*, demonstrate somewhat more derived features than those of *D. fraudator* from Ertemte. The Pliocene records (4.7 and 3.5 Ma) appear to postdate Ertemte considerably. They are also a bit small in comparison with typical Ertemte representatives, and particularly the early Pleistocene specimen from YS120 (2.5–2.2 Ma) is small for that species. The *Dipus* lineage seems to be a peripheral representative of a much richer dipodid radiation that is becoming better known in northern Asia, particularly in more inland (more xeric) settings.

Acknowledgments Gratitude is expressed to my reviewers, especially Everett Lindsay and Yuri Kimura, who offered many constructive comments on this chapter.

References

Cai, B.-Q. (1987). Late Pliocene micromammals from Yuxian and Yangyuan, Hebei. *Vertebrata PalAsiatica, 25,* 124–136 (in Chinese).

Daxner-Höck, G. (1999). Family Zapodidae. In G. E. Rőssner & K. Heissig (Eds.), *The Miocene land mammals of Europe* (pp. 337–342). München: Verlag Friedrich Pfeil.

Erbajeva, M. (1976). Fossiliferous bunodont rodents of the Transbaikal area. *Geologiya i Geofizika, 194,* 144–149.

Fahlbusch, V., Qiu, Z.-D., & Storch, G. (1983). Neogene mammalian faunas of Ertemte and Harr Obo in Nei Monggol, China. 1. Report on field work in 1980 and preliminary results. *Scientia Sinica, B26,* 205–224.

Kimura, Y. (2011). The earliest record of birch mice from the Early Miocene Nei Mongol, China. *Naturwissenschaften, 98,* 87–95.

Li, Q., & Qiu, Z.-D. (2005). Restudies in *Sminthoides* Schlosser, a fossil genus of three-toed jerboa from China. *Vertebrata PalAsiatica, 43,* 24–35.

Qiu, Z.-D. (1985). The Neogene mammalian faunas of Ertemte and Harr Obo in Inner Mongolia (Nei Mongol), China. 3. Jumping mice − Rodentia: Lophocriceinae. *Senckenbergiana lethaea, 66,* 39–67.

Qiu, Z.-D. (1988). Neogene micromammals of China. In J. S. Aigner, N. G. Jablonski, G. Taylor, D. Walker, & P. Wang (Eds.), *The palaeoenvironment of East Asia from the mid-Tertiary, 2* (pp. 834–848). Hong Kong: Hong Kong University Press.

Qiu, Z.-D. (2003). The Neogene mammalian faunas of Ertemte and Harr Obo in Inner Mongolia (Nei Mongol), China. 12. Jerboas – Rodentia: Dipodidae. *Senckenbergiana lethaea, 83,* 135–147.

Qiu, Z.-D., & Li, Q. (2008). Late Miocene micromammals from the Qaidam Basin in the Qinghai-Xizang Plateau. *Vertebrata PalAsiatica, 46,* 283–306.

Qiu, Z.-D., & Storch, G. (2000). The early Pliocene micromammalian fauna of Bilike, Inner Mongolia, China (Mammalia: Lipotyphla, Chiroptera, Rodentia, Lagomorpha). *Senckenbergiana lethaea, 80,* 173–229.

Qiu, Z.-D., Wang, X., & Li, Q. (2006). Faunal succession and biochronology of the Miocene through Pliocene in Nei Mongol (Inner Mongolia). *Vertebrata PalAsiatica, 44,* 164–181.

Qiu, Z.-D., Zheng, S.-H., & Zhang, Z.-Q. (2008). Sciurids and zapodids from the late Miocene Bahe formation, Lantian, Shaanxi. *Vertebrata PalAsiatica, 46,* 111–123.

Savinov, P. R. (1970). Jerboas (Dipodidae, Rodentia) from the Neogene of Kazakhstan. *Byulleten' Moskoskovo Obshchestva Ispytatelei Prirody, Otdel Biologicheskii,* 91–134.

Schaub, S. (1934). Über einige fossile Simplicidentaten aus China und der Mongolei. *Abhandlungen der Schweizerische Palaeontologische Gesellschaft, 54,* 1–40.

Schlosser, M. (1924). Tertiary vertebrates from Mongolia. *Palaeontologia Sinica, C, 1,* 1–119.

Simpson, G. G. (1945). The principles of classification and a classification of mammals. *Bulletin of the American Museum of Natural History, 131,* 1–350.

Topachevsky, V. A. (1965). *Insectivora and Rodentia of the late Pliocene fauna of Nogaisk*. Kiev: Naukova Dumka.

Zazhigin, V. S., & Lopatin, A. V. (2000). The history of the Dipodoidea (Rodentia, Mammalia) in the Miocene of Asia: 1. *Heterosminthus* (Lophocricetinae). *Paleontological Journal, 34,* 319–332.

Zazhigin, V. S., Lopatin, A. V., & Pokatilov, A. G. (2002). The history of the Dipodoidea (Rodentia, Mammalia) in the Miocene of Asia: 5. *Lophocricetus* (Lophocricetinae). *Paleontological Journal, 36,* 180–194.

Zheng, S.-H. (1976). Small mammals of middle Pleistocene in Heshui, Gansu. *Vertebrata PalAsiatica, 14,* 112–119 (in Chinese).

Zheng, S.-H. (1982). Pliocene micromammals from Locality 2 of Songshan, Tianzhu, Gansu. *Vertebrata PalAsiatica, 20,* 138–147 (in Chinese).

Chapter 8
A Dormouse (Gliridae, Rodentia) from Yushe Basin

Wen-Yu Wu

Abstract This work documents the first dormouse known as a component of the Pliocene small mammal assemblages of Yushe Basin, Shanxi Province. It is the youngest dormouse in the Chinese fossil record. Due to their small body size and tiny teeth, dormice are generally underrepresented in fossil assemblages, and were previously unknown in Yushe Basin. The technique of screen-washing allowed the Sino-American field team to recover a single specimen in 1988. It represents a species of dormouse that may be identical with the taxon recorded to the north at the older sites of Ertemte and Bilike in Inner Mongolia. It is currently unknown whether more than one lineage of dormouse characterized the paleocommunities of Shanxi Province, and whether they were present throughout the Miocene of China. The occurrence of this group is consistent with a stable ecology promoting high rodent diversity during the Pliocene of Yushe Basin. Dormice are not yet known from Pleistocene deposits of North China, and in China today, the only known representatives are *Dryomys* in Xinjiang and *Chaetocauda* in Sichuan Province.

Keywords Yushe Basin • North China • Pliocene • Gliridae • Dormouse

Gliridae Muirhead, 1819
Subfamily Myomininae Daams, 1981
Myomimus Ognev, 1924
Myomimus sp.

Material, locality, and stratigraphic position: A single right m2 (V 13689; Fig. 8.1) from locality YS97, about 4.3 Ma in the Culiugou Member of the Gaozhuang Formation, Yuncu Subbasin, Shanxi Province.

Description: This lower molar constitutes the first and the only record of the family recovered from the Yushe Basin to date. It is wider than long (1.08 × 1.17 mm), narrowing distinctly posteriorly by reduction at the posterolingual corner of the tooth. It shows almost no occlusal wear and has no posterior interdental facet. Like other *Myomimus*, V 13689 has a concave occlusal surface and slightly inflated ends of ridges. The centrolophid is short and thins labially, crossing half the tooth. The extra ridge between the anterolophid and metalophid (anterior accessory ridge) is absent. The single extra ridge present on this tooth, between the mesolophid and the posterolophid, is thin. Three roots are present (the anterior root is divided into two roots).

Size and morphology are consistent with *Myomimus sinensis* Wu, 1985 from Ertemte 2 and Harr Obo 2, Inner Mongolia. There is no question that the specimen is assignable to the genus *Myomimus* based on (1) the concave occlusal surface, (2) presence of the extra ridge lying between the mesolophid and posterolophid, and absence of the extra ridge between the anterolophid and metalophid, (3) the mesolophid being relatively straight and inclined labially, and (4) presence of three roots. However, definitive identification as *M. sinensis* is not justified by this single specimen, and it is left open for the time being.

Discussion: The Ertemte fauna, type locality for *Myomimus sinensis,* represents the latest Miocene Baodean Land Mammal stage/age, while the slightly younger Harr Obo fauna is likely earliest Pliocene in age. Qiu and Storch (2000) illustrate and describe a good sample of *Myomimus sinensis* from Bilike, Inner Mongolia, which is early Pliocene, younger than Harr Obo, probably between 4.5 and 5 Ma (Qiu et al. 2013). The Yushe specimen V 13689 narrows posteriorly, a characteristic of *M. sinensis* m2, in contrast to the greatly reduced and narrower m3. V 13689 shows the same size and morphology as the morphology encompassed by the Bilike sample of m2. YS97, at an age of 4.3 Ma based on

W.-Y. Wu (✉)
Laboratory of Paleomammalogy, Institute of Vertebrate Paleontology and Paleoanthropology, Chinese Academy of Sciences, 142 Xizhimenwai Ave., Beijing 100044, People's Republic of China
e-mail: wuwenyu@ivpp.ac.cn

Lawrence J. Flynn and Wen-Yu Wu (eds.), *Late Cenozoic Yushe Basin, Shanxi Province, China: Geology and Fossil Mammals, Volume II: Small Mammal Fossils of Yushe Basin*, Vertebrate Paleobiology and Paleoanthropology,
DOI 10.1007/978-94-024-1050-1_8

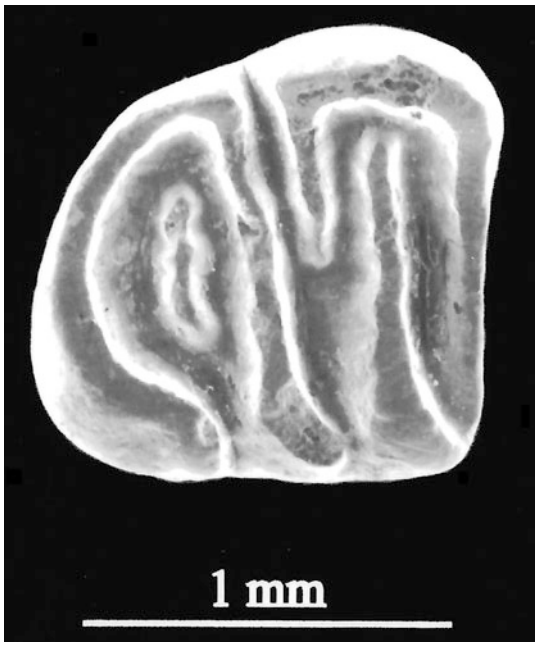

Fig. 8.1 *Myomimus* sp. from locality YS97. Right m2 (V 13689), Pliocene Culiugou Member, Gaozhuang Formation, anterior to right

magnetostratigraphic interpolation (Opdyke et al. 2013), records the youngest record for *Myomimus* in China.

The traditional usage of "Gliridae" is followed here as the formal family level designation for dormice. Myoxidae Gray, 1821 has been preferred as the appropriate name by some specialists. However, McKenna and Bell (1997) point out that, with *Glis* Brisson accepted as valid, then Gliridae, Muirhead (not Gliridae, Thomas) is validated. These nomenclatural nuances aside, Gliridae were never very successful in eastern or southern Asia, but they are an important complement to the small mammal record of Yushe.

Unlike the many dormice that live in moist, forested habitats, the extant species of *Myomimus* is a ground-dweller, living in relatively open, rocky terrain or shrubland (Storch 1978; IUCN red list 2015). While not necessarily an indicator of dry conditions, this glirid cannot be taken to indicate tree cover for Yushe Basin.

Acknowledgements The specimen was recovered through the care and attention of our colleague, the late Will Downs, by his pains-taking sorting of concentrate under magnification. Ms. Renate Liebreich from the Institut für Paläontologie und historische Geologie, Universität München, kindly made the photomicrograph with a Leitz AMR scanning electron microscope of that institution. The careful reading and additions by I. Casanovas-Vilar, Z.-D. Qiu, and L. Flynn are gratefully acknowledged.

References

IUCN red list of threatened species (2015). *International Union for Conservation of Nature and Natural Resources*. Retrieved January 13, 2016, from http://www.iucnredlist.org.

McKenna, M. C., & Bell, S. K. (1997). *Classification of mammals above the species level*. New York: Columbia University Press.

Opdyke, N. D., Huang, K., & Tedford, R. H. (2013). The paleomagnetism and magnetic stratigraphy of the Late Cenozoic sediments of the Yushe Basin, Shanxi Province, China. In R. H. Tedford, Z.-X. Qiu, & L. J. Flynn (Eds.), *Late Cenozoic Yushe Basin, Shanxi Province, China: Geology and fossil mammals Volume I: History, geology, and magnetostratigraphy* (pp. 69–78). Dordrecht: Springer.

Qiu, Z.-D., & Storch, G. (2000). The early Pliocene micromammalian fauna of bilike, Inner Mongolia, China (Mammalia: Lipotyphla, Chiroptera, Rodentia, Lagomorpha). *Senckenbergiana lethaea, 80,* 173–229.

Qiu, Z.-D., Wang, X., & Li, Q. (2013). Neogene faunal succession and biochronology of Central Nei Mongol (Inner Mongolia). In X. Wang, L. J. Flynn, & M. Fortelius (Eds.), *Fossil mammals of Asia: Neogene biostratigraphy and chronology* (pp. 155–186). New York: Columbia University Press.

Storch, G. (1978). Familie Gliridae Thomas, 1897—Schläfer. In J. Niethammer & F. Krapp (Eds.), *Handbuch der Säugetiere Europas* (pp. 201–280). Wiesbaden: Akademische Verlagsgesellschaft.

Wu, W.-Y. (1985). Neogene mammalian faunas of Ertemte and Harr Obo in Nei Mongol, China–6. Gliridae (Rodentia, Mammalia). *Senckenbergiana lethaea, 66,* 69–88.

Chapter 9
The Zokors of Yushe Basin

Shao-Hua Zheng

Abstract Myospalacinae from the Yushe Basin include ten species representing two tribes: Prosiphneini and Mesosiphneini. Of four Prosiphneini, the late Miocene *Prosiphneus murinus* spans the Mahui Formation to the Taoyang Member, low in the Gaozhuang Formation (~6.5–5.7 Ma), *Pliosiphneus antiquus* n. sp. occurs in the middle of the Nanzhuanggou Member of the Gaozhuang Formation (~4.7–4.5 Ma), and *Pliosiphneus lyratus* spans the Nanzhuanggou Member of the Gaozhuang Formation to the lower Mazegou Formation (~4.7–3.6 Ma). The derived *Eospalax fontanieri* appears much later in the Lishi Loess and younger sediments. The record of six Mesosiphneini begins with *Chardina truncatus* in the Nanzhuanggou Member (~4.7–4.5 Ma). *Mesosiphneus praetingi* spans the Culiugou Member of the Gaozhuang Formation to the lower Mazegou Formation (~4.3–3.4), and is followed by *Mesosiphneus intermedius* higher in the Mazegou Formation (~3.4–2.9 Ma). The mesosiphneine *Yangia trassaerti* is present in the early Pleistocene Haiyan Formation and *Y. tingi* occurs higher in the Haiyan Formation, both pre-Reunion magnetostratigraphic event, estimated ~2.5 to 2.2 Ma. *Yangia epitingi* in the Pleistocene Wucheng Loess is the youngest Yushe mesosiphneine. Zokor distribution reflects the Teilhard de Chardin Yushe biostratigraphy: the Mahui Formation to the Taoyang Member of the Gaozhuang Formation is equivalent to Teilhard's Yushe Zone I; the Nanzhuanggou and Culiugou members through the Mazegou Formation is equivalent to Yushe Zone II; and the Haiyan Formation represents Yushe Zone III. The data propose a lineage of Mesosiphneini evolving from a primitive form to extinction: *Chardina truncatus* → *Mesosiphneus praetingi* → *M. intermedius* → *Yangia trassaerti* → *Y. tingi* → *Y. epitingi.* The transformation from the rooted *M. intermedius* to the rootless *Y. trassaerti* (by the earliest Pleistocene) clearly reflects a major change in environmental conditions. Among the rooted myospalacines, specific differentiation is recognized by sudden increases in tooth crown height. Among the rootless forms, taxa are distinguished by the increase of clinomegodonty (decrease in angle α), which is correlated with increased dental stress during feeding, likely due to changing environment.

Keywords North China • Neogene • Siphneids • Zokors • Myospalacinae

9.1 Introduction

The Yushe Basin is one of the most fossiliferous areas for Late Cenozoic mammals in China. A characteristic component of the Yushe faunas is the group of large, burrowing rodents known today informally as the zokors. Zokors are found readily during surface prospecting, and thus are a key faunal element in the classical works of early paleontologists. Teilhard de Chardin (1942) recognized the biostratigraphic importance of zokors and other large body-size rodents early in his investigations, and characterized three Yushe faunal zones according to their occurrences. Zokors are primitive muroid rodents and were originally recognized as a group under the family level name Siphneidae. Currently they are considered Subfamily Myospalacinae, and placed in Family Spalacidae (allied with Spalacinae and Rhizomyinae) according to molecular work, but not without controversy (de Bruijn et al. 2015). As documented within the basin by

Note: This chapter includes one or more new nomenclatural-taxonomic actions, registered in Zoobank, and for such purposes the official publication date is 2017.

S.-H. Zheng (✉)
Laboratory of Paleomammalogy, Institute of Vertebrate Paleontology and Paleoanthropology, Chinese Academy of Sciences, 142 Xizhimenwai Ave., Beijing 100044, People's Republic of China
e-mail: zhengshaohua@ivpp.ac.cn

Lawrence J. Flynn and Wen-Yu Wu (eds.), *Late Cenozoic Yushe Basin, Shanxi Province, China: Geology and Fossil Mammals, Volume II: Small Mammal Fossils of Yushe Basin*, Vertebrate Paleobiology and Paleoanthropology,
DOI 10.1007/978-94-024-1050-1_9

Teilhard de Chardin (1942), Yushe myospalacines encompass approximately one-fourth of the known taxonomic diversity for the group. Among these, the rooted taxa (five species) constitute one-third of the known forms. Because these species occur in distinct stratigraphic intervals, they are extremely important for understanding the phylogeny and evolutionary history of the subfamily. The Yushe Basin occurrences are generally chronologically constrained, but some difficulties persist for specimens that lack precise stratigraphic or chronological data.

From 1987 to 1991 under the direction of Drs. R.H. Tedford and Z.-X. Qiu, a joint Sino-American field investigation was launched entitled "Neogene Rocks and Faunas, Yushe Basin, Shanxi," with express objectives to document stratigraphic positions and determine chronological ages for paleontological specimens collected in the past, in addition to the compilation of new data, and thus establishment of a biostratigraphic sequence for Asia. From 1987 to 1991, substantial micro-mammalian collections were amassed by Z.-D. Qiu, W. R. Downs, W.-Y, Wu, and L.J. Flynn. At the end of 1993, Flynn and Wu urged this author to undertake a study of the Yushe myospalacines, which were derived from 34 localities (with stratigraphic control) in the Mahui, Gaozhuang, Mazegou, and Haiyan formations, and the overlying loess. Of these localities, 29 produced fossils worthy of study, although a majority of the specimens consist of isolated teeth. During the course of this work, supplemental descriptions were written for several significant specimens that were collected by Teilhard de Chardin but not described in his 1942 monograph. Skulls collected by an IVPP field team in 1958 from Honggou and Jingnangou of the Gaozhuang area of Yushe are included in this study.

9.1.1 Taxonomy of the Subfamily Myospalacinae Lilljeborg, 1866

Myospalacine taxonomy has become increasingly complex since the discovery of the rooted "*Siphneus eriksoni"* from Ertemte, Inner Mongolia (Schlosser 1924), which was long ago synonymized under the genus name *Myotalpavus* by Miller (1927). Earlier Teilhard de Chardin (1926) had erected the genus *Prosiphneus*, with its type *P. licenti,* to represent the rooted myospalacines from the *Hipparion* Red Clay beds of Qingyang, Gansu Province. Later, Teilhard de Chardin and Young (1931) first applied the family designation "Siphneidae" and included two genera, *Prosiphneus* (rooted) and "*Siphneus*" (rootless). Also three groups were recognized: the "*psilurus* group", the "*fontanieri* group", and the "*tingi* group", which were meant to reflect occiput architecture that is flat, convex, or concave. Allen (1938) assigned several extant species to the genus *Myospalax* and species with convex occiputs to the genus *Eospalax*, combining both within the subfamily Myospalacinae. Leroy (1940) later elevated those genera to subfamily rank as "Prosiphneinae" and "Siphneinae", and recognized a "flat-occiput group", "concave-occiput group", and "convex-occiput group". Subsequently, Teilhard de Chardin (1942) preserved the name "Siphneidae" for the rooted *Prosiphneus* and the rootless "*Siphneus*" grades but emphasized that it was important to subdivide the latter into three genera based on cranial structure (clades). Much later, Kretzoi (1961) redesignated the family as Myospalacidae and erected the genera *Mesosiphneus, Episiphneus,* and *Allosiphneus,* based upon species then recognized (*Prosiphneus praetingi, P. pseudarmandi,* and "*Siphneus*" *arvicolinus*, respectively). He further proposed *P. licenti* as the type species for *Prosiphneus,* and that "*Siphneus fontanieri*" and "*Mus myospalax*" would represent *Eospalax* and *Myospalax,* elevating them from subgenera to generic status. Lawrence (1991) treated myospalacines under Myospalacinae as a murid subfamily, and placed all extant and fossil taxa within the genus *Myospalax.* McKenna and Bell (1997) used the Myospalacinae as a subfamily of the Muridae, placing the rooted taxa within the genus *Prosiphneus* and the rootless taxa within the genus *Myospalax*. Musser and Carleton (2005), following Tulberg (1899), assigned the extant myospalacines (including the genera *Eospalax* and *Myospalax*) with the genera *Spalax*, *Rhizomys,* and *Tachyoryctes* together within the muroid Family Spalacidae.

Based upon the radiations of cranial morphologies (clades) Zheng (1994) assigned the flat occiput crania to the Subfamily Myospalacinae, which was to include the rooted *Episiphneus* and the rootless *Myospalax*. The convex occiput crania were designated as the Subfamily Prosiphneinae, including the rooted genera *Prosiphneus, Myotalpavus, Pliosiphneus* and the rootless *Allosiphneus* and *Eospalax*. The concave occiput crania were assigned to the Subfamily Mesosiphneinae, including the rooted *Chardina* and *Mesosiphneus* and the rootless *Yangia*. This taxonomic division is the basis for the description of the Yushe fossils. Because "siphneids" are a muroid radiation here treated at the subfamily level, the zokors of this study are placed into two tribes: Prosiphneini and Mesosiphneini within Subfamily Myospalacinae Lilljeborg, 1866.

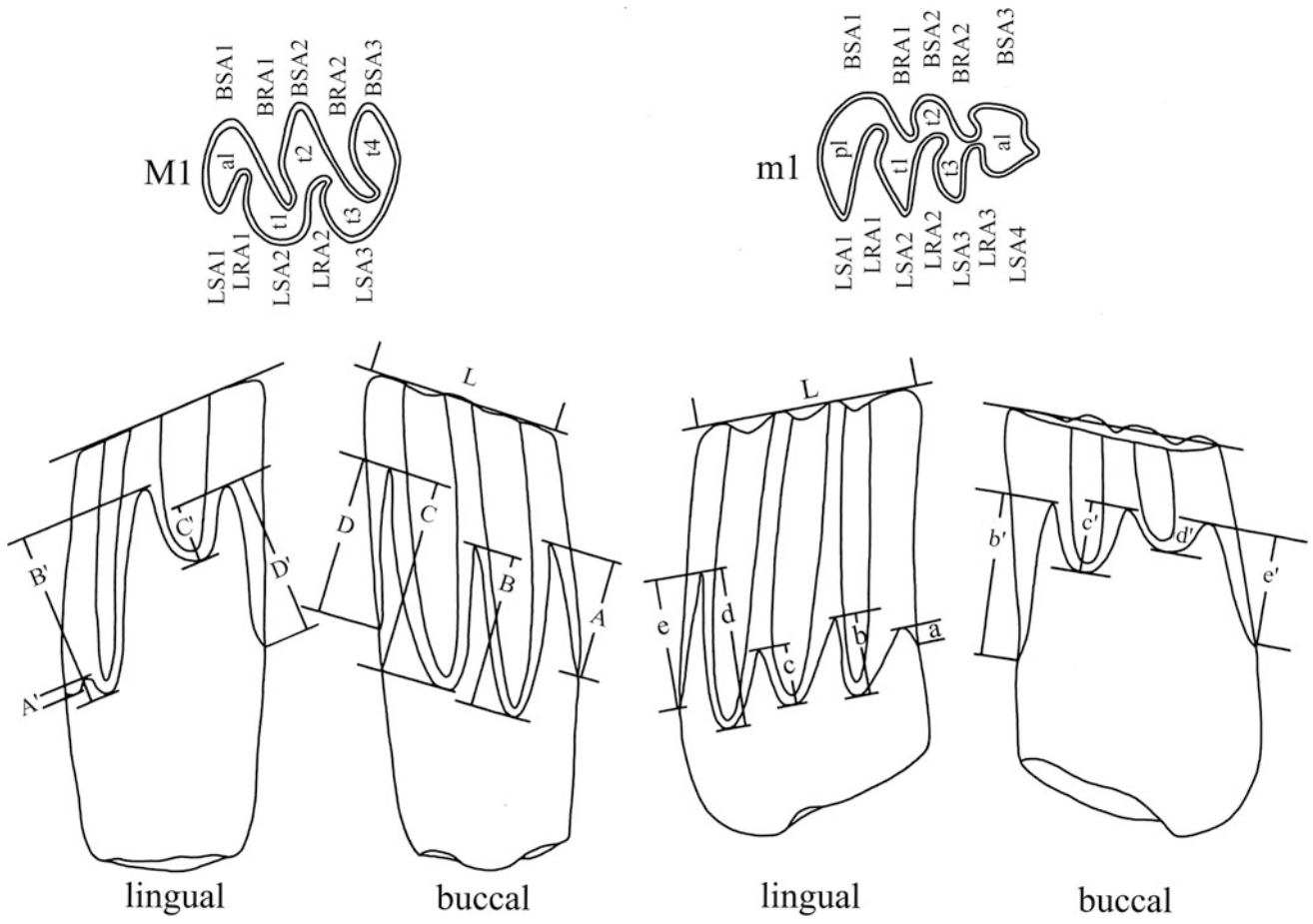

Fig. 9.1 Terminology for rooted molars, M1 (left, anterior to left) and m1 (left, anterior to right). al-anterior loop, BRA-buccal reentrant angle, BSA-buccal salient angle, LRA-lingual reentrant angle, LSA-lingual salient angle, pl-Posterior loop, t-triangle, parameters A′–D′ and a–e on lingual side and A–D and b′–e′ on buccal side for the height of dentine tracts

9.1.2 Terminology

Cranial terminology follows Teilhard de Chardin (1942), Lawrence (1991), and Zheng (1994). Dental terminology will follow Martin's (1987) application to the Microtinae due to the basically prismatic morphology of myospalacine molars. Buccal dentine tract parameters are applied to express variation in the base of the enamel on the side of the crown, stronger undulation correlating with increasing hypsodonty. Diagnosis is based upon the dentine tract (or sinuous line) parameters utilized by Zheng (1994) who recognized tracts A, B, C, D on the buccal side of the upper molars and a, b, c, d, e on the lingual side of lower molars; upper molar lingual dentine tracts are designated A′, B′, C′, D′ and lower molar buccal dentine tracts are b′, c′, d′, e′ (Fig. 9.1). In addition, Teilhard de Chardin's (1942) orthomegodont-clinomegodont terminology is applied to reflect the angle (α) of M2 between its lingual border and the anterior wall of its lingual reentrant. Primitively the tooth is short and α is nearly a right angle, but as the tooth lengthens in rootless clinomegodont forms, the angle α becomes strongly acute (Fig. 9.2). The decline in (α) is correlated with an increased length/width ratio for M2.

Specimens discussed here reside primarily in collections of IVPP with numbers having the prefix V, or in collections of the Tianjin Natural History Museum. The latter may have prefixes of THP or TNP, but old registration numbers have a prefix derived from the French name for the museum, *Musée Hoang-ho Pai-ho de Tientsin*, yielding acronym HHPHM. Some specimens bear designations of the earlier Cenozoic Laboratory of the Geological Survey of China; these are fossils numbered with a "C" numerator over a specimen number, usually transcribed as a prefix "C/" over a number. New fossils found by the Yushe research team of 1987–1991 have V numbers and localities with site number prefixes of "YS" for Yushe Site.

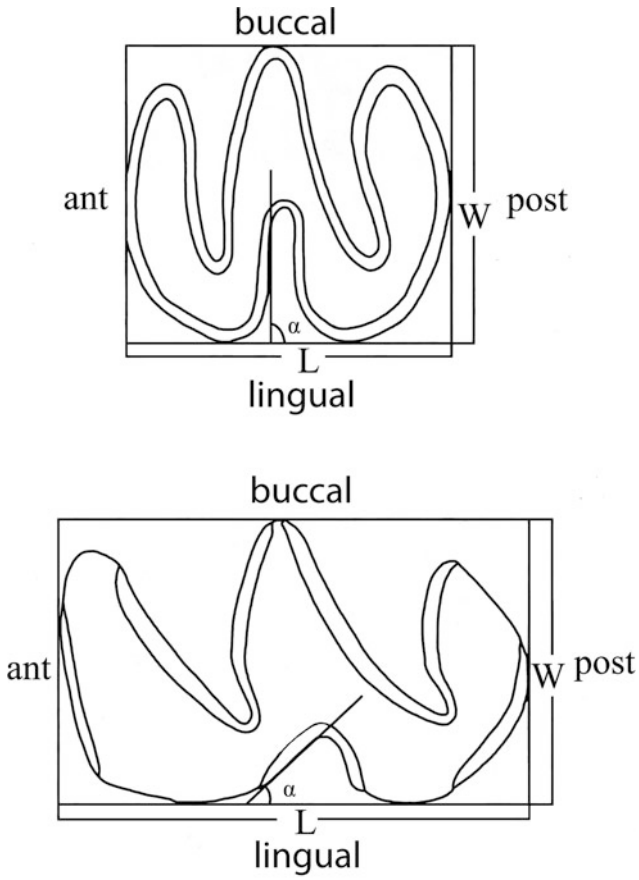

Fig. 9.2 Crown morphology of idealized myospalacine left M2, rooted above and rootless below (clinomegodont) showing the angle (α) of the anterior wall of the lingual reentrant

9.2 Systematics

9.2.1 Tribe Prosiphneini Leroy, 1940

Diagnosis: Occiput convex, squamosal/parietal suture not intersecting temporal crest. Long incisive foramen bisected by premaxilla/maxilla suture. Anterior margin of the parapterygoid fossa nearly at the same level as the mesopterygoid fossa; posterior pterygoid canal situated on the posterior wall of the pterygoid fossa. In taxa with rooted molars, interparietals located posterior to the lambdoid crest or situated between its wings; anterior cap (ac) of the lower first molar is elliptical and slightly displaced buccally, and the third lingual reentrant angle (LRA3) is opposite or obliquely opposite the second buccal reentrant angle (BRA2). In rootless taxa, the interparietal is absent, anterior end of the m1 lacks enamel, and the LRA3 is distinctly broader and shallower than the BRA2.

Included genera: *Prosiphneus* Teilhard de Chardin, 1926, *Pliosiphneus* Zheng, 1994; *Eospalax* Allen, 1938, *Allosiphneus* Kretzoi, 1961.

Prosiphneus Teilhard de Chardin, 1926 (Including *Myotalpavus* Miller, 1927)

Revised generic diagnosis: Small to medium sized myospalacines with narrow interorbital region. No squamosal in occipital region. The interparietal is quadrilateral and located posterior to the lambdoid crest. The first upper molar has two or three roots. Dentine tract parameter A of M1 and a, d and e of m1 are approximately zero. Anterior cap (ac) of the m1 is located buccally or on the longitudinal axis of the tooth.

Type species: *P. licenti* Teilhard de Chardin, 1926

Included species: *P. licenti*, *P. eriksoni* (Schlosser, 1924), *P. murinus* Teilhard de Chardin, 1942, *P. tianzuensis* (Zheng and Li, 1982), *P. qinanensis* Zheng et al. 2004, *P. qiui* Zheng et al. 2004 and *P. haoi* Zheng et al. 2004.

Prosiphneus murinus Teilhard de Chardin, 1942

1942 *P. murinus*, Teilhard de Chardin, p. 33, Figs. 27–29, 33
1961 *P. murinus*, Kretzoi, p. 126
1982 *Prosiphneus* ex gr. *ericksoni*, Mats et al., p. 118, Fig.12 (2); Pl.XIV, Figs. 2–12
1984 *P. murinus*, Li et al., Table 5
1991 *P. murinus*, Flynn et al., Fig. 4; Table 2
1991 *P. murinus*, Tedford et al., Fig. 4
1991 *Myospalax murinus,* Lawrence, p. 282
1994 *Prosiphneus murinus,* Zheng, Figs. 2, 4, 7, 9–12; Table 1
2004 *P. murinus*, Zheng et al., Figs. 6, 7; Tables 1, 2.

Revised species diagnosis: Equivalent in size to *P. licenti,* but slightly more hypsodont. Tooth roots are relatively long and bifurcate rather late in ontogeny. Average parameters A, B, C, and D of M1 are 0.18, 1.02, 0.62, 0.22 and a, b, c, d, e of m1 are 0, 0.59, 0.51, 0.2, 0.

Localities and material: YS1, left M1 (V11151.1) and left m1 (V11151.2); YS8, fragmentary left mandible with m1–2 (V11152.1), left mandible with m1–3 (V11152.2) and right m1 (V11152.3), right M2 and two right m2 (V11152.4-6); YS7 right M2 (V11153.1) and two right m2 (V11153.2-3); YS9 right M1 (V11154.1), damaged left M1 (V11154.2) and damaged right m3 (V11154.3); YS3 left m1 lacking the posterior loop (V11155); YS32, two left and one right m1 (V11156.1-3), left m2 (V11156.4), and two right m3 (V11156.5-6); YS141, left M1 (V11157.1), right M2 (V11157.2), left M3 (V11157.3), right m1 (V11157.4) and damaged right m2 (V11157.5); YS29, skull with damaged occiput and parietal, associated left and right mandibles (V11158); YS145 right M1 (V11159); YS156, left mandible portion with m1-2 (V11160); YS161, left mandible fragment with m1-3 (V11161). Measurements in Tables 9.1, 9.2, 9.3 and 9.4.

Stratigraphic range: Mahui Formation to basal Taoyang Member of the Gaozhuang Formation.

Description: Suture fusion and degree of dental wear indicate an adult individual, but missing on the YS29 skull (V11158) are the nasals, infraorbital foramen, both zygomas, posterior parts of frontals, parietals and dorsal occipital region. The nasal-frontal suture is very slightly convex anteriorly, and projects very slightly posterior to the posterior margin of the infraorbital foramen. Lacrimal foramen is narrow, long, and located anteroventral to the infraorbital foramen. Interorbital region is slightly concave. The supraorbital crests are shifted medially into the interorbital region. Incisive foramen is approximately one half the length of the diastema.

Mandibular symphysis terminates rostral to the mental foramen, and the foramen is large and situated anterior to the mesial margin of the m1. The masseteric crest ends beneath the second buccal reentrant of the m1 and comprises a weak ventral branch and an indistinct dorsal branch. The masseteric fossa is flat anteriorly but concave posteriorly, without a bump formed by root tips. The ascending ramus rises between the m1–2. Coronoid process is missing, although the notch between the coronoid and condyle is narrow and deep. A deep pit beneath the condyle-coronoid notch is due to the projecting terminus of the incisor. The condyloid process extends posteromedially. Although the ventral margin of the angular process is broken, it is estimated that it was not well developed and hence the notch between it and the condyle is rather broad and shallow (Fig. 9.3).

Upper and lower incisors resemble those of extant taxa but are distinctly smaller. The orange enamel surface is smooth and glossy, with a median longitudinal ridge on the lower incisor.

The mesial wall of M1 is flat or slightly convex, and the anterior loop is frequently narrower than posterior part of the tooth. In occlusal view, the anterolingual reentrant is slightly shallower than the posterolingual reentrant and both are perpendicular to the long axis of the tooth. Both buccal reentrants are posterolingually inclined. Lingual salient angles are rounded but buccal salient angles are acute, hence t1 and t3 are not as distinctly triangular as t2 and t4 (Fig. 9.3f). Buccal dentine tracts are higher than the bases of

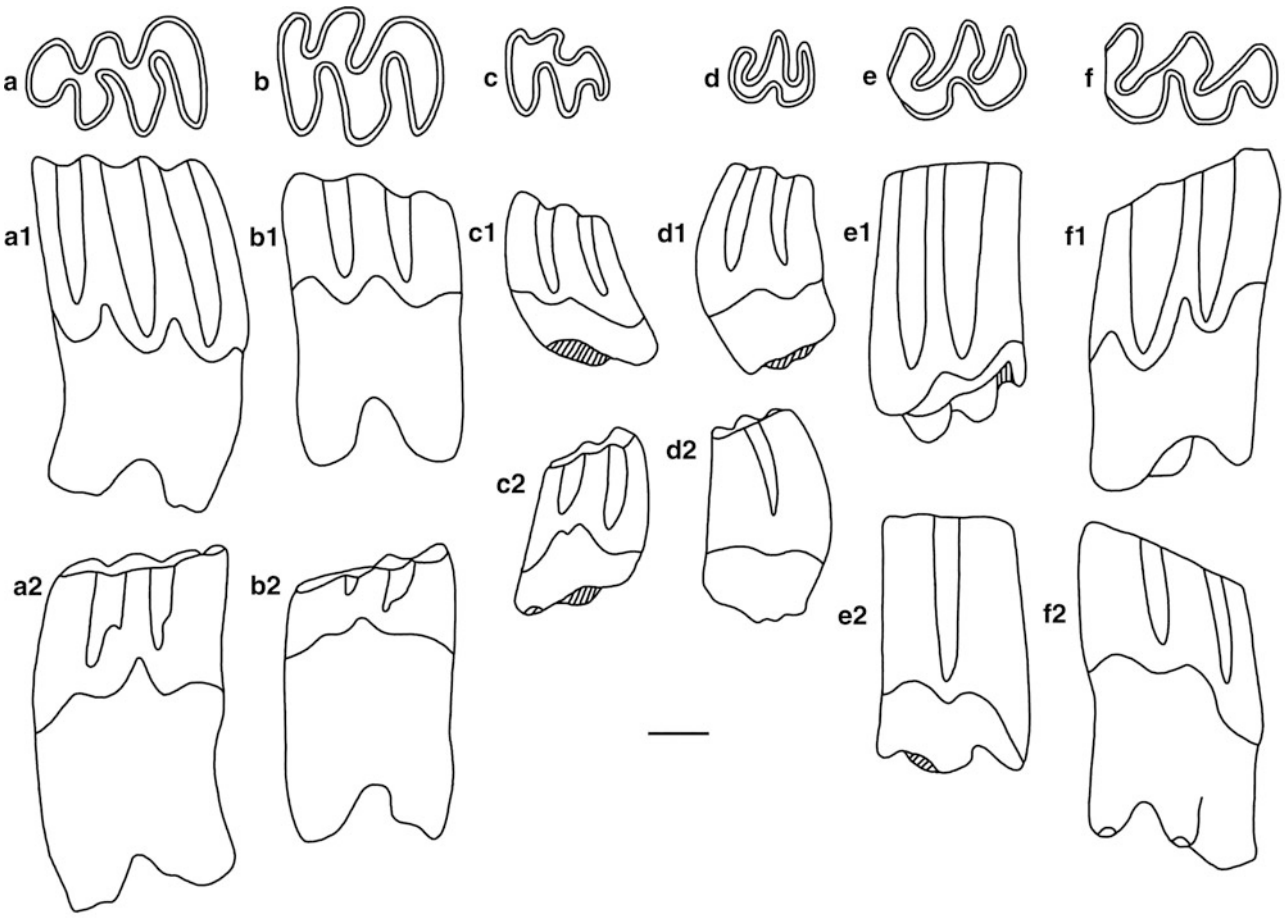

Fig. 9.3 Upper and lower molars of *Prosiphneus murinus*. Occlusal view (top row), lingual view (middle row), buccal view (bottom row); 1 mm scale. **a–a2** r m1 (V11152.3); **b–b2** r m2 (V11152.5); **c–c2** r m3 (V11156.5); **d–d2** l M3 (reversed, V11157.3); **e–e2** r M2 (V11152.4); **f–f2** l M1 (reversed, V11157.1). **a–c** anterior to left; **d–f** anterior to right

the reentrant folds, giving the enamel configuration a W-pattern (Fig. 9.3f1). The lingual dentine tracts, lower than the bases of the reentrant folds, make the enamel configuration broad and gently undulating (Fig. 9.3f2). In mature individuals the crown height is less than root length. Of the four roots, the buccal two are rather closely spaced, with their bases fused to compose a ridge.

Among the M2's are three juvenile specimens from YS 3, 8, and 141 which lack completely developed roots. Given their age, the anterior walls of the lingual reentrants are distinctly posterobuccally inclined, while the two buccal reentrants are very slightly inclined posterolingually (Fig. 9.3e). Length-breadth ratios along the occlusal surface are respectively 0.71, 0.70 and 0.71. The base of the buccal enamel is low with single-peak, double-valley. The enamel base at the anterior and posterior ends of the tooth is nearly equivalent to the bases of the reentrant valleys (Fig. 9.3e1). The basal enamel configuration on the lingual side is double-peak, single-valley (Fig. 9.3e2).

M3 is represented by a juvenile specimen from YS141 (V11157.3, Fig. 9.3d) and in the skull from YS29. It resembles M2 in basic morphology but is distinctly compressed. The third buccal salient angle is particularly reduced. The base of the enamel on both sides resembles the M2 but with less undulation. Parameters are low and reentrant angles terminate above the enamel base.

The m1 displays four lingual salient and three reentrant angles, while buccally there are three salient and two reentrant angles (Fig. 9.3a). The buccal reentrants penetrate the crown less than the lingual reentrants and in aged individuals these frequently become worn to enamel loops. There is a wide range of variation in occlusal morphology. Of seven specimens, three display anterior loops (=anterior caps) that are narrow and to the buccal (or buccal) side, while the other four have broad anterior loops that are symmetrically aligned with the long axis of the tooth. On two specimens the third lingual and second buccal reentrants are opposed. On three specimens the third lingual reentrant is more anterior, and on two specimens this reentrant is more posterior. Dentine tracts are higher than (lingually) or equivalent to (bucally) the bases of the reentrant folds, with configurations of two-peak/three-valley on the lingual side, and three-peak/two-valley on the buccal side (Fig. 9.3a1–2). A small spur occurs at the mouths of the bases of the buccal reentrants. Adult specimens have longer roots than crowns. Two roots are present.

The m2 has three salient angles and two reentrant angles on each side, with the anterior buccal reentrant (BRA2) angle being the shallowest. With the exception of the loss of the third lingual reentrant, the morphology resembles that of the m1. The dentine tracts are slightly below the bases of reentrants, with a configuration of two-peak/two-valley lingually, and two-peak/single valley or single peak/double valley on the buccal side (Fig. 9.3b1–2). With increase in age, the crown wears and the roots gradually lengthen and bifurcate.

The m3 is similar in morphology to m2, but with distinctly shallower first and second buccal reentrants. The posterior loop is greatly reduced, and the tooth curves buccally. Configuration of lingual and buccal enamel is double peak with a single valley (Fig. 9.3c).

Comparison: The new material collected from the Yushe Basin is completely consistent with *P. murinus* originally described by Teilhard de Chardin (1942) in characters such as size, nasal/frontal suture generally at the same level as the posterior margin of the infraorbital foramen, concave interorbital region, weak and medially shifted supraorbital crest, placement of the incisive foramen, morphology of the mandible, and degree of molar hypsodonty.

Table 9.1 Comparison of cranial measurements for *Prosiphneus murinus* (mm)

	P. murinus				
	YS29	Teilhard de Chardin, 1942			*P. licenti*
	V11158	Skull I	Skull II	Skull III	Type
Cranial length	36.12	35.14	>36.84	37.84	>35.5
Interorbital breadth	8.1	6.4	6.9	7.5	8.1
Occiput breadth between condyles	9.7	9.7	9.9		10.3
Cranial breadth before lambdoid crest	20.4	20	19		18.4
Diastema length	12	12	11.5	11.7	13.1
Incisive foramen length	6		6.3	6.3	
Mandible articular process – incisor	28.8	28.2			28.4
Mandible articular process-mental foramen	22.4	21.3			21
Mandible diastema length	6.4	6.9			6.4
Mandible height under the m1 (lateral)	6.9	6.8			6.7

Table 9.2 *Prosiphneus murinus* dental measurements (mm)

		M1-3	M1	M2	M3	m1-3	m1	m2	m3
	N	1	6	4	2	2	10	7	4
L	Range		2.8–3.3	2.23–2.5	1.4–2.1	8.2–8.5	2.64–3.23	2.3–2.8	1.7–2.57
	Mean	8.28	3.03	2.37	1.75	8.35	2.93	2.63	2.14
	N		6	4	2		10	7	4
W	Range		1.6–2.2	1.6–2.08	1.25–1.8		1.57–2.33	1.6–2.55	1.5–2.1
	Mean		1.91	1.83	1.53		2.51	2.11	1.85

The cranial morphology and size of *Prosiphneus murinus* are close to the type of *P. licenti* Teilhard de Chardin, 1926 from Qingyang, Gansu Province (Table 9.1), but the type for the latter is a poorly preserved articulated maxilla and mandible, making detailed comparisons difficult. Teilhard de Chardin (1942) indicated that the cranium of *P. licenti* is relatively broader (distance between lateral margins of supraoccipital process is 16 mm versus 13 mm for *P. murinus*), interorbital region is wider (8 vs. 7 mm), and the M1 anterolingual reentrant (LRA1) of *P. licenti* in occlusal view is lost and does not form the enamel ring of *P. murinus*. A reevaluation of the two species indicates very little distinction in either size or morphology. The distinctions may in fact reflect the poor preservation of the type of *P. licenti*, which suffered compressional distortion. The loss of the anterolingual reentrant occurs only on a single specimen and is influenced by wear. Furthermore, a number of isolated teeth referred to *P. licenti* by Zheng et al. (2004) display a first lingual reentrant frequently extending further than the second lingual reentrant.

Zheng et al. (2004) undertook a review of the genus *Prosiphneus* and referred seven species to it. Of these seven congeners, *P. murinus* provides the most cranial data, but the other six species have little to no comparable cranial material. Thus, comparison was based largely on isolated molars. From the aspects of crown height and tooth root development, *P. murinus* and *P. licenti* are together easily differentiated from the other five species. *Prosiphneus murinus* and *P. licenti*, share the same lengths of roots and extremely similar dentine tract parameters of molars. The m1 root height, i.e., the distance between the root bifurcation to the lowest enamel curvature under the second lingual reentrant, is 1.5 mm for both. The average values of m1 lingual dentine tract parameters a, b, c, d, e of *P. licenti* (nine specimens) are 0, 0.51, 0.59, 0.2, 0, while those of *P. murinus* (nine specimens) are 0.03, 0.53, 0.44, 0.31, 0.07; m1 buccal dentine tract indices b′, c′, d′, e′ of *P. licenti* (six specimens) are 0.10, 0.49, 0.14, 0.36, while those of *P. murinus* (four specimens) are 0.09, 0.66, 0.30, 0.92; M1 buccal dentine tract parameters A, B, C, D of *P. licenti* (six specimens) are 0.2, 0.77, 0.57, 0.38, while

Table 9.3 *Prosiphneus murinus* upper molar dentine tract values (mm)

		A	B	C	D	A’	B’	C’	D’
	N	6	6	6	6	4	4	4	4
M1	Range	0.0–0.4	0.55–1.1	0.5–0.7	0.0–0.3	0.0–0.0	0.65–0.9	0.0–0.4	0.55–1.0
	Mean	0.13	0.83	0.5	0.13	0	0.74	0.21	0.76
	N	3	3	3	3		2	2	2
M2	Range	0.0–0.0	0.68–0.7	0.3–0.7	0.0–0.1		1.05–1.15	0.4–0.7	0.2–0.4
	Mean	0	0.69	0.53	0.07		1.1	0.55	0.3
M3	N = 1	0	–0.6	–0.3	0		–0.4	–0.3	0

Table 9.4 *Prosiphneus murinus* lower molar dentine tract values (mm)

		a	b	c	d	e	b’	c’	d’	e’
	N	8	8	8	8	8	4	4	4	4
m1	Range	0.0–0.1	0.1–0.8	0.3–0.7	0.2–0.5	0.0–0.2	0.0–0.2	0.45–0.75	0.15–0.5	0.63–1.15
	Mean	0.03	0.53	0.44	0.31	0.07	0.09	0.66	0.3	0.92
	N		4	4	4	4	2	2	2	2
m2	Range		0.15–0.40	0.3–0.6	0.35–0.45	0.0–0.0	0.4–0.5	0.23–0.4	0.1–0.2	0.25–0.5
	Mean		0.24	0.4	0.4	0.0	0.45	0.32	0.15	0.38
	N		2	2	2	2	1	1	1	1
m3	Range		0.1–0.1	0.2–0.35	0.25–0.3	0.0–0.0				
	Mean		0.1	0.28	0.28	0.0	0.0	0.7	0.1	0.5

those *P. murinus* (six specimens) are 0.13, 0.83, 0.56, 0.13; M1 lingual dentine tract indices A′, B′, C′, D′ of *P. licenti* (three specimens) are 0.12, 0.52, 0.25, 0.40, while those of *P. murinus* (four specimens) are 0, 0.74, 0.21, 0.76. Thus, dental morphology, tooth crown height (dentine tract parameters) and available cranial measurements, and other aspects indicate little differentiation between *P. murinus* and *P. licenti,* so it is possible that they are synonymous, but new cranial data are required to test this hypothesis.

Prosiphneus murinus occurs in much of the Mahui Formation throughout Yushe Basin. Specimens were recovered from YS8 at 6.3 Ma in Yuncu subbasin, and it is found in lower (older) exposures of the formation at YS1 in Tancun subbasin. The species is produced throughout upper Mahui levels in both subbasins. Locality YS161 represents the latest dated record of *P. murinus* at the top of the Mahui Formation, approximately 5.8 Ma, and the species occurs at Dengyucun, Tancun subbasin locality YS145, which is in horizontal beds of basal Gaozhuang Formation, overlying locality YS141 in the gently dipping Mahui Formation (see Tedford et al. 2013: 57). Other scanty remains also indicate likely survival into the Taoyang Member of the Gaozhuang Formation.

Given an age estimate of 11.7 Ma for the appearance of *Prosiphneus* (Zheng et al. 2004), the genus spans 6 m.y. at least. *P. murinus* precedes temporally *Pliosiphneus*, but the species is not considered its ancestor. The latter genus is much closer in crown height and root length to latest Miocene *Prosiphneus eriksoni* as noted by Zheng (1994). Judging from the age range, *P. murinus* in Yushe Basin (∼6.5–5.7 Ma) succeeded *P. licenti* from the Qinan district, Gansu, with age range ∼7.6–6.5 Ma, as estimated by Guo et al. (2002) and Liu et al. (2011).

Prosiphneus ex gr. *eriksoni* (Mats et al. 1982), from the lower section of exposure 520 in the central Baikal region, has a lingual m1 bifurcation point of approximately 1.5 mm, in addition to upper and lower lingual/buccal dentine tract configurations that are consistent with *P. murinus*. This indicates the broad geographic range of *P. murinus*, and suggests comparable environmental conditions from North China to the Baikal region at the Miocene-Pliocene boundary.

Pliosiphneus Zheng, 1994

Diagnosis: Medium to large size. Convex skull with triangular squamosal adjacent to the occipital region. The interparietal is shuttle-shaped and located between the lambdoid crests. Supraorbital crest is shifted medially in primitive species, but not in derived ones. Roots of M1 are fused into a single one. The anterior cap of m1 is located on the long axis of the tooth. M1 dentine tract parameter A and m1 parameter e are well above zero.

Type species: *Pliosiphneus lyratus* Teilhard de Chardin, 1942

Included species: *P. lyratus* and *P. antiquus,* sp. nov.

Pliosiphneus lyratus (Teilhard de Chardin, 1942)

1942 *Prosiphneus lyratus,* Teilhard de Chardin, p. 46, Figs. 34B; 36–36a
1961 *Prosiphneus lyratus,* Kretzoi, p. 126
1984 *Prosiphneus lyratus,* Li et al., Table 5
1986 *Prosiphneus lyratus,* Zheng and Li, Table 5
1990 *Prosiphneus lyratus,* Zheng and Li, pp. 434, 439
1991 *Myospalax lyratus,* Lawrence, p. 206
1994 *Pliosiphneus lyratus,* Zheng, Figs. 2, 4, 7, 9–12; Table 1
2001 *Pliosiphneus lyratus*, Zheng and Zhang, Table 3
2003 *Pliosiphneus lyratus*, Zhang et al., Fig. 1

Revised species diagnosis: Skull supraorbital crest not shifted medially, and temporal crests very weakly developed on juveniles but robust on adults, sagittal region expansive and concave, and narrowing distinctly posteriorly. Nasals posteriorly extended to the margin of the infraorbital foramen. Premaxilla/maxilla suture traverses the incisive foramina 2/5 the way from their posterior margin. Molars moderately hypsodont, M1 parameters A, B, C and D are 1.45–1.5, 0.85–1.6, 1.5–2.1 and 1.1–1.2; m1 parameters a, b, c, d, e are 0, 1.9, 1.7, >4.6, >3.6.

Material and localities: YS69, fragmentary skull (V11162); YS50, aged right m1 (V11163); YS43, right m1 (V11164); locality unknown-anterior portion of skull (V11165 = 31.077); measurements in Table 9.5.

Stratigraphic range: Nanzhuanggou and Culiugou members of the Gaozhuang Formation, and basal Mazegou Formation.

Description: The holotype (HHPHM 31.076) originally ascribed to *Prosiphneus* as "*Prosiphneus lyratus*" consists of an aged skull (Teilhard de Chardin 1942, Fig. 36). Juvenile individuals are now recognized for this taxon and are discussed here. Specimens from the Tianjin Museum collection include an undescribed anterior skull part from Yushe (31.077 = V11165) and a relatively complete skull assigned to the "*murinus* group" (Teilhard de Chardin 1942, Fig. 34b).

Nasals gradually expand rostrally at their midpoint and extend caudally to the posterior margin of the infraorbital foramen. Interorbital region of frontal is broad and flat. Supraorbital crests are not medially shifted but posteriorly they expand laterally. The parietal region is concave with parasagittal crests well developed, and distinctly laterally projected at the rostral third of the parietals, but caudally they gradually migrate medially. Temporal crest does not intersect squamosal/parietal suture. Interparietal, large and shuttle-shaped, is situated between the wings of the lambdoid crests, and is nearly as broad as the posterior sagittal region. The occipital shield is flat but projects posteriorly from the junction of the lambdoid crests. A supraoccipital process is weak, lateral occipital crests are well developed compared to the medial crest, lateral occipital fossae are shallow, and the squamosal is triangular. The foramen

Table 9.5 Cranial measurements of *Pliosiphneus lyratus* (mm)

	Teilhard 1942	31.077	YS69	Teilhard 1942 Fig. 36 (31.076)
	Fig. 34B	V11165	V11162	
Cranial length	39.6		≥42.4	45.1
Diastema length	12	12.2	13	14.5
Incisive foramen length	5.3	5.7	5.4	5.1
Post. incis.for.- ant. mesopter. fossa	19.7	20.5	21.7	22.8
Ant. mesopter.-post.occ.condyle	17.5		≥ 17.5	19.4
Interorbital breadth	8.5	8.8		7.7
Cranial breadth (ant. to lambdoid)	21.9			24.6
Occiput breadth	21.8			29
Occiput height	16.7			19.3
Condyles breadth	10.6			12.5
Palate breadth (M1)	3.1	3.2	3.4	4.4
Palate breadth (ant. M3)	4.4	4.6	4.5	5.5
Interparietal breadth	9.6			11.4
Molar row length	9.7	9.3	9.4	10.8
M1 length/width		3.57/2.5	3.8/2.5	4.1/2.6
M2 length/width		2.3/2.6	2.9/2.6	3.2/2.8
M3 length/width				2.9/2.3

magnum is large and nearly circular. Incisive foramina are relatively short and may be less than half the length of the diastema. Rostral palatal vacuity is large with midpoint located between the M1 and M2. The midpoint of the caudal palatal foramen is located between the M2 and M3. The rostral pterygoid fossa reaches beyond the anterior margin of the middle pterygoid fossa. Caudal pterygoid fossa is largest and elliptical in shape. Caudal pterygoid canal is located dorsal to the posterior wall of the caudal pterygoid fossa, and has an inclined crest anteriorly. Anterolateral angle of the basioccipital is undeveloped, hardly bulging ventrally. A large hypoglossal foramen is located at the rostrolateral side of the occipital condyle. Auditory bulla is small with a ventral margin that is nearly at the same level as the basioccipital. From a lateral perspective the dorsal line is distinctly elevated and attains its greatest height at the frontal/parietal suture. The sphenopalatine fossa is a small, deep, triangular basin with the divergence of the ethmoid and optic foramina located at the rostrodorsal and the caudoventral region of the posterior wall. The sphenopalatine foramen is not seen, either concealed by dental opercula or obliterated.

The upper cheek tooth rows are in parallel alignment and moderately hypsodont (Fig. 9.4). Their lingual reentrant angles are nearly perpendicular to the long axis of the teeth, although buccal reentrant angles are slightly posterolingually inclined. The first lingual reentrant angle (LRA1) on M1 penetrates the crown as deeply as LRA2. On the M2 and M3 the second buccal salient angle (BSA2) projects slightly more than the BSA1 and BSA3. Dentine tracts for M1 are in the three-peak, two-valley configuration (Fig. 9.4c, d); parameters A, B, C, D for V11162 are 1.5, 1.6, 2.1, and 1.1; on specimen 31.077: 1.45, 0.85, 1.5, and 1.2.

The right m1 from YS50 is an aged individual with the occlusal surface on the buccal reentrant angles worn to enamel rings. The occlusal enamel surfaces of lingual salient angles 1, 2 and 3 are truncated although the surface on salient angle 4 is retained. Consequently, dentine tract configuration is three-peak, three-valley with peak beneath salient angle 4 undeveloped. Root bifurcation is high, 4.2 mm (lingual root bifurcation to the lowest point of the enamel at reentrant angle 2).

The damaged skull from locality YS69 is an extremely old individual with crowns nearly worn to their roots. Consequently lingual reentrants are transformed into enamel rings (Fig. 9.4b) and dentine tract parameters cannot be measured.

Comparison: *P. lyratus* has rather derived cranial morphology compared to the more primitive *Prosiphneus murinus*. Additionally, it is nearly contemporaneous with the concave occiput *Chardina truncatus*. Comparisons between the three taxa are shown in Table 9.6. Dentine tracts of *P. lyratus* most closely resemble *Chardina sinensis* (Teilhard de Chardin and Young 1931) with A, B, C and D parameter values of 1.5, 1.6, 2.1, 1.1 and 1.6, 1.7, 1.7, 2.05. However the latter (type is an anterior portion of skull) differs with shorter incisive foramina contained completely in the premaxilla.

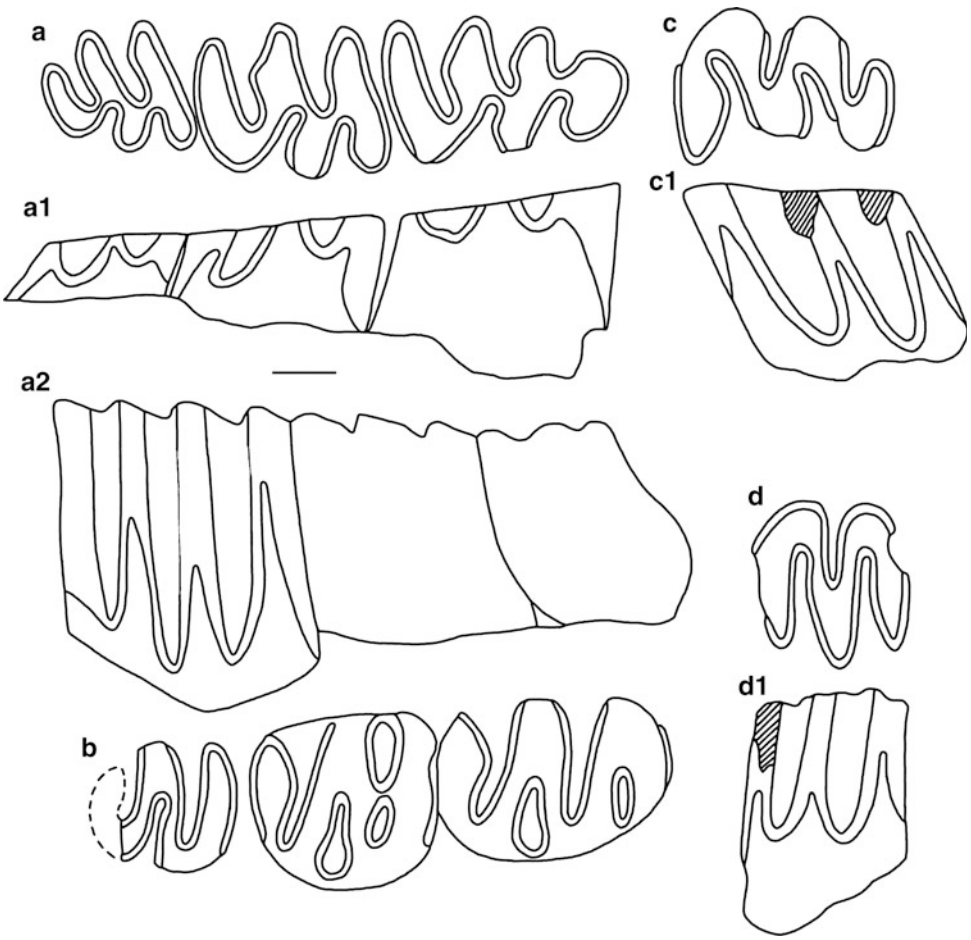

Fig. 9.4 Upper and lower dentition of *Pliosiphneus lyratus*, 1 mm scale. **a** Occlusal view of right m1–3 from Huabaogou, Nihewan (anterior to right); **a1** Buccal view, **a2** Lingual view; **b** Occlusal view of right M1-3 (V11162); **c** Occlusal view of left M1 (31.077, V11165), **c1** Buccal view of **c**; **d** Occlusal view of left M2, locality unknown, **d1** Buccal view of **d**

Table 9.6 Comparisons of cranial features of *P. murinus*, *Pliosiphneus lyratus* and *Chardina truncatus*

	Pr. murinus	*Pl. lyratus*	*Chardina truncatus*
Body size	Small	Medium	Large
Nasal expands	From half-way point suddenly	From half-way point suddenly	Gradually from posterior
Caudal end of nasal	Slightly caudal to infraorbital foramen	Slightly caudal to infraorbital foramen	Well caudal of infraorbital foramen
Interorbital region	Narrow, concave	Wide, flat	Moderate, concave
Supraorbital crest	Weak, shifted medially	Strong, not shifted medially	Strong, shifted medially
Temporal crest and parietal/squamosal suture	Not intersecting	Not intersecting	Intersecting
Sagittal region	Flat	Strongly concave	Slightly concave
Interparietal	Quadrilateral, caudal to lambdoid crest	Shuttle-form, between lambdoid crests	Semi-circular, rostral to lambdoid crest
Occipital shield	Flat	Flat	Slightly concave
Supraoccipital process	Weak	Moderate	Strong
Squamosal in occipital region	Absent	Absent	Present
Incisive foramen	In premax/maxilla, 1/2 length of diastema	In premax/maxilla, 1/2 length of diastema	In premaxilla, 2/5 length of diastema
Ventral tympanum	Projected to basioccipital	Same level as basioccipital	Projected to basioccipital
Dorsal line	Gentle	Strongly arched	Gentle
Arrangement of molar rows	Approximately parallel	Approximately parallel	Strongly divergent posteriorly

Discussion: Of the referred material, skull 31.077 represents a relatively small individual with weakly developed supraorbital, parietal, and lambdoid crests, and light degree of dental wear (enamel loops not developed), which are characters suggestive of a juvenile. Skull V11162 from YS69 is an aged individual that lacks the dorsal occipital region, and elements posterior to the basisphenoid. Its different preservation, not stained black as other specimens, may call into question its provenance, but assignment to *P. lyratus* is supported by several characters, including small size, long incisive foramina, and relatively hypsodont dentition in parallel alignment. The two m1's from YS43 and YS50 are extremely worn, prohibiting determination of lingual dentine tracts, but their hypsodonty and lingual root bifurcation (3.1–3.2 mm) are distinctly greater than *P. murinus* (1.5–1.7 mm). Furthermore, their dentine tract parameter "a" (=0) differs from the later *Mesosiphneus praetingi* (greater value, 1.7 mm). This low value is also seen in *Chardina truncatus.*

A right mandible collected from the Pliocene of Huabaogou, Nihewan Basin, Hebei Province (Fig. 9.4a1–2), was initially assigned to *Pliosiphneus lyratus* based upon its hypsodonty (m1 a, b, c, d, e parameters: 0, 2.0, 2.0, 3.2, 3.04; Zheng 1994, Fig. 10). Being a mandible rather than a skull, and a much younger individual than the aged crania representing *P. lyratus* and *Chardina truncatus* the assignment is difficult to evaluate. Considering proportional dental values, specifically the M1 A, B, C, D in relation to the m1 b, c, d, e average values, then it will be noted that primitive species, like *Prosiphneus licenti, P. murinus, P. tianzuensis* (Zheng and Li 1982), and *P. eriksoni* display average A values that are less than b values, and average B and C values greater than c and d values. In more derived taxa including *Chardina sinensis* and *Mesosiphneus intermedius* the average A, B and C values are smaller than their b, c and d values. Assuming the constancy of this relationship, the Huabaogou mandible is reasonably assigned to *P. lyratus,* as its m1 b, c, d, e values are generally smaller than M1 A, B, C and D values for HHPHM 31.077. *Pliosiphneus lyratus* would represent a transitional or intermediate form between primitive and derived taxa.

Pliosiphneus antiquus, sp. nov.

1991?*Prosiphneus eriksoni* Flynn et al., Fig. 4; Table 2

1991?*Prosiphneus eriksoni,* Tedford et al., Fig. 6

1994 *Pliosiphneus* sp. 1, Zheng, Figs. 2, 7, 10, 11, 12; Table 1

2000 *Prosiphneus* cf. *eriksoni*, Qiu and Storch, p. 196, Pl. 10, Figs. 7–12

2013 *Pliosiphneus* cf. *P. lyratus*, Liu et al., p. 227

Type: Anterior portion of skull with incisors and left and right M1-3 (V11166 [31.323], locality within the Yushe Basin unknown).

Table 9.7 Dental measurements of *Pliosiphneus antiquus* sp. nov. (mm)

		M1	M2	m1–3	m1	m2	m3
Length	N	1	2	1	2	4	2
	Range		1.80–2.50		3.20–3.23	2.90–3.12	1.90–2.30
	Mean	2.82	2.15	8.60	3.22	2.99	2.10
Breadth	N	1	2		2	4	2
	Range		1.45–1.78		1.80–2.03	1.80–2.30	1.30–1.70
	Mean	1.93	1.62		1.92	2.04	1.50

Locality and material: YS39, left M1 (V11167); YS57, right M1 (V11168.1), right M2 (V11168.2), left M2 (V11168.3), anterior half of right m1 (V11168.4), left m2 (V11168.5), right m3 (V11168.6); YS50, damaged right M2 (V11169.1), right m1 and m2 (V11169.2-3); YS36, partial left mandible with incisor and m1-3 (V11170); see Table 9.7.

Stratigraphic position: Nanzhuanggou Member of the Gaozhuang Formation.

Diagnosis: Supraorbital crests of skull converge medially and rapidly fuse. Interorbital region is narrow; nasals are distinctly laterally inflated rostrally; premaxilla/maxilla suture traverses the incisive foramen at its posterior third. Degree of hypsodonty between that of *Prosiphneus eriksoni* and *Pliosiphneus lyratus.* M1 average values of dentine tracts A, B, C and D are 0.43, 1.43, 0.93 and 1.50; m1 averages for a, b, c, d and e are 0.07, 0.73, 1.07, 1.55 and 0.6.

Etymology: From the Latin *antiquus*.

Description: The black coloration and the holotype (V11166) indicates derivation from the Yushe Basin. Incisor tips, posterior nasals, and infraorbital foramen are damaged. Rostrally, the nasals widen rapidly from the anterior margin of the infraorbital foramen, so that the anterior nasal breadth is twice that of the posterior breadth. The interorbital region is narrow (6.1 mm), supraorbital crests migrate strongly medially such that they would fuse as a single sagittal crest. From a lateral perspective the rostrum is distinctly depressed. Incisive foramina are relatively long (6.7 mm) with the premaxilla/maxilla suture traversing them at the posterior third of the foramina. At the caudal region of the incisive foramina there is a spur created by a coarse medial line that extends to the posterior palatine. The anterior palatine foramen extends to the second lingual salient angle of M1. Dental rows are nearly parallel.

Incisors are triangular in cross-section with a triangular pulp cavity and mesiodistal and transverse diameters of 2.5 and 2.2 mm, respectively. Termini of incisors are not housed in conspicuously swollen or projecting capsules. In molar morphology the first buccal salient angles on M2 and M3 are relatively reduced while the second salient angle projects prominently (Fig. 9.5a). M1 lingual reentrants penetrate the tooth crown to an equivalent depth. Buccal dentine tract parameters A, B, C, D are 0.43, 1.43, 0.93 and 1.5. On the

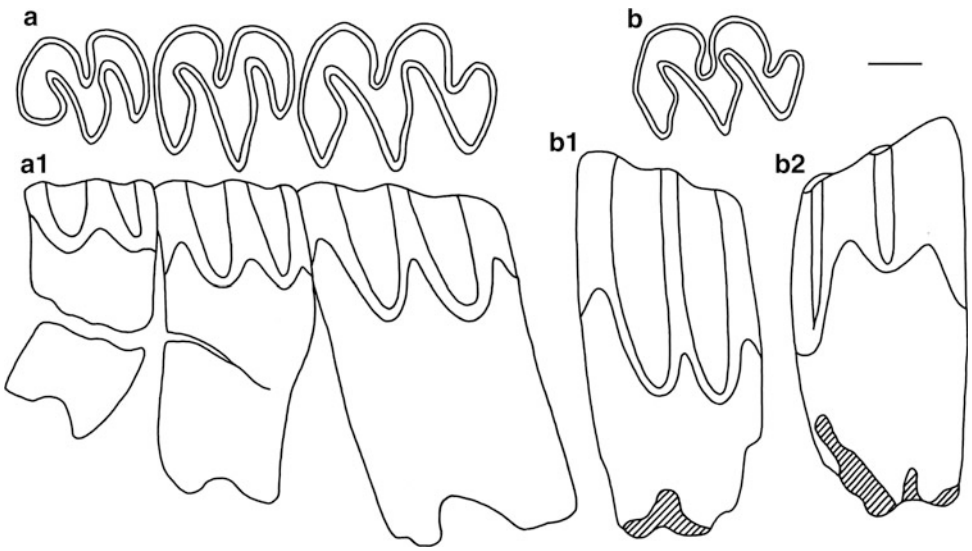

Fig. 9.5 Upper molar morphology of *Pliosiphneus antiquus* sp. nov., 1 mm scale. **a** occlusal view of left M1-3 of holotype V11166 (31.323), locality unknown, **a1** buccal view; **b** occlusal view of left M1 (V11167), **b1** buccal view, **b2** lingual view. Anterior to right for **a** and **b**

M2 these values are 0.4, 0.7, 0.7 and 0.6, and on the M3: 0.3, 0.2, 0.6 and 0.5. The roots on the holotype are extremely long and bifurcated. The lowest point of the buccal second reentrant fold to the root bifurcation is 3.6 mm. Other root termini (Figs. 9.5b, 9.6e) are broken but represent adults.

The M1 assigned to this species (Fig. 9.6e) is an adult specimen. The anterior wall of the anterior loop is flat and buccally oblique. The first lingual reentrant fold penetrates the crown further than the second reentrant fold, and penetrates the tooth toward the roots rather deeply. A small stylar conule blocks the base of the valley of both reentrant folds. Lingual dentine tracts are not pronounced with parameters A′, B′, C′ and D′ as 0, 1.7, 0.25 and 1.55. Buccal roots are broken and dentine tracts are rather pronounced with A, B, C parameters as 0.25, 0.65 and 1.70.

The M2 specimens are adult (Fig. 9.6d–d2). The lingual reentrant is conspicuously posteriorly oblique, a small stylar conule blocks the base of the valley, and the sinuous line descends distinctly anteriorly and posteriorly with parameters B′, C′ and D′ as 1.65, 0.10, and 1.34. The second and third buccal salient angles project equivalently, while the first salient angle is relatively narrow.

The mandibular diastema is 6.1 mm, the mental foramen is large and located ventral to the anterior margin of the m1, masseteric fossa is flat with a circular anterior margin ventral to the buccal second reentrant fold of the m1, and there is a deep trough anterodorsally. The ascending ramus initiates at the buccal side of the third salient angle of the m1.

The anterior wall of the m1 in juveniles is concave but in worn adults becomes convex. The buccal second and lingual third reentrants are in opposition. In juveniles there is a rather broad dentine isthmus between them but in adults this narrows greatly (Fig. 9.6). An extremely well developed stylar conule lies at the base of the first buccal reentrant fold. The posterobuccal dentine tract is lower than its anterior counterpart and b′, c′, d′ and e′ parameters as 0.5, 0.2, 0.25, and 1.5 (Fig. 9.6a2). Depths of the three lingual reentrant angles gradually increase posteriorly in occlusal view, and lingually dentine tracts consist of three peaks and three valleys with the posterior peak and valley as the deepest and highest. Average a, b, c, d and e parameter values (three specimens) are 0.07, 0.73, 1.07, 1.55, and 0.6 (Fig. 9.6a1).

The anterior wall of the m2 is flat. The second buccal reentrant angle penetrates the crown slightly less than the first (Fig. 9.6b). Among the four specimens, three of them possess this fold anterior to its lingual counterpart, but on the remaining specimen this fold is in direct opposition to its lingual counterpart. Buccal dentine tracts extend deeply anteriorly and posteriorly with little undulation between. Average b′, c′, d′, and e′ parameter values are 2.25, 0.3, 0.3 and 1.93 (Fig. 9.6b2). The two lingual reentrant angles penetrate the crown to equivalent depths. Lingual dentine tract configuration is three-peak, two-valley with average b, c, d, e parameters (three specimens) of 0.6, 0.93, 1.10, and 0.6 (Fig. 9.6b1).

The anterior wall of the m3 is flat, buccal reentrant angles are shallow and salient angles are small. The second buccal reentrant angle lies anterior to its lingual counterpart. The first lingual salient angle is greatly reduced. The first lingual reentrant angle penetrates the crown less than the second reentrant (Fig. 9.6c). The buccal dentine tracts undulate very little; b′, c′, d′ and e′ values as 0.5, 0.3, 0.1, and 0.3 (Fig. 9.6c2). Lingual

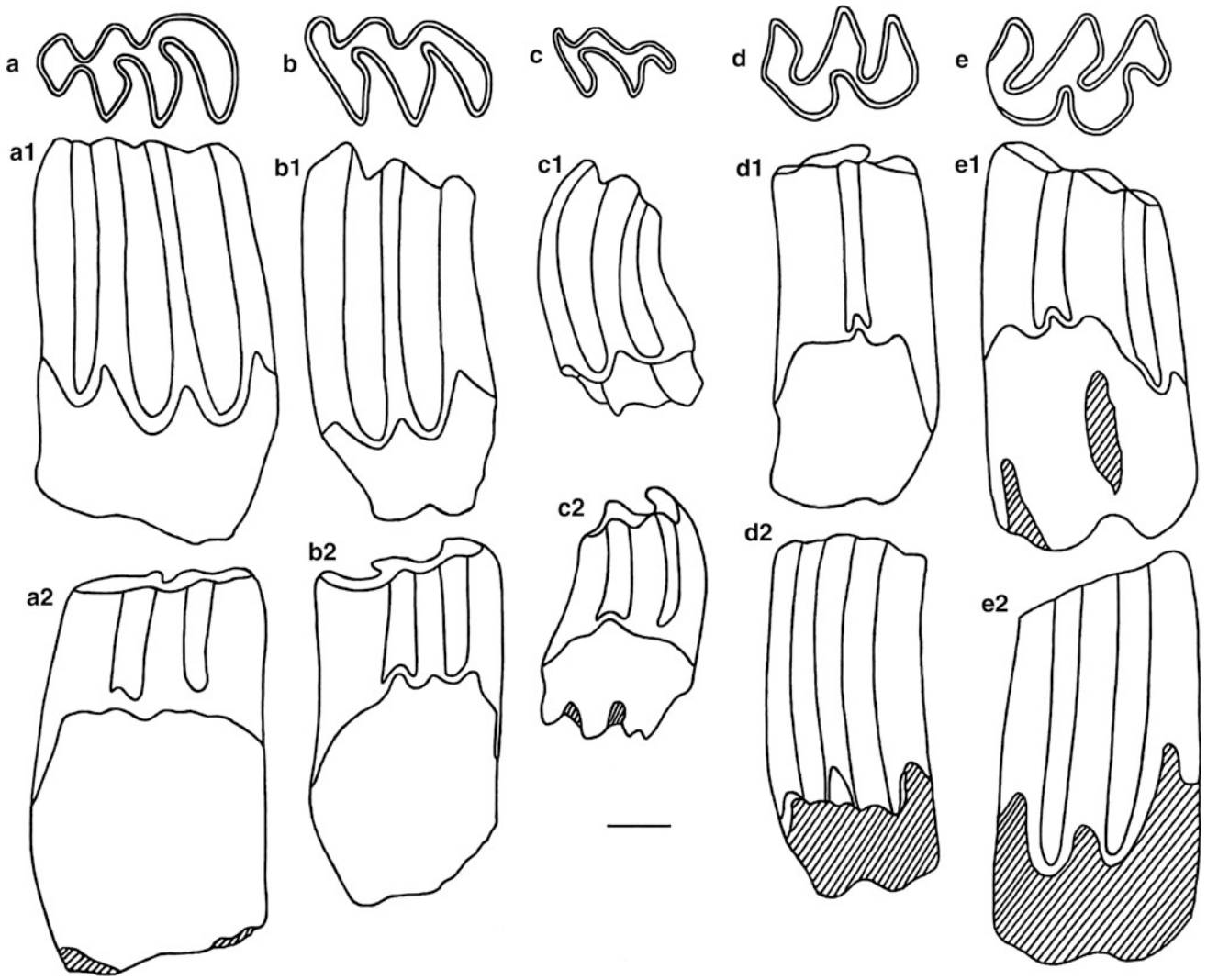

Fig. 9.6 Dental morphology for *Pliosiphneus antiquus* sp. nov., 1 mm scale. **a–e** occlusal views, **a–c** anterior to left, **d–e** anterior to right; **a1–e1** lingual view; **a2–e2** buccal view; **a–a1–a2** r m1 (V11169.2); **b–b1–b2** left m2 (reversed V11168.6); **c–c1–c2** r m3 (V11168.7); **d–d1–d2** r M2 (V11168.2); **e–e1–e2** r M1 (V11168.1)

dentine tracts undulate rather more with average b, c, d and e values of 0.3, 0.6, 0.6 and 0.2 (Fig. 9.6c1).

Comparison: The new taxon is referred to the convex occiput myospalacines based upon the position of the incisive foramina and the parallel alignment of the dentition. This species differs from all species of *Prosiphneus* but resembles *Pliosiphneus lyratus* in the increase in lateral dentine tracts and the distinct lengthening of the tooth-roots. It differs from *P. lyratus* in the relatively longer incisive foramen (6.7 vs. 5.3–5.7 mm), more slender rostrum (breadth anterior to infraorbital foramen 9.3 vs. 10.2–10.5 mm), narrower interorbital region (6.1 vs. 8.0–9.2 mm), the strongly medially shifted supraorbital crests that fuse as a sagittal crest, and distinctly greater brachydonty (M1 parameters A, B, C and D values 0.43, 1.43, 0.93 and 1.5 vs. 1.9, 2.4, 2.0 and 1.65).

Considering dental and dentine tract parameter similarity between *Pliosiphneus antiquus* from Yushe Basin and isolated molars referred to *Prosiphneus* cf. *eriksoni* from early Pliocene Bilike, Inner Mongolia (Qiu and Storch 2000), the latter are assigned to *P. antiquus*. *P. antiquus* differs from *Prosiphneus eriksoni* (skull unknown) by larger size (M1 length 3.2–3.6 vs. 2.8–3.2 mm), greater hypsodonty (*P. eriksoni* A, B, C and D values as 0.28, 1.03, 1.17 and 0.32), and longer M1 buccal root bifurcation (3.6 vs. 3.0–3.1 mm).

Discussion: Precise locality and stratigraphic data within Yushe Basin for the holotype of *P. antiquus* are unknown.

The additional material from YS39 and other localities confirms that this species occurs in the lower part of the Nanzhuanggou Member of the Gaozhuang Formation (4.7–4.4 Ma), which is close to the age of the Bilike fauna (Qiu and Storch 2000). From the perspective of molar root fusion and lengthening, or late bifurcation, there is a suggestion of close relationship between *Pliosiphneus* and *Prosiphneus eriksoni*.

The *P. antiquus* character of supraorbital crests that strongly converge medially and fuse as a single sagittal crest posterior to the interorbital region is consistent with the extant convex-occiput *Eospalax smithi* and quite distinct from the condition of *P. lyratus,* confirming that the new species is not a direct ancestor to the latter. The new taxon is more likely a relatively primitive off-shoot of the convex occiput myospalacines and may represent a distant ancestor to the *Eospalax* group, though intermediate taxa are unknown.

Eospalax Allen, 1938

Revised diagnosis: Convex-occiput zokors with rootless and clinomegodont molars. Triangular portion of the squamosal contributes to the occiput; interparietal usually absent. Posterior symphysis of mandible extends beneath the m1. Third lingual reentrant angle on m1 is shallow and second buccal reentrant angle is deep, but enamel lacking on its anterior end. A shallow anterior fold on M1 may be present. M3 and m3 not greatly reduced, M3 with two to three buccal and one to two lingual reentrant angles.

Type species: *Eospalax fontanieri* (Milne-Edwards, 1867)

Included species: *E. fontanieri*, *E. youngianus* (Kretzoi, 1961), *E. rufescens* (Allen, 1909), *E. rothschildi* (Thomas, 1911), *E. smithi* (Thomas, 1911), *Eospalax simplicidens* (Liu et al., 2014), *Eospalax lingtaiensis* (Liu et al., 2014).

Eospalax fontanieri (Milne-Edwards, 1867)

1927 *Siphneus fontanieri*, Young, p. 43
1928 *S.* cf. *fontanieri*, Boule and Teilhard de Chardin, p. 100, Fig. 28
1931 *S*. cf. *fontanieri*, Teilhard de Chardin and Young, p. 18, Pl. V, Figs. 23–24
1931 *S.* cf. *cansus*, Teilhard de Chardin and Young, p. 19, Pl. II, Fig. 6; Pl. III, Fig. 7
1931 *S. chanchenensis*, Teilhard de Chardin and Young, p. 20, Pl. III6, IV10, V19
1932 *S.* cf. *fontanieri*, Young, p. 6, Fig. 1; Pl.I, Fig. 2
1935 *S. fontanieri*, Young, p. 15
1936 *Siphneus* sp. (cf. *fontanieri*), Teilhard de Chardin, p. 19, Fig. 9
1939 *S. fontanieri*, Pei, p. 154
1940 *S. fontanus*, Takai, p. 209, Fig. 4; Pl. XXI, Figs. 1–6
1942 *S. fontanieri*, Teilhard de Chardin, p. 67, Figs. 46–48
1965 *Myospalax fontanieri*, Chow and Chow, p. 228, Pl. I, Fig. 6a, b
1965 *M.* cf. *fontanieri*, Chow and Li, p. 380, Pl. I, Fig. 3
1978 *Myospalax fontanieri*, Hu and Qi, p. 15, Pl. II, Figs. 6–8
1994 *Eospalax fontanieri*, Zheng, pp. 61–62, Figs. 2–4
1997 *E. fontanieri*, Zheng, Fig. 1
2004 *Eospalax fontanieri*, Cai et al., Table 2

Revised species diagnosis: Maximum body size for zokors; posterior margin of nasals not surpassing posteriorly the naso-frontal suture. Premaxilla-maxilla suture subdivides the incisive foramina into about equivalent parts. Supraorbital crests migrate medially to converge or form a bell-shape in adult males. Molars are clinomegodont. On M1 there is normally one shallow fold on the anterior wall. Based on M3, subspecies may be discerned: three buccal reentrant angles and one lingual reentrant angle characterize *E. f. fontanieri*; two buccal reentrant angles and one lingual reentrant angle distinguish *E. f. cansus*.

Material and locality: YS129, anterior portion of skull with broken incisors, left M1-2 and right M1 (V15266); YS123, damaged right mandible with incisor and m2–3 (V15266.1); YS133, left mandible fragment with incisor and m1–2 (V15266.2).

Stratigraphic position: Reddish Lishi Loess and Malan Loess.

Measurements: Skull V15266 diastema length 15.8 mm; length of incisive foramina 9.6 mm; breadth of palate between M1 s 5.7 mm; interorbital breadth 10.5 mm; alveolar length of m1–3, 12 mm; lengths/breadths of M1, M2, m1, two m2, m3: 4.0/2.3, 3.2/2.2, 4.5/2.2, 3.8/2.1 and 4.0/2.1, ~3.3/1.9.

Description: Nasals are slightly convex dorsally, expand very gently rostrally, and project distinctly beyond the posterior margin of the infraorbital foramen. The interorbital region is rather broad with distinct postorbital process. The supraorbital crests are weak and do not converge medially. The incisive foramina are relatively long and narrow (approximately 3/5 the length of the diastema) and located in the premaxilla and maxilla. Running caudally along the midline of the palate is a distinct crest.

The ascending ramus of the dentary, not well-preserved, initiates at the m1. The mental foramen is extremely small and located anteroventral to the anterior margin of the m1. The masseteric crest initiates at the anterior margin of m1 and maintains a well-developed ventral branch although its dorsal branch is obscure. The bone is distinctly inflated at the termini of the three molar roots. The masseteric fossa is shallow. The caudal extent of the mandibular symphysis ends posterior to the anterior margin of m1.

The m1 anterior wall (without enamel) is slightly convex. The third lingual reentrant angle is broad and shallow and nearly opposite the deep second buccal reentrant angle. The other two lingual reentrants penetrating the crown are distinctly deeper than the two buccal reentrants. The three

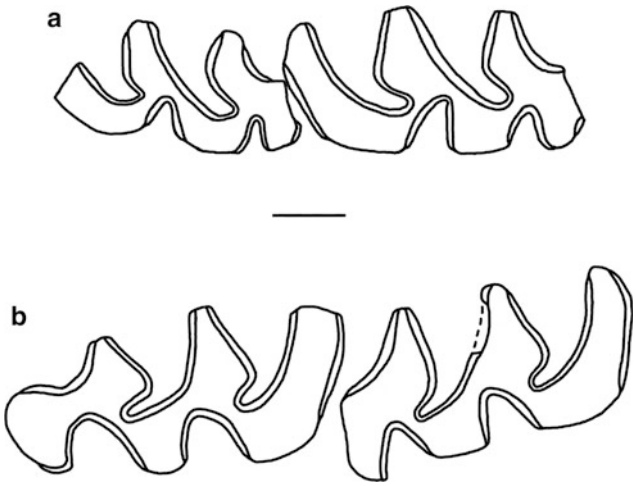

Fig. 9.7 Lower dentition of *Eospalax fontanieri* in occlusal view: **a**, right m2-3 (V15266.1) anterior to right; **b**, left m1-2 (V15266.2) anterior to left. 1 mm scale

lingual salient triangles are nearly vertical to the long axis of the tooth, but the first is inclined posteromedially (Fig. 9.7b).

The m2 and m3 have flat and straight anterior walls that also lack enamel. The first and second lingual reentrants penetrate the crown to the same degree as those of m1. The first and second buccal reentrants on both molars penetrate the crown to an equivalent degree. Both molars are clinomegodont. The m3 is less reduced (Fig. 9.7a).

The upper molars of V15266 are seriously damaged. The anterior wall of the M1 is slightly depressed. Two buccal reentrant angles penetrate the crown further than two lingual reentrants, while three buccal salient angles are sharper than three lingual salients. There are two buccal and one lingual reentrant angle, and three sharp buccal and two rounded lingual salient angles on the M2. Both M1 and M2 are clinomegodont.

Comparison and discussion: Teilhard de Chardin (1942) reported about 40 skulls of *E. fontanieri* from Yushe Basin, but they were not described in detail and only a few were illustrated. These specimens were collected from "praeloessic concretionary red clays" (equivalent to the presently recognized Lishi Loess) with the exception of one skull from a lacustrine deposit (equivalent to the Haiyan Formation).

The skull V15266 from YS129 agrees with Yushe Basin *E. fontanieri* in size, position of incisive foramen, and shape of supraorbital crests and molars. The maxillary suture intersects the incisive foramina near their midpoint in V15266 as in skulls figured by Teilhard de Chardin (1942: Figs. 47, 48). One skull illustrated by Teilhard de Chardin (1942, Fig. 46) erroneously shows the foramina to lie entirely within the premaxillae.

In China, many materials referred to this species could be reassigned to different species or subspecies, for instance, the left mandible (C/66) from Shihteshan, Wubao, Shaanxi (*Siphneus* cf. *fontanieri* of Teilhard de Chardin and Young 1931) belongs to the concave-occiput species *Yangia epitingi* given its larger size (m1–3 length of 13.4 mm), more reduced m3, deeper third lingual reentrant angle and especially less inclined, orthomegodont dentine pattern. The Chenjiawo, Lantian, Shaanxi specimen (Chow and Li 1965: "*Myospalax* cf. *fontanieri*") should be transferred to the subspecies *E. f. cansus* due to smaller size and simplicity of M3 with only two buccal and one lingual reentrant angles.

The only known extinct species of the genus is *E. youngianus* Kretzoi, 1961 that was originally described as "*Siphneus minor*" by Teilhard de Chardin and Young (1931). This species is characterized by its abnormally smaller cranium (diastema length 16.2 mm, interorbital breadth 7 mm) but longer tooth-row (length of upper tooth row 9.5 mm; M1 3.8 and M2 2.8 mm), with simple M3 as in *E. f. cansus.* All are distinct from the YS129 specimen.

Boule and Teilhard de Chardin (1928) described a right m1–2 from gravels at the base of Grand Loess, Qingyang, Gansu under the name "*Siphneus cf. myospalax*". It may represent a new species of the genus *Eospalax* because its m1 has no enamel on the anterior wall, but has broad and shallow third lingual and deep second buccal reentrants, and slightly inclined dentine lobe of m1–2 (generic character), and smaller size and lack of the second buccal reentrant of m2 (specific character).

The genus *Eospalax* includes extant *E. fontanieri*, *E. rufescens*, *E. rothschildi* and *E. smithi* (Luo et al. 2000; Wang 2003). Comparing the YS129 skull, it is similar to that of *E. fontanieri* in posterior margin of the nasals not extending caudal to the naso-frontal suture, half of the incisive foramina being in the premaxilla, and in diastema length and interorbital region breadth. *E. fontanieri* differs from *E. rufescens* in posterior margin of the nasals being rostral to rather than at or caudal to the naso-frontal suture, breadth of the supraorbital crests equaling rather than less than that of the temporal crests, half to two-thirds incisive foramina in the premaxilla (but M3 is similar in having three buccal, one lingual reentrant). *E. smithi* is characterized by its supraorbital crests approaching each other and even fusing into a strong sagittal crest, posterior margin of the nasals being equivalent or caudal to the premaxilla-frontal suture, most of incisive foramina in premaxilla, and M3 normally with three buccal and two lingual reentrants. *E. rothschildi* is smallest among recent species and has distinct supraorbital and temporal crests and faint medio-occipital crest, half or most of incisive foramina in premaxilla, and M3 normally possessing two reentrants on each side.

9.2.2 Tribe Mesosiphneini Zheng, 1994

Diagnosis: Convex occiput in primitive taxa, concave in derived taxa, with short incisive foramen located entirely in the premaxilla. Rostral margin of the parapterygoid fossa is situated distinctly rostral to the anterior margin of the mid-pterygoid fossa. The posterior pterygoid canal links two foramina at the medial and lateral ends on the platform of the pterygoid fossa. Parietal-squamosal suture intersects the temporal crest at mid-parietal. Semicircular interparietal is situated rostral to two wings of the lambdoid crest (primitively) or is absent in derived forms. Dentine tract parameter "a" of m1 is close to 0 in primitive forms, >0 in derived forms. Primitive taxa with rooted molars have m1 with a short and broad, buccally-displaced cap with interrupted enamel, and the lingual third reentrant angle situated distinctly anterior to the buccal second reentrant angle. In derived taxa with rootless molars, m1 has an anterior cap with enamel restricted mesially at the midline of tooth, and the lingual third reentrant angle is opposite the buccal second reentrant angle.

Included genera: *Chardina* Zheng, 1994, *Mesosiphneus* Kretzoi, 1961 and *Yangia* Zheng, 1994.

Chardina Zheng, 1994

Diagnosis: Skull with convex-occiput projecting slightly posterior to lambdoid crest and with a weak supraoccipital process. Squamosal in the occiput is triangular and interparietal is large, semicircular, and located rostral to lambdoid crest. Caudally, breadth of sagittal region is about 1.8 times that of the interorbital region. Posterior mandibular symphysis is anterior to the mesial margin of m1. Molars are rooted and relatively brachydont. The m1 parameter "a" value is close to zero. Roots of M1 tend to fuse.

Type species: *Chardina truncatus* (Teilhard de Chardin, 1942)

Included species: *C. truncatus*, *C. sinensis* (Teilhard de Chardin and Young, 1931), *C. teilhardi* (Zhang, 1999), *C. gansuensis* Liu et al., 2013.

Chardina truncatus (Teilhard de Chardin, 1942)

1942 *Prosiphneus truncatus,* Teilhard de Chardin, p. 43, Figs. 35–35a
1961 *P. truncatus,* Kretzoi, p. 126
1984 *P. truncatus,* Li et al., Table 5
1986 *P. truncatus,* Zheng and Li, Table 5
1990 *P. truncatus,* Zheng and Li, pp. 432, 439
1991 *P. truncatus,* Flynn et al., Fig. 4; Table 2
1991 *P. truncatus,* Tedford et al., Fig. 4
1991 *Myospalax truncatus*, Lawrence, p. 282
1994 *Chardina truncatus,* Zheng, Figs. 2, 4, 7, 10–12; Table 1
1997 *C. truncatus*, Zheng, Figs. 3, 5, 6

Table 9.8 Cranial and mandibular measurements of *Chardina truncatus* (mm)

	Type	V756	V758
Skull length	45.9	≥40.0	43.4
Narrowest interorbital breadth	7.4	≥7.2	7.4
Occipital condyle breadth	12.9	?11.5	12.2
Cranial breadth (rostral to lambdoid crest)	24.7	≥23.0	22.5
Diastema length	15.3	13.5	13.4
Incisive foramen length	5.3	5.4	5.3
M1–M3 length	10.8	9.3	10.5 (alveolar)
Articular process to lower incisor		32	
Articular process-mental foramen		22.8	
Mandible diastema length		6.3	
Mandibular height (at m1)		8.0	
Length of m1–m3		9.9	

2000 *C. truncatus*, Zheng and Zhang, Fig. 2
2000 *C. truncatus*, Zhang and Zheng, Fig. 1
2001 *C. truncatus*, Zheng and Zhang, Fig. 3
2013 *C. truncatus*, Liu et al., p. 233

Locality and material: In addition to the holotype skull (HHPHM 29.480), a skull with incisors and left and right M1 but missing its zygomatic arches (V758) from Honggou, and a skull and full mandible with complete dentition but missing the zygomatic arches (V756) from Jingnangou, both Gaozhuang area. See Table 9.8 for measurements.

Revised species diagnosis: Molars are relatively hypsodont. Average values of dentine tract parameters a, b, c, d and e of the m1 are 0.0, 3.3, 2.0, >4.7 and >4.4; M1 parameters A, B, C and D are >3.8, >4.5, 4.0 and 4.9 mm.

Stratigraphic position: Nanzhuanggou Member of the Gaozhuang Formation.

Description: The light-red clayey matrix adhering to the two specimens in addition to the absence of or very slight degree of staining, particularly V758, resemble identically the condition of the holotype (HHPHM 29.480, Teilhard de Chardin 1942, Fig. 35), so they may derive from the same rock unit.

Nasals are slightly convex dorsally, expand very gradually rostrally, and the caudal ends project conspicuously behind the posterior margin of the infraorbital foramen. The nasal/frontal suture line projects distinctly rostrally along the sagittal line. The interorbital region is relatively narrow and there is a distinct postorbital process. The supraorbital crests migrate medially on the interorbital region to become nearly confluent (3 mm apart). The temporal crests contact the supraorbital crests, gradually expand caudolaterally, reach their maximum separation at the mid-parietal, continue parallel, and extend to the lambdoid crest; the sagittal region

looks like a distinctly concave inverted bell. The temporal-parietal suture lies extremely close to the temporal crest. The interparietal is semicircular with its arched side lying nearly on the same line as the lambdoid crest and its breadth is equivalent to the caudal breadth of the sagittal region. The lambdoid crest is interrupted in the sagittal region. Due to the relative weakness of the supraoccipital process and the medial occipital crest, the occipital shield is relatively flat, nearly at a right angle intersection with the parietal. Lateral occipital crests are relatively well developed but lateral fossae are extremely weak. Occipital breadth (25 mm) is distinctly larger than its height (19 mm). Dorsoventral diameter of the foramen magnum (7.0 mm) is very slightly larger than its transverse diameter (6.4 mm). The squamosal is elongated in the occipital region (Fig. 9.8a).

Incisive foramina are relatively short and broad (approximately 2/5 the length of the diastema) and are located entirely within the premaxillae. Caudal to these and running along the midline of the palate is a well-developed crest. The midpoint of the anterior palatine foramen is located at the midpoint of the M1, the posterior palatine foramen is located at the mesial end of M2, the rostral margin of the parapterygoid fossa reaches the midpoint of the M2, the rostral margin of the midpterygoid fossa reaches the mesial margin of the M3, and the post-pterygoid canal is located on the platform of the post-pterygoid fossa (Fig. 9.8a1).

The basioccipital is distinctly concave and lacks well developed anterolateral angles. The auditory bulla is large and projects strongly from the dorsal basioccipital. From the lateral perspective and initiating from the nasals, the dorsal line ascends very gradually caudally, descends very slightly at the frontals, and then ascends very slightly, finally descending very gradually caudal to the intersection of the frontal and parietal. The sphenopalatine cavity is deep, broad, and triangular. The sphenopalatine foramen is deep and grooved. The optic and ethmoid foramina are both located on the orbital portion of the frontal (Fig. 9.8a2–3).

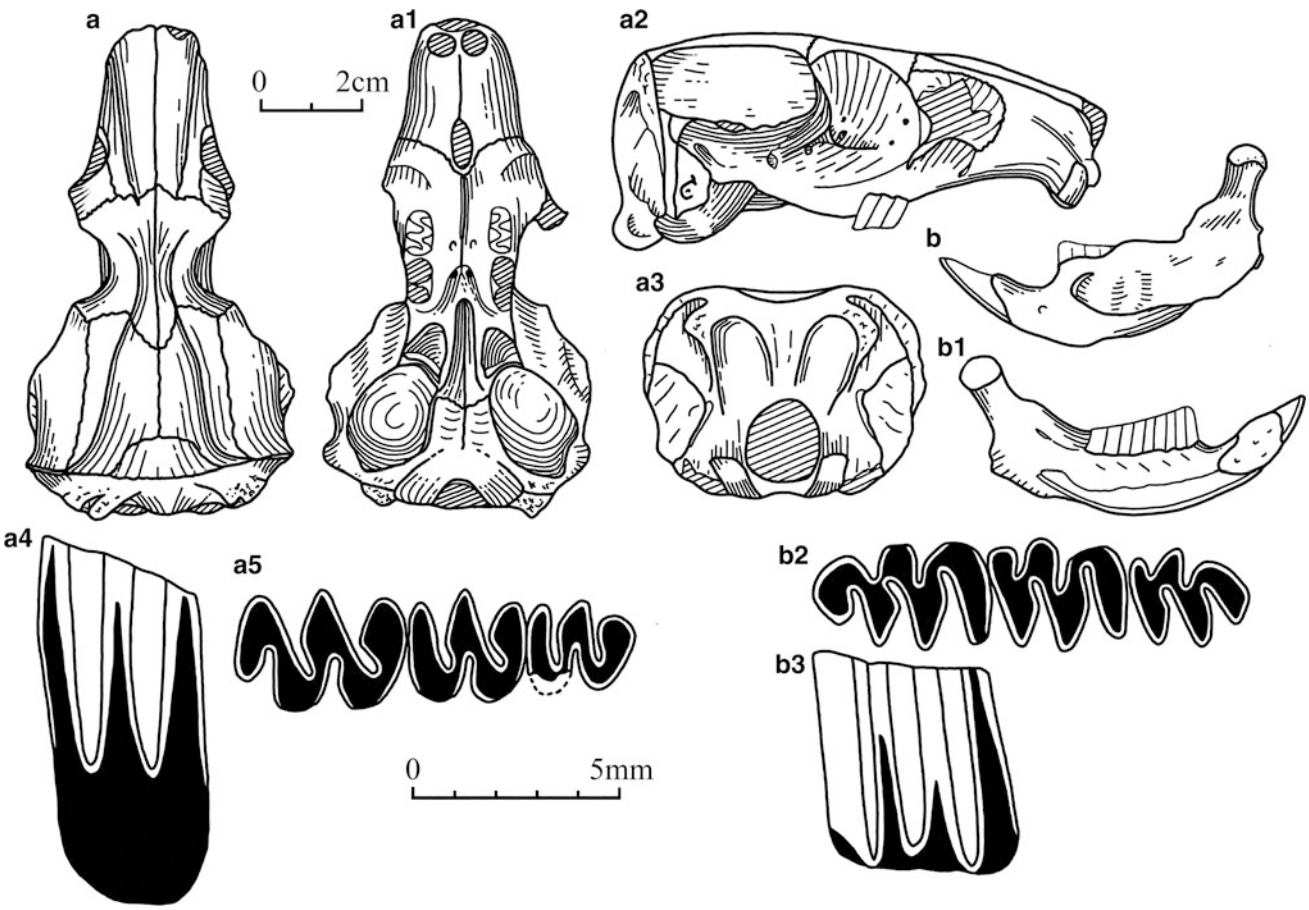

Fig. 9.8 Skull, mandible and molar morphology of *Chardina truncatus*. a, skull from Honggou, Gaozhuang (V758): **a** dorsal view, **a1** ventral view, **a2** right lateral view, **a3** occiput; **b** lateral view of left mandible from Jingnangou, Gaozhuang (V756): **b1** medial view, **b2** occlusal view of right lower dentition, **b3** lingual view of right m1, **a4** buccal view of M1 and **a5** occlusal view of left upper dentition of V756. Anterior to left for a5 and b2

The ascending ramus of the mandible is not well preserved but it initiates between the m1 and m2. The mental foramen is located anteroventral to the anterior margin of the m1. The masseteric crest initiates on the mandible at the anterobuccal reentrant angle (BRA2) of the m1 and maintains a well-developed ventral branch although its dorsal branch is obscure. The masseteric fossa is deep, and associated with it is a conspicuous lateral inflation at the root of the m2. The terminus of the incisor root is a distinct and strong projection laterally at the base of the condyloid process. The angular process is completely reduced but also distinctly laterally curved. The mandibular foramen is deep, narrow, and located at the base of the coronoid process. The posterior margin of the mandibular symphysis is located anterior to the mesial margin of the m1 (Fig. 9.8b1).

Dentition is semi-hypsodont (Fig. 9.8). Upper molar buccal reentrant angles and lower molar lingual reentrant angles penetrate the crown conspicuously deeper than the opposite reentrants on the same tooth. Upper and lower third molars are somewhat reduced. The anterior wall of the m1 is convex anteriorly. The anterolingual reentrant angle (LRA3) is distinctly more anteriorly situated than the anterobuccal reentrant angle (BRA2). The M1 (length 4.2 mm) buccal enamel configuration is three-peak, two-valley with A, B, C, D dentine tract parameters >3.8, >4.5, 4.0, and 4.9. The m1 (length 4.2 mm) lingual enamel configuration is three-peak, three-valley with a, b, c, d, e parameters 0, 3.3, 2.0, >4.7 and >4.4.

Comparison: The two skulls described above represent younger adult individuals than the holotype HHPHM 29.480 (Teilhard de Chardin, 1942, pp. 42–43, Fig. 35) and are consistent morphologically with it, except for being slightly smaller. Table 9.6 illustrates the distinctions between *Chardina truncatus, Prosiphneus murinus,* and *Pliosiphneus lyratus. C. truncatus* differs from *Pliosiphneus antiquus* in that the rostral ends of its nasals do not expand laterally conspicuously. The rostral breadth of nasals is approximately 1.7 times the caudal breadth of nasals for *C. truncatus*, whereas this ratio is 2.0 for *P. antiquus.* Interorbital region is relatively broad in *C. truncatus* (7.2–7.4 mm) but 6.1 mm in *P. antiquus*. Supraorbital crests in the interorbital region of *C. truncatus* are not confluent, but on *P. antiquus* they converge to form a single parasagittal crest. Incisive foramina are relatively broad and confined to the premaxilla, but on *P. antiquus* they are narrow, long, and extend into the maxilla. Upper dentition of *C. truncatus* is not parallel but diverges posteriorly, while the molar rows are parallel in *P. antiquus*. The m1 anterolingual reentrant angle LRA3 is situated anterior to the anterobuccal BRA2, but they are in direct opposition in *P. antiquus*. *C. truncatus* molars are relatively hypsodont with M1 A, B, C, D dentine tract parameters >3.8, >4.5, 4.8, and 4.9 and m1 a, b, c, d, e parameters 0, 3.3, 2.0, >4.7, >3.9. This contrasts with *P. antiquus* in which corresponding measurements are 0.43, 1.43, 0.93, 1.5 and 0.07, 0.73, 1.07, 1.55, 0.6.

Characters shared with *Chardina sinensis* (Teilhard de Chardin and Young, 1931) include the short and broad incisive foramen contained in the premaxilla, non-parallel upper dentition, and the alternate arrangement of LRA3 and BRA2. *C. sinensis* differs in its relatively short rostrum (diastema of 10.6 mm) and more brachydont dentition (lower M1 A, B, C and D parameters: 0.9, 1.8, 1.8 and 1.5).

Chardina truncatus is similar to "?*Mesosiphneus teilhardi*" of Zhang (1999) in some characters, such as convex anterior wall of the m1, parameter "a" value close to zero, and similar parameter A for M1. However, "?*Mesosiphneus teilhardi*" from Ningxian, Gansu, differs in its smaller size (length of M1 2.9–3.4 mm, m1 3.3–3.7 mm), larger m1 parameter b and c values (3.5–4.5 and 3.3–3.9), smaller d and e values (4.1–4.8 and 4.7), and smaller M1 parameter B, C and D values of (4.3, 3.6 and 4.3). The Ningxian species may be a member of the genus *Chardina* due to its m1 morphology, and *Chardina teilhardi* is possibly intermediate between *C. sinensis* and *C. truncatus* based on degree of hypsodonty.

Discussion: The holotype of *C. truncatus* (HHPHM 29.480) is a skull representing an aged individual. Having long lacked complementary data for the species, information based only on isolated teeth and mandibles, has been of limited use. Description of the two referred skulls and their associated mandibles facilitates research greatly. For upper and lower molar dentine tract parameters: (1) The M1 A value is slightly larger than the m1 b value. (2) The M1 B value is approximately twice that of the m1 c value. (3) The M1 C value is smaller than the m1 d value. (4) The M1 D value is slightly larger or equivalent to the m1 e value.

Using these dentine tract parameter proportions as a guideline "*?Chardina truncatus*" of Zheng (1994), later considered "*Prosiphneus* cf. *eriksoni*" by Qiu and Storch (2000), is not assignable to *Chardina truncatus*; m1 lingual dentine tract parameters a, b, c, d, e of 0.03, 1.48, 1.51, 2.72, 2.21 (average) indicate close b and c values. Furthermore, the m1 anterobuccal reentrant angle (BRA2) and the anterolingual reentrant (LRA3) are nearly in opposition, suggesting identity with the species *P. antiquus* (above).

The degree of hypsodonty of *C. truncatus* indicates that it is a derived species of the genus while still primitive among the myospalacines. The type C/21 of *C. sinensis* (Teilhard de Chardin and Young, 1931) is an anterior portion of skull that shares characters with *C. truncatus* including the short and broad incisive foramen located completely on the premaxilla and the non-parallel upper dentition. An anterior skull fragment of *C. sinensis* recovered from Lingtai, Gansu Province, has the same brachydont dentition as C/21, but in lateral perspective the dentine tract configuration is like that of *C.*

truncatus. The first molar of the mandible C/22 referred to *C. sinensis* by Teilhard de Chardin and Young (1931) may represent a hitherto unknown species. It now appears that placement of the species *sinensis* into the flat-occiput genus *Episiphneus* by Zheng (1994) is inappropriate.

Mesosiphneus Kretzoi, 1961

Revised genus diagnosis: Medium to large myospalacine. Breadth of caudal sagittal region 2–2.3 times that of interorbital region. Concave upper occiput extends rostral to the confluence of the lambdoid crest. Squamosal contributes a narrow strip to the occipital region. Interparietal absent, but the supraoccipital process is strong. Caudal symphysis of the mandible located beneath the midpoint of m1. Dentition is rooted and hypsodont; dentine tract parameter "a" of m1 considerably greater than that observed in *Chardina*.

Type species: *M. praetingi* (Teilhard de Chardin, 1942)

Included species: *M. praetingi*, *M. intermedius* (Teilhard de Chardin and Young, 1931 = *Prosiphneus paratingi* Teihard de Chardin, 1942), *M. primitivus* Liu et al., 2013.

Mesosiphneus praetingi (Teilhard de Chardin, 1942)

1942 *Prosiphneus praetingi,* Teilhard de Chardin, p. 49; Figs. 37–39
1942 *Prosiphneus praetingi*, Teilhard de Chardin and Leroy, p. 28
1961 *Mesosiphneus praetingi,* Kretzoi, p. 127
1984 *Prosiphneus praetingi,* Li et al., p. 175; Table 5
1986 *Prosiphneus praetingi,* Zheng and Li, Table 5
1990 *Prosiphneus praetingi*, Zheng and Li, pp. 432, 439, Fig. 1 h
1991 *Prosiphneus praetingi,* Flynn et al., Fig. 4; Table 2
1991 *Prosiphneus praetingi,* Tedford et al., Fig. 4
1991 *Myospalax praetingi,* Lawrence, pp. 269, 282
1994 *Mesosiphneus praetingi,* Zheng, pp. 59–62, Figs. 2–4, 7, 9, 12; Table 1
1997 *Mesosiphneus praetingi,* Zheng, Figs. 1, 3, 5, 6
2000 *M. praetingi*, Zheng and Zhang, Fig. 2
2001 *M. praetingi*, Zheng and Zhang, Fig. 3
2004 *M. praetingi*, Hao and Guo, Table 1
2008 *M. praetingi*, Li et al., Tables 2, 8
2013 *M. praetingi*, Liu et al., p. 236

Revised species diagnosis: Relatively small in size with caudal sagittal region slightly depressed and with breadth approximately twice that of the interorbital region. Parasagittal crests well separated. Lambdoid crest and supraoccipital process relatively weakly developed. Dentition relatively low-crowned with average dentine tract parameters A, B, C, D of M1: >5.5, >4.2, 3.7, 6.2, and a, b, c, d, e of m1: 2.25, 4.3, 4.4, >5.0 and >5.0.

Localities and material: YS4, three left M1 (V11171.1-3), two right M3 (V11171.4-5), fragmentary left mandible with m1-2 (V11171.6), left m1 and two right m3 (V11171.7-9); YS90, fragmentary left mandible with incisor and m1-3 (V11172.1), fragmentary left mandible with incisor and m1-2 (V11172.2), left m3 (V11172.3); YS136, fragmentary left mandible with m1-3 (V11173). See Table 9.9 for measurements.

Table 9.9 Dental measurements of *Mesosiphneus praetingi* (mm)

		M1	M3	m1–3	m1	m2	m3
	N	3	1	2	5	4	5
L	Range	3.6–4.0		9.9–10.3	3.6–4.5	3.0–3.6	2.5–2.8
	Mean	3.82	2.53	10.1	4.16	3.25	2.6
	N	3	2		5	4	5
W	Range	2.6–2.75	2.1–2.15		2.4–2.9	2.6–3.1	2.1–2.3
	Mean	2.68	2.13		2.66	2.85	2.18

Stratigraphic range: Culiugou Member, Gaozhuang Formation, to lower Mazegou Formation, 4.3 to 3.4 Ma.

Description: Anterior wall of M1 projects very slightly or is flat. Both the first lingual and buccal reentrants penetrate the crown slightly deeper than the second lingual and buccal reentrants (Fig. 9.9a). Dentine tract of the first lingual salient angle is relatively low with an A′ value of 2.1. Anterior and posterior enamel terminates at the level of the base of the LRA1 reentrant. Buccally, the dentine continues up the salient angles to reach the occlusal surface, although mesially the enamel terminates at the base of the first reentrant (BRA1) and distally the enamel terminates at the base of the second reentrant (BRA2, Fig. 9.9a1).

The M3 has relatively reduced second lingual and third buccal salient angles. Lingual reentrants penetrate half of the crown (Fig. 9.9c). Lingual dentine tract configuration is two-peak and single valley, with B′, C′, D′ values of 1.8, 1.0, and 1.85 (Fig. 9.9c1). Buccal dentine tracts are three-peak, two-valley with B, C, D values of 1.1, 1.6, and 1.4 (Fig. 9.9c2).

The mental foramen on the mandible is large and located anterior to the anterior margin of the m1. The anterior margin of the masseteric fossa is located at the third buccal salient angle of the m1 (BSA3) and the lower branch of the masseteric crest is well developed. The terminus of the m2 root is not very inflated. Ascending ramus initiates between m1 and m2. Mandibular symphysis terminates beneath the posterior margin of the m1. On the buccal side the mandible depth at m1 is 8.9 mm.

The m1 anterior wall is slightly convex. The anterior cap is inclined lingually, salient angles are robust, and reentrants are slender. Buccally the second reentrant (BRA2) penetrates the crown less than the first and is consistently located posterior to the third lingual reentrant (LRA3) (Fig. 9.9b, d). All the new fossils show that buccal reentrants wear to enamel rings. Lingual dentine tract configuration is four-peak and three-valley, and it is only the dentine on the fourth salient angle (LSA4) (parameter a value 2.25) that does not reach the occlusal surface. Anteriorly the base of

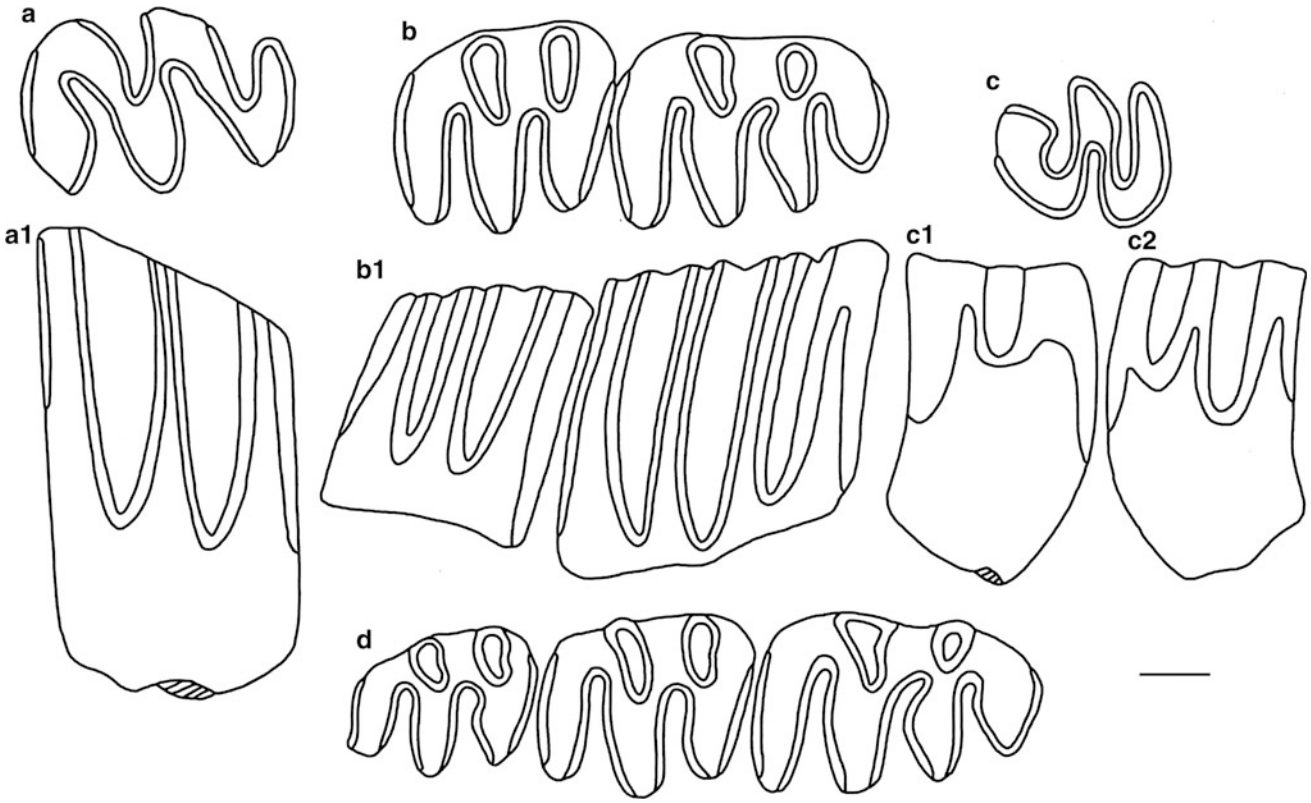

Fig. 9.9 Dental morphology of *Mesosiphneus praetingi*, 1 mm scale. **a**–**d**: Occlusal view, **a1** and **c2**: buccal view, **b1** and **c1**: lingual view, **a**–**a1**: left M1 (V11171.1), **b**–**b1**: left m1-2 (V11172.2), **c**–**c2**: right M3 (V11172.2), **d**: left m1–3 (V11171.4)

the enamel terminates at the base of LRA3, while posteriorly it terminates at the base of the first lingual reentrant (Fig. 9.9b1).

The anterior wall of m2 is posteromedially inclined. Reentrants all approach or surpass the longitudinal axis of the tooth. Lingual dentine tracts are three-peak and two-valley, and anterior and posterior enamel terminates beneath the base of the neighboring folds.

The posterior m3 is reduced. The second buccal reentrant angle is slightly deeper than the first one. Lingual dentine tract configuration is three-peak, two-valley. Anterior and posterior enamel terminates beneath the base of the neighboring folds with b, c, d, e values of 1.85, 1.7, 0.85, 1.2 mm (Fig. 9.9d).

Comparison and discussion: Although the new Yushe specimens are aged individuals they are consistent in size and morphology with *Mesosiphneus praetingi* described by Teilhard de Chardin (1942). The anterior and posterior enamel on the sides of M1 terminates at the bases of neighboring folds; the m1 second buccal reentrant is positioned posterior to the third lingual reentrant; there is a relatively short dentine tract on LSA4; m2 and m3 have a deep second buccal reentrant, robust salient angles of lower molars are associated with slender reentrants; inflated m2 terminal root at the ventral branch of the masseteric crest, and the posterior symphysis extends to the posterior margin of the m1.

"*Prosiphneus* ex gr. *praetingi*" from Beregovaya in the Outer Lake Baikal region of Siberia (Bazarov et al. 1976) is relatively small (M1 and m1 average lengths 2.84 and 3.0 mm) with a flat anterior wall and first lingual reentrant shallower than the second on M1; m1 second buccal reentrant in opposition to the third lingual reentrant; M1 lingual dentine tracts as two-peak, two-valley, anterior and posterior enamel terminating high; m1 dentine tracts poorly developed on lingual salient angles and particularly the fourth angle, buccal anterior and posterior enamel terminating low on the tooth; and shallow second buccal reentrants on m2, m3. These characters are clearly distinct from *M. praetingi* and are closer to the Chinese *Episiphneus*. As the Beregovaya form is relatively hypsodont, it may constitute a new species.

"*Prosiphneus* ex gr. *praetingi*" from Sushon, Bashkir, Southern Urals (Sushov 1970), is also distinctly smaller (M1 and m1 average lengths 3.2 and 3.09 mm). The m1 occlusal morphology resembles the material from Beregovaya, but buccal dentine tracts do not resemble any known species of myospalacines. First upper and lower molar morphology suggests that it may be a relatively primitive flat occiput form.

"*Prosiphneus praetingi*" from exposures 520 and 525 in the middle Lake Baikal region, Siberia, (Mats et al. 1982) is low crowned and also small (M1 and m1 lengths 2.75–3.1 and 2.8–3.4 mm). The second buccal and third lingual reentrants in opposite position on m1 indicate consistency with the fossils above. None of these taxa show diagnostic characters of *M. praetingi*, but they appear to match more closely flat occiput forms.

Mesosiphneus intermedius (Teilhard de Chardin and Young, 1931)

1931 *Prosiphneus eriksoni*, Teilhard de Chardin and Young, p. 14; Pl. IV. 2–3, 6–7; Pl. V. 1–4, 13
1931 *P. intermedius*, Teilhard de Chardin and Young, p. 15; Pl. V, Fig. 21
1942 *P. paratingi,* Teilhard de Chardin, p. 54; Figs. 40–40a
1942 *P. intermedius*, Teilhard de Chardin and Leroy, p. 28
1961 *Mesosiphneus paratingi,* Kretzoi, p. 127
1984 *Prosiphneus* paratingi, Li et al., Table 5
1985 *P. intermedius*, Liu et al., p. 123; Fig. 52
1986 *P. paratingi,* Zheng and Li, p. 99
1987 *Prosiphneus* sp., Cai, p. 128
1990 *P. paratingi* Zheng and Li, p. 439
1990 *P. paratingi,* Qiu and Qiu, p. 251
1991 *P. paratingi,* Flynn et al., Fig. 4; Table 2
1991 *P. paratingi,* Tedford et al., Fig. 4
1991 *Myospalax paratingi,* Lawrence, pp. 269, 282
1991 *M. intermedius*, Lawrence, pp. 269, 282
1994 *M. paratingi,* Zheng, p. 62; Figs. 2–4, 7, 9–12, Table 1
1994 *M. intermedius*, Zheng, p. 62; Figs. 9, 10
1997 *M. paratingi,* Zheng, p. 138; Figs. 3, 5, 6
1997 *M. intermedius*, Zheng, p. 138; Figs. 3, 6
2000 *M. intermedius*, Zheng and Zhang, Fig. 2
2001 *M. intermedius*, Zheng and Zhang, Fig. 3
2004 *M. paratingi*, Cai et al., Table 2
2008 *M. paratingi*, Li et al., Tables 2, 4, 7, 8
2013 *M. intermedius*, Liu et al., p. 237

Revised species diagnosis: Larger than *M. praetingi* with sagittal region concave caudally and 2.3 times the breadth of the interorbital region. Compared to *M. praetingi*, the sagittal region between the parietals is narrower, supraoccipital process is more robust, basal occipital shield projects slightly caudally, and sphenopalatine fossa is narrower. Molars are hypsodont with dentine tract parameters a, b, c, d, e of m1: 5.5, 6.8, 6.9, 7.3 and 7.0 mm.

Locality and material: YS5, portion of palate with left M1-2 and right M1-3 (V11174.1), left M1 (V11174.2), two right m1 and two left m2 (V11174.3-6); YS87 left m2 (V11175.1), damaged left m3 (V11175.2); YS99 left M1 (V11176.1), right m1 (V11176.2), right m1 damaged posteriorly (V11176.3), right m3 (V11176.4); YS95, fragmentary left mandible with m1-2 (V11177). Measurements in Table 9.10.

Table 9.10 Dental measurements of *Mesosiphneus intermedius* (mm)

		M1–3	M1	M2	M3	m1	m2	m3
L	N	1	3	1	1	4	4	1
	Range	8.6	3.1–3.84			3.3–4.0	2.5–3.1	
	Mean		3.45	2.6	1.8	3.7	2.78	2.6
W	N		3	1	1	4	4	
	Range		1.8–2.3			2.2–2.4	1.75–2.5	
	Mean		2.12	2.5	2.2	2.3	2.16	1.8

Stratigraphic range: middle to upper Mazegou Formation, 3.4 to 3.0 Ma.

Description: Upper dentition is not parallel but v-shaped with a distinctly elongated M1 that is 1.5 times the length of the M2. The anterior wall of M1 is flat and the anterior loop is not greatly inclined. The M1 first lingual reentrant angle penetrates the crown to the same depth or more than the second reentrant and also remains open distinctly further down the tooth, approaching the base of the crown. A strongly undulating dentine tract is present on the third lingual salient angle. Enamel on both sides terminates mesially and distally at the base of the crown. V11176.1 from YS99 has A′, B′, C′, D′ values of 6.1, >7.7, >5.8 and >8.0 mm. The anterior and posterior buccal enamel reaches the crown base. The dentine tract on the second buccal salient angle is relatively narrow. A, B, C and D values are 7.2, 5.5, 5.8 and 7.6 mm (Fig. 9.10c, d).

M2 and M3 lingual and buccal reentrants penetrate far beyond the long axis of the tooth. The posterior part of M3 is greatly reduced.

The mental foramen on the mandible is large and located anteroventral to the m1. Anterior end of the masseteric crest terminates beneath the second buccal reentrant of the m1. The m2 root is distinctly inflated on the lower branch of the masseteric crest.

The m1 mesial wall is slightly convex. The second buccal reentrant is situated distinctly posterior to the third lingual reentrant (Fig. 9.10a). The anterior and posterior buccal enamel extends to the base of the crown, while the dentine tract on three buccal salient angles penetrates the crown surface at an early stage. On a majority of specimens, the anterior lingual reentrant fold remains open later than the posterior one, but on a few specimens the anterior reentrant is not as deep (Fig. 9.10a).

The m2 and m3 (Fig. 9.10b) have flat anterior walls that are inclined posteromedially. The second buccal reentrant penetrates the crown nearly to the same degree as the first reentrant. Enamel extends downward to the base of the crown on all lateral salient angles. Dentine tracts on both sides of m2 undulate more strongly than those of m3.

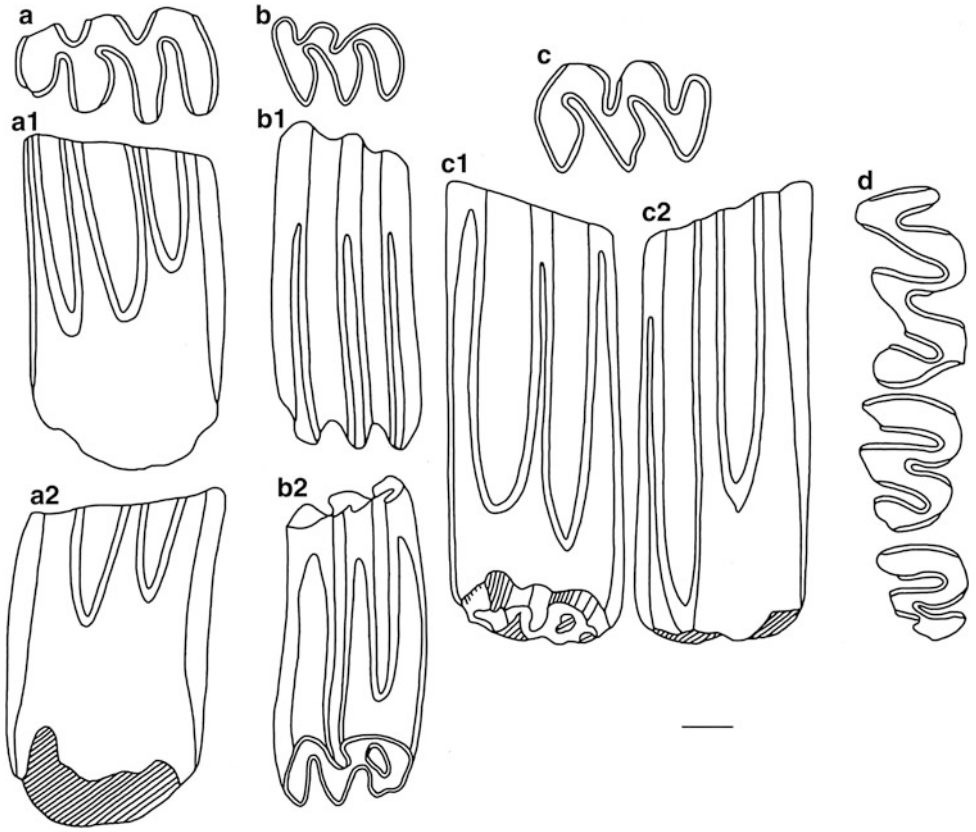

Fig. 9.10 Dental morphology of *Mesosiphneus intermedius*, 1 mm scale. **a** occlusal view of right m1 (V11174.3), **a1** lingual view, **a2**: buccal view; **b** occlusal view of right m3 (V11176.4), **b1** lingual view, **b2** buccal view; **c** occlusal view of left M1 (V11176.1), **c1** buccal view, **c2** lingual view; **d** occlusal view of right M1-3 (V11174.1)

The wide disparity of individual age among the specimens prohibits accurate measurement of dentine tracts.

Comparison and discussion: *M. intermedius* is distinguished from *M. praetingi* by the following characters: The former is slightly larger (new measurements of lengths of skulls studied by Teilhard de Chardin (1942) are 44.0 and 42.3 mm) with posterior sagittal region broader and more concave; ventral occipital shield projects less posteriorly; more robust supraoccipital process and lambdoid crests; anterior nasals descend further; narrower sphenopalatine fossa; molar enamel descends further mesially and distally, with higher dentine tracts on salient angles; and M1 is longer than M2.

Several isolated teeth recovered from the Daodi Formation of Nihewan Basin ("*Prosiphneus*" sp., Cai 1987) possess characters consistent with *M. intermedius*, including M1 first lingual reentrant penetrating the crown further than the second reentrant, m1 second buccal reentrant positioned posterior to the third lingual reentrant, deep second buccal reentrants on m2 and m3, and similar enamel distribution and dentine tract values.

The new Yushe Basin material documents for *M. intermedius* a paleomagnetic range of 3.4–2.9 Ma in the Mazegou Formation (Flynn et al. 1991; Tedford et al. 1991). Previous studies cited Yushe *M. paratingi*, but Liu et al. (2013) synonymize this name with *M. intermedius*. This links the species in a continuum with *M. praetingi* (4.3–3.4 Ma), consistent with a direct ancestor-descendent relationship. This also indicates that at approximately 3.4 Ma there was a punctuated increase in molar hypsodonty, a speciation event among the concave occiput forms that may reflect climatic change. Also from 3 Ma onwards, hypsodonty in these rodents attained high values, suggesting abrasive nutrition and related climatic degeneration. Subsequently the lineage was forced to extinction and replaced by rootless zokors.

Yangia Zheng, 1994

Diagnosis: Rootless, moderate to large-size myospalacine with a caudal sagittal skull breadth that is 2.4–3.0 times that of the interorbital region. Squamosal in the occipital region is ribbon-shaped, supraoccipital process varied from weak to strong, and interparietal is indistinct or lost. Caudal mandibular symphysis located beneath the midpoint of the m1; M2 varied from orthomegodont to clinomegodont. Third lingual reentrant angle relatively deep, and the mesial wall of the oval anterior cap possesses enamel on m1.

Type species: *Yangia tingi* (Young, 1927)

Included species: *Yangia tingi, Y. omegodon* (Teilhard and Young, 1931), *Y. chaoyatseni* (Teilhard and Young, 1931), *Y. epitingi* (Teilhard and Pei, 1941), *Y. trassaerti* (Teilhard, 1942).

Yangia trassaerti (Teilhard de Chardin, 1942)

1942 *Siphneus trassaerti,* Teilhard de Chardin, p. 62; Figs. 42, 43
1961 *Myospalax trassaerti,* Kretzoi, p. 128
1986 *Myospalax trassaerti,* Zheng and Li, p. 99
1990 *Myospalax trassaerti,* Zheng and Li, pp. 435, 439
1991 *Myospalax trassaerti*, Zheng and Han, p. 108
1991 *Myospalax trassaerti,* Flynn et al., Table 2
1991 *Myospalax trassaerti,* Lawrence, pp. 269, 282
1994 *Youngia trassaerti,* Zheng, Fig. 12; Table 1
1997 *Yangia trassaerti,* Zheng, Fig. 6

Revised species diagnosis: Moderate in size with caudal sagittal region approximately 2.4 times the breadth of the interorbital region. Parasagittal crests confined to the mid-section of the parietal. Supraoccipital process rather robust with lateral sides incompletely overlapping wings of the lambdoid crest. Upper molars are closed orthomegodont.

Material and locality: YS119, left anterior mandible with incisor (V11178); YS120, right M2 and right m2 (V11179.1-2); YS6, left M2 and damaged right m3 (v11180.1-2). Measurements in Table 9.11.

Stratigraphic position: Haiyan Formation.

Description: Diastema of the damaged mandible is 6.3 mm long, buccal depth of mandible at m1 is 9.6 mm, the mental foramen is large and located in the center of the ramus beneath the anterior margin of the m1. The masseteric fossa projects in a distinctly inflated configuration reflecting the terminal ends of the molars. Caudal end of the mandibular symphysis terminates beneath the m2.

The M2 (Fig. 9.11a, b) is represented by two individuals in early wear with mesio-distal margins that very slightly project anteriorly and posteriorly. Buccal reentrants penetrate the crown rather deeply. The angle α between the anterior wall and lingual side on both specimens is 64° and 71°. The second and third buccal salient angles extend very slightly posterolingually. Enamel breaks are relatively narrow on the occlusal surface at salient angles. The ratio of breadth to length: 0.63 and 0.69.

The m2 and m3 are also immature. The m2 second lingual salient angle is nearly perpendicular to the long axis of the molar, but this same angle on the m3 is slightly posterolingually inclined. First and second buccal reentrants on both molars penetrate the crown to an equivalent degree.

Comparison and discussion: Despite the scarcity and immaturity of new Yushe specimens, *Yangia trassaerti* can be distinguished from the other species of the genus by size and morphology (Table 9.11). The new material is equivalent in size to *Y. omegodon* and *Y. trassaerti.* The M2

Table 9.11 Upper molar measurements for selected species of *Yangia* (mm)

		Y. omegodon	*Y. trassaerti*	*Y. chaoyatseni*	*Y. tingi*	*Y. epitingi*	YS6, 120	YS110	YS83
	N	5	2	4	6	5		1	1
M1–3 length	Range	9.0–10.0	10.1–11.0	10.1–11.0	10.8–12.5	13.4–14.4			
	Mean	9.4	10.6	10.4	11.7	13.8		10.7	13.1
	N	4	2	4	7	7	2	1	1
M2 length	Range	2.9–3.0	3.0–3.2	3.3–3.8	3.5–4.4	4.0–4.7	2.9–3.0		
	Mean	2.93	3.1	3.5	3.89	4.41	2.95	3.6	4.1
	N	4	2	4	7	7		1	1
M2/M1 ratio of lengths	Range	0.71–0.75	0.67–0.70	0.81–0.86	0.77–0.86	0.80–0.88			
	Mean	0.74	0.69	0.83	0.8	0.84		0.72	0.87
	N	5	2	4	6	5		1	1
M3/M1 ratio	Range	0.56–0.68	0.59–0.60	0.58–0.68	0.56–0.72	0.67–0.76			
	Mean	0.64	0.6	0.61	0.62	0.72		0.52	0.82
	N	5	2	4	6	5		1	1
M3/M2 ratio	Range	0.76–0.99	0.87–0.90	0.74–0.82	0.72–0.81	0.77–0.93			
	Mean	0.9	0.89	0.76	0.79	0.90		0.72	0.93
	N	5	2	4	6	5		1	1
M3/M1–3 ratio	Range	0.25–0.29	0.26–0.26	0.25–0.27	0.25–0.29	0.26–0.28			
	Mean	0.27	0.26	0.26	0.26	0.27		0.24	0.29
	N	4	2	4	7	5	2	1	1
M2 W/L	Range	0.67–0.80	0.78–0.78	0.55–0.66	0.61–0.67	0.57–0.65	0.63–0.69	0.61	0.56
	Mean	0.74	0.78	0.61	0.63	0.59	0.66	0.61	0.56
	N	4	2	4	7	7	2	1	1
α angle of M2	Range	60°–87°	64°–65°	38°–60°	48°–59°	30°–54°	64°–71°		
	Mean	76°	65°	46°	52°	44°	68°	57°	47°

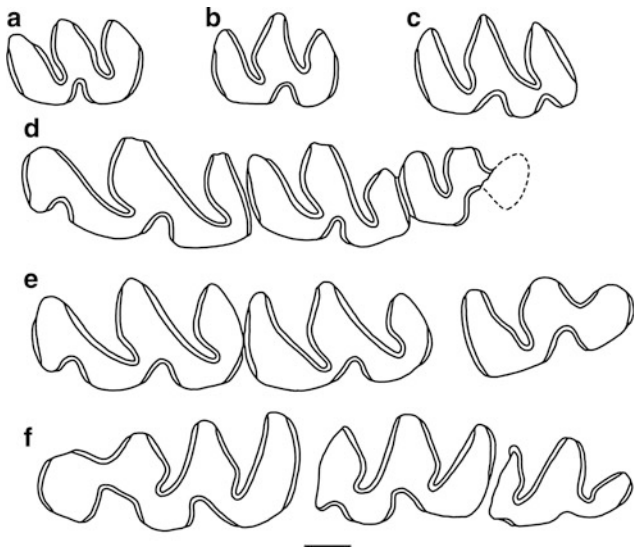

Fig. 9.11 The occlusal morphology of three species of *Yangia*, 1 mm scale. **a–b** *Y. trassaerti*: **a** left M2 (V11179.1), **b** right M2 (V11180.1, reversed); **c–d** *Y. tingi*: **c** right m2 (V11181.2), **d** left M1-3 (V11181.1); **e–f** *Y. epitingi*: **e** left M1-3 (V11182), **f** left m1–3 (V11183)

measurements lie between *Y. chaoyatseni* and *Y. trassaerti,* but the angle α is consistent with *Y. trassaerti*.

Teilhard de Chardin (1942) diagnosed *Y. trassaerti* as "a *Siphneus* of the *tingi* group resembling *Siphneus omegodon* in orthomegodont pattern of the upper molars, but larger and stronger supra-occipital process." He further indicated that in cranial size and morphology it was completely consistent with *Y. tingi,* but in molar morphology was closer to *Y. omegodon*. It differs from *Y. chaoyatseni* in its orthomegodont dentition and the distinctly depressed sagittal region.

The type of *Y. trassaerti* (THP 20.786) is a fragmentary compressionally-distorted posterior cranium, so Teilhard de Chardin's (1942) assertion that the sagittal region is more depressed compared to *Y. chaoyatseni* appears inaccurate. When comparing the Yushe specimen referred to "*Y. chaoyatseni*" by Teilhard de Chardin (1942; Fig. 42) to *Y. trassaerti,* one cannot help suspecting misidentification. The sagittal region of *Y. chaoyatseni* is generally an inverted bell form with the parasagittal crests making an abrupt turn one-third of the way posteriorly on the parietal. On both *Y. trassaerti* and *Y. tingi,* in contrast, the sagittal regions are trough-like caudally with parietal crests that do not conspicuously turn but rather gently extend posterolaterally.

From the distributional data at hand it appears that *Y. chaoyatseni* evolved in the more arid western Loess Plateau region, as opposed to the other two taxa, which are principally derived from the more mesic eastern fluviolacustrine region. The Haiyan Formation of Yushe Basin is contemporaneous with the Wucheng Loess but is fluviolacustrine in nature. It is therefore reasonable that *Y. chaoyatseni* is not present at Yushe Basin.

Yangia tingi (Young, 1927)

1927 *Siphneus tingi,* Young, p. 45; Pl.II, Figs. 32–36
1930 *Siphneus tingi*, Teilhard de Chardin and Piveteau, p. 122; Figs. 37–39
1930 *Siphneus cf. tingi,* Pei, p. 375
1931 *Siphneus tingi,* Teilhard de Chardin and Young, p. 23; Plates I.1; III.3; V.15-16
1935 *Siphneus tingi,* Young, p. 7
1936 *Siphneus tingi,* Teilhard de Chardin, p. 17; Fig. 8
1940 *Siphneus tingi,* Leroy, pp. 173–174; Fig. 1
1942 *Siphneus tingi,* Teilhard de Chardin and Leroy, p. 29
1942 *Siphneus tingi,* Teilhard, p. 65; Fig. 44
1961 *Myospalax tingi,* Kretzoi, p. 128
1975 *Myospalax tingi,* Ji, p. 170, Pl. I, Fig. 1
1976 *Myospalax tingi,* Ji, p. 60; Pl. 1, Fig. 2
1978 *Myospalax tingi,* Hu and Qi, p. 15; Pl. II, Fig. 5
1986 *Myospalax tingi,* Zheng and Li, pp. 88–89
1990 *Myospalax tingi,* Zheng and Li, pp. 435, 439
1991 *Myospalax tingi,* Zheng and Cai, p. 117; Fig. 2:1–4
1991 *Myospalax tingi,* Flynn et al., Fig. 4; Table 2
1991 *Myospalax tingi,* Zheng and Han, pp. 103, 106
1991 *Myospalax tingi,* Lawrence, pp. 269, 282
1994 *Yangia tingi,* Zheng, Figs. 4, 7, 12; Table 1
1997 *Y. tingi*, Zheng, Figs. 1–2, 5–6
2004 *Y. tingi*, Cai and Li, p. 441
2004 *Y. tingi*, Cai et al., Table 2
2006 *Y. tingi*, Zheng et al., Table 2

Revised species diagnosis: Slightly larger than *Y. trassaerti.* Dorsal occipital shield slightly concave and penetrating rostrally to the junction of the lambdoid crests. Interorbital region is relatively narrow and concave. Breadth of caudal sagittal region is approximately three times the interorbital region. Parasagittal crest projects slightly laterally. Supraoccipital process robust but not completely overlapping the two wings of the lambdoid crests. Nasals very gently expand rostrally. Upper molars clinomegodont.

Locality and material: YS110, anterior portion of skull with left M1-2 and right M1-3, and right m2 (V11181.1-2).

Stratigraphic position: Haiyan Formation.

Measurements: Diastema length, 14.5 mm; length of incisive foramina, 6.5 mm; 4.2 mm breadth of palate at M1; 6.1 mm breadth of palate at mesial face of M3; interorbital breadth, 8.4 mm; M1-3 length, 10.3 mm (see also Tables 9.10, 9.11).

Description: Nasofrontal sutures make an inverted V; nasals extend to the caudal margin of the infraorbital foramen. Rostrally from the infraorbital foramen, the nasals generally

expand laterally. Concave interorbital region with the supraorbital crest migrated distinctly medially. Incisive foramina lie completely in the premaxilla with a foramen/diastema length ratio of 0.45. Caudal to the foramina on the midline of the palate a bony crest extends as a sharp spur on the posterior palatine. The anterior palatine foramen is long and large with its rostral margin at the second lingual reentrant of the Ml. The posterior palatine foramen lies within the anterior pterygoid fossa, the mid-point of which is between M2 and M3. The rostral margin of the anterior pterygoid fossa extends to the lingual reentrant of M2. The rostral margin of the medial pterygoid fossa lies at the mesial margin of the M3. Dental rows diverge posteriorly.

The mesial wall of the M1 is slightly convex. The first lingual reentrant penetrates the crown less deeply than the second reentrant and a large dentine tract is present on the occlusal surface at the buccal angle. The mesial wall of the M2 is straight and the three buccal salient angles are anterolaterally inclined making it clinomegodont. Breadth/length ratio is 0.63 and its length is 0.7 that of the M1. Although broken, the M3 is clearly reduced, half the length of the M1 (Fig. 9.11d). The m2 mesial and distal walls are flat and slightly posterolingually inclined. The first buccal reentrant is slightly deeper than the second buccal reentrant (Fig. 9.11c).

Comparison and discussion: The YS110 fossils are consistent with *Yangia tingi* in both size and morphology of the anterior part of the skull. Dental measurements (Tables 9.11, 9.12) are close to those of both *Y. tingi* and *Y. chaoyatseni*, although total molar row length and the angle α of M2 more closely match the former. The conspicuous lateral inflation of the nasals, concave interorbital region, and distinctly medial supraorbital crest are characteristic of *Y. tingi.*

Yangia tingi possesses cranial characters that suggest relationship to *Y. trassaerti,* including the narrow interorbital region, the concave sagittal region which broadens posteriorly, the robust supraoccipital process, and the slight lateral projection of the parsagittal crests. These differ greatly from structures in *Y. omegodon* and *Y. chaoyatseni.* Dental characters of *Y. tingi* shared with *Y. chaoyatseni* include the shallow reentrants on the lingual sides of upper molars and buccal sides of lower molars, partial clinomegodonty, and the reduced M3, which differ from the more primitive conditions of *Y. trassaerti* and *Y. omegodon.* The fossil record may support derivation of *Y. tingi* from *Y. trassaerti* based on cranial structures, while the dentition of *Y. tingi* evolved in parallel with *Y. chaoyatseni. Yangia tingi* and *Y. chaoyatseni* both occur in the "Reddish Clays Zone B" or the upper Wucheng Loess at Hefeng, Jingle (Loc.1); Xujiaping, Zhongyang (Loc. 17); Xiapodi, Daning (Loc. 19; Teilhard de Chardin and Young 1931); Peichen, Fushan (Loc. 30; Young 1935); and Laochihe, Lantian (Ji 1975). These two species probably represent two lineages, which may have a common origin in *Mesosiphneus*. Zheng and Han (1991) proposed the following evolutionary sequences:

Mesosiphneus intermedius → *Y. trassaerti* → *Y. tingi* → *Y. epitingi*

Mesosiphneus intermedius → *Y. omegodon* → *Y. chaoyatseni*

Biogeographic considerations suggest that the first lineage was predominantly concentrated in the fluviolacustrine sediments of east North China, while the second tended to inhabit the western loess regions. Obviously, the localities recording both *Y. tingi* and *Y. chaoyatseni*, would represent overlapping ranges. The current data also suggest that the

Table 9.12 Lower molar lengths and length ratios for selected species of *Yangia* (mm)

		Yangia omegodon	*Yangia chaoyatseni*	*Yangia tingi*	*Yangia epitingi*	YS 83
N		5	4	7	6	1
	Range	8.8–9.6	10.4–11.7	10.1–12.7	10.6–15.8	
m1–3 L	Mean	9.22	10.78	11.07	13.3	12.9
	Range	3.6–3.7	4.3–5.1	4.4–5.4	4.6–7.0	
m1 L	Mean	3.7	4.68	4.91	5.75	5.7
	Range	2.7–3.0	3.3–3.7	3.3–3.9	3.3–4.8	
m2 L	Mean	2.9	3.45	3.64	4.1	4.0
	Range	2.3–2.9	2.7–3.2	2.8–3.7	2.9–4.15	
m3 L	Mean	2.68	2.98	3.22	3.54	3.10
	Range	0.39–0.42	0.41–0.45	0.4–0.44	0.42–0.44	
m1/m1–3	Mean	0.4	0.43	0.42	0.43	0.44
	Range	0.73–0.83	0.7–0.86	0.68–0.8	0.69–0.72	
m2/m1	Mean	0.79	0.75	0.74	0.71	0.7
	Range	0.62–0.8	0.57–0.69	0.6–0.73	0.59–0.67	
m3/m1	Mean	0.73	0.64	0.66	0.62	0.54
	Range	0.85–0.97	0.8–0.91	0.8–0.95	0.83–0.95	
m3/m2	Mean	0.92	0.86	0.88	0.87	0.78
	Range	0.26–0.31	0.26–0.29	0.26–0.29	0.26–0.28	
m3/m1–3	Mean	0.29	0.28	0.27	0.27	0.24

common ancestor for both lineages resembled *Mesosiphneus intermedius.*

With regard to *Yangia tingi* from Haiyan Formation locality YS110, in reversed sediments of the lower part of the Matuyama Chron, so somewhat older than 2.2 Ma, other occurrences of the species in North China are of about the same age. The section at Luochuan indicated *Y. chaoyatseni* principally in the upper Wucheng Loess (Liu et al. 1985), which agrees with early Pleistocene age for *Y. tingi.* The lowest stratigraphic occurrence of *Y. tingi* at Nihewan is unit Do-5 in the Danangou section (~1.8 Ma, Zheng and Cai 1991; the species continues to unit Do-6, ~0.73 Ma). This entire phase is basically the age of the Nihewan strata of Teilhard de Chardin and Piveteau (1930) and successive assemblages, and encompasses the age of the Gongwangling fauna of 1.15 Ma (Hu and Qi 1978; An and Ho 1989) or 1.25 Ma (Ding et al. 2002). After the appearance of *Y. tingi* in the Nihewan assemblage (Teilhard de Chardin and Piveteau 1930), more advanced representatives of the Chinese early Pleistocene appeared, but Young (1927) did not stress this. However, Liu (1964) proposed that *Y. tingi* was constrained to the middle Pleistocene, his "Zone B of the Reddish Loess", which would represent the (younger) lower Lishi Loess. This concept could be applied for the Jingou fauna of Heshui, Gansu (Zheng 1976).

Yangia epitingi (Teilhard de Chardin and Pei, 1941)

1931 *Siphneus* cf. *fontanieri,* Teilhard de Chardin and Young, p. 18 (in part).
1935 *Siphneus tingi,* Young, p. 32; Pl. VI, Fig. 4a
1941 *Siphneus epitingi,* Teilhard de Chardin and Pei, p. 52, Figs. 40–47
1942 *Siphneus epitingi,* Teilhard de Chardin and Leroy, p. 29
1957 *Myospalax epitingi,* Chia and Chai, p. 49; Pl. III, Fig. 2
1961 *Myospalax epitingi,* Kretzoi, p. 128
1961 *Myospalax epitingi,* Chao and Tai, pp. 374, 376; Pl. I, Fig. 2
1965 *Myospalax tingi,* Chow and Li, P. 379; Pl.I, Fig. 4
1981 *Myospalax tingi,* Zong, p. 174; Pl.I, Fig. 5
1990 *Myospalax epitingi,* Zheng and Li, pp. 435, 439
1991 *Myospalax epitingi,* Zheng and Han, pp. 103, 106
1991 *Myospalax epitingi,* Lawrence, pp. 269, 282
1994 *Yangia epitingi* Zheng, Figs. 2, 4, 7, 12; Table 1
1997 *Yangia epitingi*, Zheng, Figs. 2, 4–6

Revised species diagnosis: Noticeably larger than *Y. tingi*. Skull occipital shield distinctly concave and penetrating rostral to the confluence of the lambdoid crests. Caudal sagittal region is 2.9 times broader than the interorbital region. Supraorbital crests less medially placed. Supraoccipital process is extremely robust, with lateral sides nearly completely overlapping the lateral wings of the lambdoid crests. Nasals distinctly rostrally expanded for two-fifths of their length. Molar reentrants are relatively shallow on upper lingual and lower buccal sides. M2 α angle is low. M3 large, but m3 rather reduced. Shallow second buccal reentrants on m2 and m3 lost early in occlusal wear.

Locality and Material: YS83, palate with left and right M1-M3 and fragmentary right mandible with m1-3 (V11182, V11183). Measurements in Table 9.12.

Stratigraphic position: Red loam correlated with the Wucheng Loess.

Description: The anterior palatine foramen is small and round with a rostral margin that attains the second lingual reentrant of the M1. Posterior palatine foramen is relatively large with a caudal margin that reaches the distal end of M2. A bony crest extends from the incisive foramina along the midline of the palate to the mid-pterygoid fossa. The rostral margin of the anterior pterygoid fossa reaches the lingual reentrant of M2, while the rostral margin of the mid-pterygoid fossa reaches the anterior margin of M3. The posterior pterygoid fossa is deep, triangular, and expands laterally to the termination of the dentition. The posterior pterygoid canal extends rostrolaterally-caudomedially with a rostrolateral angular foramen penetrating the dorsal pterygoid. Dentition is distinctly non-parallel, the palate being 5.2 mm wide at M1, 7.3 mm at the mesial margin of M3.

The mesial wall of the M1 is slightly convex, and the two lingual reentrants are shallow. The buccal salient angles on the M1 and M2 extend anterobuccally, hence the M2 is typically clinomegodont with α angle 47°, and elongated. The M3 lingual reentrant is deep, but the second buccal reentrant is shallower, the second buccal salient angle is correspondingly narrow, and the third buccal salient angle is wide and extends posterolaterally (Fig. 9.11e).

The m1 anterior loop is nearly circular. The U-shaped second buccal reentrant is deeper than the V-shaped third lingual reentrant, while both are in opposition and separated by a wide bridge of dentine. The mesial wall of the second buccal salient angle is distinctly curved but the third lingual salient angle is narrow and long. The m2 and m3 second buccal reentrant angles penetrate the crown to a lesser degree than the first and are lost early due to occlusal wear. The m3 first lingual salient angle is correspondingly reduced (Fig. 9.11f).

Comparison and discussion: The YS83 material is fundamentally consistent with *Y. epitingi* in its large size (Table 9.12), slightly reduced M3 and more reduced m3, α of 47°, low on M2, shallow upper molar lingual reentrants and lower molar buccal reentrants, and anterobuccal reentrants on m2-3 that are lost at an early stage of wear.

Yangia epitingi is distinctly larger than *Y. tingi*, its interorbital region is broader and flatter, the supraoccipital process is more robust, and the nasals expand rapidly laterally toward the anterior. Teilhard de Chardin and Pei (1941) indicated that *Y. epitingi* also displays a more sculptured cranium, but this appears to be a minor difference (or perhaps sexual dimorphism is a factor) because the crests and other projecting portions are rather weakly developed and "sculpturing" is not striking. These two taxa do not differ greatly in dental morphology, so there is some suspicion of synonymy (Zheng and Cai 1991).

Teilhard de Chardin and Pei (1941) stated "the possibility remains that some Shansi specimens referred to *Siphneus tingi* by Young and Teilhard represent in reality incompletely grown *S. epitingi*." A comprehensive survey of all the specimens indicates that several finds may be included in *Yangia epitingi*: "*Siphneus cf. fontanieri*" specimen C/66 from Shiteshan (Loc. 13), Wubu Co. (Teilhard de Chardin and Young 1931) and "*Siphneus tingi*" from Fancun (Loc. 31), Fushan Co. (Young 1935). The skull from Chenjiawo, Lantian (Chow and Li 1965), is completely consistent with that of *Y. epitingi* (despite its small juvenile size), as it possesses a broad and flat interorbital region, robust supraoccipital processes, and an occipital shield that surpasses the confluence of lambdoid crests. A partial juvenile skull from Xiaochangcun, Tunliu Co. called "*Myospalax tingi*" by Zong (1981) is more appropriately assigned to *Y. epitingi* due to the breadth and shallowness of the lingual reentrants on the upper molars and the posterobuccally extended posterior lobe on the M3.

In contrast, the smaller of two "*Myospalax epitingi*" mandibles from layer 11 of locality 1 at Zhoukoudian (formerly Choukoutien) (Chao and Tai 1961: plate I, Fig. 2) is reassigned here to *Eospalax fontanieri* as its unreduced m3 has two buccal reentrants, lower molar valleys are distinctly inclined, and the m1 anterolingual reentrant is undeveloped.

The fauna from the type locality of *Yangia epitingi*, Zhoukoudian Loc. 13, is generally regarded as early middle Pleistocene. Continuation of *Y. epitingi* into the lower deposits of Zhoukoudian Loc. 1 (layer 11) indicates its general age range (Zheng and Han 1991). Fission track analysis on layer 10 from the latter locality (Hu 1985) indicates the species to predate 0.46 Ma. At Chenjiawo, paleomagnetic stratigraphy gives an age of 0.65 Ma (An and Ho 1989) or 0.684–0.710 Ma (Ding et al. 2002). Consequently, the age span of *Y. epitingi* is at least 0.65–0.46 Ma, or the Chenjiawo Stage (Zheng and Han 1991). This is the last record of *Yangia* (Zheng 1994, 1997), and indicates an age of < 1 Ma for YS83.

9.3 Biostratigraphy of the Myospalacinae

The 800 m composite section of Yuncu subbasin represents 6 million years of geological history and records ten species of myospalacine rodents (approximately one-third of Subfamily Myospalacinae diversity), making the area one of the most favorable for the study of this group.

Teilhard de Chardin (1942) subdivided the fluviolacustrine sediments he deemed as the "Yushe Series" into Zones I, II, and III (then considered Pontian stage and the younger Villafranchian faunal unit equivalents). He considered *Prosiphneus murinus* (including his *Prosiphneus* sp.) to be restricted generally to Zone I. *Chardina truncatus, Pliosiphneus lyratus, Mesosiphneus praetingi* and *M. intermedius* occurred in Zone II, and *Yangia omegodon, Y. trassaerti* (including "*Siphneus chaoyatseni*"), *Y. tingi* and *Eospalax fontanieri* were restricted to Zone III. This stratigraphic subdivision and its associated phylogenetic sequence is the basis for a long-standing biostratigraphically significant concept of zokor evolution. Until now, the lack of precise stratigraphy and inaccuracies in provenance created problems for modern workers. Results of the Sino-American collaboration include a redefined stratigraphic nomenclature for the Yushe Basin and more refined zokor biostratigraphy (Fig. 9.12): *Prosiphneus murinus* is restricted to the Mahui Formation and base of the Taoyang Member of the Gaozhuang Formation. *Pliosiphneus antiquus* and *Chardina truncatus* are characteristic of the Nanzhuanggou Member of the Gaozhuang Formation. *Pliosiphneus lyratus* appears in the Nanzhuanggou Member and continues through the Culiugou Member into the base of the Mazegou Formation. *Mesosiphneus praetingi* largely overlaps this range, but continues stratigraphically higher. *M. intermedius* appears high in the Mazegou Formation at the time of the last occurrence of *M. praetingi*. *Yangia tingi* and *Y. trassaerti* are restricted to the Haiyan Formation and *Yangia epitingi* and *Eospalax fontanieri* occur in overlying loess deposits. Figure 9.12 places the biostratigraphy in the Yushe Basin paleomagnetic framework of Opdyke et al. (2013). The new zokor biostratigraphy is compared with the previous scheme in Table 9.13.

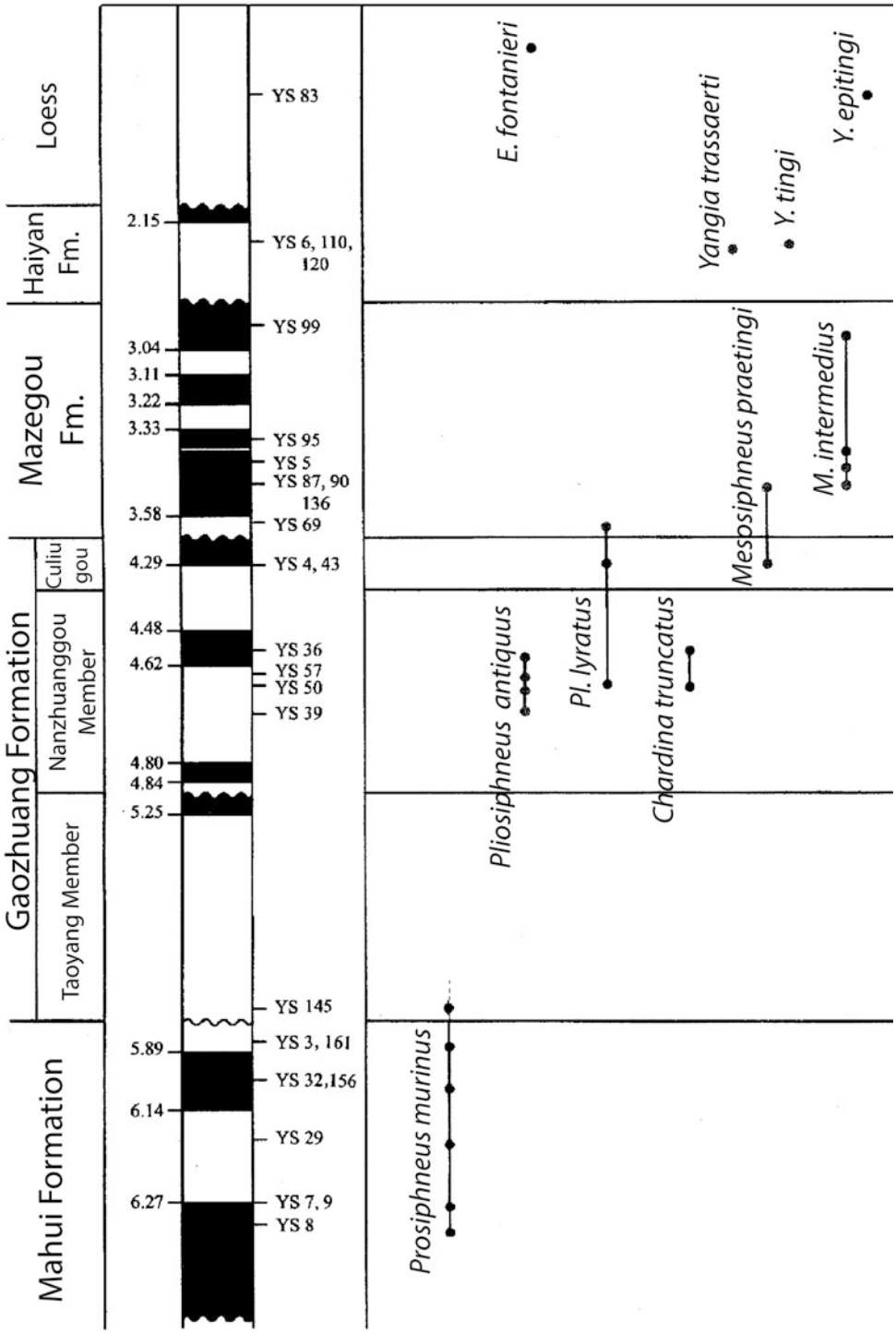

Fig. 9.12 Yushe myospalacine biostratigraphic ranges, with localities as calibrated by magnetostratigraphy. Reversal stratigraphy of Opdyke et al. (2013) with localities in magnetic sections shown on left, next to lithostratigraphic units. Some localities not in magnetic sections (e.g., loess sites YS83, YS123) are plotted based on stratigraphy. Yushe genera are *Prosiphneus*, *Pliosiphneus*, *Chardina, Mesosiphneus, Yangia*, *Eospalax*

Elsewhere than Yushe Basin, *Y. epitingi* occurs in the upper reddish clay at Wuchengzhen, Xixian Co., Shanxi (Teilhard de Chardin and Young 1931), the upper Sanmenian reddish loess at Fushan Co., Shanxi (Young 1935), Zhoukoudian Loc. 13 and the basal portion of Loc. 1 (Chao and Tai 1961), the red fine sandy soils at Nangouling, Chicheng Co., Hebei (Chia and Chai 1957), the Lishi Loess at Chenjiawo, Lantian Co., Shaanxi (Chow and Li 1965),

Table 9.13 Zokor biostratigraphic correlation in the Yushe basin

This study			Teilhard de Chardin 1942	
Wucheng & Lishi loess		*E. fontanieri* *Y. epitingi*	Red clays	*E. fontanieri*
Haiyan Fm.		*Y. tingi* *Y. trassaerti*	Zone III	*E. fontanieri* *Y. tingi* *Y. trassaerti* ("*M.*" *chaoyatseni*)
Mazegou Fm.		*M. intermedius* *M. praetingi* *P. lyratus*	Zone II	*Y. omegodon* *M. "paratingi"* *M. praetingi* *C. truncatus* *P. lyratus*
Gaozhuang Fm.	Culiugou	*M. praetingi*		
	Nanzhuanggou	*C. truncatus* *P. lyratus* *P. antiquus* n.sp.		
	Taoyang	*P. murinus*	Zone I	*P. murinus* (*Prosiphneus* sp.)
Mahui Fm.		*P. murinus*		

and the Lishi Loess of Xiaochangcun, Tunliu Co. Shanxi (Zong 1981). Based upon the 0.684–0.71 Ma paleomagnetic age estimate for Chenjiawo (Ding et al. 2002) and the approximate 0.46 Ma date of basal Loc. 1 at Zhoukoudian, one may deduce the time of deposition of the reddish Lishi Loess in the Yushe Basin.

Prosiphneus murinus and *Pliosiphneus* do not show an ancestor-descendent relationship but are successive, in keeping with the hypothesis (Zheng 1994) that *Prosiphneus eriksoni* represented a stage that preceded both *Pliosiphneus* and *Chardina*. The biogeographic distribution of *P. eriksoni* is restricted to the continental interior at the higher latitude Inner Mongolian locality of Ertemte. An evolutionary event transformed *P. eriksoni* by 4.7 Ma, as exemplified by its small M1 A, B, C, D average values (0.28, 1.03, 1.17, 0.32), with increased hypsodonty compared to higher crowned *Pliosiphneus antiquus* with average values of (0.43, 1.43, 0.93, 1.5), and by the lesser m1 a, b, c, d, e average values (0.05, 1.21, 1.07, 0.51, 0.40) compared with *P. antiquus* average values (0.07, 0.73, 1.07, 1.55, 0.6). Possibly climatic conditions in the Yushe Basin, or more broadly in northeastern Asia, resulted in a more demanding zokor habitat and a more abrasive diet for which *Pliosiphneus* and *Chardina* were adapted. The temporal range of *Chardina* was short and the transition from *P. antiquus* to *P. lyratus* was rapid, further reflecting climatic instability.

At approximately 4.3 Ma *Mesosiphneus praetingi* replaced *Chardina* (Fig. 9.12). The dentine tracts of the former are noticeably higher than those of the latter (Figs. 9.13, 9.14) and the rapid increase in hypsodonty would reflect further climatic alteration. At approximately 3.4 Ma *M. intermedius* replaced *M. praetingi*, attaining the greatest hypsodonty value for the genus, possibly correlated with further changes affecting the diet and habitat.

At the beginning of the Pleistocene, a major event occurred among the concave occiput myospalacines as the hypsodont rooted *Mesosiphneus* was replaced by the rootless *Yangia*. At the same time, the Wucheng Loess began to accumulate to the west (Liu 1985), which undoubtedly reflects widespread environmental change.

The rootless (ever-growing) molars of *Yangia* are recognized as useful for processing coarse food, although *Y. trassaerti* retained a rooted orthomegodont occlusal pattern for its upper molars (Fig. 9.15), and its occlusal surface area had not increased dramatically. *Y. trassaerti* likely had limited adaptability to a nutrition that was increasing in toughness. By about 2.2 Ma *Yangia tingi* appeared, with a hypsodont dentition adapted for heavy wear. Its upper molars were fully clinomegodont, with low M2 α angle and low breadth to length ratio. (Average breadth/length ratio for M2 is over 0.66, and α angle above 65° in the orthomegodont pattern; below these values the clinomegodont pattern is recognized; see Fig. 9.11). With clinomegodonty, tooth length increases and therefore the occlusal wear surface increases. *Y. epitingi* accentuated these changes, attaining the largest occlusal surface area in the *Yangia* lineage, but apparently it did not tolerate further environmental degradation. *Yangia* and the concave occiput myospalacines became extinct.

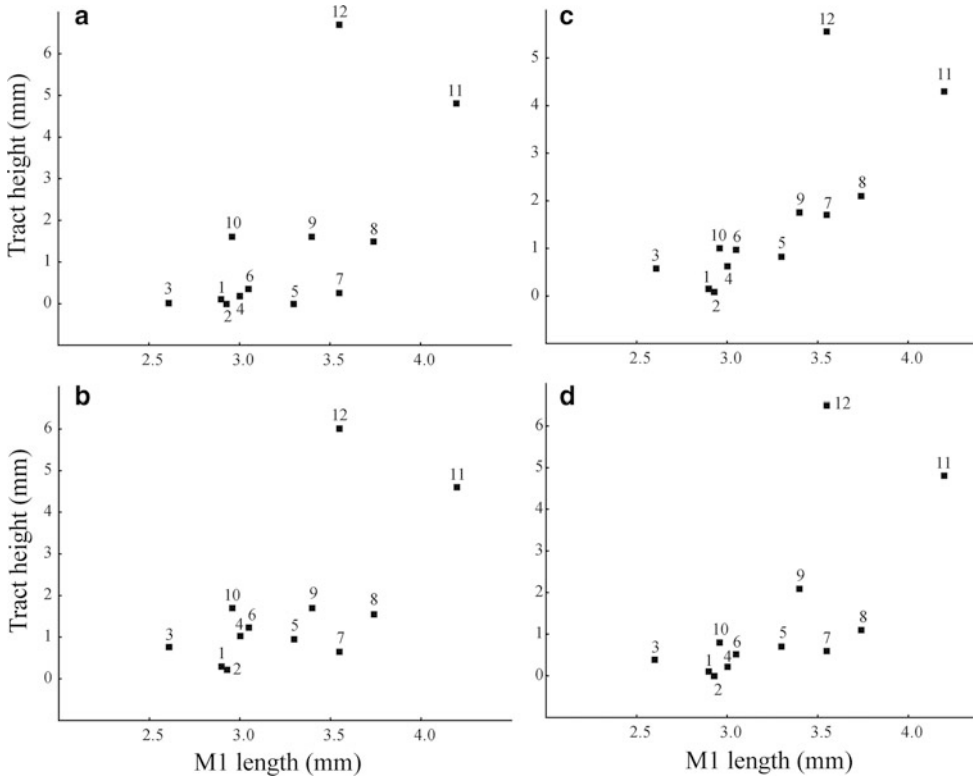

Fig. 9.13 Bivariate plot of average M1 length (mm) to average dentine tract height in mm for various myospalacine species (**a**–**d** correspond to parameters A to D, respectively). 1. *Prosiphneus qinanensis*, 2. *Pr. qiui*, 3. *Pr. licenti*, 4. *Pr. murinus*, 5. *Pr. tianzuensis*, 6. *Pr. ericksoni*, 7. *Pliosiphneus antiquus*, 8. *Pliosiphneus lyratus*, 9. *Chardina sinensis*, 10. *C. truncatus,* 11. *Mesosiphneus praetingi*, 12. *M. intermedius*

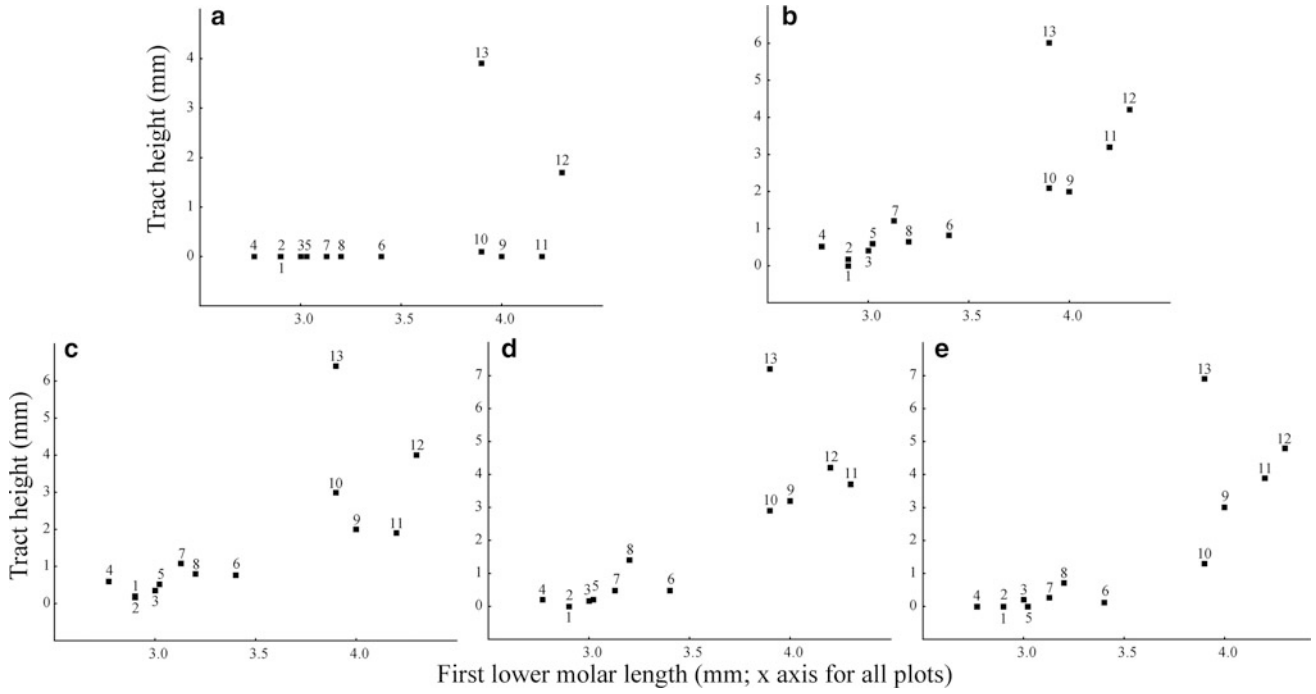

Fig. 9.14 Bivariate plot of average m1 length (mm) to average dentine tract height (mm) for parameters **a**, **b**, **c**, **d** and **e** of various myospalacine species. 1. *Prosiphneus qinanensis*, 2. *Pr. qiui*, 3. *Pr. haoi*, 4. *Pr. licenti,* 5. *Pr. murinus,* 6. *Pr. tianzuensis*, 7. *Pr. ericksoni*, 8. *Pliosiphneus antiquus*, 9. *Pliosiphneus lyratus,* 10. *Chardina sinensis*, 11. *C. truncatus*, 12. *Mesosiphneus praetingi*, 13. *M. intermedius*

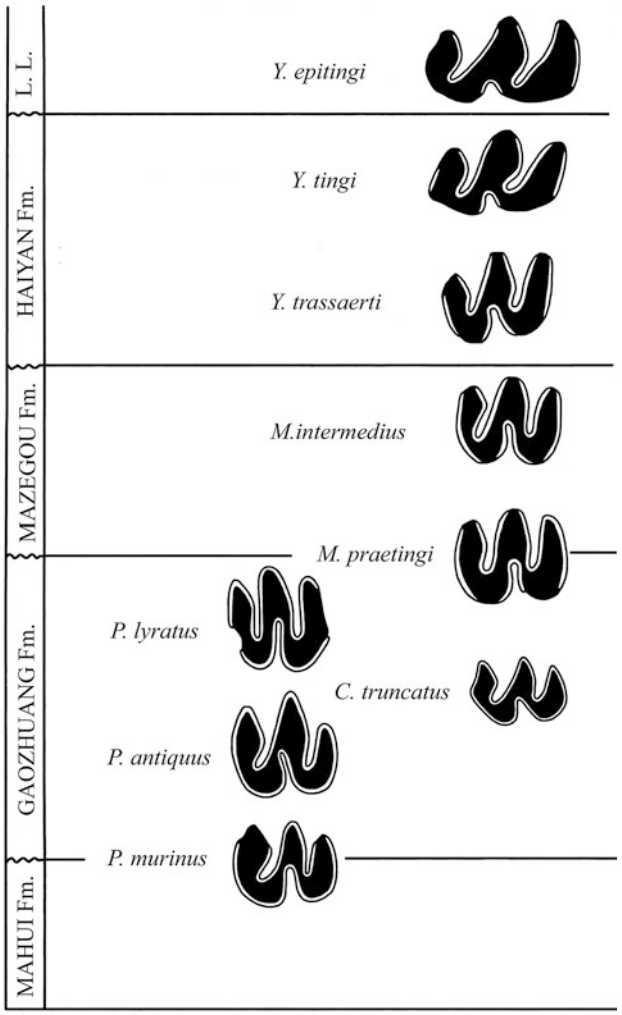

Fig. 9.15 Morphology of M2 for Yushe Basin myospalacines, illustrating rooted orthomegodont taxa preceding rootless clinomegodont morphology

In summary, myospalacine evolutionary events in the Yushe Basin indicate episodic change after 5 Ma, which is consistent with a climatic shift from relatively mesic (woodland) to xeric (grassland) conditions. Zokor evolutionary events at about 4.7, 4.3, 3.5, and 2.6 Ma in Yushe Basin may have reflected regional climatic changes. Within the Yushe Basin the concave occiput myospalacines are the most evolutionarily complete lineage. The *Chardina truncatus* → *Mesosiphneus praetingi* → *M. intermedius* → *Yangia trassaerti* → *Y. tingi* → *Y. epitingi* sequence illustrates a complete lineage from origin to extinction. The lineage further suggests rapid replacement events followed by intervals of gradual change for these rodents. Within this series, species evolutionary rates were inconstant, with greatly varying residence times in the Yushe record, some taxa surviving about 1 m.y. and others much less.

Acknowledgements The author expresses his gratitude to colleagues Wen-Yu Wu and Jie Ye for providing initial field data and comments on the manuscript, to Zhu-Ding Qiu and L.J. Flynn for support and encouragement during the research, and to the reviewers of the manuscript, Qiang Li, Thomas Stidham, Yingqi Zhang, and Samantha Hopkins. The author thanks especially the late William R. Downs for great assistance in translating the text to English.

References

Allen, G. M. (1938). The mammals of China and Mongolia. Natural history of central Asia. *American Museum of Natural History, 11,* 1–620.

An, Z.-S., & Ho, C.-K. (1989). New magnetostratigraphic dates of Lantian *Homo erectus*. *Quaternary Research, 32,* 213–221.

Bazarov, D. B., Erbaeva, M. A., & Rezanov, I. N. (1976). *Geology and fauna of the Anthropogene reference sections in western Transbaikal*. Moscow: Akademiya Nauka (in Russian).

Boule, M., & Teilhard de Chardin, P. (1928). Paléontologie. In M. Boule, H. Breuil, E. Licent & P. Teilhard de Chardin (Eds.), *Le paléolithique de la Chine, deuxieme partie* (Mémoire 4, pp. 26–102). Paris: Archives de L'Institut de Paléontologie Humaine.

Cai, B.-Q. (1987). A preliminary report on the Late Pliocene micromammalian fauna from Yangyuan and Yuxian, Hebei. *Vertebrata PalAsiatica, 25,* 124–136.

Cai, B.-Q., & Li, Q. (2004). Human remains and the environment of Early Pleistocene in the Nihewan basin. *Science in China, D47,* 437–444.

Cai, B.-Q., Zhang, Z.-Q., Zheng, S.-H., Qiu, Z.-D., & Li, Q. (2004). New advances in the stratigraphic study on representative sections in the Nihewan Basin, Hebei. *Professional Papers of Stratigraphy and Paleontology, 28,* 267–285.

Chao, Z.-K., & Tai, E.-J. (1961). Report on the excavation of the Choukoudian *Sinanthropus* site in 1960. *Vertebrata PalAsiatica, 4,* 374–378.

Chia, L.-P., & Chai, J.-C. (1957). Quaternary mammalian fossils from Chihcheng, Hopei. *Vertebrata PalAsiatica, 1,* 47–55.

Chow, M.-C., & Li, C.-K. (1965). Mammalian fossils in association with the mandible of Lantian Man at Chen-Chia-Ou, in Lantian, Shensi. *Vertebrata PalAsiatica, 9,* 377–393.

De Bruijn, H., Bosma, A. A., & Wessels, W. (2015). Are the Rhizomyinae and Spalacinae closely related? Contradistinctive conclusions between genetics and palaeontology. *Palaeobiodiversity and Palaeoenvironments, 95,* 257–269.

Ding, Z.-L., Derbyshire, E., Yang, S.-L., Yu, Z.-W., Xiong, S.-F. & Liu, T.-S. (2002). Stacked 2.6-Ma grain size record from the Chinese loess based on five sections and correlation with the deep-sea $\delta^{18}O$ record. *Palaeoceanography, 17*, 5.1–21

Flynn, L. J., Tedford, R. H., & Qiu, Z.-X. (1991). Enrichment and stability in the Pliocene mammalian fauna of North China. *Paleobiology, 17,* 246–265.

Gromov, I. M., & Baranova, G. J. (1981). *Catalogue of the Pliocene-recent mammals of the USSR*. Leningrad: Akademiya Nauka (in Russian).

Guo, Z.-T., Ruddiman, W.F., Hao, Q.-Z., Wu, H.-B., Qiao, Y.-S., Zhu, R.-X. et al. (2002). Onset of Asian desertification by 22 Myr ago inferred from loess deposits in China. *Nature, 416*, 159–163.

Hao, Q.-Z., & Guo, Z.-T. (2004). Magnetostratigraphy of a late Miocene-Pliocene loess-soil sequence in the western Loess Plateau in China. *Geophysical Research Letters, 31,* 1–4.

Hu, C.-K. (1985). The history of mammalian fauna of Locality 1 of Zhoukoudian and its recent advances. In IVPP (Eds.), *Multidisciplinary study of the Peking man site at Zhoukoudian* (pp. 107–113). Beijing: Science Press.

Hu, C.-K., & Qi, T. (1978). Gongwangling Pleistocene mammalian fauna of Lantian, Shaanxi. *Palaeontologia Sinica new series, C21,* 1–64.

Ji, H.-X. (1975). The Lower Pleistocene mammalian fossils of Lantian district, Shensi. *Vertebrata PalAsiatica, 13,* 169–177.

Ji, H.-X. (1976). The Middle Pleistocene mammalian fossils of Laochihe, Lantian district, Shaanxi. *Vertebrata PalAsiatica, 14,* 59–66.

Kretzoi, M. (1961). Zwei Myospalaxiden aus dem Nordchina. *Vertebrata Hungarica, 3,* 123–136.

Lawrence, M. A. (1991). A fossil *Myospalax* cranium (Muridae, Rodentia) from Shanxi, China with observations on zokor relationships. In T.A. Griffiths & D. Klingener (Eds.), *Contributions to mammalogy in honor of Karl F. Koopman* (Vol. 206, pp. 261–286). New York: Bulletin American Museum of Natural History.

Leroy, P. (1940). Observations on living Chinese mole-rats. *Bulletin of the Fan Memorial Institute of Biology. Zoology, 10,* 167–193.

Li, C.-K., Wu, W.-Y., & Qiu, Z.-D. (1984). Chinese Neogene: Subdivision and correlation. *Vertebrata PalAsiatica, 22,* 163–178.

Li, Q., Zheng, S.-H., & Cai, B.-Q. (2008). Pliocene biostratigraphic sequence in the Nihewan Basin, Hebei, China. *Vertebrata PalAsiatica, 46,* 210–232.

Liu, D.-S. (1964). *Loess in the middle reaches of the Huanghe River*. Beijing: Science Press (in Chinese).

Liu, D.-S. (1985). *Loess and the environment*. Beijing: Science Press (in Chinese).

Liu, L.-P., Zheng, S.-H., Cui, N., & Wang, L.-H. (2013). Myospalacines (Cricetidae, Rodentia) from the Miocene-Pliocene red clay section near Dongwan Village, Qin'an, Gansu, China and the classification of Myospalacinae. *Vertebrata PalAsiatica, 51,* 211–241.

Liu, L.-P., Zheng, S.-H., Cui, N., & Wang, L.-H. (2014). Rootless myospalacines from upper Pliocene to Pleistocene of Wenwanggou section, Lingtai, Gansu. *Vertebrata PalAsiatica, 52,* 440–466.

Liu, L.-P., Zheng, S.-H., Zhang, Z.-Q., & Wang, L.-H. (2011). Late Miocene-Early Pliocene biostratigraphy and Miocene/Pliocene boundary in the Dongwan section, Gansu. *Vertebrata PalAsiatica, 49,* 229–240.

Luo, Z.-X., Chen, W., Gao, W., Wang, Y.-X., Li, C.-Y. & Li, H. (2000). Mammalia 6. Rodentia, Part III: Cricetidae. In Z.-X. Luo, W. Chen & W. Gao (Eds.) *Fauna Sinica* (pp. 121–128). Beijing: Science Press.

Martin, R. A. (1987). Notes on the classification and evolution of some North American fossil *Microtus* (Mammalia, Rodentia). *Journal of Vertebrate Paleontology, 7,* 270–283.

Mats, V. D., Pokatilov, S. M., Popova, A. J., Kranchynsky, N. V., Kulagina, N. V., & Shymaraeva, M. K. (1982). *Central Baikal in Pliocene and Pleistocene time*. Novosibirsk, Siberian Branch: Akademiya Nauka (in Russian).

McKenna, M. C., & Bell, S. K. (1997). *Classification of mammals above the species level*. New York: Columbia University Press.

Miller, G. S. (1927). Revised determinations of some Tertiary mammals from Mongolia. *Palaeontologia Sinica C, 5*(2), 1–20.

Musser, G. G., & Carleton, M. D. (2005). Superfamily Muroidea. In D. E. Wilson & D. M. Reeder (Eds.), *Mammal species of the world—A taxonomic and geographic reference* (pp. 894–1531). Baltimore: Johns Hopkins University Press.

Opdyke, N. D., Huang, K. & Tedford, R. H. (2013). The Paleomagnetism and magnetic stratigraphy of the Late Cenozoic sediments of the Yushe Basin, Shanxi Province, China. In R. H. Tedford, Z.-X. Qiu & L. J. Flynn (Eds.) *Late Cenozoic Yushe Basin, Shanxi Province, China: Geology and fossil mammals, Volume I: History, geology, and magnetostratigraphy* (pp. 69–78). Dordrecht: Springer.

Pei, W. C. (1930). On a collection of mammalian fossils from Chiachiashan, near Tongshan (Hopei). *Bulletin of the Geological Society of China, 9,* 371–378.

Qiu, Z.-D. (1988). Neogene micromammals of China. In E. K. Y. Chen (Ed.), *The Paleoenvironment of East Asia from the mid-Tertiary 2* (pp. 834–848). Hong Kong: Center for Asian Studies.

Qiu, Z.-D., & Storch, G. (2000). The Early Pliocene micromammalian fauna of Bilike, Inner Mongolia, China (Mammalia: Lipotyphla, Chiroptera, Rodentia, Lagomorpha). *Senckenbergiana Lethaea, 80,* 173–229.

Qiu, Z.-X., & Qiu, Z.-D. (1990). Neogene local mammalian faunas, succession, and ages. *Journal of Stratigraphy, 14,* 241–260.

Schlosser, M. (1924). Tertiary vertebrates from Mongolia. *Palaeontologia Sinica C, 1*(1), 1–131.

Suchov, V. P. (1970). *Micromammals of Bashkiria (Southern Ural)*. Moscow: Akademiya Nauka.

Tedford, R. H., Flynn, L. J., Qiu, Z.-X., Opdyke, N. D., & Downs, W. R. (1991). Yushe Basin, China, Paleomagnetically calibrated mammalian biostratigraphic standard for the Late Neogene of Eastern Asia. *Journal of Vertebrate Paleontology, 11,* 519–526.

Tedford, R. H., Qiu, Z.-X., & Ye, J. (2013). Cenozoic geology of the Yushe Basin. In R. H. Tedford, Z.-X. Qiu, & L. J. Flynn (Eds.), *Late Cenozoic Yushe Basin, Shanxi Province, China: Geology and fossil mammals, Volume I: History, geology, and magnetostratigraphy* (pp. 35–67). Dordrecht: Springer.

Teilhard de Chardin, P. (1926). Mammifères Tertiaires de Chine et de Mongolie. *Annales de Paléontologie, 15,* 1–51.

Teilhard de Chardin, P. (1936). Fossil mammals from Locality 9 of Choukoutien. *Palaeontologia Sinica, C, 7*(4), 1–70.

Teilhard de Chardin, P. (1942). New rodents of the Pliocene and lower Pleistocene of North China. *Publications de l'Institut de Géobiologie, Pékin, 9,* 1–101.

Teilhard de Chardin, P., & Leroy, P. (1942). Chinese fossil mammals. A complete bibliography, analyzed, tabulated, annotated, and indexed. *Publications de l'Institut de Géobiologie, Pékin, 8,* 1–142.

Teilhard de Chardin, P., & Piveteau, J. (1930). Les mammifères fossiles de Nihowan (Chine). *Annales de Paléontologie, 19,* 1–134.

Teilhard de Chardin, P., & Pei, W. C. (1941). The fossil mammals of Locality 13 in Choukoutien. *Palaeontologia Sinica, C11,* 1–106.

Teilhard de Chardin, P., & Young, C. C. (1931). Fossil mammals from northern China. *Palaeontologia Sinica, C, 9*(1), 1–66.

Wang, H. (1988). An Early Pleistocene mammalian fauna from Dali, Shaanxi. *Vertebrata PalAsiatica, 26,* 59–72.

Wang, Y.-X. (2003). *A complete checklist of mammal species and subspecies in China. A taxonomic and geographic reference*. Kunming: China Forestry Publishing House.

Young, C. C. (1927). Fossile Nagetiere aus Nord-China. *Palaeontologia Sinica, C, 5*(3), 1–82.

Young, C. C. (1935). Miscellaneous mammalian fossils from Shansi and Honan. *Palaeontologia Sinica, C, 9*(2), 1–42.

Zhang, Z.-Q. (1999). Pliocene micromammal fauna from Ningxian, Gansu Province. In Y. Q. Wang & T. Deng (Eds.), *Seventh Annual Meeting of the Chinese Society of Vertebrate Paleontology Proceedings* (pp. 167–177). Beijing: China Ocean Press.

Zhang, Z.-Q., & Zheng, S.-H. (2000). Late Miocene–Early Pliocene biostratigraphy of Loc. 93002 section, Lingtai, Gansu. *Vertebrata PalAsiatica, 38,* 274–286.

Zhang, Z.-Q., & Zheng, S.-H. (2001). Late Miocene–Pliocene biostratigraphy of Xiaoshigou section, Lingtai, Gansu. *Vertebrata PalAsiatica, 39,* 54–66.

Zhang, Z.-Q., Zheng, S.-H., & Liu, J.-B. (2003). Pliocene micromammalian biostratigraphy of Nihewan basin, with comments on the stratigraphic division. *Vertebrata PalAsiatica, 41,* 306–313.

Zheng, S.-H. (1976). Small mammals of Middle Pleistocene in Heshui, Gansu. *Vertebrata PalAsiatica, 14,* 112–119.

Zheng, S.-H. (1994). Classification and evolution of the Siphneidae. In Y. Tomida, C.-K. Li, & T. Setoguchi (Eds.), *Rodent and lagomorph families of Asian origins and diversification* (pp. 57–76). Tokyo: National Science Museum Monograph 8.

Zheng, S.-H. (1997). Evolution of the Mesosiphneinae (Siphneidae, Rodentia) and environmental change. In Y.-S. Tong, Y.-Y. Zhang, W.-Y. Wu, J.-L. Li & L.-Q. Shi (Eds.), *Evidence for evolution. Essays in honor of Prof. Chungchien Young on the hundredth anniversary of his birth* (pp. 137–150). Beijing: China Ocean Press.

Zheng, S.-H. & Cai, B.-Q. (1991). Micromammalian fossils from Danangou of Yuxian, Hebei. In IVPP (Ed.), *Contributions to the XIII INQUA* (pp. 100–131). Beijing: Beijing Science and Technology Publishing House (in Chinese with English summary).

Zheng, S.-H., & Han, D.-F. (1991). Quaternary mammals of China. In T.-S. Liu (Ed.), *Quaternary geology and environment in China* (pp. 101–114). Beijing: Science Press.

Zheng, S.-H., Huang, W.-P., Zong, G.-F., & the Yellow River Elephant Research Team (1975). *Huanghe River Stegodon* (pp. 1–46). Beijing: Science Press.

Zheng, S.-H., & Li, C.-K. (1986). A review of Chinese *Mimomys* (Arvicolidae, Rodentia). *Vertebrata PalAsiatica, 24,* 81–109.

Zheng, S.-H., & Li, C.-K. (1990). Comments on fossil arvicolids of China. In O. Fejfar & W.-D. Heinrich (Eds.), *International symposium: Evolution, phylogeny and biostratigraphy of arvicolids (Rodentia, Mammalia)* (pp. 431–442). Prague: Geological Survey.

Zheng, S.-H., & Li, Y. (1982). Some Pliocene lagomorphs and rodent from Loc. 1 of Songshan, Tianzuxian, Gansu Province. *Vertebrata PalAsiatica, 20,* 35–44 (in Chinese with English abstract).

Zheng, S.-H., & Zhang, Z.-Q. (2000). Late Miocene–Early Pleistocene micromammals from Wenwanggou of Lingtai, Gansu, China. *Vertebrata PalAsiatica, 38,* 58–71.

Zheng, S.-H., & Zhang, Z.-Q. (2001). Late Miocene–Early Pleistocene biostratigraphy of the Leijiahe area, Lingtai, Gansu. *Vertebrata PalAsiatica, 39,* 215–228.

Zheng, S.-H., Zhang, Z.-Q., & Cui, N. (2004). On some species of *Prosiphneus* (Siphneidae, Rodentia) and the origin of Siphneidae. *Vertebrata PalAsiatica, 42,* 297–315.

Zong, G.-F. (1981). Pleistocene mammals from Tunliu, Shanxi. *Vertebrata PalAsiatica, 19,* 174–183.

Chapter 10
The Hamsters of Yushe Basin

Wen-Yu Wu and Lawrence J. Flynn

Abstract Fossil hamsters are a minor but constant microfauna component in the succession of Yushe Basin deposits. They indicate considerable hamster diversity for North China during the late Neogene, with at least six genera and eight species recorded from late Miocene to early Pleistocene assemblages. *Neocricetodon* is a long-ranging late Neogene hamster, with closely related species widespread throughout Europe and Asia. Yushe Basin famously produced the type material of *Neocricetodon grangeri*, which we show to come from the late Miocene Mahui Formation south of the town of Yushe. *Neocricetodon grangeri* ranges from late Miocene (6.3 Ma) to early Pliocene (4.7 Ma) deposits. Later long-ranging Pliocene hamster lineages are *Allocricetus* and *Cricetinus*, for each of which we define a new species. Joining the latter two genera during the Late Pliocene, the living *Cricetulus* brings to three the number of coeval hamster genera. Finally, by the early Pleistocene, the modern genus *Phodopus* appears and coexists with *Cricetulus* in Yushe Basin.

Keywords Yushe Basin • North China • Late Neogene • Hamsters • Cricetidae

Note: This chapter includes one or more new nomenclatural-taxonomic actions, registered in Zoobank, and for such purposes the official publication date is 2017.

W.-Y. Wu (✉)
Laboratory of Paleomammalogy, Institute of Vertebrate Paleontology and Paleoanthropology, Chinese Academy of Sciences, 142 Xizhimenwai Ave., Beijing 100044, People's Republic of China
e-mail: wuwenyu@ivpp.ac.cn

L.J. Flynn
Department of Human Evolutionary Biology, and the Peabody Museum of Archaeology and Ethnology, Harvard University, Cambridge, MA 02138, UK
e-mail: ljflynn@fas.harvard.edu

10.1 Introduction

Previously, the only cricetine rodent (hamster) recorded from the Neogene of the Yushe Basin was described by Young (1927) as *Cricetulus grangeri*. It was collected one-half kilometer southeast of the village of Jiayucun (Chia-yu-tsun), which is three kilometers south of the Yushe County seat. The specimen consists of an incomplete skull, a pair of mandibles, a left humerus, tibia, and several vertebrae. *C. grangeri* was recognized as distinctive and made the type species for *Neocricetodon* Schaub, 1934. We redescribe the original dentitions below. The cricetine collection of the 1987 and 1988 field seasons by the Sino-American Yushe field team contains only 136 specimens. The 1991 investigation extended our field study into the Tancun subbasin, the area including the type locality of *C. grangeri*. Although only a handful of specimens were recovered from several localities, key hamster material was found at Jiayucun.

Most Yushe hamster specimens are fragmentary isolated teeth, although there are several maxillae and mandibles, but they show moderate diversity. Current research on the phylogeny of Neogene cricetines is not greatly advanced, which creates a certain degree of difficulty due to lack of a phylogenetic framework. Our systematic analysis is based therefore on size and morphology of dentitions compared with taxa from the Neogene of Eurasia. The following cricetines are recognized in the Yushe collection:

Neocricetodon grangeri (Young, 1927)
Cricetinus mesolophidos sp. nov.
Allocricetus primitivus sp. nov.
Allocricetus cf. *A. ehiki* Schaub, 1930
Cricetulus sp.
Cricetulus barabensis Pallas, 1773
Cricetulus barabensis obscurus (Milne – Edwards, 1867)
Phodopus sp.
Nannocricetus? sp.
Cricetinae gen. et spp. indet.

Lawrence J. Flynn and Wen-Yu Wu (eds.), *Late Cenozoic Yushe Basin, Shanxi Province, China: Geology and Fossil Mammals, Volume II: Small Mammal Fossils of Yushe Basin*, Vertebrate Paleobiology and Paleoanthropology,
DOI 10.1007/978-94-024-1050-1_10

Dental terminology is adapted from Li (1977). Measurements (in mm) were taken with a Wild M7A binocular microscope. Plates were photographed by Lian Ouyang at the Institute of Vertebrate Paleontology and Paleoanthropology (IVPP) with a JSOM-T200 scanning electron microscope. Due to poor reflectivity, original photomicrographs appeared slightly distorted, with the longitudinal axis 19.9–22.9 times the original and transverse axis 16.7–20.5 times the original. We have corrected the error by computer processing. The supplemental 1991 specimens were photographed with a JSM-6100 scanning electron microscope. The data permit construction of hamster biostratigraphic ranges for the Yuncu and Tancun subbasins.

10.2 Systematics

Family Cricetidae Rochebrune, 1883
Subfamily Cricetinae Rochebrune, 1883
Neocricetodon Schaub, 1934
Neocricetodon grangeri (Young, 1927)
1927 *Cricetulus grangeri* Young
1930 *Cricetulus grangeri* Schaub
1934 *Neocricetodon grangeri* Schaub
1991 *Kowalskia* Flynn et al., Fig. 4
1991 *Kowalskia* Tedford et al., Fig. 4
1997 *Neocricetodon grangeri* Flynn et al., Fig. 5

Type: Yu She #173 in the Uppsala University Lagrelius collection.

Type Locality: "Chia yu Tsun", (currently Jiayucun) Yushe County, Shanxi Province, China.

Referred material and localities: Yuncu subbasin YS8: half M1, two M2 (one damaged), half m1 or m2, half m3 (V9875.1-5); YS9: half M1 (V9876); YS32: three M1, two M2, three M3, four m1, three m2, fragmentary left mandible with m2 and damaged m1 (V9877.1-16); YS3: M1, two M3 (incomplete) (V9978.1-3); YS39: M2 and M3 (V9879.1-2); YS50: left maxilla with heavily worn M1-3, right mandible with m1; M2, M3, m1, m2 (V9880.1-6); YS97: two fragmentary M1, m2 (V9881.1-3); YS4: two M1, two M2, two M3, m1, m2 (V9882.1-8). Tancun subbasin: YS161, fragmentary right maxilla with damaged M1 (V11326); YS145: m2 and m3 (V11332.1-2); YS142: M1 (V11327); YS152, right mandible with m2-m3 (V11328); YS139, m2 (V11329). See Table 10.1; Fig. 10.1.

Stratigraphy and age range: Late Miocene Mahui Fm. through early Pliocene Gaozhuang Fm. (Nanzhuanggou and Culiugou members), 6.3 to 4.7 Ma.

Description: Only anterior portions of two mandibles are preserved, with the masseteric crest on V9877.16 from YS32 more robust than on V9880.4 from YS50. The latter has a mental foramen anteroventral to the m1 and a ramus that is 3.42 mm deep at the anterior part of the m1.

Table 10.1 Dental measurements of *Neocricetodon grangeri* from Yuncu subbasin

	Length			Width	
	Range	$\bar{x}$	n	Range	$\bar{x}$
M1	1.63–1.81	1.71	4/4	1.03–1.18	1.13
M2	1.22–1.46	1.36	8/8	1.00–1.29	1.13
M3	1.02–1.19	1.12	5/5	0.98–1.10	1.02
m1	1.57–1.82	1.68	6/6	0.95–1.08	1.02
m2	1.27–1.47	1.39	6/6	1.07–1.27	1.15

The differences among the specimens collected from the various stratigraphic positions in the Yuncu subbasin are insignificant. Molars are brachydont; the M1 anterocone is posteriorly bifid, and the labial spur of its anterolophule may reach the buccal margin on some specimens; the mesoloph is short on M1 and M2, only about one half its possible length, and frequently lies on the anterior wall of the metacone; and the mesoloph is extremely short or lost on M3. M1 and M2 usually possess protolophule I and II, and metalophule I and II, though these crests may not be present on all specimens. M3 consistently has protolophule I and II, and metalophule I but not II. M1 has four roots: a large anteriorly projecting root, two lingual roots (large root under the protocone, smaller under the hypocone), and a posterobuccal root. M2 has four roots, one supporting each corner of the tooth.

The anteroconid on m1 is very slightly bifid and never more complicated (trifid), and the single anterolophulid usually extends from labial anteroconid or lingual anteroconid (only one case) to the anterior arm of the protoconid. Lower molars possess long mesolophids that extend to the lingual margin of the tooth, with the exception of only one specimen on which it ends short of the lingual wall. An ectomesolophid is absent. The lower third molar is large, its length nearly equal to that of m2.

The specimens collected in 1991 from the Jiayucun area of the Tancun subbasin are described in detail here. The broken M1 of fragmentary right maxilla V11326 is 1.27 mm wide and rather heavily worn, but it is clear that the anterocone is bifid. The anterolophule links lingually to the anterior arm of the protocone. Although the buccal part of the anterocone is isolated, a labial spur of the anterolophule extends to its posterolingual side. The paracone is linked to the protocone by protolophules I and II. The metacone is linked to the posterolabial corner of the hypocone by metalophule II. Metalophule I is absent. The mesoloph extends across two-thirds of the tooth with slight obliquity, and posteriorly to connect with the anterior wall of the metacone. Morphology, root structure and size are comparable to the Type.

M1 V11327 (length × width = 1.72 × 1.14 mm) is well-preserved, has a double anterocone with the buccal part isolated and a labial spur of the anterolophule ending with an

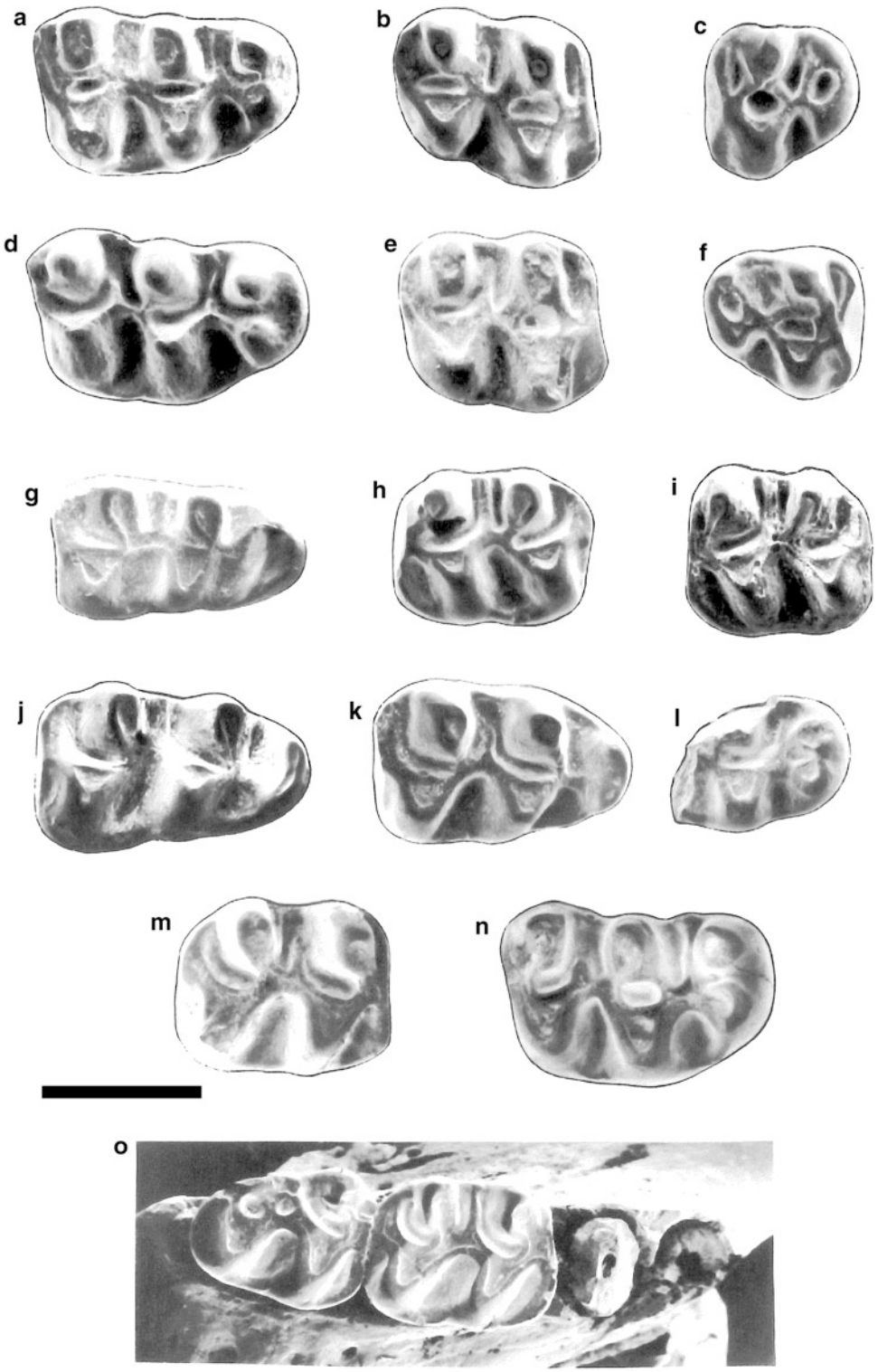

Fig. 10.1 SEM images of *Neocricetodon grangeri* (Young, 1927) from Yushe Basin, scale bar = 1 mm. **a**–**c** right M1 V9882.2, right M2 V9882.3, right M3 V9883.5, from YS4, Gaozhuang Formation; **d**, **e** right M1 (V9878.1) and M2 (V9875.2) from YS3 and YS8, Mahui Formation; **f**–**h** right M3 V9880.3, right m1 V9880.4, left m2 V9880.6 from YS50, Gaozhuang Formation; **i** left m2 V9881.3 from YS97, Gaozhuang Formation; **j**, **k** right m1 V9877.10 and V9877.9 from YS32, Mahui Formation; **l**–**o** right M1 fragment V9876 (YS9), right m2 V11329 (YS139), right M1 V11327 (YS142), and right m2-3 V11328 (YS152), all Mahui Formation. Scale bar = 1 mm

inflated cuspule at the wall of the tooth. The mesoloph crosses a third of the tooth, with an isolated termination. Protolophules I and II are present as is metalophule II, which links to the posterior corner of the hypocone, but metalophule I is absent.

The right mandible V11328 (m2: 1.28 × 1.08, m3: 1.27 × 0.98) has an m2 with mesolophid that extends to the lingual wall with a slightly inflated terminus. The m3 mesolophid extends posteriorly to intersect with the entoconid. Worthy of note is that the m3 is nearly equivalent in length to the m2, which is the same condition as for the Type. The long m3 is a diagnostic character for the species.

The m2 V11329 (1.38 × 1.17) mesolophid is low, crosses half the tooth, and extends transversely to rest against the posterior wall of the metaconid. The m2 V11332.1 (1.32 × 1.04) and m3 V11332.2 (1.10 × 0.88) both have well developed lingual anterolophids and mesolophids, with the mesolophid on the m3 extending to the lingual margin.

Comparison and discussion: The specimens from the successive Mahui and Gaozhuang formations of the two subbasins are few and poorly preserved, but they display no distinct differences. All specimens therefore can be referred to a single taxon. *Neocricetodon grangeri* is smaller than *Kowalskia neimengensis* Wu, 1991, and differs from the latter in the shorter mesoloph on upper molars, simpler m1 anteroconid, single (labial) anterolophulid, lack of ectomesolophid and the 4-rooted M1 and M2. In *Kowalskia neimengensis* the mesoloph reaches the labial margin on more than half M1 and M2, 27% of M1 are 3-rooted, the anteroconid is tripartite ("trifid") on 30% of m1, two anterolophulids are present on 14% of m1, and an ectomesolophid is present on 16% of m1.

Schaub (1930) restudied C.C. Young's *Cricetulus grangeri* and excluded it from *Cricetulus* based upon its robust rostrum, broad nasals, constricted interorbital region, broad supraorbital foramen, and its mandibular and dental characters. In a more detailed description of the type material of the species, Schaub (1934) erected the genus *Neocricetodon.* The senior author (Wu) studied the Type at Uppsala University in 1992, which is labeled "Chia yu Tsun, Yu She 173." After more detailed preparation, the dental characters were clearly revealed, but unfortunately the specimen is incomplete. Figure 10.2 illustrates the dorsal view of the skull, left mandible, left and right lower dentitions, and right maxillary dentition, which are basically consistent with the description of Schaub (1934). Daxner-Hőck et al. (1996) record the complete description of the type material. The only contradiction noted in that study concerns the short M2 mesoloph, which was considered originally as long. Type specimen measurements are recorded in Table 10.2. Morphology and size of the new Yushe specimens match these, and a maxilla with M1 (V11326) was recovered from the area described by Young (1927) at our site YS161 (0.5 km south of Jiayucun). Given the limited local outcrop we consider YS161 as the Type Locality for this species (Table 10.2 and Fig. 10.2).

Controversy has surrounded the status of *Kowalskia* Fahlbusch, 1969, *Neocricetodon* Kretzoi, 1930, and *Neocricetodon* Schaub, 1934. Schaub (1930) discussed the Yushe *Cricetulus grangeri,* and Kadic and Kretzoi (1930: 49) published cricetids from Csáckvár, Hungary, in the same year, erecting *Neocricetodon schaubi,* but unfortunately without any description or figure. Schaub redescribed *Cricetulus grangeri* from Yushe in detail in 1934 and at that time created for the species his new genus also named *Neocricetodon.* According to the International Commission on Zoological Nomenclature (1999), Kretzoi's genus should be regarded as *nomen nudum* while Schaub's name is a *nomen validum* or *nomen usuale*. Fahlbusch (1969) later published cricetids from the Pliocene of Poland and erected the genus *Kowalskia*, but was unaware of *Neocricetodon* in Hungary and China and hence made no comparison to either. Workers currently recognize these three genera published diachronously as being extremely similar in morphology, but as to nomenclature, consider that *Neocricetodon* Schaub, 1934 holds priority over *Neocricetodon* Kretzoi, 1930.

Freudenthal and Kordos (1989) regard Kretzoi's genus as *nomen nudum* because he neglected to provide a description. However they acknowledge that a description is provided in Kretzoi (1954) and that his hypodigm exists in the Hungarian Institute of Geology, and these are eligible for establishment of a *nomen validum*. They concurrently recognized synonymy with *Kowalskia* and hence, under the International Code of Nomenclature, the latter was considered as junior synonym. Kretzoi (1978: 355) himself also considered *Kowalskia* as synonym of *Neocricetodon* by his notation *Neocricetodon* ("*Kowalskia*") *schaubi* ssp.

We agree that Schaub retains priority based upon his detailed descriptions and plates despite Kretzoi's (1954) description.

The question of synonymy of *Neocricetodon* and *Kowalskia* has lingered. Freudenthal et al. (1998) promoted the viewpoint that *Neocricetodon* Schaub, 1934 is the senior synonym of *Kowalskia* Fahlbusch, 1969. Daxner Höck et al. (1996) had addressed the problem by provisionally retaining both genera and awaiting further data prior to final conclusions, largely because the several features noted earlier demonstrate considerable variation for a single genus. De Bruijn et al. (2012) endorsed the Freudenthal et al. (1998) conclusion that *Kowalskia* is a junior synonym of *Neocricetodon* Schaub, 1934. Most recently, Sinitsa and Delinschi (2016) published an analysis of nearly twenty species of hamster and found *N. grangeri* to be embedded well within

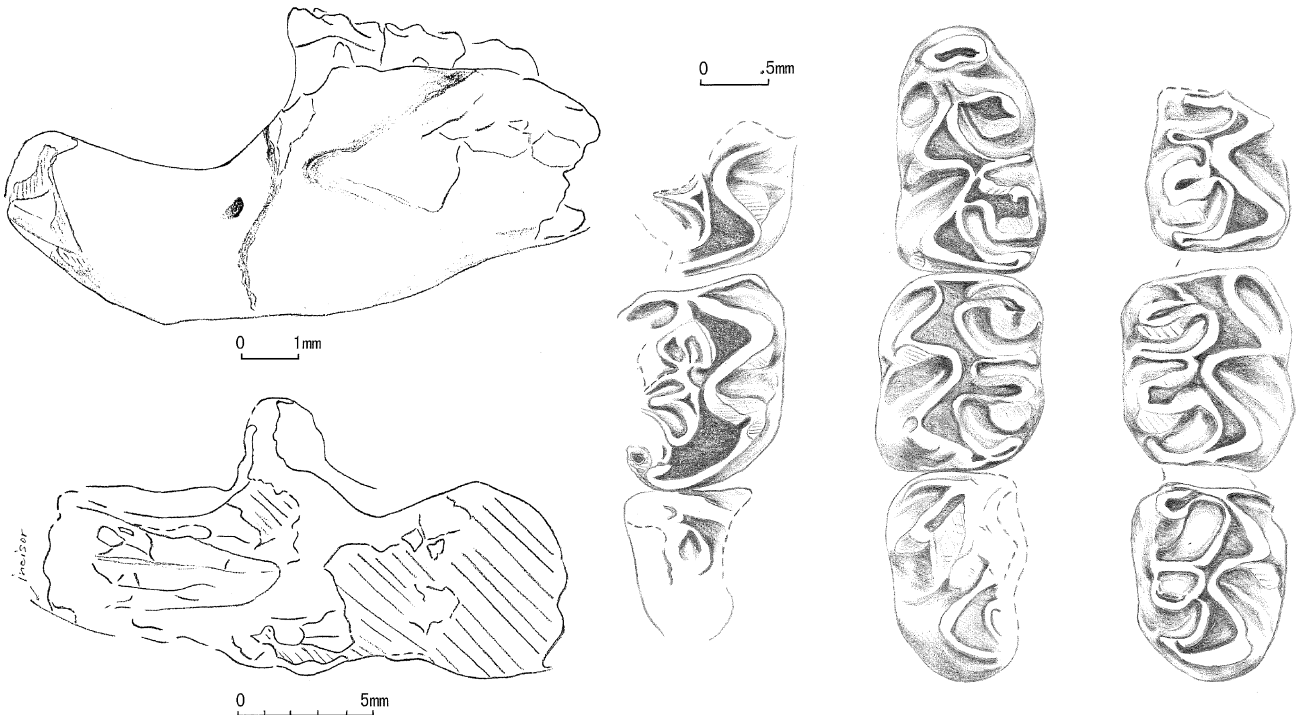

Fig. 10.2 Original line drawings by W.-Y. Wu of the *Neocricetodon grangeri* holotype housed at Uppsala University. Left ramus in lateral view and dorsal view of incomplete cranium to left; on the right are the damaged right maxillary dentition, left m1–m3, and right m1 (broken) followed by m2–3 (anterior upward)

Table 10.2 Dental measurements for the type of *Neocricetodon grangeri* (Chia yu Tsun, Yu She 173)

Lm1	1.80 × 1.10	Rm1	– × 1.05
Lm2	1.45 × 1.25	Rm2	1.50 × 1.23
Lm3	1.40 × ~1.10	Rm3	1.40 × 1.15
RM2	1.50 × ~1.25		

an array of fourteen species of *Neocricetodon*. Discovery of cranial and mandibular material of both genera would provide a comparative basis for definitive resolution of the question of synonymy.

Cricetinus Zdansky, 1928

Cricetinus mesolophidos sp. nov.

Type: Left m1 (V9885.1), 2.39 × 1.37 mm.

Paratypes: V9885.2-6: left M2 (1.90 × 1.65 mm), left M3, and fragmentary m1, M2, and m3 from the type locality YS97.

Type Locality and age: YS97, early Pliocene Culiugou Member, Gaozhuang Fm., 4.3 Ma.

Etymology: Species adjective is based on the lower molar crest, the mesolophid, plus the Greek masculine suffix, "*os*".

Diagnosis: A large hamster, close in size to Chinese Pleistocene *Cricetinus varians,* but with an elongate, well-developed mesolophid reaching the lingual tooth margin on the lower molars; upper molars are broad, their cusps nearly opposite in position, including the large double anterocone on M1; anteroconid is bifid on m1, a cingulum encloses labial sinusids, and the posterolophid encloses a large posterior lake.

Referred material: V9884.1-12: four M1, M2, two M3, two m1, two m2, m3 from YS50; V9886.1-22: six M1, two M2, three M3, three m1, three m2, four m3, and an incomplete right mandible with heavily worn and damaged m2-3 from YS4; V9887.1-2: damaged M3 and m3 from YS90; V9888.1-5: two M1, M3, m1, m2 from YS87; V9883: worn and fragmentary right maxilla with M1-2 from YS59 (Fig. 10.3; Table 10.3).

Stratigraphic range: Pliocene Gaozhuang and Mazegou formations, about 4.7 to 3.3 Ma.

Differential diagnosis: *Cricetinus mesolophidos* sp. nov. is about the same size as *Cricetinus varians* Zdansky, 1928 (Pleistocene of China) and *Cricetinus europaeus* Kretzoi, 1959 (Csarnóta, Hungary), but both of the latter lack the m1 mesolophid. Also the m1 of *C. europaeus* is a short tooth relative to the other lower molars. *C. janossyi* Hir, 1996 has a short mesolophid, but is larger. *C. beremendensis* Hir, 1994, Pliocene of Hungary, is smaller, has

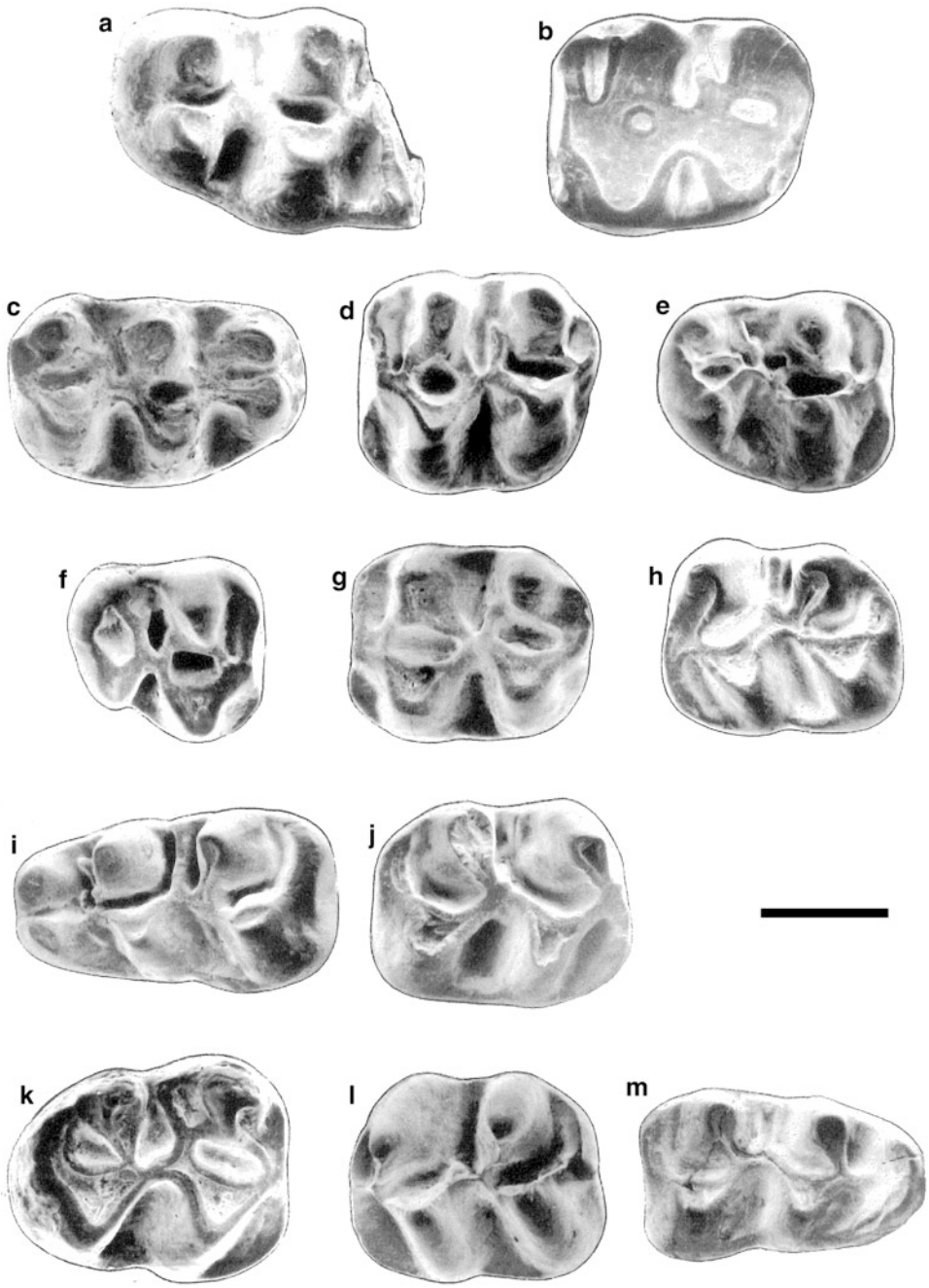

Fig. 10.3 SEM images for the Yuncu subbasin hamster *Cricetinus mesolophidos* sp. nov, scale bar = 1 mm. **a** left M1 V9888.1 from YS87, Mazegou Formation; **b** paratype left M2 V9885.2 from YS97, Gaozhuang Formation; **c–e** right M1 V9886.3, left M2 V9886.7, right M3, V9886.9 from YS4, Gaozhuang Formation; **f–h** right M3 V9884.7, left M2 V9884.5, left m2 V9884.10 from YS50, Gaozhuang Formation; **i**, holotype left m1 V9885.1 from YS97, Gaozhuang Formation; **j** right m2 V9888.5 from YS87, Mazegou Formation; **k–m** right m3 V9884.12, left m2 V9884.11, right m1 V9884.8 from YS50, Gaozhuang Formation. Scale bar, 1 mm

m1 with a weakly divided anteroconid on m1, and no mesolophid. *Cricetinus mesolophidos* resembles superficially some large cricetines, such as *Kowalskia yinanensis* Zheng, 1984b, Pliocene of Yinan, Shandong, which has similar lower molar morphology; principal distinctions of *K. yinanensis* include long mesolophs that completely cross M1 and M2, and a well-developed lingual anterolophid on m2.

Description: The slightly worn m1 of the holotype (V9885.1) has robust and rounded cusps and crests. The anteroconid is broad and bisected by a groove which is deeper posteriorly than anteriorly. The labial anteroconid is

Table 10.3 Dental measurements for *Cricetinus mesolophidos* sp. nov. (mm)

	Length			Width	
	Range	$\bar{x}$	n	Range	$\bar{x}$
M1	2.22–2.49	2.32	6/8	1.42–1.55	1.52
M2	1.57–1.90	1.80	6/4	1.47–1.65	1.56
M3	1.34–1.72	1.56	7/5	1.26–1.48	1.36
m1	2.10–2.39	2.23	7/6	1.26–1.39	1.35
m2	1.77–2.00	1.90	6/7	1.44–1.62	1.53
m3	1.71–2.10	1.90	6/6	1.27–1.66	1.43

connected to the anterior arm of the protoconid by a short anterolophulid, and a crest extends anterolingually from the metalophid to terminate at the posterolingual wall of the lingual anteroconid; homology of this crest as a "lingual spur of the anterolophulid" is questionable since it is not seen on other m1. The mesolophid is extremely well developed and extends to the lingual margin of the tooth. The posterosinusid is lingually enclosed by the lingual end of the posterolophid. Labially, the sinusid and protosinusid are enclosed by a low cingulum.

The paratype M2 (V9885.2) is well worn but displays a robust labial anteroloph that extends to the labial margin from the anterior arm of the protocone. The lingual anteroloph is low, but extends to the lingual side of the tooth. Labial cusps oppose the lingual cusps but lie slightly posterior to the lingual cusps. Lingual and labial sinuses are nearly perpendicular to the long axis of the tooth. The sinus is blocked by a low cingulum lingually, while protolophule I and II, metalophule I and II are equivalently developed and form deep fossae together with the protocone and hypocone respectively. The fossae form enamel islets after deep wear. A mesoloph extends half way across the tooth and posteriorly connects to the anterolingual side of the metacone. Referred M2 specimens resemble V9885.2 and have robustly rounded cusps and four roots.

M1 specimens are broad and short in outline with robust and rounded cusps and crests. Lingual and labial cusps are only slightly staggered, sinuses are perpendicular to the long axis of the tooth, and anterocone is relatively broad and bisected by a groove into two equal-size cusps. The lingual anterocone is connected to the anterior arm of the protocone by a rather robust anterolophule, while the labial anterocone is connected to the labial side of the anterolophule by a weak crest. Protolophule I and protolophule II are well developed on five out of seven specimens. Of 13 M1, 12 have a short mesoloph that cannot be distinguished from metalophule I. The exception is one heavily worn specimen (YS50: V9884.4) with isolated labial anterocone, a low and weak labial spur of the anterolophule that extends to the labial margin of the tooth, and a relatively long, free mesoloph. First molars also have a metalophule II and four roots.

The best preserved M3 (YS50, V9884.7) resembles M2 morphologically, but it narrows posteriorly. The metacone and hypocone are small but well-developed, and metalophule II is absent.

The m1 anteroconid of referred specimens is posteriorly bifid to varying degrees. An anterolophulid is present on four specimens. On three this crest extends from the labial anteroconid to the anterior arm of the protoconid, but on one specimen it extends from between the two anteroconids to the anterior arm of the protoconid. Two additional specimens display paired anterolophulids extending from both the lingual and labial anteroconids to connect with the anterior arm of the protoconid in addition to intersecting the metalophid. Mesolophids are low and all extend to the lingual margin of the tooth. The posterosinusid is enclosed on all specimens.

All well-preserved m2 specimens have an undeveloped lingual anterolophid, in addition to a well developed labial anterolophid. Nearly all specimens have a mesolophid that extends to the lingual margin, but in one specimen (YS87: V9888.5; Fig. 10.3j) this crest is weak and discontinuous. The posterosinusid is large and enclosed. One unworn specimen (YS50: V9884.11; Fig. 10.3l) with a short lingual anterolophid and an abbreviated mesolophid that extends to the posterolabial side of the metaconid is included with reservation in this species.

The m3 is large (similar average length as m2), and its structures resemble those of m2 although the tooth narrows posteriorly. A strong posterolophid sweeps lingually from the large hypoconid toward the reduced entoconid. Consequently the enclosed posterior sinusid is smaller than that of m2.

Discussion: *Cricetinus mesolophidos* sp. nov. is a distinctive early member of the genus, and helps to characterize the early Pliocene small mammal fauna of North China. Zheng and Zhang (2000, 2001) found fossils representing this species in Pliocene deposits of Gansu Province. They compared the fossils to the Yushe sample, using manuscript name *Cricetinus mesolophidus* [sic] which is *nomen nudum*. The correct name, *Cricetinus mesolophidos*, applies to the Gansu fossils.

The Yushe species is consistent in size and general morphology with the younger *Cricetinus varians* (Zheng 1984a, his Table 4) with robust, bulbous cusps and sinuses that are nearly perpendicular to the long axis of the tooth. Upper molar similarities are very close. Both species have M1 anterocones that are split posteriorly with the labial anterocone being connected to the anterolophule by a ridge. A protolophule I and a well developed metalophule II are always present on M1 and M2. On the M2, the lingual anteroloph is well developed. M3 is short and attenuates posteriorly. Dentition lengths also resemble *C. varians* with M3 shorter than M2, and m3 nearly equivalent to m2. Lower

molar morphology and length differ, however, and the extremely elongated mesolophid terminates at the lingual margin on the vast majority of specimens. On *C. varians* m1, the mesolophid is short or lost, while it is retained as a partial to complete crest on m2 and m3.

Of the referred material, the maxilla with M1-2 from YS59 (V9883), the incomplete mandible from YS4 (V9886.22) and M1s from YS50 (V9884.2), YS87 (V9888.3), and two from YS4 (V9886.2 & 5) are provisionally assigned to this species. The molars of the right maxilla from YS59 (V9883) are extremely worn such that the occlusal surface morphology is difficult to distinguish and inclusion in the species is based solely on size. It is even possible that this specimen is not a fossil. The incomplete mandible from YS4 is relatively close to *C. varians* both in size and morphology; it has a weak masseteric crest that terminates beneath the anterior root of m1, its masseteric fossa is slightly depressed, and a mental foramen is located ventral to the m1 anterior root. The M1s are all worn or incomplete, but the anterocones are quite large, so they are assigned tentatively to *Cricetinus mesolophidos*.

Because the YS59 maxilla, low in the Taoyang Member of the Gaozhuang Fm., may be Recent it should not be taken as the earliest stratigraphic record of the genus, and instead the YS50 specimen in the Nanzhuanggou Member has that status. Records of this taxon occur also at YS87 in the Mazegou Fm. *Cricetinus mesolophidos* age is Pliocene, generally equivalent to the European mammal zones MN14-16, and its youngest occurrence is one million years earlier than *Cricetinus varians* from Locality 9 of Zhoukoudian.

Allocricetus Schaub, 1930

Allocricetus primitivus sp. nov.

Type: Incomplete left maxilla with M1-2 (V9895.1); size of M1: 2.00 × 1.23, M2: 1.53 × 1.25 mm (Fig. 10.4d–h; Table 10.4).

Paratypes: three M1, three M2, two m1, m2, m3, and four fragmentary mandibles with m1-2, m1-3, m2-3, several of which are damaged (V9895.2-15).

Type Locality, age: YS4, Culiugou Member, Gaozhuang Fm., Yuncu subbasin, 4.3 Ma.

Etymology: From the Latin *primitivus*, being an early species of the genus.

Species diagnosis: A primitive *Allocricetus* with relatively narrow anterocones and anteroconids; anterocones doubled; distinctive x-pattern on M2 and posterior of M1 formed by the four principal cusps connected through the entoloph; anteroconids weakly bifid anteriorly with a slight sulcus dividing them; M1 anterocone with extremely low and weak posterior crests from both halves; M1 and M2 with metalophule I stronger than metalophule II; mesolophid absent or short on m1, more frequent on m2, well developed on m3. The m3 is large, on one paratype only 4% shorter than m2.

Table 10.4 Dental measurements for *Allocricetus primitivus* sp. nov. (mm)

	Length			Width	
	Range	$\bar{x}$	n	Range	$\bar{x}$
M1	1.81–2.00	1.87	6/6	1.15–1.23	1.21
M2	1.37–1.53	1.48	5/5	1.25–1.37	1.28
M3		1.03	1/1		1.03
m1	1.61–1.86	1.76	8/8	1.07–1.14	1.11
m2	1.22–1.51	1.40	6/6	1.00–1.22	1.16
m3	1.28–1.46	1.35	5/5	1.07–1.17	1.10

Differential diagnosis: *Allocricetus primitivus* differs from other *Allocricetus* species in the less strongly bifurcated anterocones and anteroconids. The anterolophules running posteriorly from the two parts of the anterocone are low and poorly defined. The lower last molar is not reduced in size relative to the second molar. About equal in size to *A. bursae* Schaub, 1930, the species smaller than *A. ehiki* Schaub, 1930, and about two thirds the size of *A. teilhardi* Zheng, 1984a.

Referred material: YS39: m1, m3 (V9890.1-2); YS50: m1, m2 (possibly incorrectly assigned) (V9892.1-2); YS44: m1, a fragmentary left mandible with m2-3 (V9892.1-2); YS97: M1, m1, m3 (V9893.1-3); YS43: fragmentary right maxilla with M1-3 (V9894).

Age range: Early Pliocene, Nanzhuanggou and Culiugou members, Gaozhuang Formation, about 4.7 to 4.3 Ma.

Description: The holotype consists of an incomplete left maxilla with incisive foramina that terminate slightly posterior to the anterior margin of the anterior root of M1. Molars are rather worn. The M1 anterocones are close and are bifid only anteriorly. Crests extend from both anterocones and represent a doubled anterolophule. Both of the crests are low, weak, and closely spaced. Protolophule I is extremely weak while protolophule II is well developed. Metalophule I is well developed and linked to the anterior arm of the hypocone. Despite wear the metalophule II is discernible as a short, low crest running to the posterior cingulum. A conspicuous "x" configuration is composed of the four principal cusps joined at the relatively long entoloph. Labial cusps are placed slightly posterior to lingual cusps and form distinct parallel crests and sinuses that are slightly oblique to the longitudinal axis of the tooth. All labial and lingual cusps are rather widely spaced, and in the absence of a mesoloph, the transverse valley (sinus) is rather broad). Other first molars from YS4 are either deeply worn or damaged, but morphologically they resemble the holotype in that the anterocones are all closely situated, the lingual anterocone being somewhat smaller. On two of three specimens the buccal anterocone is isolated or connected to the anterolophule by a very weak crest, and protolophule I is absent or very weak.

The M2 has well developed labial and lingual anterolophs though the former is higher than the latter, and both are at a right angle to the anterior arm of the protocone. Protolophules I and II and metalophule I on M2 are very well developed, and metalophule II is distinct but less developed. Thus the M2 has a morphology that is consistent with the posterior portion of M1. M1 and M2 both have four roots.

Mandible V9895.8 is rather completely preserved with a shallow masseteric fossa, and a masseteric crest that terminates posteroventral to the anterior root of the m1. The ramus is 3.5 mm deep at the level of the m1 anterior root. A mental foramen is just anteroventral to the anterior root of the m1. Four specimens of m1 are present from the type locality YS4. The anteroconid is wide, slightly bifid, the two anteroconids are closely appressed. All have only a single anterolophulid that extends from the anterior arm of the protoconid to the labial anteroconid. The mesolophid is absent on two specimens and the other two specimens have a very short mesolophid that leans against the base of the posterolabial wall of the metaconid. The posterolophid descends low so that the posterosinusid is open lingually. Specimens from YS50 and YS39, older than the type series, are morphologically similar, but the anteroconids on m1 are more weakly divided.

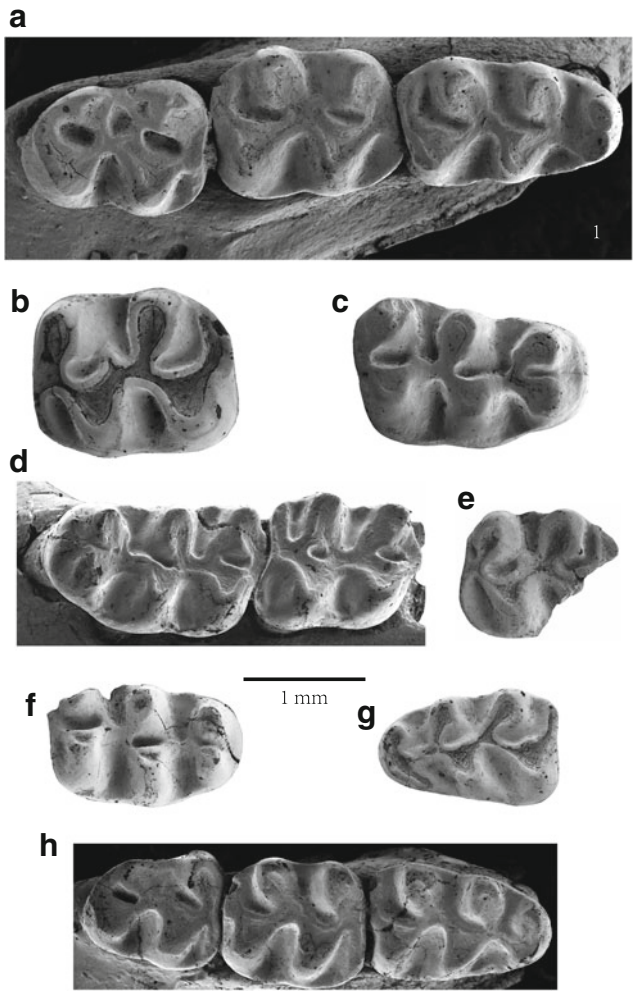

Fig. 10.4 SEM images for Yuncu subbasin *Allocricetus*. *Allocricetus* cf. *A. ehiki* , **a**–**c**; **a** right m1-3 V9921 from YS111, **b** left m2 V9926 from YS5, **c** right M1 V9920.1 from YS87, all Mazegou Formation. *Allocricetus primitivus* sp. nov., **d**–**h**; holotype left M1-2 V9895.1, left m2 V9895.14, right M1 V9895.4, left m1 V9895.12, right m1-3 V9895.10, all from YS4, Gaozhuang Formation. Scale bar = 1 mm

All five m2 are worn. The labial anterolophid is well developed and extends to the labial side of the protoconid while a lingual anterolophid is short and merges with the metaconid short of the lingual tooth margin. On three specimens the lingual anterolophid is moderately long (shorter on the other), and three of four m2 have a short mesolophid that extends toward the posterior wall of the metaconid (the fourth lacks a mesolophid). On two of three specimens, the posterosinusid is enclosed lingually by the posterolophid but on the other it is open.

V9895.10 shows the large but posteriorly reduced m3 relative to m2. As in this specimen an unworn but fragmentary m3 (V9895.15) displays well-developed lingual and labial anterolophids, a mesolophid that extends directly to the slightly reduced entoconid, and a posterosinusid enclosed lingually by the posterolophid. A distinct cingulum blocking the labial sinusid is present on most m3.

Specimens from YS43, 97, and 44, which are stratigraphically equivalent to the type locality YS4, are morphologically similar to YS4 specimens, but show some variation. The right maxilla with M1-3 (V9894) from YS43 has the posterior margin of the incisive foramen at the level of the anterior margin of the anterior root of M1. M1 and M2 are morphologically identical to those of the holotype. The M3 of V9894, although damaged, preserves morphology that resembles M2, but is slightly shorter and is narrower posteriorly. The M1 from YS97 (V9893.1) is extremely worn, lacks a protolophule I, and has four roots. The m1 (V9893.2) anteroconids are slightly open posteriorly but the two cusps are joined at the base. The m3 (V9893.3) lacks both lingual anterolophid and connection from protoconid to entoconid. The mandible from YS44 (V9892) is damaged but is slightly more robust than that from YS4 and its masseteric crest curves anterodorsally. Its m2 and m3 have relatively long lingual anterolophids, the m2 lacks a mesolophid, and m3 has a mesolophid that extends nearly to the lingual cingulum.

Discussion: The Yushe material, while limited, includes a partial maxilla, four mandibles and ten isolated teeth (some of which are incomplete). The teeth are brachydont with bifid first molar anterocones and anteroconids, a distinct "x" configuration composed of the four principal cusps connected by a relatively long entoloph on upper molars, occasional presence of a short mesolophid on m1 and m2, usually well developed on m3, and m3 nearly as long as m2.

These characters are consistent with those for *Allocricetus* as described by Schaub (1930), Fahlbusch (1969), and Fejfar

(1970). *Allocricetus primitivus* is similar in size to the younger *A. bursae* from Rębielice, Kadzielnia, and Kamyk, Poland (Fahlbusch 1969). The Yushe specimens are distinctly more primitive in their lesser degree of bifurcation of anterocones and anteroconids on M1 and m1. The anterocone of M1 is narrow with weak and low lingual and labial anterolophules; these crests running posterior from the anterocones are equivalent and have a small sinus between them. The m1s from the stratigraphically low YS39 and YS50 have particularly poorly bifid anteroconids, which is consistent with a concept of early Pliocene acquisition of the double anterocones (-ids) in this genus. The new species *A. primitivus* represents this early stage in *Allocricetus* evolution.

Allocricetus was erected by Schaub (1930) in his study of cricetids from Siebenbürgen (present Romania, a part of Hungary before 1918). Cranial morphology approaches that of *Cricetus,* dental morphology is typical of *Cricetulus*, but limb morphology is unlike either. Its size approaches *Mesocricetus,* but the dentition (incisor and molars) and the zygomatic arches are unlike the latter. After the study by Schaub, new European collections were principally isolated teeth (Fahlbusch 1969, Fejfar 1970) with time range spanning the mid-Pliocene to early Pleistocene, MN15-17. Paunovic and Rabeder (1996) named the early Pleistocene *Allocricetus croaticus* from southern Croatia. Of a size intermediate between *A. ehiki* and *A. bursae*, it is somewhat larger than *Allocricetus primitivus*. This species is derived in its broad anterocones and anteroconids and its reduced m3. Bate (1943), Haas (1966), and Tchernov (1968) assigned populations from the Pleistocene of Israel to this genus. Daxner-Höck (1995, MN13/14) and Rummel (1998, MN11 or 12-13) reported older *Allocricetus* from the late Miocene and early Pliocene of the Mediterranean region, and Kälin (1999) accepted latest Miocene fossils (MN13) as early *Allocricetus*. Ünay et al. (2006) recognized early late Miocene *Allocricetus aylasevimae* from Anatolia. This species is about the size of *A. primitivus*, has broader and more distinct anterocones, and its cusps are more alternating in position.

In China, Zheng (1984a) transferred specimens previously considered *Cricetinus* or *Cricetulus varians* from Zhoukoudian localities 12 and 18 (including cranial, mandible, and dental specimens) to *Allocricetus ehiki,* and erected *Allocricetus teilhardi* for some large skulls, maxillae and mandibles from Zhoukoudian localities 9 and 13 formerly identified as *Cricetinus varians*. He also reassigned *Cricetinus varians* from Xichawan (Chi 1975) and Gongwangling (Hu and Qi 1978), both Shaanxi Province, to *Allocricetus teilhardi*. Additional reports of *Allocricetus* were made for Chinese Pliocene fossils from Daodi (Cai 1987), Jingle (Zhou 1988), Dali (Wang 1988), Lingtai (Zheng and Zhang 2000, 2001) and Yushe (Flynn et al. 1997). Based on these records, the temporal distribution of the genus in China spans the early Pliocene to early middle Pleistocene. As the majority of the Yushe Basin fossils are dentitions and isolated teeth, taxonomic identification was made solely upon dental morphology and size. In fact it is extremely difficult to differentiate the isolated teeth of *Allocricetus* from those of *Cricetulus*. Isolated teeth of *Nannocricetus* also may be confused with *Allocricetus*, but almost all *Allocricetus* m3 and some m2 possess a mesolophid, whereas no mesolophid exists on m2-3 of *Nannocricetus*.

In her comprehensive review of hamster phylogeny, Cuenca Bescós (2003) found *Allocricetus* to be paraphyletic, similar hamster populations having been assigned to the genus, erroneously in some cases. From the viewpoint of China, we see *Allocricetus primitivus* at the early Pliocene base of an endemic group of *Allocricetus* that thrived and continued as Pleistocene *A. teilhardi*.

Allocricetus cf. A. ehiki Schaub, 1930

Material and localities: YS87: right M1 (length × width = 2.10 × 1.33 mm) and a damaged and heavily worn right M3 (V9920.1-2); YS111: right mandible with moderately worn m1-3 (V9921); YS5: left m2 (V9926); damaged right m3 (V9919). Figure 10.4a–c.

Stratigraphy and age range: Late Pliocene Mazegou Formation, about 3.4 to 3.3 Ma.

Description: The anterocone of M1 is strongly bifid with a slightly concave anterior wall. A well-developed posterior crest of the labial anterocone connects posteriorly with the anterolophule, forming a well-developed anteriorly-open sinus. Protolophule I is absent but protolophule II, metalophules I and II are distinct, and there is a relatively long entoloph. The M3 is deeply worn but is narrow posteriorly, longer than wide. Its protolophules I, II and metalophules I, II all are well-developed.

Mandible V9921 from YS111 has a slightly concave masseteric fossa and well-developed masseteric crest that terminates between the m1 anterior and posterior roots. A mental foramen is located anteroventral to the m1 anterior root. The length of m1-3 is 5.7 mm, and teeth measure respectively: m1: 2.10 × 1.22, m2: 1.80 × 1.46, m3: 1.85 × 1.30 mm. The m1 is narrow and long, anteroconid is bifid, a mesolophid is absent, and the anterolophulid is low, extending from the posterior side of the labial anteroconid to the anterior arm of the protoconid. The posterosinusid is open lingually but the lingual base of the posterolophid is slightly expanded. The m2 is also narrow and long, has a well-developed labial anterolophid, and the lingual anterolophid merges with the metaconid short of the labial tooth margin. The protosinusid is low and wide, and a short structure that we consider a mesolophid intersects the posterolabial wall of the metaconid. The m3 is nearly equivalent in length to the m2, but narrower posteriorly, and has a

well-developed labial anterolophid although the lingual anterolophid appears to merge with the metaconid. A mesolophid extends to the metaconid. Posteriorly, the m3 narrows with a slight reduction of the hypoconid and much smaller entoconid. On both the m2 and m3 the posterolophid encloses the posterosinusid on the lingual side.

The YS5 m2 is moderately worn (1.90 × 1.58 mm), larger than the YS111 specimen, and has a very short mesolophid extending anteriorly to rest against the posterior wall of the metaconid. A well-developed labial anterolophid is present but the lingual anterolophid was short if one was present. The YS5 m3 is damaged posterolabially but a short lingual anterolophid can be recognized, and the posterior arm of the protoconid inclines posteriorly to intersect the developed entoconid. Morphology and size are comparable to *A. ehiki.*

Discussion: These specimens are generally consistent in size and morphology with Plio-Pleistocene *Allocricetus* from Europe, although the anteroconids of the m1 are narrower, which might be plesiomorphic due to the greater age of the strata whence the Yushe specimens were collected. Teeth are 20% larger than *Allocricetus primitivus*, close in size to European *A. ehiki,* and show a strongly bifurcated anterocone on M1 with strong anterolophules. The few specimens from the late Pliocene Mazegou Fm. are allocated as *Allocricetus* cf. *A. ehiki* since their firm identification or eventual diagnosis must await the recovery of new data to verify whether they represent immigrants from Europe or an endemic Chinese lineage.

Phodopus Miller, 1910

Phodopus sp.

Referred material and locality: YS120: left M2, 1.22 × 0.93; left m1, 1.32 × 0.78; right m2, 1.10 × 0.90 (V9925.1-3, Fig. 10.5a–c).

Stratigraphy and age: Early Pleistocene Haiyan Formation (>2.2 Ma).

Description: The teeth are narrow and long with labial cusps offset posteriorly to lingual cusps. The elongated m1 has a bifid anteroconid with cuspids that merge in early wear. The anterolophulid is low, and lies nearly on the midline of the tooth. Lophids and sinusids are parallel but oblique to the long axis of the tooth. The metalophid joins the protoconid anterior arm and the hypolophid joins the oblique ectolophid. A mesolophid is notis not detected, and cin detected, and cingula are all low. The subrectangular m2 has a long labial anterolophid that approaches the base of the protoconid; the lingual anterolophid is absent. A prominent, oblique metalophid joins the protoconid anterior arm and a parallel hypolophid joins the oblique ectolophid; the posterolophid descends lingually to terminate at the base of the entoconid. Mesolophid is absent as on m1. The posterosinusid is lingually open.

The M2 is a parallelogram in outline, with well-developed labial anteroloph and low lingual anteroloph. Protolophule I is absent, protolophule II runs posterolingually to connect to the posterior arm of the protocone/entoloph near the midline. Metalophule I descends anterolingually to join the entoloph at the anterior arm of the hypocone. Metalophule II is short and joins the posterior arm of the hypocone and posteroloph near the midline of the tooth in between. The posteroloph thins and descends labially. The deep sinus and mesosinus are both narrow, forming oblique valleys parallel to the anterior and posterior margins of the tooth, and dividing the tooth into anterior and posterior moieties.

Discussion: Size and morphology resemble *Phodopus* but with conspicuous distinction from the two living species in China, *P. roborovskii* and *P. sungorus*. Specimens housed at the Zoological Institute, Chinese Academy of Sciences, were studied and measured to determine that the Yushe m1 is smaller than the extant forms, while M2 and m2 are comparable in size to *P. sungorus*. Morphologically these teeth are distinct from both species. Extant species have a protolophule I on M2, which is absent on the Yushe specimens. Lower molars of *P. roborovskii* have a metalophulid II, which is absent on the Yushe m1 and m2 but like the condition in *P. sungorus.* Consequently the status of the Yushe specimens is presently indeterminate. The geographic range of extant *Phodopus* in North China includes Shanxi Province. The genus is recorded from Zhoukoudian Locality 3 (Zheng 1984a), but the Yushe record is older.

Cricetulus Milne-Edwards, 1867

Cricetulus sp.

Referred material and localities: YS5: left m3, 1.42 × 1.03 (V9916); YS87: left M1, 1.85 × 1.19 (V9917); YS103: right mandible with incisor, m1, 1.73 × 1.15 mm (V9918) (Fig. 10.5d–f).

Stratigraphy and age range: Late Pliocene Mazegou Formation, 3.4 to 3.2 Ma.

Description: The YS103 mandible is 4.15 mm high at the anterior root of m1. Incisor anteroposterior diameter is 1.44 mm and transverse width is 0.58 mm. The mandible is very close in morphology to the YS4 *Allocricetus primitivus* (V9895.8) mandible but is much larger. With occlusal wear the m1 anteroconid facet is kidney shaped but not strongly bifid. The anteroconid is single cusped but slightly asymmetrical, with a short anterolophulid directed posteriorly from slightly labial to the midline. Tooth cusps are all very slightly anteriorly inclined, a minute mesolophid may be discerned, and the lingual side of the ectolophid opposite the mesolophid is slightly convex. The YS87 left M1 anterocone is posteriorly bifid with the labial anterocone slightly larger than the lingual anterocone, both securely joined anteriorly. A low anteroloph is directed from the lingual anterocone

toward the anterior arm of the protocone. A less prominent crest joins the buccal anterocone to the protocone arm and a distinct sinus lies between the anterocones. Protolophule I is absent but a short protolophule II joins the posterior arm of the protocone near the midline. A short metalophule II joins the hypocone posterior arm near the midline and a low mesoloph extends buccally toward the anterior wall of the metacone. The midline entoloph is long, and the sinus and mesosinus are open and wide. The YS5 m3 lingual and buccal anterolophids are short, the protoconid is larger than the hypoconid and the slightly smaller metaconid, the entoconid is minute, and there is no mesolophid.

Discussion: These specimens are evidence of a hamster distinctly smaller than either *A.* cf. *A. ehiki* or *Cricetinus mesolophidos* of the same stratigraphic range. They represent a species of *Cricetulus* that differs from younger *Cricetulus* in the undeveloped anteroconid bifurcation of m1 and incompletely doubled anterocone on M1, and in the absence of a protolophule I on M1. They are characterized by the presence of a developed metalophule II on M1, and the absence of a mesolophid on lower molars, which indicate a primitive form of the genus.

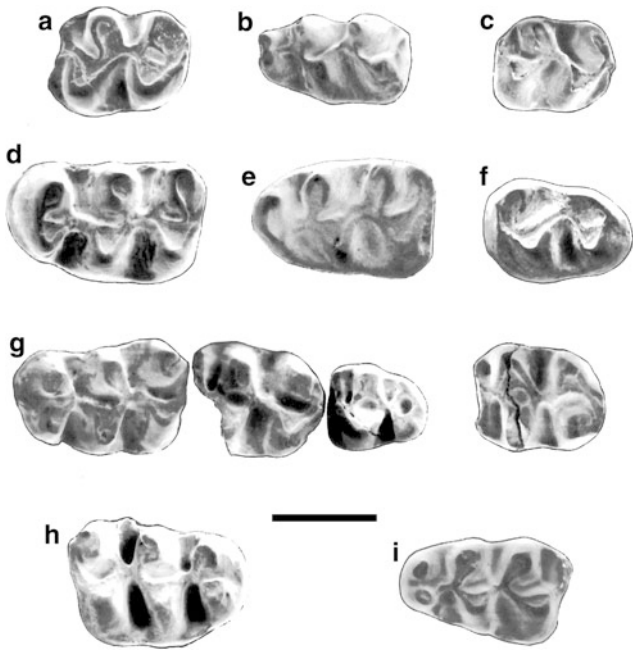

Fig. 10.5 SEM images of Late Pliocene – Pleistocene hamsters from Yuncu subbasin, *Phodopus* sp. and *Cricetulus* spp. *Phodopus* sp., **a–c** V9925.1-.3, left M2, left m1, right m2 from YS120, Haiyan Formation. *Cricetulus* sp., **d–f** V9917 (left M1), 9918 (left m1), 9916 (left m3) from Mazegou Formation. *Cricetulus barabensis obscurus,* **g** V9924, left M1-3 and right M2 on the right, from YS83. *Cricetulus barabensis*, **h–i** V9922.1 (right M1) and V9923.1 (left m1) from Haiyan Formation. Mesial is to the left for all but c and h. Scale bar = 1 mm

Cricetulus barabensis Pallas, 1773

Referred material and localities: YS120 right M1, 1.66 × 1.29 (V9922.1); damaged right m2, 1.08 mm wide (V9922.2); YS109: left m1, 1.54 × 1.01 and damaged right m1, 0.99 mm wide (V9923.1-2), and damaged right M1 (V9923.3).

Stratigraphy and age range: Early Pleistocene Haiyan Formation (>2.2 Ma).

Description: The YS109 m1 (Fig. 10.5i) is nearly unworn with a highly bifid anteroconid associated with a deep groove such that the lingual anteroconid is isolated; the labial anteroconid is linked to the anterior arm of the protoconid by a low anterolophulid. Metalophid I is well developed and joins the anterior arm of the protoconid. Metalophid II is low, directed toward the hypoconid and weakly joining the junction of the hypolophid and the short posterior arm of the protoconid. Hypolophid I is well developed, similar to metalophid I, and joins the hypoconid anterior arm near the midline; hypolophid II is very low, uniting the posterior entoconid and the posterior hypoconid only after deep wear. A mesolophid is absent. The posterolophid descends rapidly lingually, curving anteriorly toward the posterior entoconid and partially closing a broad and shallow posterosinusid.

The YS120 m2 is represented by a posterior fragment resembling the end of m1, but the posterolophid on V9922.2 is higher and curves toward the posterolingual base of the entoconid.

The YS120 M1 (V9922.1, Fig. 10.5h) is well preserved. It is short with moderately narrow anterior portion, although the anterocone is strongly bifid and invaded anteriorly by a shallow valley. Short lophs from the larger lingual and smaller labial anterocones join the anterior arm of the protocone near the midline. Protolophule II and metalophule I are well developed, while protolophule I and metalophule II are weak or absent. A posterior spur from the labial margin of the paracone descends and flares labially at the base of the cusp to partially close, but not constrict the labial mesosinus. The YS109 half M1 shares this morphology.

Size and morphology of these specimens are consistent with extant *Cricetulus barabensis* in the m1 anteroconid bifurcation, the isolation of the lingual anteroconid, and the anterolophulid that connects only the labial anteroconid to the anterior arm of the protoconid. They probably do not represent subspecies *C. b. obscurus* or *C. b. fumatus* due to the well developed M1 and M2 metalophule I, but may represent *C. b. xianganensis* Wang due to the strong m1 anteroconid bifurcation, although this subspecies does not occur in Shanxi Province today.

The current geographic range for *Cricetulus barabensis* in North China includes Shanxi Province. The Yushe record extends the species in time to the early Pleistocene.

Cricetulus barabensis obscurus (Milne-Edwards, 1867)

Material and locality: YS83, left M1-3 and right M2 from the same individual (V9924, Fig. 10.5g).

Stratigraphy and age estimate: late early Pleistocene Red Loess (correlated with the Wucheng Loess, probably ~1 Ma).

Description: Small in size as M1-3 length is 3.7 mm, M1: 1.66 × 1.15, M2: ~1.25 × 1.08, M3: 0.99 × 0.84, and right M2: 1.27 × 1.05. The M1 anterocone is strongly bifid with lingual cusp larger than labial cusp, and well-developed crests and anteriorly opened narrow valley between the anterocone cusps. Protolophule I and metalophule II are absent or weak; protolophule II is well developed and metalophule I is short, joining the hypocone after moderate wear. M2 lingual and labial anterolophs are well developed, though the lingual loph is low. Protolophules I and II are conspicuous, metalophule I is low, and metalophule II is variable. The M3, subtriangular in outline, is longer than wide, narrow posteriorly with a small hypocone and a minute metacone. The protocone is larger than the paracone, protolophules I, II are well-developed and metalophule I is short, but metalophule II is absent.

This fossil hamster from the red loess is very similar to its predecessor in the older Haiyan Formation. However, the morphology, particularly the reduction or absence of metalophule I on M1 and M2, suggests an affinity to *C. barabensis obscurus,* a subspecies that occurs in Shanxi today and at middle Pleistocene Zhoukoudian localities 13 and 1, and the Upper Cave (Zheng 1984a). This find extends the geographical range of the subspecies to the Yushe region in the late early Pleistocene.

?Nannocricetus sp.

Referred material and locality: YS132, early Pliocene, basal Nanzhuanggou Member, Gaozhuang Formation (4.8 Ma, Fig. 10.6): right mandible with m1-3 but lacking ascending ramus and angular process (V 9889). An isolated incisor may belong to this specimen.

Description: A small cricetid, the ramus is 2.83 mm deep at the lingual side beneath the two m1 roots and 2.10 mm at the lingual side from the posterior margin of m3 to the most concave portion of the ramus. Molar row length is 3.76 mm, m1: 1.51 × 0.88, m2: 1.22 × 0.97, m3: 1.12 × 0.83. Mandible morphology is typical of *Cricetulus* with a relatively weak masseteric crest that terminates ventral to the anterior root of m1 and with a shallow masseteric fossa. The long incisor is gracile, anteroposterior diameter and transverse width being 0.91 and 0.59 mm. This specimen resembles *Nannocricetus mongolicus* from the late Baodean (terminal Miocene) Ertemte fauna, Inner Mongolia, in absence of mesolophids, but it is smaller with gracile tooth cusps, and m1 is narrow, long, and not much broadened posteriorly. Among the Yushe cricetids it is larger than only *Phodopus.* Unlike *Phodopus,* the m1 anteroconid is not bifid, and the anterolophulid extends from the labial portion of the anteroconid toward the anterior arm of the protoconid and base of the metalophid. Zhang et al. (2008, 2011)

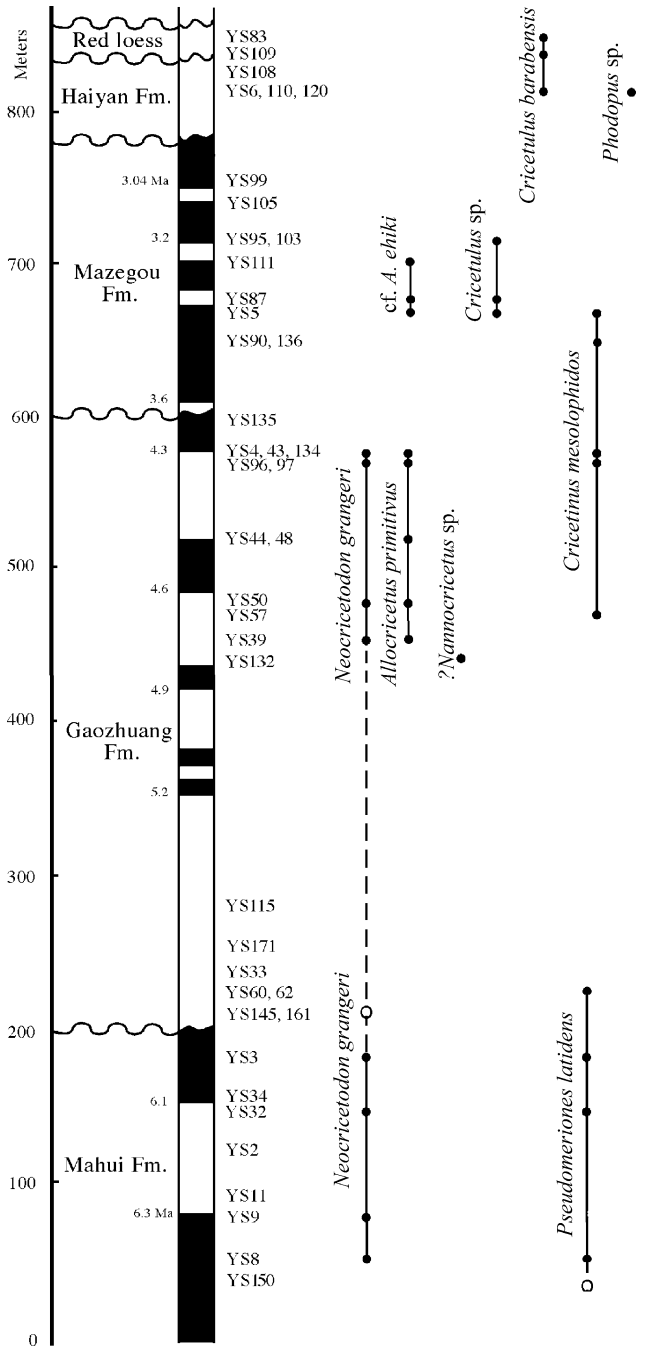

Fig. 10.6 Biostratigraphic distribution of hamsters and the gerbil *Pseudomeriones* in the Yushe Basin composite section, with magnetostratigraphic zonation to provide approximate dating. Points representing stratigraphic occurrences of single species are joined by solid lines; records of *Neocricetodon* are joined despite a long hiatus in occurrences (dashed line) of one million years. Tancun subbasin *Neocricetodon* and *Pseudomeriones* occurrences are shown by open circle

described primitive and older Miocene species of *Nannocricetus* in Tunggurian and early Baodean assemblages.

Cricitinae gen. et sp. indet. 1

A left mandible with m1-3 (V11331) from YS170, late Miocene Mahui Fm., cannot be identified due to its great occlusal wear. V11331 has a long m1 with an anterior root that extends obliquely anteriorly, a bifid but narrow anteroconid that is worn more lightly than posterior principal cusps, and no mesolophid. Dentition length is 4.19 mm, m1: 1.56 × 0.89, m2: 1.37 × 1.08, m3: 1.22 × 1.02, small for *Neocricetodon grangeri*. Size and morphology indicate it may represent *Nannocricetus mongolicus.*

Cricitinae gen. et sp. indet. 2

A right mandible (V11330) from YS155, late Miocene Mahui Fm. is small and fragmentary, with m1-3, broken incisor, and disassociated angular and articular processes. This specimen has a short m1 with an anterior root that extends directly ventrally. Anteroconid is narrow and slightly bifid, and all molars possess mesolophids, although their lengths cannot be determined, except in m3 where it extends to the lingual side. Dentition length is 3.70 mm, m1: 1.42 × 0.93, m2: 1.19 × 1.02, and m3 1.07 × 0.93. It is too small to be *Neocricetodon grangeri.*

10.3 Summary

Fossil hamsters collected from the Yushe Basin are neither abundant nor well preserved. Specimens are derived predominantly from the Yuncu subbasin, where they occur in every major rock unit (Fig. 10.6), supplemented by material from the Tancun subbasin. Their discovery is significant for basin biostratigraphic subdivision and correlation, and for the temporal and geographical distribution of several Late Neogene taxa. Following are the principle conclusions.

1. *Cricetinus mesolophidos* predates Chinese *C. varians*, and is more primitive in several features. Although it is uncertain that *Cricetinus mesolophidos* is a direct ancestor of *C. varians*, relationship of the two species appears to be close.

2. *Allocricetus primitivus* displays primitive characters of weak anterocone and anteroconid bifurcation and low posterior connections from these. Found in early Pliocene deposits, it is currently the oldest record of the genus in China, and it predates the late Pliocene European *A. ehiki*. Sparse remains of younger *Allocricetus* similar to *A. ehiki* from the late Pliocene of Yushe Basin may indicate endemic evolution of the genus in China.

3. Three specimens assigned as *Cricetulus* sp. display slightly bifurcated anterocones and anteroconids and a well-developed metalophule II, and represent a late Pliocene record of the genus in the Mazegou Formation of Yushe Basin. These characters are primitive relative to any extant *Cricetulus*.

4. The occurrences of *Cricetulus barabensis* and *Phodopus* sp. in the Haiyan Formation constitute their first appearances in the early Pleistocene. The former taxon is identical in size and morphology to the extant species and the latter is smaller than, but similar in morphology to extant *Phodopus*. A still younger hamster from the red loess with strongly bilobed anterocone on M1 appears identical with the living subspecies *Cricetulus barabensis obscurus*.

5. The *Neocricetodon grangeri* occurrences in the Yuncu subbasin are restricted to the Mahui and upper Gaozhuang formations, including a temporal hiatus of about one million years between occurrences. This hiatus probably reflects low fossil productivity in the Taoyang Member of the Gaozhuang Formation. However, in the Tancun subbasin the species occurs in both the Mahui and basal Gaozhuang formations, and partly fills the gap (open circle in Fig. 10.6). YS161 near the village of Jiayucun in the Tancun subbasin represents the Type Locality. *Neocricetodon grangeri* differs from other Eurasian species assigned to *Kowalskia,* but current studies demonstrate a morphological breadth for *Neocricetodon* that encompasses *Kowalskia*, consistent with seniority of *Neocricetodon* as the genus name for these widespread hamsters.

Acknowledgements Gratitude is expressed to Dr. Solweig Stuenes of the Paleontological Museum of Uppsala University for her generous assistance in allowing W.-Y. Wu the opportunity to study the holotype of *Neocricetodon grangeri*. Staff of the Zoological Institute, Chinese Academy of Sciences, kindly enabled our comparisons with extant hamsters. The careful reviews of Everett Lindsay, Hans de Bruijn, and Jon Baskin led to significant improvements of the manuscript.

References

Bate, D. M. A. (1943). Pleistocene Cricetinae from Palestine. *Annals and Magazine of Natural History, 11,* 813–838.

Cai, B.-Q. (1987). A preliminary report on the Late Pliocene micromammalian fauna from Yangyuan and Yuxian, Hebei. *Vertebrata PalAsiatica, 25,* 124–136 (in Chinese with English summary).

Chi, H.-X. (1975). The Lower Pleistocene mammalian fossils of Lantian district, Shensi. *Vertebrata PalAsiatica, 13,* 169–177 (in Chinese with English summary).

Cunca Bescós, G. (2003). Análisis filogenético de *Allocricetus* del Pleistoceno (Cricetidae, Rodentia, Mammalia). *Coloquios de Paleontología, 1,* 95–113.

Daxner-Höck, G. (1995). The vertebrate locality Maramena (Macedonia, Greece) at the Turolian-Ruscinian boundary (Neogene), 9. Some glirids and cricetids from Maramena and other late Miocene localities in Northern Greece. *Münchner Geowissenschaftliche Abhandlungen, A, 28,* 103–120.

Daxner-Höck, G., Fahlbusch, V., Kordos, L., & Wu, W.-Y. (1996). The Late Neogene cricetid rodent genera *Neocricetodon* and *Kowalskia*.

In R. L. Bernor, V. Fahlbusch, & H. W. Mittmann (Eds.), *The evolution of western Eurasian Neogene mammal faunas* (pp. 220–226). New York: Columbia University Press.

de Bruijn, H., Doukas, C. D., van den Hoek Ostende, L. W., & Zachariasse, W. J. (2012). New finds of rodents and insectivores from the Upper Miocene at Plakias (Crete, Greece). *Swiss Journal of Palaeontology, 131,* 61–75.

Fahlbusch, V. (1969). Pliozäne und pleistozäne Cricetinae (Rodentia, Mammalia) aus Polen. *Acta Zoologica Cracoviensia, 14,* 99–138.

Fejfar, O. (1970). Die plio-pleistozänen Wirbeltierfaunen von Hajnácka und Ivanovcé (Slowakei, CSSR) VI. Cricetidae (Rodentia, Mammalia). *Bayerische Staatssammlung für Paläontologie und Histische Geologie, Mitteilungen, München, 10,* 277–296.

Flynn, L. J., Wu, W.-Y., & Downs, W. R. (1997). Dating vertebrate microfaunas in the late Neogene record of northern China. *Palaeogeography, Palaeoclimatology, Palaeoecology, 133,* 227–242.

Freudenthal, M., & Kordos, L. (1989). *Cricetus polgardiensis* sp. nov. and *Cricetus kormosi* Schaub, 1930 from the Late Miocene Polgardi localities (Hungary). *Scripta Geologica, 89,* 71–100.

Freudenthal, M., Mein, P., & Martin-Suarez, E. (1998). Revision of Late Miocene and Pliocene Cricetinae (Rodentia, Mammalia) from Spain and France. *Treballs del Museu de Geologia de Barcelona, 7,* 11–93.

Haas, G. (1966). *On the vertebrate fauna of the lower Pleistocene site 'Ubeidiya*. Jerusalem Central Press.

Hir, J. (1994). *Cricetinus beremendensis* sp. n. (Rodentia, Mammalia) from the Pliocene fauna of Beremend 15. (S Hungary). *Fragmenta Mineralogica et Palaeontologica, 17,* 71–89.

Hir, J. (1996). *Cricetinus janossyi* sp. n. (Rodentia, Mammalia) from the Pliocene fauna of Osztramos 7. (N Hungary). *Fragmenta Mineralogica et Palaeontologica, 18,* 79–90.

Hu, C.-K., & Qi, T. (1978). Gongwangling Pleistocene mammalian fauna of Lantian, Shaanxi. *Palaeontologia Sinica, new series C, 21,* 1–64.

International Commission on Zoological Nomenclature (1999). *International code of zoological nomenclature*. London: The International Trust for Zoological Nomenclature.

Kadic, O., & Kretzoi, M. (1930). Ergebnisse der weiteren Grabungen in der Esterházyhöhle (Csákvárer Höhlung). *Mitteilungen über Höhlen und Karstforschung. Zeitschrift des Hauptverbundes deutscher Höhlenforsche, 2,* 45–49.

Kälin, D. (1999). Tribe Cricetini. In G. E. Rőssner & K. Heissig (Eds.), *The Miocene land mammals of Europe* (pp. 373–387). München: Verlag Dr. Friedrich Pfeil.

Kretzoi, M. (1951). The Hipparion-fauna from Csákvár. *Földtani Közlöny, 81,* 384–417.

Kretzoi, M. (1954). Rapport final des fouilles paléontologiques dans la grotte de Csákvár. *Földtani Intézet Évi Jelentése, 1952,* 37–68.

Kretzoi, M. (1959). Insectivoren, Nagetiere und Lagomophen der jüngstpliozänen Fauna von Csarnóta im Villányer Gebirge Südungarn. *Vertebrata Hungarica, 1,* 237–244.

Kretzoi, M. (1978). Wichtigere Streufunde in der wirbeltierpalaontologischen Sammlung der ungarischen geologischen Anstalt. *Földtani Intézet Évi Jelentése, 1978,* 347–358.

Li, C.-K. (1977). A new Miocene cricetodont rodent of Fangshan, Nanking. *Vertebrata PalAsiatica, 15,* 67–75 (in Chinese with English abstract).

Paunovic, M., & Rabeder, G. (1996). Die altpleistozänen Kleinsäugerfaunen Razvodje und Tatinja draga in Süd-Kroatien. *Beiträge zur Paläontologie, Wien, 21,* 69–84.

Rummel, M. (1998). Die Cricetiden aus dem Mittel- und Obermiozän der Türkei. *Documenta Naturae, 123,* 1–300.

Schaub, S. (1930). Quartäre und jungtertiäre Hamster. *Schweizerische Paläontologische Gesellschaft, Abhandlungen, 49,* 1–49.

Schaub, S. (1934). Über einige fossile Simplicidentaten aus China und der Mongolei. *Schweizerische Paläontologische Gesellschaft, Abhandlungen, 54,* 1–40.

Sinitsa, M. V., & Delinschi, A. (2016). The earliest member of *Neocricetodon* (Rodentia: Cricetidae): a redescription of *N. moldavicus* from Eastern Europe, and its bearing on the evolution of the genus. *Journal of Paleontology, 90,* 771–784.

Tchernov, E. (1968). *Succession of rodent faunas during the upper Pleistocene of Israel*. Hamburg, Berlin: Verlag Paul Parey.

Ünay, E., de Bruijn, H., & Suata-Alpaslan, F. (2006). Rodents from the upper Miocene hominoid locality Çorakyerler (Anatolia). *Beiträge zur Paläontologie, Wien, 30,* 453–467.

Wang, H. (1988). An early Pleistocene mammalian fauna from Dali, Shaanxi. *Vertebrata PalAsiatica, 26,* 59–72 (in Chinese with English abstract).

Wu, W.-Y. (1991). The Neogene mammalian Faunas of Ertemte and Harr Obo in Inner Mongolia (Nei Mongol), China.–9. Hamsters: Cricetinae (Rodentia). *Senckenbergiana Lethaea, 71,* 257–305.

Young, C. C. (1927). Fossile Nagetiere aus Nord-China. *Palaeontologia Sinica, C, 5*(3), 1–82.

Zdansky, O. (1928). Die Säugetiere der Quartärfauna von Chou-K'ou-Tien. *Palaeontologia Sinica, C, 5*(4), 1–146.

Zhang, Z.-Q., Wang, L.-H., Liu, Y., & Liu, L.-P. (2011). A new species of late Miocene hamster (Cricetidae, Rodentia) from Damiao, Nei Mongol. *Vertebrata PalAsiatica, 49,* 201–209 (in Chinese with English summary).

Zhang, Z.-Q., Zheng, S.-H., & Liu, L.-P. (2008). Late Miocene cricetids from the Bahe Formation, Lantian, Shaanxi Province. *Vertebrata PalAsiatica, 46,* 307–316 (in Chinese with English summary).

Zheng, S.-H. (1984a). Revised determination of the fossil cricetinae (Rodentia, Mammalia) of Choukoutien district. *Vertebrata PalAsiatica, 22,* 179–197 (in Chinese with English summary).

Zheng, S.-H. (1984b). A new species of *Kowalskia* (Rodentia, Mammalia) of Yinan, Shandong. *Vertebrata PalAsiatica, 22,* 251–260 (in Chinese with English summary).

Zheng, S.-H., & Zhang, Z.-Q. (2000). Late Miocene-early Pleistocene micromammals from Wenwanggou of Lingtai, Gansu, China. *Vertebrata PalAsiatica, 38,* 58–71 (in Chinese with English summary).

Zheng, S.-H., & Zhang, Z.-Q. (2001). Late Miocene-early Pleistocene biostratigraphy of the Leijiahe Area, Lingtai, Gansu. *Vertebrata PalAsiatica, 39,* 215–228 (in Chinese with English summary).

Zhou, X.-Y. (1988). The Pliocene micromammalian fauna from Jinle, Shanxi – a discussion of the age of Jinle Red Clay. *Vertebrata PalAsiatica, 26,* 181–197 (in Chinese with English summary).

Chapter 11
Yushe Basin Prometheomyini (Arvicolinae, Rodentia)

Wen-Yu Wu and Lawrence J. Flynn

Abstract Absent from Miocene and Pleistocene assemblages of Yushe Basin, prometheomyine Arvicolinae are a common and characteristic element of Pliocene faunas. Two time-successive species of the genus *Germanomys* are well represented in the Gaozhuang and Mazegou formations and serve as index fossils for Gaozhuangian and Mazegouan faunas. The genus *Germanomys* is well known in the Pliocene of Europe, but the oldest Yushe *Germanomys* (at about 4.7 Ma) is appreciably older than the European records, yet relatively derived in stage of evolution of crown height and sinuousity of the base of the enamel on molars. The younger *Germanomys* species is late Pliocene in age, higher crowned, and shows a more derived sinuous line. In addition to the *Germanomys* lineage that is well represented in the Yushe Pliocene sequence, we find evidence of the distinct genus *Stachomys* and perhaps another prometheomyine in Yushe Basin.

Keywords Yushe Basin • North China • Late Neogene • *Germanomys* • Prometheomyini

Note: This chapter includes one or more new nomenclatural-taxonomic actions, registered in Zoobank, and for such purposes the official publication date is 2017.

W.-Y. Wu (✉)
Laboratory of Paleomammalogy, Institute of Vertebrate Paleontology and Paleoanthropology, Chinese Academy of Sciences, 142 Xizhimenwai Ave., Beijing 100044, People's Republic of China
e-mail: wuwenyu@ivpp.ac.cn

L.J. Flynn
Department of Human Evolutionary Biology, and the Peabody Museum of Archaeology and Ethnology, Harvard University, Cambridge, MA 02138, USA
e-mail: ljflynn@fas.harvard.edu

11.1 Introduction

The Pliocene strata of Yushe Basin are characterized by the addition of arvicoline rodents to the zokor/mouse/hamster-dominated microfaunas of the late Miocene. Pliocene deposits reveal *Germanomys* and *Mimomys* in abundance. We follow common practice in using the term "arvicoline" for the core monophyletic group of small muroids with prismatic molars, but acknowledge that *Germanomys*, here considered a member of Tribe Prometheomyini, has a deep common ancestry with *Mimomys* and its Tribe Arvicolini. Given the diversity and distinct evolutionary trends of the prometheomyinin and arvicolinin rodents, they are treated separately in successive chapters of this Volume II on the Yushe small mammals. The present chapter focusses on the Prometheomyini.

Among the microfauna assemblages of Yushe Basin, we expected to find evidence of the "microtoid" cricetid *Microtoscoptes*, because it is well-represented at the latest Miocene site Ertemte, Inner Mongolia (Schaub 1934; Fahlbusch 1987). Instead, these were absent from the Miocene of Yushe Basin, but we found abundant *Germanomys* (and *Mimomys*) in Pliocene age deposits. Whereas Arvicolini remained common in Pleistocene deposits of Yushe, the Prometheomyini disappeared by the end of the Pliocene. Our study of Yushe arvicolines came to depend on the Russian and European literature, as well as Chinese work, e.g., the indispensable study by Zheng and Li (1986), which summarized knowledge of Chinese arvicolines up to that time.

The Arvicolinae of Yushe Basin are not only intrinsically interesting, but they shed light on the changing paleoecology of the region. They may indicate decreasing mean annual temperature, but also likely demonstrate that moisture remained significant in the region. In addition, these rodents are useful in correlation of localities over long distances, and in testing correlations with the European biochronology. Although some localities produce both *Germanomys* and

Lawrence J. Flynn and Wen-Yu Wu (eds.), *Late Cenozoic Yushe Basin, Shanxi Province, China: Geology and Fossil Mammals, Volume II: Small Mammal Fossils of Yushe Basin*, Vertebrate Paleobiology and Paleoanthropology,
DOI 10.1007/978-94-024-1050-1_11

Mimomys, an interesting pattern is apparent in which individual small mammal assemblages produce dominantly one or the other genus. Perhaps the partially exclusive occurrence of these forms reflects differing microhabitat preference or oscillations in dominant climate.

Terminology used in the descriptions below follows that of Carls and Rabeder (1988). The term "sinuous line" used in this paper also has been termed "linea sinuosa", "basal enamel margin" and "dentine tract" by some authors. Measurements of the occlusal surfaces of teeth are expressed as length times width (L × W) in mm. Prism height is measured at the first buccal reentrant on upper molars and at the last lingual reentrant on lower molars (see Carls and Rabeder 1988).

11.2 Systematics

Since the establishment of Tribe Prometheomyini Kretzoi, 1955, the content of the group has lacked consensus. Although Repenning (1987) preferred to include *Microtoscoptes* in the tribe, we follow Fejfar (1999) in excluding that genus as a "microtoid" cricetid. Most authors, e.g., Mckenna and Bell (1997) and Musser and Carleton (2005) include the extinct *Stachomys* in Prometheomyini; we consider the fossil genera *Germanomys* and *Ungaromys* here, as well.

11.2.1 *Genus* Germanomys *Heller, 1936*

Germanomys yusheica sp. nov.

Type: Left m 1 (V11313.1).

Paratypes: A fragmentary right mandible lacking incisor but bearing m1 (V11313.2); two m1, four m2, and m3 (V11313.3-9); nine M1 (two missing posterior ends); seven M2 (damaged), and M3 (V11313.10-26).

Type locality: YS4, early Pliocene, Culiugou Member, Gaozhuang Formation, 4.3 Ma.

Etymology: Derived from the name of the county where the type locality is situated.

Species diagnosis: Compared to *Germanomys weileri,* larger in size, with tooth crown and sinuses slightly higher. The protosinus on the M1 is the highest but all other sinuses are nearly equivalent. The M3, after heavy wear, is "W"-shaped like M2, but relatively longer and narrower (higher length-width ratio). M1 is 3-rooted, M2 and M3 are 2-rooted, and lower molars are 2-rooted.

Referred material: Incomplete left mandible with m1-2 and broken incisor (V11314.1), and one m1 (V11314.2, now lost) from YS 97 (4.3 Ma) of the Culiugou Member; five M1 and one m2 (V11315.1-6) from YS50 (4.7 Ma), Nanzhuanggou Member, Gaozhuang Formation.

Description: The Type (left m1, V11313.1) is lightly worn, and measures 2.44 × 1.17 mm at the occlusal surface. Prisms are 2.44 mm in height lingually; three slightly alternate salient angles are present between the anteroconid complex and posterior lobe. The anteroconid complex is composed of two anteriorly directed projections, with the anterolingual projection longer than the anterolabial one. The fold between the two projections thins out (becomes shallow) toward the base of the tooth and disappears near the anterosinuid. Lingual reentrant and salient angles are symmetrically V-shaped, while the labial salient angles display a longer mesial side than distal side and hence the labial salient angles and reentrant angles are asymmetrically V-shaped, and the lingual reentrant angles are obviously deeper than the labial ones. Salient angles on both sides are in alternate arrangement with confluent dentine space between them. Enamel is thick, labial sinuids are all higher than lingual ones, the hyposinuid is 0.56 mm in height, and the hyposinulid is nearly 0.05 mm high (Fig. 11.1). Two tooth roots are present, the anterior root laterally compressed and posterior root anteroposteriorly compressed.

The m1 on the paratype mandible (V11313.2) displays two roots labial to the incisive alveolus. The diastema is 3.13 mm in length, and a mental foramen is situated just anterior to the anterior root of the m1. All four slightly worn m1 specimens display bifid anterior projections on the anterior cap. On the heavily worn specimen (V11313.4) with the labial enamel of the anteroconid complex worn off nearly completely, no trace of the anterior projections is observed and the labial reentrants are sealed to form two enamel islets. On one specimen the hyposinuid is 0.44 mm high. On two specimens the hyposinulids differ in height: 0.13 and 0.28 mm, respectively.

The m2 (4 specimens) is composed of a posterior lobe and two alternate lingual and labial salient angles and reentrant angles with tooth prism slightly posteriorly curved. The distinct anteromedial ridge becomes weak and disappears with progressive occlusal wear of the tooth. Sinuids are relatively shallow. The hyposinuid height varies from 0.09 to 0.25 mm (3 cases), and the hyposinulid varies from 0.09 to 0.31 mm (4 cases). Two roots occur.

The single m3 resembles the m2 in crown morphology, but the prisms and tooth-roots are distinctly more posteriorly curved and sinuids are even shallower. Hyposinuid and hyposinulid height are both 0.09 mm.

Nine M1 specimens are present, of which two are deeply worn and two are seriously damaged. The tooth crown is composed of an anterior lobe and two pairs of slightly alternate salient angles and reentrant angles (Fig. 11.2).

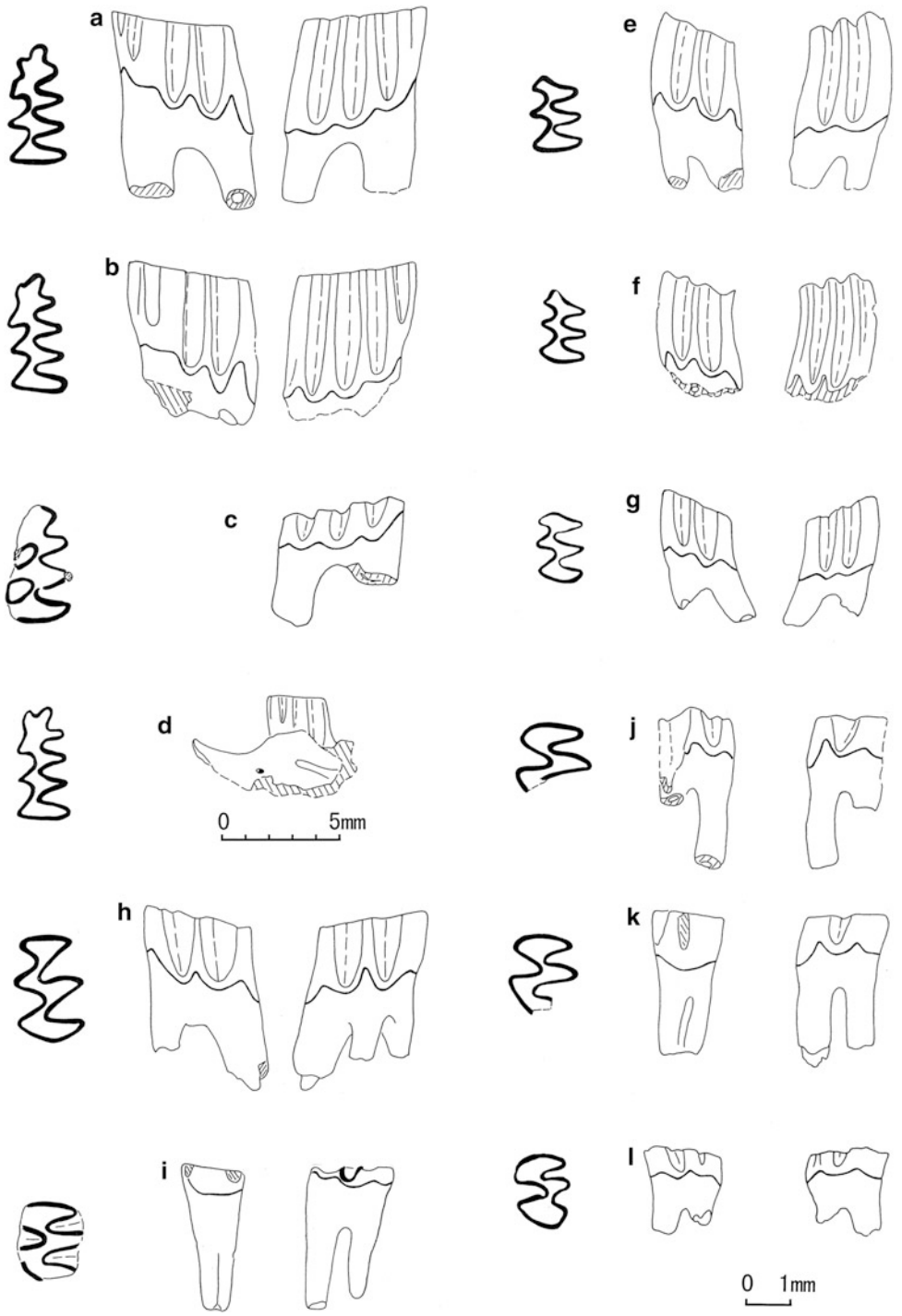

Fig. 11.1 *Germanomys yusheica* **sp. nov. from YS4, Culiugou Member, Gaozhuang Formation**. **a** Type left m1 V11313.1; **b** right m1 V11313.3 (inverted); **c** left m1 V11313.4; **d** right dentary with m1 V11313.2 (inverted); **e** left m2 V11313.5; **f** left m2 V11313.6; **g** right m3 V11313.9 (inverted); **h** left M1 V11313.10; **i** right M2 V11313.19 (inverted); **j** left M2 V11313.21; **k** right M2 V11313.20 (inverted); **l** left M3 V11313.26. Anterior toward top for occlusal views here and in subsequent figures. Occlusal (left), labial (middle) and lingual (right) views except d; the middle figures of 11.1i and 11.1k show anterior views

The labial reentrant angles are transversely deeper in occlusal view than the lingual ones. The dentine space of the opposite angles is confluent. The distal ridge on all specimens is not distinct, probably reflecting wear. Sinuses are conspicuously curved and relatively high lingually. The observed range of protosinus height is 0.34–1.0 mm (n = 6, $\bar{x}$ = 0.69) while the

anterosinus height is 0.15–0.31 mm (n = 6, $\bar{x}$ = 0.23). Three roots are present with the anterior root the most robust and the lingual root relatively gracile.

All seven M2 are incomplete. The M2 is composed of an anterior lobe and three alternating salient angles and reentrant angles with wide, confluent dentine space. Because of heavy wear it is impossible to determine if a distal ridge were present or absent. The crowns are distinctly "w" shaped (Fig. 11.1i–k). The protosinus varies from 0.56–0.88 mm in height. Two roots are present and on two specimens a shallow vertical groove is present on the anterior surface of the anterior root, which could represent a remnant scar caused by the fusion of two roots.

M3 (only one specimen) shares the same morphology as M2, but is comparatively narrower and longer. The labial reentrants and salient angles are distinctly smaller than the lingual ones. The metacone-talon complex (posterior loop) is simple and relatively long (Fig. 11.1l). Sinuses are extremely shallow, the protosinus is 0.09 mm in height and the anterosinus is nearly absent. Two roots are present. This tooth is determined to be an M3 rather than M2 due to the lack of a posterior dental pressure facet.

The specimens from YS50 and YS97 are morphologically identical to those from YS4. The lowest stratigraphic level producing this species is locality YS50. Of the five M1 specimens from YS50, three are relatively lightly worn, the third lingual and labial salients are both well-developed and the distal ridge is distinct (Fig. 11.2b). The salient angles and distal ridge gradually weaken upon increased occlusal wear, and the degree of sinus development is nearly the same as at YS4. The protosinus height ranges from 0.44–0.59 mm (n = 4, $\bar{x}$ = 0.52) and the anterosinus height ranges from 0.19–0.28 (n = 4, $\bar{x}$ = 0.24). Three roots are present. Heights of the YS50 m2 hyposinuid and hyposinulid are 0.25 and 0.20, respectively.

YS97 produced a left mandible lacking its ascending ramus, angular process, and anterior portion of the incisor. Diastema length is 3.66 mm, and the ramus is 3.42 mm deep on the lingual side of m1. A mental foramen is situated anterior to the anterior root of the m1 and a masseteric ridge is very well-developed. The m1 and m2 are well worn. The two projections on the m1 anterior cap are only vestigially traced, and as such, give the anteroconid complex a trapezoid form. The heights of the hyposinuid and hyposinulid are 0.31 and 0.09 mm, respectively, while on the m2 these features are 0.16 and 0.13 mm high.

Discussion: *Germanomys yusheica* resembles *G. weileri* from Europe but is larger in size and has a more sinuous line at the base of the enamel on the sides of molars (higher dentine tracts). Although older than *G. weileri*, its sinuous line is more derived. Other species of *Germanomys* have been named (see below) but these resemble *G. weileri* in size and morphology. The species *Ungaromys altenburgensis* resembles the slightly larger *G. yusheica* but has more

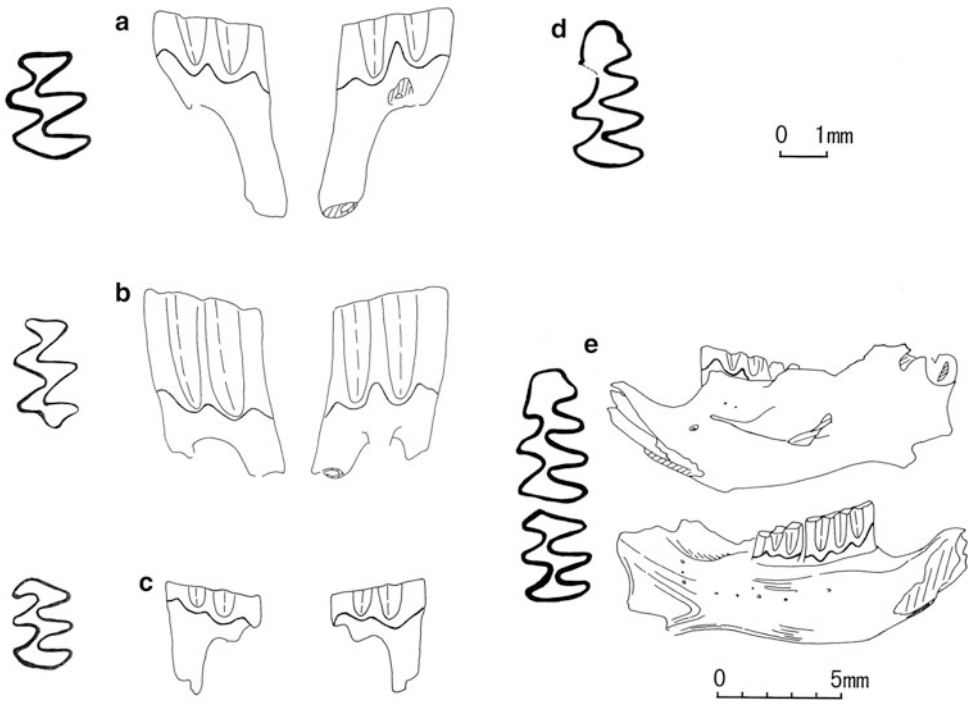

Fig. 11.2 *Germanomys yusheica* **sp. nov. from YS50 and YS97, Gaozhuang Formation**. **a** left M1 V11315.3; **b** left M1 V11315.5; **c** right m2 V11315.6 (inverted); **d** left m1 V11314.2 (missing); **e** left dentary with m1-2 V11314.1. Occlusal (left), labial (middle) and lingual (right) views for 11.2a–c

sinuous dentine tracts, and we suggest below that it should be transferred to *Germanomys*. Other *Ungaromys* species have very strong sinuousity, stronger than that of any *Germanomys,* and show derived molar enamel microstructure. *Stachomys trilobodon* is close in size to Yushe *Germanomys* but differs in features discussed below.

Germanomys shares general prismatic occlusal surface structure with *Microtodon*, but the latter is mesodont, not hypsodont, and has a simple anteroconid complex on m1. *Microtodon atavus* is smaller than *G. yusheica*, and shows only slight undulation of the sinuous line. *M. atavus* is common at the late Miocene site Ertemte, Inner Mongolia, but only a single tooth was found at Bilike (early Pliocene, Inner Mongolia). However, Bilike does produce a primitive arvicolinin, *Aratomys bilikeensis*, which is close in size to *G. yusheica* and shows molar morphology that is superficially comparable. The difference of this arvicolinin from the prometheomyinin lies in the position of the angles and reentrants: they are strongly alternating in arvicolinins, but in *Germanomys* they tend to be more opposite in position. In m1, the buccal salient angles are shifted posteriorly so that they lie more opposite the lingual salient angles.

Germanomys progressiva sp. nov.

Type: Right M1 (V11316.1).

Paratypes: M1, two M2, two m1 (one deeply worn and one lacks anterior cap), m2 damaged anteriorly (V11316.2-7).

Type locality: YS87, late Pliocene, Mazegou Formation, 3.4 Ma.

Etymology: An indication of the more derived state compared to *G. yusheica*.

Species diagnosis: Although size is indistinguishable from that of *G. yusheica* (Tables 11.1 and 11.2), *G. progressiva* is more hypsodont and displays higher lateral sinuses and sinuids (Tables 11.3 and 11.4). On M1 the parasinus is lowest, while the other sinuses are nearly equivalent in height. M3 differs from that of *G. yusheica* in occlusal morphology, with two reentrant angles on each side and relatively high sinuses. *Germanomys progressiva* has much higher tooth prisms and sinuous lines than *G. weileri*, moderately more strongly sinuous lines than *Ungaromys altenbergensis*.

Referred material: YS90 (3.5 Ma, Mazegou Formation); posterior section of m1, two m2, two broken m3, two M1 (one lacks the anterior lobe), M2 and M3 (V11317.1-9). YS99 (3.0 Ma, upper part of the Mazegou Formation); right mandible with incisor and m1-2, but lacking the ascending ramus and angular process (V11318).

Description: The type specimen (right M1, V11316.1) is lightly worn, with occlusal surface measuring 2.10 × 1.20 mm, prism height 3.42 mm. The crown is composed of an anterior lobe, and two pairs of alternate salient and reentrant angles, which are all rounded V-shaped (Fig. 11.3). No trace of a third lingual reentrant is present. The anterior

Table 11.1 Measurements of lower molars of *Germanomys yusheica* and *Germanomys progressiva* at occlusal surface (L × W in mm; number of specimens in parentheses)

Germanomys		m1	m2	m3
G. yusheica	YS50		1.86 × 1.22 (n = 2)	
	YS97	2.64 × 1.42	1.85 × 1.35	
	YS4	2.25–2.48(3) × 1.07–1.22(2) mean 2.39 × 1.16	1.51–1.91(4) × 1.00–1.37(4) mean 1.70 × 1.22	1.47 × 1.03 (1)
G. progressiva	YS90		1.71–2.00 × 1.22–1.27(2) mean 1.85 × 1.24	– × 0.78
	YS87	– × 1.12–1.17(3) mean – × 1.14		
	YS99	2.54 × 1.22	1.71 × 1.32	

Table 11.2 Measurements of upper molars of *Germanomys yusheica* and *Germanomys progressiva* at occlusal surface (L × W in mm)

Germanomys		M1	M2	M3
G. yusheica	YS50	2.05–2.34 × 1.22–1.42(5) mean 2.16 × 1.31		
	YS97			
	YS4	2.10–2.49(4) × 1.46–1.62(6) mean 2.26 × 1.55	1.67–1.72 × 1.35–1.46(2) mean 1.70 × 1.41	1.59 × 1.18
G. progressiva	YS90	2.15(1) × 1.28–1.42(2) mean 2.15 × 1.35	1.61 × 1.17	1.32 × 0.98
	YS87	2.10–2.31 × 1.22–1.51(2) mean 2.20 × 1.36	1.67–1.72 × 1.22–1.37(2) mean 1.70 × 1.30	
	YS99			

Table 11.3 Measurements (mm) of lower molar sinuid heights for *Germanomys yusheica* and *Germanomys progressiva*

Germanomys		m1		m2		m3	
		hsd*	hsld**	hsd	hsld	hsd	hsld
G. yusheica	YS50			0.25	0.20		
	YS97	0.31	0.09	0.16	0.13		
	YS4	0.44–0.56(2) mean 0.50	0.13–0.28(2) mean 0.20	0.09–0.25(3) mean 0.19	0.09–0.31(4) mean 0.20	0.09(1)	0.09(1)
G. progressiva	YS90	~1.06	0.78–>0.81 ca. 0.79				
	YS87	1.56	0.75				
	YS99						

*hsd – hyposinuid, **hsld – hyposinulid

Table 11.4 Measurements (mm) of upper molar sinus heights of *Germanomys yusheica* and *Germanomys progressiva*

Germanomys		M1		M2		M3	
		Prs*	As**	Prs	As	Prs	As
G. yusheica	YS50	0.44–0.59(4) mean 0.52	0.19–0.28(4) mean 0.24				
	YS97						
	YS4	0.34–1.0(6) mean 0.69	0.15–0.31(6) mean 0.23	0.56–0.88(2) mean 0.72		0.09 (1)	
G. progressiva	YS90	1.27–~1.40(2) mean ca.1.34	>1.13	1.22	ca. 0.54	0.73	0.34
	YS87	1.46	1.27	1.22	0.38–~0.47(2) mean 0.42		
	YS99						

*Prs – protosinus, **As – anterosinus

lobe is triangular in shape with a flat and straight mesial wall. The distal ridge is distinct but blunt. The dentine space in between the salient angles is confluent, and enamel thickness is almost uniform, about 0.1 mm. The labial parasinus is the lowest, while the anterosinus and metasinus are nearly equivalent in height. The lingual anterosinulus, protosinus, and hyposinus are also nearly equivalent in height, with the protosinus 1.46 mm and anterosinus 1.27 mm high. M1 is three-rooted.

The paratype M1 (V11316.2) is rather worn and has a slightly anteriorly arched mesial wall. Enamel wall thickness is nearly uniform at ~0.15 mm. Lingual sinuses are truncated as are the anterosinus and metasinus. A distal ridge and third lingual reentrant are absent. Prism height is 1.66 mm. Three roots are present.

The M2, w-shaped in occlusal outline, lacks a distal ridge. Protosinus and hyposinus are nearly equivalent in height, while the anterosinus is the lowest and the metasinus is highest. The protosinus is 1.22 mm in height (n = 1), and the anterosinus is 0.38–0.47 (n = 2). Two roots are present.

The m1 that represents this taxon is missing its anterior cap and part of the anteroconid complex. Lingual and labial salients and reentrants resemble the configuration of *G. yusheica,* however the prisms are higher, 3.43 mm at the posterior lobe. Hyposinuid is 1.56 mm and hyposinulid is 0.75 mm (n = 1). Of the labial sinuids, the hyposinuid is the highest while the anterosinuid is the lowest. Among the lingual sinuids, the hyposinulid is the highest, while the endosinuid and metasinuid are nearly equivalent in height.

The m2 is damaged anteriorly and is heavily worn (Fig. 11.3e). Labial sinuids have been truncated at their apices. Among the lingual sinuids, the hyposinulid is the highest though it also has been truncated, and the metasinuid is the lowest.

Dental characters of the referred material are identical with the type and paratype. On the two specimens of m2 from YS90 (Fig. 11.4f) the labial hyposinuid and anterosinuid are nearly equivalent in height while the protosinuid is lowest. Lingually, the hyposinulid is highest while the endosinuid and metasinuid are relatively low. Height of hyposinuid is 1.06 (n = 1), hyposinulid 0.78 to >0.81 (n = 2). One broken m3 (V11317.5 from YS90, Fig. 11.4g) is assigned to this taxon with hesitation. Judging from the preserved portion the crown appears to resemble the m2 in

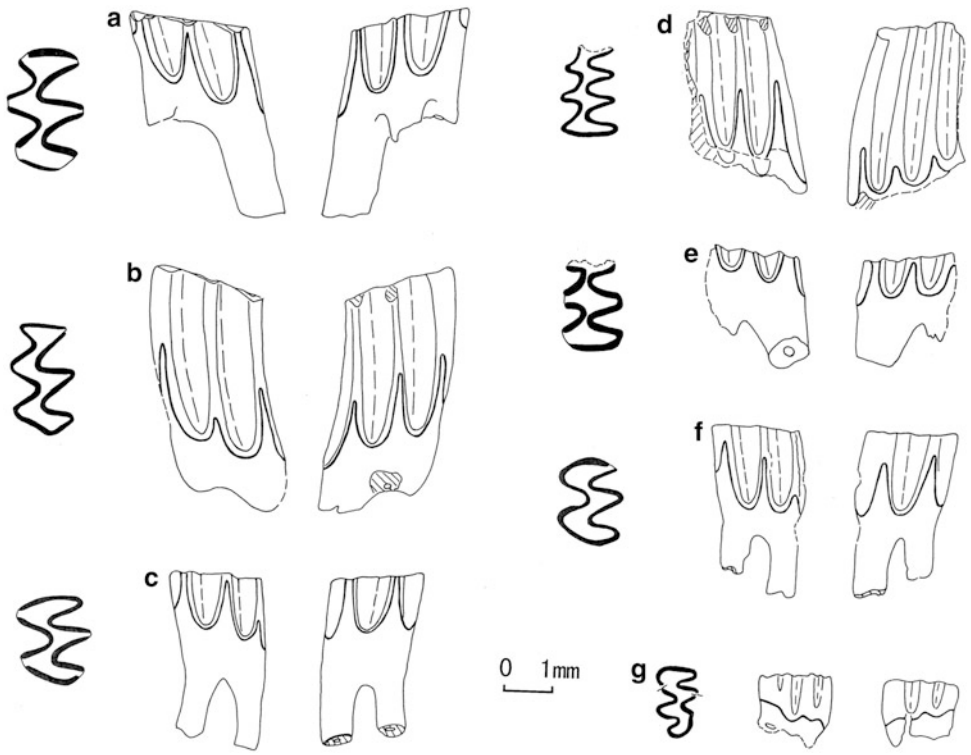

Fig. 11.3 *Germanomys progressiva* **sp. nov. (a–f) and cf.** *Stachomys* **sp. (g) from YS87, Mazegou Formation. a** left M1 V11316.2; **b** holotype right M1 V11316.1 (inverted); **c** right M2 V11316.3 (inverted); **d** left m1 V11316.6; **e** left m2 V11316.7; **f** right M2 V11316.4 (inverted). **g** left M3 V11320

morphology. That is to say, it resembles the m3 of *G. yusheica* but is distinctly narrower and longer than the latter, and the hyposinuid and hyposinulid are shallow. Two roots are present.

On the M3 from YS90 (V11317.9, Fig. 11.4d) there are two lingual and three labial reentrants, and correspondingly two lingual and three labial salient angles, alternately arranged. The first and second labial reentrants are U-shaped and the third reentrant is very shallow, the first and second labial salients are nearly equivalent but larger than the third one, the first labial reentrant is deeper than the second reentrant. The first lingual reentrant is wider and deeper than the second one, and the first lingual salient is somewhat larger than the second one. The posterior lobe is narrow and long, and slightly lingually directed. The sinuses are high with the lingual protosinus and hyposinus nearly equivalent. The labial anterosinus and parasinus are nearly equivalent in height, but the metasinus is relatively low. Protosinus is 0.73 mm and anterosinus is 0.34 mm in height. Two roots are present.

YS99 produced a right mandible with incisor and m1-2 (V11318, Fig. 11.4j), which resembles the YS97 mandible in morphology and size. Its diastema is 3.70 mm long, mandible depth is 3.42 mm measured lingually beneath the m1, the m1 anterior lobe (anteroconid complex) and first lingual salient angle are broken at its upper portion, prohibiting the study of sinus morphology. The anterior projections are absent low on the tooth. Refer to Tables 11.3 and 11.4 for measurements of sinus and sinuid height. Unfortunately, few specimens of *G. progressiva* m1 are available and the anteroconid complex of m1 is damaged so that the shape of the anteroconid complex of m1 cannot be exactly figured.

Discussion: Among other Late Pliocene records of *Germanomys* in China, Zhou (1988) described a tooth from Hefeng, Jingle, (V8664) under the name ?*Ungaromys*. It displays the same sinuids and occlusal surface morphology as two m1 described above (V11316.6) from YS87 and the m2 (V11317.3) from YS90. It is therefore suggested that the Hefeng form should be assigned to *Germanomys progressiva*. Similarly, the upper and lower molars of *Germanomys* sp. from Daodi (Cai 1987) demonstrate the same occlusal patterns and same sinuous lines as *G. progressiva* from Yushe. All Daodi specimens were observed in detail by the senior author. These observations are consistent with our conclusion (Flynn et al. 1997) that the faunas from the Mazegou Formation, Hefeng, and Daodi are contemporary.

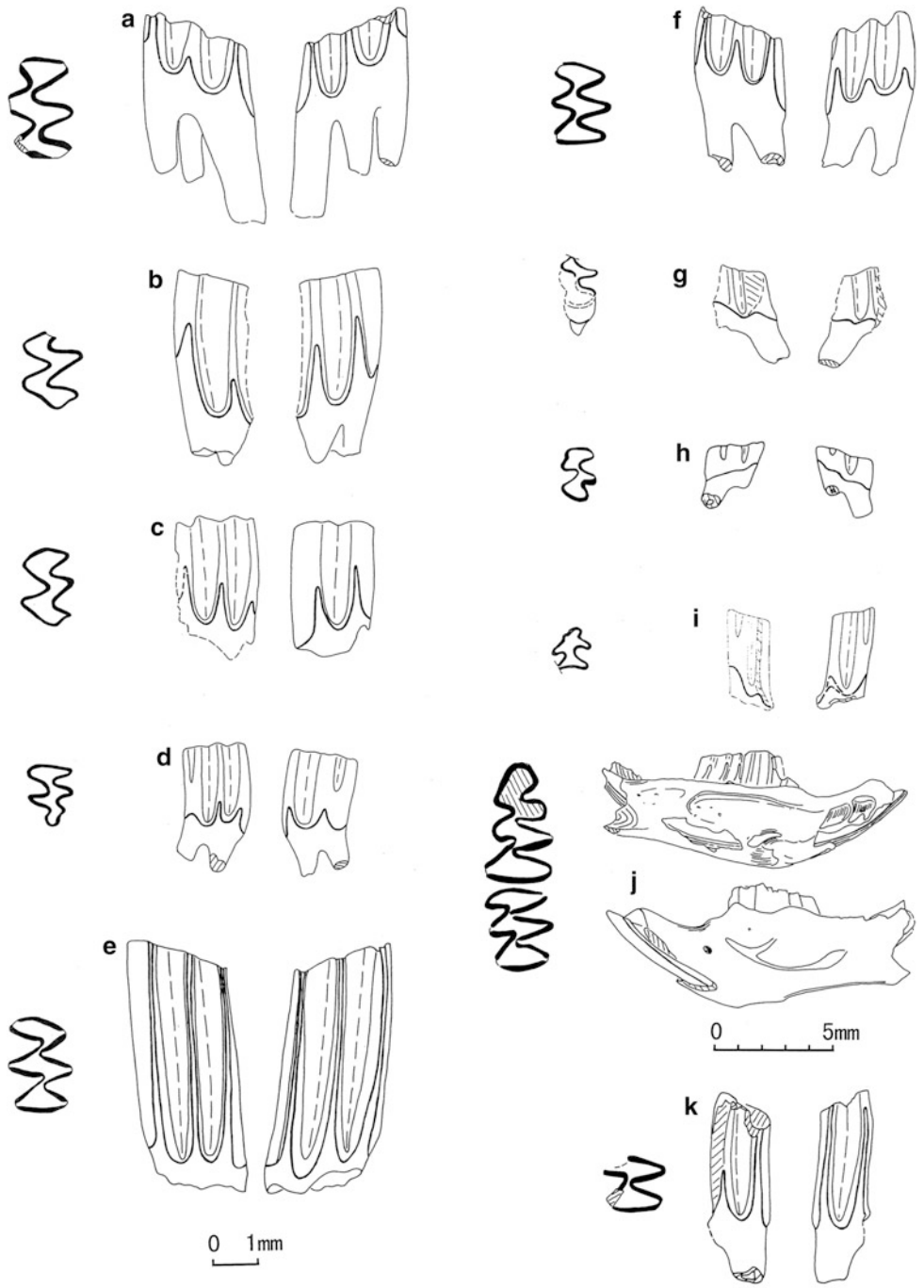

Fig. 11.4 *Germanomys progressiva* **sp. nov. (a–d, f–g from YS90 and j, YS99), cf.** *Stachomys* **sp. (h, from YS90), Prometheomyini gen. et sp. indet. (e, i, k). a** left M1 V11317.6; **b** right M1 fragment V11317.7 (inverted); **c** right M2 V11317.8 (inverted); **d** left M3 V11317.9; **e** right m2 V11321 (inverted); **f** left m2 V11317.3; **g** right m3 fragment V11317.5 (inverted); **h** right m3 V11319 (inverted); **i** left m1 fragment V11323; **j** right dentary with m1-2 V11318 (inverted, separate scale bar); **k** left lower molar fragment V11324

11.2.2 Other Yushe Prometheomyini

cf. *Stachomys* sp.

Material: A single left M3 (V11320) from YS87 (Fig. 11.3g), and a single right m3 (V11319) from YS90, both Mazegou Formation, late Pliocene, about 3.5 Ma (Fig. 11.4h).

Description: The M3 (V11320) is long and narrow (1.37 × 0.83), and well worn, such that only 1.07 mm of height remains. Two reentrant folds are present on both the lingual and labial sides, and the two lingual reentrants are equivalent in depth, being one-half the breadth of the tooth. The first labial reentrant is short and deep, the second one is relatively shallow. This condition creates relatively confluent dentine space between the salient angles. The shallow anterosinus and parasinus are both 0.06 mm high. Tooth root count, probably 2, is unclear.

The m3 (V11319) is also narrow and long (1.17 × 0.78) and well-worn such that the remaining prism height is merely 0.54 mm. Two reentrant folds are present both labially and lingually, with the second lingual and first labial reentrant much deeper than the other two, dividing the tooth surface into two distinct portions; the second labial reentrant is extremely shallow. An anterior medial ridge is absent. The sinuids, not measurable, undulate only slightly. Two roots are present.

Discussion: These specimens were collected from the Mazegou Fm., together with those of *G. progressiva*. However, their crown morphology and sinus height are quite different from *G. progressiva*, but more closely resemble the Pliocene *Stachomys trilobodon* Kowalski, 1960 from Węże, Poland; hence they are provisionally assigned to genus *Stachomys*. This genus co-exists with *Germanomys* in Europe, and its presence in Yushe is reasonable. We do not agree with Sulimski (1964) that *Stachomys* is a synonym of *Germanomys* (see below). We should recall that the M3 from YS 87 is probably 2-rooted, which is unusual for *Stachomys*.

Stachomys, established by Kowalski (1960) for *Stachomys trilobodon* from Węże, is well known from Ivanovce (Fejfar 1961, as "*Leukaristomys vagui*"). *Stachomys* also has Pliocene Russian records, for example on the Don River (Agadjanian 1993) and on the Olchon Peninsula of Lake Baikal in Siberia (Mats et al. 1982).

Prometheomyini gen. et sp. indet.

Material: A right m2 (V11321) from YS115, Taoyang Member, about 5.5 Ma (Fig. 11.4e), and an unfigured anterior loop of right M1 (V11322) from YS39, Nanzhuanggou Member, both Gaozhuang Formation; a possible right anterior fragment of m1 (V11323) from YS90, and a posterior portion of a left m1 or m2 (V11324) from YS105, both Mazegou Formation (Fig. 11.4i, k). Although generic assignment is impossible at present, these specimens are considered Prometheomyini based upon their "V" shaped salient angles and reentrants in addition to the uniform enamel thickness. The YS 115 and YS39 records represent the first occurrences of Prometheomyini in Yushe Basin.

Description: The slightly worn YS115 m2 is 1.96 × 1.37 mm, and is hypsodont, with prisms = 4.6 mm. The crown is composed of two lingual and two labial salient angles and the posterior loop. All reentrants are "V"-shaped. Enamel thickness is uniform, tooth roots not yet formed, and sinuses (dentine tracts) penetrate the entire prism, surpassing the worn occlusal surface. The YS39 M1 (V11322) preserves only the anterior loop with a prism height of 4.01 mm. Height of the anterosinus is approximately 0.73 mm, higher than in *G. yusheica* and lower than on *G. progressiva*. The enamel thickness is uniform.

The fragmentary V11323 from YS90 is determined with uncertainty as the anterior part of a right m1. It includes the anteroconid complex and the third lingual salient angle. The anteroconid complex is composed of anterior cap, the fourth lingual salient angle and the third labial salient angle (=prism edge). The labial side of the anterior cap maintains a small projection. Enamel thickness is uniform and cementum is absent. Greatest measurable width is 0.83 mm. The labial sinus is distinct but the metasinuid is indistinct; dashed lines in Fig. 11.4i indicate two possible metasinuid morphologies.

The YS105 m1 or m2 fragment (V11324) preserves its posterior loop, second lingual salient angle and incomplete second labial salient angle with prism height of 2.8 mm. Enamel thickness is uniform, cementum is absent and sinuses are quite high with the lingual hyposinulid and labial hyposinuid extending into the occlusal surface. The entosinuid is 2.7 mm high and the protosinuid is relatively low at approximately 1.2 mm.

11.3 Comparison of *Germanomys*, *Ungaromys* and *Stachomys*

Germanomys yusheica and *G. progressiva* are from successive stratigraphic units. *G. yusheica* is produced from Yushe Basin at localities YS97, YS50, and YS4 which are in the higher levels of the Gaozhuang Formation (Nanzhuanggou and Culiugou members). *G. progressiva* is from YS90, YS87, and YS99, of the Mazegou Formation. Characters for both taxa are stable. With the exception of the M3, the occlusal outline of the molars and the mandibular morphology of the two species are similar. Distinctions lie in the height of tooth prisms, and sinuous lines (Tables 11.3 and 11.4): *G. progressiva* displays much higher prisms, sinuses and sinuids. The M1 of *G. yusheica* has its protosinus as the highest and other sinuses are nearly equal. In the M1 of derived *G. progressiva* the parasinus is the lowest while the

remaining sinuses are nearly equal in height. The HH-index value is 0.32–0.54 for *G. yusheica* m1, 1.72–1.73 for *G. progressiva* m1; and the PA-index value is 0.57–0.73 for *G. yusheica* M1, 1.75–1.94 for *G. progressiva* M1. Only two specimens of M3 are present in Yushe: one M3 of *G. yusheica* from YS4 and one of *G. progressiva* from YS90. Although these may not represent the species fully in M3 morphology due to unknown variation, we suggest that *G. yusheica* is primitive insofar as M3 approaches M2 in its single lingual reentrant fold and relatively low sinuses. The *G. progressiva* M3 possesses a complicated metacone-talon complex and higher sinuses.

These two species resemble European species of *Germanomys, Ungaromys,* and *Stachomys* in occlusal morphology. The genus *Germanomys* was erected by Heller (1936) based on the species *G. weileri* from the German locality of Gundersheim. Later, Fejfar (1961) erected two new species *G. helleri* and *G. parvidens* from Ivanovce, Slovakia, based on the anteroconid complex shape, enamel thickness, and size of m1, which were thought to differ from the type species *G. weileri*. In actuality, the distinctions in m1 among these samples of *Germanomys* are very slight. Sulimski (1964) synonymized *G. weileri* with *G. helleri* when he studied the rich material of *G. weileri* from Węże 1. In our opinion *G. parvidens* could also be the junior synonym of *G. weileri* because the labial sinuids of the unique m1 of Ivanovce *G. parvidens* are almost the same as *G. helleri* of the same locality (Fejfar, 1961, Fig. 8c, e), and dimensions fall into the range for *G. weileri* from Węże 1 (Sulimski, 1964, Table 14), though the enamel thickness of *G. parvidens* is somewhat thinner and the anteroconid is more complicated, possibly reflecting individual variation. According to Fejfar and Storch (1990) and Fejfar and Repenning (1998), European *Germanomys* is mid-Pliocene, ranging from late Ruscinian (MN15b) to early Villányian (MN16b).

Ungaromys was erected by Kormos (1932) based upon the early Pleistocene species *U. nanus* with type locality Episcopia (Püspökfürdö=Betfia II, early Biharian), Romania. Van der Meulen (1973) described Biharian *Ungaromys nanus* from Monte Peglia, Italy. Subsequently, Rabeder (1981) created the species *U. altenburgensis* for a single m1 from Deutsch-Altenburg 21 in his study of Pliocene and early Pleistocene arvicolids of Lower Austria, and he differentiated the Monte Peglia *U. nanus* as new species *U. meuleni,* given the more evolved sinuids, and the longer and wider anterior cap of the m1 of this species. Carls and Rabeder (1988) erected another new species *U. dehmi* for an early Pleistocene arvicoline from Schernfeld (MN17), Germany. *U. dehmi* had been known to be slightly more primitive than *U. nanus* in the sinuous line and the occlusal morphology of m1. They considered *U. dehmi*, *U. nanus* and *U. meuleni* (late Villányian, MN17 to MN18) to constitute a phylogenetic lineage but without reference to *U. altenburgensis* from Deutsch-Altenburg 21. Subsequently Mörs et al. (1998) described this species more fully from late Pliocene Reuver Clay of Hambach (early Villányian, MN16a) by a relatively large sample, including all upper and lower molars. We note that the sinuous lines of *U. altenburgensis* from both Deutsch-Altenburg 21 and Hambach are comparable with those of *Germanomys weileri* but more derived, and also comparable with those of *G. yusheica* from China. More interesting is that the hyposinuid-height, hyposinulid-height, and HH-index of the m1 (holotype) of *U. altenburgensis* from Deutsch-Altenburg 21 are within the range of variation for *G. yusheica*. On the contrary, we find no special relationship between *U. altenburgensis* and the *U. dehmi* - *U. nanus* - *U. meuleni* lineage in terms of sinuous lines. We consider it plausible to assign *U. altenburgensis* to *Germanomys*. According to Carls and Rabeder (1988), all upper molars of *Ungaromys* are two-rooted. Unfortunately the number of roots in upper molars of *U. altenburgensis* is unsurveyed.

The genus *Stachomys* Kowalski, 1960 was based on material from Węże, Poland. The type species *S. trilobodon* at the type locality is associated with *Germanomys weileri*. These two species also co-occur at Gundersheim-Findling (Storch and Fejfar 1990). The occlusal surface morphology of *Germanomys* and *Stachomys* molars are similar, but the anterior cap of *Germanomys* m1 is bifid. Kowalski (1960: 458, 464) did not identify, and thus neither described nor figured the upper molars of *Germanomys weileri*, but mentioned that all the upper molars of *S. trilobodon* are three-rooted. *Stachomys* was regarded (Kowalski 1960) as the progenitor of extant *Prometheomys,* which is the only surviving member of the tribe Prometheomini and lives in the Caucasus Mountains and Turkey (Ognev 1926; Çolak et al. 1999). According to Çolak et al. (1999), the upper and lower molars of *Prometheomys* have only two roots in adults. The sinuous line of *Prometheomys* is unknown, prohibiting further comparison.

Kowalski (1960, 2001), van der Meulen (1973) and Mörs et al. (1998) consider *Germanomys* and *Ungaromys* as synonyms. However, other European workers (Fejfar 1961; Sulimski 1964; Fejfar and Heinrich 1987; Carls and Rabeder 1988; Fejfar and Storch 1990; Fejfar and Repenning 1998) hold *Germanomys* as a legitimate taxon. We support the latter opinion with the following arguments.

(1) The sinuous line pattern of *Germanomys* is quite different from that of *Ungaromys* though the molars are extremely similar in occlusal surface pattern. *G. weileri* (=*U. helleri* and *G. parvidens*) displays low and not very differentiated sinuous lines. In contrast, the sinuous lines of *U. dehmi*, *U. nanus* and *U. meuleni* are well differentiated. Figure 11.5 displays the M1 and m1 sinuous

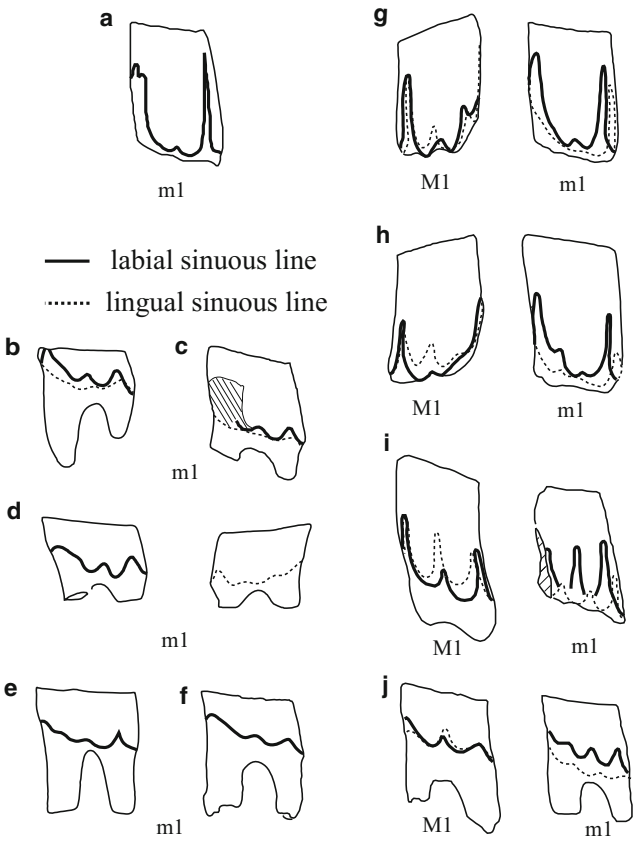

Fig. 11.5 Comparisons of the m1 and M1 sinuous line in *Ungaromys* and *Germanomys*. **a** *U. meuleni* from Monte Peglia (after van der Meulen 1973); **b** *U. altenburgensis* from Deutch-Altenburg 21 (after Rabeder 1981); **c** *G. weileri* from Wölfersheim (after Fejfar and Repenning 1998); **d** *U. altenburgensis* from Hambach (after Mörs et al. 1998; labial sinuid, left, and lingual sinuid, right); **e** *G. weileri* from Węże (after Kowalski 1960); **f** *G. weileri* (= *G. helleri*) from Ivanovce (labial sinuid of m1, after Fejfar 1961); **g** *U. nanus*, Deutch-Altenburg 2 C_1 (after Rabeder 1981); **h** *U. dehmi* from Schernfeld (after Carls and Rabeder 1988); **i** *G. progressiva* from YS87, Yushe; **j** *G. yusheica* from YS4, Yushe

lines of *Germanomys* and *Ungaromys*. Except for *G. progressiva,* sinuous lines of other species of *Germanomys* undulate slightly, but *Ungaromys* has dramatic undulation, yet no phylogenetic relationship can be traced between these two extremes. The sinuous lines of *G. progressiva* likely derived from the state represented by *G. yusheica* despite the obvious hiatus between species ranges in Yushe Basin.

(2) Fejfar and Repenning (1998: 166) enumerated the typical features of *Germanomys*, one trait being "thick enamel with simple not differentiated microstructure of radial type". When describing *Ungaromys altenburgensis* from Hambach, Mörs et al. (1998: 147) mentioned: "In *U. dehmi*, Carls and Rabeder found lamellar enamel in the tip of the anticlines, while the Hambach teeth have only radial enamel". The enamel microstructure of *Ungaromys* is different from that of *Germanomys*, and *U. altenburgensis* shows the *Germanomys* pattern. This is another argument that *Ungaromys altenburgensis* should be transferred to *Germanomys* but other species of *Ungaromys* are distinct.

(3) All upper molars of *Ungaromys* are 2-rooted (Carls and Rabeder 1988: 210). All upper molars of *Stachomys* are 3-rooted, while Yushe *Germanomys* displays 3 roots in M1, but 2 roots in M2 and M3. Root counts differentiate these rodents, although we acknowledge that number of roots for other genera may vary at the species level.

G. yusheica is similar to *G. weileri* not only in occlusal morphology of molars, but also in the m1 sinuous line. The Yushe upper molars are more similar to those of *G. weileri* from Ivanovce (Fejfar and Repenning 1998) in occlusal morphology than to *S. trilobodon* (Kowalski 1960, Fig. 4H–J). The sinuous lines of all molars of *G. yusheica* are quite different from those of *Ungaromys*. Moreover the root number of the *G. yusheica* molars differs from both *Stachomys* and *Ungaromys*. This is why we assign the Yushe species to *Germanomys* although the root number of the upper molars of European *Germanomys* is currently unknown. Enamel microstructure of the Yushe species should be studied to test their assignment.

In summary, the Chinese *G. yusheica* differs from European *G. weileri* mainly in larger size and slightly higher sinus and sinuid. The younger *G. progressiva* is in turn more derived than *G. yusheica* in its much higher tooth prisms, sinuous lines and M3 occlusal morphology. An obvious stratigraphic gap separates the two evolutionary stages, and includes the disconformity between the Gaozhuang and Mazegou formations. The time difference between the last occurrence of *G. yusheica* (YS4, 4.3 Ma) and the first occurrence of *G. progressiva* (YS90, 3.5 Ma) is considerable, ca. 800,000 years.

11.4 The Origin of *Germanomys*

In Europe *Germanomys* spans the late Ruscinian (MN15b) to late Villafranchian interval (and possibly early Villányian). In China the first occurrence of *Germanomys yusheica* at locality YS50, in the lower Gaozhuang Formation of the Yushe sequence, (MN14 age) is about 4.7 Ma; the last occurrence of *G. progressiva* is at YS99, high in the Mazegou Fm. about 3.0 Ma in age.

The first occurrence of *Germanomys weileri* in Europe (MN15b) is much later than the more derived *Germanomys yusheica* of China. However, if we transfer *U. altenburgensis* to *Germanomys*, which is MN16a in age, we note sinuous lines similar to those of *G. yusheica*, yielding a similar stage

of evolution, but still the difference in age is apparent. How do we explain the earlier occurring Chinese *G. yusheica* with a more derived sinuous line than the younger European *G. weileri,* and the "more advanced" stage of evolution of the sinuous line of Chinese *Germanomys*? We suppose that the genus *Germanomys* descended from a *Microtodon*-like ancestor in Asia where the earliest records are, or in Europe where the less derived *Germanomys* species are. *Microtodon* sp. occurs earliest in the late Miocene Bilutu fauna (MN12/13) of Inner Mongol (Qiu et al. 2013), where it is rare. It is abundant in the younger latest Miocene Ertemte fauna, but uncommon in the early Pliocene Bilike fauna (Qiu and Storch 2000). *Germanomys* and *Microtodon* have similar molar occlusal surfaces, and 3-rooted M1. However, *Microtodon atavus* from Ertemte differs in its 3-rooted M2 and M3 (Fahlbusch and Möser 2004) and its M3 structure, which in occlusal view is unlike that of the simple *Germanomys yusheica* M3. In this case the ancestor of *Germanomys* is unlikely to be *Microtodon atavus* but could be another *Microtodon*-like taxon. When and where does *Germanomys* originate (Asia or Europe), and are the European and Asian lineages separate? Did the lineages originate independently and converge morphologically as crown height increased? If they are convergent lineages, the Chinese *Germanomys* would need its own generic name. All these questions await discovery of more material.

11.5 Conclusion

Muroids of the Yushe Basin that display prismatic structure of the molars comprise two tribes, Prometheomyini and Arvicolini. Small mammal specialists currently recognize that these tribes, sometimes considered at the subfamily level, are distinct and may not form a monophyletic group. Indeed, the Prometheomyini seem to be older, originating in the late Miocene, and Yushe representatives are described here. The latest Miocene Ertemte, Inner Mongolia, fauna produces abundant remains of the primitive "microtoid" cricetid *Microtoscoptes*. We find no evidence of *Microtoscoptes* in the Miocene of Yushe Basin, but *Germanomys* appears in the basin by the early Pliocene. We discovered one undetermined, high crowned prometheomyine tooth dated to about 5.5 Ma in Yushe Basin (Fig. 11.4e).

Two time-successive species of *Germanomys* are well represented in Yushe Basin and were recognized as distinct in previous publications where we called them *Germanomys* A and B (e.g., Flynn et al. 1997). *Germanomys yusheica* sp. nov. is abundant in the upper part of the Gaozhuang Formation, 4.7 to 4.3 Ma. Although an early species, earlier than counterparts in Europe, it is already moderately derived in crown height and sinuosity of the enamel border. It is succeeded in the Mazegou Formation by the more derived *Germanomys progressiva* sp. nov. (3.5 to 3.0 Ma). The clear difference in these species coincides with the large gap in their temporal ranges and the depositional disconformity between them. They are part of the distinction between Gaozhuangian and Mazegouan faunas and may be taken as index fossils to those Land Mammal Stage/Ages.

Our study shows *Ungaromys* and *Germanomys* to be distinct genera with different features and trajectories of evolution, and argues that European *Ungaromys altenburgensis* from Deutsch-Altenburg 21, Germany, should be transferred to *Germanomys*. A few Yushe Basin fossils hint at greater prometheomyine diversity in Yushe Basin, including possible *Stachomys* in the Mazegou Formation.

Acknowledgements Many thanks are due Prof. Dr. G. Rabeder from Institute of Palaeontology, University of Vienna and Priv.-Doz. Dr. U. Göhlich, Natural History Museum of Vienna, for providing critical references. Drs. Q. Li, Y.-Q. Zhang, and S.-H. Zheng kindly reviewed the manuscript, offering many improvements. We also thank Miss H.-W. Si for improving the figures.

References

Agadjanian, A. K. (1993). A new volelike rodent (Mammalia, Rodentia) from the Pliocene of the Russian Plain. *Paleontological Journal, 27,* 126–140.

Cai, B.-Q. (1987). A preliminary report on the Late Pliocene micromammalian fauna from Yangyuan and Yuxian, Hebei. *Vertebrata PalAsiatica, 25,* 124–136 (in Chinese with English abstract).

Carls, N., & Rabeder, G. (1988). Die Arvicoliden (Rodentia, Mammalia) aus dem Älter-Pleistozän von Schernfeld (Bayern). *Beiträge zur Paläontologie von Niederösterreich, 14,* 123–237.

Çolak, E., Yiğit, N., Sözen, M., & Verimli, R. (1999). A study on morphology and karyology of *Prometheomys schaposchnikowi* Satunin, 1901 (Mammalia: Rodentia) in Turkey. *Turkish Journal of Zoology, 23,* 415–421.

Fahlbusch, V. (1987). The Neogene mammalian faunas of Ertemte and Harr Obo in Inner Mongolia (Nei Mongol), China. 5. The genus *Microtoscoptes* (Rodentia: Cricetidae). *Senckenbergiana lethaea, 67,* 345–373.

Fahlbusch, V., & Möser, M. (2004). The Neogene mammalian faunas of Ertemte and Harr Obo in Inner Mongolia (Nei Mongol), China. – 13. The genera *Microtodon* and *Anatolomys* (Rodentia, Cricetidae). *Senckenbergiana lethaea, 84,* 323–349.

Fahlbusch, V., Qiu, Z.-D., & Storch, G. (1983). Neogene mammalian faunas of Ertemte and Harr Obo in Nei Monggol, China. 1. Report on field work in 1980 and preliminary results. *Scientia Sinica, B26,* 205–224.

Fejfar, O. (1961). Die plio-pleistozänen Wirbeltierfaunen von Hajnáčka und Ivanovce (Slowakei), ČSR. II. Microtidae und Cricetidae inc. sed. *Neues Jahrbuch für Geolologie und Paläontologie, 112,* 48–82.

Fejfar, O. (1999). Microtoid cricetids. In G. E. Rössner & K. Heissig (Eds.), *The Miocene land mammals of Europe* (pp. 365–372). München: Verlag Dr. Friedrich Pfeil.

Fejfar, O., & Heinrich, W. D. (1987). Zur biostratigraphischen Gliederung des jüngeren Känozoikums in Europa an Hand von Muriden und Cricetiden (Rodentia, Mammalia). *Časopis pro mineralogii a geologii, 32,* 1–16.

Fejfar, O., & Repenning, C. A. (1998). The ancestors of the lemmings (Lemmini, Arvicolinae, Cricetindae, Rodentia) in the early Pliocene of Wölfersheim near Frankfurt am Main, Germany. *Senckenbergiana lethaea, 77,* 161–193.

Fejfar, O., & Storch, G. (1990). Eine pliozäne (ober-ruscinische) Kleinsäugerfauna aus Gundersheim, Rheinhessen—1. Nagetiere: Mammalia Rodentia. *Senckenbergiana lethaea, 71,* 139–184.

Flynn, L. J., Wu, W.-Y., & Downs, W. R. (1997). Dating vertebrate microfaunas in the late Neogene record of northern China. *Palaeogeography, Palaeoclimatology, Palaeoecology, 133,* 227–242.

Heller, F. (1936). Eine oberpliocäne Wirbeltierfauna aus Rheinhessen. *Neues Jahrbuch für Mineralogie, Geolologie, und Paläontologie, Beilagebände, B76,* 99–160.

Kormos, T. (1932). Neue Wühlmäuse aus dem Oberpliocän von Püspökfürdö. *Neues Jahrbuch für Mineralogie, Geolologie, und Paläontologie, Beilagebände, B69,* 323–346.

Kowalski, K. (1960). Cricetidae and Microtidae (Rodentia) from the Pliocene of Węże (Poland). *Acta Zoologica Cracoviensia, 5,* 447–504.

Kowalski, K. (2001). Pleistocene rodents of Europe. *Folia Quaternaria, 72,* 1–389.

Kretzoi, M. (1955). *Promimomys cor* n. gen. n. sp., ein altertümlicher Arvicolide aus dem Ungarischen Unterpleistozän. *Acta Geologica Hungarica, 3,* 89–94.

Mats, V. D., Pokatilov, S. M., Popova, A. J., Kranchynsky, N. V., Kulagina, N. V., & Shymaraeva, M. K. (1982). Pliocene and Pleistocene of middle Baikal. Academy of Sciences of the USSR, Siberian Branch, Novosibirsk (in Russian).

McKenna, M. C., & Bell, S. K. (1997). *Classification of mammals above the species level*. New York: Columbia University Press.

Mörs, T., von Königswald, W., & von der Hocht, F. (1998). Rodents (Mammalia) from the late Pliocene Reuver Clay of Hambach (Lower Rhine Embayment, Germany). *Mededelingen Nederlands Instituut voor Toegepaste Geowetenschappen TNO, 60,* 135–160.

Musser, G. G., & Carleton, M. D. (2005). Superfamily Muroidea. In D. E. Wilson & D. M. Reeder (Eds.), *Mammal species of the world: A taxonomic and geographic reference* (3rd ed., Vol. 2, pp. 956–1038). Baltimore: The John Hopkins University Press.

Ognev, S. (1926). *Prometheomys*, a remarkable rodent from the Caucasus. *Journal of Mammalogy, 7,* 215–220.

Qiu, Z.-D., & Storch, G. (2000). The early Pliocene micromammalian fauna of Bilike, Inner Mongolia, China (Mammalia: Lipotyphla, Chiroptera, Rodentia, Lagomorpha). *Senckenbergiana lethaea, 80,* 173–229.

Qiu, Z.-D., Wang, X., & Li, Q. (2013). Neogene faunal succession and biochronology of central Nei Mongol (Inner Mongolia). In X. Wang, L. J. Flynn, & M. Fortelius (Eds.), *Fossil mammals of Asia: Neogene biostratigraphy and chronology* (pp. 155–186). New York: Columbia University Press.

Rabeder, G. (1981). Die Arvicoliden (Rodentia, Mammalia) aus dem Pliozän und dem älteren Pleistozän von Niederösterreich. *Beiträge zur Paläontologie von Niederösterreich, 8,* 1–373.

Repenning, C. A. (1987). Biochronology of the microtine rodents of the United States. In M. O. Woodburne (Ed.), *Cenozoic mammals of North America: Geochronology and biostratigraphy* (pp. 236–268). Berkeley and Los Angeles: University of California Press.

Schaub, S. (1934). Über einige fossile Simplicidentaten aus China und der Mongolei. *Schweizerische Paläontologische Gesellschaft, Abhandlungen, 54,* 1–40.

Storch, G., & Fejfar, O. (1990). Gundersheim – Findling, a Ruscinian rodent fauna of Asian affinities from Germany. In E. H. Lindsay, V. Fahlbusch, & P. Mein (Eds.), *European Neogene mammal chronology* (pp. 405–412). New York: Plenum Press.

Sulimski, A. (1964). Pliocene Lagomorpha and Rodentia from Węże 1 (Poland). *Acta Palaeontologica Polonica, 9,* 149–261.

Van der Meulen, A. J. (1973). Middle Pleistocene smaller mammals from the Monte Peglia (Orvieto, Italy) with special reference to the phylogeny of *Microtus* (Arvicolidae, Rodentia). *Quaternaria, 17,* 1–144.

Zheng, S.-H., & Li, C.-K. (1986). A review of Chinese *Mimomys* (Arvicolidae, Rodentia). *Vertebrata PalAsiatica, 24,* 81–109 (in Chinese with English summary).

Zhou, X.-Y. (1988). The Pliocene micromammalian fauna from Jingle, Shanxi – a discussion of the age of Jingle Red Clay. *Vertebrata PalAsiatica, 26,* 181–197 (in Chinese with English summary).

Chapter 12
Fossil Arvicolini of Yushe Basin: Facts and Problems of Arvicoline Biochronology of North China

Ying-Qi Zhang

Abstract Six forms of arvicolines discovered from the Pliocene and Pleistocene fluvial and lacustrine deposits of the Yushe Basin and its capping loess are systematically described. Biochronological distributions are discussed in the present chapter based on their biostratigraphic occurrences in different localities and sections in North China. From the arvicoline point of view and compared to other localities and sections in North China, the correlations between faunal assemblages and paleomagnetic age calibration in the Yushe Basin are fundamentally acceptable if ruling out one conflicting occurrence of apparently younger *Mimomys gansunicus* at YS5 (late Pliocene). However, a systematic study of the dental morphology of all the existing arvicoline species and establishment of several key evolutionary lineages based on such characters are still urgently needed for the future study of fossil arvicolines, especially in the hope of establishing a more robust biochronological framework for interregional correlations.

Keywords Yushe Basin • Arvicoline biochronology • Stage of evolution • Land mammal ages • Chinese Neogene Mammal Faunal Units

12.1 Introduction

Arvicolines have a history of more than 5 million years, and a Holarctic distribution during the Late Cenozoic (Repenning et al. 1990). Among micromammals, fossil arvicolines usually draw much attention especially when chronology and biostratigraphy of continental deposits of the late Cenozoic are taken into account. This is not only owing to the facts that they have abundant fossil records and a relatively rapid evolutionary rate like other rodent taxa, but also that they display strong evolutionary trends during the Late Cenozoic, such as: (1) increasing hypsodonty; (2) appearance of crown cement; (3) increasing undulation of the linea sinuosa; (4) disappearance of enamel islet on the first lower molar; (5) reduction of roots; and (6) change of enamel band microstructure from *Mimomys*-type (negative type) to *Microtus*-type (positive type). Furthermore, some of these changes, like (3) and (6), can be quantified to demonstrate evolutionary gradualism through time. Repenning et al. (1990) stated that when combined with external age control data, it is possible to distinguish age differences as brief as 100,000 years during the past 5 million years if arvicoline history is well known in the region of concern. It is due to this merit that particular attention has been paid to fossil arvicolines, which leads to a tremendous accumulation of literature and knowledge about this group. At the same time, since the first fossil arvicoline from the Issoire region of France was referred to as *Arvicola amphibius cizae* by Croizet and Jobert in 1828 (Kretzoi 1990), an excessive nomenclature has plagued the group on a global scale, and the taxonomy is still growing, so that it is nearly impossible for every researcher or researchers from single regions to discuss the phylogeny of arvicoline species on a regional scale, or propose interregional correlations of their faunas on a panoramic global view or, more specifically, from a panoramic Holarctic view without interregional cooperation. For that reason, in this chapter, discussion of arvicoline species will focus mainly on the Chinese records.

The study of fossil arvicolines in China began with Kormos (1934), who named a right mandible with m1-3 (Teilhard de Chardin and Piveteau 1930: 123, text-Fig. 40) from Xiashagou, Nihewan as *Mimomys chinensis*. Reports on fossil arvicolines from scattered localities greatly increased thereafter (e.g., Young 1935; Pei 1939; Zheng 1976; Xue 1981; Zheng et al. 1985a, b; Zong et al. 1982; Zong 1987).

Y.-Q. Zhang (✉)
Key Laboratory of Vertebrate Evolution and Human Origins of Chinese Academy of Sciences, Institute of Vertebrate Paleontology and Paleoanthropology, Chinese Academy of Sciences, Beijing 100044, People's Republic of China
e-mail: zhangyingqi@ivpp.ac.cn

Lawrence J. Flynn and Wen-Yu Wu (eds.), *Late Cenozoic Yushe Basin, Shanxi Province, China: Geology and Fossil Mammals, Volume II: Small Mammal Fossils of Yushe Basin*, Vertebrate Paleobiology and Paleoanthropology,
DOI 10.1007/978-94-024-1050-1_12

Most of these localities have just a single fossil-bearing layer, and almost all of them lack external age controls. The comprehensive reviews on Chinese fossil arvicolines carried out by Zheng and Li (1986, 1990) established the initial arvicoline biochronological framework based on the materials described up to then. Since 1990, numerous new arvicoline-bearing fossil localities from the Pliocene and Pleistocene of China have been discovered, such as Bilike and Gaotege, Inner Mongolia (Qiu and Storch 2000; Li et al. 2003; Li 2006; Qiu and Li 2016), Lingtai, Gansu (Zheng and Zhang 2000, 2001; Zhang and Zheng 2000, 2001), and Renzidong, Anhui (Jin and Liu 2009). The Gaotege and Lingtai studies include sections with multiple arvicoline-bearing layers and paleomagnetic age control. In addition to these localities, six arvicoline-bearing layers, with tens of arvicoline specimens including several jaws were found from the Gaozhuang, Mazegou, and Haiyan formations of Yushe Basin, and these are tied directly to the composite magnetostratigraphy and lithostratigraphy of the basin (Tedford et al. 1991; Flynn et al. 1991, 1997; Flynn and Wu 2001; Tedford et al. 2013). Due to its length and continuous depositional record up to the early Pleistocene, the Yushe magnetostratigraphic record is perhaps the most reliable paleomagnetic composite for the Late Neogene of North China. Description of these specimens will contribute greatly to the establishment of the arvicoline biochronological framework in North China.

The descriptive terminology for the occlusal view of molars follows van der Meulen (1973) and Zhang et al. (2008b), and the enumeration system of Kawamura (1988) is used to describe the isthmuses. Linea sinuosa stands for the basal boundary line of the enamel on the lateral sides of molars. For the convenience and clarity of description, the terminology of Rabeder (1981) for the linea sinuosa is adopted.

12.2 Systematic Paleontology

Order Rodentia Bowdich, 1821
Family Cricetidae Gray, 1821
Subfamily Arvicolinae Gray, 1821
Tribe Arvicolini Kretzoi, 1955
Genus *Mimomys* Forsyth-Major, 1902
Type species: *Mimomys pliocaenicus* Forsyth-Major, 1902

Diagnosis: Molars rooted. Cementum absent or slight in ancestral forms, but abundant in advanced forms. Enamel islet and *Mimomys*-kante on m1 strongly developed in ancestral forms, but becoming relatively shallower or totally absent in advanced forms. Upper molars all with three roots in ancestral forms, and loss of roots occurring with the progress of evolution. Only M1 even in advanced forms retains three roots, but with the anterior two fused together. M3 with two enamel islets in ancestral forms, but the anterior one reduced in advanced forms. Linea sinuosa flat in ancestral forms, but sinuses (sinuids) rise during the progress of root loss.

Mimomys sp.

1991 *Mimomys* sp. Tedford et al., p. 524, Fig. 4
1991 *Mimomys* sp. Flynn et al., p. 251, Fig. 4; p. 256, Table 2
1997 *Mimomys* sp. Flynn et al., p. 239, Fig. 5
2001 *Mimomys* Flynn and Wu, p. 197

Stratigraphic distribution: Culiugou Member, Gaozhuang Formation, about 4.3 Ma.

Biochronology: Gaozhuangian Stage/Age.

Horizon and material: **YS4,** left m1, left M3 (V22607.1–2); **YS97,** left m1 (V22608.1).

Description: See Fig. 12.1. No cementum is seen in reentrant angles of the molars.

M3: V22607.2, the single specimen, belongs to a juvenile individual. The occlusal pattern is composed of an anterior loop, a simple and semicircular posterior loop (PL) and a small triangle between them. There are two buccal reentrant angles and one on the lingual side. The lingual reentrant angle LRA2 is conspicuously deeper and wider than the buccal ones. A feeble BSA3 appears on buccal side of the PL. The apex of BRA2 is nearly opposite to that of LRA2. An extra reentrant fold is developed on the lingual side of the posterior loop, which will separate and fade away by the necking of it at the lingual side with wear and it will form an enamel islet on the PL at about midpoint of the crown height (Fig. 12.1: B3). An enamel islet will also appear around the anterior loop by the buccal withdrawal of the apex of BRA1 at about midpoint of the whole crown height (Fig. 12.1: B2). The linea sinuosa on the lingual side is nearly flat, while that on the buccal side slightly rises at As (anterosinus). The root formation has not started yet.

m1: The two m1s from YS4 and YS97 are deeply worn, V22607.1 (Fig. 12.1A) to a much greater extent. Its enamel wall on buccal side has been almost completely worn down. There are three alternating triangles between anteroconid complex (ACC) and the posterior loop on m1. No enamel islet can be seen on the anterior cap probably because of deep wear of the teeth. The ACC is semi-rounded in outline, and no extra salient or reentrant angles are developed. A faint trace of *Mimomys*-kante can be observed on the buccal side of ACC of V22608.1 (Fig. 12.1C). The apex of LRA3 is obliquely opposite to that of BRA2. The undulation of linea sinuosa is weak, but higher positioned Hsd (hyposinuid) and Asd (anterosinuid) can be observed. The linea sinuosa undulates less on the lingual side. The tooth has two roots.

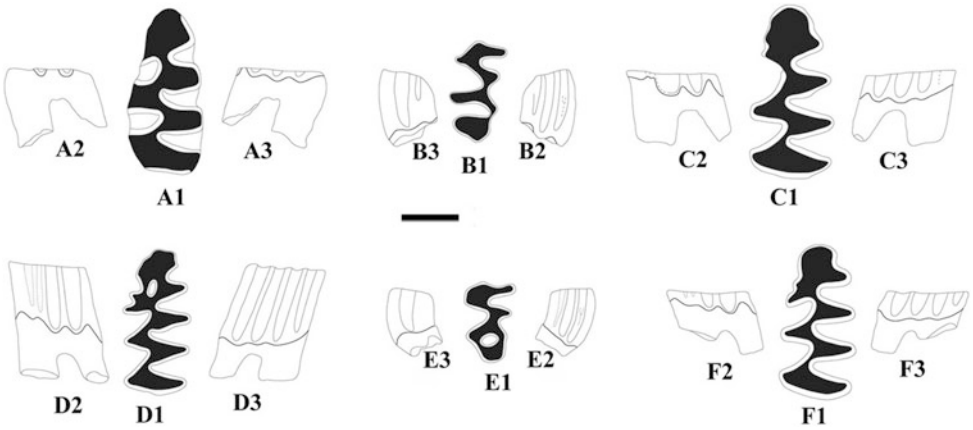

Fig. 12.1 *Mimomys* sp. from YS4 and YS97 of the Gaozhuang Formation and comparable stage of evolution in *Mimomys* sp. nov. from Gaotege, Inner Mongolia. *Mimomys* sp.: **YS4**, A. left m1 (V22607.1), B. left M3 (V22607.2); **YS97**, C. left m1 (V22608.1). *Mimomys* sp. nov.: **Gaotege**, D. left m1 (DB02-3-547), E. left M3 (DB02-2-380), F. left m1 (DB02-2-547). 1. occlusal view (mesial toward top), 2. buccal view, 3. lingual view. Scale bar = 1 mm for occlusal view, and 2 mm for lateral view

Comparisons and discussion: *Mimomys* sp. of the Culiugou Member, Gaozhuang Formation, represents a very primitive form of the genus, but there are too few specimens to make a specific identification. From the stage of evolution point of view, there are very few *Mimomys* forms comparable to *Mimomys* sp. in China. One of them is a new primitive form of *Mimomys* from the locality Gaotege, situated about 73 km southwest of Xilinhaote City, Inner Mongolia Autonomous Region. Gaotege section with an exposed thickness less than 70 m was lithologically divided into eight layers from the top down (Li et al. 2003: Fig. 2). The arvicoline materials were collected from layer 3, 4 and 5. In the faunal list of Li et al. (2003), only one arvicoline species, *Mimomys* cf. *M. bilikeensis* (=*Aratomys* cf. *A. bilikeensis*) was identified. In his doctoral dissertation, Li (2006) described three forms of arvicolines: *Mimomys* sp. nov.[1] from the same layers (DB02-5–6 and DB02-1–4) as *Mimomys* cf. *M. bilikeensis* listed by Li et al. (2003) plus one new layer (DB03-1), and *Mimomys* cf. *M. orientalis* and ?*Borsodia* sp. from a new higher layer (DB03-2). *Mimomys* sp. nov. of Gaotege shows great morphological resemblance with *Mimomys* sp. of YS4 and YS97, Gaozhuang Formation. The magnetostratigraphic study by Xu et al. (2007) constrained the age of DB02-5–6 of layer 3 to 4.38 Ma, the age of DB02-1–4 of layer 4 to 4.34 Ma, and DB03-1 of layer 5 to 4.15 Ma. Combined with Xu et al. (2007), O'Connor et al. (2008) also correlated the Gaotege section with Chrons C2Ar to C3n.2n (3.6–4.6 Ma). So *Mimomys* sp. nov. of Gaotege is chronologically equivalent with *Mimomys* sp. of the Yushe Gaozhuang Formation.

Teeth of *Mimomys* sp. nov. of Gaotege show morphological similarity to *Mimomys* sp. of Gaozhuang Formation (Fig. 12.1). The linea sinuosas of both forms show nearly the same level of undulation on m1 and M3. The apices of LRA3 and BRA2 on m1 of both forms are similarly obliquely opposite to each other. M3 of both has two enamel islets. All these similarities demonstrate a comparable stage of evolution in the genus *Mimomys*. However, *Mimomys*-kante (Fig. 12.1: D, F) and enamel islet (Fig. 12.1: D) are clearly developed on m1 of *Mimomys* sp. nov. These characters cannot be observed on m1 of the Gaozhuang *Mimomys* sp., given the deep wear of the two m1s. Furthermore, LRA4 and BRA3 on m1 of *Mimomys* sp. are not as distinctly developed as in *Mimomys* sp. nov. from Gaotege, which is also probably due to the deep wear of the two m1s of *Mimomys* sp. Because V22608.1 and DB02-2-547 (Fig. 12.1: C, F) are at similar levels of deep wear, *Mimomys* sp. looks somewhat more primitive based on the ACC morphology.

Mimomys cf. *M. youhenicus* Xue, 1981

1991 *Mimomys* cf. *M. orientalis* Tedford et al., p. 524, Fig. 4 (part)

1991 *Mimomys orientalis* Flynn et al., p. 251, Fig. 4; p. 256, Table 2 (part)

1997 *Mimomys irtyshensis* Flynn et al., p. 239, Fig. 5 (part)

2001 *Mimomys irtyshensis* Flynn and Wu, p. 197 (part)

[1]During final preparation of this volume, Qiu and Li (2016) published a monograph on Neogene rodents from Central Nei Mongol. Therein, two of the three forms from Gaotege, *Mimomys* sp. nov. and ?*Borsodia* sp. were officially established as new species *Mimomys teilhardi* and *Borsodia mengensis*, respectively. *Mimomys* cf. *M. orientalis* was determined as *Mimomys orientalis*. Here usage of *Mimomys* sp. nov. and *Mimomys* cf. *M. orientalis* is retained for the two Gaotege *Mimomys*, without further discussion, to avoid delay in publication of this volume.

Holotype: 75-WEI①-1.1, a right m1 of a young individual

Type locality: Youhe, Weinan, Shaanxi

Stratigraphic distribution: Mazegou Formation, Yushe Basin, about 3.0 Ma.

Biochronology: Mazegouan Stage/Age.

Horizon and material: **YS99**: right M1 (V22609.1), right M2 (V22609.2), broken left mandible with m1-2 (V22609.3); **YS105**: left M1 (V22610.1), see Fig. 12.2.

Description: The two M1s underwent moderate (V22610.1, Fig. 12.2C) and deep wear (V22609.1, Fig. 12.2B). Their occlusal pattern comprises four alternating triangles behind the anterior loop. The dentine field is separated at every isthmus; all isthmuses are equally closed. Cementum can be observed on all the reentrant angles of V22610.1, but not on V22609.1. Prs (protosinus) of lingual linea sinuosa rises very high and penetrates through the crown on both specimens. The buccal linea sinuosa also

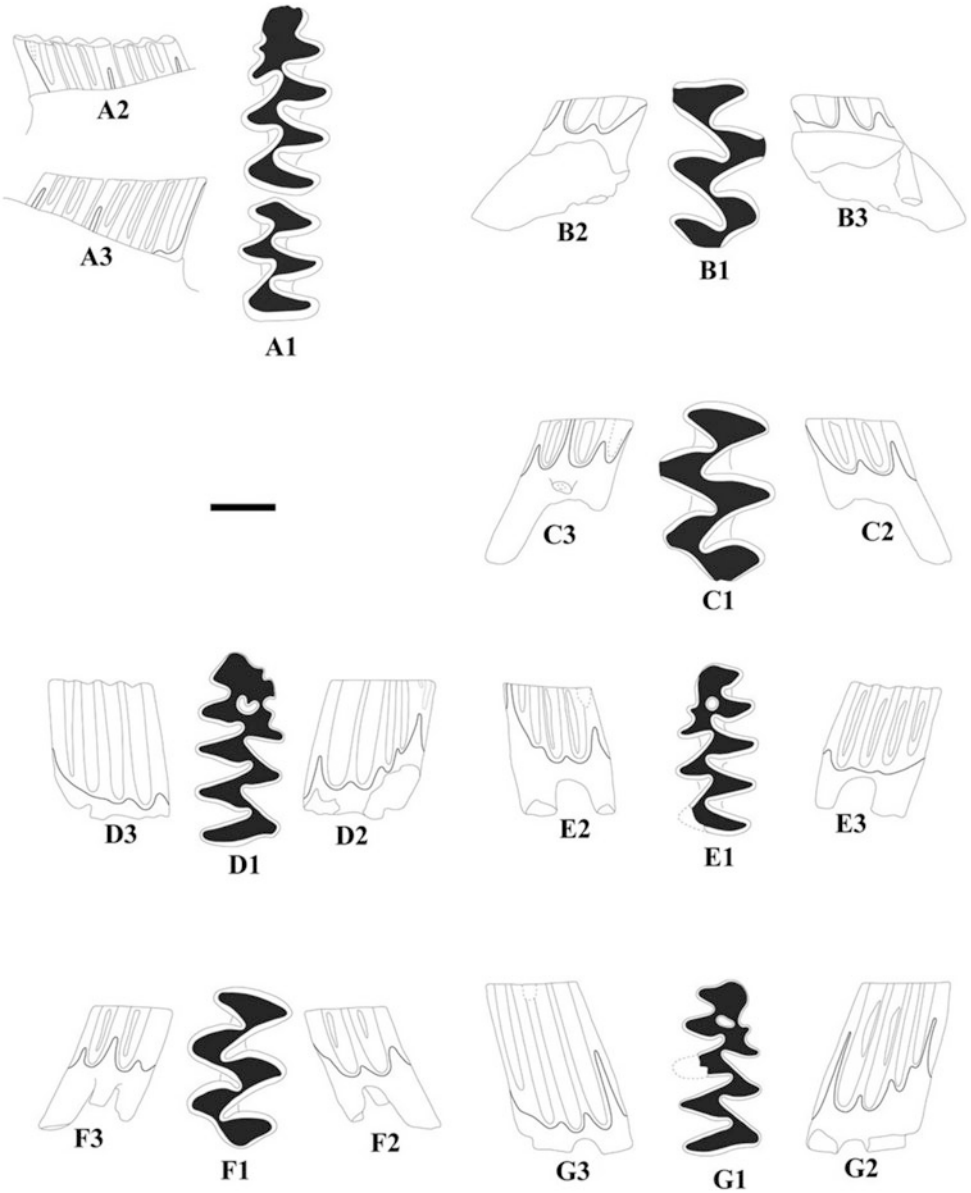

Fig. 12.2 *Mimomys* cf. *M. youhenicus* from YS99 and YS105 of the Mazegou Formation compared with *Mimomys orientalis* and *Mimomys youhenicus* from Youhe, Weinan, Shaanxi, and *Mimomys* cf. *M. orientalis* from Gaotege, Inner Mongolia. *Mimomys* cf. *M. youhenicus*: **YS99**, A. broken left mandible with m1-2 (V22609.3), B. right M1 (V22609.1); **YS105**, C. left M1 (V22610.1). *Mimomys orientalis*: **Youhe**, D. right m1 (75-WEI①-1.4). *Mimomys youhenicus*: **Youhe**, G. right m1 (75-WEI①-1.1). *Mimomys* cf. *M. orientalis*: **Gaotege**: E. left m1 (DB03-2-Li200705-03), F. left M1 (DB03-2-008). 1. occlusal views (mesial toward top), 2. buccal view, 3. lingual view. Scale bar = 1 mm for occlusal view, and 2 mm for lateral view

penetrates through the crown of the more worn V22609.1, but Asl (anterosinulus) of lingual linea sinuosa positions below the occlusal surface. On V22610.1, both Asl and As rise high towards the occlusal surface but do not penetrate the crown with the former lower than the latter. The roots of V22609.1 are preserved in a small piece of maxillary fragment, and it is certain that both specimens have three independent roots.

m1: The only m1 belongs to the broken mandible (V22609.3), which has been moderately worn. There are three alternating triangles between ACC and the posterior loop. No enamel islet can be seen on the anterior cap probably due to deep wear. *Mimomys*-kante is conspicuously developed. The development of LRA4 on lingual side of the anterior cap is also prominent. The apex of LRA3 is obliquely opposite that of BRA2 and slightly anteriorly positioned. The isthmus IS3 is slightly wider than IS1, 2, and 4. Cementum is abundantly deposited in all the reentrant angles behind the anteroconid complex. Hsd of buccal linea sinuosa and Hsld (hyposinulid) of lingual linea sinuosa rise high above the alveolus level, but do not penetrate the crown.

m2: The single moderately worn m2 also belongs to the broken mandible (V22609.3). There are four alternating triangles in front of the posterior loop. T1 and T2 are semi-confluent with each other. Dimensions of lower and upper molars are given in Tables 12.1 and 12.2 for comparison.

Mandible: The ascending ramus and angular process of the left mandible (V22609.3) are broken. The anterior part of the incisor is not preserved. The mental foramen is small and situated antero-inferiorly to m1. The lower masseteric crest is stout and originates from a position about 0.5 mm posterior to the mental foramen. The crest is slightly convex ventrally. The upper masseteric crest runs parallel to the remnant anterior edge of the ascending ramus and connects to the lower masseteric crest by an acute angle somewhat below BRA1 of m1. The anterior edge of the ascending ramus originates from the position beside the posterior loop of m1. The internal temporal fossa between the ascending ramus and the alveoli of the molars is shallow.

Comparisons and discussion: *Mimomys youhenicus* was established by Xue (1981) based on twelve specimens, including four right m1, collected from greenish deposits, the "Youhe Formation" of the lower reach of the You River, Weinan, Shaanxi Province. Zheng and Li (1986) reclassified one m1 of the *Mimomys youhenicus* type collection, 75-WEI①-1.4, as *Mimomys orientalis*, a species established

Table 12.1 Measurements (mm) for lower molars of arvicoline species of Yushe Basin

Species	Loc.	m1			m2			m3		
		No.	L	W	No.	L	W	No.	L	W
Mimomys sp.	YS4	V22607.1	2.96	1.38						
	YS97	V22608.1	3.12	1.52						
Mimomys cf. *M. youhenicus*	YS99	V22609.3	2.96	1.41	V22609.3	1.94	1.31			
Mimomys gansunicus	YS5	V22611.6	3.28	1.44	V22611.6	2.04	1.29	V22611.6	1.68	0.99
		V22611.7	2.67+	1.40	V22611.7	2.04	1.40	V22611.7	1.65	0.99
		V22611.8	2.81	1.43	V22611.8	1.88	1.30	V22611.8	1.72	1.03
		V22611.9	2.89	1.44	V22611.9	1.92	1.27			
		V22611.10	3.24	1.45	V22611.10	2.03	1.30			
		V22611.12	2.53	1.16						
		V22611.13	2.65	1.23						
	YS6							V22612.2	1.39	0.92
	YS120	V22613.6	2.86	1.31				V22613.9	1.40	0.87
		V22613.7	2.75	1.16				V22613.10	1.42	0.88
		V22613.8	2.71	1.37				V22613.11	1.47	0.86
Villanyia fanchangensis	YS6	V22616.2	2.42-	1.12						
		V22616.3	2.50	1.06						
	YS120							V22617.2	1.15	0.64
	YS109							V22618.4	1.50	0.96
								V22618.5	1.39	0.83
Borsodia chinensis	YS120				V22620.15	1.48	0.92	V22620.16	1.49	0.83
		V22620.12	2.53+	1.21	V22620.19	1.59	0.99	V22620.17	1.40	0.74
		V22620.13	2.42	1.01				V22620.18	1.35	0.72
								V22620.20	1.44	0.75
Microtus cf. *M. complicidens*	YS123	V22622.1	2.27	1.07						

Table 12.2 Measurements (mm) for upper molars of arvicoline species of Yushe Basin

Species	Loc.	M1			M2			M3		
		No.	L	W	No.	L	W	No.	L	W
Mimomys sp.	YS4							V22607.2	1.83	1.03
Mimomys cf. *M. youhenicus*	YS99	V22609.1	2.64	1.52						
	YS105	V22610.1	2.80	1.80						
Mimomys gansunicus	YS5	V22611.1	2.79	1.60	V22611.1	2.08	1.37	V22611.4	1.83	0.99
					V22611.3	1.81	1.27	V22611.5	1.63	0.95
	YS6	V22612.3	2.26	1.40	V22612.1	1.85	0.81			
	YS120	V22613.1	2.69	1.64	V22613.3	1.86	1.18	V22613.4	1.87	1.03
		V22613.2	2.55	1.60				V22613.5	1.72	0.97
Villanyia fanchangensis	YS6				V22616.1	1.67	1.11			
	YS120				V22617.1	1.88	0.97			
	YS109				V22618.1	1.81	1.12	V22618.2	1.68	0.86
								V22618.3	1.34	0.78
Borsodia chinensis	YS6							V22619.1	1.47	0.85
	YS120				V22620.1	1.88	1.09	V22620.5	1.53	0.80
					V22620.2	1.88	1.03	V22620.6	1.47	0.76
					V22620.3	1.88	1.08	V22620.7	1.49	0.84
					V22620.4	1.73	1.03	V22620.8	1.23	0.80
								V22620.9	1.53	0.79
								V22620.10	1.62	0.79

by Young (1935), but the type specimen of which was missing. Comparison between 75-WEI①-1.1 (Fig. 12.2G), which is taken as the type specimen of *Mimomys youhenicus*, and 75-WEI①-1.4 (Fig. 12.2D) shows that there are, indeed, conspicuous morphological differences from the stage of evolution point of view. The linea sinuosa of the former (Fig. 12.2:G2, G3) rises much higher than the latter (Fig. 12.2:D2, D3). There are several extra secondary folds on the anterior cap of 75-WEI①-1.4 (Fig. 12.2:D1), but not on that of 75-WEI①-1.1 (Fig. 12.2:G1). There is very little cementum deposited in BRA1 and BRA2 of 75-WEI①-1.1 (Fig. 12.2:G2), but no cementum can be seen in any of the reentrant angles of 75-WEI①-1.4 (Fig. 12.2:D2, D3). Because Xue (1981) provided no detailed information about the stratigraphic distribution of the type collection, there is the possibility that 75-WEI①-1.1 and 75-WEI①-1.4 came from different stratigraphic layers. Because 75-WEI①-1.4 holds some primitive characters, it is possible that the m1 came from a lower stratigraphic layer than 75-WEI①-1.1. Zheng and Li (1986) also referred some other specimens from Yushe to *Mimomys orientalis*. However, there are no absolute age constraints for these specimens except faunal correlations based on stage of evolution. *Mimomys* cf. *M. youhenicus* from YS99 and YS105 of the Mazegou Formation described here represents a species comparable to *Mimomys youhenicus* based on stage of evolution. Although half covered by alveoli, the linea sinuosa of m1 of *Mimomys* cf. *M. youhenicus* (V22609.3, Fig. 12.2: A2, A3) shows a similar extent of rise towards the occlusal surface at major sinuids as the type specimen of *Mimomys youhenicus* (75-WEI①-1.1, Fig. 12.2: G2, G3). *Mimomys*-kante is equally developed on both specimens, but V22609.3 has much more cementum deposited in every reentrant angle behind ACC than 75-WEI①-1.1. Differing from 75-WEI①-1.1, enamel islet is not seen on ACC of the m1 of V22609.3, but this is possibly because it has been worn away. There is no M1 in the type collection of *Mimomys youhenicus*. However, Li (2006) identified one arvicoline form from layer DB03-2 as *Mimomys* cf. *M. orientalis*. That m1 morphology (Fig. 12.2: E) resembles that of *Mimomys orientalis* (75-WEI①-1.4, Fig. 12.2: D) very much not only in the aspect of the extent of linea sinuosa undulation, but also in ACC morphology (enamel islet, *Mimomys*-kante). Comparison of M1 between *Mimomys* cf. *M. youhenicus* of Mazegou Formation (Fig. 12.2: B, C) and *Mimomys* cf. *M. orientalis* of Gaotege (Fig. 12.2: F) shows that there are no distinct differences in the morphology of the occlusal surface. All have three independent roots. The only conspicuous difference between them is the linea sinuosa morphology, which rises higher at major sinuses of *Mimomys* cf. *M. youhenicus* than *Mimomys* cf. *M. orientalis*. It may be inferred that *Mimomys* cf. *M. youhenicus* of the Mazegou Formation represents a morphologically more advanced form than *Mimomys orientalis*, but comparable to *Mimomys youhenicus* based on these comparisons.

Mimomys gansunicus Zheng, 1976

1991 *Cromeromys gansunicus* Tedford et al., p. 524, Fig. 4

1991 *Mimomys* cf. *M. orientalis* Tedford et al., p. 524, Fig. 4 (part)

1991 *Cromeromys gansunicus* Flynn et al., p. 251, Fig. 4; p. 256, Table 2

1991 *Mimomys orientalis* Flynn et al., p. 251, Fig. 4; p. 256, Table 2 (part)

1997 *Cromeromys gansunicus* Flynn et al., p. 239, Fig. 5

1997 *Mimomys irtyshensis* Flynn et al., p. 239, Fig. 5 (part)

2001 *Cromeromys gansunicus* Flynn and Wu, p. 197

2001 *Mimomys irtyshensis* Flynn and Wu, p. 197 (part)

Holotype: V4765, right m1 of an adult individual.

Type locality: Jingou, Hesui, Gansu.

Stratigraphic distribution: Mazegou Formation (YS5, about 3.4 Ma) and Haiyan Formation (YS6, YS109, YS120), 2.5–2.2 Ma, Yushe Basin.

Biochronological distribution: Mazegouan and Nihewanian Stage/Ages.

Horizon and newly referred material: **YS5**: broken maxilla with left M1-2 and right M2 (V22611.1), right M1, left M2, left M3, right M3 (V22611.2-5), broken right mandible with m1-3 (V22611.6), broken left mandible with m1-3 (V22611.7), broken right mandible with m1-3 (V22611.8), broken right mandible with m1-2 (V22611.9), broken left mandible with m1-2 (V22611.10), two left m1 and right m1 (V22611.11-13); **YS6**: right M2 (V22612.1), right m3 (V22612.2), right m2 (V22612.3); **YS120**: left and right M1 (V22613.1-2), left M2 (V22613.3), two left M3 (V22613.4-5), two right m1 and left m1 (V22613.6-8), two left m3 and right m3 (V22613.9-11); **YS109**: broken left m1 (V22614.1). See Figs. 12.3 and 12.4.

Description: There is plentiful cementum in all reentrant angles of the molars. Both walls of all triangles are seemingly posteriorly curved on lower molars, and anteriorly curved on upper molars. The linea sinuosa is of *Mimomys* type. Usually, on lower molars, the sinuids Hsd, Hsld and Asd rise towards the occlusal surface so high that they will penetrate the whole crown at a relatively early stage of tooth wear, which makes the enamel bands interrupted at the apices of BSA1, LSA1 and anterior ends of molars in occlusal view. On upper molars, the sinuses As, Asl and Ds show the same effect.

M1: The occlusal pattern of M1 comprises four alternating triangles behind the anterior loop. The dentine field is completely separated at all isthmuses. Besides the usual high positioned sinuses As, Asl and Ds, Prs is also very high and usually interrupts the enamel band at the apex of LSA2 in occlusal view. V22613.1 and V22613.2 have three roots, but the anterior two are nearly completely fused together (Fig. 12.4D, E). The situation for the M1 of V22611.1 is unclear because the tooth is still held in its alveolus.

M2: There are three alternating triangles behind the anterior loop. Among all the salient angles, BSA1 looks slimmer and LSA2 more blunt than the others. The dentine field is separated at all the isthmuses. The tooth has two roots.

M3: The occlusal pattern of M3 is basically composed of an anterior loop, a posterior loop and two triangles (T2 and T3) between them. There are always two buccal reentrant angles (BRA1, 2), and one, sometimes two (Fig. 12.3: C; Fig. 12.4: H) reentrant angles on the lingual side. Salient angles are always three and two on buccal and lingual sides, respectively. On some specimens, BSA3 is very pointed (Fig. 12.3: C, D), but blunt on the others. BSA1 looks much slimmer than the other salient angles. LSA2 is comparatively robust and blunt. The apex of BRA2 is distinctly posterior to that of LRA2. An enamel islet appears on the posterior loop but will be worn away after the roots are formed. There is no enamel island developed around the anterior loop, so IS2 is nearly closed. All the specimens have two roots.

m1: There are three alternating triangles between ACC and the posterior loop. No enamel islet can be observed on any specimen, even on the very young individual (Fig. 12.4: J). The anterior cap is usually lingually pointed on younger individuals. An extra feeble salient angle, or the so-called *Mimomys*-kante, can be observed on some specimens (Fig. 12.3: G, I, K; Fig. 12.4: J). This extra salient angle is located far away from the apex of BSA3, which makes it more like an independent salient angle than a normal *Mimomys*-kante. LRA4 is very deep on most specimens, but much shallower than the reentrant angles behind the anterior loop. BRA3 is broad and shallow. The apex of LRA3 is located in front of that of BRA2. Dentine IS1-4 are equally closed. All the specimens have two roots.

m2: There are four alternating triangles in front of the posterior loop. T1 and T2 are separated from each other. T3 and T4 are semi-confluent with each other, which means that the dentine isthmuses IS1-3 are closed, but IS4 is widely open. Two roots occur on this tooth.

m3: There are four alternating triangles in front of the posterior loop. T1-T2 and T3-T4 are semi-confluent with each other, respectively. As a result, IS1 and 3 are closed, while IS2 and 4 are widely open. Buccal triangles are distinctly smaller than lingual ones. There are two roots.

Comparisons and discussion: *Mimomys gansunicus* was established by Zheng (1976) based on materials from Hesui,

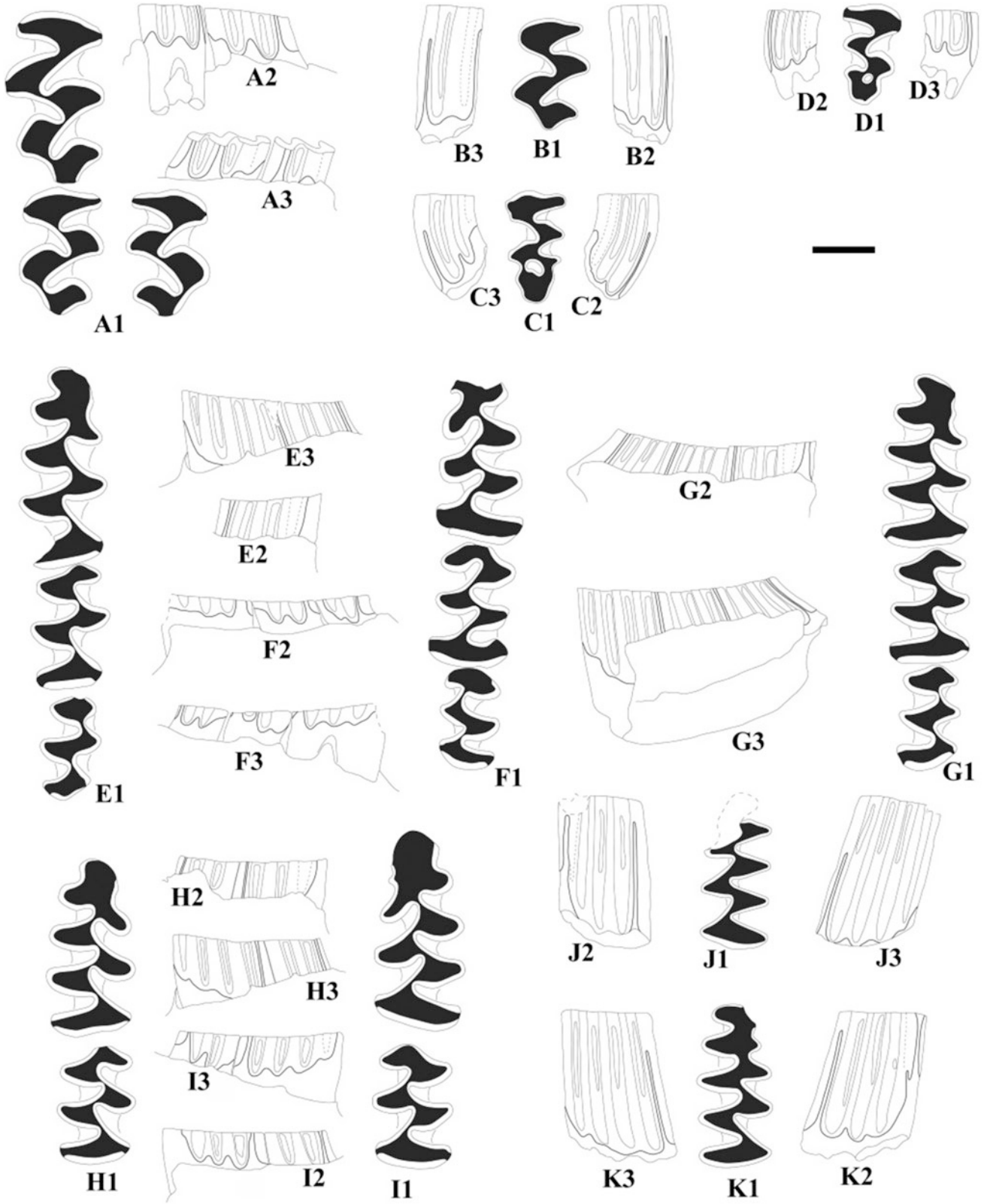

Fig. 12.3 *Mimomys gansunicus* form YS5 of the Mazegou Formation. A. broken maxilla with left M1-2 and right M2 (V22611.1), B. left M2 (V22611.3), C. left M3 (V22611.4), D. right M3 (V22611.5), E. broken right mandible with m1-3 (V22611.6), F. broken left mandible with m1-3 (V22611.7), G. broken right mandible with m1-3 (V22611.8), H. broken right mandible with m1-2 (V22611.9), I. broken left mandible with m1-2 (V22611.10), J. left m1 (V22611.12), K. right m1 (V22611.13). 1. occlusal views (mesial toward top), 2. buccal view, 3. lingual view. Scale bar = 1 mm for occlusal views, and 2 mm for lateral views

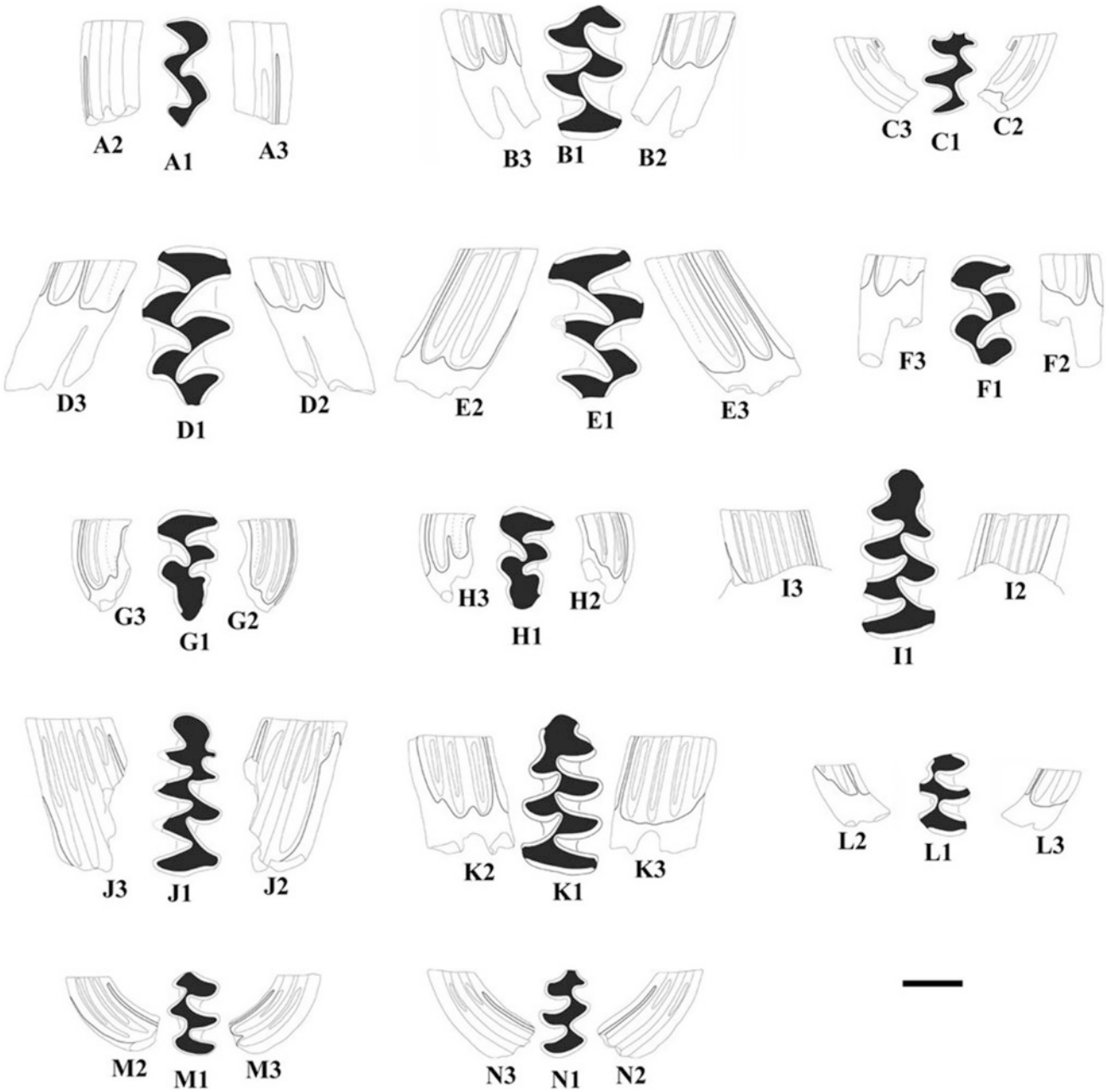

Fig. 12.4 *Mimomys gansunicus* from YS6, and YS120, Haiyan Formation. **YS6**: A. right M2 (V22612.1), B. right m2 (V22612.3), C. right m3 (V22612.2); **YS120**: D. left M1 (V22613.1), E. right M1 (V22613.2), F. left M2 (V22613.3), G. left M3 (V22613.4), H. left M3 (V22613.5), I. right m1 (V22613.6), J. right m1 (V22613.7), K. left m1 (V22613.8), L. left m3 (V22613.9), M. left m3 (V22613.10), N. right m3 (V22613.11). 1. occlusal views (mesial toward top), 2. buccal view, 3. lingual view. Scale bar = 1 mm for occlusal view, and 2 mm for lateral view

Gansu Province. Zheng and Li (1986) re-described the type collection and provided more detailed morphological definition for the species. The morphology of the specimens from YS5 of the Mazegou Formation and YS6, YS120 and YS109 of the Haiyan Formation described above coincides with the description of the type collection by Zheng (1976) and Zheng and Li (1986), especially the type specimen (V4765, Fig. 12.5: A): weak *Mimomys*-kante, plentiful cementum in all reentrant angles, M1 with three roots, high-rising linea sinuosa and so on. So it is reasonable to refer these specimens to *Mimomys gansunicus*.

Besides the type collection, abundant fossil material of this species has been discovered from localities 93001 and 72074(4) of Lingtai, Gansu Province (Zheng 1994; Zheng and Zhang 2000, 2001; Zhang and Zheng 2000, 2001;

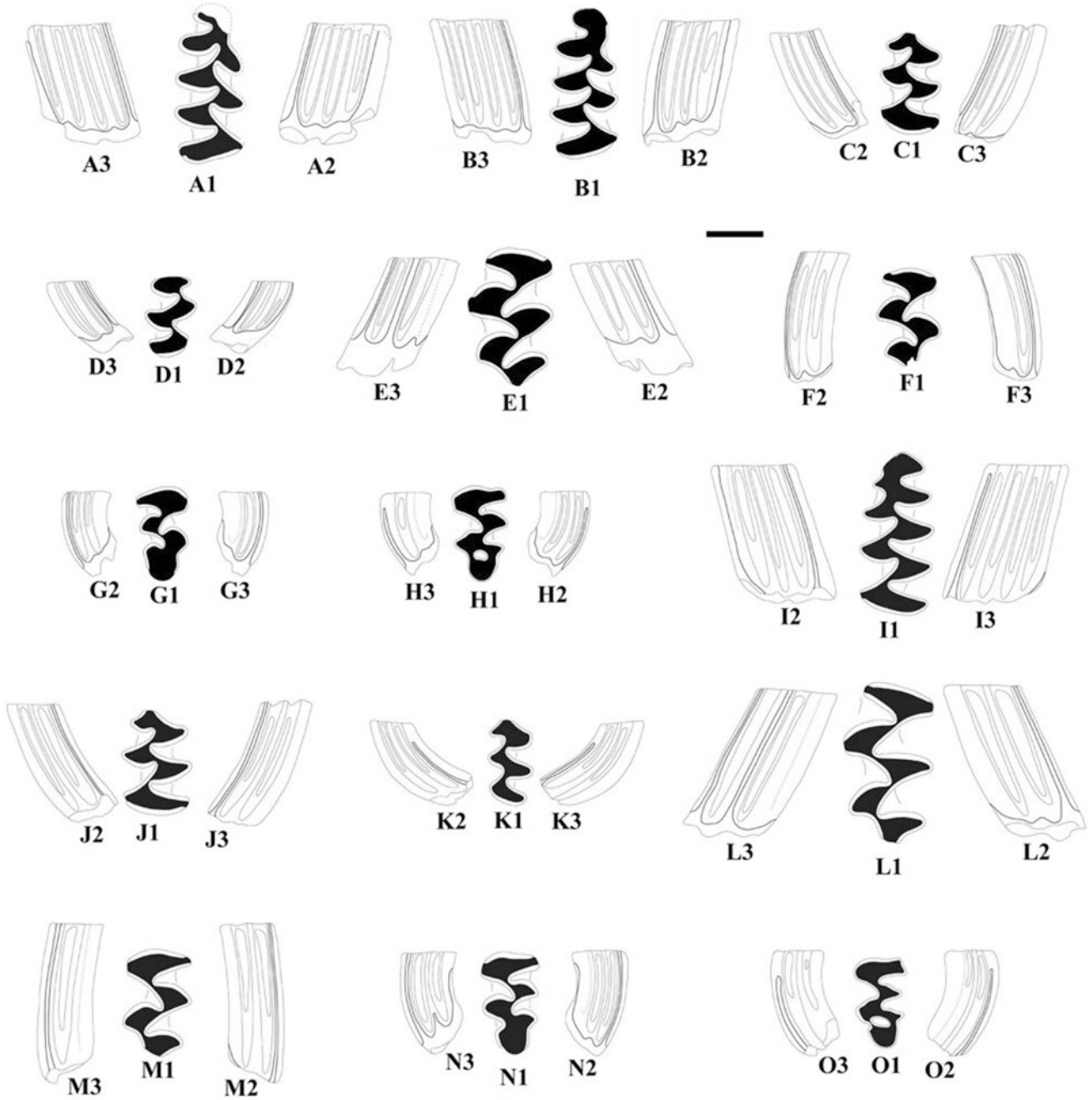

Fig. 12.5 *Mimomys gansunicus* from Jingou, Hesui and Locality 93001, Lingtai, Gansu and Renzidong Cave, Fanchang, Anhui. **Hesui**: A. right m1 (V4765, TYPE); **Loc. 93001**: B. right m1 (V18076.105, WL8), C. left m2 (V18076.10, WL11), D. right m3 (V18076.1, WL15), E. left M1 (V18076.90, WL8), F. right M2 (V18076.41, WL10), G. right M3 (V18076.68, WL10), H. left M3 (V18076.101, WL8); **Renzidong**: I. left m1 (V13990.97), J. left m2 (V13990.213), K. left m3 (V13990.368), L. left M1 (V13990.454), M. left M2 (V13990.655), N., O. left M3 (V13990.791, V13990.810). 1. occlusal views (mesial toward top), 2. buccal view, 3. lingual view. Scale bar = 1 mm for occlusal view, and 2 mm for lateral view

Zhang et al. 2011) and Renzidong Cave, Fanchang, Anhui Province (Jin et al. 2000; Jin and Liu 2009).

Zheng and Zhang (2000) reported the comprehensive biostratigraphic study of the 93001 section. Paleomagnetic correlation of the section was based on the magnetostratigraphic study of Wei et al. (1993), and new chronological interpretation was given owing to the fact that there is a big hiatus in the section. Zheng and Zhang (2001) combined the three sections, 93001, 93002 and 72074(4), into one composite biostratigraphy based on biological and stratigraphic principles, and perceived six biozones. All the *Mimomys gansunicus* layers fell into Zone V, to which the time

interval 3.6–2.6 Ma was assigned. Zhang et al. (2011) described the arvicoline materials from 93001 and 72074(4) sections and found that the stratigraphic distribution of *Mimomys gansunicus* was not limited to Zone V of the composite section proposed by Zheng and Zhang (2001), and the first appearance of *Mimomys gansunicus* in 93001 section was actually in WL15, which would represent Zone III of the composite biostratigraphic section and chronologically correlated to the upper part of the Gaozhuang Formation by Zheng and Zhang (2001). Jin et al. (2000) listed more than 67 forms of mammals from Renzidong Cave and thought the age of the site fell into the interval between 2.0 and 2.4 Ma based on faunal correlation. Jin and Liu (2009) later suggested it was more appropriate to restrict the age of Renzidong fauna to about 2.0 Ma. There are several hundreds of *Mimomys gansunicus* teeth unearthed from the cave deposits of this site.

There is only one right m3 (Fig. 12.5: D) from WL15 of 93001 section, and all the other *Mimomys gansunicus* specimens are from WL11, WL10 and WL8, which are confined to Zone V of the composite biostratigraphic section. The right m3 from WL15 shows no distinct morphological differences compared with those from YS5 of the Mazegou Formation (Fig. 12.3: E, F, G) and those from YS6, YS120 and YS109 of the Haiyan Formation. All other teeth of the Mazegou Formation and the Haiyan Formation (Figs. 12.3 and 12.4) also display almost identical stage of evolution and similar morphology of occlusal surface and linea sinuosa comparable to those of site 93001 (Fig. 12.5: B–H) and those of Renzidong Cave (Fig. 12.5: I–O), e.g. all M1 s have two roots, very high-rising linea sinuosa penetrating the crown before or around root formation, plentiful cementum, and so on. The two M3 s (Fig. 12.3: C, D) from YS5 of the Mazegou Formation both have a long-lasting posterior enamel islet, while the two younger M3 s from the Haiyan Formation (Fig. 12.4: G, H) both lack a posterior enamel islet even at similar extent of wear. Both morphotypes are seen in the M3 from both 93001 section (Fig. 12.5: G, H) and Renzidong Cave (Fig. 12.5: N, O). It is reasonable to consider the existence of a posterior enamel islet on M3 as variation within the species and not a significant morphological difference. The same consideration applies to the existence of a feeble *Mimomys*-kante on ACC of m1. There are several m1 from the Mazegou Formation (Fig. 12.3: G, K, I) and the Haiyan Formation (Fig. 12.4: J) that have a feeble *Mimomys*-kante variously developed on ACC. Two morphotypes can be observed in the Renzidong *Mimomys gansunicus* collection (Fig. 12.5: I, morphotype with feeble *Mimomys*-kante). This would also be considered a variation without significance.

Genus *Villanyia* Kretzoi, 1956

Type species: *Villanyia exilis* Kretzoi, 1956

Diagnosis: Rooted vole with cementless molars; M1 with three roots; M2 with three roots in primitive species, but with two roots in advanced species; M3 with one or two enamel islets, of which the anterior one tends to be reduced in advanced species; posterior loop of M3 short and broad; m1 without enamel islet; *Mimomys*-kante present in primitive species; enamel band differentiation quotient (SDQ) close to or more than 100; posterior root of M2 sits on the incisor in primitive species, but shifted to its buccal side in advanced species.

Villanyia fanchangensis Zhang et al., 2008

1991 *Borsodia chinensis* Tedford et al., p. 524, Fig. 4 (part)

1991 *Mimomys* cf. *M. orientalis* Tedford et al., p. 524, Fig. 4 (part)

1991 *Borsodia chinensis* Flynn et al., p. 251, Fig. 4; 256, Table 2 (part)

1991 *Mimomys orientalis* Flynn et al., p. 251, Fig. 4; p. 256, Table 2 (part)

1997 *Borsodia chinensis* Flynn et al., p. 239, Fig. 5 (part)

1997 *Mimomys irtyshensis* Flynn et al., p. 239, Fig. 5 (part)

2001 *Mimomys irtyshensis* Flynn and Wu, p. 197 (part)

2001 *Borsodia chinensis* Flynn and Wu, p. 197 (part)

Holotype: V13991, a left mandible with incisor and m1-3

Type locality: Layer 3–4 of Renzidong Cave, Fanchang, Anhui

Stratigraphic distribution: Mazegou Formation (YS5, about 3.4 Ma) and Haiyan Formation (YS6, YS109, YS120), 2.5–2.2 Ma, Yushe Basin.

Biochronology: Mazegouan and Nihewanian Stage/Ages.

Horizon and newly referred material: **YS5**: broken right M3 (V22615.1); **YS6**: right M2 (V22616.1), two left m1 (V22616.2, 3); **YS120**: right M2 (V22617.1), left m3 (V22617.2); **YS109**: left M2 (V22618.1), two right M3 (V22618.2, 3), left m3 (V22618.4), right m3 (V22618.5). See Fig. 12.6.

Description: Medium-size. There is no cementum in reentrant angles of the molars. The linea sinuosa is of typical *Mimomys*-type. Usually, on lower molars, the sinuids Hsd, Hsld, and Asd rise so high that they will penetrate the whole crown before or right after the roots are formed, which makes the enamel bands interrupted at the apices of BSA1, LSA1 and anterior end in occlusal view, respectively, and on upper molars, the sinuses As, Asl and Ds act in the same way. Both walls of all the triangles are straight and uncurved.

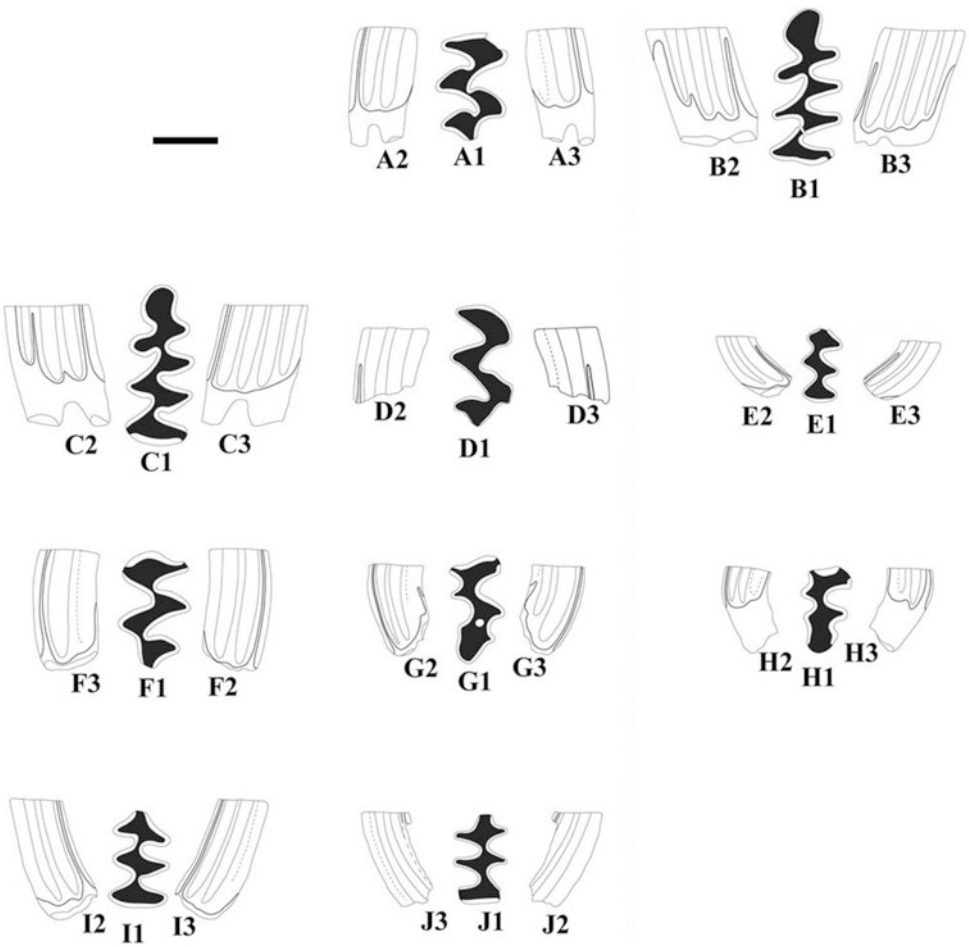

Fig. 12.6 *Villanyia fanchangensis* from YS5 of the Mazegou Formation, and YS6, YS120 and YS109 of the Haiyan Formation. **YS6**: A. right M2 (V22616.1), B. left m1 (V22616.2), C. left m1 (V22616.3); **YS120**: D. right M2 (V22617.1), E. left m3 (V22617.2); **YS109**: F. left M2 (V22618.1), G. right M3 (V22618.2), H. right M3 (V22618.3), I. left m3 (V22618.4), J. right m3 (V22618.5). 1. occlusal views (mesial toward top), 2. buccal view, 3. lingual view. Scale bar = 1 mm for occlusal view, and 2 mm for lateral view

M2: The occlusal pattern comprises three alternating triangles behind the anterior loop. BSA1 usually looks slimmer than the other salient angles. On some specimens, the anterior wall of AL is sometimes concave on its buccal side. On some teeth, the anterior wall of T3 is nearly parallel to the posterior wall of T2, so T3 and T2 are completely confluent and make a parallelogram (Fig. 12.6F). On the teeth of older or younger individuals, however, the two walls are not parallel. All specimens have two roots.

M3: The occlusal pattern comprises two alternating triangles (T2 and T3) between the anterior and posterior loop. No enamel islet can be observed on the anterior loop of the two specimens from YS109, where BRA1 is very shallow and the anterior loop is widely confluent with T2. The anterior wall of the anterior loop is somewhat concave. LSA2 is relatively robust and blunt. The isthmus between T2 and T3 is nearly closed. T3 and the posterior loop are confluent, and form a large dentine field, which accommodates the posterior enamel islet on the much younger specimen V22618.2 (Fig. 12.6:G). LSA3 is well developed, but LRA3 is shallow and feeble. BSA3 is also indistinct. The two roots of V22618.3 (Fig. 12.6:H) are fused together.

m1: The occlusal pattern comprises five alternating triangles between the anterior cap and the posterior loop. The anterior cap is simple and rounded in shape, without enamel islet. LRA4 is much shallower than the other lingual reentrant angles. The isthmus between the anterior cap and T5 is broad, which makes ACC trilobed in shape. T5 and T4 are obliquely opposite to and confluent with each other. There is no *Mimomys*-kante developed on the anterior wall of T4. The apices of LRA3 and BRA2 are obliquely opposite to each other and IS4 is nearly closed. The IS2 is distinctly wider than IS1, 3, and 4. Two roots.

m3: The occlusal pattern comprises three dentine fields. T4 and T3 are opposite to each other in position, and completely confluent to form a rhombus. T2 and T1 are also opposite and confluent to form the middle field with a more

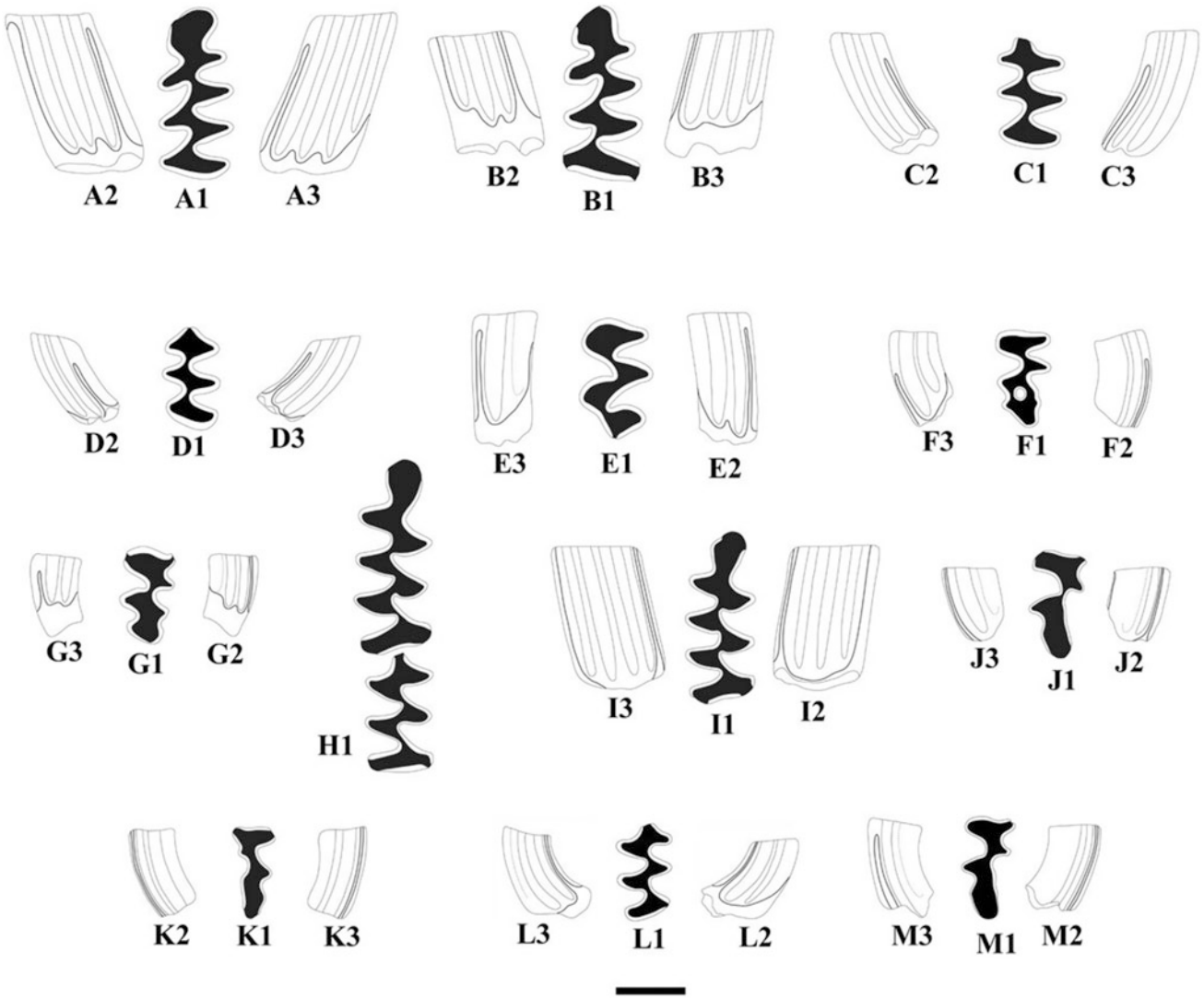

Fig. 12.7 *Villanyia fanchangensis* from Renzidong Cave, Fanchang, Anhui, *Borsodia chinensis* from Xiashagou and Xiaochangliang, Nihewan, and *Borsodia* sp. from Locality 93001, Lingtai, Gansu. *Villanyia fanchangensis*: **Renzidong**, A. left m1 (V13991.52), B. left m1 (V13991.251), C. left m2 (V13991.520), D. left m3 (V13991.754), E. left M2 (V13991.1122), F. left M3 (V13991.1264), G. left M3 (V13991.1332). *Borsodia chineinsis*: **Xiashagou**, H. right m1-2 (RV30011, TYPE); **Xiaochangliang**, I. right m1 (V15323.41), J. left M3 (V15323.26), K. right M3 (V15323.31). *Borsodia* sp.: **Loc. 93001**, L. right m3 (V18079.3), M. left M3 (V18079.7). 1. occlusal views (mesial toward top), 2. buccal view, 3. lingual view. Scale bar = 1 mm for occlusal view, and 2 mm for lateral view

transversely elongated rhombus shape. The isthmuses between the anterior and middle fields and that between the middle field and posterior loop are closed. The lingual reentrant angles are deeper than the buccal ones. Two roots.

Comparisons and discussion: *Villanyia fanchangensis* was named by Zhang et al. (2008b) based on more than a thousand specimens unearthed from the Renzidong Cave, Fanchang, Anhui Province, as mentioned earlier. The specimens from Yushe referred to this species are from YS6, YS120 and YS109 of the Haiyan Formation and one older M3 from YS5 of the Mazegou Formation. The morphology of these teeth coincides with that of the type collection very well, especially the m1, which is morphologically most important for the definition and identification of the species. There are nearly identical morphotypes in the type collection (Fig. 12.7: A, B) for the two m1 s of YS6 (Fig. 12.6: B, C), respectively. The high rise of Pmsd (prismosinuid, sinuid of prismenkante) on V22616.3 (Fig. 12.6: C) is a quite unusual situation. Similar morphotypes for the two M3 of YS109 (Fig. 12.6: G, H) can also be found in the type collection (Fig. 12.7: F, G). Although BRA1 of the left M3 of the type collection (V13991.1264, Fig. 12.7: F) looks much deeper than that of the right M3 of V22618.2, this is due to the different extent of wear. After the shallowing of BRA1 on V13991.1264, its morphology will look more similar to V22618.2 (Fig. 12.6: G). The morphologies of the other

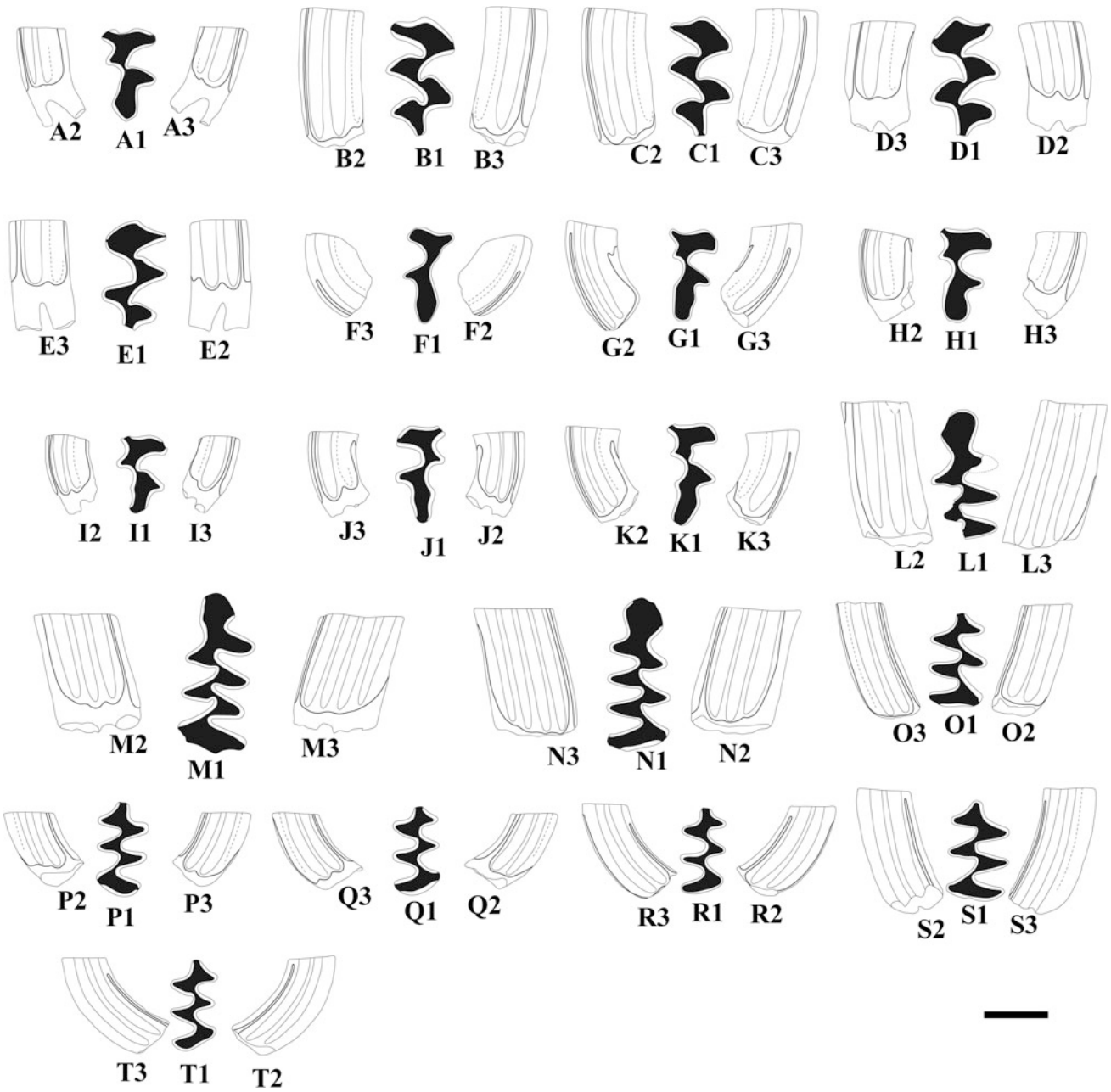

Fig. 12.8 *Borsodia chinensis* from YS6, and YS120, Haiyan Formation. **YS6**: A. right M3 (V22619.1); **YS120**: B. right M2 (V22620.1), C. right M2 (V22620.2), D. left M2 (V22620.3), E. left M2 (V22620.4), F. left M3 (V22620.5), G. right M3 (V22620.6), H. right M3 (V22620.7), I. right M3 (V22620.8), J. left M3 (V22620.9), K. right M3 (V22620.10), L. broken left m1 (V22620.11), M. broken left m1 (V22620.12), N. right m1 (V22620.13), O. right m2 (V22620.15), P. left m3 (V22620.16), Q. right m3 (V22620.17), R. right m3 (V22620.18), S. left m2 (V22620.19), T. right m3 (V22620.20). 1. occlusal views (mesial toward top), 2. buccal view, 3. lingual view. Scale bar = 1 mm for occlusal view, and 2 mm for lateral view

teeth also display significant similarities to the type collection. It is appropriate to refer these specimens to *Villanyia fanchangensis,* including the single broken M3 V22615.1 from the Mazegou Formation.

Zhang et al. (2011) reported the occurrence of *Villanyia* cf. *V. fanchangensis* in WL11, WL10, WL8, and WL7 in the 93001 section. The faunal assemblage WL13-WL7 of 93001 was correlated to that of the Mazegou Formation by Zheng and Zhang (2001).

Genus *Borsodia* Jánossy and van der Meulen, 1975

Type species: *Borsodia hungaricus* (Kormos, 1938)

Diagnosis (following Jánossy and van der Meulen 1975): No cementum deposited in the reentrant angles of the

molars. The differentiation of the enamel band is *Microtus*-type or positive.

Borsodia chinensis (Kormos, 1934)

1991 *Borsodia chinensis* Tedford et al., p. 524, Fig. 4 (part)

1991 *Borsodia chinensis* Flynn et al., p. 251, Fig. 4; 256, Table 2 (part)

1997 *Borsodia chinensis* Flynn et al., p. 239, Fig. 5 (part)

2001 *Borsodia chinensis* Flynn and Wu, p. 197 (part)

Holotype: RV30011, a right mandible with m1-3.

Type locality: Xiashagou Village, Huashaoying, Yangyuan, Hebei.

Stratigraphic distribution: Haiyan Formation, 2.6 to 2.2 Ma, Yushe Basin.

Biochronology: Nihewanian Stage/Age.

Horizon and newly referred material: **YS6**: right M3 (V22619.1); **YS120**: two right M2, and two left M2 (V22620.1-4), left M3 (V22620.5), three right M3 (V22620.6-8), left and right M3 (V22620.9, 10), two broken left m1 (V22620.11-12), right m1 (V22620.13), broken right m1 (V22620.14), right m2 (V22620.15), left m3 and two right m3 (V22620.16-18), left m2 (V22620.19), right m3 (V22620.20); **YS109**: broken left m1 (V22621.1). See Fig. 12.8.

Description: The molars are rooted and lack cementum in the reentrant angles. The enamel band is differentiated as the *Microtus*-type (positive). On the occlusal surface, the enamel is usually interrupted at the apices of LSA1, BSA1 and, as is common in arvicoline species, at posterior edges on upper molars, and anteriorly on lower molars.

M2: There are three alternating triangles behind the anterior loop. BSA1 is much slimmer and more acute compared with the other salient angles. No so-called "*Lagurus*-angle" can be observed on any specimens. The anterior wall of the anterior loop is concave on its buccal side. All the dentine isthmuses are closed. The posterior end of the tooth is acute and pointed posteriorly like a spur. Two roots are observed.

M3: Usually there are two triangles behind the anterior loop, but the specimen V22620.5 (Fig. 12.8: F) is an exception, on which there is only one triangle behind the anterior loop. This is because V22620.5 belongs to a very young individual; from the buccal view (Fig. 12.8: F2), we can tell that BSA2 required deeper wear to be expressed on the occlusal surface. The mesial wall of the anterior loop is concave. Because AL-T2 and T3-PL are confluent with each other, respectively, IS3 is the only closed isthmus on this tooth. As a result, the dentine is normally divided into two fields. On 2 of 7 specimens, the vestige of BSA3 is visible. A weak *Lagurus*-angle is observed at the apex of LRA2 on V22620.10 (Fig. 12.8: K). The posterior loop is slim, long, bar-like, and extends posteriorly or slightly posterobuccally. Two roots.

m1: Between ACC and the posterior loop, there are three alternating triangles. The anterior loop is rounded in shape, and somewhat extended anterobuccally. The apex of LRA3 is positioned in front of that of BRA2. The anterior cap, T4 and T5 are confluent, and make ACC trilobed in shape; IS1–4 are closed. Two roots.

m2: Anterior to the posterior loop, there are 4 alternating triangles; IS1 and 3 are closed. Usually, IS2 is slightly more open than these and IS4 is open. The anterior end of the tooth is spur-like and anteriorly pointed. Two roots.

m3: There are four alternating triangles anterior to the posterior loop. Other than IS4, all dentine isthmuses are closed, but, usually, IS2 is a little more open. The anterior end of the tooth is spur-like and anteriorly pointed. Two roots.

Comparisons and discussion: *Borsodia chinensis* was first discovered from the Xiashagou locality of the classic Nihewan Fauna (Teilhard de Chardin and Piveteau 1930; Kormos 1934). This species usually co-occurrs with *Allophaiomys deucalion* in many sections of the Nihewan area, such as Majuangou (Cai and Li 2004), Donggou (Zheng et al. 2006), Xiaochangliang (Zhang et al. 2008a). Cai and Li (2004) estimated the age of a new Paleolithic layer of the Majuangou section as earlier than 1.8 Ma, possibly 2.0 Ma based mainly on the coexistence of *Borsodia chinensis* and *Allophaiomys deucalion*, the occurrences of which in other sections usually provide correlation and age estimation. Zheng et al. (2006) pointed out contradictions between the magnetostratigraphy and the biostratigraphy, but biostratigraphically, the age of the *Borsodia chinensis* and *Allophaiomys deucalion* layers (Layer 11 and Layer 16) of Donggou section could be estimated as 2.4–2.0 Ma. Xiaochangliang is one of the *Borsodia chinensis* and *Allophaiomys deucalion* sites with convincing absolute age control other than the Haiyan Formation, Yushe Basin. Zhu et al. (2001) paleomagnetically dated the culture layer as 1.36 Ma. Zhang et al. (2008a) reported the small mammal fauna collected from the culture layer, in which *Borsodia chinensis* and *Allophaiomys decaulion* also co-occur. This is believed to be the last appearance datum of *Borsodia chinensis* by Zheng et al. (2006). Zhang et al. (2011) also described *Borsodia* sp. from WL11, WL10, WL8 and WL3 of the 93001 section. As mentioned above, WL13-WL7 was correlated to the faunal assemblage of the Mazegou Formation, while WL3 was thought to predate the fauna of the Haiyan Formation (Zheng and Zhang 2001, Fig. 4).

Morphological comparisons show that *Borsodia chinensis* of the Haiyan Formation does not differ from that of the Xiashagou type specimen (Fig. 12.7: H1), that of the Xiaochangliang culture layer (Fig. 12.7: I, J), and *Borsodia* sp. of the 93001 section (Fig. 12.7: L, M). ACC of V22620.11 (Fig. 12.8: L1) and occlusal morphology of V22620.13 (Fig. 12.8: N1) demonstrate great similarities to the type specimen and the right m1 of Xiaochangliang (Fig. 12.7: I1). As for M3, occlusal morphology of V22619.1, V22620.6, and V22620.7 (Fig. 12.8: A1, G1,

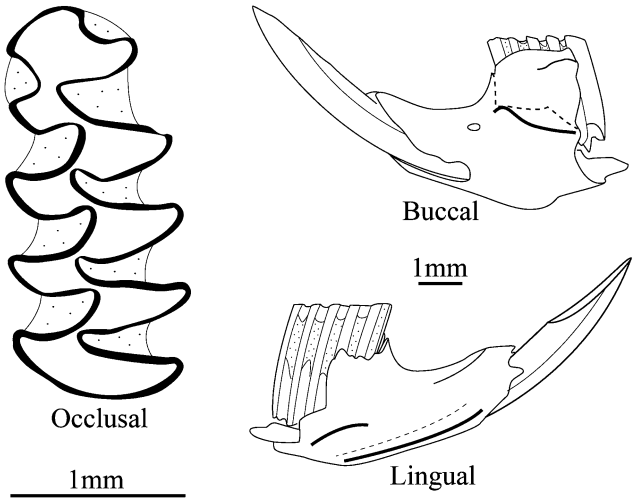

Fig. 12.9 *Microtus* cf. *M. complicidens* from YS123, Yushe, V22622.1, left dentary with incisor and m1, occlusal view of m1 on left, mesial toward top

H1) is also nearly identical to that of the left M3 of Xiaochangliang (Fig. 12.7: J1) and the left M3 of WL10 of 93001 section (Fig. 12.7: M1). There is virtually no morphological difference between the Haiyan specimens and any *B. chinensis* from the stage of evolution point of view.

Genus *Microtus* Schrank, 1798

Microtus cf. *M. complicidens* Pei, 1936

Stratigraphic distribution: Lishi loess, YusheBasin, less than 1 Ma.

Horizon and referred material: **YS123**: broken left mandible with incisor and m1 (V22622.1), Fig. 12.9.

Description: The molars are rootless. The salient angles of m1 are sharply pointed. All the reentrant angles are filled with rich cementum. The thickness of enamel is well differentiated, which means the enamel band is generally thicker on the concave side of each triangle than on convex sides. The lingual triangles are larger than the buccal ones. IS1-6 are closed, so five alternating closed triangles (T1–T5) are formed between the anterior and posterior loops. LRA4 extends deeply toward but does not reach the apex of BRA4, which makes a partial sixth triangle (T6). BSA4 is much weaker than the other buccal salient angles. The most anterior reentrant angles (LRA5 and BRA4) are much shallower than the posterior ones.

Comparisons and discussion: Flynn et al. (1997) reported the occurrence of *Microtus brandtioides* from YS83, which lies in the older red loess correlated to the Wucheng Loess (Tedford et al. 2013, Fig. 3.15). Zheng et al. (1985b) reported the species from the Lishi Loess. But *Microtus* cf. *M. complicidens* from YS123 shows several more advanced characters than *Microtus brandtioides*. According to Young (1934) and Pei (1936), five and six closed triangles are present in *Microtus brandtioides* and *Microtus complicidens*, respectively, and the anterior loop of *Microtus brandtioides* is simpler and usually lacks BRA4 and well-developed BSA4. Both BRA4 and BSA4 are well developed on the m1 of *Microtus* cf. *M. complicidens* from YS123. From the stage of evolution point of view, this may indicate that YS123 is younger than YS83. The identity of the limited YS83 material remains an issue, but it is also possible that the two forms, *Microtus brandtioides* from YS83 and *Microtus* cf. *M. complicidens* from YS123, were in part contemporary because their phylogenetic relationship is still not clear. However, in either case, both forms from the loess capping the Yushe Group undoubtedly indicate younger ages than those of the arvicolines typical of the Yushe Group.

12.3 Pliocene-Early Pleistocene Arvicoline Biocrhonology in North China: Facts and Problems

Biochronological concepts, including "stage of evolution", have been employed for decades by vertebrate paleontologists to order faunal assemblages of mammals collected from terrestrial deposits. As a result, several independent frameworks have been proposed and become widely accepted and applied by vertebrate paleontologists all over the world. These biochronological systems include NALMA (North America Land Mammal Ages, Wood et al. 1941; Woodburne 1987, 2004), MN (Mammal Neogene Zones of Europe, Mein 1975, 1979, 1990), NMU (Chinese Neogene Mammal Faunal Units, Qiu et al. 1999; Deng 2006), RZ (North American Rodent Zone, Martin 2003) and have proven to be effective and practical for the correlation of terrestrial deposits between regions. In China, fossil arvicolines have not played as important a role as in the NALMA and MN systems, although the Chinese Neogene Mammal Faunal Unit system has been used for over 30 years (Qiu et al. 1999; Deng 2006). This is due largely to the lack of external age controls and a clear phylogeny of related arvicoline species, despite the landmark review and summary by Zheng and Li (1986, 1990). More arvicoline localities have been discovered and more external age controls, most of which are paleomagnetic, have been applied to these localities or sections in recent years as mentioned above, but there remain some problems that need to be solved before fossil arvicolines can make a significant contribution to the Chinese Neogene Mammal Faunal Unit system.

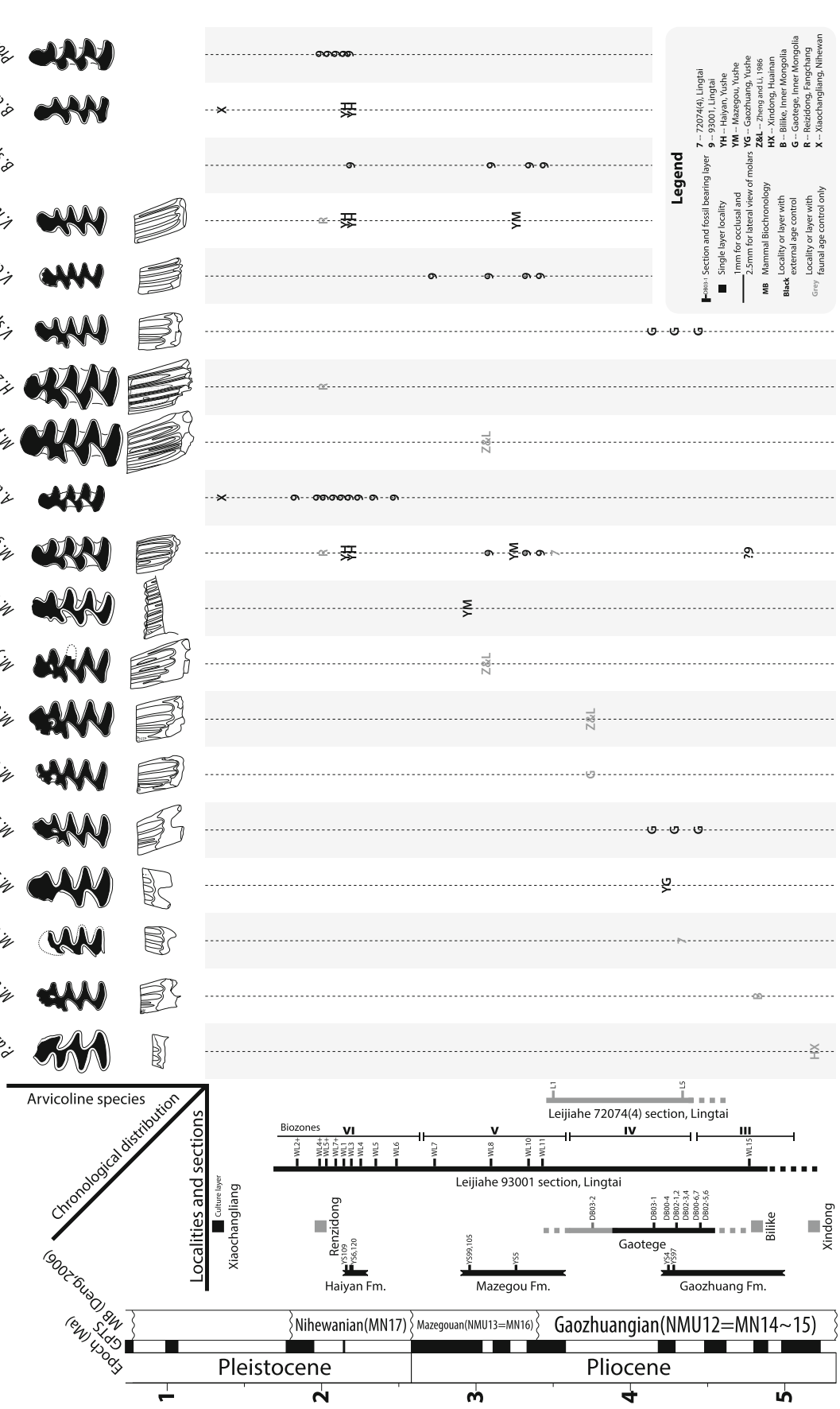

Fig. 12.10 Pliocene ~ early Pleistocene arvicoline biochronology of North China

The biggest problem is the unclear phylogeny of Pliocene – early Pleistocene arvicolines, which is also a byproduct of incongruities between stage of evolution and chronological correlations. Except for the *Mimomys banchiaonicus* – *Mimomys peii* – *Heteromimomys zhengi* lineage (Zheng et al. 2010), there has been no other Chinese arvicoline lineage established. Almost all Pliocene – early Pleistocene arvicoline species are aligned at the top (left side) of Fig. 12.10, with the chronological distribution and biostratigraphic position shown below. *Promimomys asiaticus* from Huainan, Anhui Province, is still the oldest arvicoline species in China (Jin and Zhang 2005). The morphology of *Promimomys asiaticus* is apparently more primitive than that of *Mimomys bilikeensis* from Bilike, Inner Mongolia (Qiu and Storch 2000). There are no external age controls for these two species. Their chronological placements are based mainly on faunal correlation. The next arvicoline species in a chronological sequence should be *Mimomys* sp. nov. from Gaotege, Inner Mongolia (Li et al. 2003; Li 2006; Xu et al. 2007; O'Connor et al. 2008). The age of this species was well-constrained magnetostratigraphically, and *Mimomys* sp. from YS4 and YS97 of the Yushe Gaozhuang Formation (4.3 Ma) occupies a comparable stage of evolution and its magnetostratigraphic correlation agrees. Both *Mimomys orientalis* Xue, 1981 and *Mimomys youhenicus* Zheng and Li, 1986 were collected from the greenish deposits of the lower You River, Weinan, Shaanxi Province. Based on their stage of evolution, *Mimomys orientalis* is a little more primitive than *Mimomys youhenicus*. *Mimomys* cf. *M. youhenicus* from YS99 and YS105 of the Mazegou Fm. (3.0 Ma) exhibits a comparable stage of evolution. *Mimomys gansunicus* is the most advanced Chinese species in the genus *Mimomys* from a stage of evolution point of view. Its linea sinuosa runs very close to the occlusal surface and penetrates the crown early in tooth wear at major sinuses and/or sinuids, and its *Mimomys*-kante is much less developed than in older species. *Allophaiomys deucalion* is a rootless arvicoline form that may have evolved from *Mimomys gansunicus*. In brief, we hypothesize that *Promimomys asiaticus*, *Mimomys bilikeensis*, *Mimomys* sp. nov., *Mimomys orientalis*, *Mimomys youhenicus*, *Mimomys gansunicus*, and *Allophaiomys deucalion* constitute an evolutionary lineage that demonstrates morphological differences representing distinct evolutionary grades. However, applying the stage of evolution concept in the sense of Lindsay (2003), the biostratigraphic and biochronologic placement of *Mimomys gansunicus* and *Allophaiomys deucalion* on Fig. 12.10 demonstrates a conflict between the evolutionary level and the chronological correlation. The morphology of *Mimomys gansunicus* appears to be more advanced than *Mimomys youhenicus*, but it first occurs at lower levels than *Mimomys youhenicus* in the Mazegou Formation. In the 93001 section of Lingtai, Gansu Province, the first occurrence of *Mimomys gansunicus* is also apparently earlier than *Mimomys* cf. *M. youhenicus* of the Mazegou Fm., if the correlation is correct. The 93001 occurrence appears to correlate to a low level, approximately comparable even to that of *Mimomys bilikeensis* from Bilike, Inner Mongolia, which seems hard to believe. The first occurrence of *Allophaiomys deucalion* at 93001 in the section of Lingtai, Gansu Province, also shows overlap with the morphologically less advanced *Mimomys gansunicus,* both from Renzidong Cave and the Haiyan Formation. These discrepancies suggest reexamining specimen identifications and local age determinations.

Except for the problems caused by *Mimomys gansunicus* and *Allophaiomys deucalion*, the evolutionary levels of all the other Pliocene – early Pleistocene arvicoline species show great congruity with biochronological placement based on the concept of stage of evolution. The phylogeny of the other species noted on the top of Fig. 12.10 is not as clear as these seven species mentioned above, so it is much harder to discuss their biostratigraphic and biochronologic distributions. However, *Villanyia fanchangensis* from the Haiyan Formation and the Mazegou Formation of the Yushe Basin shows similar biochronological distribution to *Villanyia* cf. *V. fanchangensis* in the 93001 section of Lingtai, Gansu Province. On the other hand, the FAD of *Borsodia* sp. at 93001 is much lower than *Borsodia chinensis* in Yushe Basin, because there is no occurrence of *Borsodia chinensis* in the Mazegou Formation; in Yushe it is restricted to the Haiyan Formation.

The *Mimomys gansunicus* and *Allophaiomys deucalion* conflict caused by disagreement of the biochronological correlation and evolutionary level, illustrates why more arvicoline-yielding stratigraphic layers combined with high quality age controls are still needed to accomplish an arvicoline biochronological framework robust enough to be used to calibrate the biostratigraphy of North China.

12.4 Conclusions

Although many arvicoline fossils and species have been discovered in the Pliocene and the Pleistocene of North China, their phylogeny is still a matter of unsolved problems because in many cases there are no concrete absolute age controls. This in turn leads to circular reasoning problems when discussing the biostratigraphy and biochronology of arvicoline species. A typical example for this is the occurrence of *Mimomys gansunicus* in Lingtai locality 93001, where the contradiction between stage of evolution and paleomagnetic calibration is outstanding. This is the essential reason why fossil arvicolines have not yet played the role they ought to play in the establishment of the biochronological framework for North China.

From the arvicoline point of view, the correlations between faunal assemblages and paleomagnetic age calibration in

Yushe Basin are fundamentally acceptable if ruling out the conflicting occurrence of *Mimomys gansunicus* in YS5 compared to other localities or sections in North China.

However, a systematic study of the dental morphology of all the existing arvicoline species and establishment of several key evolutionary lineages based on characters are still urgently needed to help solve these problems.

Acknowledgements For careful editing, I am grateful to Dr. Lawrence Flynn, Harvard University, and to Professor Wen-Yu Wu of the Institute of Vertebrate Paleontology and Paleoanthropology, Chinese Academy of Sciences. Reviewers Robert Martin and Richard Zakrzewski offered many improvements. Li Qiang kindly allowed use of his drawing for Fig. 12.9.

References

Cai, B.-Q., & Li, Q. (2004). Human remains and the environment of Early Pleistocene in the Nihewan Basin. *Science in China D, Earth Sciences, 47,* 437–444.

Deng, T. (2006). *Chinese Neogene mammal biochronology. Vertebrata PalAsiatica, 44,* 143–163.

Flynn, L. J., Tedford, R. H., & Qiu, Z.-X. (1991). Enrichment and stability in the Pliocene mammalian fauna of North China. *Paleobiology, 17,* 246–265.

Flynn, L. J., & Wu, W.-Y. (2001). The late cenozoic mammal record in North China and the Neogene mammal zonation of Europe. *Bollettino della Società Paleontologica Italiana, 40,* 195–199.

Flynn, L. J., Wu, W.-Y., & Downs, W. R. (1997). Dating vertebrate microfaunas in the late Neogene record of Northern China. *Palaeogeography, Palaeoclimatology, Palaeoecology, 133,* 227–242.

Jánossy, D., & van der Meulen, A. J. (1975). On *Mimomys* (Rodentia) from Osztramos-3, North Hungary. *In Proceedings of the Koninklijke Nederlandse Akademie van Wetenschappen, B78,* 381–391.

Jin, C.-Z., Zheng, L.-T., Dong, W., Liu, J.-Y., Xu, Q.-Q., Han, L.-G., et al. (2000). The early Pleistocene deposits and mammalian fauna from Renzidong, Fanchang, Anhui Province, China. *Acta Anthropologica Sinica, 19,* 184–198.

Jin, C.-Z., & Liu, J.-Y. (Eds.). (2009). *Paleolithic site – The Renzidong Cave, Fanchang, Anhui Province*. Beijing: Science Press.

Jin, C.-Z., & Zhang, Y.-Q. (2005). First discovery of *Promimomys* (Arvicolidae) in East Asia. *Chinese Science Bulletin, 50,* 327–332.

Kawamura, Y. (1988). Quaternary rodent faunas in the Japanese Islands (Part I-&II). *Memoirs of the Faculty of Science, Geology and Mineralogy, Kyoto University, 53,* 31–348.

Kormos, T. (1934). Première preuve de l'existence du genre *Mimomys* en Asie Orientale. *Travaux du Laboratoire de géologie de la Faculté des sciences de Lyon*, *24, mém. 20*, 3–8.

Kretzoi, M. (1990). History of research of fossil arvicolids. In O. Fejfar & W.-D. Heinrich (Eds.), *International symposium: Evolution, phylogeny and biostratigraphy of Arvicolids (Rodentia, Mammalia)* (pp. 305–312). Prague, Rohanov (Czechoslovakia): Geological Survey.

Lindsay, E. (2003). Chronostratigraphy, biochonology, datum events, land mammal ages, stage of evolution, and appearance event ordination. In L. J. Flynn (Ed.), *Vertebrate fossils and their context* (pp. 212–230). New York: American Museum of Natural History.

Li, Q. (2006). Pliocene rodents from the Gaotege fauna, Nei Mongol (Inner Mongolia). Ph. D. dissertation of the Chinese Academy of Sciences.

Li, Q., Wang, X.-M., & Qiu, Z.-D. (2003). Pliocene mammalian fauna of Gaotege in Nei Mongol (Inner Mongolia), China. *Vertebrata PalAsiatica, 41,* 104–114.

Martin, R. A. (2003). Biochronology of latest Miocene through Pleistocene arvicolid rodents from the central Great Plains of North America. *Coloquios de Paleontologia Volumen Extraordinario, 1,* 373–383.

Mein, P. (1975). Résultats de groupe de travail des vertébrés: Biozonation du Néogène méditerranéen àpartir des mammifères. In: J. Senes (Ed.), *Report on activity of the RCNMS working groups (1971–1975)* (pp. 78–81). Bratislava.

Mein, P. (1979). Rapport d'activité de travail vertébrés mise à jour de la biostratigraphie du Néogène basée sur les mammifères. *Annales géologiques des Pays Helléniques, Tome hors serie, 1979,* 1367–1372.

Mein, P. (1990). Updating of MN zones. In E. H. Lindsay, V. Fahlbusch, & P. Mein (Eds.), *European Neogene mammal chronology* (pp. 73–90). New York: Plenum Press.

O'Connor, J., Prothero, D. R., Wang, X., Li, Q., & Qiu, Z.-D. (2008). Magnetic stratigraphy of the lower Pliocene Gaotege Beds, Inner Mongolia. *New Mexico Museum of Natural History and Science Bulletin, 44,* 431–436.

Pei, W. C. (1936). On the mammalian remains from Locality 3 at Choukoutien. *Palaeontologia Sinica, C, 7*(5), 1–108.

Pei, W. C. (1939). New fossil material and artifacts collected from the Choukoutien region during the years 1937–39. *Bulletin of the Geological Society of China, 19,* 207–234.

Qiu, Z.-D., & Storch, G. (2000). The early Pliocene micromammalian fauna of Bilike, Inner Mongolia, China (Mammalia: Lipotyphla, Chiroptera, Rodentia, Lagomorpha). *Senckenbergiana Lethaea, 80,* 173–229.

Qiu, Z.-X., Wu, W.-Y., & Qiu, Z.-D. (1999). Miocene mammal faunal sequence of China: palaeozoogeography and Eurasian relationships. In G. E. Rössner & K. Heissig (Eds.), *The Miocene land mammals of Europe* (pp. 443–455). München: Verlag Dr. Friedrich Pfeil.

Rabeder, G. (1981). Die Arvicoliden (Rodentia, Mammalia) aus dem Pliozän und dem älteren Pleistozän von Niederösterreich. *Beiträge zur Paläontologie von Österreich, 8,* 1–373.

Repenning, C. A., Fejfar, O., & Heinrich, W.-D. (1990). Arvicolid rodent biochronology of the Nothern Hemisphere. In O. Fejfar & W.-D. Heinrich (Eds.), *International symposium: evolution, phylogeny and biostratigraphy of arvicolids (Rodentia, Mammalia)* (pp. 385–418). Prague, Rohanov (Czechoslovakia): Geological Survey.

Tedford, R. H., Flynn, L. J., Qiu, Z. X., Opdyke, N. D., & Downs, W. R. (1991). Yushe Basin, China; Paleomagnetically calibrated mammalian biostratigraphic standard for the Late Neogene of Eastern Asia. *Journal of Vertebrate Paleontology, 11,* 519–526.

Tedford, R. H., Qiu, Z.-X., & Flynn, L. J. (Eds.). (2013). *Late Cenozoic Yushe Basin, Shanxi Province, China: Geology and fossil mammals. Volume I: History, geology, and magnetostratigraphy*. Dordrecht: Springer.

Teilhard de Chardin, P. T., & Piveteau, J. (1930). Les mammifères fossiles de Nihowan (Chine). *Annales de Paléontologie, 19,* 1–134.

van der Meulen, A. J. (1973). Middle Pleistocene smaller mammals from the Monte Peglia (Orvieto, Italy) with special reference to the phylogeny of *Microtus* (Arvicolidae, Rodentia). *Quaternaria, 17,* 1–144.

Wei, L.-Y., Chen, M.-Y., Zhao, H.-M., & Sun, J. M. (1993). Magnetostratigraphic study on the Late Miocene-Pliocene lacustrine sediments near Leijiahe. *Monograph of the meeting in honor of Prof. Yuan Fuli on the Hundredth Anniversary of his Birth* (pp. 63–69). Beijing: Geological Publishing House.

Wood, H. E., Chaney, R. W., Clark, J., Colbert, E. H., Jepsen, G. L., Reeside, J. B., et al. (1941). Nomenclature and correlation of the North American continental Tertiary. *Geological Society of America Bulletin, 52,* 1–48.

Woodburne, M. O. (1987). *Cenozoic mammals of North America*. Berkeley: University of California Press.

Woodburne, M. O. (2004). *Late Cretaceous and Cenozoic mammals of North America*. New York: Columbia University Press.

Xu, Y-.L., Tong, Y-.B., Li, Q., Sun, Z.-M., Pei, J.-L., & Yang, Z.-Y. (2007). Magnetostratigraphic dating on the Pliocene mammalian

fauna of the Gaotege section, Central Inner Mongolia. *Geological Review*, *53,* 250–261.

Xue, X.-X. (1981). An Early Pleistocene mammalian fauna and its stratigraphy of the River You, Weinan, Shensi. *Vertebrata PalAsiatica, 19,* 35–44.

Young, C. C. (1934). On the Insectivora, Chiroptera, Rodentia and Primates other than *Sinanthropus* from Locality 1 at Choukoutien. *Palaeontologia Sinica C, 8*(3), 1–139.

Young, C. C. (1935). Miscellaneous mammalian fossils from Shansi and Honan. *Palaeontologia Sinica C, 9*(2), 1–42.

Zhang, Y.-Q., Jin, C.-Z., & Kawamura, Y. (2010). A distinct large vole lineage from the Late Pliocene – Early Pleistocene of China. *Geobios, 43,* 479–490.

Zhang, Y., Kawamura, Y., & Cai, B. (2008a). Small mammal fauna of Early Pleistocene age from the Xiaochangliang site in the Nihewan Basin, Hebei, northern China. *Quaternary Research*, *47,* 81–92.

Zhang, Y., Kawamura, Y., & Jin, C. (2008b). A new species of the extinct vole *Villanyia* from Renzidong Cave, Anhui, East China, with discussion on related species from China and Transbaikalia. *Quaternary International*, *179*, 163–170.

Zhang, Y., Zheng, S., & Wei, G. (2011). Fossil arvicolines from the Leijiahe section, Lingtai, Gansu Province and current progress of Chinese arvicoline biochronology. *Quaternary Sciences, 31,* 622–635.

Zhang, Z.-Q., & Zheng, S.-H. (2000). Late Miocene-Early Pliocene biostratigraphy of Loc. 93002 Section, Lingtai. *Gansu. Vertebrata PalAsiatica, 38,* 274–286.

Zhang, Z.-Q., & Zheng, S.-H. (2001). Late Miocene-Pliocene biostratigraphy of Xiaoshigou Section, Lingtai, Gansu. *Vertebrata PalAsiatica, 39,* 54–66.

Zheng, S.-H. (1976). A Middle Pleistocene micromammal fauna from Heshui, Gansu. *Vertebrata PalAsiatica, 14,* 112–119.

Zheng, S.-H. (1994). Preliminary report on the Late Miocene-Early Pleistocene micromammals collected from Lingtai of Gansu, China in 1992 and 1993. *Northern Hemisphere Geo-Bio Traverse, 2,* 44–56.

Zheng, S.-H., Cai, B.-Q., & Li, Q. (2006). The Plio-Pleistocene small mammals from Donggou section of Nihewan Basin, Hebei, China. *Vertebrata PalAsiatica, 44,* 320–331.

Zheng, S.-H., & Li, C.-K. (1986). A review of Chinese *Mimomys* (Arvicolidae, Rodentia). *Vertebrata PalAsiatica, 24,* 81–109.

Zheng, S.-H., & Li, C.-K. (1990). Comments on fossil arvicolids of China. In O. Fejfar & W.-D. Heinrich (Eds.), *International symposium: Evolution, phylogeny and biostratigraphy of arvicolids (Rodentia, Mammalia)* (pp. 431–442). Prague, Rohanov (Czechoslovakia): Geological Survey.

Zheng, S.-H., Wu, W.-Y., Li, Y., & Wang, G.-D. (1985a). Late Cenozoic mammalian faunas of Guide and Gonghe Basin, Qinghai Province. *Vertebrata PalAsiatica, 23,* 89–134.

Zheng, S.-H., Yuan, B.-Y., Gao, F.-Q., & Sun, F.-Q. (1985b). Paleovertebrate biology and paleoecology of the loess in China. In D.-S. Liu (Ed.), *Loess and the environment* (pp. 113–140). Beijing: Science Press.

Zheng, S.-H., & Zhang, Z-.Q. (2000). Late Miocene-Early Pleistocene micromammals from Wenwanggou of Lingtai, Ganus, China. *Vertebrata PalAsiatica*, *38*, 58–71.

Zheng, S.-H., & Zhang, Z.-Q. (2001). Late Miocene-Early Pleistocene biostratigraphy of the Leijiahe Area, Lingtai, Gansu. *Vertebrata PalAsiatica, 39,* 215–228.

Zhu, R.-X., Hoffman, K. A., Potts, R., Deng, C.-L., Pan, Y.-X., Guo, B., et al. (2001). Earliest presence of humans in northeast Asia. *Nature, 413,* 413–417.

Zong, G.-F. (1987). Note on some mammalian fossils from the Early Pleistocene of Di-Qing County, Yunnan. *Vertebrata PalAsiatica, 25,* 69–76.

Zong, G.-F., Tang, Y.-J., Xu, Q.-Q., & Yu, Z.-Q. (1982). The Early Pleistocene in Tunliu, Shanxi. *Vertebrata PalAsiatica, 20,* 236–247.

Chapter 13
The Shanxi Gerbils

Lawrence J. Flynn and Wen-Yu Wu

Abstract Despite the wealth of small mammals in the Late Neogene of Yushe Basin, gerbils are not an abundant or diverse element. A single genus, *Pseudomeriones* Schaub, 1934, is known in the Miocene-Pliocene deposits of Yushe, although the Pleistocene introduces a new fauna containing *Meriones* Illiger, 1811. The well-known species *Pseudomeriones abbreviatus* (Teilhard de Chardin, 1926) is recorded in the Pliocene deposits of Zhangcun subbasin, south of Yushe. Whereas this species remains undocumented for Yuncu subbasin, Miocene age sediments have produced a lower crowned member of the genus, *P. latidens* Sen, 2001. We describe these remains and summarize their stratigraphic occurrence. The low crowned Miocene Yushe material suggests that the *Pseudomeriones* lineage involves increasing hypsodonty, with latest Miocene and Pliocene *Pseudomeriones abbreviatus* showing greater crown height than older late Miocene *P. latidens*.

Keywords Yushe Basin • North China • Miocene • Gerbillinae • *Pseudomeriones*

13.1 Introduction

Modern gerbils are a distinctive component of the microfauna of central Asia. While all genera are not necessarily indicators of aridity, they are adapted to life in open environments and construct burrows in which they may spend long intervals of time (Nowak and Paradiso 1983). Gerbils occur in North China and Mongolia today, but at low diversity. The jird *Meriones,* Tribe Gerbillini, is the characteristic gerbil today of Shanxi and Gansu Provinces (distributed throughout northwestern China and into Shanxi); closely related *Brachiones* and *Rhombomys* occur in deserts of northwestern China and Mongolia.

The diversity among fossil representatives of the subfamily is as low as that of modern gerbils in China. In recent years the tribe Taterillini has been recognized in the Neogene fossil record of China with the discovery of *Abudhabia* in the early Late Miocene of Shaanxi Province (Qiu et al. 2004). More basal gerbils, not clearly assignable to crown tribe groups, also occur in the fossil record of China. Qiu et al. (2004) describe two species of *Myocricetodon*, a genus otherwise represented by diverse species in the Neogene of North Africa, and the widespread genus *Pseudomeriones* is known from the eastern Mediterranean (Wessels 1999) and across Asia, to Inner Mongolia and Yushe Basin. The Sino-American Yushe expeditions of 1987 to 1991 found gerbils to be a minor component of the Yushe Basin Late Neogene small mammal assemblages. Yushe Group gerbils are represented only by *Pseudomeriones*, which is not clearly related to living species groups. Here we discuss previous records of *Pseudomeriones*, and describe the fragmentary remains of the genus that we recovered as surface finds and by wet screening. These specimens are stored in the collections of the Institute of Vertebrate Paleontology and Paleoanthropology, Beijing.

13.2 Systematics

Family Muridae Illiger, 1811
Subfamily Gerbillinae Gray, 1825
Pseudomeriones Schaub, 1934

L.J. Flynn (✉)
Department of Human Evolutionary Biology and the Peabody Museum of Archaeology and Ethnology, Harvard University, Cambridge, MA 02138, UK
e-mail: ljflynn@fas.harvard.edu

W.-Y. Wu
Laboratory of Paleomammalogy, Institute of Vertebrate Paleontology and Paleoanthropology, Chinese Academy of Sciences, 142 Xizhimenwai Ave., Beijing 100044, People's Republic of China
e-mail: wuwenyu@ivpp.ac.cn

Lawrence J. Flynn and Wen-Yu Wu (eds.), *Late Cenozoic Yushe Basin, Shanxi Province, China: Geology and Fossil Mammals, Volume II: Small Mammal Fossils of Yushe Basin*, Vertebrate Paleobiology and Paleoanthropology,
DOI 10.1007/978-94-024-1050-1_13

Type species: *Pseudomeriones abbreviatus* (Teilhard de Chardin, 1926)

Discussion. Teilhard de Chardin (1926) based *Lophocricetus abbreviatus* on several specimens recovered from "*Hipparion* red beds" of Qingyang, Gansu. In 2008 an IVPP reconnaissance team revisited the locality (Flynn et al. 2011), which is considered Baodean in age, but we note that it is not securely dated. Schaub (1934) recognized the gerbil affinity of this material and coined the name *Pseudomeriones*. Although *P. abbreviatus* is a high crowned species, *Pseudomeriones* presents a number of primitive features that led Tong (1989) to place it with *Myocricetodon* in a basal, extinct group of gerbils.

Sen (1983) advanced understanding of diversity within *Pseudomeriones* based on dental remains. He recognized species level differences among samples of this genus from Rhodes and Çalta. Sylvestrou and Kostopoulos (2007) added the distinctively large species *P. megistos* under this genus for the "latest" Miocene of Greece. Souata-Alpaslan (2009) described *P. hansi* from the early Pliocene of Turkey; this species is high crowned. *P. complicidens* from the Pliocene of Gansu, China, is also high crowned, and rather small for the genus (Zhang 1999).

Inner Mongolia has produced additional records of *Pseudomeriones*, and these samples are clearly assignable to *P. abbreviatus* based on comparable size and crown height. The species is richly sampled at Ertemte (Fahlbusch et al. 1983), which is late Baodean in age. It is also well represented at Bilike and Gaotege, both early Pliocene (Qiu and Storch 2000; Li et al. 2003). Coupled with the Afghan record of *P. abbreviatus* at Pul-e Charkhi (Sen 1983), early Pliocene, it appears that this species is restricted in time to the terminal Miocene and early Pliocene.

Prof. S.-T. Liu and the 1954 IVPP Yushe field team recovered remains of *Pseudomeriones* from near the town Qiuyuan in the Zhangcun subbasin of Yushe Basin. This is not far from Renjianao and the area in which Emile Licent had collected fossils (Qiu and Tedford 2013). Modern field work shows that Zhangcun strata are early Pliocene in age (Shi 1994; Opdyke et al. 2013). The Zhangcun specimens were carefully examined by Li (1981) and found to match the Qingyang, Gansu, type material of *P. abbreviatus*. Our observations agree; it is indistinguishable from Qingyang and Ertemte examples of the species, and it is equally high crowned.

In summary, the evidence places *Pseudomeriones abbreviatus* as a high crowned member of the genus at the end of the Miocene into early Pliocene age, probably restricted to 6 to 4 Ma, and the species is represented in the early Pliocene of Yushe Basin. We describe here older, lower crowned specimens of the genus.

Pseudomeriones latidens Sen, 2001

Material and localities: V 8825 from YS60, one right maxilla fragment with M1 and M2 (length × width in mm: M1 = 2.45 × 1.50, M2 = 1.25 × 1.45); V 8822 from YS8, one damaged left M1 (est. 1.9+ × 1.55); V 8824 from YS3, one right M1 (2.25 × 1.40, preserved crown height, 1.1 mm); V 8823 from YS32, one damaged left m1 (2.15 × 1.55, preserved crown height, 1.3 mm); V 8826.1−4 from YS150, Tancun subbasin, a right and left m1, each in a dentary fragment, and additional isolated right and left m1 (2.10 × 1.40, 2.20 × 1.50, 2.25 × 1.45, 2.20 × 1.40, preserved crown height for V 8826.1, 1.0 mm).

Stratigraphic position and age: All specimens are late Miocene; all from Mahui Formation, except YS60, which is basal Gaozhuang Formation. The interpolated range of locality ages is 6.3 to 5.7 Ma; Tancun subbasin site YS150, not in the paleomagnetic section, is probably about 6.5 Ma.

Description: The maxillary bone is represented by the specimen from YS60 (V8825, Fig. 13.1a). It shows a long incisive foramen that ends posteriorly opposite the anterior root of M1. The preserved bone indicates that the premaxillary/maxillary suture is >3 mm anterior to the root of M1. A large, long palatine foramen begins opposite the hypocone of M1 and continues past M2. A large palatine foramen or fenestra is shared with modern gerbils; its position and that of the incisive foramen are reminiscent of the arrangement in *Ammodillus*; less so that of *Meriones*.

Given the few molars, crown height is difficult to quantify, but the maximum observed is less than that of *Pseudomeriones abbreviatus*. M1 is characterized by three transverse lophs joined longitudinally. The first loph is short. The lingual protocone and hypocone are somewhat anterior to the buccal cusps. The posterior loph gives hardly a hint of a posterior cingulum. There are three major roots, anterior, posterior and a large one located lingually, and variably a tiny, central buccal rootlet.

M2 of V 8825 has two transverse lophs, the anterior one slightly broader. They are joined by a longitudinal crest buccal to the midline of the tooth. There is an anterobuccal cingulum on the anterior loph. At least two roots anchor the tooth, a large posterior one is exposed.

The lower first molar is represented by 5 specimens, one from YS32 and four from YS150 (Fig. 13.1d–h). Of the latter, two are in small dentary fragments, one of which shows the anterior scar of the masseteric crest to extend just beyond the front root of m1. The three lophs of m1 are joined longitudinally and slightly diagonally. The anterior loph is shortest and is asymmetrical, with a long, low buccal extension that curves posteriorly as it descends. The protoconid and hypoconid are distinctly posterior to the meta-

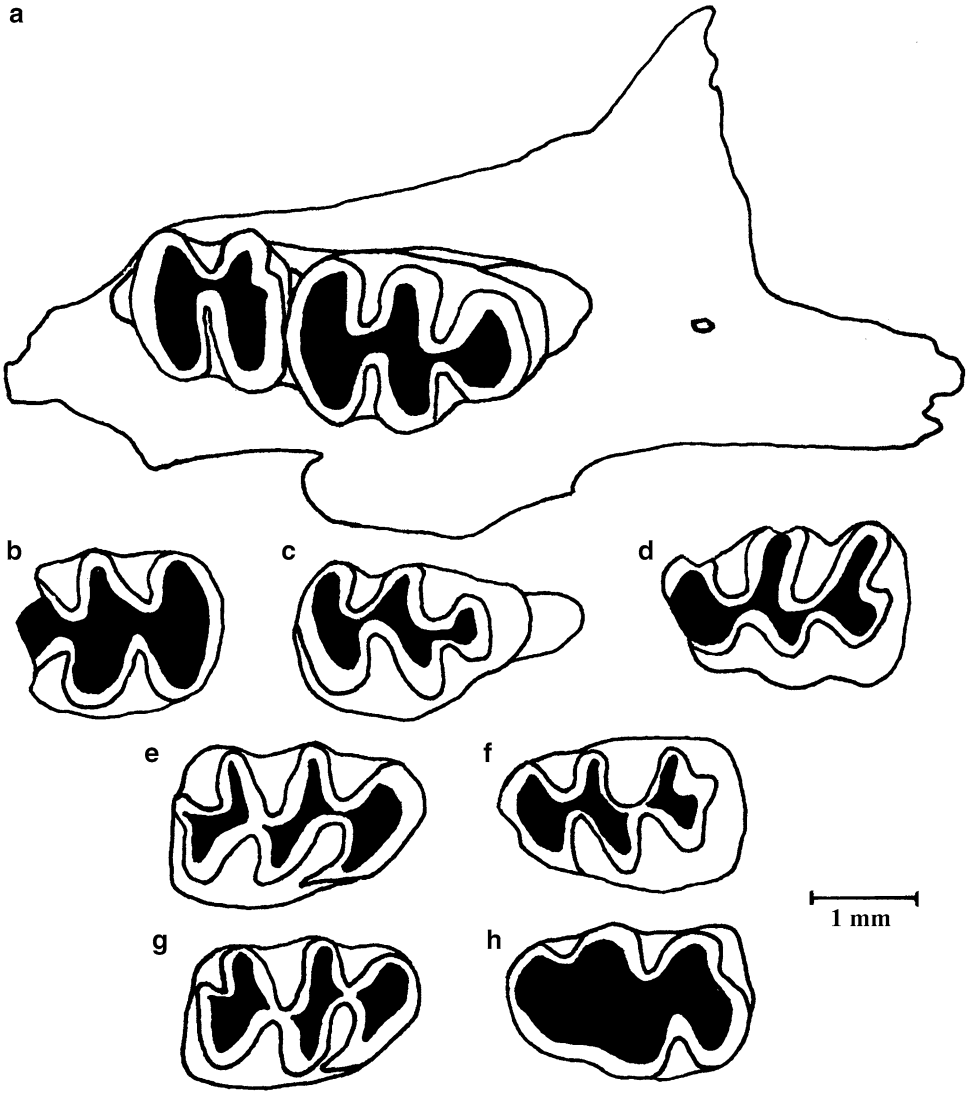

Fig. 13.1 Line drawings of occlusal surfaces of all specimens assigned to *Pseudomeriones latidens*. **a** V 8825 from YS60, right maxilla fragment with M1 and M2; **b** V 8822 from YS8, damaged left M1; **c** V 8824 from YS3, right M1; **d** V 8823 from YS32, damaged left m1; **e** to **h** V 8826.1–.4, respectively, four m1 from YS150. Anterior to right for **a**, **c**, **e**, **g**; anterior to left for **b**, **d**, **f**, **h**

conid and entoconid, lending an oblique aspect to the transverse lophs. There is a short posterior cingulum, which is the posterior arm of the hypoconid. There are two roots. The YS-32 specimen, V 8823, has a shorter buccal extension of the anterior loph, and is higher crowned (Fig. 13.2) than the YS150 specimens.

Discussion: The fossils recovered from the Mahui Formation and base of the Gaozhuang Formation conform to the primitive gerbil genus *Pseudomeriones*. Previously (e.g., Flynn et al. 1997), we recorded these as *Pseudomeriones abbreviatus*. While length and width of teeth agree with that identification, our Miocene age Yushe specimens are lower crowned than observed in any sample of *Pseudomeriones abbreviatus*. The sand rats described by Li (1981) from the Zhangcun subbasin of Yushe are younger (Pliocene, see Volume I) and higher crowned, like the type material from Qingyang described by Teilhard de Chardin (1926). In their discussion of the Bilike, Inner Mongolia, *Pseudomeriones abbreviatus*, Qiu and Storch (2000) concluded that the species shows increasing crown height through time. We believe that Qiu and Storch (2000) are correct. The older Miocene *Pseudomeriones* specimens from Yushe are readily identified with *Pseudomeriones latidens* from the Miocene of Afghanistan (Sen 2001). We do note that one of the younger specimens, V 8823 from YS32 (6 Ma) is higher crowned than specimens from YS150 or the sample from

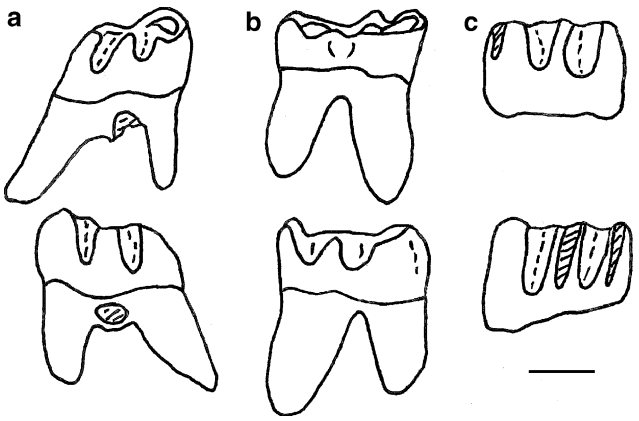

Fig. 13.2 Sketched crown height for selected less-worn *Pseudomeriones latidens* specimens, scale bar = 1 mm, labial view above, lingual view below. **a** right M1 V 8824 from YS3; **b** right m1 V 8826.3 from YS150; **c** left m1 V 8823 from YS32. Diagonal cross-hatching indicates breakage

Molayan, Afghanistan (Sen 2001: Fig. 7), but it is lower crowned than *P. abbreviatus*, and we assign all Yushe Miocene specimens to *P. latidens*.

The Yushe Basin appears to record successive low to high crowned gerbils, consistent with a *Pseudomeriones* chronocline lineage showing increasing hypsodonty. Difficulties with this simplistic interpretation include the apparently tight timing of turnover: *P. latidens* in Yushe is Baodean in age, around 6 Ma and older, but *P. abbreviatus* occurs in the late Baodean Ertemte fauna and the Qingyang fauna which is considered Baodean. It is possible that *P. latidens* persisted as a contemporary of *Pseudomeriones abbreviatus*, or that both Ertemte and Qingyang are younger than 6 Ma. Also, only one specimen of *P. latidens*, V 8825, occurs in the Gaozhuang Formation, at 5.7 Ma; this mature individual could be a worn higher-crowned *Pseudomeriones*.

The gerbil *Pseudomeriones* has a wide distribution, from China to the Mediterranean, and it may prove very useful as an index fossil for biochronological correlation. However, the genus is not known from high latitudes or from South China, and did not penetrate the Indian subcontinent. Agreeing with Qiu and Storch (2000), we suggest that the trend of increasing crown height through time probably characterized the group throughout its Asian range.

Meriones Illiger, 1811
Meriones meridianus (Pallas, 1773)

Material and localities: V 8827, left dentary from Dong Gou, YS60, with incisor and m1 (2.40 × 1.55 mm). From Tancun subbasin site YS144 (Dengyucun), V 8828, left dentary fragment with incisor stub and m1-2 (2.35 × 1.50, 1.40 × 1.65); site YS141 (Taiqiu), V 8829, right m1 (2.20 × 1.45), slightly worn height = 2.0 mm.

These specimens, found on surface exposures, are likely Pleistocene to Recent in age. They are consistent with *Meriones* in their high-crowned, simple tri-lophate m1 structure with central connection and simple anterior loop (m2 is bilobed). *Meriones meridianus* currently lives in the Yushe region and is of the same size.

13.3 Conclusion

Our field work recovered *Pseudomeriones* from older strata of the Yushe Basin complex. It is a characteristic element, although not common, in Mahui assemblages and the lower Gaozhuang Formation (Taoyang Member; see Fig. 10.6). All specimens are significantly lower crowned than *Pseudomeriones abbreviatus*, comparable to Late Miocene *Pseudomeriones latidens* from Molayan, Afghanistan (Sen 2001). The stratigraphically lowest *Pseudomeriones* of Yushe Basin are 6 to 7 Ma in age and the youngest of these shows increased crown height (Fig. 13.2), still less than that of *P. abbreviatus*. The youngest specimen attributed here to *P. latidens* in Yushe Basin is from YS60 (5.7 Ma), but the dentition is worn (Fig. 13.1); it is conceivable that this specimen is a representative of *Pseudomeriones abbreviatus.* We do recognize *Pseudomeriones abbreviatus* in younger Pliocene deposits of Zhangcun subbasin, in agreement with Li (1981). Yushe Basin, therefore, demonstrates the successive occurrence of *Pseudomeriones* species, and the evolution of the genus may involve chronoclinal increase in crown height. The record suggests that the transition between these species was about 6 Ma.

Pseudomeriones is distributed westward across Asia, through Afghanistan, to the Mediterranean region, including Turkey and Spain, and therefore constitutes a useful biochronological marker for the late Neogene. The genus is not known from the high latitude Palaearctic and never invaded the Oriental (Indomalayan) biogeographic province to the south.

The extant gerbilline *Meriones* appears in the Pleistocene of Yushe Basin and persists in the region today.

Acknowledgements We thank our colleagues at IVPP who made original collections of *Pseudomeriones abbreviatus* from the type locality and from Zhangcun subbasin available to us, especially C.-K. Li and Z.-D. Qiu. Our reviewers suggested many improvements in the manuscript and we thank Sevket Sen, Wilma Wessels, and Zhao-Qun Zhang for this and for their encouragement.

References

Fahlbusch, V., Qiu, Z.-D., & Storch, G. (1983). Neogene mammalian faunas of Ertemte and Harr Obo in Nei Monggol, China. 1. Report on field work in 1980 and preliminary results. *Scientia Sinica, B 26,* 205–224.

Flynn, L. J., Deng, T., Wang, Y., Xie, G.-P., Hou, S.-K., Pang, L.-B., et al. (2011). Observations on the *Hipparion* red clays of the Loess Plateau. *Vertebrata PalAsiatica, 49,* 275–284.

Flynn, L. J., Wu, W.-Y., & Downs, W. R. (1997). Dating vertebrate microfaunas in the late Neogene record of northern China. *Palaeogeography, Palaeoclimatology, Palaeoecology, 133,* 227–242.

Illiger, C. (1811). *Prodromus systematis mammalium et avium*. Berlin: C. Salfeld.

Li, C.-K. (1981). Pontian sand-rat from Yushe Basin, Shansi. *Vertebrata PalAsiatica, 19,* 321–326.

Li, Q., Wang, X., & Qiu, Z.-D. (2003). Pliocene mammalian fauna of Gaotege in Nei Mongol (Inner Mongolia), China. *Vertebrata PalAsiatica, 41,* 104–114.

Opdyke, N. D., Huang, K., & Tedford, R. H. (2013). The paleomagnetism and magnetic stratigraphy of the late cenozoic sediments of the Yushe Basin, Shanxi Province, China. In R. H. Tedford, Z.-X. Qiu, & L. J. Flynn (Eds.), *Late Cenozoic Yushe Basin, Shanxi Province, China: Geology and fossil mammals Volume I: History, geology, and magnetostratigraphy* (pp. 69–78). Dordrecht: Springer.

Qiu, Z.-D., Zheng, S.-H., & Zhang, Z.-Q. (2004). Gerbillids from the Late Miocene Bahe formation, Lantian, China. *Vertebrata PalAsiatica, 42,* 193–204.

Qiu, Z.-D., & Storch, G. (2000). The Early Pliocene micromammalian fauna of Bilike, Inner Mongolia, China (Mammalia: Lipotyphla, Chiroptera, Rodentia, Lagomorpha). *Senckenbergiana Lethaea, 80,* 173–229.

Qiu, Z.-X., & Tedford, R. H. (2013). History of scientific exploration of Yushe Basin. In R. H. Tedford, Z.-X. Qiu, & L. J. Flynn (Eds.), *Late Cenozoic Yushe Basin, Shanxi Province, China: Geology and fossil mammals, Volume I: History, geology, and magnetostratigraphy* (pp. 7–34). Dordrecht: Springer.

Schaub, S. (1934). Űber einige fossile Simplicidentaten aus China und der Mongolei. *Abhandlungen der Schweizerischen Palaeontologischen Gesellschaft, 54*, 1–40, 1 plate.

Sen, S. (1983). Rongeurs et lagomorphes du gisement pliocène de Pul-e Charkhi, bassin de Kabul, Afghanistan. *Bulletin du Muséum National d'Histoire Naturelle, Paris, 5*(*5C*), 33–74.

Sen, S. (2001). Rodents and insectivores from the Upper Miocene of Molayan, Afghanistan. *Palaeontology, 44,* 913–932.

Shi, N. (1994). The Late Cenozoic stratigraphy, chronology, palynology and environmental development in the Yushe Basin, North China. *Striae, 36,* 1–90.

Suata-Alpaslan, F. (2009). *Pseudomeriones hansi* nov. sp. (Rodentia, Mammalia) from the early Pliocene (Ruscinian) fauna of Iğdeli (Turkey). *The Open Journal of Geology, 3,* 58–63.

Sylvestrou, I. A., & Kostopoulos, D. S. (2007). *Pseudomeriones megistos* nov. sp. (Gerbillinae, Mammalia) from the latest Miocene of Northern Greece and its phylogenetic relationships. *Geobios, 40,* 833–848.

Tong, H.-Y. (1989). Origine et évolution des Gerbillidae (Mammalia, Rodentia) en Afrique du Nord. *Mémoires de la Société Géologique de France, 155,* 1–120.

Teilhard de Chardin, P. (1926). Description de Mammifères Tertiares de Chine et de Mongolie. *Annales de Paléontologie, Paris, 15,* 1–52.

Wessels, W. (1999). Family Gerbillidae. In G.E. Rössner & K. Heissig (Eds.), *The Miocene land mammals of Europe* (pp. 395–400). Munich: Verlag Dr. Friedrich Pfeil.

Zhang, Z.-Q. (1999). Pliocene micromammal fauna from Ningxian, Gansu Province. *Proceedings Seventh Annual Meeting of the Chinese Society of Vertebrate Paleontology, 1999,* 167–177.

Chapter 14
The Murine Rodents of Yushe Basin

Wen-Yu Wu, Lawrence J. Flynn, and Zhu-Ding Qiu

Abstract We review and expand the systematics and biostratigraphic record of murine rodents in Yushe Basin. Several new taxa were established for the Pliocene fossil record of North China following our initial field work of the 1980s. The rodent collection was expanded and developed by complementary field work in 1991, and subsequent study. Herein we present a new Late Miocene genus and review all occurrences of Yushe Murinae. Relatively primitive taxa characterize the Late Miocene of Yushe, and these appear to be related to early lineages that diversified in the Indian Subcontinent. The interval of about 6–5 Ma in Yushe records several murines that occur at Ertemte, Inner Mongolia: *Karnimatoides hipparionus*, *Apodemus orientalis*, and *Micromys chalceus. Chardinomys* is an additional genus that distinguishes Yushe microfaunas from other Asian assemblages, and the common *C. yusheensis* ranges from latest Miocene through early Pliocene. With *Chardinomys,* the genus *Huaxiamys* characterizes Late Neogene Yushe murine assemblages. The Pliocene of Yushe Basin records successive species of *Chardinomys, Micromys, Huaxiamys*, and *Apodemus*. Derived species of *Chardinomys, Micromys*, and *Apodemus* persist into the Pleistocene.

Keywords Yushe Basin • North China • Late Neogene • Murinae • Biogeography

14.1 Introduction

For nearly a century, the late Miocene to Pleistocene deposits of Yushe Basin have produced the classic faunas that stand as the basis for concepts of terrestrial life in eastern Asia. Yushe Basin, in Shanxi Province, northern China, contains thick accumulations of fluvial and lacustrine sediments with vertebrate faunas spanning six million years, late Miocene through early Pleistocene. These provide an excellent opportunity to build a precise biostratigraphy of the entire fauna, toward which goal this contribution is one element.

Since 1978, teams from the Institute of Vertebrate Paleontology and Paleoanthropology (IVPP) led by Zhan-Xiang Qiu have concentrated on the geology of the Yushe Basin in order to place all collections in a stratigraphic and temporal framework, and to supplement these with new material. When Richard Tedford of the American Museum of Natural History in New York (AMNH) became interested in Yushe Basin for the parallel goal of increasing information retrievable for the Frick collection of Yushe fossils, we engaged in a collaborative Sino-American project to document and date the Yushe sequence. It became clear that the microfauna could be better represented through systematic screening of fossiliferous sediment. With Will Downs, then of the Bilby Research Center at Northern Arizona University, the present authors initiated an intensive program of screening. Field programs of 1987–1991 focused on the Yuncu and Tancun subbasins, throughout which occur fossil localities (YS prefix).

Prior to 1987 the only fossil murid rodent reported from the Yushe Basin was *Chardinomys yusheensis* Jacobs and

Note: This chapter includes one or more new nomenclatural-taxonomic actions registered in Zoobank and for such purposes the official publication date is 2017.

W.-Y. Wu (✉) · Z.-D. Qiu
Laboratory of Paleomammalogy, Institute of Vertebrate Paleontology and Paleoanthropology, Chinese Academy of Sciences, 142 Xizhimenwai Ave., Beijing 100044, People's Republic of China
e-mail: wuwenyu@ivpp.ac.cn

Z.-D. Qiu
e-mail: qiuzhuding@ivpp.ac.cn

L.J. Flynn
Department of Human Evolutionary Biology, and the Peabody Museum of Archaeology and Ethnology, Harvard University, Cambridge, MA 02138, USA
e-mail: ljflynn@fas.harvard.edu

Lawrence J. Flynn and Wen-Yu Wu (eds.), *Late Cenozoic Yushe Basin, Shanxi Province, China: Geology and Fossil Mammals, Volume II: Small Mammal Fossils of Yushe Basin*, Vertebrate Paleobiology and Paleoanthropology,
DOI 10.1007/978-94-024-1050-1_14

Li, 1982. This was represented by several specimens collected by IVPP in 1957 from Yagou, near the village of Gaozhuang. We relocated this site and added murine localities throughout the Yushe Basin section. Current finds far surpass the original sample in both quantity and diversity (~500 versus the original five specimens). Moreover, the current collection is extremely significant in a biostratigraphic context, for it is associated with precise geographic and chronostratigraphic data.

Wu and Flynn (1992) published new taxa based on fossils recovered from the field seasons of 1987 and 1988, and the reader is referred to that source for original observations and metric data. The present chapter reviews all Yushe Basin species known in the late 1980s, and presents new material collected in 1991. The 1991 collection supplements the basis of documentation of Yushe murids, and provides for recognition of a new genus and species, because the Tancun subbasin localities found in 1991 sample a late Miocene interval that is poorly represented in Yuncu subbasin.

Measurements (L × W, length × width in mm) were taken under a Wild M7A binocular microscope while a majority of the photographic plates were taken by Peling Fong with a Zeiss 950 digital scanning electron microscope (5 kV, low magnification) and the remaining photographs were taken by Lian Ouyang with a Joel JSM-6100 scanning electron microscope. Dental terminology for murids, especially upper first molars, can be complex. We use the terminology of Storch (1987), who described murids from Inner Mongolia, and give the homologous Cope-Osborn terms for those structures (Table 14.1), following Jacobs (1977, 1978). Studies by Zheng (1981), Zhou (1988), and Zheng and Zhang (2001) on Nihewan, Jingle, and Gansu rodents also provide important morphological and stratigraphic details. Specimens are catalogued at the IVPP, Beijing, with prefix "V".

Table 14.1 Murid terminology for upper and lower molars, with Cope-Osborn homologies for tubercles 1 to 12 following Jacobs (1977, 1978)

	Upper first molar	Lower first molar
t1	Anterostyle	tma = Medial anteroconid
t2	Lingual anterocone	Lingual anteroconid
t3	Labial anterocone	Labial anteroconid
t4	Enterostyle	Protoconid
t5	Protocone	Metaconid
t6	Paracone	Hypoconid
t7	Posterostyle	Entoconid
t8	Hypocone	Posterior cingulum
t9	Metacone	
t12	Posterior cingulum	C1 to C4, from posterior to anterior position = small cusps on labial cingulum

14.2 Systematics

Family Muridae Illiger, 1811
Subfamily Murinae Illiger, 1811
Chardinomys Jacobs and Li, 1982

Type species: *Chardinomys yusheensis* Jacobs and Li, 1982

Included species: *Chardinomys yusheensis*, *Chardinomys nihowanicus* (Zheng, 1981), *Chardinomys bilikeensis* Qiu and Storch, 2000.

Chardinomys yusheensis Jacobs and Li, 1982

Emended diagnosis: Posteriorly positioned t1 and t4; t5 with a spindle-shaped occlusal surface; oblique t3–t5–t4 ridge oriented at a right angle to the connection between t2–t3. Species characterized by moderately inclined cusps on M1 and m1. On M1 the t1 and t4 are nearly columnar, anterior cingulum (some specimens with prestyle, a small, medial anterior cusp) is well developed on 75% of the specimens, t5 and t6 are connected on over 50% of specimens, c3 is present on over half m1 specimens, M1 is five-rooted, and m1 is three-rooted.

Referred material (Fig. 14.1). YS49: incomplete I2 (V8868); YS57b: M2 (V8869); YS50: two M1, m1 (damaged), m2, two left mandibles with m1 and m1–2 respectively, two I2 (V8870.1-8); YS96: left mandible with m1–3 (V8871); YS97: four M1 (one damaged), three M2 (one damaged), m1, two m2, three I2 (V8872.1-13); YS43: left mandible with m1–m2 (V8873); YS4: two fragmentary maxillae with M1 (one bearing half M2), 11 M1 (three damaged or eroded), 7 M2, two incomplete right mandibles with m1 and m2 respectively, 15 m1 (six damaged or eroded), 10 m2, 6 m3, and 2 I2 (V8874.1-55); YS134: damaged M2, (V8874.56); from Tancun subbasin YS161: m1 (V11345). Measurements in Table 14.2.

Stratigraphic range and age: Early Pliocene upper Taoyang and Culiugou members of the Gaozhuang Fm. in Yuncu subbasin; late Miocene lowest Gaozhuang Fm. in Tancun subbasin; time span is ca. 5.8–4.2 Ma.

Description: The zygomatic arch initiates approximately 1 mm anterior to the M1. The incisive foramen extends posteriorly to one third of M1 length. The maximal depth of the mandible is of 3.65 mm at the level of m1. The masseteric crest is conspicuous and anteriorly swollen, the masseteric fossa is broad and shallow, and a mental foramen lies anteroventral to the anterior terminus of the masseteric crest. Upper incisor (dI2) enamel surface is smooth and glossy with a distinct longitudinal groove that divides the tooth into two unequal sections: the medial part is broader and its antero-posterior dimension is distinctly greater than the lateral part, and consequently, it is asymmetrically heart-shaped in cross-section. The groove affects the dentine-enamel junction. Additionally, there is a gracile

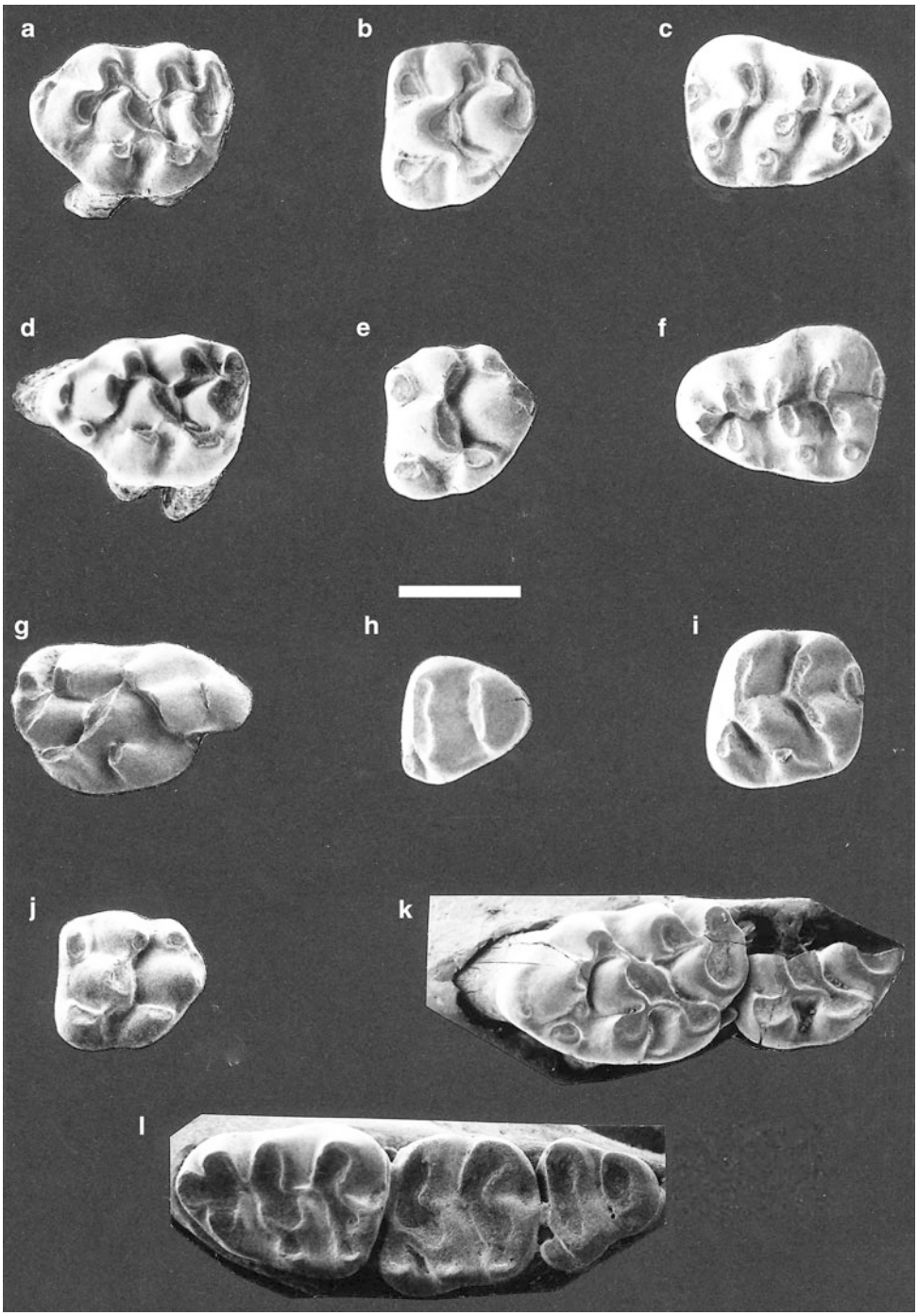

Fig. 14.1 *Chardinomys yusheensis* Jacobs and Li, 1982 from YS4 (**a**–**f**, **h**, **i**, **k**), YS50 (**g**), YS57b (**j**), and YS96 (**l**), all Gaozhuang Formation. **a** Left M1 V8874.4; **b** left M2 V8874.17; **c** right m1 V8874.32; **d** left M1 V8874.3; **e** left M2 V8874.16; **f** left m1 V8874.23; **g** right M1 V8870.1; **h** left m3 V8874.50; **i** left m2 V8874.38; **j** left M2 V8869; **k** left M1–2 V8874.1; **l** left m1–3 V8871. Scale bar = 1 mm

longitudinal groove and ridge medial to it running along the anteromedial margin of the enamel (Fig. 14.2). This feature is not reflected in the underlying dentine.

Main cusps on the M1 are posteriorly inclined with t1 nearly columnar, positioned slightly posterior to t3, isolated from t2 by a broad valley, but in close proximity and linked to t5 by a weak crest. The t2 is close to and linked to t3 by a short crest. The t4 is anteroposteriorly extended and equivalent to or slightly larger than t1. The t5 is anterolabial-posterolingually expanded with a spindle-shaped occlusal surface that connects to t3 and t4 at both ends, and forms a distinct diagonal crest on the tooth. The morphology of t6 resembles t3 but is more

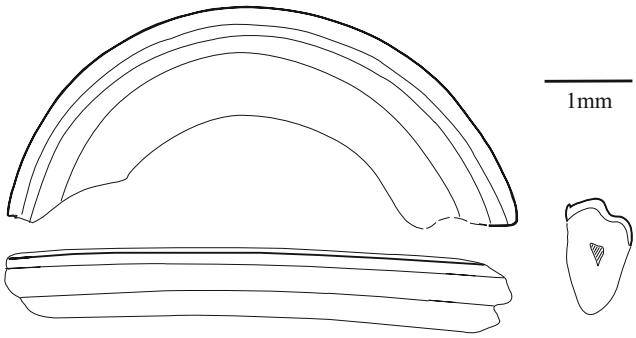

Fig. 14.2 Upper left incisor of *Chardinomys yusheensis* Jacobs and Li, 1982 (V8870.8) from YS50 in lateral (above left) and labial (below it) views, as well as cross-section (right)

robust. Of 17 specimens 12 have a weak t5–t6 connection of varying degree, while on the remaining specimens this link is absent. With one exception, on all specimens the t6 possesses a posterior crest which, in the majority (9), is linked to t8. On several specimens (4) this crest is connected to the junction of t8 and t9, but on only one specimen is there a connection to only t9. There is no t7, and t9 is transversely oriented and nearly fused to t8. To varying degrees of development t0 is present on 12 specimens, absent on only two. This cusp is aligned with t2 and t3 approximately at a right angle to the t3–t5–t4 oblique crest. Among 11 relatively well-preserved specimens, nine display a distinct anterior cingulum. Five roots always occur and several specimens possess an additional small central rootlet.

On M2, t1 is slightly larger than t3. In general, t1 is linked to t5 by a posterolabial crest, the t3 is close to t5 and occasionally has a posterolingual spur, and t4 is posterior to and usually connected to t5 (only on one specimen are they not connected). The t6 is slightly anterior to t4 and located near t5 with connections between the two always present. The t6 is linked to t9 by a low crest on one specimen, while the remaining specimens all have t6 isolated from t9. A t7 is absent. The t4 is either separated from t8 by a groove or linked to the lingual side of t8 by a low crest. Five-rooted (5 cases); one is 4-rooted.

The m1 is posteriorly broadened, creating an isosceles triangle in occlusal view. Cusps are slightly anteriorly inclined with a well-developed medial anteroconid (tma) present. On half the specimens this cusp is isolated but on the other half it is connected to the lingual anteroconid. Lingual and labial anteroconids are either nearly equivalent to or slightly larger than the tma in size, and frequently posteriorly weakly connected. An anterior mure varies from being distinct to totally absent. Protoconid is slightly posterior to and connected anteriorly to the metaconid by a low crest. A medial ridge is present on eight specimens and usually extends to the protoconid. The anterior mure and medial ridge are parallel to the lingual side of the tooth. All specimens possess c1 and c2. The c1 is smaller than c2 with the exception of four specimens where the c1 is equivalent to or just slightly smaller than the c2. Nearly half the specimens possess a small or discernible c3. The posterior cingulum is simply a transversely-oriented oval to ridge-like cusp, positioned slightly lingually. Three roots are present.

The YS161 record (one isolated and well-worn m1, V11345, length × width = 1.80 × 1.21 mm) is identical with the species in size and morphology. The tma is developed. The posterior cingulum is ridge-shaped and weak. This extends downward the range of *Chardinomys* in Yushe Basin to the base of the Gaozhuang Fm. (latest Miocene), and based on this tooth, places the first occurrence of *C. yusheensis* at this age.

On m2 a well-developed labial anteroconid is connected lingually by a crest to the protoconid. Approximately half the specimens display a low and weak medial ridge that occasionally extends to the base of the protoconid. A conspicuous c2 is present on all specimens, but c1 is present on only two-thirds of the specimens, and is generally quite small, with only one exception where the c1 is as large as the c2. A majority of specimens possess a small ovoid posterior cingulum. Four or five roots may be present. Among the four observable specimens from YS4, two are 5-rooted and the other two 4-rooted, but all the specimens derived from localities stratigraphically lower than YS4 (4 teeth) have only four roots.

On m3 the labial anteroconid is low, weak, and isolated. The metaconid-protoconid ridge and entoconid-hypoconid ridge are either straight or slightly curved. The medial ridge and labial accessory cuspids are absent. Three (two of five teeth) or four roots are present (three teeth). On the 4-rooted specimens the fourth root is small and between the two anterior roots.

Comparison and discussion: The morphology described here is consistent with the diagnosis for the genus *Chardinomys* which includes posteriorly positioned t1 and t4; a t5 with a spindle-shaped occlusal surface; an anterolabial-posterolingually oriented t3–t5–t4 oblique ridge; the t0 (or "t1 bis"), t2, and t3 aligned as a crest perpendicular and anterior to the oblique ridge; t6–t8 connection frequent; and m1 with two or three labial accessory cuspids, c2 nearly always larger than c1. These characters, in addition to size, and the majority of specimens having a relatively distinct anterior cingulum on M1, diagnose the specimens to *C. yusheensis.*

Chardinomys yusheensis was erected for a left and right M1–M3 from Yagou arroyo, near Gaozhuang village, Yushe Co., Shanxi Province (Jacobs and Li 1982). The new data greatly increase knowledge of the species. Our field locality YS57b in Yagou is believed to be the Type locality, but only one M2 (consistent with the Type specimen) was found there in 1987. Occurrences indicate that *C. yusheensis* ranged from 5.8 to 4.2 Ma in Yushe Basin.

Although Cui (2003) erected latest Miocene-earliest Pliocene species of *Chardinomys* (*C. primitivus* and *C. lingtaiensis* from Lingtai, Gansu Province), which would be contemporaneous with the type species, we agree with Qiu and Li (2016) that these forms pertain to the distinct genus *Orientalomys,* which occurs also at Ertemte, Inner Mongolia. Qiu and Li (2016) note that the characteristic shuttle-shaped wear surface on t5 of M1 of *Chardinomys* is a character that readily distinguishes the genus from *Orientalomys*.

Two additional species of *Chardinomys* are known. The younger *C. nihowanicus* (Zheng 1981; Zheng and Cai 1991; Cai and Qiu 1993) was first recognized in the late Pliocene-early Pleistocene of Dongyaozitou and Daodi, in Hebei Province, Jingle in Shanxi Province, and Dali in Shaanxi Province. It is identical with late Pliocene-early Pleistocene fossils from Yushe Basin (below). A contemporary of *C. yusheensis* is the early Pliocene *C. bilikeensis* from Bilike, Inner Mongolia (Qiu and Storch 2000). These species are now based on large samples.

Chardinomys yusheensis differs from *C. nihowanicus* in slightly larger size (Table 14.2); M1 with a well-developed anterior cingulum and a majority of specimens with this feature, and a relatively high frequency of M1 with t5–t6 connection; M2 with weak posterior spurs on t3 and t6 (tendency to stephanodonty), and with t1, t4, t5 and t6 flat column-shaped; the m1 with more developed c3; and the m2 with less roots (4–5 roots), in contrast to 5 roots in *C. nihowanicus.*

Qiu and Storch (2000) listed the differences between *C. bilikeensis* and *C. yusheensis*. *Chardinomys yushensis* differs from *C. bilikeensis* from Bilike, Inner Mongolia, in (1) its higher crowns, with less inclined cusps, (2) its M1 with more columnar and less inclined cusps, weaker precingulum, and a relatively weak t5–t6 connection, (3) the M2 shows less developed stephanodonty, (4) m1 has a relatively weak c3, and (5) M1 and m1 have more roots, m1 with three, M1 with five, in contrast to the 2 or 3-rooted m1 and 3 or 4-rooted M1 of *C. bikikeensis.*

Chardinomys nihowanicus (Zheng, 1981)

Material: YS90: M1, two M2, fragmentary mandible with m1–2, and m1 (V8875.1-5); YS5: fragmentary mandible with m1–2, and 1 m1, (V8876.1-2); YS87: three M1 and M2, fragmentary mandible with m1, and m2 (V8877.1-6); YS99: anterior half of M1, m1 and m2 (V8878.1-3); YS120: M1 and M2 (V8879.1-2); YS109: posterior half of M1, m1, m2, anterior half of m2, two I2 (V8890.1-6); YS83: heavily corroded M1 (V8891). Figure 14.3a–f; measurements in Table 14.3.

Stratigraphic ranges and age: Late Pliocene Mazegou Formation to early Pleistocene Haiyan Formation (about 3.5 to 2 Ma), and Red Loess (YS83, about 1 Ma).

Description: Mandible and incisor are extremely close in size and morphology to *C. yusheensis.* M1 cusps are posteriorly inclined with t1 sub-columnar, situated posterior to t3, and extremely close to t5, separated from t2 by a broad valley. The t2 lies close to t3 and is linked by a short ridge. The t4 is larger than t1 and anteroposteriorly extended. The t5 is anterolabial-posterolingually extended with a spindle-shaped occlusal surface. The t5 is linked to both t3 and t4, forming the distinct oblique ridge, with the exception of one specimen that lacks a t3–t5 connection. Among the five M1, one has t5 and t6 isolated and the others show t5–t6 weakly connected, two with a gracile crest. A crest posterior to t6 links to either t8 or to the junction of t8 and t9, or directly to t9 as on V8879.1 from YS120. The t9 is nearly fused with t8. On two specimens a tiny t0 is present. An extremely weak anterior cingulum is seen on only one specimen. M1 has five roots.

On M2 the t1 is nearly equivalent to or slightly larger than t3 in size, and smaller than t4. With the exception of one specimen on which the t3 lacks a posterior spur, the remaining specimens have t3–t5 connections. The t4 is posterior to t5 and t6, the three linked by thin ridges, forming an anteriorly convex arc. A t7 is absent. Five-rooted.

The m1 is shaped as an anteriorly narrow and posteriorly broadened triangle with slightly anteriorly inclined cusps. A well-developed tma is slightly smaller than, or equivalent in size to the lingual and labial anteroconids and is linked to, or isolated from them. Frequently, the labial and lingual anteroconids are weakly connected posteriorly. All specimens possess an anterior mure of varying degrees of strength. The protoconid lies posterior to metaconid, but they are connected anteriorly at their bases. All specimens display a gracile and weak medial ridge that extends to the protoconid. The c1 is equivalent in size to or slightly smaller than the c2, and only one specimen possesses a distinct c3. A weak posterior cingulum is transversely extended, slightly lingually positioned. Three-rooted.

The m2 labial anteroconid is developed and linked to the protoconid lingually. The main labial cuspids resemble roughly the lingual ones in morphology, while the anterior pair of cuspids is slightly larger than the posterior pair. The medial ridge is variable in strength: from a distinct ridge connected to the protoconid to its complete absence. The c2

Table 14.2 Dental measurements of *Chardinomys yusheensis* (mm)

	Length			Width		
	N	$\bar{x}$	Range	N	$\bar{x}$	Range
M1	10	1.94	1.70–2.15	13	1.31	1.20–1.40
M2	9	1.27	1.05–1.40	9	1.29	1.20–1.40
m1	19	1.77	1.65–1.95	16	1.28	1.15–1.35
m2	16	1.33	1.20–1.50	16	1.32	1.20–1.40
m3	5	1.11	1.00–1.15	6	1.11	1.00–1.15

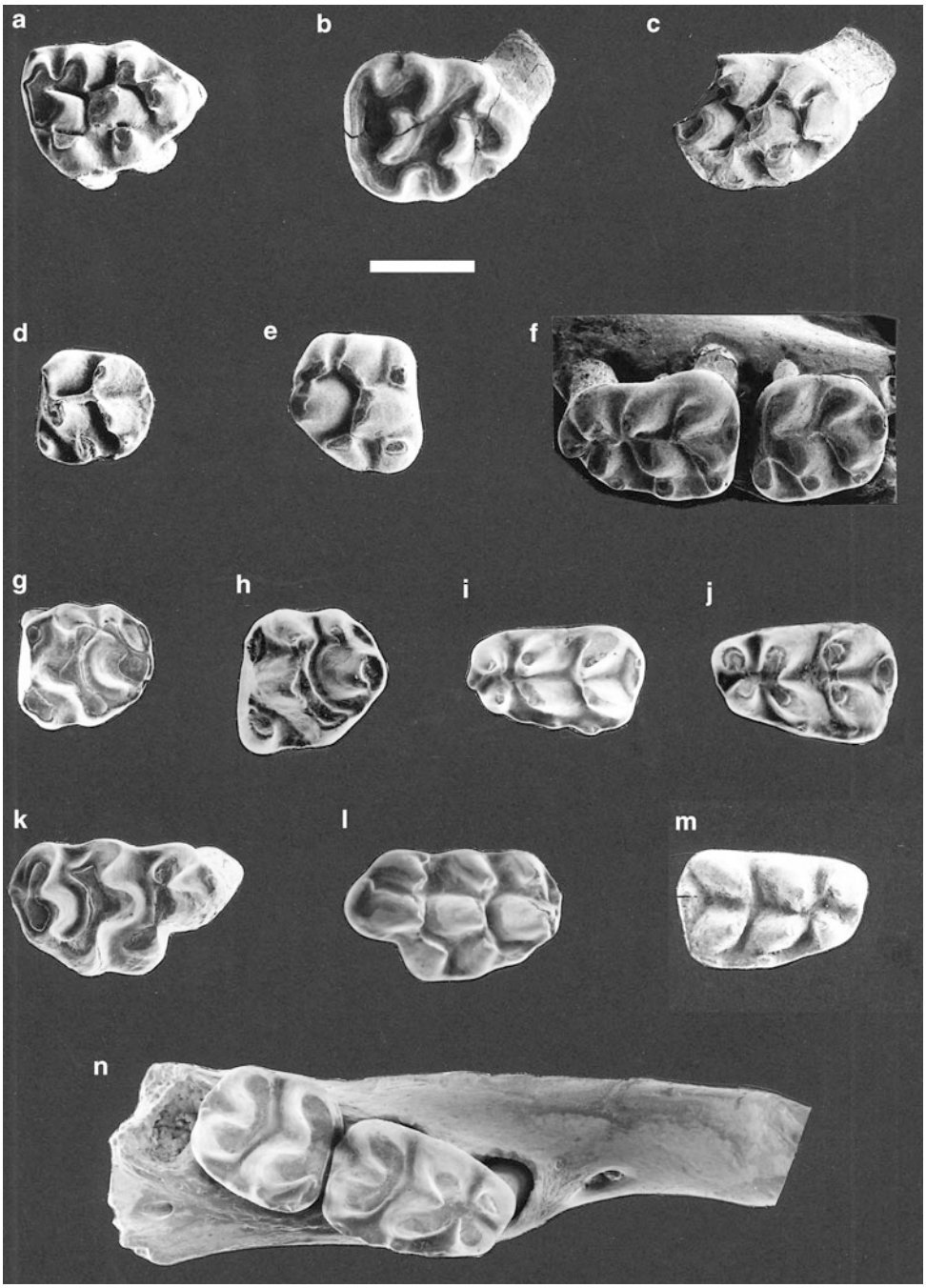

Fig. 14.3 *Chardinomys nihowanicus* (**a**–**f**). **a** Right M1 V8879.1; **b** right M1 V8875.1; **c** right M1 V8877.3; **d** left m2 V8880.3; **e** right M2 V8877.4; **f** left m1–2 V8876.1. *Apodemus orientalis* **g** left M2 V11343. *Tedfordomys jinensis* gen. et sp. nov. (**h**–**n**). **h** left M2, V11336.19; **i** left m1 V11336.3; **j** left m1 V11336.2; **k** right M1 V11336.26; **l** left M1 holotype V11336.24; **m** right m1 (YS8) V8867; **n** right m1–2 V11336.8. Scale bar = 1 mm

Table 14.3 Dental measurements of *Chardinomys nihowanicus* from Yushe, Shanxi

	Length			Width		
	N	$\bar{x}$	Range	N	$\bar{x}$	Range
M1	5	1.92	1.80–2.00	5	1.31	1.25–1.40
M2	4	1.23	1.15–1.30	4	1.26	1.15–1.30
m1	5	1.85	1.80–1.90	6	1.27	1.25–1.30
m2	4	1.33	1.25–1.40	4	1.29	1.15–1.35

is distinct on all specimens, while the c1 is small, present on 3 specimens out of 4. The posterior cingulum is small and oval-shaped, positioned slightly lingually. There are three anterior and two posterior roots.

Comparison and discussion: Both in size and morphology, the Yushe Basin specimens fall within the range of variation for *Chardinomys nihowanicus* from the late Pliocene of Jingle, Shanxi; Daodi and Dongyaozitou, Hebei (Zhou 1988; Cai and Qiu 1993; Zheng and Cai 1991). Shared characters include a weak t5–t6 connection, undeveloped t0 and anterior cingulum on M1, a very weak c3 on m1, and 5-rooted m2. The species recovered from the Mazegou and Haiyan formations, and red loess at Yushe, therefore, differs from *C. yusheensis* described from the Gaozhuang Fm. and from early Pliocene *C. bilikenesis* from Bilike, Inner Mongolia.

Zhou (1988) carefully distinguished differences of a late Pliocene sample of murines (Jingle, Shanxi) from *Chardinomys yusheensis* and named *Chardinomys louisi* for them. He was correct in this, but the distinguishing features of *C. louisi* are those that define *C. nihowanicus*. Cai and Qiu (1993) synonymized *C. louisi* with *C. nihowanicus*.

Chardinomys nihowanicus is an end member in the evolution of *Chardinomys* (Cai 1987; Zhou 1988; Cai and Qiu 1993) and its features indicate principally increase in crown height and decrease in cusp inclination, t1 and t4 becoming nearly columnar, and reduction of the anterior cingulum on M1 and labial accessory cuspids on m1. In addition, the t5–t6 connection on M1 weakens, and the number of molar roots increases on average. Recognizing these changes generally requires many specimens due to trait variability; to determine the evolutionary relationships of the partly contemporary *C. yusheensis* and *C. bilikeensis* will require more fossils.

Karnimatoides Qiu and Li, 2016

Type species: *Karnimatoides hipparionus* (Schlosser, 1924), only named species.

Karnimatoides hipparionus (Schlosser, 1924)

Material: Yuncu subbasin, YS34: fragmentary mandible with m1 (V8844); YS32: 13 M1 (5 damaged), 6 M2 (2 damaged); M3, 8 m1 (1 damaged), 12 m2, 2 m3 (V8845.1-42); YS3: 13 M1 (3 damaged), 11 M2 (1 damaged), 2 M3, 9 m1 (3 damaged), 11 m2, 4 m3 (V8846.1-50); YS60: maxilla with M1–2 and mandible with m1–2, both broken (V8847.1-2); YS62: maxilla with M1–3 and mandible with m1–3, both broken (V8848.1-2); YS33: mandible fragment with m1–2 (V8849); YS39: mandible fragment with m2-3, 4 M1 (one damaged), M3, 5 m2 (V8856.1-11); YS171 (Jiangou): M1, M2, m1, damaged m2 (V11346.1-4). Tancun subbasin, YS144: m1 (V11339); YS145: m1 (V11340); YS161: right mandible fragment with m1–3; left mandible with heavily worn m1; right maxilla with M1–3, heavily worn left and right M1–M3 of the same individual; m1, damaged M1, damaged M2, and three m2 (V11341.1-10). See Figs. 14.4 and 14.5m–p; measurements in Table 14.4.

Stratigraphic range and age: Late Miocene Mahui Fm. to early Pliocene Taoyang Member, Gaozhuang Fm., about 6 to 4.7 Ma.

Description: The zygomatic arch initiates above the anterior margin of the M1 and the incisive foramen extends to the anterior margin of the M1. The ramus is 4.7 mm in depth beneath m1, masseteric crest is distinct but not particularly inflated at its anterior terminus, and a mental foramen is close and anterolateral to the m1 anterior root and on the diastema; the diastema is conspicuously concave and 3.5 mm long. Ascending ramus initiates lateral to m2 (V8848.2).

The t1 of M1 is frequently larger than t3 and is posterior to both t2 and t3. The t2 and smaller t3 are closely situated and linked by a crest. In half the specimens t3 possesses a weak posterior spur. The t4 and t6 are almost equivalent in size, equally somewhat posterior to t5, and both linked to t5 by crests. A t6 is slightly larger or equivalent to t9. On 24 of 26 variably worn specimens a connection between t6 and t9 is present; on two unworn teeth, the connection is present on one, but absent on the other, indicating some variability in the t6–t9 connection. No t7 occurs. A t4–t8 connection is extremely low or absent. On nine specimens there is an extremely weak t12. Of 30 specimens 13 possess a prestyle which is distinct on six. Three-rooted, occasionally plus a small central root, as in the Ertemte population.

The M2 has a t1 distinctly larger than t3 usually with a low crest that links to the anterior t5. On one specimen the t1 is twinned. The t3 is frequently isolated. The relative position and morphology of t4, t5, and t6 resemble that on the M1, though t6 is occasionally slightly anterior. The t6 is slightly larger than t9. Among 17 specimens, six have a very low and weak t6–t9 connection while on the rest these cusps are isolated. The t4–t8 connection is generally low and weak although on nine specimens this connection only appears after occlusal wear. Five specimens have an obscure t12; all have four roots.

The M3 has a robust t1 that is isolated or is linked to the anterolingual side of t5 by a very weak crest. The t4 and t5 are equivalent in size, and the latter constitutes the anterolabial corner of the tooth because t3 is absent. The t6 is nearly fused to the t5, while t8 and t9 are fused into a single cusp. Three-rooted or 4-rooted (as on YS32, V8845.20).

The tma is present on 18 out of 20 m1 at varying degrees of development, ranging from a cuspule to an extremely obscure cingulum. In general, a low and weak anterior mure is present between the lingual anteroconid and the metaconid, though on four specimens this feature is either incomplete or absent. A medial ridge is absent. A labial cingulum is frequently well developed. The c1 is consistently larger than c2, which is not present on two specimens. On a number of specimens the posterior cingulum is ovoid, but in a minority it is transversely extended. Two roots are observed.

The m2 has a distinct labial anteroconid that is either isolated or linked by a crest at its lingual side to the protoconid anteriorly. A medial ridge is absent while a labial cingulum is

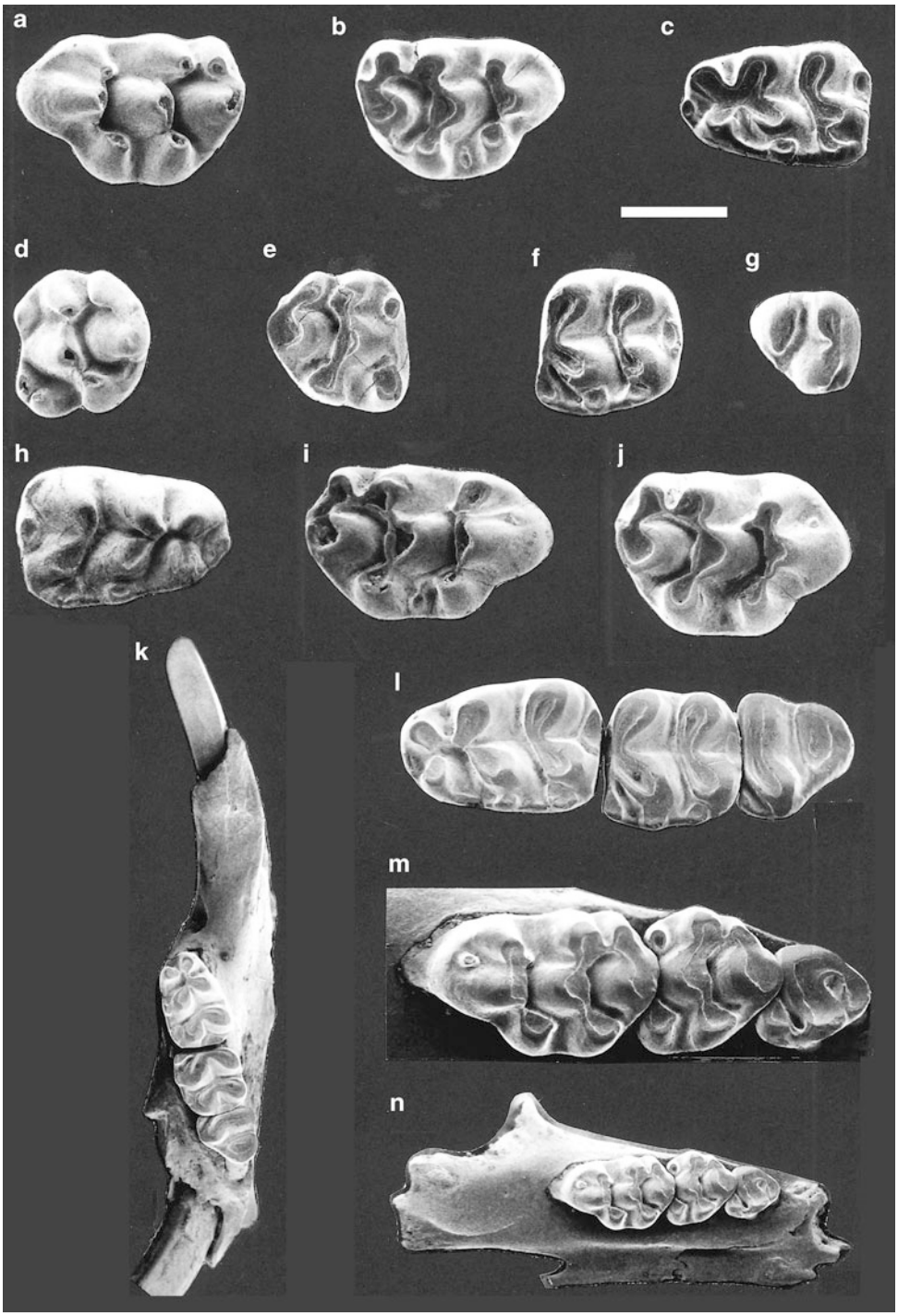

Fig. 14.4 *Karnimatoides hipparionus* (Schlosser, 1924); **a**–**g** from YS3, **h**–**j** from YS32, **k**–**n** from YS62. **a** Left M1 V8846.6; **b** right M1 V8846.9; **c** left m1 V8846.27; **d** left M2 V8846.17; **e** right M2 V8846.19; **f** left m2 V8846.40; **g** right m3 V8846.50; **h** right m1 V8845.27; **i** right M1 V8845.6; **j** right M1 V8845.5; **k** left dentary with incisor and molars V8848.2; **l** m1–3, left to right, of V8848.2; **m** M1–3, left to right, of V8848.1; **n** left maxilla with molars V8848.1. Scale bar = 1 mm; 2 mm for (**k**) and (**n**)

distinct and frequently bears a c1 and c2, the c2 is generally larger than the c1, however on four specimens the c1 is obscure or absent, and on one specimen the c2 is also absent. Posterior cingulum resembles that on the m1. Two-rooted.

The labial anteroconid of m3 is small – extremely small on some specimens. A medial ridge is absent, as are labial cingula and accessory cuspids. On only one specimen is there a vestigial hypoconid. Two-rooted.

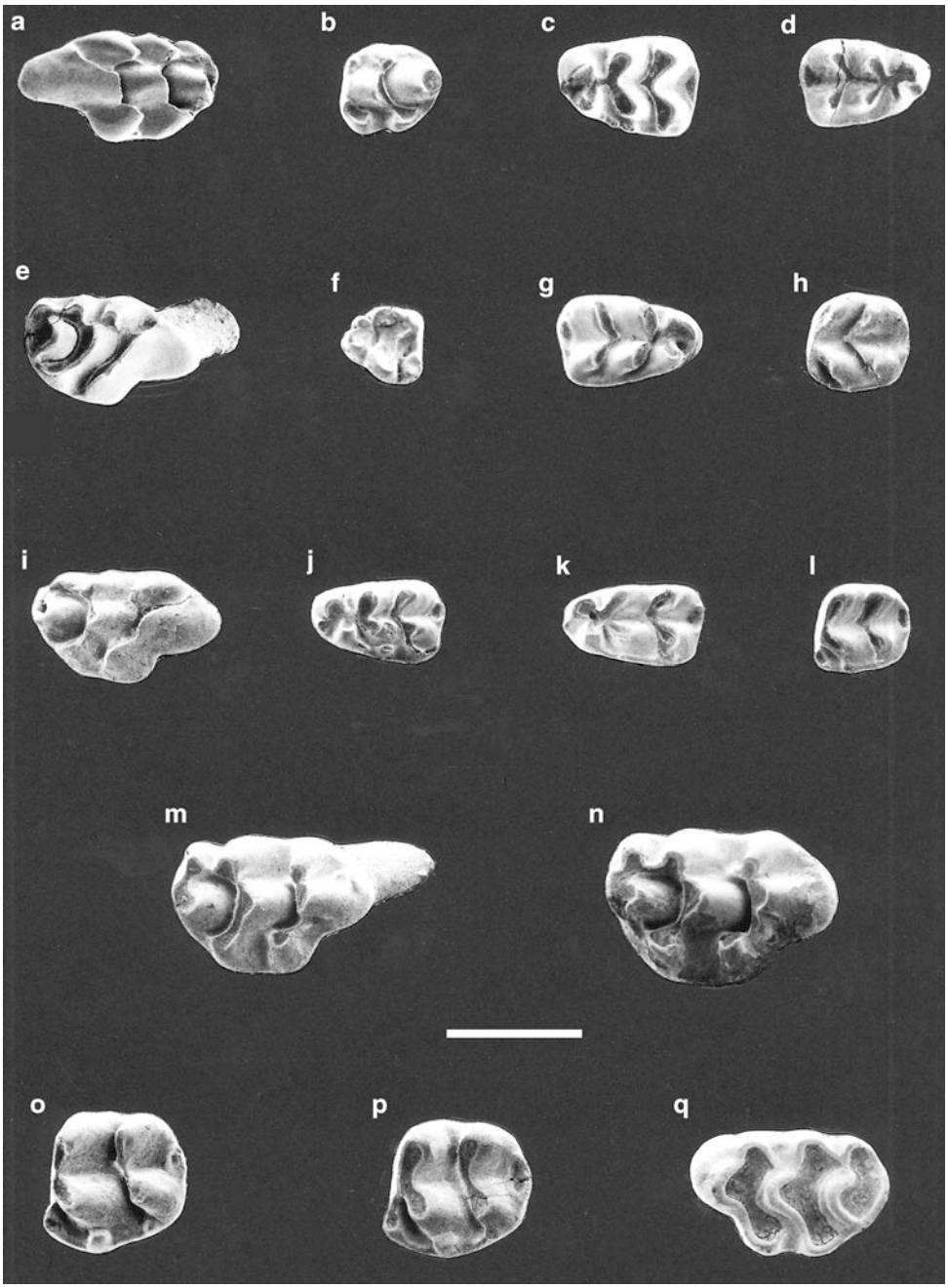

Fig. 14.5 *Huaxiamys downsi* Wu and Flynn, 1992, **a–h** from YS4; *Huaxiamys primitivus* Wu and Flynn, 1992, **i–l** from YS32 and YS3; *Karnimatoides hipparionus* (Schlosser, 1924), **m–p** from YS39; *Karnimatoides* sp., **q** from YS11. **a** Holotype, left M1 V8855.7; **b** left M2 V8855.22; **c** left m1 V8855.28; **d** right m1 V8855.35; **e** right M1 V8855.13; **f** right M3 V8855.25; **g** right m1 V8855.36; **h** left m2 V8855.47; **i** holotype, right M1 V8850.1; **j** left m1 V8851.1; **k** left m1 V8851.2; **l** left m2 V8850.5; **m** right M1 V8856.2; **n** right M1 V8856.3; **o** left m2 V8856.9; **p** left m2 V8856.7; **q** left M1 V8843. Scale bar = 1 mm

The Jiangou YS171 sample collected by Will Downs in 1991, low in the Taoyang Member, was a sandstone block that he reduced by acid treatment. It yielded molars like the material above in morphology, but somewhat larger size (M1: 2.30 × 1.50, M2: 1.30 × 1.35, m1: 1.92 × 1.30 mm). The 1991 Tancun subbasin fossils from YS144, 145, and 161 are from low in the Gaozhuang Formation, and resemble Yuncu subbasin samples both in morphology and size: three m1 length × width, 1.80–1.90 × 1.22–1.30 (ranges); m2, 1.35 × 1.30; m3, 1.05 × 1.00; M1, 2.00 × 1.42; M2, 1.40 × 1.42; M3, 1.00 × 1.00 mm.

Comparisons: Specimens attributed to *Karnimatoides hipparionus* from Yushe Basin come from the late Miocene Mahui Fm. and the overlying Gaozhuang Fm., extending into

Table 14.4 Dental measurements of *Karnimatoides hipparionus* from Yuncu subbasin

	Length			Width		
	N	$\bar{x}$	Range	N	$\bar{x}$	Range
M1	24	2.05	1.85–2.25	31	1.40	1.25–1.55
M2	19	1.34	1.25–1.45	19	1.42	1.35–1.50
M3	5	0.92	0.90–0.95	5	0.94	0.85–1.00
m1	18	1.87	1.75–2.00	18	1.25	1.20–1.35
m2	31	1.29	1.20–1.35	31	1.29	1.15–1.40
m3	8	1.02	0.90–1.10	8	1.05	1.00–1.20

the early Pliocene. Previously (e.g., Flynn et al. 1991) we considered that the youngest sample of this species (Fig. 14.5 m–p) from YS39 might differ from the type material from Ertemte, Inner Mongolia. The younger Yushe Basin material is slightly smaller and shows a stronger t3 spur, but we consider such differences as insignificant for species distinction. Possibly this indicates chronoclinal change (decreasing size, increasing stephanodonty) in the early Pliocene *K. hipparionus* lineage.

Although the Ertemte population was referred by Storch (1987) to genus *Karnimata*, Storch and Ni (2002) reexamined the rich material of Ertemte and pointed out that the Ertemte species should be excluded from *Karnimata*. Qiu and Li (2016) erected the new genus *Karnimatoides* for that species. We see no significant morphological or metric contrast of Yushe *Karnimatoides* of 6.0–4.7 Ma with the type material of *Karnimatoides hipparionus*, but a difference is apparent with an older Yushe mouse as noted in the following.

Karnimatoides sp. (Fig. 14.5q)

At about the 100 m level in the late Miocene Mahui Fm. (about 6.2 Ma), locality YS11 produced a small M1 (V8843, 1.78 × 1.18 mm) that is deeply worn. The t1 and t3 are posterior to t2, and t1 is situated slightly posterior to t3. The t3 has a moderately developed posterior spur. The t4 and t6 are both posterior to and almost symmetrical to t5. The t6 is in contact with but not fused to t9. A t7 and t12 are absent, and t4 is isolated from t8. The tooth has three roots; its length/breadth ratio is 0.67. This smaller, non-stephanodont *Karnimatoides* from YS11 is not assignable to *K. hipparionus*. Although morphologically distinct, the lack of material makes naming a new species imprudent.

Discussion on Yushe Basin *Karnimatoides*: The report of *Karnimata* sp. from Daodi, Hebei Province (Cai and Qiu 1993) may be questioned. The damaged M1 and m1 fall within the range of variation in size for Yushe Basin specimens, but the M1 has a t6–t9 connection and a distinct t7 with developed stephanodonty. Furthermore the morphology of m1 is quite different from that of *Karnimatoides* of Yushe basin.

The genus *Karnimata* was erected by Jacobs (1978) for a late Miocene lineage of murines from the Siwaliks of Pakistan. Brandy (1979) recognized several species from the late Miocene and Pliocene of Afghanistan, and Storch (1987) and Mein et al. (1993) attributed species from China and Spain to the genus. Some of these species are quite distinctive in morphology and are now recognized as being derived from separate lineages. Sen (1983) suggested reassignment of *K. afghanensis* to the genus *Saidomys*. Both Storch (1987) and Cai and Qiu (1993) recognized distinct discrepancies between the Siwalik and the Chinese forms of *Karnimata*, particularly the stephanodonty of the M1 of the latter. Subsequently, from the viewpoint of fossils from Spain, Mein et al. (1993) proposed that the type species *Karnimata darwini* is a synonym of *Progonomys woelferi* Bachmayer and Wilson, 1970, and that all Siwalik *Karnimata darwini* should be transferred to *Progonomys*.

The Siwaliks do produce a lineage of *Progonomys*. *Progonomys debruijni* Jacobs (1978) is a derived member of the genus, of about 9 Ma. Older *Progonomys* with more blunt cusps is also present in the Siwaliks. Cheema et al. (2000) named *Progonomys hussaini* for Siwalik samples of about 11–10 Ma. This material is so close to European *Progonomys* that Wessels (2009) proposed synonymy of *P. hussaini* with *P. cathalai*.

Qiu et al. (2004) confirmed the generic attribution of the Siwalik species and added a new Lantian species *Progonomys sinensis*, also early late Miocene. Storch and Ni (2002) reviewed the Ertemte murines attributed to *Karnimata*. Their analysis reaffirms the distinctiveness of Siwalik *Karnimata* from *Progonomys*, but demonstrates that *"K. hipparionum"* is not *Karnimata*. While *Karnimata* evolved in the Indian Subcontinent, another lineage evolved in China. Whether *Karnimata* was present in Europe is unresolved. The species *Karnimatoides hipparionus* from Ertemte and Yushe Basin represents a distinct Miocene/Pliocene lineage in China.

Most recently, Kimura et al. (2015a, b) demonstrated definitively that early late Miocene Siwalik mice represent two separate lineages that diverged at the *Mus/Arvicanthis* phylogenetic split, and that *Karnimata darwini* is a member of the *Arvicanthis* group, whereas *Progonomys debruijni* is in the *Mus* lineage.

Huaxiamys Wu and Flynn, 1992

Type species: *Huaxiamys downsi* Wu and Flynn, 1992.

Included species: *H. downsi*, *H. primitivus* Wu and Flynn, 1992.

Localities, age, and stratigraphic range: Late Miocene Mahui Fm. through early Pliocene Nanzhuanggou and Culiugou Members, Gaozhuang Fm., Yuncu and Tancun subbasins, Yushe Co., Shanxi Province; early Pliocene of Gaotege, Abag Qi, and of Bilike, Huade County, Inner Mongol; late Pliocene Daodi Fm. of Yangyuan-Yuxian Basin, Hebei Province.

Generic diagnosis: A small murid with brachy-stephanodont molars and upper tooth cusps strongly posteriorly inclined. Anterior wall of t2 on M1 is greatly extended anteriorly, t3 is extremely posteriorly positioned with a broad valley between it and t2, and the connected t1–t2 forms an anterolabial-posterolingually oriented crest. A t7 is absent. The tma on m1

is either small or absent, the lingual anteroconid is anterolabial-posterolingually inflated to varying degrees between individuals, and is more anteriorly extended than the labial anteroconid. Upon occlusal wear, the tma is connected to the lingual anteroconid, and an asymmetrical X-pattern is formed by connections between the lingual, labial anteroconids, protoconid, and metaconid. A medial ridge is incomplete and the labial accessory cuspids are undeveloped. M1 is 3-rooted, M2 4-rooted, and m1, m2 are 2- or 3-rooted.

Differential diagnosis: This rodent genus overlaps in size with several species of *Micromys*, but differs greatly in morphology with strongly inclined cusps on upper molars. The M1 t1 is more posteriorly positioned, a broad valley is present between t2 and t3, t7 is absent on M1–2, and m1 lacks distinct tma and labial accessory cuspids. *Huaxiamys* differs from *Mus* in its stephanodont molars with distinct t6–t9 connection on upper molars, broad valley between t2–t3 on M1, and more developed medial ridge, anterior mure, labial accessory cuspids or cingula on lower molars.

Huaxiamys downsi Wu and Flynn, 1992

Type: Left M1 (V8855.7; L × W = 1.88 × 1.00 mm).

Paratypes: 20 M1, 3 M2, 2 M3, 14 m1, 7 m2, 4 m3, 5 fragmentary mandibles with m1 or m1–2 (V8855.1-6, 8-56) (Fig. 14.5a–h).

Type locality, age, and stratigraphic range: YS4, 4.3 Ma, Yushe Co. Shanxi Province, early Pliocene, Culiugou Member, Gaozhuang Fm. Stratigraphic range extends down into Nanzhuanggou Member, Gaozhuang Fm. (YS50 and YS97).

Species diagnosis: A derived species with anterior wall of t2 on M1 rapidly attenuates anteriorly (extends and narrows as it descends). Both t3 and t6 are more posterior than on *H. primitivus,* and a t12 is absent. The tma on m1 is usually absent, and the posterior cingulum and labial accessory cusps on m1–2 are frequently reduced to crest-like structures. The m1 and m2 are 2- or 3-rooted.

Huaxiamys primitivus Wu and Flynn, 1992

Type: Right M1 (V8850.1; L × W = 1.72 × 1.00 mm).

Paratypes: Broken M1, M2; m1 and left m2 (V8850.2-5) (Fig. 14.5i–l)

Type locality, age, and stratigraphic range: YS32, 6.0 Ma, Yushe Co., Shanxi Province, late Miocene Mahui Fm. Stratigraphic range is late Miocene: upper part of Mahui Fm., extending up to basal Taoyang Member, Gaozhuang Fm. (YS3 and YS60).

Species diagnosis: Less stephanodont than *H. downsi.* On M1 the t3 is not shifted posteriorly in position, mesial wall of t2 is extends anteriorly but does not rapidly attenuate, and a t12 (cusp-like posterior cingulum) is present. More developed tma on m1, and more developed or ridge-like labial cingulum cuspids on m1 and m2. The posterior cingulum on lower molars is ovoid. The m1 and m2 are 2-rooted.

Additional specimens: Type material and referred specimens were measured and described by Wu and Flynn (1992). In 1991, Tancun subbasin locality YS161 produced a fragmentary right mandible with m1–2 and incisor, in addition to two heavily worn left and right m2 specimens (V11344.1-3). The locality is basal Gaozhuang Formation equivalent. A mental foramen is located anterior to the distinctly inflated anterior terminus of the masseteric crest. The masseteric fossa is extremely shallow. The ramus is 2.0 mm deep beneath the lingual side of m1, the diastema is 1.95 mm long, and lower incisor is thin and gracile. The tma on m1 is small and round. The labial cingulum is a gracile crest. The m1 is 1.30 × 0.80 mm; two m2 are 0.86–0.87 × 0.81–0.84 mm.

Discussion: Being more primitive and older, *Huaxiamys primitivus* is a likely ancestor to *H. downsi. Huaxiamys* has been reported from Late Pliocene Daodi Fm. of Yangyuan-Yuxian Basin, Hebei Province (Cai and Qiu 1993); late Miocene to mid-Pliocene of Lingtai, Gansu Province (Zhang and Zheng 2000, 2001; Zheng and Zhang 2000, 2001), early Pliocene of Gaotege, Abag Qi (Qiu and Li 2016) and Bilike of Huade County (Qiu and Storch 2000), both Nei Mongol. Qiu and Li (2016), in their study of the rich material of *H. downsi* from Gaotege, note that the absence of t12 on M1 should not be used as a criterion to differentiate *H. downsi* from *H. primitivus* because the recognition of t12 on *H. downsi* M1 depends on the wear stage of the tooth.

Micromys Dehne, 1841

Micromys chalceus Storch, 1987

Material: M1 (V8857.1), 1.42 × 0.94; m2 (V8857.2), 0.93 × 0.81 mm (Fig. 14.6m).

Locality, age, and stratigraphic position: YS39, 4.7–4.8 Ma, early Pliocene Taoyang Member, Gaozhuang Fm.

Description: The specimens are consistent in small size and morphology with *M. chalceus* from Ertemte 2, Inner Mongolia, showing primitive characters for the genus such as absence of t7 on M1, which is 3-rooted.

Micromys cf. *M. chalceus*

YS145 of the basal Gaozhuang Fm. (about 5.7 Ma) produced 2 M1 and 1 m2 (V11342.1-3). The t3 on both M1 (Fig. 14.6l) has a posterior spur which is particularly pronounced and linked to the anterolabial side of the t5 on V11342.1. In the position of t7 is a slightly inflated crest with a constriction between it and the t4, as in many of the type series of M1 (Storch 1987). A t6–t9 connection is present and there is a well-developed t12. M1 is 3-rooted. The m2 is extremely worn but a weak medial ridge is still discernible. The labial cingulum is a narrow crest and the posterior cingulum is

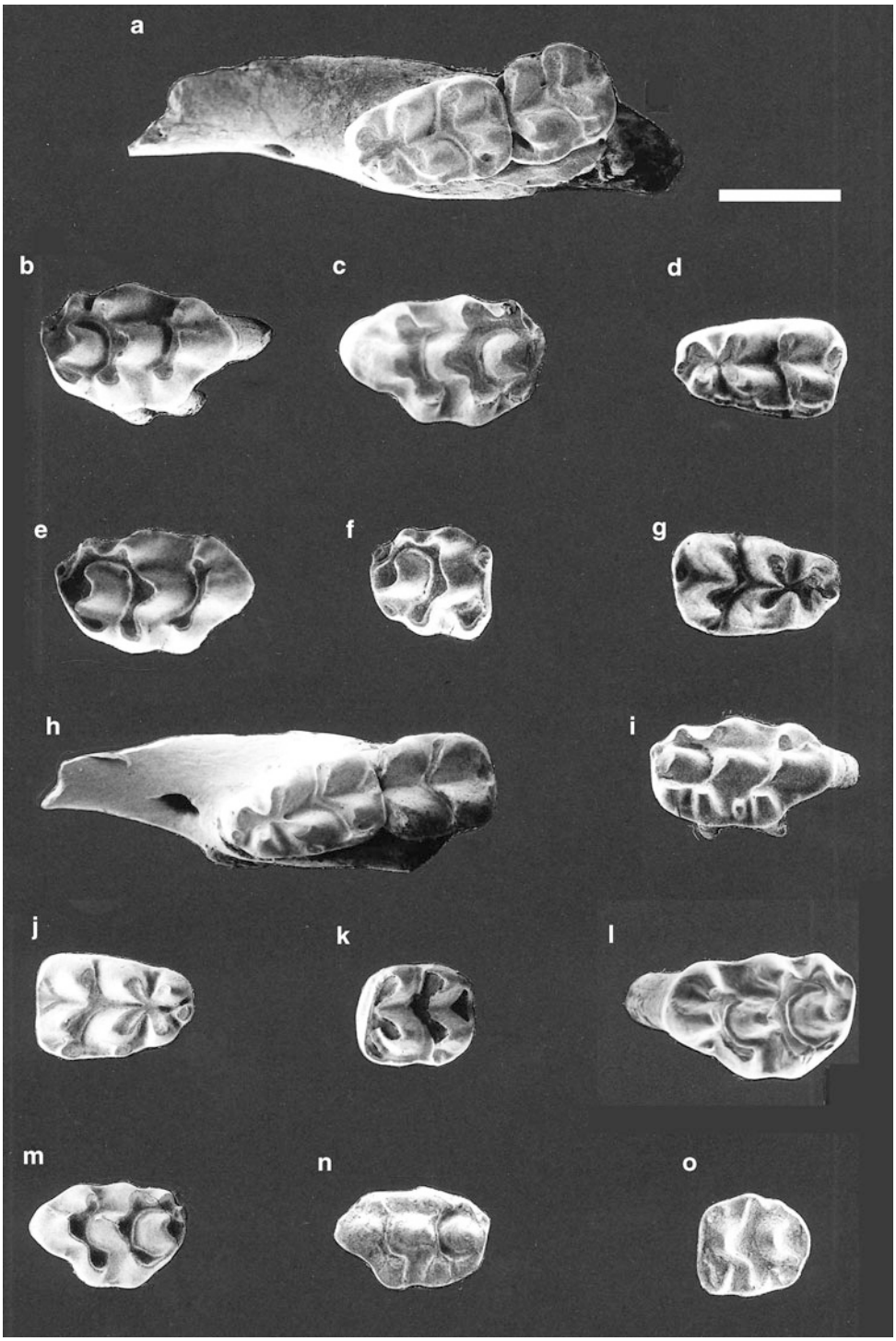

Fig. 14.6 *Micromys tedfordi* Wu and Flynn, 1992, **a**–**g** from Gaozhuang Formation; *Micromys* aff. *M. tedfordi,* **h**–**k** from Haiyan Formation; cf. *M. chalceus* (**l**) from the Gaozhuang Formation and *Micromys chalceus* Storch, 1987 (**m**); *Micromys* cf. *M. minutus* (**n**, **o**) from the Haiyan Formation. **a** Left dentary with m1–2 V8859.3; **b** right M1 V8861.8; **c** left M1 V8858.1; **d** left m1 V8858.3; **e** right M1 V8861.7; **f** right M2 V8861.11; **g** right m1 V8861.23; **h** left dentary with m1–2 V8865; **i** right M1 V8866; **j** right m1 V8864.4; **k** left m2 V8864.5; **l** left M1 V11342.1; **m** left M1 V8857.1; **n** left M1 V8863.1; **o** left M2 V8863.2. Scale bar = 1 mm

obscure. Morphologically, the specimens resemble *M. chalceus* from Ertemte 2, but they are almost 10% larger (M1 1.55 × 1.03, 1.51 × 0.97; m2 1.00 × 0.90).

Micromys tedfordi Wu and Flynn, 1992

Type: Left mandible (V8859.3), with m1: 1.56 × 0.96, m2: 1.14 × 1.00 mm (Fig. 14.6a–g).

Paratypes: Left M1 (V8859.1) 1.67 × 1.09, and right m2 (V8859.2) 1.09 × 0.94 mm.

Type locality, age, and stratigraphic range: YS50, 4.7 Ma, Yuncu subbasin, early Pliocene, Nanzhuanggou Member, Gaozhuang Fm.

Emended diagnosis: *Micromys* of large size with moderate stephanodonty and with the mental foramen located laterally on the dentary, well rostral and below the diastema. M1 always with t7 and t12 and is 5-rooted. Small but distinct tma on m1, but undeveloped labial accessory cuspids, 2-rooted. The m2 is occasionally 3-rooted.

This is the largest member of the genus and possesses derived characters including the presence of five roots on M1, three roots on several m2, the small t9 on M1, t4 isolated from t7. Lower molars have accessory labial cuspids that are small or uninflated ridges. The tma is small but constant, and m1 has a short medial ridge terminating anterior to the hypoconid-entoconid chevron; its strong posterior cingulum is lingual in position. Complete description is given in Wu and Flynn (1992).

This species occurs in Yuncu subbasin from localities YS50, YS57b, YS4, YS97 and YS90. The stratigraphic range extends through the Pliocene from Nanzhuanggou and Culiugou members of the Gaozhuang Fm. to the Mazegou Fm., about 4.7 to 3.4 Ma.

Micromys aff. *M. tedfordi*

Material: YS109: M1 (V8866); YS6: left fragmentary mandible with m1–2 (V8865); YS120: M1, three m1, and m2 (V8864.1-5) (Fig. 14.6h–k).

Age and stratigraphic range: early Pleistocene, ~2.5–2.2 Ma, Haiyan Fm.

Measurements: M1: 1.73 × 1.05, 1.66 × 1.14; m1: 1.52 × 0.88, 1.46 × 0.82, 1.44 × 0.85, 1.49 × 0.91; m2: 1.10 × 0.98, 1.13 × 0.89 mm.

Description: Average size is slightly smaller than *M. tedfordi* but slightly larger than *M. praeminutus,* in tooth morphology it is precisely consistent with the former. Primary distinction is in mandibular morphology, with *M.* aff. *M. tedfordi* having a mental foramen more caudally placed on the diastema and a more robust masseteric crest that terminates nearly at the mental foramen. Other morphological characters worthy of note are on the YS109 M1 (V8866), where there is a cuspule respectively lingual and labial to t2, namely t0 and prestyle, and a cuspule between t1 and t4, the latter posteriorly shifted. Well-developed c1 and c2 on two m1; ridge-shaped on the other two specimens.

Micromys cf. *M. minutus* (Pallas, 1771)

The entire sample consists merely of three specimens from the Haiyan Fm., ~2.5–2.2 Ma: relatively deeply worn M1 from YS6 (V8863.3: 1.30 × 0.85 mm); and from YS120, M1 (V8863.1: 1.46 × 0.94 mm) and M2 (V8863.2: 1.06 × 0.91 mm; Fig. 14.6n, o). Morphologically, these resemble the living species *M. minutus* in small-size, the small t9 on M1–2, t7 distinctly separated from t4, 5-rooted M1, and the twinned t1 on M2. The "confer" status reflects the small sample.

Discussion on Yushe Basin *Micromys*: Four species of *Micromys*, two large and two small, were recovered from the late Neogene of the Yuncu subbasin. For the small species, two million years interrupt the records of *M. chalceus* and *M.* cf. *minutus* and, no phylogenetic hypothesis is attempted here. *M.* cf. *minutus* probably has a close relationship with the extant *M. minutus* based on similar dental morphology. *M. tedfordi* and *M.* aff. *M. tedfordi* share similar dental morphology, but have mental foramina in different positions on the mandible, with that of the latter positioned further caudally on the diastema dorsally and close to the terminus of the masseteric crest. Though their occurrences are separated by over one million years, they may represent members of one lineage. We hypothesize a tendency for the position of the mental foramen to shift from the lateral side to the dorsal surface of the diastema.

Specimens of the extant *M. minutus* were studied in the collections of the Museum of Comparative Zoology (MCZ), Harvard University: *M. minutus ussuricus* (MCZ 43401, 43404, 43405) from Korea; *M. m. hygmaceus* (23464, 43631, 56415) from South China, and *M. minutus* (24106) from Siberia. All specimens display a mental foramen positioned posterodorsally on the diastema, with the exception of *M. ussuricus* where it is slightly more laterally placed.

Apodemus Kaup, 1829

Apodemus orientalis (Schaub, 1938)

Material: Left M2 (V11343.1), 1.12 × 1.03 (Fig. 14.7i), and two broken M1 (V11343.2-3), ~1.65 × 1.12 and 1.70 × 1.21 mm from YS145; right M2 (V8881) from YS32, 1.14 × 1.08 mm.

Locality, age, and stratigraphic position: Late Miocene YS32 (V8881), Mahui Fm., 6.0 Ma; and YS145 (V11343), basal Gaozhuang Fm. equivalent (~5.7 Ma).

This species, type locality being Ertemte, Inner Mongolia, is represented at YS32 by a well-worn M2 with a large t1 that is linked to the lingual side of t5 by a weak crest. There are t6–t9 and t4–t7 connections, t9 is slightly smaller than t6, and t7 is smaller than t4. A t12 is conspicuous. Three roots are present with a vertical groove along the lingual root. The

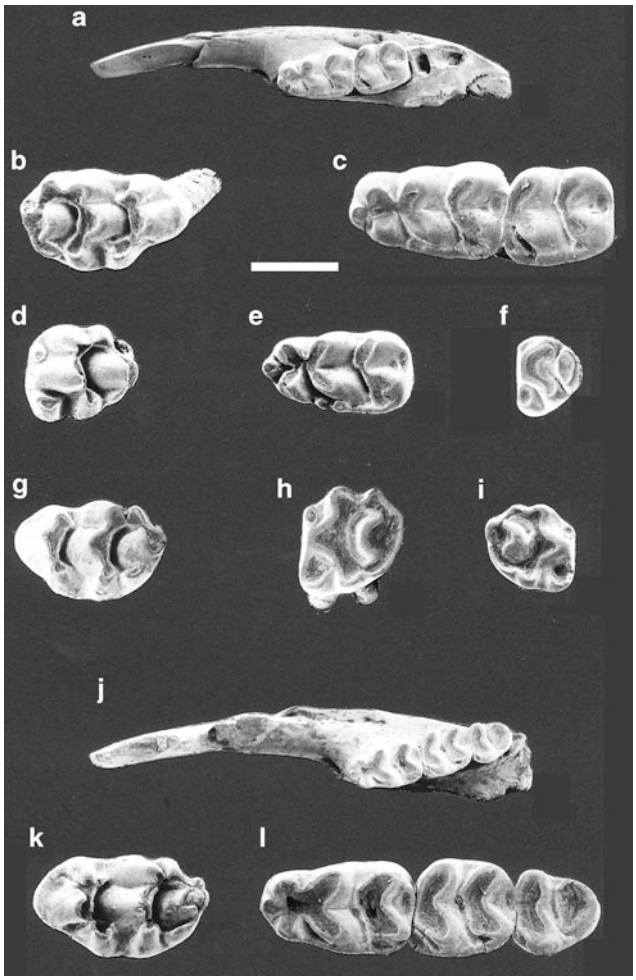

Fig. 14.7 *Apodemus qiui* Wu and Flynn, 1992 (**a**–**h**) from the Gaozhuang Formation; *Apodemus orientalis* (Schaub, 1938) (**i**) from the Mahui Formation; *Apodemus zhangwagouensis* Wu and Flynn, 1992 (**j**–**l**) from the Mazegou Formation. **a** Holotype left dentary with incisor and m1–2 V8883.15; **b** right M1 V8883.4; **c** m1–2 of dentary V8883.15; **d** left M2 V8883.6; **e** left m1 V8886.10; **f** left M3 V8886.9; **g** left M1 V8886.1; **h** left M2 V8886.8; **i** right M2 V8881; **j** Holotype, left dentary with incisor m1–3 V8887.5; **k** left M1 V8887.1; **l** m1–3 of dentary V8887.5. Scale bar = 1 mm; 2 mm for (**a**) and (**j**)

YS145 M2 is moderately worn, with double cusped t1, t4–t8 and t6–t9 connections, well-developed t12, and four roots. The two damaged M1 from YS145 are 3-rooted, with no t7 but a crest connecting t4–t8.

Apodemus qiui Wu and Flynn, 1992

Type: Left mandible with m1–2 (V8883.15): m1, 2.00 × 1.15; m2, 1.41 × 1.23 mm.

Paratypes: Five M1 (two damaged), M2, six m1 (four damaged), and two m2 (one damaged) (V8883.1-14; Fig. 14.7a–h).

Type locality, age, and stratigraphic position: YS50, 4.7 Ma, early Pliocene, Yuncu subbasin Nanzhuanggou Member, Gaozhuang Fm.

Species diagnosis: A moderate sized species of the genus with 3-rooted M1, 4-rooted M2, and a mental foramen below the anterior terminus of the masseteric crest.

Referred material and stratigraphic range: YS4: seven M1, M2, M3, six m1, and two m2 (V8886.1-17); YS97: two M1, m2 (V8885.1-3); YS48: fragmentary right mandible with m1 (V8884). Nanzhuanggou and Culiugou Members, Gaozhuang Fm., early Pliocene, 4.6 to 4.3 Ma.

Apodemus zhangwagouensis Wu and Flynn, 1992

Type: A fragmentary left mandible (V8887.5) with m1–m3, measurements: 1.89 × 1.13, 1.39 × 1.23, 1.13 × 1.07 mm (Fig. 14.7j–l).

Paratypes: M1, M2, M3, m1 (V8887.1-4).

Type locality, age, and stratigraphic position: YS87, 3.5 Ma, late Pliocene, Mazegou Fm.

Species diagnosis: A moderate sized species of the genus with 3-rooted M1, 4-rooted M2, and a mental foramen located just anterior to the anterior terminus of the masseteric crest.

Referred material: YS135: fragmentary right mandible with m1–2 (V8882) from early Pliocene Culiugou Member, of Gaozhuang Fm., about 4.3 Ma.

Apodemus sp.

The Pleistocene loess locality YS83, probably less than 1 Ma, produced an m2 (V8888, 1.35 × 0.98 mm) with a labial anteroconid that is anterolingual-posterolabially extended, a slightly lingually positioned ovoid posterior cingulum, a circular c1, c2 absent, c3 weak, and a weak medial ridge. This demonstrates this small mouse persisting into the Pleistocene.

Discussion on Yushe Basin *Apodemus*: Four taxa of *Apodemus* occur from the late Miocene to early Pleistocene in the Yuncu subbasin (6–1 Ma). Specimens from Mahui Formation (YS32) and basal Gaozhuang Formation are consistent in size and morphology with the relatively primitive late Miocene *A. orientalis* from Ertemte, Inner Mongolia. *A. qiui* from the middle to upper Gaozhuang Formation and *A. zhangwagouensis* from the Mazegou Formation are equivalent in size to *A. dominans* (Kretzoi) (see de Bruijn and van der Meulen 1975) from Tourkobounia-1, Greece, but the Chinese forms differ in having a four-rooted M2, while the Greek forms have a three-rooted M1 and M2. The Yushe Basin *Apodemus* tooth root characters (four in M2) in addition to their brachydonty distinguish these species from *A.* cf. *A. atavus* (Cai and Qiu 1993) from the Daodi Fm. in the Nihewan region. After comparison to 19 extant Eurasian subspecies among 12 species at the Museum of Comparative Zoology, the two Yushe Basin fossil species most closely resemble the Chinese *A. agrarius ningpoensis* (MCZ 24280) from Ningbo, *A. a. pallidior* (MCZ 23491-23496) from the foot of Taibai Mountain of Qin Ling and Wanxian and *A. a. mantschuricus*

(MCZ 23487) from Dongling, Hebei Province. Furthermore, the Yushe specimens are consistent with *A. agrarius* in the undeveloped labial accessory cuspids of lower molars, 4-rooted M2, and more elongated M1 and m1. However, *A. agrarius* exhibits more derived characters: greater stephanodonty, better developed t1 and t3 posterior spurs, well developed medial ridges on m1 and m2, four roots on M1, and more reduced upper and lower third molars.

A. zhangwagouensis is distinguished from *A. qiui* by the position of its mental foramen, which is at the anterior terminus of the masseteric crest, and is consistent with *A. agrarius*. *A. zhangwagouensis* appears to be closely related to *A. agrarius,* while *A. qiui* is more primitive.

Tedfordomys gen. nov.

Type species: *Tedfordomys jinensis*, new and only known species.

Generic diagnosis: Small-sized murid with low crowned molars and inclined cusp(-id)s, and absence of longitudinal ridges between cusp(-id)s. The t1 on M1 is in anterior position relative to *Mus*. The t1 and t3 on M1 and M2 have no posterior spurs; stephanodonty is undeveloped. The t7 is absent. The t4 has a low connection to t8, occasionally ridgelike on M1. No t6–t9 connection is present. The t12 is a low, undeveloped crest present in that position. M1 possesses 3 roots and a small central rootlet; M2 is 4-rooted. The labial and lingual cuspids on lower molars are angled (not transverse). On m1 tma is absent or small and low, as are the anterior mure and medial ridge. The medial ridge on m2 is absent. The labial accessory cuspules on m1 and m2 are undeveloped, and constitute a low and thin cingulum, sometimes with a small c1 and c2. The posterior pair of cusps on m1–2 are angled, rather than transverse, and the posterior cingulum is a transversely-extended crest or constitutes an ovoid cusp. The m1 is 2-rooted without a small central rootlet.

Etymology: In honor of Richard H. Tedford who conceived and built the Yushe project with Zhan-Xiang Qiu in the 1980s. He would love to have a mouse named in his memory.

Tedfordomys jinensis gen. et sp. nov.

Type: Left M1 (V11336.24; Fig. 14.3l).

Paratypes: A right mandible with m1–2, and 11 m1 (four damaged, two very worn), six m2, M1, and seven M2 (two damaged, 1 heavily worn, V11336.1-23, 25-26). Figure 14.3h–n.

Table 14.5 Dental measurements of *Tedfordomys jinensis* from YS145 (mm)

	Length			Width	
	N	$\bar{x}$	Range	$\bar{x}$	Range
M1	2	1.79	1.78–1.79	1.11	1.11
M2	5	1.22	1.18–1.27	1.17	1.14–1.20
m1	8	1.53	1.45–1.58	0.93	0.86–0.97
m2	6	1.17	1.14–1.20	1.04	0.95–1.11

Type locality: YS145, basal Gaozhuang Fm. about 5.7 Ma, Tancun subbasin, Shanxi Province.

Referred material: Tancun subbasin: left m1–2 (V11337) from YS141, and left m1 (V11338) from YS159, both upper Mahui Fm.; Yuncu subbasin: from YS8 (middle Mahui Fm., 6.3 Ma), right m1, V8867. Measurements are given in Table 14.5.

Stratigraphic range: Late Miocene, Mahui Fm. to basal Gaozhuang Fm.

Etymology: "Jin" is the appellation of a kingdom of ancient China and also the abbreviation of current Shanxi Province.

Species diagnosis: The same as the generic diagnosis; differential diagnosis developed in Discussion.

Description: The molars are low-crowned and with inclined cusps (-ids).

The holotype is a left, lightly worn M1 on which the t1 and t3 are slightly posteriorly positioned relative to t2 and connected to t2 by low ridges; a prestyle is anterolabial to the t2, a posterior spur from t3 is absent, the t4 and t6 are a little posterior to t5 and connected to it by low ridges, t6 lacks a posterior spur and the t6 and t9 are well separated from each other, the t4 is connected to the lingual base of t8 by a thick and low ridge, the t12 is an uninflated low ridge, roots are broken off. On one M1 (V11336.26) is a distinct posterior spur from t6 is present, but it does not contact t9, and there are 3 roots and a central rootlet.

All seven M2 are uniform in morphology. The t1 is relatively large and high, lacks a posterior spur, and is linked to the anterior base of t5 by a low crest. The t3 is a small and low transverse crest that is linked lingually to the anterior base of t5. The t4 is posterior to t6 and is linked to the posterolingual corner of t8 by a crest. A t7 is absent, t6 is slightly posterior to t5, lacks a posterior spur, and lies distant from and unconnected to t9. It is only on a relatively worn specimen that there is a t6–t9 contact, in which the t9 extends to the labial base of t6. As on the M1, t12 is present as a low and weak ridge. Four roots are present with two on the lingual side.

The right dentary (V11336.8) preserves m1–2, and diastema. The diastema is strongly concave, 2.8 mm long. A mental foramen is situated slightly below the diastema dorsal margin and 0.5 mm anterior to the anterior root of the m1. The masseteric crest terminates with a swollen terminus ventral to the anterior root of the m1 at nearly the same height as the mental foramen. The m1 and m2 (1.58 × 0.99, 1.18 × 1.11 mm) are brachydont, and the axes of the labial and lingual cuspids form a distinct angle (not nearly transverse as in *Progonomys*). The protoconid-metaconid cusp pair forms an angle only somewhat greater than a right angle. The m1 is long, narrow, not distinctly broadened posteriorly, lacks a tma, lingual anteroconid is slightly anterior to the labial anteroconid, and both are linked to the protoconid and metaconid at their base, forming an asymmetrical x-shaped

connection. A medial ridge is absent, labial accessory cuspids are not well developed: c1 and c2 are elongated ovals, c3 small and round. All three cuspules are linked by a cingulum. A low posterior cingulum extends as a transverse crest that connects to the posterior margins of the entoconid and hypoconid. The m2 is an anteriorly broadened rectangle with a ridge-like labial anteroconid connecting the protoconid with the labial cingulum. The labial accessory cuspules are on a cingulum and only the low c2, labial to the protoconid, is developed. Posterior cingulum resembles that on m1.

On the seven isolated m1 a small and low tma (medial anteroconid) is present on all but one specimen. The lingual anteroconid is placed slightly anterior, the anteroconids are linked to the protoconid and metaconid by a very weak crest (two out of seven) or are not linked at all (five out of seven) except on one heavily worn specimen where the ridge-like connections are present. A medial ridge is absent from all specimens and labial accessory cuspules are submerged in a cingulum on the majority of specimens, but on two there are a relatively well developed low and conical c1 and weaker c2. The posterior cingulum is a crest-like cuspid that extends transversely as a thick ridge or is oval. Two-rooted.

The remaining m2 specimens resemble the m2 of the jaw V11336.8, but the labial cingulum is less developed. All have two roots.

The m1–2 measurements from V11337 (YS141) are m1: 1.50 × 1.00, and m2: 1.10 × 1.05; V11338 (YS159) m1 is 1.63 × 1.00 mm. These specimens have undergone relatively heavy occlusal wear but resemble teeth from the type locality in morphology. A medial anteroconid is extremely small and low, anterior mure and medial ridge are absent, and a labial cingulum is undeveloped. They are all two-rooted without central rootlet.

A single specimen from the Yuncu subbasin is attributed to this taxon, an unworn right m1 derived from YS8 in the Mahui Fm. (V8867, 1.70 × 1.07). It is larger than the m1s from Tancun subbasin. The specimen has an extremely weak and crest-shaped medial anteroconid (tma), the isolated lingual anteroconid is anterior to the labial anteroconid, the labial anteroconid is linked to the metaconid-protoconid crest lingually, c1 and c2 are ridge-like, a medial ridge is absent, and the posterior cingulum is slightly lingually located.

Discussion: *Tedfordomys jinensis* is of small size, larger than *Micromys*, about the size of *Huaxiamys*, which differs in its stephanodonty and greatly derived M1 morphology. *Tedfordomys* is not stephanodont (no posterior spurs on t1 or t3; t6 isolated from t9), lacks t7, has a very weak posterior cingulum (t12), and its lower molars have a very weak labial cingulum; there is, however, a strong connection between t4 and t8, and all M2 have four roots, both of which appear to be derived conditions. *Tedfordomys jinensis* is somewhat smaller than *Progonomys cathalai*, but very similar to this and other primitive murines. The careful work of Wessels (2009) documented considerable variation in large samples of *P. cathalai*, which encompasses the range of morphologies observed in Yushe *Tedfordomys*. It is the combination and frequencies of variations that separates these genera: *Tedfordomys* has a stronger t4–t8 connection, a much weaker t12, a weaker labial cingulum on m1–2, and M2 with four roots (usually three in *Progonomys*, see Wessels 2009).

Tedfordomys is similar to *Linomys* in having lengthened and slender molars, M1 with a separate t6 and t9, and stronger connection between t4 and t8. *Tedfordomys jinensis* differs from *Linomys yuannanensis* (=*Progonomys yunnanensis* Qiu and Storch, 1990) in having no t7, weak t12, no posterior spur of t3 on M1, and undeveloped tma and weak c1 on m1 and lack of longitudinal ridges on lower molars. In *Linomys* a minute t7 occurs in almost 20% of M1, t3 has a posterior spur in more than 2/3 of M1, t12 is always developed, over half the m1 have a distinct tma, the medial ridge is variably present in lower molars, and only 1/3 M2 of *Linomys* are four-rooted (Qiu and Storch 1990; Storch and Ni 2002). Also, the axes of the posterior cusps on m1 of *Tedfordomys* (entoconid and hypoconid) make an angle much less than 180°.

Karnimatoides is larger than *Tedfordomys*, with stronger cusps and and shows posterior spurs on t3, t6 and t1of M1, and more developed labial accessory cuspules on m1 and m2. *Tedfordomys* is comparable to *Huerzelerimys* from Qinghai (see Qiu and Li 2008) in M1 having no t7, and a weak t12, and in m1 with a small tma and a low angle between the entoconid and hypoconid, but differs in having lengthened and slender molars, more anteriorly extended t2 and t3 on M1, narrower labial cingulum and weaker c1 on m1–2. The new genus is easily distinguished from *Hansdebruijnia* in completely lacking stephanodonty on M1, and a much less pronounced c1 on m1 (see Storch and Ni 2002; Qiu and Li 2016). *Tedfordomys* resembles *Parapodemus* in t7 weak or absent on upper molars, but the latter has relatively well developed longitudinal ridges, is more stephanodont (spurs present on t1, t3, t6, t6–t9 connected), and has a well-developed t12 on M1 and M2, and a well-developed tma on m1 (see Martín-Suárez and Mein 1998).

The primitive murid *Tedfordomys* is morphologically close to *Progonomys*, as revised by Mein et al. (1993) and documented by Wessels (2009). The similarities between the new genus and *Progonomys* include slender molars with weak longitudinal crests, t1 not greatly posteriorly positioned on M1, t6 isolated from t9, and t7 absent on M1 and M2; the tma on m1 is absent or weak and the anterior mure is undeveloped. *Tedfordomys* differs from *Progonomys* in the 4-rooted M2, weak t12, smaller accessory buccal cuspules on m1, and the axes of the entoconid and hypoconid of the lower molars make a smaller angle than in *Progonomys*. The resemblance to *Progonomys* suggests close phylogenetic relationship.

Allorattus Qiu and Storch, 2000
Allorattus cf. *A. engesseri* Qiu and Storch, 2000

Material, locality, age, and stratigraphic position: YS39 produced a damaged left M1 (V8890, Fig. 14.8a) from the early Pliocene upper part of the Taoyang Member (4.7–4.8 Ma), Gaozhuang Formation.

Broken left M1 (V8890) is large, the width being 1.61 mm. The t1 and t3 are nearly symmetrically positioned around t2. The t6 is slightly anterior to and larger than the t4. The t4 is larger than and confluent with the t7. A large t8 is posteromedially positioned and is also confluent with t7. There are 4 roots plus a central rootlet. The tooth is consistent with *Allorattus engesseri* from Bilike, Inner Mongolia (Qiu and Storch 2000), both in morphology and size. Because of its incompleteness we refer it tentatively as *A.* cf. *A. engesseri*.

Niviventer Marshall, 1976
cf. *Niviventer* sp.

Material, locality, age, and stratigraphic position: YS39 produced a single deeply worn right M1 (V8889, Fig. 14.8b) from the early Pliocene upper part of the Taoyang Member, 4.7–4.8 Ma, Gaozhuang Formation. Length × width: 2.40 × 1.44 mm.

The large M1 is simple in morphology with t1 and t3, t4 and t6 symmetrically arranged in relation to the midline cusps t2 and t5, respectively. The t1 is larger than t3 and t4 is larger than t6, while t8 is large, isolated and positioned posteromedially. The t7, t9 and t12 appear to be absent at this stage of moderate wear. Three roots are present, the large lingual root broken, but with a vertical groove present on its remaining portion (Fig. 14.8b). A small medial rootlet is present between the anterior and posterior buccal roots. This specimen differs from V8890 (above). Although identification is uncertain, this large rat is similar to *Niviventer* in occlusal morphology.

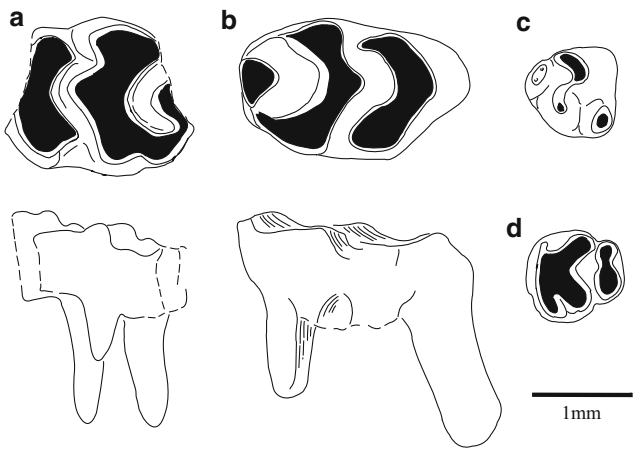

Fig. 14.8 Line drawings of **a** *Allorattus* cf. *A. engesseri*, left M1 (V8890) from YS39: occlusal (above) and lingual (below) views; **b** cf. *Niviventer* sp., right M1 (V8889) from YS39: occlusal (above) and lingual (below) views; **c** *Karnimatoides hipparionus*, right M3 (V8846.26) from YS3, occlusal view; **d** indeterminate Muridae left M3 (V8892) from YS3, occlusal view

Muridae gen. et sp. indet.

A single left M3 (V8892, Fig. 14.8d) collected from YS3 at the top of the late Miocene Mahui Fm. in Yuncu subbasin (5.8 Ma) is relatively deeply worn, but the t1 is distinctly larger than t3, the second chevron formed by t4, t5 and t6 is anteriorly convex and confluent anteriorly with the t1 and t3, and both t8 and t9 are well developed and united to compose a transverse posterior crest. The tooth is three-rooted; length, width are 1.00 × 0.94 mm. Size falls between that expected for *Chardinomys yusheensis* and *Huaxiamys primitivus*. The third molar of *Karnimatoides hipparionus*, shown (Fig. 14.8c) for comparison, has a single posterior cusp.

14.3 Conclusions

Seven genera encompassing at least 17 murine species (Fig. 14.9) we recovered in Yushe Basin faunal assemblages:

Chardinomys yusheensis Jacobs and Li, 1982
Chardinomys nihowanicus (Zheng, 1981)
Karnimatoides hipparionus (Schlosser, 1924)
Karnimatoides sp.
Huaxiamys downsi Wu and Flynn, 1992
Huaxiamys primitivus Wu and Flynn, 1992
Micromys chalceus, Storch, 1987
Micromys cf. *M. chalceus* Storch, 1987
Micromys tedfordi Wu and Flynn, 1992
Micromys aff. *M. tedfordi* Wu and Flynn, 1992
Micromys cf. *M. minutus* Pallas, 1771
Apodemus orientalis (Schaub, 1938)
Apodemus qiui Wu and Flynn, 1992
Apodemus zhangwagouensis Wu and Flynn, 1992
Apodemus sp.
Tedfordomys jinensis gen. et sp. nov.
Allorattus cf. *A. engesseri* Qiu and Storch, 2000
cf. *Niviventer* sp.
Muridae gen. et sp. indet.

The murine fauna of Yushe Basin shows Pliocene diversity and the roots of the modern murine fauna of North China. Because murines had been unknown in the Miocene assemblages of Baode, Wu and Flynn (1992) suggested that the Mahui Formation of Yushe Basin recorded the earliest (late Miocene) record of murines in North China. Mahui mice are conservative morphologically, which would seem to be consistent with an early phase of diversification, but the end-Miocene Ertemte fauna from Inner Mongolia is rich

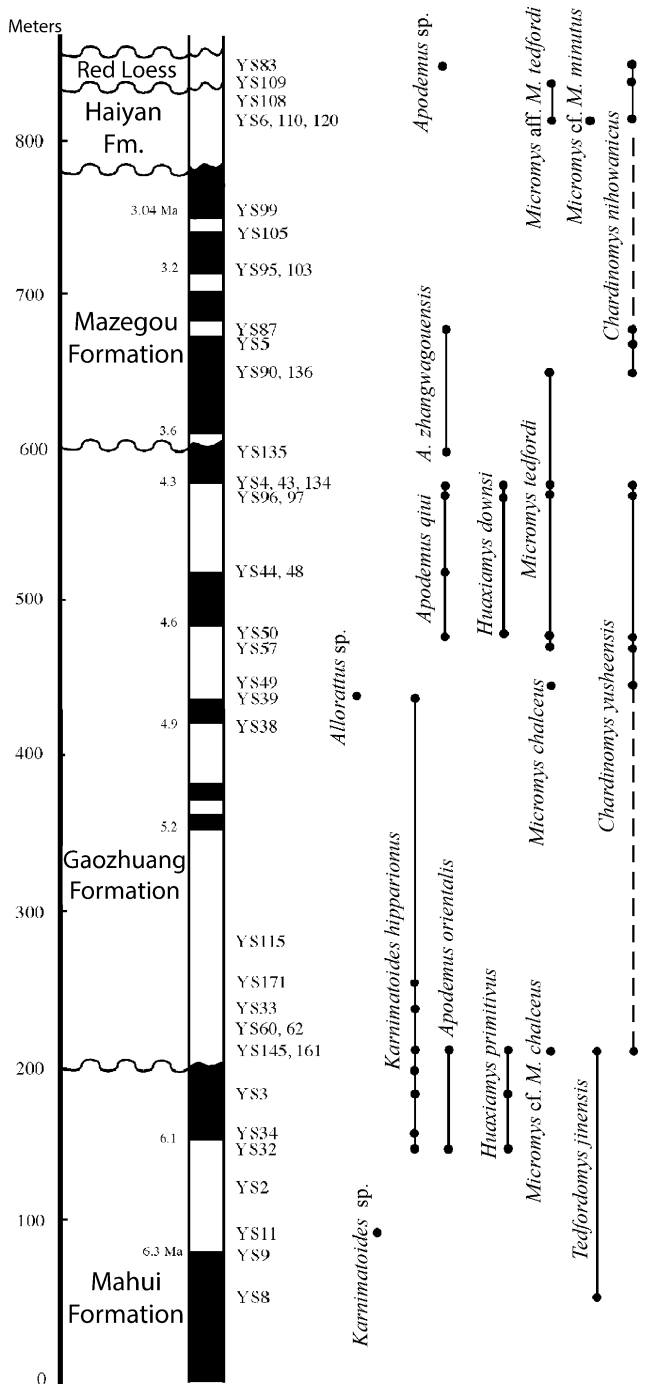

Fig. 14.9 Biostratigraphic ranges of murine species in Yushe Basin, with magnetostratigraphic time scale. Dashed lines hypothesize continuous species presence in Yushe Basin

with diverse murines, which should call into question a simplistic scenario of mouse introduction into North China by Mahui time (~6.5 Ma). More recently, murines have been found in the Lantian faunas of Shaanxi Province (Qiu et al. 2004). These show that murines were part of late Miocene communities of North China since about 10 Ma (Zhang et al. 2013). Probably the lack of mice at Baode itself is an artifact of limited screen washing there.

The mice of the Lantian assemblages, early late Miocene, are conservative and include *Progonomys,* which is characteristic of older murine faunas from South Asia and the circum-Mediterranean region. *Progonomys* is not known from Yushe Basin, but we recognize *Tedfordomys*, a small murine in the later Miocene that is derived in some features and separate at the genus level. Another primitive murine found in the Miocene of Yushe Basin formerly was attributed to the South Asian genus *Karnimata*, but is now recognized as distinct. This North Asia lineage is derived in cusp orientation and connections, and in the pattern of cusp connections known as stephanodonty. Restudy of a well-represented population from the latest Miocene locality Ertemte, of Inner Mongolia, led Qiu and Li (2016) to define *Karnimatoides*. Remains from Yushe Basin are indistinguishable from *Karnimatoides hipparionus* of Ertemte, Inner Mongolia. An older mouse of Yushe Basin, about 6.2 Ma, indicates a more primitive species of *Karnimatoides*.

As much as *Tedfordomys* is a late Miocene derivative of *Progonomys* in China, *Karnimatoides hipparionus* is also a late Miocene counterpart of older *Karnimata* from Pakistan. Both murine lineages show biogeographic connection with South Asia, but the connection was probably not direct. More likely, the lineages were widespread across South Asia to the Middle East and dispersed from there, eastward to China (Flynn and Wessels 2013).

The late Miocene of Yushe Basin also produces the Ertemte taxa *Micromys chalceus* and *Apodemus orientalis*. These affirm correlation of upper Mahui/lower Gaozhuang assemblages with those of Ertemte and Harr Obo, Inner Mongolia, and suggest an age of about 6 Ma or younger for Ertemte. These genera are typical of the late Miocene across Eurasia, and speak to dispersal of some murines across the Palaearctic biogeographic province. Successive species of both genera are recorded throughout the Pliocene of Yushe Basin.

The large murine *Chardinomys*, with distinctive diagonal connection of cusps on its broad M1, is perhaps a hallmark of Yushe Basin. Unlike widespread *Apodemus* and *Micromys*, *Chardinomys* is known only from China. This long-lived genus, quite common at many localities, occurs elsewhere in North China, but not in the late Miocene Ertemte fauna where one finds the large, derived genus *Orientalomys* instead. Both genera are apomorphic, but in different ways making their diagnoses clear. *Chardinomys yusheensis* has a contemporary sister species, *C. bilikeensis*, in the Bilike fauna of the early Pliocene of Inner Mongolia. In Yushe Basin *Chardinomys yusheensis* ranges from the late Miocene of Tancun subbasin (dashed line in Fig. 14.9) through the early Pliocene. *Chardinomys* continues as *C. nihowanicus* through the late Pliocene and early Pleistocene,

and has a later early Pleistocene record in the red loess of Yushe Basin. Another murine in the Yushe assemblages also appears to reflect local evolution – endemism within China. *Huaxiamys* was named for time-successive species observed in the basin. The distinct lineage appears to be closely related to *Mus*.

Yushe Basin also records the rat-like *Allorattus* in the early Pliocene Gaozhuang Fm. This form was first noted in Bilike, also early Pliocene. Another interesting rat from the same locality is assigned with some hesitation to *Niviventer*. If accurate, this identification would be the oldest record of this species-rich genus so common in the modern faunas of southeastern Asia.

The murines of Yushe Basin are diverse with elements shared across Eurasia. They show mixing of Palaearctic species, as well as a degree of endemism. There is only indirect faunal connection with South Asia, two distinctly Chinese lineages being possibly related to Siwalik *Progonomys* and *Karnimata,* but perhaps via the Mideast. There is by Pliocene time already a characteristic species composition in Yushe Basin that reflects the origin of the modern murine assemblages of China.

Acknowledgements We express our gratitude to the Academia Sinica and US National Science Foundation without whose support our project could not have been accomplished. The encouragement and guidance of Zhan-Xiang Qiu and Richard H. Tedford were the underlying forces that brought success to our work. Of course, Will Downs, our long-time collaborator and friend in vertebrate paleontology, especially for the paleontology of China, brought the micromammal effort to fruition. Will, Dong Weilin, insisted that YS145 would produce rich fossil remains and, of course, he was correct. C.-K. Li, L.L Jacobs, and S.-H. Zheng provided valuable counsel and information. Drs. Jacobs, Wilma Wessels, and Yuri Kimura kindly reviewed the manuscript, offering many improvements. We thank all members of the Yushe field parties, and the people of Yushe. Guy Musser (AMNH) and Maria Rutzmoser and Judy Chupasko (MCZ) kindly made mammalian comparative material available.

References

Brandy, L. D. (1979). Étude des rongeurs muroïdes de Néogène supérieur et du Quaternaire d'Europe, d'Afrique du Nord, et d'Afghanistan. Évolution, biogéography, correlations. Thèse de troisième cycle, Université Montpellier.

Brandy, L. D. (1981). Rongeurs muroïdes du Néogène supérieur d'Afghanistan. Évolution, biogéographie, correlations. *Palaeovertebrata, 11,* 133–179.

Cai, B.-Q. (1987). A preliminary report on the late Pliocene micromammalian fauna from Yangyuan and Yuxian, Hebei. *Vertebrata PalAsiatica, 25,* 124–136.

Cai, B.-Q., & Qiu, Z.-D. (1993). Murid rodents from the Late Pliocene of Yangyuan and Yuxian, Hebei. *Vertebrata PalAsiatica, 31,* 267–293 (in Chinese with English summary).

Cheema, I. U., Mahmood Raza, S., Flynn, L. J., Rajpar, A. R., & Tomida, Y. (2000). Miocene small mammals from Jalalpur (District Jhelum) and their biochronologic implications. *National Science Museum Bulletin, 26,* 57–77.

Cui, N. (2003). Fossil *Chardinomys* (Muridae, Rodentia, Mammalia) from Leijiahe sections, Lingtai, Gansu. *Vertebrata PalAsiatica, 41,* 289–305.

de Bruijn, H., & van der Meulen, A. J. (1975). The Early Pleistocene rodents from Tourkobounia-1 (Athens, Greece), I. *Koninklijke Nederlandse Akademie van Wetenschappen, Proceedings, B78,* 314–327.

Flynn, L. J., Tedford, R. H., & Qiu, Z.-X. (1991). Enrichment and stability in the Pliocene mammalian fauna of North China. *Paleobiology, 17,* 246–265.

Flynn, L. J., & Wessels, W. (2013). Paleobiogeography and South Asian small mammals: Neogene latitudinal faunal variation. In X. Wang, L. J. Flynn, & M. Fortelius (Eds.), *Fossil mammals of Asia: Neogene biostratigraphy and chronology* (pp. 445–460). New York: Columbia University Press.

Jacobs, L. L. (1977). A new genus of murid rodent from the Miocene of Pakistan and comments on the origin of the Muridae. *PaleoBios, 25,* 1–11.

Jacobs, L. L. (1978). Fossil rodents (Rhizomyidae & Muridae) from Neogene Siwalik deposits, Pakistan. *Museum of Northern Arizona Press, Bull Series, 52,* 1–103.

Jacobs, L. L., & Li, C.-K. (1982). A new genus (*Chardinomys*) of murid rodents (Mammalia, Rodentia) from the Neogene of China, and comments on its biogeography. *Géobios, 15,* 255–259.

Kimura, Y., Hawkins, M. T. R., McDonough, M. M., Jacobs, L. L., & Flynn, L. J. (2015a). Corrected placement of *Mus-Rattus* fossil calibration forces precision in the molecular tree of rodents. *Scientific Reports, 5*, 9 pages. doi:10.1038/srep14444.

Kimura, Y., Flynn, L. J., & Jacobs, L. L. (2015b). A palaeontological case study for species delimitation in diverging fossil lineages. *Historical Biology, 28,* 189–198.

Martín-Suárez, E., & Mein, P. (1998). Revision of the genera *Parapodemus*, *Apodemus*, *Rhagamys* and *Rhagapodemus* (Rodentia, Mammalia). *Géobios, 31,* 87–97.

Mein, P., Martín-Suárez, E., & Agustí, J. (1993). *Progonomys* Schaub, 1938 and *Huerzelerimys* gen. nov. (Rodentia); their evolution in Western Europe. *Scripta Geologica, 103,* 41–64.

Qiu, Z.-D., & Li, Q. (2008). Late Miocene micromammals from the Qaidam Basin in the Qinghai-Xizang Plateau. *Vertebrata PalAsiatica, 46,* 285–306.

Qiu, Z.-D., & Li, Q. (2016). Neogene rodents from central Nei Mongol, China. *Palaeontologia Sinica 198, New Series C30*, 1–684. Beijing: Science Press.

Qiu, Z.-D., & Storch, G. (1990). New murids (Mammalia, Rodentia) from the Lufeng hominoid locality, late Miocene of China. *Journal of Vertebrate Paleontology, 10,* 467–472.

Qiu, Z.-D., & Storch, G. (2000). The early Pliocene micromammalian fauna of Bilike, Inner Mongolia, China (Mammalia: Lipotyphla, Chiroptera, Rodentia, Lagomorpha). *Senckenbergiana Lethaea, 80,* 173–229.

Qiu, Z.-D., Zheng, S.-H., & Zhang, Z.-Q. (2004). Murids from the Late Miocene Bahe Formation, Lantian, Shaanxi. *Vertebrata PalAsiatica, 42,* 67–76 (in Chinese with English summary).

Schaub, S. (1938). Tertiär und Quartär Murinae. *Schweizerische Paläontologische Gesellschaft, Abhandlungen, 61,* 1–39.

Schlosser, M. (1924). Tertiary vertebrates from Mongolia. *Palaeontologia Sinica, C1,* 1–119.

Sen, S. (1983). Rongeurs et lagomorphes du gisement pliocène de Pul-e Charkhi, bassin de Kabul, Afghanistan. *Bulletin du Muséum National d'Histoire Naturelle, Paris, 5*(5C), 33–74.

Storch, G. (1987). The Neogene mammalian faunas of Ertemte and Harr Obo in Inner Mongolia (Nei Mongol), China. – 7. Muridae (Rodentia). *Senckenbergiana Lethaea, 67,* 401–431.

Storch, G., & Ni, X. (2002). New Late Miocene murids from China (Mammalia, Rodentia). *Géobios, 35,* 515–521.

Wessels, W. (2009). Miocene rodent evolution and migration: Muroidea from Pakistan, Turkey, and northern Africa. *Geologica Ultraiectina, 307,* 1–290.

Wu, W.-Y., & Flynn, L. J. (1992). New murid rodents from the Late Cenozoic of Yushe Basin, Shanxi. *Vertebrata PalAsiatica, 30,* 17–38.

Zhang, Z.-Q., Kaakinen, A., Liu, L.-P., Lunkka, J. P., Sen, S., Gose, W. A., et al. (2013). Mammalian biochronology of the Late Miocene Bahe Formation. In X. Wang, L. J. Flynn, & M. Fortelius (Eds.), *Fossil mammals of Asia: Neogene biostratigraphy and chronology* (pp. 187–202). New York: Columbia University Press.

Zhang, Z.-Q., & Zheng, S.-H. (2000). Late Miocene – Early Pliocene biostratigraphy of Loc. 93002 section, Lingtai, Gansu. *Vertebrata PalAsiatica, 38,* 274–286 (in Chinese with English summary).

Zhang, Z.-Q., & Zheng, S.-H. (2001). Late Miocene – Pliocene biostratigraphy of Xiaoshigou section, Lingtai, Gansu. *Vertebrata PalAsiatica, 39,* 54–66 (in Chinese with English summary).

Zheng, S.-H. (1981). New discovered small mammals in the Nihowan Bed. *Vertebrata PalAsiatica, 19,* 348–358 (in Chinese with English summary).

Zheng, S.-H., & Cai, B.-Q. (1991). Micromammalian fossils from Danangou of Yuxian, Heibei. In Institute of Vertebrate Paleontology and Paleoanthropology (Eds.), *Contributions to INQUA XIII* (pp. 100–131). Beijing: Beijing Scientific and Technological Publishing House (in Chinese with English summary).

Zheng, S.-H., & Zhang, Z.-Q. (2000). Late Miocene-Early Pleistocene micromammals from Wenwanggou of Lingtai, Gansu, China. *Vertebrata PalAsiatica, 38,* 58–71 (in Chinese with English summary).

Zheng, S.-H., & Zhang, Z.-Q. (2001). Late Miocene-Early Pleistocene biostratigraphy of the Leijiahe Area, Lingtai, Gansu. *Vertebrata PalAsiatica, 39,* 215–228 (in Chinese with English summary).

Zhou, X.-Y. (1988). The Pliocene micromammalian fauna from Jingle, Shanxi – A discussion of the age of Jingle red clay. *Vertebrata PalAsiatica, 26,* 181–197 (in Chinese with English summary).

Chapter 15
The Bamboo Rats and Porcupines of Yushe Basin

Lawrence J. Flynn and Wen-Yu Wu

Abstract Surface finds of small mammal fossils tend to be large body-size species; small species are retrieved more readily by applying special collecting techniques. The bias against small fossil recovery from Yushe Basin was greatly diminished by screen washing, beginning in 1987. Prior to that time, the historical monographic study by Teilhard de Chardin on the rodents of Yushe Basin focused on relatively large body-size species, especially beavers and zokors. Two other large kinds of rodents, bamboo rats and porcupines, were known to Teilhard and are reviewed here. Of these, the bamboo rats include *Brachyrhizomys shansius* Teilhard de Chardin, 1942 named for fossils from the Pliocene of Yushe, and a smaller late Miocene bamboo rat recovered by the Sino-American collaborative field team in 1991. This species is the oldest rhizomyine in North China, and the oldest species assignable to the extant *Rhizomys* group. Specimens representing the Old World porcupine *Hystrix* have stratigraphic importance, with a higher crowned species replacing *Hystrix gansuensis* by the early Pleistocene.

Keywords Yushe Basin • North China • Neogene • *Rhizomys* • *Hystrix*

15.1 Introduction

Before the adoption of modern screening techniques by our paleontological field parties, fossil representation of rodents and other small mammals was greatly limited. The bias against recovery and documentation of most rodent groups led to underestimation of their prominence in the fossil record. We now know rodents, insectivorans, lagomorphs, and other small body-size mammals to have been quite diverse and well-represented in the microfossil record. Despite the bias against the retrieval of small mammals, years of careful collecting allowed Teilhard de Chardin (1942) to proceed with monographic treatment of the rodents of Yushe Basin. His key paper included large collections of beavers and zokors, which are treated in separate chapters in this volume. He also noted limited squirrel material, and the important Lagomorpha (leporids and ochotonids), which we treat in Chap. 4.

Teilhard de Chardin's (1942) monograph included a few specimens of bamboo rats and porcupines. Demonstrably more primitive than living *Rhizomys*, he named the fossil bamboo rat as new. The porcupine from Yushe Basin was a single tooth, equivocally identified. The subject of this chapter is our current understanding of the Yushe bamboo rats and porcupines. Our field work and screening efforts added some material, but for these groups the older collections stored in museums in Tianjin and New York remain particularly important.

15.2 Systematics

15.2.1 Family Spalacidae Gray, 1821

Subfamily Rhizomyinae Winge, 1887
Tribe Rhizomyini Winge, 1887
Rhizomys Gray, 1831
Rhizomys (*Brachyrhizomys*) Teilhard de Chardin, 1942

L.J. Flynn (✉)
Department of Human Evolutionary Biology, and the Peabody Museum of Archaeology and Ethnology, Harvard University, Cambridge, MA 02138, USA
e-mail: ljflynn@fas.harvard.edu

W.-Y. Wu
Laboratory of Paleomammalogy, Institute of Vertebrate Paleontology and Paleoanthropology, Chinese Academy of Sciences, 142 Xizhimenwai Ave., Beijing 100044, People's Republic of China
e-mail: wuwenyu@ivpp.ac.cn

Lawrence J. Flynn and Wen-Yu Wu (eds.), *Late Cenozoic Yushe Basin, Shanxi Province, China: Geology and Fossil Mammals, Volume II: Small Mammal Fossils of Yushe Basin*, Vertebrate Paleobiology and Paleoanthropology,
DOI 10.1007/978-94-024-1050-1_15

Included species: *Rhizomys* (*Brachyrhizomys*) *shansius, Rhizomys* (*B.*) *shajius*.

Rhizomys (*Brachyrhizomys*) *shansius* Teilhard de Chardin, 1942.

Holotype: RV42017 (THP 31.096) right dentary with incisor, m1–3; locality unrecorded, but likely from Yushe Zone II (Pliocene; usage of Licent and Trassaert 1935).

Referred Material: THP 14.183, right dentary fragment with incisor, m2–3 from Baihaicun, upper Gaozhuang Fm. or lower Mazegou Formation, and THP 14.244, left dentary fragment with incisor and m1 (both Tianjin Museum specimens); F:AM 117337, cranium and mandible with complete dentition and associated postcrania from Zhaozhuang, Mazegou Formation, age about 3.5 Ma; V8830 from YS5, lateral wall of right dentary fragment showing masseteric crest with round termination, but no teeth, Mazegou Formation, 3.4 Ma.

Age Range: All specimens from Pliocene deposits of Yushe Basin, Shanxi Province, China. The age range for known fossils, at most 4.5–3 Ma, is quite possibly shorter, ~4–3.3 Ma.

Diagnosis (after Flynn 2009): *Brachyrhizomys* about the size of smaller individuals of *Rhizomys sinensis* or *R. pruinosus* but with less elevated cranium and lower crowned molars; skull with proodont incisors, weak lambdoid crest, gently convex occiput nearly vertical and not expanded dorsoventrally; lingual reentrant on M1 short and not convergent with middle buccal reentrant, M1 and M2 retain mesoloph, m2 not wider than long and with persistent anterolingual enamel lake, mandible with unshortened diastema. Molar row length of RV42017 is 15.4 mm.

Discussion: Teilhard de Chardin (1942) recognized a bamboo rat among the larger rodent fossils recovered from Yushe Basin, although Yushe is northeast of the present distribution of *Rhizomys*. He found it to be distinct from living *Rhizomys* in its proodonty evident from the lower jaw, and in its lesser molar crown height, which distinguished it as his *Brachyrhizomys*. Flynn (2009) reevaluated the taxon based on an excellent Yushe Basin fossil in the Frick collection of the American Museum, F:AM 117337 (Fig. 15.1). This skull demonstrates proodonty clearly, the derived rhizomyine condition of a dorsally confined, round infraorbital foramen (ventral slit closed), and less dorso-ventral expansion of the cranium than observed in modern species. *Brachyrhizomys* molars, less high crowned than those of modern *Rhizomys*, retain some primitive connections between lophs. *Brachyrhizomys shansius* represents a subgenus basal to all living *Rhizomys* and was fully fossorial based on skull and postcranial morphology (Flynn 2009), but lacked some of the overprint of cranial features associated with subterranean life.

Fig. 15.1 Cranium and right dentary of *Rhizomys* (*Brachyrhizomys*) *shansius*, F:AM 117337, specimen in the Frick Collection of the American Museum of Natural History. Provenance is the collecting area of Zhaozhuang, Yushe Basin, age about 3.5 Ma. Cranium in ventral, dorsal and right lateral views with cm scale. Dentary below in dorsomedial view, with its own cm scale. Anterior is to the left

Rhizomys (*Brachyrhizomys*) shares with living species several modern features that are lacking in earlier Rhizomyini, *Miorhizomys* for example. *B. shansius* is a bamboo rat of modern grade, and therefore included in the genus *Rhizomys*. Being fully fossorial *B. shansius* suggests that Yushe Pliocene landscapes had appreciable rainfall (extant species generally live in areas receiving ~1 m of rain per year).

Rhizomys (*Brachyrhizomys*) *shajius* Flynn, 1993 (see Fig. 1 therein)

Holotype and only specimen: V8920, right dentary fragment with m2–3 from locality YS156, Mahui Formation in Tancun subbasin; normally magnetized sediment correlated with chron C3An, about 6.0 Ma.

Emended diagnosis: Small *Brachyrhizomys* with masseteric crest of modern grade (smooth, rounded conjunction of upper and lower portions, without anterior extension). Molar crown height less than that of *Brachyrhizomys shansius*; elongated molars, m3 with mure and short mesolophid. The first lower molar of V8920 is lost, but its alveolus remains; alveolar length of molar row would be about 10.8 mm.

Discussion: This medium size rodent, small for Rhizomyini, and smaller than *B. shansius,* retains primitive features in the dentition. Lower molars are longer than wide and retain a short mesolophid and weak connection (mure) between arms of the hypoconid and protoconid. *Rhizomys* (*Brachyrhizomys*) *shajius* indicates the presence of bamboo rats in the late Miocene of Yushe Basin. *B. shajius* is the oldest evidence of the group north of South China and the Indo-Malayan Biogeographic Province, and therefore gives a minimum age on northward dispersal of these typically South Asian rodents. It also provides a minimum age for the genetic divergence of the genus *Rhizomys*.

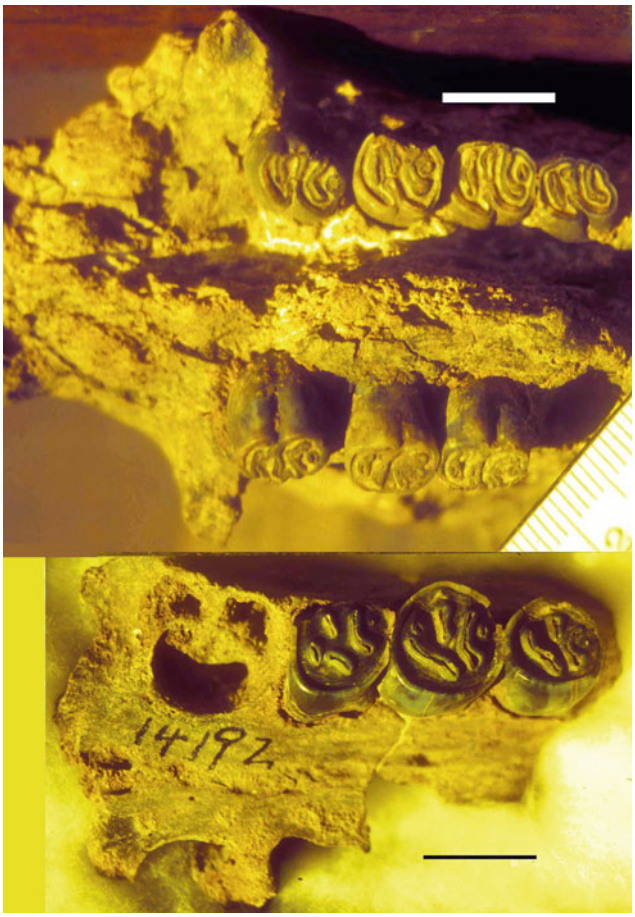

Fig. 15.2 *Hystrix gansuensis* from Yushe Basin. Above, partial skull THP 10069 in ventral view, anterior to left, showing parallel tooth rows. Below, broken palate THP 14192 with left premolar alveolus and worn M1-3, showing rounded posterior emargination of the palate adjacent to the midpoint of M3. Scales for both are 1 cm, anterior is to the left

15.2.2 Family Hystricidae Fischer, 1817

Hystrix Linnaeus, 1758

Hystrix gansuensis Wang and Qiu, 2002

Holotype: V13052, partial skull from Xiaozacun, Linxia Basin, Guanghe County, Gansu Province, late Miocene.

Referred material and localities: V8833, right M1 or M2 from YS40, Jingjiagou, and V8832, right lower incisor tip from YS57, Yaergou, both Gaozhuang Formation; V8831, molar fragment from Mahui Formation, YS32 (age range, late Miocene to early Pliocene 6.0 to 4.7 Ma); upper molar figured by Teilhard de Chardin (1942, Fig. 61A) from Zone II, Pliocene. In the Tianjin Museum collection: THP 10.069, partial skull from Beicun; THP 14.192, left maxilla with molars from Baihaicun; THP 14.236, right M1-M3 from Nan Jia Zhuang, all early Pliocene (Fig. 15.2).

Description: Materials recovered by the Sino-American team are few, the most informative specimen being upper molar V8833 (Fig. 15.3a). This tooth, probably M2, is pentalophodont. At its early stage of wear, the metaloph and posteroloph are nearly joined, but the central syncline (hypoflexus) remains open, unbridged by an enamel fold with a dentine ridge that would join the protocone and hypocone. Small interdental appression facets have not removed much enamel anteriorly or posteriorly (length = 9.1 mm) and the crown's greatest width (8.1 mm) is below the hypoflexus (sinus). Crown height is moderate, 11.8 mm preserved, and the base of the hypostria (vertical expression of the hypoflexus) is 8.4 mm above the base of the enamel; ratio of preserved height over length is 1.3, close to that of both *H. gansuensis* and *H. aryanensis* Sen and Purabrishemi, 2010. The width of incisor V8832 is 5.7 mm, somewhat less than that observed for *H. aryanensis* Sen and Purabrishemi, 2010.

The important, largely unstudied Tianjin collection includes cranial material from Yushe. THP 10.069 is a partial skull at a more advanced stage of wear than V8833, such that the molars show beginning closure of the

hypoflexus by a narrow bridge of dentine (Fig. 15.2). Upper cheek tooth rows are nearly parallel, as in the holotype of *H. gansuensis* Wang and Qiu, 2002. The posterior margin of the palate is rounded and opposite to the middle of M3. The latter feature is also evident in the partial palate THP 14.192 (Fig. 15.2), an aged individual with molars showing typically wide occlusal surfaces due to late-stage wear.

Discussion: Molar size is quite variable in *Hystrix*, but informative when differences are great. These specimens are smaller than common late Miocene-Pliocene age porcupines of northern Eurasia, such as *H. primigenia, H. depereti,* and *H. caucasica* (see, e.g., Lopatin et al. 2003). The Yushe *Hystrix* is also considerably smaller than the South Asian Myanmar porcupine of similar age, *H. paukensis* Nishioka et al., 2011. Lower crowned and smaller than the Yushe species is a late Miocene Yunnan porcupine, *H. lufengensis* Wang and Qi, 2005. However, *H. aryanensis* Sen, 2001 and *H. gansuensis* Wang and Qiu, 2002 are close enough in size to the Yushe Basin porcupine that differentiation based on size alone is unreliable. Wang and Qiu (2002) do find a difference in hypsodonty, and indicate that crown height of *H. gansuensis* is greater than height of *H. aryanensis*. As noted above, the somewhat worn V 8833 with a crown height ratio of 1.3 underestimates the crown height of the Yushe population, and tends to argue in favor of identification as *H. gansuensis*.

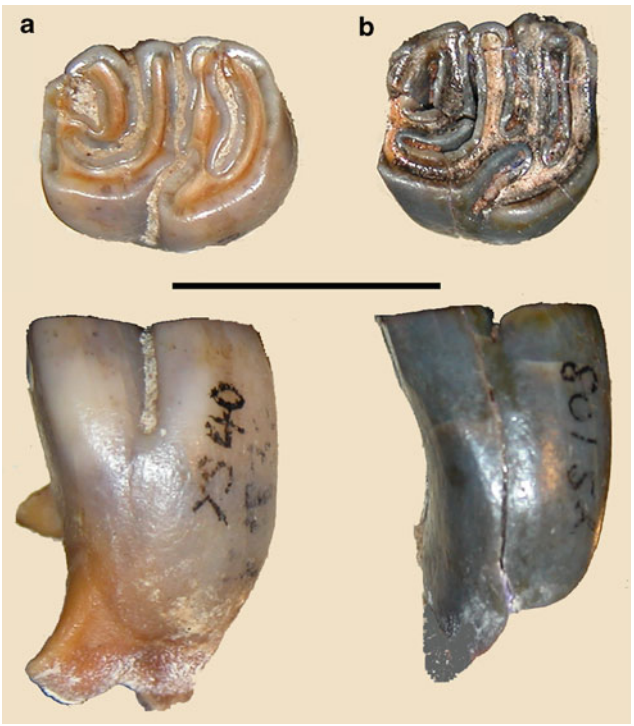

Fig. 15.3 *Hystrix gansuensis* (**a**) and *Hystrix refossa* (**b**) molars from Yushe Basin. *H. gansuensis* V8833 from YS40, Gaozhuang Formation *H. refossa* V8834 from YS108, Haiyan Formation. Scale bar = 1 cm; anterior is to the right. These are comparable molars, but the lower-crowned V8833 is longer (rectangular), reflecting its earlier stage of wear

The Yushe material does present other features to support this identification. THP 10069 shows parallel upper cheek tooth rows, rather than the anteriorly diverging maxillary dentitions illustrated by Sen (2001). The posterior border of the palate is V-shaped and reaches the M2-M3 contact in *H. aryanensis* Sen, 2001. Two Yushe specimens indicate shallower posterior emargination of the palate, a rounded border reaching only the middle of the last molar (Fig. 15.2).

These features support identification as *Hystrix gansuensis*, a species previously known from the late Miocene Linxia Basin of Gansu Province, some 900 km to the west. One Yushe specimen is late Miocene in age, but the Yushe records extend this species into the early Pliocene, up to perhaps 4 Ma. This range and age extension is not surprising given the few studied early Pliocene rodent faunas in North China.

Hystrix refossa Gervais, 1852

Holotype: right dentary fragment with p4, specimen 109, Muséum National d'Histoire Naturelle, from Perrier Hill, Val d'Issoire, France (see Rook and Sardella 2005).

Referred material and locality: V8834, right M1 or M2 from Liuping Gou, YS108, Haiyan Formation, 2.2–2.5 Ma reversed magnetic interval (Fig. 15.3b).

This upper molar is about the size of V8833, but more hypsodont, evident despite showing a somewhat greater stage of wear. Length by width is 8.5 × 8.5; height at least 13.4 mm, given the broken base of the enamel. This yields a crown height ratio of 1.6. This is greater than the ratio for V8833, but more striking is that the base of the hypostria extends to 6 mm from the base of the enamel; i.e., the fold is much deeper toward the roots in this porcupine. Enamel loss by attrition on the sides of the tooth at the interdental facets is clear, especially on the distal facet. The tooth is pentalophodont, the metaloph and posteroloph are connected by wear, and there is a narrow dentine bridge joining the protocone and hypocone.

Discussion: V8834 indicates a porcupine in the early Pleistocene of Yushe Basin that is different from the Tertiary *Hystrix gansuensis*. It is about the size of the older *H. gansuensis*, but more hypsodont. Again, the age of the Haiyan Formation is early Pleistocene, but because it falls in the long reversely magnetized chron C2r, the date is not precisely constrained. We estimate the age to be somewhat older than 2.2 Ma, around two m.y. younger than *H. gansuensis*.

Like *H. gansuensis*, V8834 represents a porcupine smaller than late Miocene *H. primigenia* and other large porcupines. However, the specimen indicates a size markedly greater than early Pleistocene *H. lagrelli* Lőnnberg, 1924. A larger early Pleistocene porcupine of North China is commonly encountered. Van Weers (2005) reviewed the many named forms, and synonymized a number of species for which he concluded that the appropriate name is *Hystrix*

refossa. Tong (2008) also noted two porcupines in Pleistocene sites of China, but came to the conclusion that appropriate names are *H. lagrelli* and *H. subcristata*. The discrepancy in the identification of the larger porcupine may be explained by different comparative material. Except for a Nihewan premolar, all of Tong's (2008) comparative material postdates considerably the Haiyan porcupine. For example, V8834 is over 1 m.y. older than and larger than the Gongwangling porcupine (see Hu and Qi 1978) that Tong (2008) discussed. *Hystrix subcristata* may be the appropriate name for large late Pleistocene porcupines in North China. Late Pleistocene porcupines aside, V8834 matches in size and hypsodonty the older early Pleistocene porcupines considered as *Hystrix refossa* by Van Weers (2005).

15.3 Conclusion

The small mammal fauna of Yushe Basin contains two large-body-size rodents that are not as commonly found as beavers and zokors, but were recognized by Teilhard de Chardin (1942) in his monographic treatment of Yushe rodents. These are bamboo rats and porcupines. Collections of the Tianjin Natural History Museum and American Museum of Natural History in New York contain excellent material of the bamboo rat *Brachyrhizomys shansius*, which is Pliocene in age. We add a smaller, older bamboo rat that shows that the group dispersed northward from South China by 6 Ma, late Miocene. Porcupines were also present in the late Miocene and Pliocene of Yushe Basin. These are assignable to *Hystrix gansuensis*, previously known only in the late Miocene of Gansu Province. Another more hypsodont porcupine is present in the early Pleistocene of Yushe Basin. Data are too sparse, at present, to specify when and how the older *H. gansuensis* was replaced by *H. refossa.*

Rhizomyini, the crown Asian bamboo rats, were confined to South Asia throughout much of their biogeographic history. Their record in the late Neogene of Yushe Basin represents a northward dispersion from South China. This is one of the few examples of direct northward expansion of a South Asian small mammal group into North China. Most other small mammal taxa shared by South Asia and North China likely spread by an indirect route, for example murines dispersing westward from South Asia, then northward and eastward to China.

The porcupine *Hystrix* may have dispersed independently to North China and to South Asia. *Hystrix* was present in Europe by about 9 Ma (Sen 1999), but younger late Miocene to Pliocene *Hystrix gansuensis* of North China appears to be distinct from porcupines of both western Eurasia and South Asia. However, South Asian *Hystrix sivalensis* at 8 Ma (Barry et al. 2002, p. 71) is indistinguishable from *H. primigenia* (Van Weers and Rook 2003; the type material is from Pikermi, Greece). Apparently bamboo rats evolved in South Asia from early Miocene Rhizomyinae, and later expanded northward into Yushe Basin, but South Asian porcupines, which have a younger record, likely invaded the Siwaliks of the Indian Subcontinent, not from China, but from the west.

Acknowledgements We thank the curators of the Tianjin Natural History Museum and the American Museum of Natural History for access to collections made in the early part of the last century. These are crucial to understanding the relationships of both the bamboo rats and the porcupines of Yushe Basin. Our visit to Tianjin on September 1, 1988, introduced us to a number of Yushe Basin specimens; photographs by Will Downs are the basis for Fig. 15.2. We appreciate the suggestions for improvements by reviewers Sevket Sen, Rajeev Patnaik and Louis Jacobs.

References

Barry, J. C., Morgan, M. E., Flynn, L. J., Pilbeam, D., Behrensmeyer, A. K., Raza, S. M., et al. (2002). Faunal and environmental change in the Late Miocene Siwaliks of Northern Pakistan. *Paleobiology Memoir, 3,* 1–71.

Flynn, L. J. (1993). A new bamboo rat from the late Miocene of Yushe Basin. *Vertebrata PalAsiatica, 31,* 95–101.

Flynn, L. J. (2009). The antiquity of *Rhizomys* and independent acquisition of fossorial traits in subterranean muroids. In R. S. Voss & M. D. Carleton (Eds.), *Systematic mammalogy: Contributions in honor of Guy G. Musser. Bulletin of the American Museum of Natural History*, *331*, 128–156.

Hu, C.-K., &, Qi, T. (1978). Gongwangling Pleistocene mammalian fauna of Lantian, Shaanxi. *Palaeontologia Sinica 155C, 21*, 1–64.

Licent, E., & Trassaert, M. (1935). The Pliocene lacustrine series in central Shansi. *Bulletin of the Geological Society of China, 14,* 211–219.

Lőnnberg, E. (1924). On a new fossil porcupine from Honan with some remarks about the development of the Hystricidae. *Palaeontologia Sinica, C, 1*(3), 1–16.

Lopatin, A. V., Tesakov, A. S., & Titov, V. V. (2003). Late Miocene-early Pliocene porcupines (Rodentia, Hystricidae) from south European Russia. *Russian Journal of Theriology, 2,* 26–32.

Nishioka, Y., Zin-Maung-Maung-Thien, Egi, N., Tsubamoto, T., Nishimura, T., Ito, T., et al. (2011). New *Hystrix* (Mammalia, Rodentia) from the late Miocene/early Pliocene of Myanmar. *Journal of Vertebrate Paleontology, 31,* 919–924.

Rook, L., & Sardella, R. (2005). *Hystrix refossa* Gervais, 1852 from Pirro Nord (early Pleistocene, southern Italy). *Rivista Italiana di Paleontologia e Stratigrafia, 111,* 489–496.

Sen, S. (1999). Family Hystricidae. In G. E. Rőssner & K. Heissig (Eds.), *The Miocene land mammals of Europe* (pp. 427–434). München: Verlag Dr. Friedrich Pfeil.

Sen, S. (2001). Rodents and insectivores from the Upper Miocene of Molayan, Afghanistan. *Palaeontology, 44,* 913–932.

Sen, S., & Purabrishemi, Z. (2010). First porcupine fossils (Mammalia, Rodentia) from the late Miocene of NW Iran, with notes on late Miocene-Pliocene dispersal of porcupines. *Paläontologische Zeitschrift, 84,* 239–248.

Teilhard de Chardin, P. (1942). New rodents of the Pliocene and lower Pleistocene of North China. *Publications de l'Institut de Géobiologie, Pékin, 9,* 1–101.

Tong, H.-W. (2008). Quaternary *Hystrix* (Rodentia, Mammalia) from North China: Taxonomy, stratigraphy and zoogeography, with discussions on the distribution of *Hystrix* in Palearctic Eurasia. *Quaternary International, 179,* 126–134.

Van Weers, D. J. (2005). A taxonomic revision of the Pleistocene *Hystrix* (Hystricidae, Rodentia) from Eurasia with notes on the evolution of the family. *Contributions to Zoology, 74,* 301–312.

Van Weers, D. J., & Rook, L. (2003). Turolian and Ruscinian porcupines (genus *Hystrix,* Rodentia) from Europe, Asia and North Africa. *Paläontologische Zeitschrift, 77,* 95–113.

Wang, B.-Y., & Qi, G.-Q. (2005). A porcupine (Rodentia, Mammalia) from *Lufengpithecus* site, Lufeng, Yunnan. *Vertebrata PalAsiatica, 43,* 11–23.

Wang, B.-Y., & Qiu, Z.-X. (2002). A porcupine from Late Miocene of Linxia Basin, Gansu, China. *Vertebrata PalAsiatica, 40,* 23–33.

Chapter 16
Dynamic Small Mammal Assemblages of Yushe Basin

Lawrence J. Flynn and Wen-Yu Wu

Abstract Targeted prospecting and screening for microfossils has revealed rich small mammal assemblages at many stratigraphic levels from late Miocene through Pliocene to early Pleistocene formations of the Yushe Basin. The recovered rodents, lagomorphs, bats, and insectivorans include species of small body size not previously known from Yushe. These assemblages represent North China small mammal communities from about 6.5 to 2 Ma and may be used to characterize four land mammal stage/ages: Baodean, Gaozhuangian, Mazegouan, and Nihewanian. The fossil succession establishes diversity and stability in Pliocene small mammal faunas for Yushe Basin before significant turnover at the beginning of the Pleistocene. The Yushe Basin habitat was relatively moist, probably without strong annual temperature extremes, supporting high species diversity.

Keywords Yushe Basin • North China • Neogene • Rodentia • Lagomorpha • Chiroptera • Lipotyphla

16.1 Introduction

The influential monograph of Teilhard de Chardin (1942) on the fossil rodents of Yushe Basin focused light on the Pliocene small mammals of northeastern Asia for the first time. Through much of the 20th century, the Pliocene Epoch was perceived to have begun about 10 to 12 million years ago largely because terrestrial *Hipparion* faunas (Pontian stage equivalent) were thought to correlate to the early Pliocene (Berggren and van Couvering 1974); many *Hipparion* faunas are now known to be late Miocene in age. The title of the monograph by Teilhard **New rodents of the Pliocene and lower Pleistocene of North China** was appropriate. We now perceive the Pliocene as a relatively short period of time, about 5.3 to 2.6 Ma on the time scale of Gradstein et al. (2004). Strata of the Yushe Basin span much of Late Neogene time, from about 7 Ma in the oldest part of the Zhuozhanghe valley to the ~2.2 Ma fluvio-lacustrine sediments at the top, with overlying loess of younger ages. There are therefore, in addition to a long Pliocene sequence, late Miocene (Baodean Stage/Age and MN 13 zone equivalent) and Pleistocene assemblages in the basin. Teilhard de Chardin's (1942) monograph title is still descriptive because we find the Pliocene microfaunas, especially in the interval of about 4.8 to 3.0 Ma, to be highly fossiliferous, with two dozen small mammal species recorded as contemporaries in successive assemblages. Yushe Basin remains one of the best areas in China to study a relatively complete and fossiliferous sequence representing successive Pliocene faunas.

The richness of Yushe Basin assemblages indicates that Pliocene habitats there supported diverse mammal communities, which implies availability of moisture throughout the year and moderate annual temperature ranges. Yushe Basin is situated at the eastern edge of the Loess Plateau, but likely had equable climatic conditions throughout the year, not the extremes one expects for the continental interior. In addition to Rodentia, the orders Lagomorpha and Eulipotyphla (specifically the less inclusive Lipotyphla) show high Pliocene diversity in Yushe Basin. Pliocene Lagomorpha, for

L.J. Flynn (✉)
Department of Human Evolutionary Biology, and the Peabody Museum of Archaeology and Ethnology, Harvard University, Cambridge, MA 02138, USA
e-mail: ljflynn@fas.harvard.edu

W.-Y. Wu
Laboratory of Paleomammalogy, Institute of Vertebrate Paleontology and Paleoanthropology, Chinese Academy of Sciences, 142 Xizhimenwai Ave., Beijing 100044, People's Republic of China
e-mail: wuwenyu@ivpp.ac.cn

Lawrence J. Flynn and Wen-Yu Wu (eds.), *Late Cenozoic Yushe Basin, Shanxi Province, China: Geology and Fossil Mammals, Volume II: Small Mammal Fossils of Yushe Basin*, Vertebrate Paleobiology and Paleoanthropology,
DOI 10.1007/978-94-024-1050-1_16

example, include up to four contemporary genera. Chiroptera (bats) are also recorded, but their diversity is greatly underrepresented compared to modern diversity. Taphonomic bias works against bat preservation, and insofar as each Yushe fossil specimen may represent a different species, likely there were many more bats in the community to be found. Other microfossils, especially fish, snakes, lizards, turtles, and some invertebrates were also recovered from 80 localities as surface finds or by organized screening (see Appendix).

In the following we summarize lipotyphlan, lagomorph and rodent biostratigraphy, noting occurrences of taxa and paleoenvironmental indicators for Yushe Basin. We then specify the succession of faunal associations to help to characterize North China land mammal stage/ages that are represented in Yushe Basin. This also provides an opportunity to review the timing of faunal turnover in the area. Finally, we attempt to analyze biogeographic patterns of taxon distributions to determine timing and direction of dispersal events.

16.2 Biostratigraphic Ranges

16.2.1 Hedgehogs, Moles, Shrews

The core group of the insectivorans is the monophyletic Lipotyphla. Few Yushe Basin fossils represent hedgehogs (Erinaceidae), but we find *Erinaceus* in the late Pliocene Mazegou Formation and in overlying Pleistocene deposits. This hedgehog is the extinct species *Erinaceus olgae*, known previously from Zhoukoudian 1 and 2. The material, although limited, may indicate size increase and survival of the species through the Pliocene-Pleistocene faunal turnover.

There are several moles (Talpidae) preserved in Late Neogene deposits of Yushe Basin. Yushe Basin records the oldest dated *Scaptochirus*, identified by its distinctive humerus and lower molar. A new species of *Yanshuella* is represented by mandibular material in the late Miocene of Yushe Basin; a younger ($\sim$3 Ma) humerus is also referred and to this species. The South China mole *Yunoscaptor* sp. occurs as dental material from early Pliocene localities of Yushe Basin, and a number of humeri represent the genus in the late Miocene. Also found in the early Pliocene is the water mole *Desmana*, an indicator of streams and ponds, therefore reinforcing a reconstruction of moist habitat in this part of Shanxi Province.

Shrew diversity suggests moist, equable climatic conditions. The Pliocene of Yushe Basin includes a neomyine shrew (*Soriculus praecursus*) and the larger beremendiines *Beremendia pohaiensis* and *Lunanosorex lii*, which occur elsewhere in North China. *Sorex* appears in the early Pleistocene of Yushe Basin, and *Crocidura* is found in younger loess. The presence of two other shrews is also indicated among the scant remains of the group in late Miocene deposits.

16.2.2 Pikas, Rabbits, Hares

The fossil pika *Ochotona lagreli,* widespread throughout North China, is well represented in the late Miocene and early Pliocene of Yushe Basin. More than one species of pika is represented, including small body size *Ochotona,* perhaps *O. nihewanica*, but the fragmentary nature of the fossils prevents diagnostic recognition at the species level. *Ochotonoides complicidens*, well known in the Pleistocene of North China, is found in loess deposits of Yushe Basin. We describe (Chap. 4) a good sample of a new, older species *Ochotonoides teilhardi* from the late Pliocene of Yushe. It first appears at about 3.3 Ma, and continues into the earliest Pleistocene.

The large rabbit *Alilepus annectens* is recorded in the late Miocene of Yushe Basin, mostly within the Mahui Formation, but ranging into the base of the overlying Gaozhuang Formation. A smaller species of the genus (*A. parvus*) is named herein based on a late Miocene skull from the Mahui Formation. A new long-jaw rabbit, *Hypolagus mazegouensis*, is found in the late Pliocene of Yushe Basin; it is preceded by a much smaller *Hypolagus* in the early Pliocene. We see two species of the leporid genus *Trischizolagus* in the early Pliocene of Yushe Basin; one is *Trischizolagus mirificus*, otherwise known from the early Pliocene of Inner Mongolia. Another new rabbit species from the late Pliocene or, possibly, early Pleistocene deposits of Yushe Basin is assigned to *Sericolagus*. Further leporid diversity is suggested by Yushe specimens, including a latest Miocene fossil that presents *Nekrolagus*-like morphology. The early Pleistocene loess adds the extant hare *Lepus* to the fossil record.

16.2.3 Rodents

The field campaigns of the Sino-American teams of 1987–1991 specifically targeted small rodents. We knew that the Yushe Basin sequence should include multiple fossiliferous horizons, and we were successful in identifying superposed microfaunas, many of which could be related directly to paleomagnetic sections, and therefore assigned interpolated dates. We applied the techniques of wet-screening to process bulk samples of sediments from Yushe Basin localities, and found the small body size microfauna to be richly represented, especially small rodents, many not previously known in Yushe Basin. The biostratigraphic ranges of all small mammals are shown in Fig. 16.1a, b.

As is generally the case in the Neogene of Asia, squirrels were diverse in Shanxi Province. The flying squirrels *Pliopetaurista* and *Hylopetes* and the chipmunk *Eutamias* characterized late Miocene and early Pliocene faunas. There is also a record of the rock squirrel *Sinotamias* in the early Pliocene and the tree squirrel *Sciurus* in the late Pliocene. *Hylopetes* persisted into the late Pliocene. Remains of the large *Marmota*, an immigrant from North America and collected as surface finds, occur in the early Pleistocene Haiyan Formation.

Yushe beavers, which are large rodents, have been known for nearly a century. Teilhard de Chardin (1942) thought there were perhaps four lineages in Yushe Basin, but one (*Eucastor*) was later to be determined an artefact of misidentification (Chap. 6). Two beaver lineages are encountered in the Miocene and Pliocene: *Sinocastor* and *Dipoides*. In our interpretation, *Sinocastor* is a subgenus of *Castor*, and is quite distinct from the castoroidine group represented by *Dipoides*. While *Castor* appears to have originated in the Palaearctic biogeographic region, with the oldest records occurring in Europe, *Dipoides* may be an immigrant to Eurasia from North America. Different species of *Dipoides* (and perhaps also *Sinocastor*) characterize Miocene and Pliocene assemblages. Such beavers are absent from the early Pleistocene of Yushe Basin; instead, the large castoroidine *Trogontherium* is encountered in the Haiyan Formation.

Zokors (Myospalacinae) also range to large size for rodents. They were diverse and well represented in Yushe Basin, and formed the basis for the analyses of Teilhard de Chardin (1942) and Zheng (1994, 1997; Zheng et al. 2004; Liu et al. 2013, 2014). Fossil zokors (Chap. 9) have considerable stratigraphic importance and their distribution through time corresponds very roughly to the tripartite division of the Yushe sequence into three zones postulated by Licent and Trassaert (1935) and adopted by Teilhard de Chardin (1942). The late Miocene Zone I is characterized by the relatively primitive *Prosiphneus murinus*, which occurs in the Mahui Formation and basal part of the Gaozhuang Formation. The Pliocene Nanzhuanggou Member of the Gaozhuang Formation (Zone II) yields *Pliosiphneus* and the earliest mesosiphneine *Chardina*. *Pliosiphneus lyratus* ranges through the uppermost Gaozhuang Formation into the base of the Mazegou Formation (also Zone II). Otherwise, the Mazegou Formation is characterized by the more advanced *Mesosiphneus*. The early Pleistocene Haiyan Formation, and arguably the overlying Yushe red loam, designated Zone III by Licent and Trassaert (1935), yield the derived *Yangia* and *Eospalax*. The large *Y. tingi* and *E. fontanieri*, respectively concave and convex occiput species, show changes in dentition (clinomegodonty: lengthened molars and inclined reentrant folds) that likely correspond to early Pleistocene changing food sources requiring more processing, either tougher or less nutritious vegetation.

Like beavers and zokors, the large-body-size bamboo rats and porcupines occur as surface finds. They are represented by extinct species of the living genera *Rhizomys* and *Hystrix*, respectively. Bamboo rats are committed fossorial species, and indicate significant rainfall. A field study of extant *Rhizomys sinensis* documents 1100 mm of rain per year in its habitat (He 1984).

Dipodoids, a group of rodents expected to be found in Yushe Basin, heretofore have been completely unknown. The very small birch mouse *Sicista* suggests vegetation cover, and modern species are capable of hibernation with seasonal temperature change. Extinct lophocricetines are also present. Known only in the Yushe Basin from the late Miocene Mahui Formation, these small rodents may be under-represented in the fossil record, or Yushe Basin may be near the southern limit of the range of both *Sicista* and *Lophocricetus*. A few specimens of a larger dipodoid, a fossil species of the modern jerboa genus *Dipus*, occur sporadically in early Pliocene to early Pleistocene deposits. Among other rodents, a tiny dormouse found by screening is documented in the Pliocene of Yushe Basin, despite bias against retrieval of such small fossils.

Several groups of small muroids present in the microfauna are recovered by screening. Hamsters are an example and show moderate diversity. A hallmark of the Mahui and Gaozhuang formations is the conservative *Neocricetodon grangeri*, which is closely related to Late Neogene hamster species distributed throughout Eurasia. Upper levels of the Gaozhuang Formation and the Mazegou Formation (Zone II) produced species of *Allocricetus* and *Cricetinus*. Two of these are new, which is not unexpected given the limited fossil record of early Pliocene deposits elsewhere in northern Asia. *Cricetulus* appears in the Mazegou Formation and with *Phodopus* characterizes Yushe Zone III. Unlike hamsters, Yushe Basin gerbils show little diversity. Until the late Pleistocene appearance of modern gerbils, only *Pseudomeriones* is encountered (Zone I). The Yushe Basin record is important because it suggests that the genus shows chronoclinal increase in crown height, with late Miocene specimens

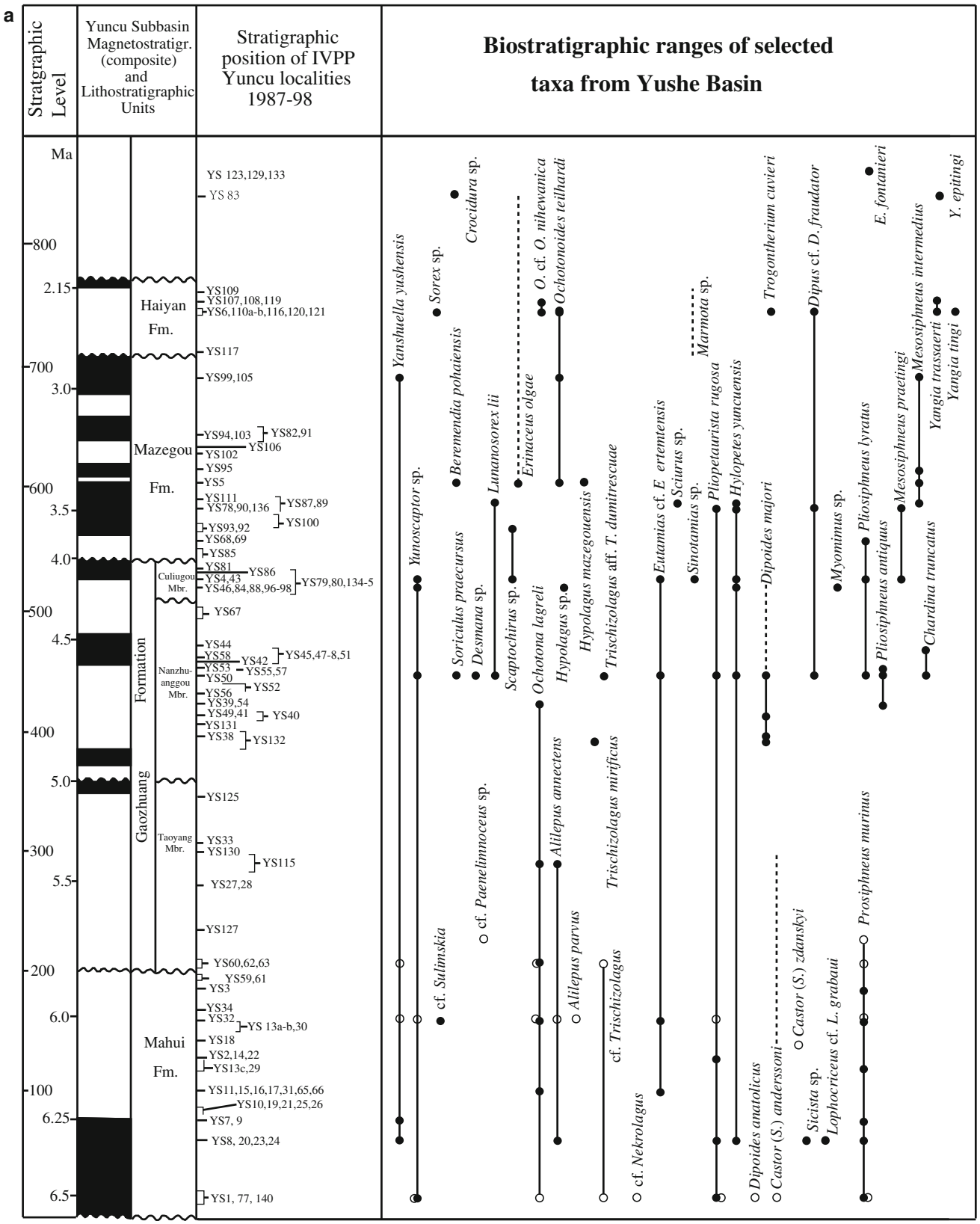

Fig. 16.1 Biostratigraphic ranges observed for small mammals of Yushe Basin. Plotted on the left side of Fig. 16.1a, b is the observed stratigraphy with composite thickness and magnetostratigraphy (after Opdyke et al. 2013), which yields estimated ages (Ma). Small mammal localities of Yushe Basin (YS numbers) are plotted by stratigraphic position. Species occurrences in Yuncu Subbasin are indicated by filled dots, vertical lines connecting single species. Tancun Subbasin species occurrences (open dots) supplement the biostratigraphic ranges (localities found in systematic accounts). These are plotted by Tancun subbasin magnetostratigraphy (see Tedford et al. 2013) and by stratigraphic reference to the C3An-C3r chron boundary and the Mahui Formation-Gaozhuang Formation contact

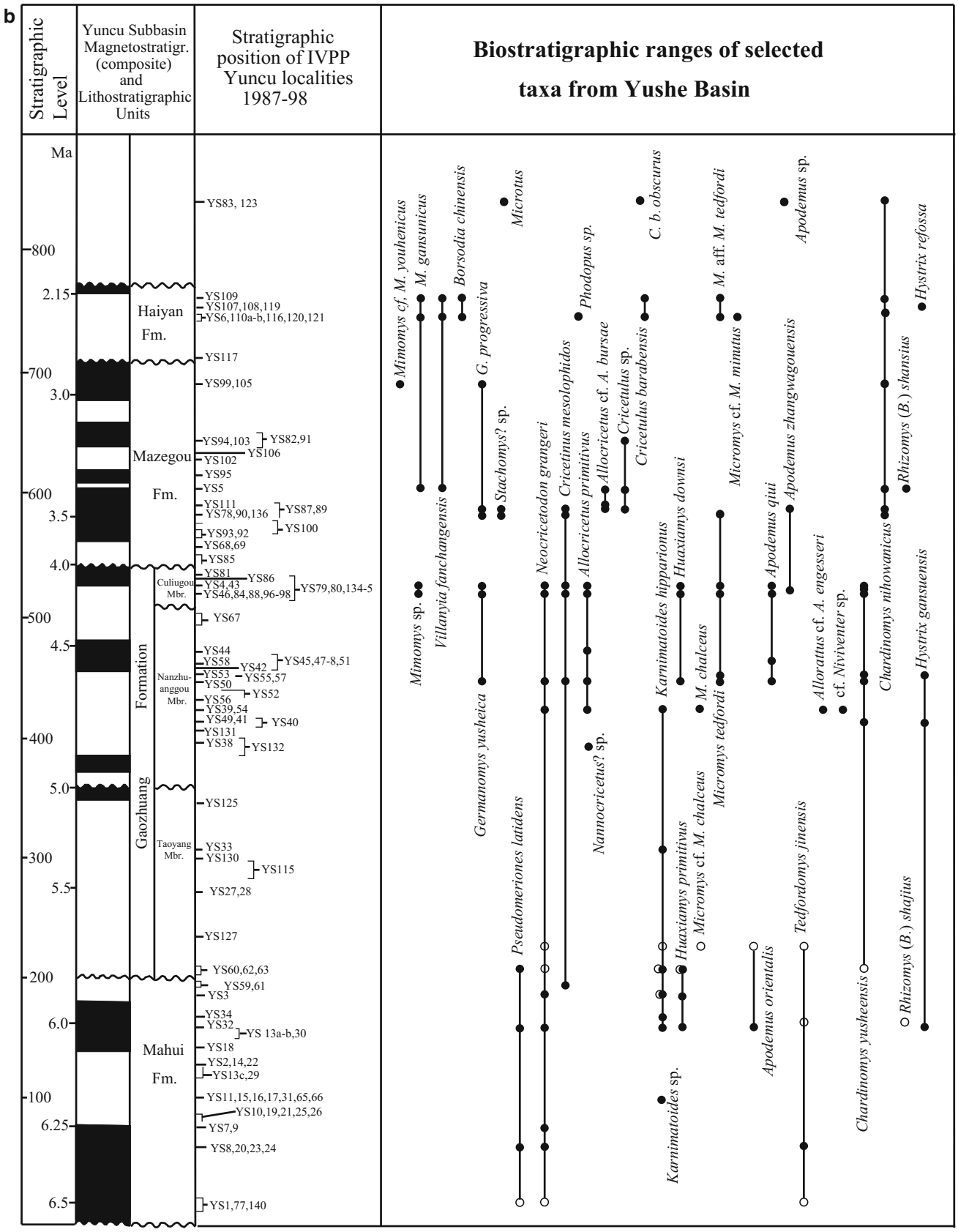

Fig. 16.1 (continued)

attributed to *P. latidens* and the type species *P. abbreviatus* restricted to the latest Miocene and Pliocene.

Derived muroids of Yushe Basin include two groups of Avicolinae. Representing the Tribe Arvicolini, an indeterminate species of *Mimomys* is encountered high in the Gaozhuang Formation at 4.3 Ma. Two species occur in the Mazegou Formation, *Mimomys* cf. *M. youhenicus* and *M. gansunicus*. The early Pleistocene Haiyan Formation produces the derived *Villanyia fanchangensis* and *Borsodia chinensis*. *Microtus* occurs in overlying loess. These records are important for the stratigraphy of Yushe Basin and of North China in general. The other arvicoline group, Prometheomyini, occurs in Yushe Basin mainly as two successive species, *Germanomys yusheica* in the Gaozhuang Formation and *Germanomys progressiva* in the Mazegou Formation, both new species. There is evidence of *Stachomys* also in Yushe Basin. Yushe Arvicolinae are absent from the Miocene Zone I. Zone II is characterized by *Mimomys* cf. *M. youhenicus* and appearance of *M. gansunicus* and by *Germanomys*. Zone III is distinguished by *Villanyia* and *Borsodia* and *Mimomys gansunicus*.

Muridae are the dominant family of rodents in the late Neogene of North China in both abundance and diversity. The murid cohort is largely stable, with congeneric species replacing earlier species. Some species are long-ranging, both *Karnimatoides hipparionus* and *Chardinomys yusheensis* spanning the Miocene-Pliocene boundary and at least 1.5 million years. Yushe Basin Zone I includes *Karnimatoides*, *Apodemus orientalis, Huaxiamys primitivus*, and *Tedfordomys jinensis*. Zone II is typified by *Karnimatoides hipparionus, Apodemus qiui* and *A. zhangwagouensis, Huaxiamys downsi, Micromys tedfordi*, and *Chardinomys yusheensis*, replaced by *C. nihowanicus*. Zone III and overlying loess continue with *C. nihowanicus* and advanced species of *Apodemus* and *Micromys*.

16.3 Faunal Units

The foregoing very briefly outlines the small mammal biostratigraphy observed in Yushe Basin, based largely through amassing samples from stratigraphically discrete screening localities. Details are given in previous chapters. These biostratigraphic observations form the basis for the conceptually distinct process of recognizing successive faunas based on small mammals, and using these to typify biochrons (see Tedford 1995), steps which lead ultimately to recognizing the stage/ages of Qiu et al. (2013). The latter authors greatly advanced the conceptual basis for Chinese Land Mammal Stage/Ages of the Neogene. Yushe Basin biostratigraphy contributes substantially to four of these, and the small mammal components are revised here.

In Yushe Basin, the late Miocene Baodean Land Mammal Stage/Age fauna is represented in the Mahui Formation, and we observe that Baodean assemblages continue into the lower part of the Gaozhuang Formation. Both the upper limit of this stage/age and the Miocene/Pliocene boundary occur near the top of the Taoyang Member of the Gaozhuang Formation. Baodean age small mammals observed in Yushe Basin are listed in Table 16.1. Characteristic Baodean elements of Yushe Basin are the talpid *Yanshuella primaeva*, the lagomorphs *Ochotona lagreli* and *Alilepus* (*A. annectens* and *A. parvus*), and the rodents *Pliopetaurista rugosa*, *Tamias* cf. *T. ertemtensis, Dipoides anatolicus*, *Prosiphneus murinus, Neocricetodon grangeri*, *Pseudomeriones latidens*, *Karnimatoides hipparionus*, *Apodemus orientalis*, *Huaxiamys primitivus*, *Tedfordomys jinensis*, *Chardinomys yusheensis*, and *Brachyrhizomys shajius.*

Table 16.1 Yushe Basin small mammals of the Baodean mammal stage/age

Lipotyphla
cf. *Paenelimnoecus* sp.
cf. *Sulimskia* sp.
Yanshuella primaeva
Lagomorpha
Ochotona lagreli
Alilepus annectens
Alilepus parvus
Rodentia
Pliopetaurista rugosa
Hylopetes yuncuensis
Tamias cf. *T. ertemtensis*
Lophocricetus sp.
Dipoides anatolicus
Sinocastor zdanskyi
Prosiphneus murinus
Neocricetodon grangeri
Pseudomeriones latidens – P. abbreviatus
Karnimatoides hipparionus
Apodemus orientalis
Huaxiamys primitivus
Micromys sp.
Tedfordomys jinensis
Chardinomys yusheensis
Brachyrhizomys shajius

Pliocene faunas of Yushe Basin embrace two successive stage/ages (Qiu et al. 2013). Characteristic mammalian players in each are similar; a number of genera are shared, but with species substitutions. The similarity of the successive assemblages suggests an enduring Yushe Basin Pliocene chronofauna. Webb (1984) applied the concept of the "chronofauna" to Miocene large mammal assemblages of North America. A chronofauna represents a community that persists without change in structure for a time interval usually greater than one m.y. Its characteristic assemblage remains largely constant, although species substitutions through time may be observed. This is the case for the Pliocene small mammal faunas of Yushe Basin, which show different species in the early and late Pliocene, but mostly the same or closely related genera.

The small mammals observed in Yushe Basin for the Gaozhuangian and Mazegouan stage/ages are listed together in Table 16.2 for comparison. In addition to species shared with the younger Mazegouan assemblage, characterizing early Pliocene Gaozhuangian components are *Yunoscaptor* sp., *Soriculus praecursus, Ochotona lagreli, Trischizolagus* spp., *Pliosiphneus antiquus, Chardina truncatus, Neocricetodon grangeri, Allocricetus primitivus, Germanomys yusheica, Mimomys* sp., *Karnimatoides hipparionus, Apodemus qiui, Huaxiamys downsi, Chardinomys yusheensis.*

Characteristic late Pliocene Mazegouan species include *Erinaceus olgae, Beremendia pohaiensis, Lunanosorex lii, Ochotonoides teilhardi, Hypolagus mazegouensis*, *Sericolagus yushecus, Mesosiphneus praetingi* (followed by *M. intermedius*), *Allocricetus* cf. *A. ehiki, Cricetulus* sp., *Germanomys progressiva,* cf. *Stachomys* sp., *Mimomys* cf. *M. youhenicus, Mimomys gansunicus, Apodemus zhangwagouensis, Chardinomys nihowanicus.*

The early Pleistocene Haiyan Formation contains assemblages that represent the early Nihewanian Stage/Age (Table 16.3). This assemblage differs considerably from the preceding faunas, and its diversity is much less, corresponding to change in climate and, presumably, different nutritional resources. Distinctive species are *Sorex* sp., *Marmota* sp., *Trogontherium cuvieri, Hystrix refossa, Yangia trassaerti, Yangia tingi*, *Cricetulus barabensis*, *Phodopus* sp, *Mimomys gansunicus*, *Villanyia fanchangensis*, *Borsodia chinensis, Chardinomys nihowanicus.*

The later Pleistocene of Yushe Basin is represented by loess deposits. The limited lateral extent of the loess, which is partly removed by erosion, and the restricted paleohabitat of loess deposits explain why we have relatively few species of that age. Recovered fossils reveal continued elements (*Erinaceus, Ochotonoides complicidens, Apodemus*) and new appearances: the white-tooth shrew *Crocidura*, modern *Lepus, Yangia epitingi, Eospalax fontanieri, Microtus* cf. *M. complicidens*, and the modern gerbil *Meriones*.

Table 16.2 Yushe Basin Pliocene small mammals of the Gaozhuangian and Mazegouan stage/ages

Gaozhuangian land mammal stage/age	Mazegouan land mammal stage/age
Lipotyphla	
Yunoscaptor sp.	*Erinaceus olgae*
Scaptochirus sp.	*Scaptochirus* sp.
Desmana sp.	*Beremendia pohaiensis*
Soriculus praecursus	*Lunanosorex lii*
Lagomorpha	
Ochotona lagreli	*Ochotona* sp.
Hypolagus sp.	*Ochotonoides teilhardi*
Trischizolagus mirificus	*Hypolagus mazegouensis*
cf. *Trischizolagus dumitrescue*	*Sericolagus yushecus*
Rodentia	
Pliopetaurista rugosa	*Pliopetaurista rugosa*
Hylopetes yuncuensis	*Hylopetes yuncuensis*
Tamias cf. *T. ertemtensis*	*Sciurus* sp.
Dipus fraudator	*Dipus fraudator*
Dipoides majori	*Dipoides majori*
Sinocastor anderssoni	*Sinocastor anderssoni*
Brachyrhizomys shansius	*Brachyrhizomys shansius*
Hystrix gansuensis	*Hystrix gansuensis*
Myomimus sp.	(no Gliridae recorded)
Pliosiphneus antiquus	*Pliosiphneus lyratus* (early only)
Pliosiphneus lyratus	*Mesosiphneus praetingi*
Chardina truncatus	*M. intermedius/M. praetingi*
Neocricetodon grangeri	*Allocricetus* cf. *A. ehiki*
Allocricetus primitivus	*Cricetulus* sp.
Cricetinus mesolophidos	*Cricetinus mesolophidos*
Germanomys yusheica	*Germanomys progressiva*
Mimomys sp.	cf. *Stachomys* sp.
Karnimatoides hipparionus	*Mimomys* cf. *M. youhenicus*
Apodemus qiui	*Mimomys gansunicus*
Huaxiamys downsi	*Apodemus zhangwagouensis*
Micromys chalceus/M. tedfordi	*Micromys tedfordi*
Chardinomys yushensis	*Chardinomys nihowanicus*

16.4 Turnover, Biogeography, and Dispersal

We have proposed that the Yushe Pliocene faunas show stability in general, with continuity of associations at the genus level, and substitution of congeners at the species

Table 16.3 Yushe Basin small mammals of the Nihewanian mammal stage/age

Lipotyphla
Sorex sp.
Lagomorpha
Ochotona cf. *O. nihewanica*
Ochotonoides teilhardi
Leporidae, indet.
Rodentia
Marmota sp.
Trogontherium cuvieri
Hystrix refossa
Dipus fraudator
Yangia trassaerti
Yangia tingi
Cricetulus barabensis
Phodopus sp.
Mimomys gansunicus
Villanyia fanchangensis
Borsodia chinensis
Micromys cf. *M. tedfordi*
Micromys cf. *M. minutus*
Chardinomys nihowanicus

level (Flynn et al. 1991). This pattern is supported by the present analysis (Fig. 16.1a, b) and is consistent with the recognition of a Yushe Pliocene chronofauna, which includes assemblages representing two mammalian stage/ages: Gaozhuangian and Mazegouan. Faunal turnover events cluster at the beginning and, especially, the end of the chronofauna.

The Yushe Basin Pliocene faunal stability is rooted in the late Baodean land mammal stage/age assemblages. The limits of the Baodean biochron are not yet fully constrained, but magnetostratigraphy shows that Baode deposits of the Lantian area date back to 7.2 Ma (Zhu et al. 2008); the younger limit of the Baodean stage/age may be best approximated in Yushe Basin. We find that Baodean assemblages persist low in the Gaozhuang Formation and that the Baodean/Gaozhuangian age boundary is quite near the Miocene/Pliocene boundary, which occurs near the top of the Taoyang Member of the Gaozhuang Formation. Faunal correlation to the key reference locality, Ertemte, agrees that the age of Ertemte is late Baodean, and suggests an age for it between 6.0 and 5.5 Ma.

Magnetostratigraphy in Yushe Basin (Opdyke et al. 2013) dates the disconformity between the Gaozhuang and Mazegou formations, which is chosen as the division between corresponding land mammal stage/ages. The hiatus is perhaps a half million years long around 4 Ma. The Mazegou Formation is truncated above by a slight angular unconformity at about 2.9 Ma. In Yushe Basin the overlying Haiyan Formation is constrained by its reversed magnetozone, which is considered chron C2r.2r, ca. 2.6–2.2 Ma (Opdyke et al. 2013). The Mazegou-Haiyan hiatus could be over a half million years in duration, and the faunal turnover at this time is profound. Possibly this stage/age boundary could be better temporally constrained in Nihewan Basin.

The geographic extent of the faunas that represent these biochrons is widespread (Tedford et al. 1991), spanning from North China to Kazakhstan, Kyrgyzstan, Tajikistan, and probably Afghanistan, and northward through Mongolia, into Siberia (see faunal lists of Erbajeva and Alexeeva 2013). Regarding historical biogeography, it appears that many of the small mammal species evolved within the Palaearctic biogeographic province, so that replacement of Baodean and Gaozhuangian taxa would have been by species derived largely from neighboring subprovinces. However, some mixing between North China and South China is evident and some long-distance dispersers may be identified.

Although Yushe Lipotyphla include widely distributed genera, the talpids and soricids are generally endemic to East Asia. The large shrew *Beremendia* and the water mole *Desmana* are known across Eurasia, and a possible late Miocene blarinine (*Sulimskia*) suggests immigration of that tribe from North America. Other insectivores are more local: the talpids *Scaptochirus*, *Yanshuella* and *Yunoscaptor*, and the shrews *Lunanosorex* and *Soriculus* are mainly endemic; some like *Soriculus* and *Yunoscaptor* suggest early Pliocene mixing of elements from South China. Pleistocene *Sorex* and *Crocidura* are, of course, widespread.

Fossil ochotonids were as diverse as they are today and, like today, may have had limited areas of distribution of species. *Ochotonoides teilhardi* appears to have originated in the biogeographic subprovince of North China. Earliest leporines of Yushe are *Alilepus* and (later) *Hypolagus*, both derived from immigrant stock from North America. Pliocene *Trischizolagus* is widespread across Eurasia, in contrast to *Sericolagus*, which appears to be endemic to northeast Asia. Pleistocene *Lepus* is an immigrant from North America, but *Ochotonoides complicidens* evolved endemically.

Like Lipotyphla and Lagomorpha, squirrels include both widespread and local elements. *Tamias, Sciurus, Pliopetaurista*, and *Hylopetes* are Eurasian (the first two Holarctic) and *Sinotamias* is Chinese; *Marmota* is a later immigrant from North America. Among dipodoids, *Lophocricetus* and *Dipus* are Asian, but the birch mouse *Sicista* is widespread across the Palaearctic, as is the glirid *Myomimus*. Beavers are distinctive in reflecting long-distance dispersal: *Dipoides* has its ancestry in North America, *Trogontherium* is pan-Eurasian in distribution, and the *Castor* group (locally *Sinocastor*) is Holarctic. *Hystrix* is also widespread in the late Miocene, but *Brachyrhizomys*, appearing by 6 Ma and thriving to about 3 Ma is one of the few rodents that likely expanded its range northward from South China.

The zokors (Myospalacinae), endemic to eastern Asia (China including Tibet, Mongolia, parts of Siberia and Kazakhstan) are a relatively young group derived from middle Miocene muroids. They diversified through the later Neogene, with species distributions of limited geographical extent in keeping with their restricted mobility, being fossorial specialists. They did not penetrate greatly into South China, but did invade Tibet (Li and Wang 2015).

Late Neogene hamsters of Yushe Basin show diversity at the generic level, with Pliocene lineages of *Neocricetodon*, *Allocricetus* and *Cricetinus*, and the addition of *Cricetulus* in the late Pliocene. Similar diversity is noted across Eurasia and makes species distinctions problematic. North China *Neocricetodon*, very close to species of *Kowalskia*, may be the senior synonym of the latter. Regardless of generic content, the hamsters are widely distributed, which indicates lack of dispersal barriers for them. Hamsters (*Kowalskia hanae* Qiu, 1995) spread to South China during the late Miocene (Ni and Qiu 2002). Like hamsters, the gerbil lineage *Pseudomeriones* occurs widely across Asia.

Arvicoline genera are also distributed throughout the Palaearctic. These rodents evolve rapidly, and quite possibly there is endemism at the species level in China. Our analysis of *Germanomys* raises the possibility that the Yushe lineage is distinct from that of Europe, which may call for a separate genus name. Chinese *Mimomys* species, too, may be distinct and until species level systematics are worked out across Eurasia, provincial names will prevail. Nonetheless, similar assemblages of *Mimomys*, *Villanyia*, and *Borsodia* are found from Europe to China.

Two late Miocene murines of Yushe Basin, *Karnimatoides* and *Tedfordomys*, are similar to older lineages of South Asia, specifically the Siwaliks of Pakistan. They are close to *Karnimata* and *Progonomys*, respectively. The biogeographic significance of this resemblance is still unclear, but Flynn and Wessels (2013) hypothesize that faunal connection of Yushe Basin and the Siwaliks was indirect – the two murine lineages dispersed westward from South Asia, spread around the Mediterranean region, and migrated eastward to China at temperate latitude. This scenario calls for wide dispersal but not a direct south-to-north connection. End-Miocene and Pliocene murines are a mix of endemic groups and widespread genera. *Chardinomys*, hallmark of Yushe Basin microfaunas, is endemic to China, as is *Huaxiamys* and *Allorattus*. If *Niviventer* is correctly identified in Yushe Basin, it would be an element shared with Southeast Asia. In contrast, the genera *Apodemus* and *Micromys*, like many other late Neogene rodents, show a great Palaearctic distribution.

The biogeographic signal presents Yushe Basin as part of a wide subprovince covering much of northern Asia to the Ural Mountains, throughout which the Baodean, Gaozhuangian, Mazegouan and Nihewanian stage/ages may be recognized (see Tedford et al. 1991). This subprovince is part of the Palaearctic biogeographic region. Throughout the later Neogene, new species appear to derive mainly from this or neighboring subprovinces within the Palaearctic region.

Notable biogeographic exceptions are late Miocene introductions of taxa: Leporidae, the beaver *Dipoides*, and a possible blarinine shrew disperse from North America. Also a bamboo rat (*Brachyrhizomys*), some insectivorans, and perhaps *Niviventer* expand to Yushe Basin from South China. Other murines appear in North China, not directly from the south, but via dispersion from the west. *Castor* (*Sinocastor*) and possibly *Hystrix* spread eastward into North China from Europe. Through the Pliocene, hamsters, arvicolines, mice, and some insectivorans show wide connections across the Palaearctic. Pleistocene assemblages introduce exotic elements, such as *Marmota* and *Lepus* ultimately from North America, and *Trogontherium* from Europe.

16.5 Closing

The Yushe Basin field campaigns of 1987–1991 succeeded in recovering diverse small mammals from all stratigraphic units of the Yuncu and Tancun subbasins. Chapter 1 of this volume outlines the techniques we used to retrieve small mammal teeth by wet screening fossiliferous sediment. Meticulous care in collecting resulted in samples from productive localities that reasonably well reflect communities of the last six million years in Shanxi Province. Research last century (e.g., Teilhard de Chardin 1942) was based on surface finds of fossils, which built good collections of beavers, zokors, and lagomorphs, and limited representation of other small mammal groups. This is the foundation for our opportunity to investigate 20 groups of small mammals.

Preliminary faunal analysis for Yushe Basin (Flynn et al. 1991) saw overall stability in the small mammal assemblages. It was apparent that the Pliocene faunas became enriched in species diversity, and that the Pleistocene ushered in considerable changes that greatly altered the mammalian community. Presently we see the Miocene-Pliocene faunal change as less than that at the Pliocene-Pleistocene boundary. The assemblages from 6 to 3 Ma remained largely similar at the level of the genus, differences lying in species substitutions, and in addition of new elements inserted into the fauna (some from Europe or North America). The Yushe Basin presented favorable habitat to maintain an evolving community through most of the Pliocene. The fauna was mainly a variant of the North China biogeographic subprovince, but with a mix of a few South China elements.

We find diverse moles (Talpidae) and shrews (Soricidae), including good material of some taxa, a diversity that

correlates with moist, mild conditions. One Pliocene genus, *Desmana*, is aquatic. Hedgehogs (*Erinaceus*) are in evidence since late in the Pliocene. Two families of bats are present, but Chiroptera are terribly under-represented. Ochotonid and leporid Lagomorpha are well represented by jaw and some cranial material. Two or three pikas (Ochotonidae) co-occur in the Pliocene of Yushe Basin, and at least three leporid genera co-occur in that epoch. Pleistocene loess yields *Ochotonoides*, *Ochotona*, and *Lepus*.

Squirrels are diverse, if under-represented, and there is good fossil material of the flying squirrel *Pliopetaurista*. This genus plus *Hylopetes* and the tree squirrel *Sciurus* imply some tree cover. So, too, the birchmouse *Sicista*, and possibly *Lophocricetus* indicate woodlands, but the jerboa *Dipus* indicates open terrain. The dormouse *Myomimus* is not arboreal but suggests thick vegetation, as does the chipmunk *Tamias* and the large body-size porcupine, *Hystrix*.

Bamboo rats prefer moist conditions and adequate vegetation to support fossorial life. A smaller species appears in the late Miocene and the larger *Brachyrhizomys shansius* typifies the Pliocene of Yushe. Two lineages of beavers coexist through the late Miocene and Pliocene. Both appear to be aquatic lineages. The larger body-size genus *Trogontherium* is the sole beaver of the Pleistocene. In contrast to these indicators of moist to aquatic conditions, the diverse zokors indicate nearby open terrain. They diversify endemically and species appear to have restricted distributions.

The extinct gerbil lineage *Pseudomeriones* accents the late Miocene fauna of Yuncu and Tancun subbasins. Fossils are clearly lower-crowned than *Pseudomeriones abbreviatus* and all but one worn specimen are older than 6 Ma. *P. abbreviatus* has been described from the Pliocene of Zhangcun subbasin. The *Pseudomeriones* lineage shows increasing hypsodonty, the earlier late Miocene fossils of Yushe Basin representing *P. latidens*. Latest Miocene *Pseudomeriones*, as at Ertemte, is the higher crowned *P. abbreviatus*. Being extinct, we do not know the environmental indications for *Pseudomeriones*, but modern gerbils indicate open conditions. The diverse hamsters (Cricetinae) also suggest open conditions, and occur in all Yushe formations.

Arvicolinae appear in the Pliocene, first the *Germanomys* lineage at 4.7 Ma, and then early *Mimomys* at 4.3 Ma. *Germanomys* disappears in the late Pliocene, but Arvicolini dominate Pleistocene microfaunas. Although we do not know the habitat preferences of *Germanomys*, and generally we reconstruct mild, moist conditions in the Pliocene of Yushe, we think of *Mimomys* and allied arvicolines as indicators of lower mean annual temperature. This is likely the climate by Pleistocene time, when we see considerable faunal turnover.

The Murinae are successful and dominant in the Pliocene of Yushe. Early genera would be consistent with warm conditions, if their close relatives are taxa of South Asian distribution, as is thought to be the case. Other terminal Miocene and Pliocene murine genera of Yushe Basin show wide Palaearctic distribution at more temperate latitudes. The hamsters, mice, and arvicolines also suggest wide dispersal with limited geographic barriers, and partly open habitat perhaps under cooling climatic conditions. Later species of these and other groups appear to be closely related to living species in the region.

Concerning small mammals in general, an ecological scenario emerges indicating well-watered, mild habitat with patchy woodlands and open terrain for the Miocene and Pliocene of Yushe Basin. In addition to several taxa that are likely aquatic or arboreal, some species suggest open, seasonally dry habitat. Yushe Basin provided an enclave of favorable habitat, likely without the extremes of more continental interior settings, and stability since the late Miocene supported a Pliocene Yushe chronofauna for the small mammals. Yushe Basin assemblages of eastern Shanxi Province may be seen as documenting the history of a late Neogene woodland fauna, contrasting with drier contemporary faunas of the interior, in affirmation of the late Miocene variation in faunal assemblages reconstructed by Kurtén (1952).

Acknowledgements We thank Lou Taylor, Jon Baskin, and Louis Jacobs, who gave generously of their time to refine the present text through their constructive reviews. We appreciate their efforts and those of all reviewers who consistently supported our efforts in producing this volume.

References

Berggren, W. A., & van Couvering, J. A. (1974). *The Late Neogene: Biostratigraphy, geochronology and paleoclimatology of the last 15 million years in marine and continental sequences*. Amsterdam: Elsevier Scientific Publishing Company.

Erbajeva, M., & Alexeeva, N. (2013). Late Cenozoic mammal faunas of the Baikalian region: Composition, biochronology, dispersal and correlation with Central Asia. In X. Wang, L. J. Flynn, & M. Fortelius (Eds.), *Fossil mammals of Asia: Neogene biostratigraphy and chronology* (pp. 495–507). New York: Columbia University Press.

Flynn, L. J., & Wessels, W. (2013). Paleobiogeography and South Asian small mammals: Neogene latitudinal faunal variation. In X. Wang, L. J. Flynn, & M. Fortelius (Eds.), *Fossil mammals of Asia: Neogene biostratigraphy and chronology* (pp. 445–460). New York: Columbia University Press.

Flynn, L. J., Tedford, R. H., & Qiu, Z.-X. (1991). Enrichment and stability in the Pliocene mammalian fauna of North China. *Paleobiology, 17,* 246–265.

Gradstein, F. M., Ogg, J. G., & Smith, A. G. (Eds.). (2004). *A geologic time scale 2004*. Cambridge: Cambridge University Press.

He, X.-R. (1984). A preliminary observation on the structure of the tunnel system of the Chinese bamboo rat (*Rhizomys sinensis*). *Acta Theriologica Sinica, 4*, 196 and 206.

Kurtén, B. (1952). The Chinese *Hipparion* fauna. *Societas Scientiarium Fennica. Commentationes Biologicae, 13*(4), 1–82.

Li, Q., & Wang, X. (2015). Into Tibet: An early Pliocene dispersal of fossil zokor (Rodentia: Spalacidae) from Mongolian Plateau to the Hinterland of Tibetan Plateau. *PLoS ONE, 10,* e0144993. doi:10.1371/journal.pone.0144993.

Licent, E., & Trassaert, M. (1935). The Pliocene lacustrine series in central Shansi. *Bulletin of the Geological Society of China, 14,* 211–219.

Liu, L.-P., Zheng, S.-H., Cui, N., & Wang, L.-H. (2013). Myospalacines (Cricetidae, Rodentia) from the Miocene-Pliocene red clay section near Dongwan Village, Qin'an, Gansu, China and the classification of Myospalacinae. *Vertebrata PalAsiatica, 51,* 211–241.

Liu, L.-P., Zheng, S.-H., Cui, N., & Wang, L.-H. (2014). Rootless myospalacines from upper Pliocene to Pleistocene of Wenwanggou section, Lingtai, Gansu. *Vertebrata PalAsiatica, 52,* 440–466.

Ni, X. J., & Qiu, Z. D. (2002). The micromammalian fauna from Leilao, Yuanmou hominoid locality: Implications for biochronology and paleoecology. *Journal of Human Evolution, 42,* 535–546.

Opdyke, N. D., Huang, K., & Tedford, R. H. (2013). The paleomagnetism and magnetic stratigraphy of the Late Cenozoic sediments of the Yushe Basin, Shanxi Province, China. In R. H. Tedford, Z.-X. Qiu, & L. J. Flynn (Eds.), *Late Cenozoic Yushe Basin, Shanxi Province, China: Geology and fossil mammals, Volume I: History, geology, and magnetostratigraphy* (pp. 69–78). Dordrecht: Springer.

Qiu, Z.-D. (1995). A new cricetid from the Lufeng hominoid locality, Late Miocene of China. *Vertebrata PalAsiatica, 33*, 61–73.

Qiu, Z.-X., Deng, T., Qiu, Z.-D., Li, C.-K., Zhang, Z.-Q., Wang, B.-Y., et al. (2013). Neogene Land Mammal Ages of China. In X. Wang, L. J. Flynn, & M. Fortelius (Eds.), *Fossil Mammals of Asia: Neogene biostratigraphy and chronology* (pp. 29–90). New York: Columbia University Press.

Tedford, R. H. (1995). Neogene mammalian biostratigraphy in China: Past, present, and future. *Vertebrata PalAsiatica, 33,* 272–289.

Tedford, R. H., Flynn, L. J., Qiu, Z.-X., Opdyke, N. D., & Downs, W. R. (1991). Yushe Basin, China: Paleomagnetically calibrated mammalian biostratigraphic standard for the Late Neogene of eastern Asia. *Journal of Vertebrate Paleontology, 11,* 519–526.

Teilhard de Chardin, P. (1942). New rodents of the Pliocene and lower Pleistocene of North China. *Publications de l'Institut de Géobiologie, Pékin, 9,* 1–101.

Webb, S. D. (1984). On two kinds of rapid faunal turnover. In W. A. Berggren & J. A. van Couvering (Eds.), *Catastrophes and Earth History: The new uniformitarianism* (pp. 417–436). Princeton: Princeton University Press.

Zheng, S.-H. (1994). Classification and evolution of the Siphneidae. In Y. Tomida, C.-K. Li, & T. Setoguchi (Eds.), *Rodent and lagomorph families of Asian origins and diversification* (pp. 57–76). Tokyo: National Science Museum Monograph 8.

Zheng, S.-H. (1997). Evolution of the Mesosiphneinae (Siphneidae, Rodentia) and environmental change. In Y.-S. Tong, Y.-Y. Zhang, W.-Y. Wu, J.-L. Li, & L.-Q. Shi (Eds.), *Evidence for evolution. Essays in honor of Prof. Chungchien Young on the hundredth anniversary of his birth* (pp. 137–150). Beijing: China Ocean Press.

Zheng, S.-H., Zhang, Z.-Q., & Cui, N. (2004). On some species of *Prosiphneus* (Siphneidae, Rodentia) and the origin of Siphneidae. *Vertebrata PalAsiatica, 42,* 297–315.

Zhu, Y., Zhou, L., Mo, D., Kaakinen, A., Zhang, Z., & Fortelius, M. (2008). A new magnetostratigraphic framework for late Neogene *Hipparion* Red Clay in the eastern Loess Plateau of China. *Palaeogeography, Palaeoclimatology, Palaeoecology, 248,* 47–57.

Appendix

Log of Surface Collections and Initial Screening Results for Microvertebrate Localities of Yushe Basin (not comprehensive faunal lists). YS means "Yushe Site", followed by number, for field localities documented by the Sino-American team. Here we list only sites that produced microfauna. Parenthetical notes after site numbers are nearby towns or stratigraphic units (see Fig. 1.2a–c).

YS1 (Haobei)
Gastropoda
Teleostei
Anura
Chelonia
Yunoscaptor humerus
Sciuridae
Prosiphneus murinus

YS2 (Lintou)
Pliopetaurista

YS3 (Top of Mahui Formation)
Gastropoda
Teleostei
Chelonia
Lacertilia
Soricidae
Leporidae
Hystrix
Pseudomeriones
Neocricetodon
Prosiphneus murinus
Huaxiamys
Karnimatoides

YS4 (Gaozhuang village)
Anura
Chelonia
Lacertilia
Aves
Scaptochirus
Yunoscaptor
Soricidae
Chiroptera
Ochotona
Leporidae
Sciuridae
Cricetini
Mesosiphneus
Germanomys
Huaxiamys
Apodemus
Chardinomys
Micromys

YS5 (Zhaozhuang village)
Teleostei
Anura
Chelonia
Erinaceus olgae
Beremendia
Talpidae
Ochotonoides teilhardi
Leporidae
Dipus fraudator
Cricetini
Mesosiphneus
Rhizomys (Brachyrhizomys)
Germanomys

Lawrence J. Flynn and Wen-Yu Wu (eds.), *Late Cenozoic Yushe Basin, Shanxi Province, China: Geology and Fossil Mammals, Volume II: Small Mammal Fossils of Yushe Basin*, Vertebrate Paleobiology and Paleoanthropology,
DOI 10.1007/978-94-024-1050-1

Mimomys
Micromys
Chardinomys

YS6 (Haiyan)
Gastropoda
Teleostei
Anura
Serpentes
Ochotonoides
Leporidae
Yangia
Borsodia
Cromeromys
Micromys

YS7 *Prosiphneus murinus*

YS8 (Low Mahui Formation)
Gastropoda
Teleostei
Yanshuella yushensis
Pliopetaurista
Lophocricetus
Sicista
Pseudomeriones
Prosiphneus murinus
Neocricetodon
Tedfordomys

YS9
Teleostei
Yanshuella yushensis
Neocricetodon
Prosiphneus murinus

YS11
Teleostei
Ochotona
Tamias
Karnimatoides sp.

YS12
Charophyta
Gastropopda
Teleostei
Lacertilia

YS23 Leporidae

YS29
Ochotona
Muridae
Prosiphneus

YS 32 (6 Ma, Mahui Fm.)
Teleostei
Lacertilia
cf. *Sulimskia* sp.
Ochotona
Hystrix
Sciuridae
Pseudomeriones
Prosiphneus murinus
Neocricetodon
Karnimatoides
Huaxiamys
Apodemus

YS33 *Karnimatoides*

YS34 *Karnimatoides*

YS35
Gastropoda
Teleostei

YS36
Ochotona
Pliosiphneus

YS37
Teleostei
Anura
Chelonia
Chiroptera, *Rhinolophus* sp.

YS38
Teleostei

Anura
Chelonia
Lacertilia
Dipoides
Pliosiphneus

YS39 (low Nanzhuanggou Member, Gaozhuang Fm.)
Gastropoda
Teleostei
Anura
Serpentes
Ochotona
Neocricetodon
Pliosiphneus
Karnimatoides
Micromys
cf. *Niviventer*

YS40
Hystrix
Dipoides

YS43
Serpentes
Cricetinae
Myospalacinae
Chardinomys

YS44 Cricetinae

YS46
Chelonia
Meles
Leporidae
Muridae

YS48
Pliosiphneus
Apodemus

YS49
Leporidae
Ochotona
Dipoides
Chardinomys
Myospalacinae

YS50 (mid-Nanzhuanggou Member, Gaozhuang Fm.)
Gastropoda
Teleostei
Anura
Chelonia
Lacertilia
Aves
Soriculus
Lunanosorex
Yunoscaptor
Desmana
Ochotona
Trischizolagus
Sciuridae
Cricetini
Pliosiphneus
Germanomys
Apodemus
Chardinomys
Micromys
Huaxiamys

YS57
Gastropoda
Teleostei
Anura
Lacertilia
Aves
?*Dipoides*
Pliosiphneus
Chardinomys yushensis
Micromys

YS60
Serpentes
Ictithere
Ochotona
Pseudomeriones
Karnimatoides
Huaxiamys

YS62 *Karnimatoides*

YS65 ?Zapodidae

YS83 (Older Red Loess)
Lacertilia
Crocidura sp.
Cricetulus barabensis
Yangia epitingi
Microtus cf. *M. brandtioides*
Chardinomys nihowanicus
Apodemus sp.

YS87 (Mazegou Formation)
Serpentes
Chiroptera
Lunanosorex
Mustelidae
Ochotona
Sciurus
Cricetini
Mesosiphneus
Germanomys
Chardinomys
Apodemus

YS88
Gastropoda
Leporidae
Myospalacinae

YS90 (Mazegou)
Anura
Chelonia
Lacertilia
Aves
Sciuridae
Pliopetaurista
Dipus fraudator
Mesosiphneus
Cricetini
Germanomys
Chardinomys
Micromys

YS93 *Scaptochirus* humerus

YS95 Dick's *Mesosiphneus*

YS96 *Chardinomys*

YS97
Gastropoda
Teleostei
Anura
Chelonia
Lacertilia
Yunoscaptor
Ochotona
Sciuridae
Myomimus
Cricetini
Germanomys
Mimomys
Chardinomys
Micromys
Huaxiamys
Apodemus

YS99 (High Mazegou Formation)
Teleostei
Yanshuella
Ochotona
Ochotonoides
Leporidae
Mesosiphneus
Germanomys
Mimomys
Chardinomys

YS103 *Cricetulus*

YS105 Will's *Mimomys*

YS107 *Ochotona*

YS108 (Haiyan Formation)
Ochotona
Hystrix
Yangia

YS109 (Haiyan Formation)
Gastropoda
Teleostei
Anura
Aves
Ochotona
Cricetini
Borsodia
Cromeromys
Chardinomys
Micromys

YS110 (Haiyan Formation)
Teleostei
Ochotona
Yangia

YS111 (Dagou)
Felid carnassial
Cricetulus

YS115
Aves
Ochotona
Leporid
Prometheomyini
Myospalacinae
Muridae

YS116
Teleostei
Ochotona
?*Rhizomys* incisor

YS117 (Haiyan Formation)
Yushe Museum *Marmota*

YS118
Ochotonoides
cf. *Chardinomys*

YS119 *Yangia*

YS120 (Haiyan Formation)
Teleostei
Anura
Anatidae
Sorex
Dipus
Cricetulus
Yangia
Borsodia
Cromeromys
Chardinomys
Micromys

YS123 (Younger Red Loess)
Yangia epitingi
Microtus cf. *M. complicidens*

YS129 Will's *Yangia* skull

YS132
Serpentes
Trischizolagus
Dipoides
Neocricetodon

YS133 Xiaofeng's *Yangia*

YS134
Chiroptera
Germanomys
Chardinomys

YS135 *Apodemus*

YS136 (Qiu Mazegou Site)
Mesosiphneus
Mimomys

YS139 (Danangou)
Teleostei
Serpentes
Ochotona

Leporidae
Pliopetaurista
Neocricetodon

YS141 (Taiqiu)
Teleostei
Lacertilia
Prosiphneus
Huxiamys

YS142 (Taiqiu)
Neocricetodon

YS143 (Taiqiu)
Yanshuella
Yunoscaptor
Alilepus
Prosiphneus

YS144 (Dengyucun)
Teleostei
Karnimatoides

YS145 (Dengyucun)
Gastropoda
Cyprinidae (probably *Cyprinus carpia* and *Siniperca* sp.)
Anura
Serpentes
Lacertilia
Chiroptera
Talpidae

YS150 (Liujiahuang-Tancun)
Teleostei
Ochotona
Pliopetaurista
Pseudomeriones

YS151 (Liujiahuang)
Yunoscaptor
Prosiphneus

YS152 (Wangxiawa)
Lacertilia
Yunoscaptor
Prosiphneus
Neocricetodon

YS154 (Jiayucun, lower level)
Chelonia
Serpentes
Ictithere
Yunoscaptor

YS155 (Jiayucun, lower level)
Teleostei
Chelonia
Serpentes
Prosiphneus
Neocricetodon

YS156 (Jiayucun, lower level)
Chelonia
Serpentes
Aves
Ochotona
Alilepus
Prosiphneus
Rhizomys (Brachyrhizomys)

YS157 (Zhongyugou)
Yunoscaptor

YS158 (Zhaigou)
Prosiphneus

YS159 (Zhaigou)
Teleostei
Serpentes
Soricidae
Yanshuella
Alilepus
Prosiphneus
Apodemus

YS161 (Jiayucun, upper level)
Gastropoda
Yanshuella
Ochotona
Alilepus
Dipoides

Prosiphneus
Neocricetodon
Karnimatoides
Huaxiamys
Chardinomys
Apodemus

YS162 (Jiayucun, upper level)
Gastropoda
Teleostei
Serpentes
Rodentia

YS167 (CAWL paleomag site)
Alilepus annectens mandible

YS169 (Daxigou, lower Jiayucun level)
Ochotona
Talpidae

YS170 Dengyucun (Mahui Formation)
Pliopetaurista
Neocricetodon

YS171 (Jiangou, Taoyang area)
Gastropoda
Teleostei
Karnimatoides

Index

Note: Page numbers followed by *f* and *t* indicate figures and tables respectively

Lawrence J. Flynn and Wen-Yu Wu (eds.), *Late Cenozoic Yushe Basin, Shanxi Province, China: Geology and Fossil Mammals, Volume II: Small Mammal Fossils of Yushe Basin*, Vertebrate Paleobiology and Paleoanthropology,
DOI 10.1007/978-94-024-1050-1